Modernization of Post-Graduate Courses in FECU
HEEPF Grant # A-045-J0

Project PI: Prof. Said M. Megahed

MPE 635: Electronics Cooling

Mechanical Power Engineering Department
Faculty of Engineering
Cairo University
Egypt

Dr. Sayed Kaseb
Dr. Gamal El-Hariry

CONTENTS

Part E: Analysis of Thermal Failure of Electronic Components

25. Analysis of Thermal Stresses and Strain
26. Effect of PCB Bending Stiffness on Wire Stresses
27. Vibration Fatigue in Lead Wires and Solder Joints

Part F: Practical Applications

28. Fan-Cooled Enclosure of a PC System
29. Flow over a Heat Sink

Part G: Appendices

G.1 Course Specifications
G.2 Problem Bank
G.3 Solved Problems
G.4 Sample Exams
G.5 Contents of Courses and Books
G.6 Internet Links
G.7 References

COURSE OBJECTIVES

The objectives of "Electronics Cooling" course are as following:

1. To establish fundamental understanding of heat transfer in electronic equipment.
2. To select a suitable cooling processes for electronic components and systems.
3. To increase the capabilities of post-graduate students in design and analysis of cooling of electronic packages.
4. To analysis the thermal failure for electronic components and define the solution.

Part A: Introduction to Electronics Cooling

Indicative Contents

- **Introduction**
- **Packaging Trends and Thermal Management**
- **Basics of Heat Transfer**

1. Introduction

As a mechanical power engineer you have passed through your undergraduate studies by thermodynamics, fluid mechanics, and heat transfer. As you have graduated you should have had a good sense of the interaction between these three fields of science. Now in your postgraduate studies you should elaborate more on the relation between what you have learned and the modern engineering applications.

The ongoing graduate course, electronics cooling, will deal with electronic equipments design and packaging from the thermal view point. The proper thermal design of electronic equipment will increase its reliability and durability as the major failure cause of electronics equipment damages results from the excessive heating of the electronic components.

1.1 Importance of Electronics Cooling

Heat transfer as a science and art has been the key for industrial development, since the industrial revolution. At the beginnings of the industrial age scientists as Watt, Stevenson …etc, made use of heat transfer as a science for the design of heat equipments to run steam power cycles, nowadays the information technology revolution have also to rely on the heat transfer as the electronic industry develop in order to maintain proper working conditions for these fast developing equipments.

As electronic devices run they consume electric power, this power needs to be dissipated or otherwise heat will be accumulated and device's temperature may exceed to dangerous levels. Consider the simplest electronic component, the resistance, as the electric current pass through it heat is generated by Equation 1.1, now if this resistance is thermally insulated allover its surface what would happen?

$$P = I^2 \times R \tag{1.1}$$

Where;

P = Represents both the electric power and heat dissipated in W
I = Electric current in A
R = Electric resistance in Ω

Now if we get to a more complicated electronic component like the processor of a personal computer, what do you think will happen if the processor fan fails to operate? The common answer here is that the computer will not respond and any process will be failed. This answer needs more elaboration, so let us start our first case study concerning this problem.

1.2 Electronics Cooling Devices

1.2.1 CPU, an Electronic Component

The CPU is an integrated circuit made of silicon. It combines a lot of electronic components like transistors, resistances, capacitors, and inductances. By this large combination mathematical operations may be done, as the time goes on, this single IC incorporate more elements and thus more operations are done per second and the operation frequency is getting much higher.

As each operation is done thousands of transistors switch on and back off again resulting in a huge heat dissipation requirement. If this heat is not dissipated properly, the processor temperature will rise to dangerous limits (above 120 ºC), which may result in the destruction of the IC's structure and components.

1.2.2 CPU, Heat Dissipation

Now considering the heat transfer area of an electronic processor, this area would not be sufficient to dissipate the large heat generated inside it, this is due to:

- Compact design of ICs.
- Low heat transfer by natural convection.
- Small allowable temperature difference (20-70 ºC)

These drawbacks need to be solved, and by common engineering sense, the use of extended surfaces seems to be a solution for the first limitation, also the PCB itself may be used as another heat sink. As for the second limitation, we may increase the heat transfer rate by forced convection instead of natural convection; this may be accomplished by the aid of a fan that increases the air velocities over the fins.

Now as the processor capability differs, the thermal design of the heat sink will change. This is your assignment to search for the various processors and the appropriate thermal design for each. Remember this is due for next week!?

1.2.3 Fans

Exercise 1.1: Submit a report for cooling by fans

1.2.4 Heat Sink

Exercise 1.1: Submit a report for cooling by heat sink

1.3 Introduction to Thermo-Fluid Issues in Electronic Manufacturing

Thermal issues in the electronic product life cycle appear to be crucial. Electronics manufacturing incorporate many stages that depend on the thermal behavior of the processing techniques such as:

- Crystal growth.
- Rapid thermal processing.
- Thin film processing.
- Soldering.
- Rework.
- Testing.

But none of the above mentioned processes are within our scope of study. Actually we are more interested in the thermal issues in electronics packaging. In this case we have to differentiate between the various electronic, optoelectronic, and power packaging requirements.

Therefore thermal management should be studied to incorporate passive or active techniques or a combination of both. The thermal characteristics may be analyzed and studied by computer modeling and experimentation.

1.3.1 Reliability and Temperature

The exponential advancement in electronic industries has led to greater emphasis being placed on reliability of electronic products; as electronic applications are used in military systems, medical instruments, aircraft control and other many sensitive applications. Reliability may be increased by improving components quality and in particular on cooling.

Recent studies of electronic equipment have shown that the field reliability of equipment is temperature related. This relation is affected by the mod of heat transfer being natural or forced convection.

The reliability of an electronic system comprising a group of components is most simply stated as the probability, expressed in percent, of operating continuously over a specified period of time with no failures. For most solid-state electronic devices, the reliability handbooks which establish a common basis for comparing competitive designs utilize an Arrhenius-type failure-rate model of the form:

$$\lambda_i = B_i e^{\left(-A_i / \lambda_j (T)\right)} + E_i \tag{1.2}$$

Where; the coefficients A_i, B_i, and E_i are independent of temperature.

Considering that each part has a particular failure rate expressed in number of failures per million hours, the mean time between failures MTBF for a group of components constituting a system is expressed as:

$$MTBF = 1 \Big/ \sum_{i=1}^{n} \lambda_i (T) \tag{1.3}$$

The reliability R, which is the probability of no failures over the operating time t, is, in terms of MTBF,

$$R = e^{-t / MTBF} \tag{1.4}$$

Therefore for a module consisting of 1000 devices, each having an assumed failure rate λ_i of 1.0 ppm, the MTBF is 1000 h [from Equation 1.3], and the probability of operating with zero failures over only 100 h is 90.5 percent [from Equation 1.4]. Furthermore, assuming there are 10 identical assemblies or modules constituting a package, the overall package MTBF is only 100 h and the reliability for a 100-h operating time is reduced to 36.8 percent. The inclusion of nine additional modules effectively lowers the reliability by 59 percent.

In some cases we would like to know the MTBF required to achieve a given reliability. For example, in the case cited, if the desired reliability of the 10-module system is 0.95, that is, 95 percent probability of failure-free operation for 100 h, the resulting system MTBF, from Equation 1.4, is 1949 h, or 19,490 h per module.

As to what is considered a proper level of operation, Figure 1.1 illustrates typical junction temperatures for equipment presently operating in a large number of field applications. The acceptable operating range for semiconductor junctions is shown to be generally 40 to 60 °C, although even fewer failures occur, down to as low as 0 °C. Below 0 °C, reliability is uncertain and some semiconductors cease operating, only to return to operation at higher temperatures with no apparent permanent damage. It must be recognized that the allowable junction temperature for any system required to meet a specified reliability may vary considerably due to many factors, including parts count, type of components and dissipation levels. Nevertheless, the upper limit for commercial applications is usually set at 85 °C, and for military equipment the acceptable upper limit is 100 to 110 °C for all semiconductors in power supplies and processors. It should also be recognized that other electronic components, diodes, capacitors, resistors, and so on, are also sensitive with respect to temperature, even though in general these components do not drive systems with regard to reliability. Nevertheless, in determining MTBF, all components become contributors and as such figure into the overall computation.

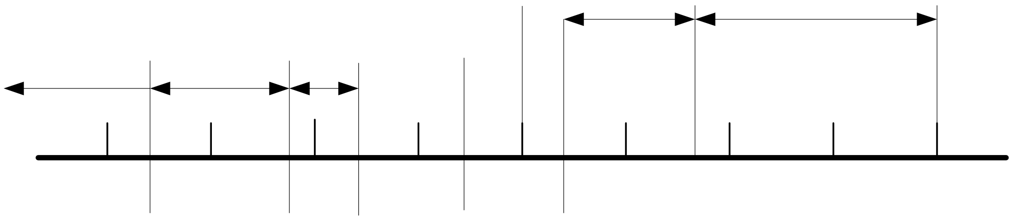

Figure 1.1 Temperature spectrum of operating junctions

1.3.2 Liquid Cooling Systems Considerations

System Types

There are two types of liquid systems used extensively in electronic cooling, direct and indirect. In the direct cooling system approach, the coolant flows over the component to remove heat from the surface and as such must be capable of sustaining a voltage gradient; alternatively in cold-plate cooling, which is indirect, there is no such requirement. The direct method is an efficient means of heat removal because the coolant is closest to the heat source. Even so, in critical applications where the heat flux rates are high, surface temperatures are best determined through actual measurements of temperature rather than exclusive dependence on analytical predictions. Some examples of direct liquid cooling of electronic equipment and the coolants used in these systems appear in Table 1.1. Common to these applications is the necessity for the maintenance of coolant purity, which is obtained through a means of filtration consistent with the dielectric requirements. Experience has shown that in direct cooling of components, the system must be absolutely airtight in order to prevent air or moisture from degrading the heat transfer performance of the coolant. In addition, moisture absorption can lead to a chemical breakdown in some coolants, which in turn lowers the flash point, hence creating a potential safety hazard. Extreme care is thus required in selecting a dielectric for direct cooling applications.

The category of indirect liquid cooling refers to the use of cold plates for the absorption of heat. Some recent examples of this type of cooling include cold plates for use in antenna array modules having solid-state circuitry and in high-heat flux power supply modules in aircraft applications. Commercial applications include mainframe computers where a refrigerant system provides a heat sink for the liquid used to cool high-heat chip packages.

Table 1.1 Common examples of direct liquid cooling

Coolant	Application
FC.77	Cray-2 supercomputer
FC-104, EWG, deionized water	Laser target illumination for electro-optical systems
C25R	Radar transmitter and TWTs on F-15 and F-16 fighter aircraft and others
FC-77, EWG	Antenna and klystron tubes for E3-AWACS radar system
C25R, PAO	

Coolant Selection

The choice of coolant in these applications, whether direct or indirect, often depends on the forced convection figures of merit (FOM) derived from the four basic coolant properties, c_p, μ, k and ρ. Table 1.2 lists these properties at 1 atm for five coolants at the three temperatures of -40, 25, 93.3 °C. It is important to note that absolute viscosity [in kg/(m.s)] varies widely with temperature and as such has significant implications in the coolant selection process. Figures 1.2 and 1.3 illustrate the coolant figures of merit as functions of temperature for straight finned or tubular channel flow operating in the laminar and turbulent regimes. These cases define typical flow conditions in liquid systems used in electronic applications. Equations 1.5 and 1.6 express the figure of merit FOM for these two cases of interest.

For laminar flow at the entrance to the cold plate,

$$FOM \approx k^{0.66} \rho^{0.33} c_p^{0.33} \tag{1.5}$$

For fully developed turbulent flow in the cold plate,

$$FOM \approx \frac{k^{0.6} \rho^{0.8} c_p^{0.4}}{\mu^{0.4}} \tag{1.6}$$

Table 1.2 Coolants properties

	PAO Chevron Chemical Company			C25R Monsanto Company			FC-77 3M Company			EWG (62-38) E.I. du pont de Nemours & Company, Inc.			Water		
	-40	25	93.33	-40	25	93.33	-40	25	93.33	-40	25	93.33	-40	25	93.33
c	2051	2261	2428	1549	1842	2177	921.1	1047	1172	2763	3098	3433	N/A	4145	4187
miu	0.22	0.006	0.001	0.076	0.005	0.001	0.008	0.001	5E-04	0.2	0.005	1E-03	N/A	9E-04	3E-04
k	0.149	0.144	0.137	0.137	0.13	0.126	0.069	0.064	0.057	0.398	0.381	0.363	N/A	0.606	0.675
rho	839.4	789.7	743.3	949.9	900.2	839.4	1938	1778	1589	1121	1080	1030	N/A	999.6	962.7

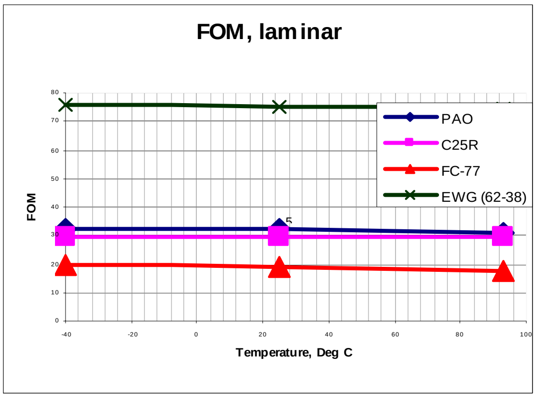

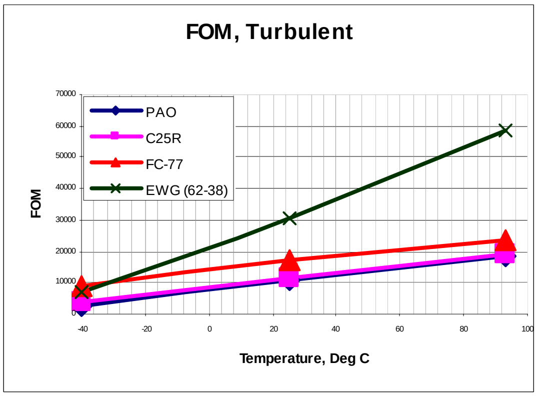

Figure 1.2 Figures of merit for liquid coolants in laminar flow	Figure 1.3 Figures of merit for liquid coolants in turbulent flow

Good design practice for cold plates operating in the laminar region, which is common in liquid systems, dictates that critical components be located near the entrance of cold plates in order to benefit from the low inlet coolant temperature but also to take advantage of the higher cold-plate film coefficients. As to coolant selection, the heat transfer figures of merit shown in Figures. 1.2 and 1.3 are to be used judiciously along with other criteria deemed important to specific applications. These parameters include the following:

- Toxicity
- Pour point
- Maximum wet wall temperature
- Flammability
- Cost per gallon Freeze point
- Material compatibility
- Corrosion
- Pressure drop characteristics
- Water absorption sensitivity

Pressure Drop and Pump Requirements

The cold plate heat transfer design is best expressed in terms of a friction factor f and a heat transfer j, both being functions of the Reynolds number. For the viscous pressure drop through the heat exchanger core, neglecting the entrance and exit losses,

$$\Delta P_{core} = 4f\frac{\ell}{d_h}\left(\frac{\rho V^2}{2}\right) = 4f\frac{\ell}{d_h}\left(\frac{G^2}{2\rho}\right) \qquad (1.7)$$

In Equation 1.7 the term of ($\rho V^2/2$) is replaced by ($G^2/2\rho$), where G is the mass flow per unit area, kg/m^2.s, a more commonly used heat exchanger parameter.

The total system pressure drop of a common system as in Figure 1.6 includes the cold-plate and heat exchanger viscous core drops and the inviscid entrance and exit losses within the exchangers as well as line pressure drops throughout. Loss coefficients through valves, expansion, and contractions may be obtained by the equation:

$$\Delta P = \frac{kG^2}{2\rho} \tag{1.8}$$

The pump characteristic curve showing flow versus pressure drop is then used together with superposition of the system resistance to obtain the operating point as shown in Figure 1.4.

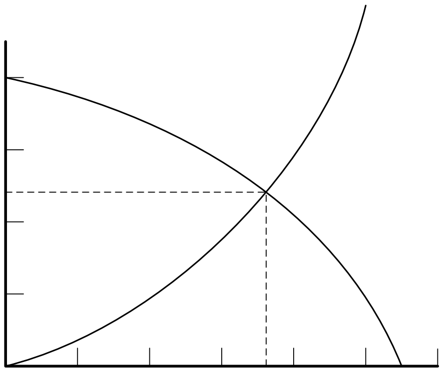

Figure 1.4 pump characteristic curves

Air Cooling System Consideration

In electronic systems, air seems to be a competitive coolant due to its availability, properties, and simple system requirements. The essential components of air cooling systems are the prime movers, fans and blowers, and the heat exchangers. For small heat dissipation, the prime mover of the air cooling system may be the draft or circulation created by density variations.

Induced or Draft Cooling

The use of induced draft air cooling in electronic application with low dissipation results in increased reliability, less number of system components, and decrease in maintenance operation. This method of cooling is applicable if the heat dissipation is less than 3500 W/m^3.

The driving force in induced-air cooling is the pressure difference caused by a change in air density between the lower and upper regions of a cabinet. This so called chimney effect produces an air motion within the enclosure which cools the component as the air moves from the bottom upward. Resisting this motive force is the internal friction and the losses associated with area changes within the enclosure. The operating point for a cabinet is where a balance exists between the system pressure or resistance and the induced draft. The latter is expressed as the flotation pressure ΔP_f (in Pa) in the equation

$$\Delta P_f = H\rho g \ln\left(\frac{T_2}{T_1}\right) \tag{1.9}$$

Here T_2 and T_1 are outlet and inlet absolute temperatures (°K), respectively. In the application of Equation 1.9, the height H (m) is related to the manner in which the cabinet heat is dissipated, that is. H is the full height whenever the entire heat is located at the console bottom, whereas for uniform heat spreading top to bottom, H is equal to one-half the cabinet height. For any other distribution of heat the centroid of heat as measured to the exit or top of the cabinet is the desired height. Figure 1.5 shows a typical cabinet, 457 by 483 by 1524 mm. with four layers or PCB buckets stacked vertically. The operating point for this cabinet is obtained from a plot of the cabinet resistance made up of the sum of friction loss and the entrance and exit losses balanced against the induced draft pressure defined by Equation 1.9.

Figure 1.6 represents the solution for the above mentioned cabinet including 42 active PCBs out of a total of 60 slots, having an average dissipation of 12 W each. If the flow rate is not suitable to dissipate the required heat a fan or a blower may be used to reach the best heat transfer design.

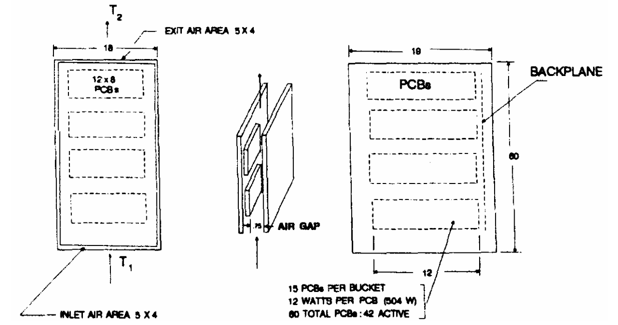

Figure 1.5 Types of induced-draft-cooled cabinet.

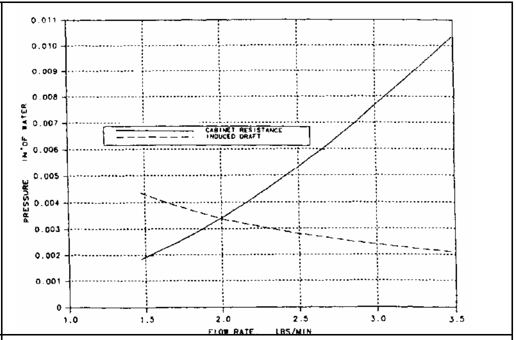

Figure 1.6 Cabinet draft and flow resistance curves.

Fans and Blowers

In the selection of fans and blowers, the flow and pressure head are the major parameters of interest, but also important are the noise level, life, ac (60 Hz or 400 Hz) or dc operation, size, and, in some cases, operation at other than sea level.

Fan laws are sometimes used to compare the operation of a specific fan under varying assumptions of speed, flow, density, and size:

Speed change

$$\dot{Q}_2 = \frac{\dot{Q}_1 N_2}{N_1} \tag{1.10}$$

$$P_2 = P_1 \left(\frac{N_2}{N_1} \right)^2 \tag{1.11}$$

Density change

$$\dot{Q}_2 = \dot{Q}_1 \tag{1.12}$$

$$P_2 = P_1 \left(\frac{\rho_2}{\rho_1} \right) \tag{1.13}$$

Size change

$$\dot{Q}_2 = \dot{Q}_1 \left(\frac{d_2}{d_1} \right)^3 \tag{1.14}$$

$$P_2 = P_1 \left(\frac{d_2}{d_1} \right)^2 \qquad (1.15)$$

The relation ships, in Equations 1.10 through 1.15, express the fan laws under the stated conditions. The assumption of constant efficiency is inherent in these equations, whereas practical fan designs will alter this assumption. The air power P_a, (in W) at a given flow (m^3/s) and pressure (Pa) is in accordance with the equation

$$P_a = \Delta P \dot{Q} \qquad (1.16)$$

Fans are sometimes used to simply purge air from a cabinet in order to prevent heat buildup, or they can provide air circulation within enclosures, as in ground equipment racks, or in many cases they provide a high-velocity air flow over components to increase the convection coefficient h These many uses cover a broad spectrum of pressure and flow conditions, leading to the development of different wheel designs tailored to match a wide range of applications. The general classification of blowers is best defined in terms of specific speed.

Specific speed, N_s, is expressed by the equation

$$N_s = \mathrm{rpm} \frac{\dot{Q}^{0.5}}{\Delta P^{0.75}} \qquad (1.17)$$

Where; in terms of the flow Q (in ft^3/min) and the pressure ΔP (in inches of water).

Figure 1.7 shows the range of specific speeds for several wheel designs commonly used in electronic cooling. These devices are illustrated in Figure. 1.8. The propeller fan is a high-pressure device used mostly as a circulating fan. The tubeaxial fan provides higher pressure versus flow than a propeller fan and represents a logical extension of fan design. Vaneaxial fans are compact high-frequency (400-Hz) units whose airflow is parallel to the motor shaft. The impeller and correctional vanes of these units are airfoil designs installed to develop maximum efficiency. The other centrifugal impellers in Figure.1.8 vary in blade configuration, which is either radial, forward, or backward curved. In small sizes, the forward- curved blades often provide the best overall performance.

The performance of fans and blowers is represented by a constant-speed plot of pressure head, Δp verses flow $\dot{Q}$. A typical example of a constant speed fan is shown in Figure. 1.9 along with a system impedance curve. The intersection of the system impedance curve and the fan curve defines an operating point.

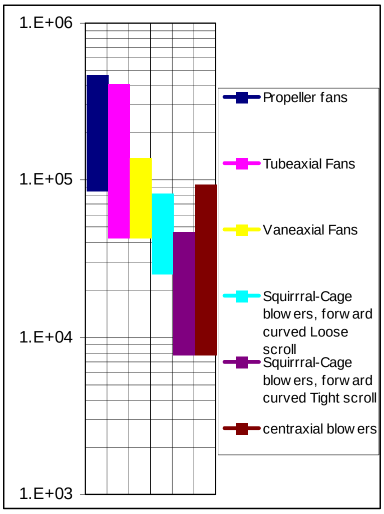

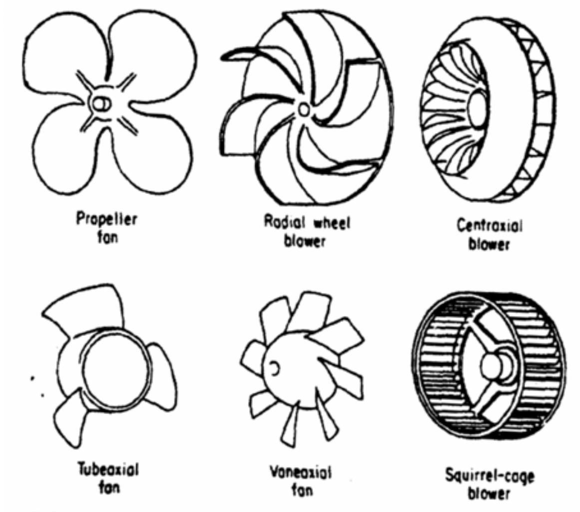

Figure 1.7 Range of specific speeds for various Fans and blowers	Figure 1.8 Fan and blower impeller designs

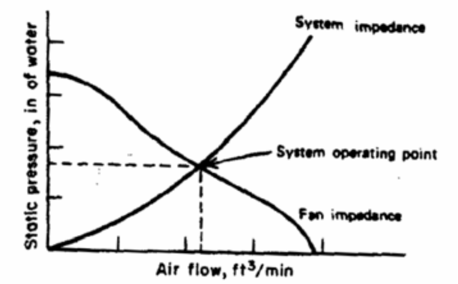

Figure1.9 Typical fan and system operating point

Exercise 1.3: Submit a report to illustrate the steps requires to obtain the operating point for a fan.

Example 1.1: The cabinet depicted in Figure. 1.5 is to be converted into a fan-cooled cabinet in order to lower the component temperatures. A further 10 PCBs are also added, each dissipating 15 W, for a total cabinet dissipation of 654 W. Select a fan based on a desired temperature rise of only 10 °C inlet to outlet having an operating speed of 1750 or 3450 rpm (60 Hz). The cabinet inlet air temperature is 21.1 °C. (Assume the airflow pressure drop in the cabinet to be 0.059 in of water.)

Solution:

1. Apply energy balance on the air flow:

$$\dot{m}_{air} c_{p_{air}} (\Delta T_{air}) = 654$$

Rearranging,

$$\dot{m}_{air} = \frac{654}{c_{p_{air}} (\Delta T_{air})} = 0.0652 \quad kg/s$$

2. The average density is

$$\bar{\rho} = \frac{P}{RT} = \frac{1.01325\times10^5}{287\times(273.15+26.1)} = 1.18 \quad kg/m^3$$

3. The air flow is

$$Q^{\bullet}_{air} = \frac{m^{\bullet}_{air}}{\bar{\rho}} = 0.0553 \quad m^3/s = 116.8 \quad ft^3/\min$$

4. The specific speed is

$$N_s = rpm\frac{\sqrt{Q^{\bullet}_{air}}}{\Delta P^{0.75}} = 1750\frac{\sqrt{116.8}}{(0.059)^{0.75}} = 157918$$

5. From the Figure. 1.8, the chart indicates a propeller fan as a likely candidate and further examination of catalog data reveals that a type BS-650l satisfies the requirements. A plot of this fan's curve along with the cabinet resistance line defines an operating point at the intersection of 120 ft^3/min and 0.062 in of water pressure drop (Figure. 1.10). The fan operates at 1750 rpm, 60 Hz. and draws only 10 W at full load.

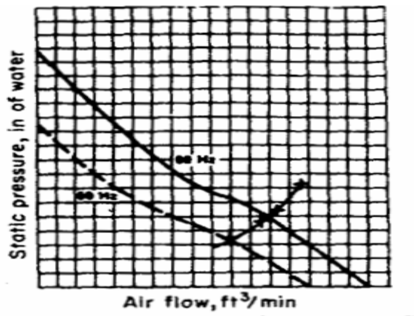

Figure 1.10 Vaneaxial fan curve

2. Packaging Trends and Thermal Management

2.1 Introduction

Packaging is one of the important stages in the electronic devices manufacturing. Proper packaging of electronic component increase reliability and lifetime but unfortunately increases its cost. Due to the nature of the design and development in the electronics industry, while the function of a computer is undeniably, the electronic failures in the field today are most often mechanical.

2.1.1 Electronic packaging and interconnection technology

Electronic packaging is the realization of the physical, electronic system, starting with block-circuit diagram. This involves choice of technology for implementation, choice of materials, detailed design in chosen technology, analysis of electrical and thermal properties, and reliability. This definition is one among many, and may shift as the field is further developed.

Due to the multi-disciplinary of the electronic packaging and interconnection technology, a combination of the following disciplines should be studied:

- Electronics
- Materials properties and materials compatibility
- Mechanics
- Chemistry
- Metallurgy
- Production technology
- Heat transfer
- Reliability, etc
-

Product development should involve experts from the various fields, and the interdependence of the fields may be the most important to make a good product.

2.1.2 Types of Electronics and Demands

Satellite Electronics

Production volume: one unit, 20 years life required, no repair, very low weight, and very high development cost acceptable.

Life Saving Medical Electronics

Similar reliability/power demand may be in harsh environment (body fluids), medium production volume.

Telephone Main Switchboard

10 year life, benign environment, very high complexity, low and high production volume, and high price pressure.

Military Electronics
Very high reliability demands, in very rough environments. High development cost (and production cost) acceptable.

Computers
High performance and reliability required. Very short product life, high production volume for some, and small volume for some products.

Consumer Products (watches, calculators...)
Extreme price pressure, very short product life, low weight and power, very big market, and no repair.

2.1.3 Automotive Electronics

Electronic content in cars and trucks has significantly increased in the last 30 years. Much of the functional content of these vehicles is now generated or controlled by electronic systems. This trend will continue in the future, as more mechanical functions are converted to electronic and electrical functions. A list of many current automotive electronic functions can be found in Table 2.1.

Table 2.1 Current Automotive Electronic Functions

Where Are We Today?

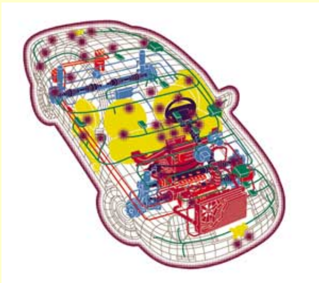

- Collision Warning Systems
- Adaptive Cruise Control
- Night Vision
- LED Displays
- Incandescent Lamp Lighting
- UV Front Lighting
- Motor Controls
- Low Tire Pressure Warning
- Reconfigurable Displays
- Electric Vehicle Propulsion Systems
- Cockpit Modules
- Automatic Wiper Control
- Automatic Head/Tail Lamp Controls

- Electronic Spark Control
- Body Control Computer
- Speakers and Enclosures
- High Fidelity Music Systems
- Compact Disc Players
- AM Radios
- Anti-Lock Brakes
- Traction Controls
- Engine Control Modules
- Suspension Controllers
- FM Radios
- Power Modules
- Remote Keyless Entry
- Cellular Telephone
- Emergency Call Service
- Satellite Radio
- Automatic/Remote Mirror Control
- Remote Start
- CB Radio

- Voltage Regulators
- Anti-Theft Systems
- Electromechanical Instrument Clusters
- Heating/Ventilation/Air Conditioning Controls
- Electronic Instrument Clusters
- Driver Information Center
- Head-Up Displays
- Steering Wheel Controls
- Air meter Electronics
- Air Bag Electronics
- Pressure Sensors
- Ignition Electronics
- Four Wheel Steering Systems
- Vehicle Stability Control Systems
- Power Train and Transmission Control Modules

Some recently introduced vehicles – hybrid cars – use internal combustion engines in conjunction with electric drive motors. Electric vehicles use electric motors alone without internal combustion engines. It is anticipated that fuel cell based electric vehicles will go into production some time late in this decade. These vehicles will use high power motor controls and drive electronics that will likely dissipate kilowatts of thermal energy.

Cost, Size, and Reliability

The requirements of low cost and small size is a given for nearly all commercial electronics applications. This is also true for automotive electronic systems and, as is the case with many consumer electronic products, price is a major driver of the hardware design. One example can be seen in the history of typical engine control modules (ECMs) shown in Figure 2.1. Over time, the size and cost of the typical ECM has decreased while the required functionality and operating temperatures have significantly increased.

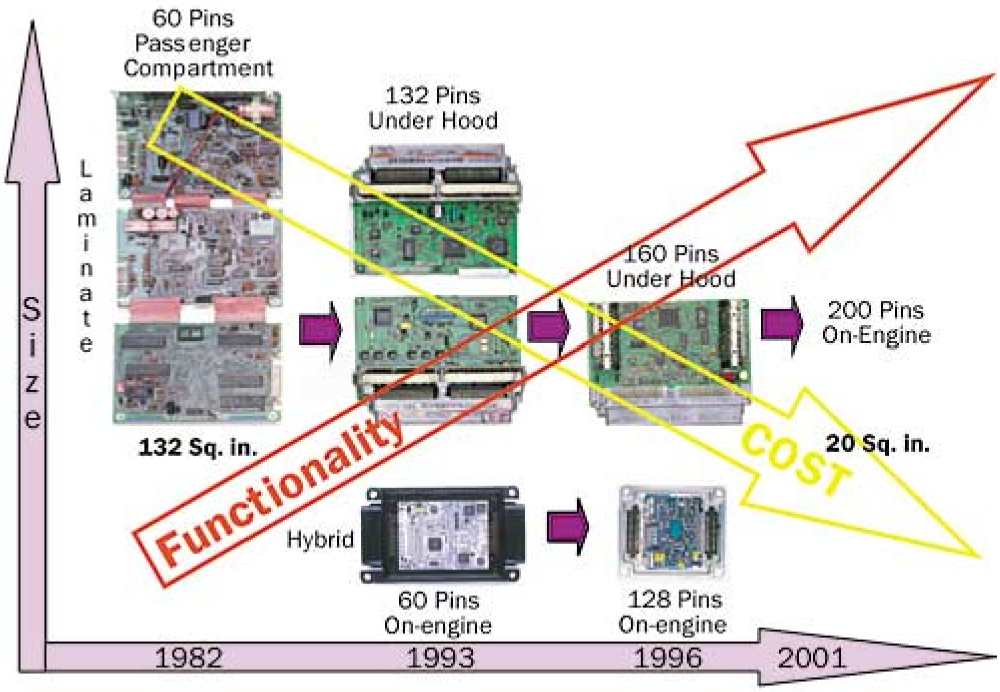

Figure 2.1 History of typical engine control modules (ECMs)

Although both consumer and automotive electronic hardware trends push suppliers toward smaller size and lower cost, there are significantly higher requirements for operating life, reliability and operating environment in automotive applications. Automotive safety issues as well as customer expectations require flawless function under all weather and operating conditions for 10 years or more. Hence, the challenge for automotive electronic hardware designs and the resident cooling technology is not only achieving small size and low cost, but also high reliability in high ambient temperatures.

2.2 Packaging Levels

There are six generally recognized levels of electronic packaging. Figure 2.2 shows the packaging hierarchy described. The six levels are:
Level 0: Bare semiconductor (unpackaged).

Level 1: Packaged semiconductor or packaged electronic functional device. The electronic device can be active, passive, or other (e.g., electromechanical).

Level 2: Printed wiring assembly (PWA). This level involves joining the packaged electronic devices to a suitable substrate material. The substrate is most often an organic material such as FR-4 epoxy-fiberglass board, or ceramic such as alumina. Level 2 is sometimes referred to as the circuit card assembly (CCA) or, more simply, the card assembly.

Level 3: Electronic subassembly. This level refers to several printed wiring assemblies (PWAs), normally two, bonded to a suitable backing functioning both as a mechanical support frame and a thermal heat sink. Sometimes this backing, or support frame, is called a sub-chassis.

Level 4: Electronic assembly. This level consists of a number of electronic subassemblies mounted in a suitable frame. An electronic assembly, then, is a mechanically and thermally complete system of electronic subassemblies.

Level 5: System. This refers to the completed product.

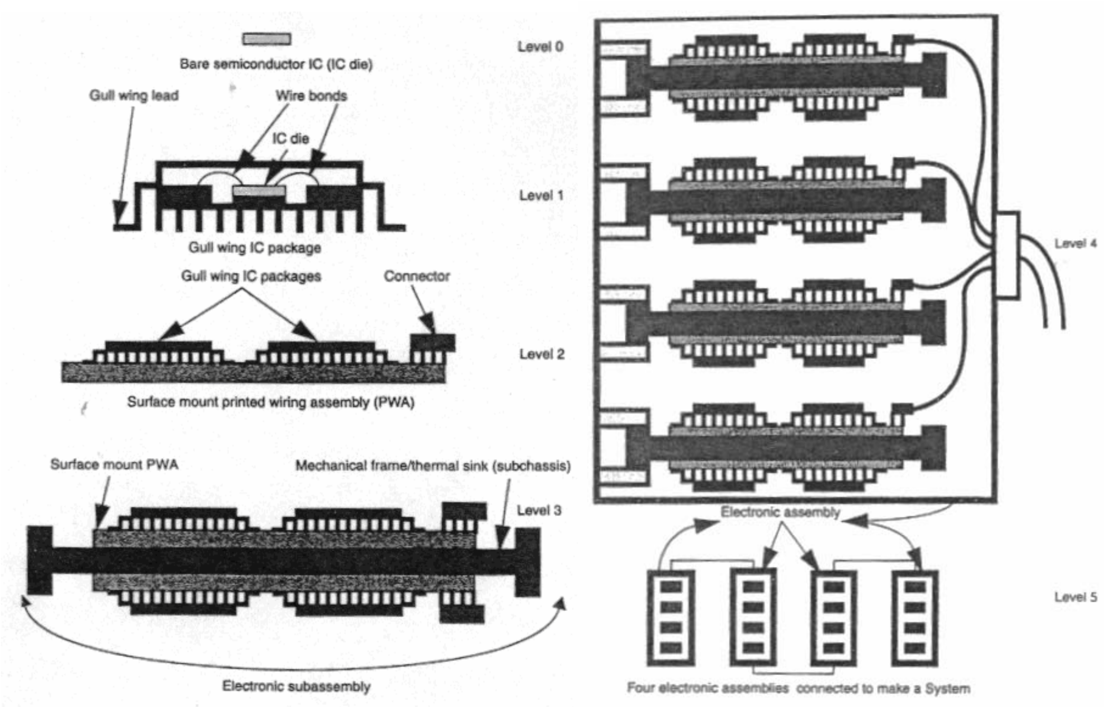

Figure 2.2 Packaging levels

The trend in electronic packaging is to simplify and/or reduce the number of packaging levels. For example, the chip-on-board technology (COB), where a bare integrated circuit die (sometimes also called a chip) is placed directed on a printed wiring board and bonded to the board, eliminating the first level of packaging by going directly from the zeroth level to the second level. COB technology is a particular example of direct chip attache (DCA).

The packaging hierarchy given above is not universal. For computer packaging, for example, Level 3 entails a number of PWAs plugged into a backplane board and supported in a suitable chassis.

2.3 Package Function

Definition

Physical implementation of the electronic design, as shown in Figure 2.3, proper package design should provide:

- Signal distribution
- Power delivery
- Thermal management
- Gentle environment
- Minimum signal delay
- Minimum cost

In the present course we will focus only on providing good thermal management and gentle environment through the scope of heat transfer design.
The thermal management strategy plays a pivotal role in:

- Establishing physical configuration
- Determining environmental/dissipation envelope
- Life - cycle cost
- System reliability

Consequently, thermal analysis techniques are of critical importance.

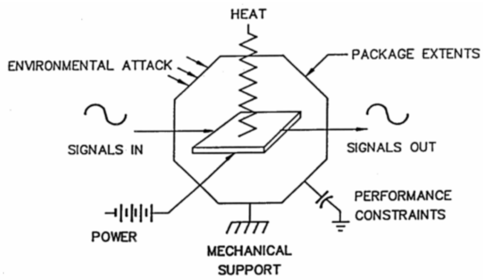

Figure 2.3 Package function

2.4 Stages in the Development of a Packaging Technology

The development of electronic packaging goes through various stages, which are:

- Environment
- Building blocks
- Enabling technology
- Modeling and simulation
- Comparison to specifications
- Preparation for manufacturing

The inter-relation-ship of these stages is shown in Figure 2.4.

2.5 Product Categories

Packaging parameters and requirements are different from one category to the other. The following product categories are illustrative examples to show the different product categories with the suggested price for each:

- Commodity <$300; disk drives, displays, micro-controllers, boom-boxes, VCR's
- Hand-Held < $1000 ; PDA's, cellular phones
- Cost/Performance <$3000; PC's and Notebooks
- High-Performance > $3000; Workstations, Servers, Supercomputers
- Harsh Environment; Automotive
- Memory; DRAMs, SRAMs

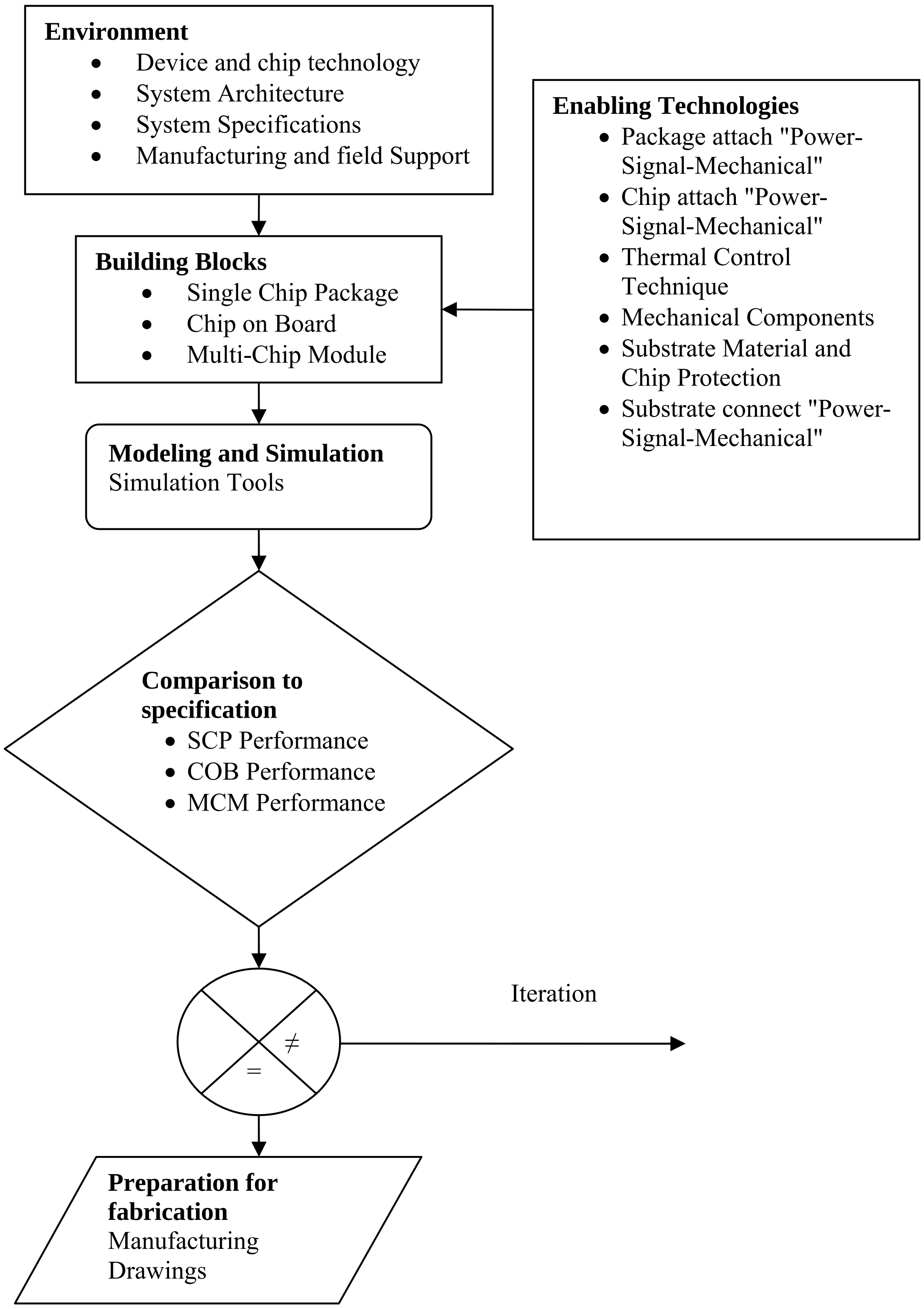

Figure 2.4 Packaging development stages

2.5.1 Packaging Parameters

As seen above the electronic products may vary in category from commodity to high performance products. As such the packaging parameters should vary. This variation is driven by the application and cost of the electronic products. Table 2.2 below shows common packaging parameters.

Table 2.2 Packaging Parameter, 1999

	Commodity	Hand-Held	Cost-Perf	High-Perf	Automot	Memory
Power Dissipation(W)	n/a	1.4	48	88	14	0.8
Chip size (mm^2)	53	53	340	340	53	400
On-Chip Frequency (MHz)	300	300	526	958	150	100
Transistors or Bits				$6M/cm^2$		1G
Junction Temperature (C)	125	115	100	100	175	100
Ambient Temperature (C)	55	55	45	45	165	45
Pin Count	40-236	117-400	300-976	1991	40-236	30-82
Chip Heat Flux (W/cm^2)	n/a	2.6	14.1	25.9	26.4	0.2
Chip/Ambient Specific Resist ($K/(W/cm^2)$)	n/a	23.1	3.9	2.1	0.38	275

2.6 Thermal Packaging Strategies

In order to reach the optimum package design for each product category, it is required to consider the market needs during the development of the end product. As a rule of thumb, the following packaging strategies may apply.

Commodity & Memory: Natural Convection

Hand-Held: Natural Convection + Spreaders

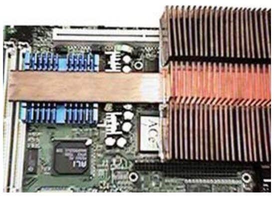

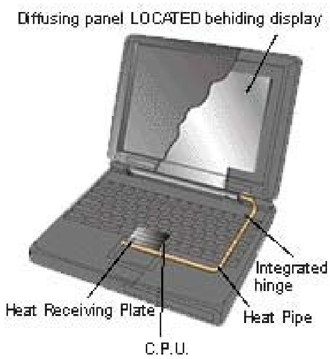

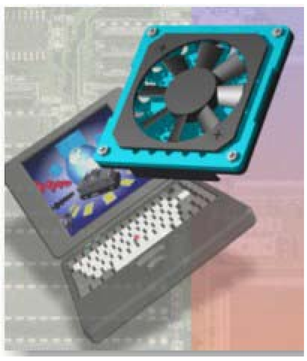

High-Performance:

Forced-Air Heat Sinks; Water-Cooled Cold Plates; Refrigeration; Immersion

Cost/Performance:

PC - Forced-Air Heat Sinks, Fan-Sinks
Notebooks - Heat Pipe Spreaders, Fans, Heat Sinks

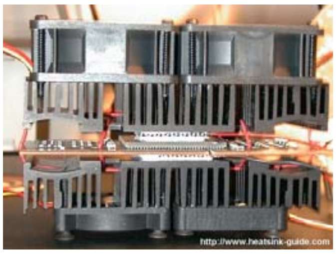

Peltier Cooling Concept

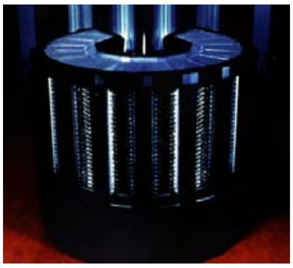

Cray-2 Supercomputer

Harsh Environment:

Forced Air Heat Sink

(3DfxCOOL BigMoFoHO-REX heat sink w/12V, 40cfm fan)

2.7 Examples of Thermal Requirements for Various Product Categories

2.7.1 Cost/Performance 2004 Microprocessor Thermal Requirements

- Power Dissipation – 200 W
- Temperatures: Junction = 95 ^oC; Ambient = 45 ^oC
- Chip Size – 15 mm x 15 mm x 0.3 mm
- Thermal "Space Claim" - 100 x 100 x 50 mm
- Thermal "Mass Claim" – 250 gm
- Flow Parameters: Pressure Drop = 40 Pa (0.15"H_2O), 40 cfm

2.7.2 Cost/Performance 2004 RF Chip Thermal Requirements

- Power Dissipation – 100 W
- Temperatures: Junction = 150 oC; Ambient = 45 oC
- Chip Size - 3mm x 1mm x 0.3mm
- Wireless Module = 10 Chips, 1 kW
- Thermal "Space Claim" - 150 x 150 x 150mm
- Thermal Resistances:

Spreading (Chip Level) = 0.6 K/W

Internal Convective (Chip Level) = 0.2 K/W
External Convective (Module Level) = 0.25 K/W

2.8 Thermal Packaging, Future Forecasting

2.8.1 Future Thermal Packaging Needs

As the technology develops, the electronic products increase its needs. Reaching the nano-technology for the ICs' manufacturing enlarge the thermal management demand and requires higher volumetric heat densities as more electronic components are packed in a smaller volume. Other future needs may result fro the market competition and the search for the least expensive product. Also the environmental pollution laid severe constraints on the manufacturing process.

- Higher power dissipation
- Higher volumetric heat density
- Market-driven thermal solutions
- Air as the ultimate heat sink
- Environmentally-friendly design

2.8.2 Future Thermal Packaging Solutions

- Thermo-fluid modeling tools
- Integrated packaging CAD
- Compact heat exchanger technology
- Design for manufacturability/sustainability
- “Commodity” refrigeration technology
- Thermal packaging options and trends

2.9 Aims of Thermal Control

2.9.1 Prevent Catastrophic Failure

- Electronic function
- Structural integrity

2.9.2 Provide Acceptable Microclimate

- Device reliability
- Packaging reliability
- Prevent fatigue, plastic deformation and creep

2.9.3 System Optimization

- Fail safe or graceful degradation
- Multilevel design
- Reduction of “cost of ownership”

2.10 Direct Air-Cooling Applications

2.10.1 Turbulator for Boundary Layer Control

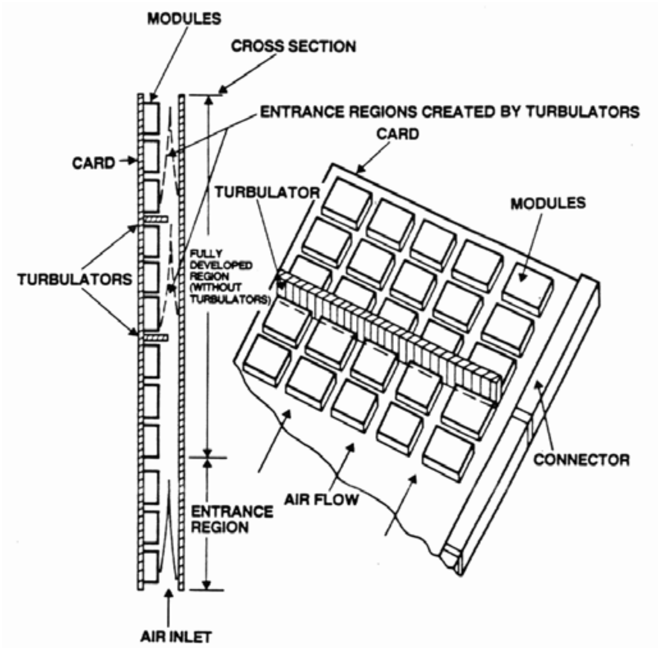

2.10.2 Air cooling of chip carriers

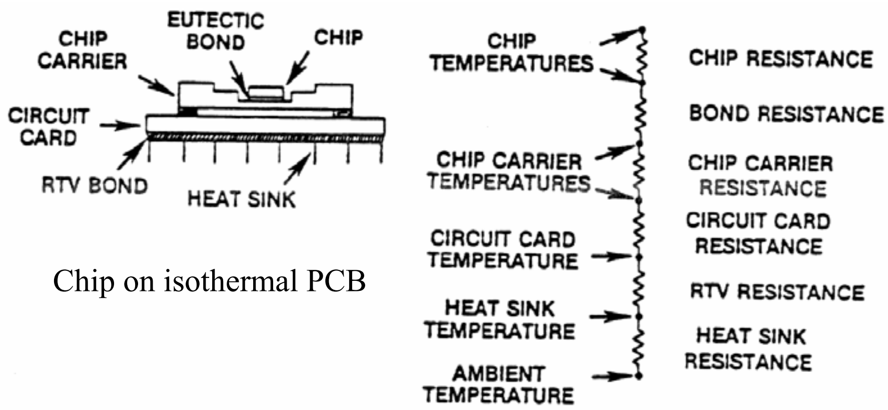

Chip on isothermal PCB

Thermal Resistance Schematic

2.11 Heat Sink Assisted Air-Cooling Applications

2.11.1 Single Chip Package with Heat Sink

42 x 37x 20 mm high chip module

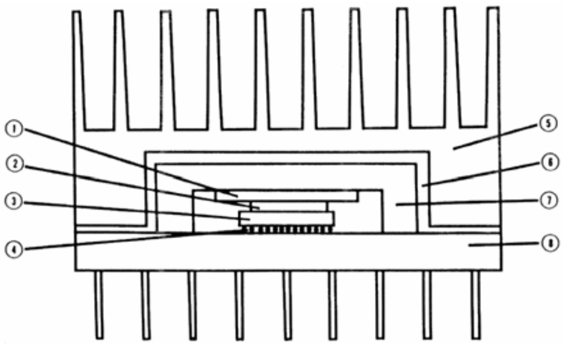

Structure of single chip package:
1. Conductive plate
2. Low temperature solder
3. Chip
4. Flip chip bonding
5. Fin
6. Thermal conductive material
7. Cap
8. Package substrate

2.11.2 PGA Package with Attached Heat Sink

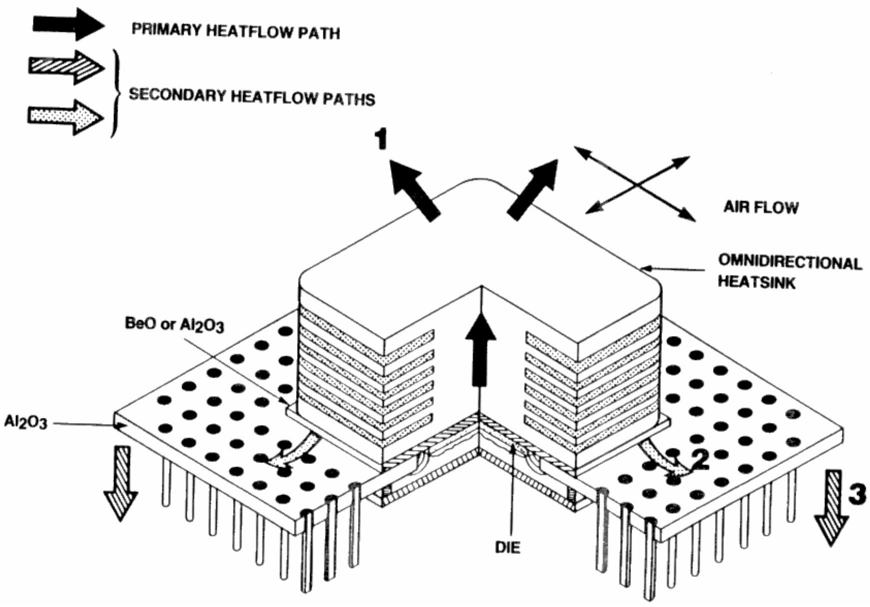

Schematic of a cavity down, 149 pin PGA package with attached heat sink to house a 12 W chip in an air cooled application, 40 x 40 x 20 mm high.

Example: UNISYS A-16 MCM
Chips: ECL, 10,000 Gate ASIC + 8 SRAMS
Size: 46 x 46 x 15 mm high
Power: 14 W ASIC + 14 W in all SRAMS
Cooling: Impinging or Streaming Air ,
Convoluted Fins (CCI)
$\theta_{ja} = 1.5\ K/W$ For module

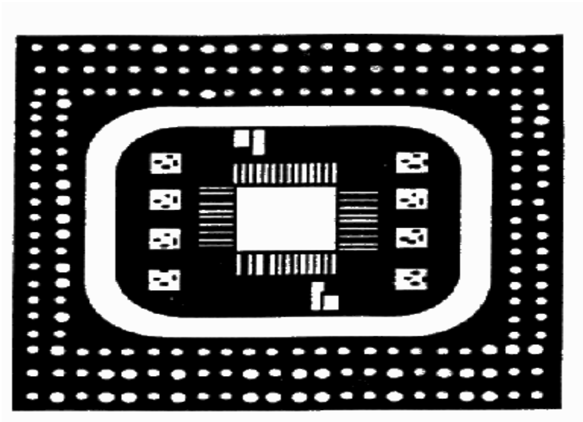

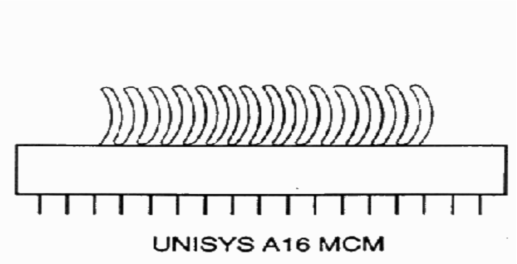

2.11.3 SIC RAM Module

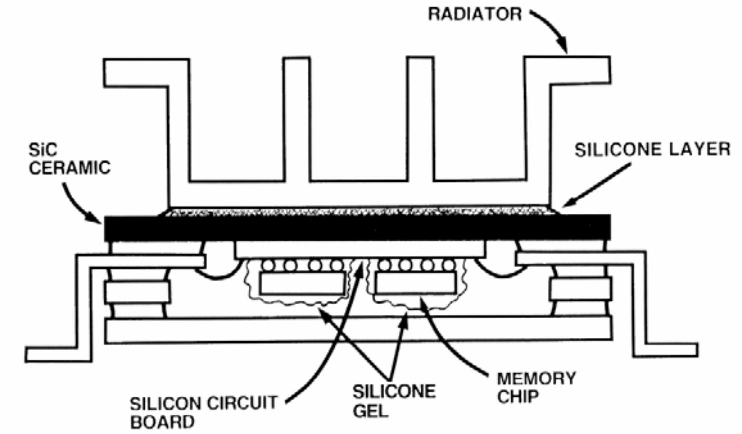

Hitachi

2.11.4 Air-Cooled Module

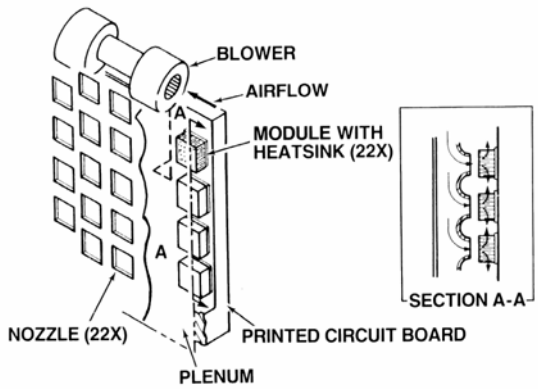

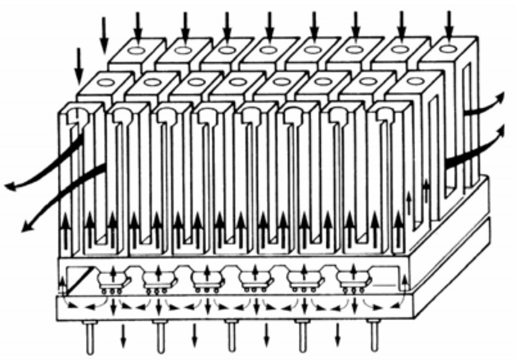

(IBM 4381) (IBM 4331) cross-sectional view

2.11.5 Thermal Conduction Module (TCM)

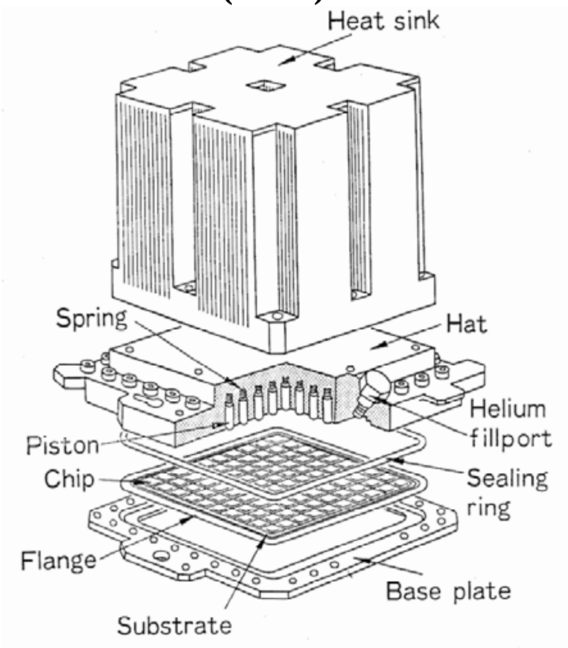

(IBM 9370 Model 90)

Example: SIEMENS H-90 MCM

Chips: 166,000 GATE LSI, 12 mm

Size: 115 x 115 x 52 mm

Power: 280 W

Cooling: Water/Dry Interface

Ultrasound Inspection for Particles

$\theta_{ja} = 0.11\ K/W$ For module

2.12 Indirect water-cooling Applications

2.12.1 Water-Cooled Cold Plate

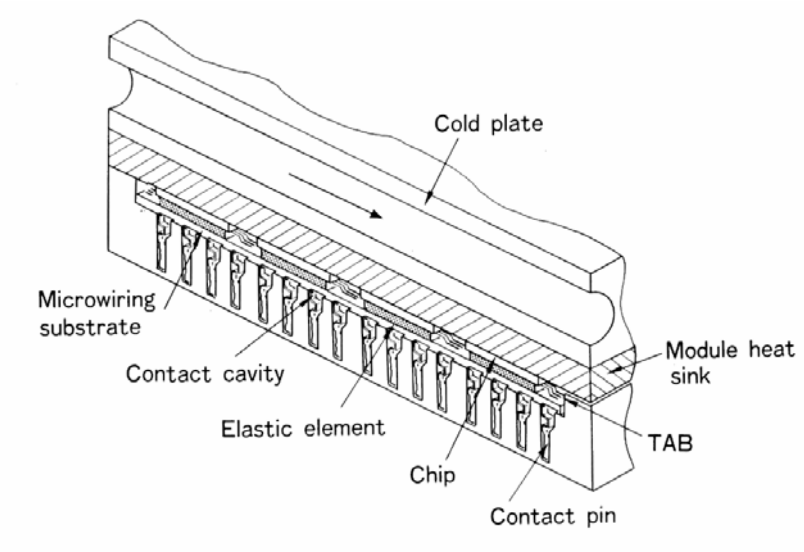

(Siemens H-90)

2.12.2 Liquid-Cooled Module

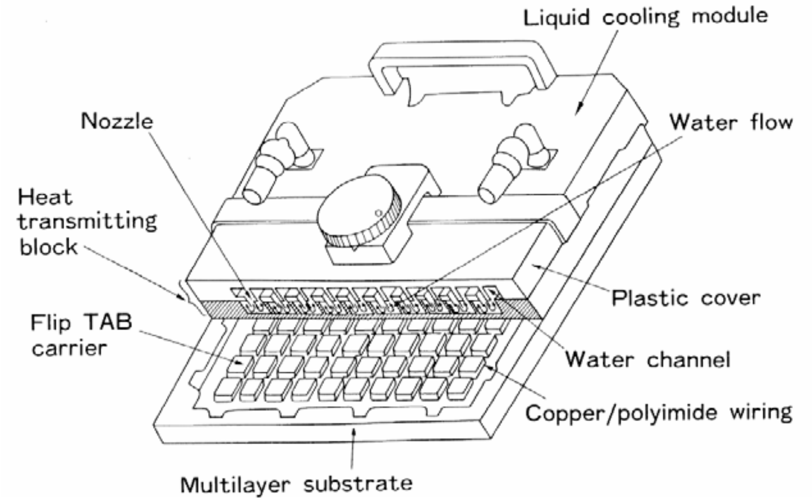

(NEC SX-3)

Example: NEC SX-3 MCP
Chips: 100 FTCs, 20,000 GATE LCLM, 18.5mm
Size: 300 x 300 x 60 mm
Power: 4000 W
Cooling: Water, Internal Jet Impingement
Dry Interface
$\theta_{ja} = 0.0075\ K/W$ For module

2.13 Passive Immersion Module
Smooth or Finned Module Walls

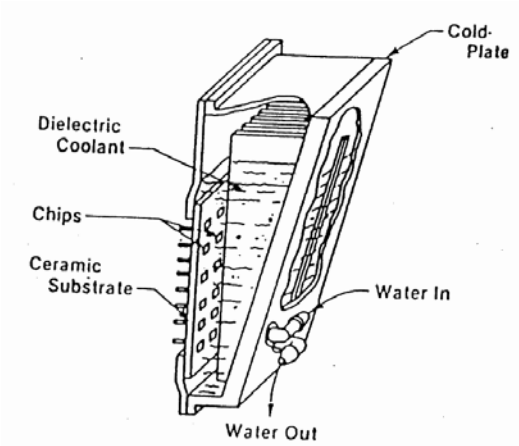

2.14 Phase Change Cooling Applications

Passive Immersion Module

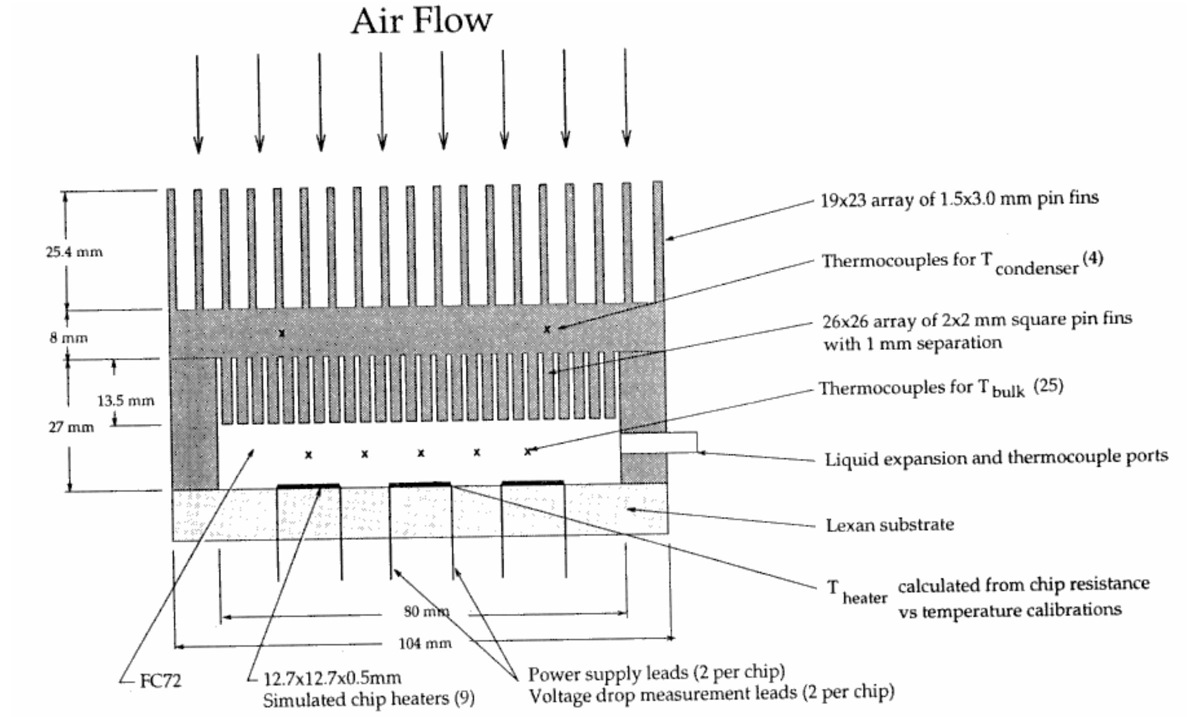

Evaporation Scheme

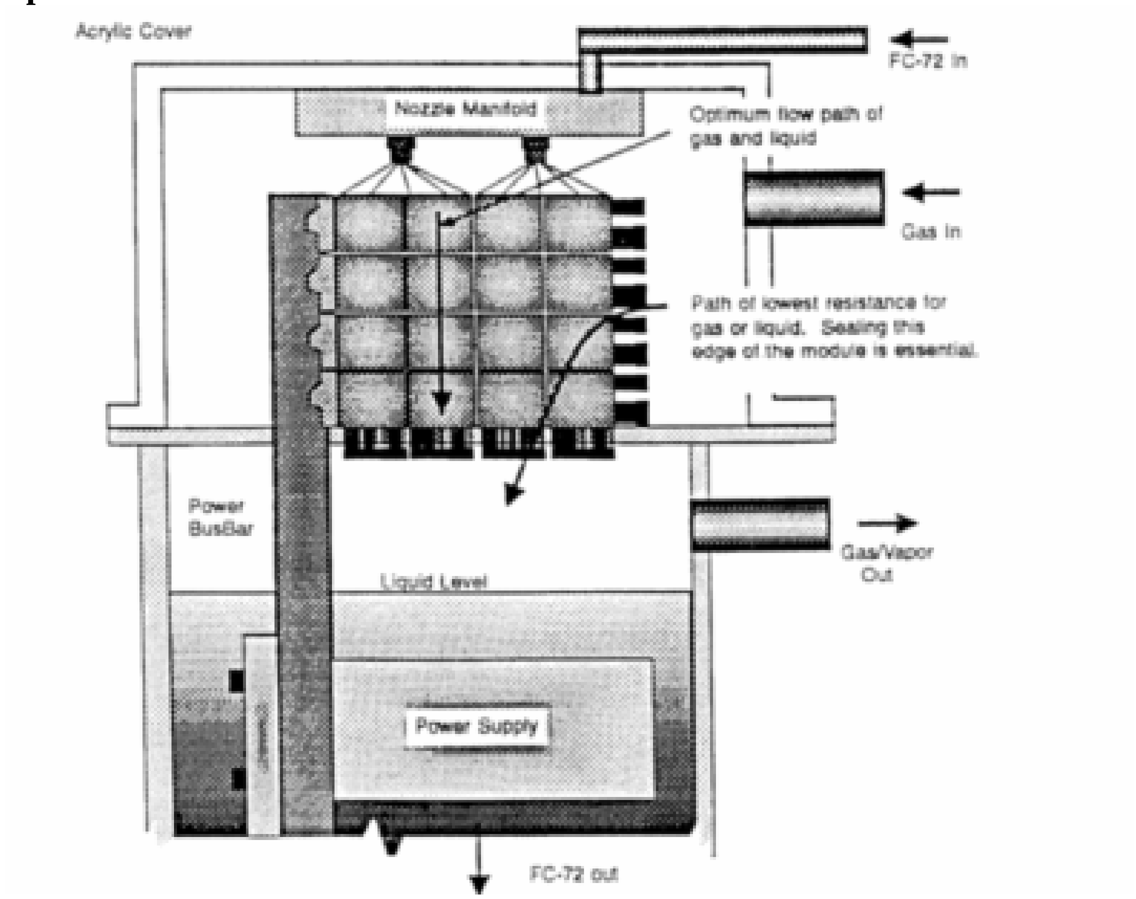

XHA-6 Semiconductor Cooler

Small

Light weight
Low cost
Low thermal resistance
Forced convection

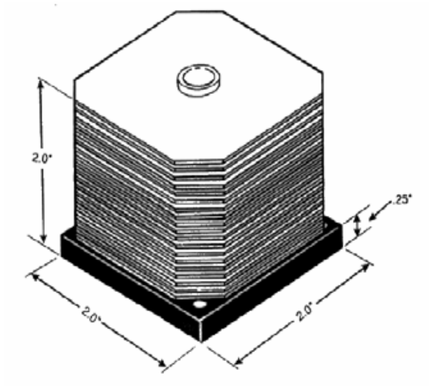

HS-7 Heat Sink
Low cost
Natural or forced convection
Low thermal resistance

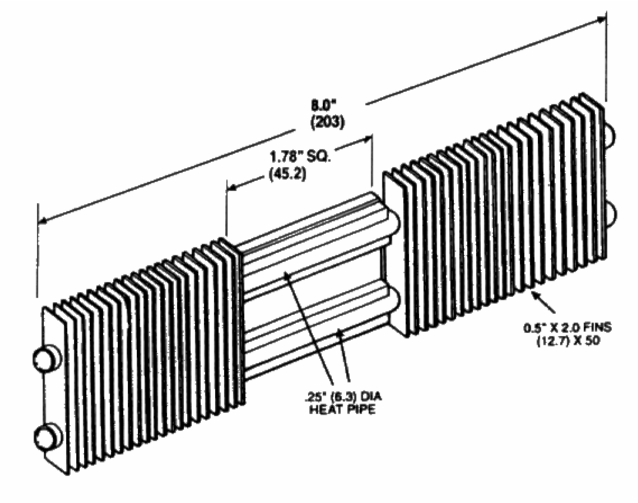

Heat Pipe to Keyboard Thermal Design
Can handle 6.5 Watts CPU power
Keyboard temperature control
Cost of thermal solution

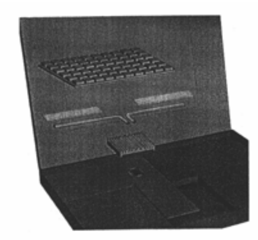

(Intel)

Heat Dissipation of Tape Carrier Package (TCP)

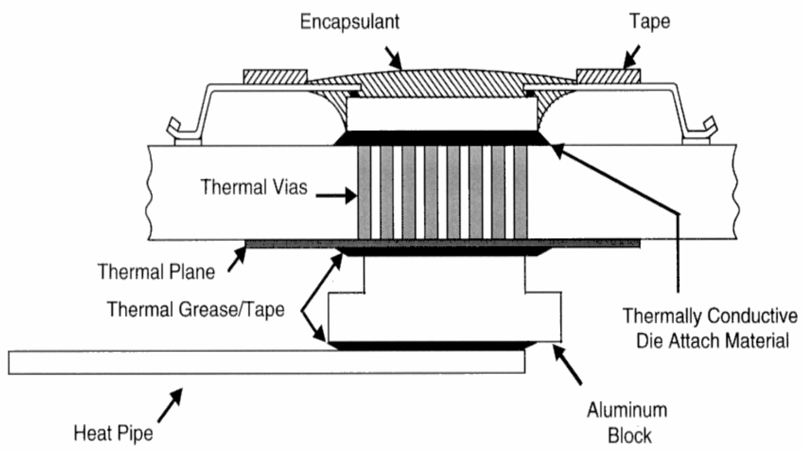

(Intel)

Concepts for High Flux Thermal Packaging

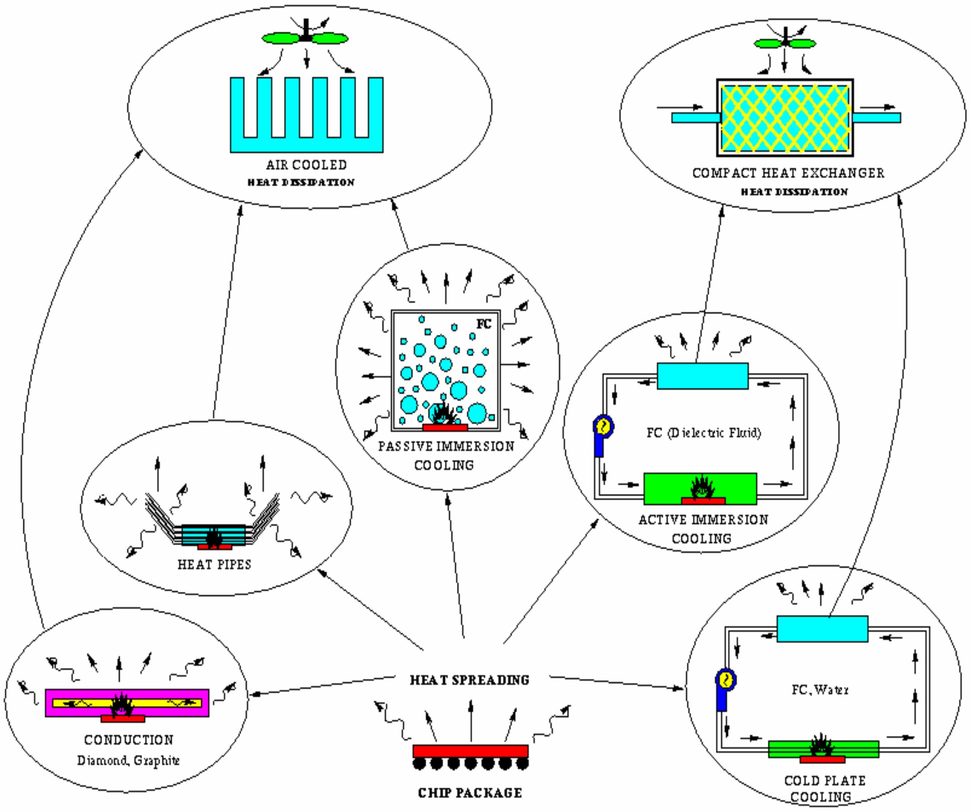

CONCEPTS FOR HIGH FLUX THERMAL PACKAGING

2.15 Future Thermal Packaging Needs

The future works should include many topics to enhancement the cooling as:

- Compact heat sinks - High performance fans
- Low resistance heat spreading
- Heat pipes - High conductivity materials
- Low interfacial resistance

- Adhesives - Mechanical – Fluid

Typical Compact Pin-Fin Heat Sinks

Advanced Immersion Cooling

2.16 Refrigerated Packaging

- CMOS chip/CPU performance
- Cost of refrigeration system
- Life cycle cost
- Volume, mass
- Power consumption
- Reliability of refrigeration/packaging
- Refrigeration hardware
- Condensation on PCBs + refrigerant lines
- Vibration

2.17 Practical Applications

IBM S/390 G4 Server, Refrigeration Cooled MCM

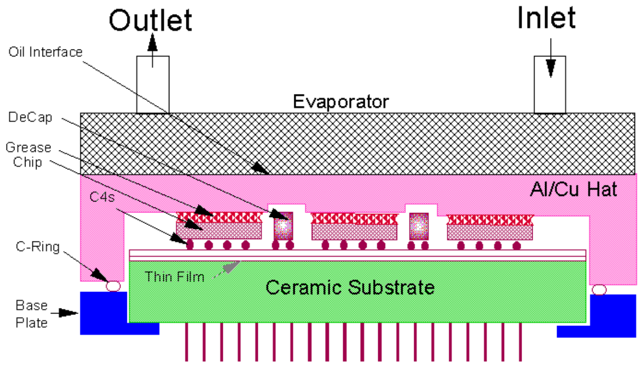

Kryotech Vapor Phase Refrigeration, Cool-Athalon 800MHz

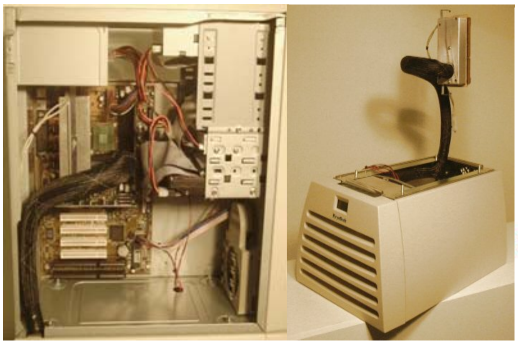

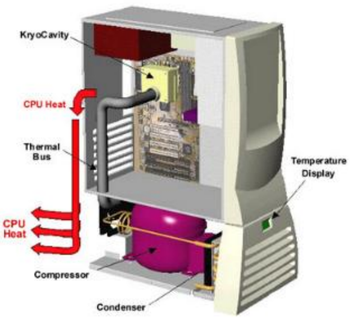

3. Basics of Heat Transfer

This lecture is intended to refresh the post graduate students memory about the basics of heat transfer regarding the various modes of heat transfer, analogy between heat transfer and electric circuits, combined modes of heat transfer and the overall heat transfer coefficient.

As a start, we will begin by the modes of heat transfer mechanism in a brief review then we will elaborate on the analogy between heat transfer and electric circuits. This will enable us to study the combined modes of heat transfer then we will end this lecture with the concept of overall heat transfer coefficient.

3.1 Modes of Heat Transfer

Heat, by definition, is the energy in transit due to temperature difference. Whenever exists a temperature difference in a medium or between media, heat flow must. Different types of heat transfer processes are called modes. These modes are shown in Figure 3.1. When a temperature gradient exists in a stationary medium, which may be a solid or a fluid, heat flows under the law of conduction heat transfer. On the other hand if the temperature gradient exists between a surface and a moving fluid we use the term Convection. The third mode of heat transfer is termed Radiation and it needs no medium to transfer through since it is driven by electromagnetic waves emitted from all surfaces of finite temperature, so there is a net heat transfer by radiation between two surfaces at different temperatures.

Conduction Through a solid or a stationary fluid	Convection from a surface to a moving fluid	Net radiation heat exchanges between surfaces

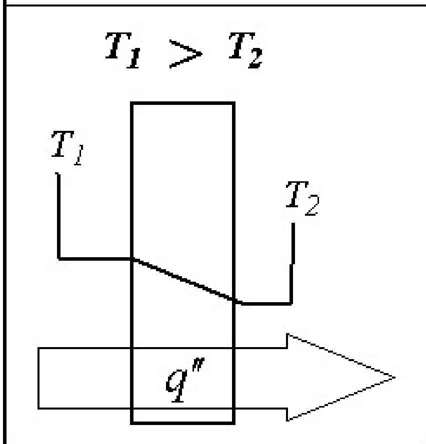

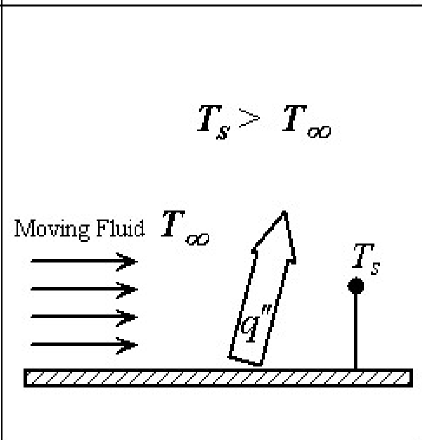

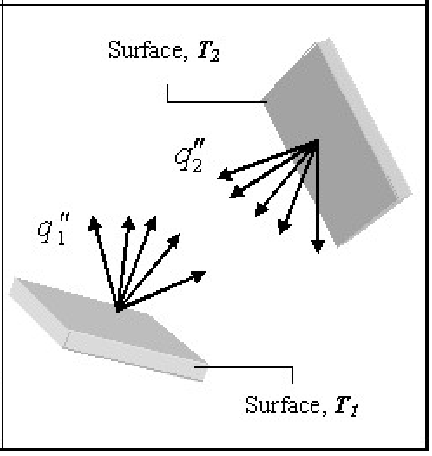

Figure 3.1 Conduction, convection and radiation heat transfer modes

3.1.1 Conduction

Conduction is the mechanism of heat transfer whereby energy is transported between parts of a continuum by the transfer of kinetic energy between particles or groups of particles at the atomic level. We should conjure up the concept of atomic and molecular activity In gases, conduction is caused by elastic collision of molecules; consider a gas in which there exist a temperature gradient and assume there is no bulk motion . The gas may occupy the space between two surfaces which are maintained at different temperatures as shown in Figure 3.2. We associate the temperature at any point with the energy of gas molecules in proximity to the point. This energy is related to the random translational motion as well as to the internal rotational and vibrational motions of the molecules. As shown in Figure 3.3. The hypothetical plane at xo is constantly being crossed by molecules from above and below due to their random motion. However, molecules from above are associated with a larger temperature than those from below, causing net transfer of energy in the positive x direction. We may speak of the net transfer of energy by the random molecular motion as a diffusion of energy.

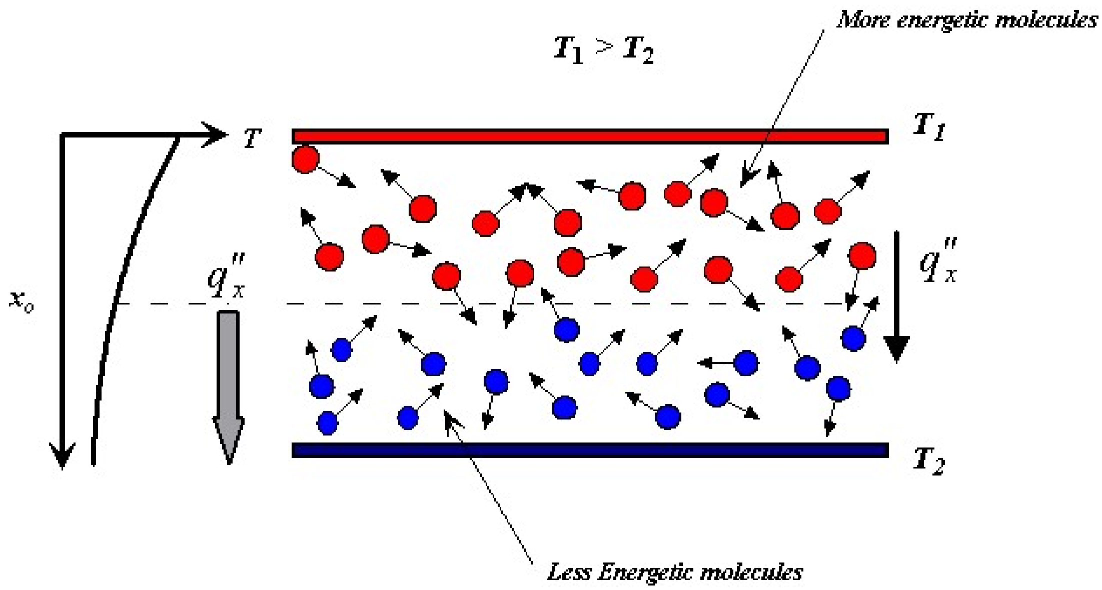

Figure 3.2 Conduction heat transfer as diffusion of energy due to molecular activity.

In liquids and electrically non conducting solids, it is believed to be caused by longitudinal oscillations of the lattice structure; it is called also lattice waves. Thermal conduction in metals occurs, like electrical conduction, through the motion of free electrons. Thermal energy transfer occurs in the direction of decreasing temperature, a consequence of the second law of thermodynamics.

In solid opaque bodies, thermal conduction is the significant heat transfer mechanism because no net material flows in the process. With flowing fluids, thermal conduction dominates in the region very close to a solid boundary, where the flow is laminar and parallel to the surface and where there is no eddy motion.

Examples of conduction heat transfer are tremendous. On a summer day there is a significant energy gain from outside air to a room. This gain is principally due to conduction heat transfer through the wall that separates room air from outside air. Also in electronics cooling process conduction is a heat transfer mechanism used in every electronics design. Even if a system is designed for convection cooling of the circuit boards, conduction is still the dominant heat transfer mechanism within the component devices and on the circuit board. This is especially true for power electronics, where concentrations of heat are developed in components such as power silicon and magnetic. This heat must be transferred via conduction to the component case, the circuit board or a heat sink before it can be handled by the system-level cooling mechanism(s). Consequently, all electronics designers must be aware with the techniques of thermal conduction and its analysis.

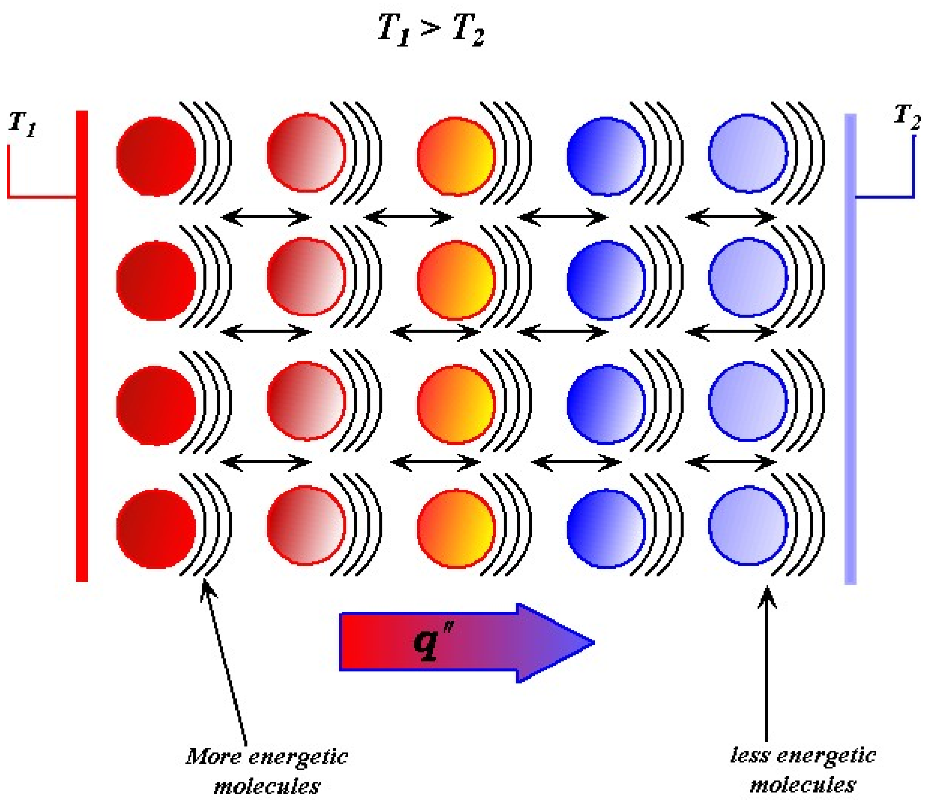

Figure 3.3 Conduction in liquids and solids ascribed to molecules vibration (solids), translational and rotational (liquids)

It is possible to quantify heat transfer processes in terms of appropriate rate equations. These equations may be used to compute the amount of energy being transferred per unit time. For heat conduction, the rate equation is known as Fourier's law.

Fourier's law is a phenomenological; that is developed from observed phenomena rather than being derived from first principles. The general rate equation is based on much experimental evidence. For the one dimensional plane wall shown in Figure 3.4 having a temperature distribution T(x), the rate equation is expressed as

$$q''_x = -k\frac{dT}{dx}$$

The heat flux q" (W/m^2) is the heat transfer rate in the x direction per unit area perpendicular to the direction of transfer, and it is proportional to the temperature gradient, dT/dx, in this direction. The proportionality constant k is a transport property known as the thermal conductivity (W/m. K) and is a characteristic of the wall material. The minus sign is a consequence of the fact that heat is transferred in the direction of decreasing temperature.

Under the steady-state conditions shown in Figure 3.4, where the temperature distribution is linear then the temperature gradient may be expressed as

$$\frac{dT}{dx} = \frac{T_2 - T_1}{L}$$

And the heat flux is then

$$q_x'' = -k\frac{T_2 - T_1}{L}$$

Note that this equation provides a heat flux, that is, the rate of heat transfer per unit area. The heat rate by conduction, q_x (W), through a plane wall of area A is then the product of the flux and the area, $q_x = q_x^{//}$ x A .

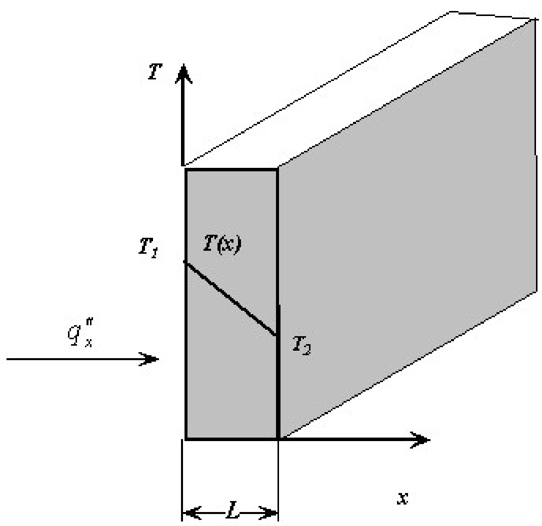

Figure 3.4 One- Dimensional heat transfer (diffusion of energy)

3.1.2 Thermal Convection

This mode of heat transfer involves energy transfer by fluid movement and molecular diffusion. Consider heat transfer to a fluid flowing over flat plate as in Figure 3.5. If the Reynolds number is large enough, three different flow regions exist.

Immediately adjacent to the wall is a laminar sublayer where heat transfer occurs by thermal conduction; outside the laminar sublayer is a transition region called the buffer layer, where both eddy mixing and conduction effects are significant; beyond the buffer layer is the turbulent region, where the dominant mechanism of transfer is eddy mixing.

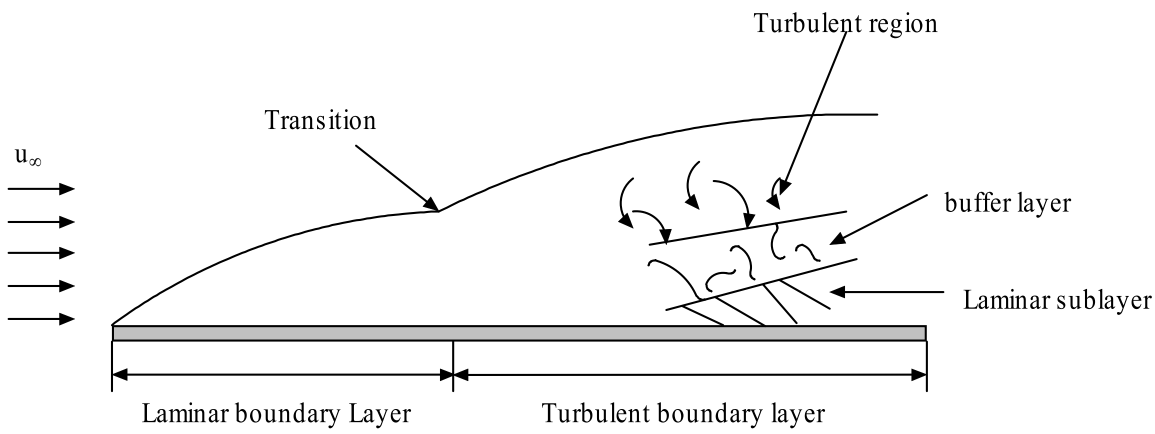

Figure 3.5 Boundary layer build up over flat plate

Convection heat transfer may be classified according to the nature of the flow for free or natural convection the flow is induced by buoyancy forces, which arise from density differences caused by temperature variations in the fluid.

An example is the free convection heat transfer that occurs from hot components on a vertical array of circuit boards in still air as shown in Figure 3.6(a).Air that makes contact with the components experiences an increase in temperature so that the density is reduced.

For a forced convection; the flow is caused by external means, such a fan, a pump, or atmospheric winds. An example of which is the use of a fan to provide forced convection air cooling of hot electrical components on printed circuit boards as shown in Figure 3.6(b).

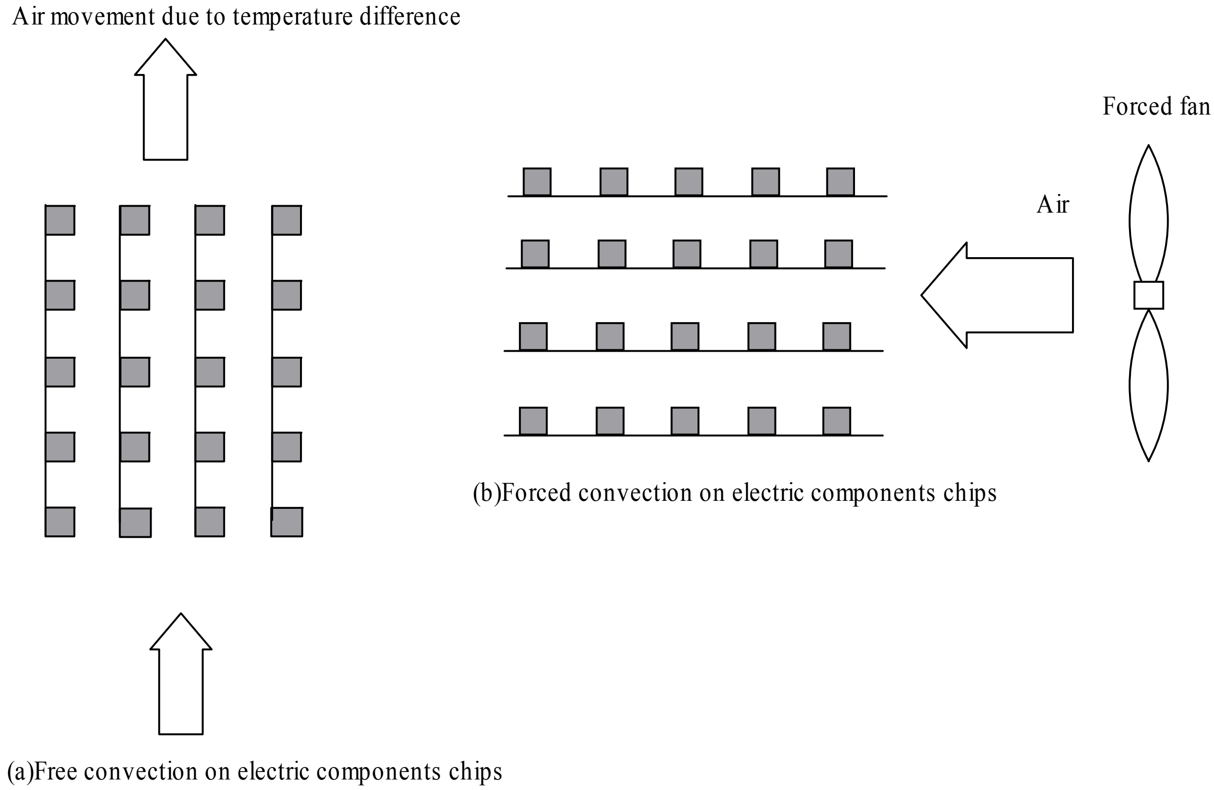

Figure3.6 (a) Free convection, (b) Forced convection

The heat transfer by convection is described by the Newton's law of cooling:

$$q = hA(T_W - T_\infty)$$

Where;

q = Heat transfer rate (W)
h = Heat transfer coefficient ($W/m^2.K$)
T_w= Wall temperature (K)
T_∞= Free stream fluid temperature (K)

The approximate ranges of convection heat transfer coefficients are indicated in Table 3.1 for both free and forced convection.

Table 3.1 Convection heat transfer ranges

Process	$h(W/m^2.K)$
Free convection	
- gases	2-25
- liquids	50-1000
Forced convection	
- gases	25-250
- liquids	50-20,000
Convection with two phase	
- boiling or condensation	2500-100,000

Example 3.1: An electric current is passed through a wire 1mm diameter and 10 cm long. This wire is submerged in liquid water at atmospheric pressure, and the current is increased until the water boils. For this situation h = 5000 $W/m^2.{}^oC$. And the water will be 100 ^oC. How much electric power must be supplied to the wire to maintain the wire surface at 114 ^oC?

Schematic:

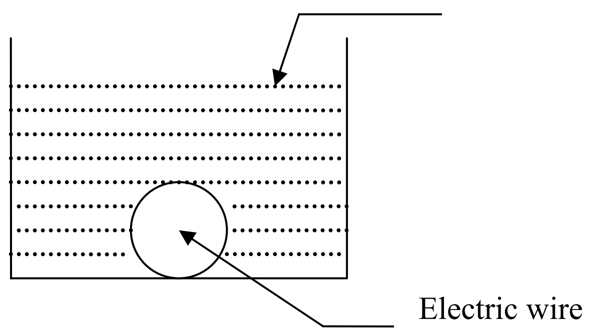

Solution:
The total convection loss from the wire is given by

$$q = hA(T_W - T_\infty)$$

For this problem the surface area of the wire is

$$A = \pi\, d\, L = \pi\,(1 \times 10^{-3})\,(10 \times 10^{-2}) = 3.142 \times 10^{-4}\ m^2$$

The heat transfer is therefore

$$q = 5000 \times 3.142 \times 10^{-4} \times (114 - 100) = 21.99\ W$$

And this is equal to the electric power which must be applied.

3.1.3 Thermal Radiation

The mechanism of heat transfer by radiation depends on the transfer of energy between surfaces by electromagnetic waves in wave length interval between 0.1 to 100 µm. Radiation heat transfer can travel in vacuum such as solar energy.

Radiation heat transfer depends on the surface properties such as colors, surface orientation and fourth power of the absolute temperature (T^4) of the surface. The basic equation for radiation heat transfer between two gray surfaces is given by:

$$q = \sigma \varepsilon f A (T_1^4 - T_2^4)$$

Where:
σ = Stefan-Boltzmann constant = 5.67x10-8 $W/m^2.K^4$
ε = Emissivity of the surface which provide of how efficiently a surface emits energy relative to a black body(no reflection) and it's ranges $0 \le \varepsilon \le 1$
f = Geometrical factor which depends on the orientation between the surfaces

Example3.2: A horizontal steel pipe having a diameter of 10 cm is maintained at a temperature of 60 ^oC in a large room where the air and wall temperature are at 20 ^oC with average heat transfer coefficient 6.5 $W/m^2.k$. The emissivity of the steel is 0.6 calculate the total heat lost from the pipe per unit length.

Solution:
The total heat lost from the pipe due to convection and radiation

$$\begin{aligned} q_{total} &= q_{convection} + q_{radiation} \\ &= \bar{h} A (T_S - T_\infty) + \sigma \varepsilon f A (T_S^4 - T_\infty^4) \end{aligned}$$

Because the pipe in a large enclosure then the geometrical factor f = 1

$$\begin{aligned} q_{total} &= 6.5(\pi x 0.1)(60 - 20) + 5.67 x 10^{-8} (0.6)(1)(\pi x 0.1)(333^4 - 293^4) \\ &= 134.33\ W/m \end{aligned}$$

3.2 Analogy between Heat Transfer and Electric Circuits

There exists an analogy between the diffusion of heat and electrical charge. Just as an electrical resistance is associated with the conduction of electricity, a thermal resistance may be associated with the conduction of heat. Defining resistance as the ratio of a driving potential to the corresponding transfer rate, it follows from Figure 3.4 that the thermal resistance for conduction is:

$$R_{t,cond} \equiv \frac{T_{s,1} - T_{s,2}}{q_x} = \frac{L}{kA}$$

As the electric resistance from Ohm's law

$$R_e = \frac{E_{s,1} - E_{s,2}}{I} = \frac{L}{\sigma A}$$

As there is a conduction resistance also there is a convection resistance.

$$q = h\,A\,(T_s - T_\infty)$$

$$R_{t,conv} \equiv \frac{T_s - T_\infty}{q} = \frac{1}{hA}$$

3.2.1 Series Circuits

In the series circuits of heat transfer, heat is transferred in a series of stages that aren't necessary of the same heat transfer mode. Figure 3.7 shows a plane wall subjected at its end to convective heat transfer. So in this case the heat is first transferred from the hot fluid to the wall surface by convection, then through the wall by conduction, and finally by convection from the second wall surface to the cold fluid. Here the heat quantity in each phase is the same so as current flowing in a series of electric resistances. Then from this analogy we may conclude that:

$$q = \frac{\Delta T_{overall}}{\Sigma R_t} = \frac{T_{\infty 1} - T_{\infty 2}}{\left(R_{t,conv}\right) + \left(R_{t,cond}\right) + \left(R_{t,conv}\right)} = \frac{T_{\infty 1} - T_{\infty 2}}{\left(\frac{1}{h_1 A}\right) + \left(\frac{L}{kA}\right) + \left(\frac{1}{h_2 A}\right)}$$

As

$$i = \frac{\Delta E}{\Sigma R_e} = \frac{E_1 - E_2}{\left(R_{e,1}\right) + \left(R_{e,2}\right) + \left(R_{e,3}\right)}$$

This thermal resistance analysis is very useful for more complex systems as composite walls and combined heat transfer modes. As examples examine Figure 3.8, if we use the analogy, the problem formulation will be much easier and less time consuming.

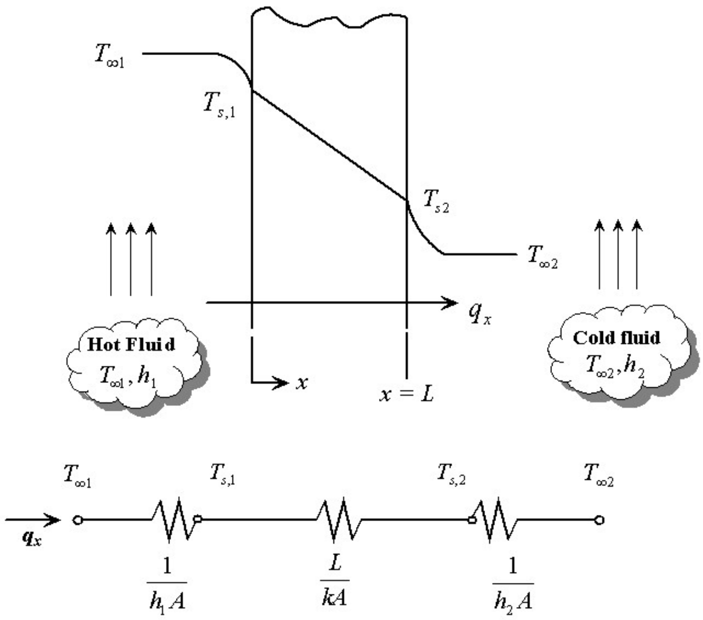

Figure 3.7 Heat transfer through a plane wall

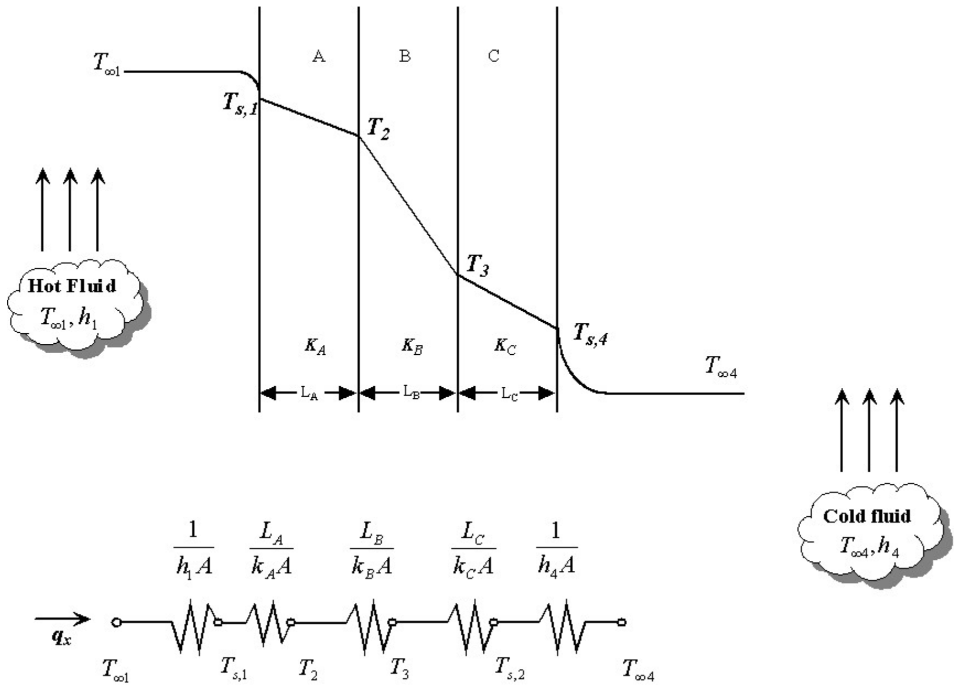

Figure 3.8 composite wall

Hence, the amount of heat transferred could be expressed as

$$q = \frac{T_{\infty 1} - T_{\infty 2}}{\left(\frac{1}{h_1 A}\right) + \left(\frac{L_A}{k_A A}\right) + \left(\frac{L_B}{k_B A}\right) + \left(\frac{L_C}{k_C A}\right) + \left(\frac{1}{h_2 A}\right)}$$

3.2.2 Parallel Circuit

In parallel thermal circuits, heat is transferred in parallel through several heat transfer conduits. These conduits may be of various heat transfer mod or from the same mod as is the case shown in Figure 3.9a and b.

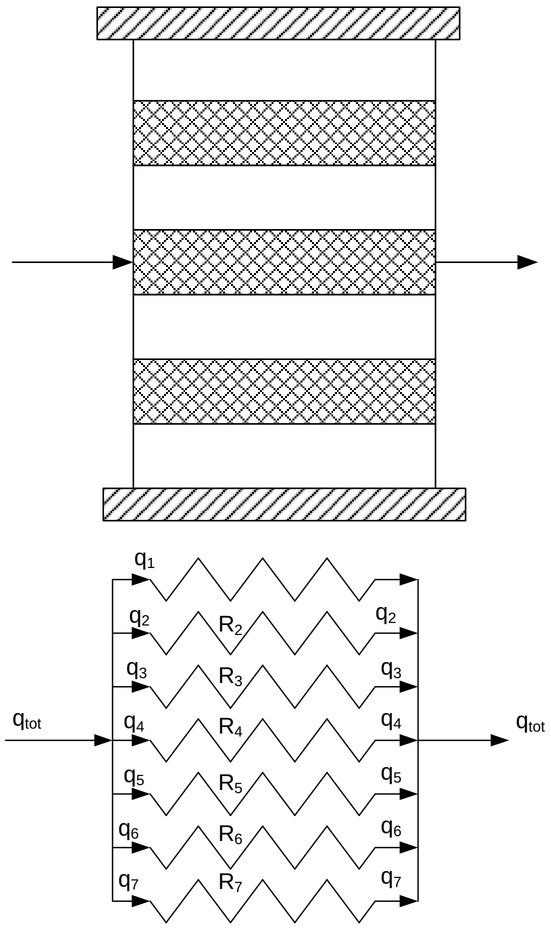

Figure 3.9 a

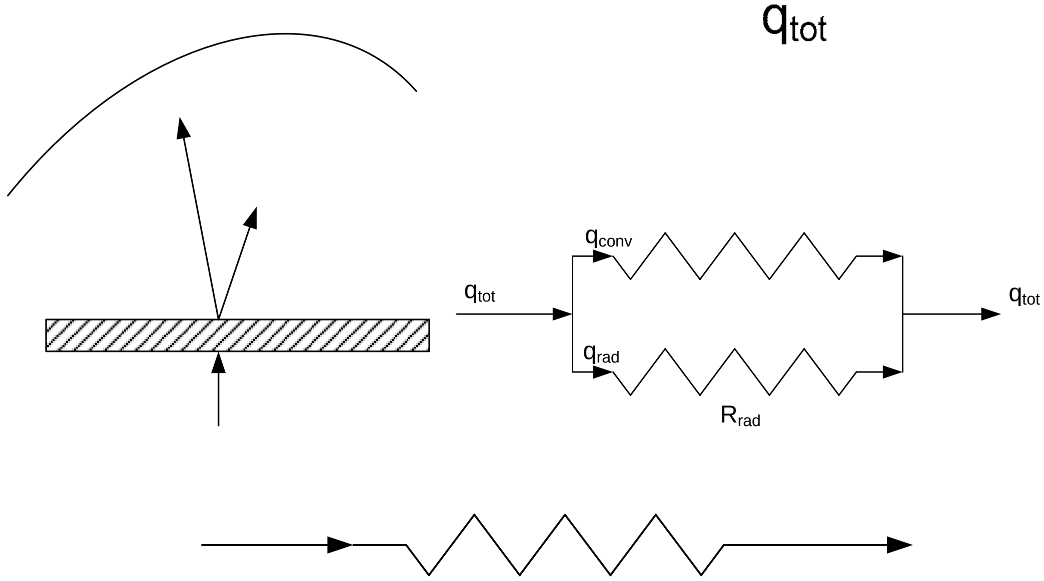

Figure 3.9 b

Now considering the case in Figure 3.9 a,

$$q_i = k_i A_i \frac{\Delta T}{L_i} = \frac{\Delta T}{R_{t,i}}$$

And;

$$q_{tot} = \Sigma q_i = \Delta T\left(\frac{1}{R_{t,1}} + \frac{1}{R_{t,2}} + \frac{1}{R_{t,3}} + \frac{1}{R_{t,4}} + \frac{1}{R_{t,5}} + \frac{1}{R_{t,6}} + \frac{1}{R_{t,7}}\right) = \frac{\Delta T}{R_{t,tot}}$$

This means that like electric circuits in parallel, the equivalent total thermal resistance would be:

$$\frac{1}{R_{t,tot}} = \sum \frac{1}{R_{t,i}}$$

3.2.3 Series-Parallel Network Reduction

A thermal network can be extremely complicated so that normal analysis would be exhaustive. In this case, the use of the analogy between thermal and electric network would simplify the analysis. In order to simplify the thermal networks, the series and parallel thermal resistance are combined in order to reach simplified analysis. The following figure shows a circuit with the method of simplification.

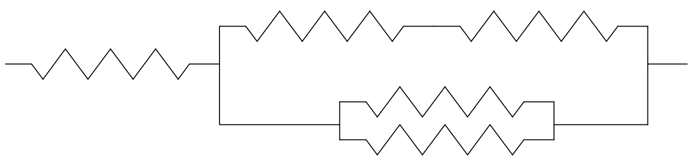

Let, $R_6 = \dfrac{1}{\dfrac{1}{R_2} + \dfrac{1}{R_3}}$ and $R_7 = R_4 + R_5$

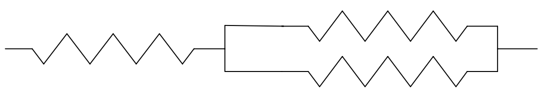

Let, $R_8 = \dfrac{1}{\dfrac{1}{R_6} + \dfrac{1}{R_7}}$

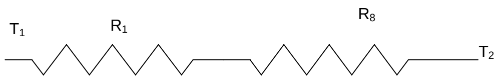

Let, $R_9 = R_1 + R_8$

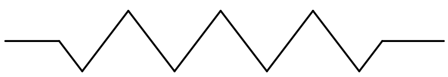

R_4

T_1 R_1

3.3 Combined Modes of Heat Transfer

Most of the practical cases under investigations, heat is transferred by more than one mode; as for examples heat may be transferred by combined convection and radiation, combined convection and conduction, etc.

3.3.1 Combined Convection and Radiation

Since these two modes of heat transfer are completely independent, there would be no mutual effect between them. Thus net heat exchange of the surface is the sum of the two

$$q_{net} = q_{conv} + q_{rad}$$

This hypothetical approach seems to be similar to the parallel electrical resistances as shown previously, but the problem here is that no radiation resistance has been defined yet. So let us use a radiant heat transfer in order to express the radiation heat transfer, q_{rad}, as a linear function in the temperature difference between the surface temperature and the fluid temperature.

$$q_{rad} = h_r \times A \times (T_s - T_f)$$

Where;

h_r = radiation heat transfer coefficient, W/m^2.K
A = heat transfer surface area, m^2
T_s = surface absolute temperature, K
T_f = enclosure absolute temperature, K

Now it is time to define how the radiation heat transfer coefficient can be obtained

$$h_r = \frac{q_{rad}}{A \times (T_s - T_f)} = \varepsilon \times \sigma \times F_{se} \times \frac{(T_s^4 - T_e^4)}{(T_s - T_f)}$$

In the above equation, T_e is used to express the enclosure temperature as this is the more general case. But for most of the cases, the fluid adjacent to the surface has the same temperature as that of the enclosure. So for this most likely circumstance the following agree:

$$h_r = \varepsilon \times \sigma \times F_{se} \times \frac{(T_s^4 - T_f^4)}{(T_s - T_f)} = \varepsilon \times \sigma \times F_{se} \times \frac{(T_s^2 + T_f^2) \times (T_s + T_f) \times (T_s - T_f)}{(T_s - T_f)}$$

$$\therefore h_r = \varepsilon \times \sigma \times F_{se} \times (T_s^2 + T_f^2) \times (T_s + T_f) = \varepsilon \times \sigma \times F_{se} \times ((T_s + T_f)^2 - 2T_sT_f) \times (T_s + T_f)$$

Now if we define the arithmetic means temperature as

$$T_m = \frac{T_s + T_f}{2}$$

If further T_s-T_e<<T_s then

$$T_m = \sqrt{T_s T_f}$$

So we may define the radiation heat transfer coefficient as

$$\therefore h_r = 4 \times \varepsilon \times \sigma \times F_{se} \times T_m^3$$

And finally;

$$q_{net} = h_{tot} \times A \times (T_s - T_f)\,.$$

Where $h_{tot} = h_{conv} + h_{rad}$

3.3.2 Combined Convection and Conduction

This combination is likely to occur with the use of extended surfaces where the primary surface exchanges heat by convection to the adjacent fluid flow and by conduction through the extended surfaces. This case may be considered in a similar manner as the above, but here the problem doesn't need extra work as the conduction thermal resistance is pre-defined.

$$q_{net} = q_{conv} + q_{cond}$$

$$q_{net} = \left(h_{conv}(T_s - T_f) + k\frac{(T_s - T_{ext})}{L} \right) \times A$$

3.4 Overall Heat Transfer Coefficient

The concept of overall heat transfer coefficient laid its importance in the heat exchanger design and industry as it combines the various modes of heat transfer in the heat exchange between two fluids.

The concept of overall heat transfer has been extensively studied in the undergraduate courses of heat transfer and heat transfer equipments, but again for reasons of memory refresh. Let's examine the defining equation and it parameters.

$$U_h A_h = U_c A_c = \cfrac{1}{\cfrac{1}{h_c(A_{c,p} + \eta_{f,c} A_{c,s})} + \cfrac{R''_{f,c}}{(A_{c,p} + \eta_{f,c} A_{c,s})} + \cfrac{x}{kA_m} + \cfrac{R''_{f,h}}{(A_{h,p} + \eta_{f,h} A_{h,s})} + \cfrac{1}{h_h(A_{h,p} + \eta_{f,h} A_{h,s})}}$$

Where;
U_c is the overall heat transfer coefficient based on the cold side area, W/m^2.K.
A_c is the total heat transfer surface area adjacent to the cold fluid side, m^2.
U_h is the overall heat transfer coefficient based on the hot side area, W/m^2.K.
A_h is the total heat transfer surface area adjacent to the hot fluid side, m^2.
h_c is the convection heat transfer coefficient based on the cold side area, W/m^2.K.
$A_{c,p}$ is the primary heat transfer surface area adjacent to the cold fluid side, m^2.
$A_{c,s}$ is the secondary heat transfer surface area adjacent to the cold fluid side, m^2.
$\eta_{f,c}$ is the cold side fin efficiency.
$R_{f,c}''$ is the fouling factor for the cold side, m^2.K/W.
x is the wall thickness, m.
k is the thermal conductivity of the interface wall material, W/m^2.K.
A_m mean heat transfer area for conduction, m^2.
h_h is the convection heat transfer coefficient based on the hot side area, W/m^2.K.
$A_{h,p}$ is the primary heat transfer surface area adjacent to the hot fluid side, m^2.
$A_{h,s}$ is the secondary heat transfer surface area adjacent to the hot fluid side, m^2.

$\eta_{f,h}$ is the hot side fin efficiency.
$R_{f,h}''$ is the fouling factor for the hot side, m^2.K/W.

The following table gives values for representative fouling factor for several applications: The heat transfer between to fluids separated by heat transfer area can then be easily calculated as:

$$Q_{net} = U_h A_h \Delta T_{overall}$$

The following table shows some values for the overall heat transfer coefficient:

Fluid	$R_{f,}''$, m^2.K/W.
Seawater and treated boiler feedwater (below 50 ºC)	0.0001
Seawater and treated boiler feedwater (above50 ºC)	0.0002
River water below 50 ºC	0.0002-0.001
Fuel oil	0.0009
Refrigerating liquids	0.0002
Steam (nonoil bearing)	0.0001

Fluid combination	U, W/m^2.K.
Water to water	850-1700
Water to oil	110-350
Steam condenser, water in tube	1000-6000
Ammonia condenser, water in tube	800-1400
Finned tube heat exchanger, water in tubes air in cross flow	25-50

Part B: Heat Transfer Principals in Electronics Cooling

Indicative Contents

- **Conduction Heat Transfer**
- **Multi-Dimensional Conduction**
- **Transient Conduction**
- **Natural Convection in Electronic Devices**
- **Forced Convection Heat Transfer**
- **Forced Convection Correlations**
- **Radiation Heat Transfer**
- **Advanced Radiation**
- **Case Study: Using EES in Electronics Cooling**

4. Conduction Heat Transfer

4.1 Fourier Equation for Conduction

Conduction is one of the heat transfer modes. Concerning thermal design of electronic packages conduction is a very important factor in electronics cooling specially conduction in PCB's and chip packages. The basic law governing the heat transfer by conduction is Fourier's law (Equation 4.1).

$$q'' = -k\frac{dT}{dx} \tag{4.1}$$

The above equation is called the rate equation it calculates the heat transferred per unit area in the direction perpendicular to the area through which it's transferred.

4.2 General Governing Equation (Energy Equation)

As a system, energy balance may be applied on any electronic component. A typical energy balance on a control volume can be described as in Equation 4.2. The amount of energy flowing into or out of the system can be described by the Fourier's law.

$$\dot{E}_{in} + \dot{E}_g = \dot{E}_{out} + \dot{E}_{stored} \tag{4.2}$$

4.2.1 Cartesian Coordinates

A differential control volume is shown in Figure 4.1. The differential control volume has the side's dx, dy, dz respectively.

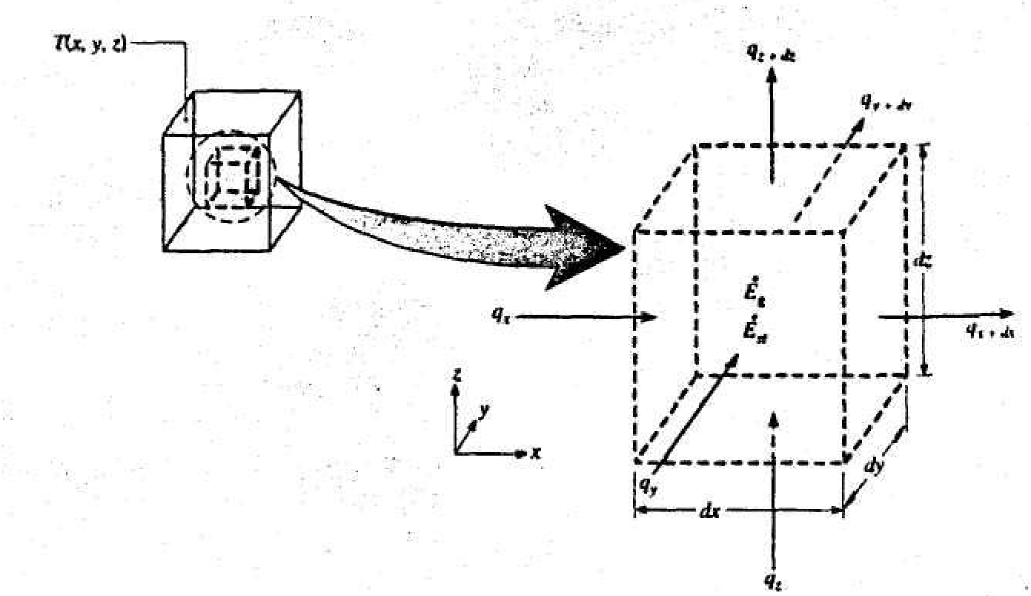

Figure 4.1 Differential control volume , dx dy dz, for conduction in cartesian coordinates.

From Fourier's law the heat flux (per unit volume) flowing into the control volume in the three Cartesian coordinates is

$$q''_x = -k\frac{\partial T}{\partial x} \qquad q''_y = -k\frac{\partial T}{\partial y} \qquad q''_z = -k\frac{\partial T}{\partial z} \tag{4.3}$$

Using Taylor expansion series and neglecting higher order terms, the surface flux for x, y and z after a displacement dx, dy and dz respectively could be expressed as

$$q_{x+dx} = q_x + \frac{\partial q_x}{\partial x}dx \tag{4.4a}$$

$$q_{y+dy} = q_y + \frac{\partial q_y}{\partial y}dy \tag{4.4b}$$

$$q_{z+dz} = q_z + \frac{\partial q_z}{\partial z}dz \tag{4.4c}$$

In the above equations the rate of heat transferred at location x + dx equals that at location x in addition to the change of this rate with respect to x multiplied by the distance dx.

If there is a thermal energy generated by an energy source through the medium .This term is expressed as

$$\dot{E}_g = \dot{q}^{///}\, dx\, dy\, dz \tag{4.5}$$

Where, $\dot{q}^{///}$ is the rate at which energy is generated per unit volume of the medium in W/m^3.

If the material shows no change in phase, we may ignore the effects of latent energy, and the energy storage term may be expressed as

$$\dot{E}_{st} = \rho C_P \frac{\partial T}{\partial t} dx\, dy\, dz \tag{4.6}$$

Where, $\rho C_p dT/dt$ is the time rate of change of the sensible internal energy of the medium per unit volume.

Substituting from Equations 4.3, 4.5 and 4.6 in Equation 4.2 yields

$$q_x + q_y + q_z + \dot{q}^{///}\, dx\, dy\, dz - q_{x+dx} - q_{y+dy} - q_{z+dz} = \rho C_P \frac{\partial T}{\partial t} dx\, dy\, dz \tag{4.7}$$

Substituting from Equations 4.4, it follows that

$$-\frac{\partial q_x}{\partial x}dx - \frac{\partial q_y}{\partial y}dy - \frac{\partial q_z}{\partial z}dz + \dot{q}^{///}\, dx\, dy\, dz = \rho C_P \frac{\partial T}{\partial t} dx\, dy\, dz \tag{4.8}$$

Using Fourier's law, we obtain the conduction rates

$$q_x = -k\,dy\ dz\,\frac{\partial T}{\partial x} \tag{4.9a}$$

$$q_y = -k\,dx\ dz\,\frac{\partial T}{\partial y} \tag{4. 9b}$$

$$q_z = -k\,dx\ dy\,\frac{\partial T}{\partial z} \tag{4.9c}$$

Substituting Equations 4.9 into Equation 4.8 and dividing by the dimensions of the control volume (dx dy dz), we obtain

$$\frac{\partial}{\partial x}\left(k\frac{\partial T}{\partial x}\right)+\frac{\partial}{\partial y}\left(k\frac{\partial T}{\partial y}\right)+\frac{\partial}{\partial z}\left(k\frac{\partial T}{\partial z}\right)+\dot{q}^{///} = \rho C_P\,\frac{\partial T}{\partial t} \tag{4.10}$$

For a constant thermal conductivity the heat equation could be rewritten as

$$\frac{\partial^2 T}{\partial x^2}+\frac{\partial^2 T}{\partial y^2}+\frac{\partial^2 T}{\partial z^2}+\frac{\dot{q}^{///}}{k} = \frac{1}{\alpha}\frac{\partial T}{\partial t} \tag{4.11}$$

Where $\alpha = k/\rho C_p$ is the thermal diffusivity.

4.2.2 Cylindrical Coordinates

Similarly we can deduce the general heat equation in the cylindrical and spherical coordinates. The general equation in the cylindrical coordinates and the infinitesimal control volume on which the energy conservation is done is shown in Figure 4.2

$$\frac{1}{r}\frac{\partial}{\partial r}\left(kr\frac{\partial T}{\partial r}\right)+\frac{1}{r^2}\frac{\partial}{\partial \phi}\left(k\frac{\partial T}{\partial \phi}\right)+\frac{\partial}{\partial z}\left(k\frac{\partial T}{\partial z}\right)+\dot{q}^{///} = \rho C_P\,\frac{\partial T}{\partial t} \tag{4.12}$$

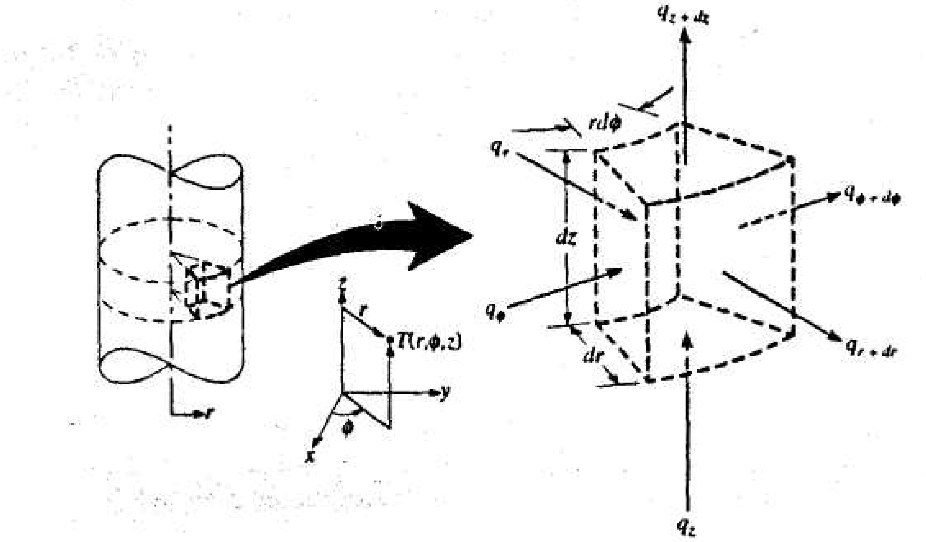

Figure 4.2 Differential control volume dr.rdφ.dx for conduction analysis in cylinderical

coordinates (r, ϕ ,z)

4.2.3 Spherical Coordinates

For the spherical coordinates also the general form and the volume on which the energy conservation is done is shown in Figure 4.3

$$\frac{1}{r^2}\frac{\partial}{\partial r}\left(kr^2\frac{\partial T}{\partial r}\right)+\frac{1}{r^2\sin^2\theta}\frac{\partial}{\partial\phi}\left(k\frac{\partial T}{\partial\phi}\right)+\frac{1}{r^2\sin\theta}\frac{\partial}{\partial\theta}\left(k\sin\theta\frac{\partial T}{\partial z}\right)+\dot{q}^{///}=\rho C_P\frac{\partial T}{\partial t} \qquad (4.13)$$

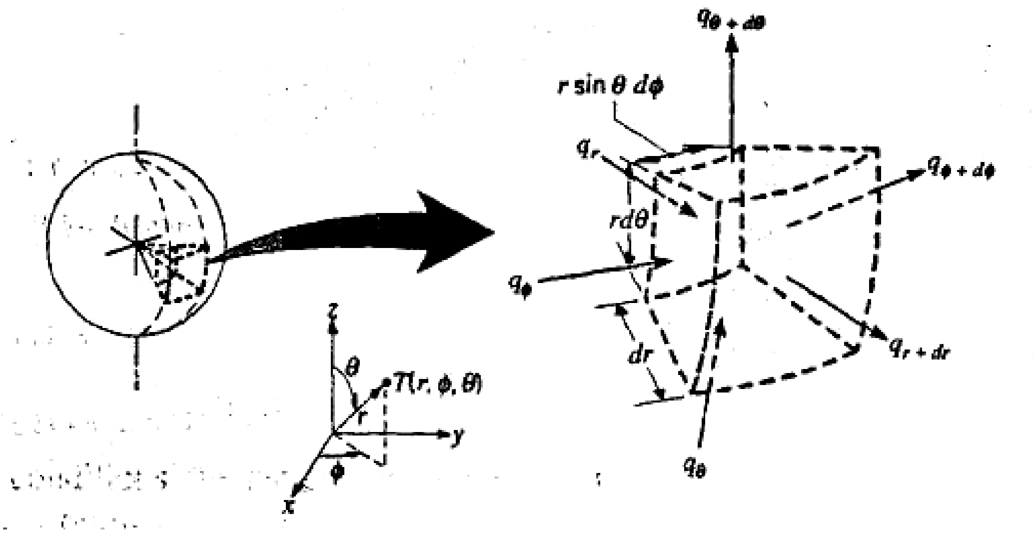

Figure 4.3 Differential control volume , dr.r sin θ dϕ .r dθ , for conduction analysis in spherical coordinates (r,ϕ,θ)

The above equations represent the general form of heat equations; these are Partial differential equation (PDE). As the heat equations are second order in the spatial coordinates, two boundary conditions must be expressed for each coordinate in order to describe the system. But since the equation is first order in time, only one condition, termed the initial condition, must be specified.

4.3 Special Cases of one Dimensional Conduction

In order to reach solutions for the conduction heat transfer equation in engineering applications, some assumptions may be made. These assumptions and approximations give reasonable results and accuracy for many engineering applications.

One of the mostly used approximations of the general heat equation is the one dimensional steady state heat transfer by conduction. As this section considers one dimensional heat flow therefore a single coordinate is needed to describe the temperature gradient and heat flow which are exclusively in that direction and if the temperature at any point is independent of time this system is to be considered one dimensional steady state heat transfer.

4.3.1 Boundary Conditions

Some of the boundary conditions usually met in heat transfer problems for one dimensional system are described below. These conditions are set at the surface x = 0, assuming transfer process in the positive direction of x- axis with temperature distribution which may be time dependent, designated as T(x, t).

Constant Surface Temperature

The surface is maintained at a fixed temperature T_s. It is commonly called a Dirichlet condition, which is the boundary condition of the first case. It can be approximated as a surface in contact with a solid or a liquid in a changing phase state (boiling, evaporating, melting or freezing) therefore the temperature is constant.

$$T(0,t) = T_s$$

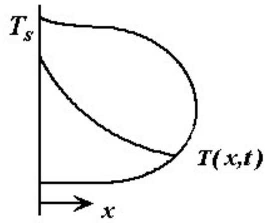

Constant Surface Heat Flux

In this case fixed or constant heat flux q" at the surface is described. At which the heat flux is a function of the temperature gradient at the surface by Fourier's law (Equation 4.1) that was stated before. This type of boundary condition is called Neumann condition. Examples of constant surface heat flux are described below.

a) Finite heat flux

$$-k\frac{\partial T}{\partial x}\bigg|_{x=0} = q''_s \qquad (4.14)$$

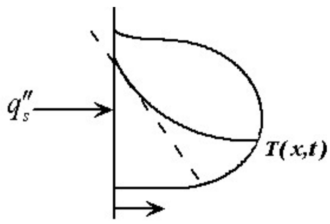

This type of boundary conditions may exist, for example, in the case of an electric heater attached to a surface.

b) Adiabatic heat flux

$$\frac{\partial T}{\partial x}\bigg|_{x=0} = 0_s \qquad (4.15)$$

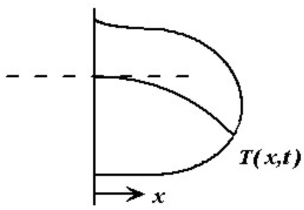

An example of the adiabatic heat flux is a surface which is perfectly insulated.

c) Convection surface condition

$$-k\frac{\partial T}{\partial x}\bigg|_{x=0} = h[T_\infty - T(0,t)] \qquad (4.16)$$

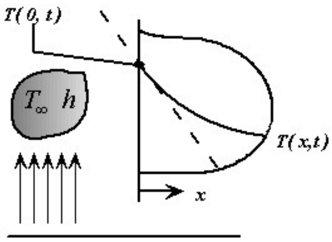

This represents the existence of convection heating (or cooling) at the surface and is determined by applying an energy balance on the surface by equating the amount of heat transferred by conduction with that transferred by convection which results yields Equation 4.16.

4.3.2 One Dimensional Steady state Conduction without Heat Generation

The assumptions made for this kind of analysis are:

- One dimensional
- Steady state
- No heat generation
- Constant material properties

Cartesian Coordinates

This model deals with a one dimensional steady state system with no heat generation. It may describe the heat flow through a plane wall. Therefore the temperature is a function of x coordinates and heat is transferred in that direction.

According to the pervious assumptions the general heat Equation 4.11 becomes

$$\frac{d}{dx}\left(k\frac{dT}{dx}\right) = 0 \qquad (4.17)$$

By integrating this equation twice assuming constant thermal conductivity of the wall to determine the general equation

$$T(x) = C_1 x + C_2 \qquad (4.18)$$

In order to obtain the constants found in Equation 4.18 we have to introduce the appropriate boundary condition. From the analysis done above, we can choose the first case (the surface is maintained at a fixed temperature T_s)

$$T(0) = T_{s,1} \qquad T(L) = T_{s,2} \qquad (4.21)$$

Substituting these conditions in Equation 4.18 we obtain the two constants as follows

At x =0 we get

$$T_{s,1} = C_2$$

Similarly at x =L

$$T_{s,2} = C_1 L + C_2$$

$$T_{s,2} = C_1 L + T_{s,1}$$

We can put the constant C_1 in the following form

$$\frac{T_{s,2} - T_{s,1}}{L} = C_1 \qquad (4.22)$$

Substituting in the general solution of the heat equation

$$T(x) = (T_{s,2} - T_{s,1})\frac{x}{L} + T_{s,1} \qquad (4.23)$$

From Fourier's law the heat flux crossing the wall is expressed by

$$q''_x = k\frac{dT}{dx}$$

Thus the amount of heat transferred through the wall of an area A is then obtained by

$$q_x = k\,A\frac{dT}{dx}$$

From the previous derivation the temperature gradient dT/dx could be obtained as

$$\frac{dT}{dx} = C_1 = \frac{T_{s,2} - T_{s,1}}{L} \qquad (4.24)$$

$$q_x = k\,A(\frac{T_{s,2} - T_{s,1}}{L}) \qquad (4.25)$$

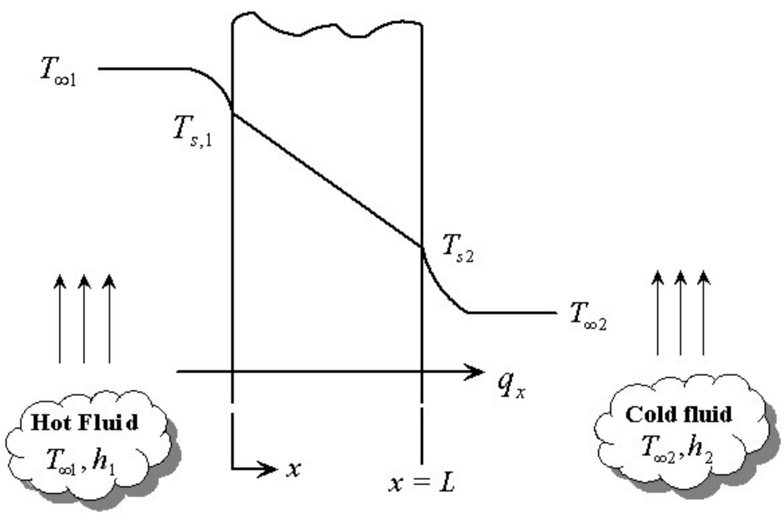

Figure 4.10 Heat transfer through a plane wall

Example 4.1: Calculate the maximum temperature the transistor base attains if it dissipates 7.5 W through the bracket shown in the Figure below. All dimensions are in mm and the bracket is made of duralumin.

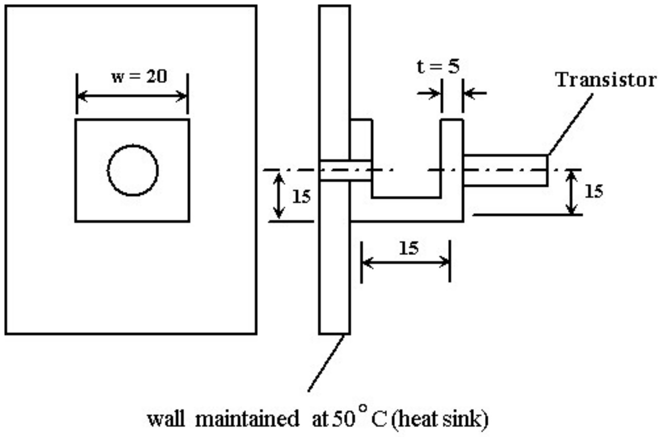

Required:
The maximum temperature attained by the transistor base.

Solution:
Given
Dimension on the figure.
$q = 7.5$ W
$t_w = 50$ º C
This problem could be approximated to one dimensional steady state conduction.
$k = 164$ W/m.K
As the dimensions of the bracket is very small we can consider that the transfer is in one dimension through the sides of the bracket for the dimensions shown on the figure
$L = 15 + 15 + 15 = 45$ mm $= 0.045$ m
$w = 20$ mm $= 0.02$ m
$\delta = 5$ mm $= 0.005$ m
$A = w \times \delta = 1 \times 10^{-4}\ m^2$
From the above values the only unknown in equation 4.23 is the temperature of the transistor base.
$q = k A (t_b - t_w)/L$
$t_b = t_w + (qL/kA)$
$t_b = 50 + (7.5 \times 0.045/164 \times 10^{-4})$
$t_b = 70.58$ ºC

Note:

Usually the maximum allowable temperature is 100 ºC; therefore, the transistor temperature base is safe with a reasonable value which compensates the approximation done in the solution.

Cylindrical Coordinates
Considering the above assumptions, dT/dr is constant and heat flow only in one spatial coordinates the general form becomes

$$q = \frac{2\pi k L (T_1 - T_2)}{\ln(r_2 / r_1)} \qquad (4.26)$$

Where subscripts 1 and 2 refer to the inner and the outer surfaces respectively

Example 4.2: A hollow stainless (25 % Cr, 20 % Ni) steel cylinder 35 mm long has an inner diameter of 50 mm and outer diameter of 105 mm. a group of resistors that generate 10 W is to be mounted on the inside surface of the cylinder as shown in figure if the resistors temperature is not to exceed 100 ºC find the maximum allowed temperature on the outer surface of the cylinder.

Solution:
From appendix the thermal conductivity of 25 % Cr, 20 % Ni stainless steel is 12.8 W/m.K from Equation 4.26; the only unknown is the temperature of the outside surface of the cylinder.

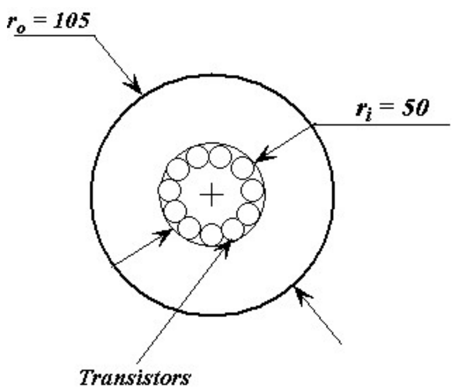

$$T_o = T_i - \frac{q(\ln(r_o / r_i))}{2\pi kL}$$

T_o= 100 – 10 × (ln (52.5/25)/ (2π × 12.8 × 0.035)

T_o = 100 – 2.64 = 97.36 ºC

Spherical Coordinates

The same assumptions are applied to the spherical system giving the following solution

$$q_r = \frac{(T_i - T_o)}{\frac{(1/r_o - 1/r_i)}{4\pi k}}$$

Where the subscripts i and o refer to the inside and the outside surfaces respectively.

4.3.3 One Dimensional Steady state Conduction with Uniform Heat Generation

The assumptions made for this kind of analysis are:

- One dimensional
- Steady state
- Uniform heat generation
- Constant material properties

Cartesian Coordinates

The heat equation becomes

$$k\frac{d^2T}{dx^2} + q''' = 0$$

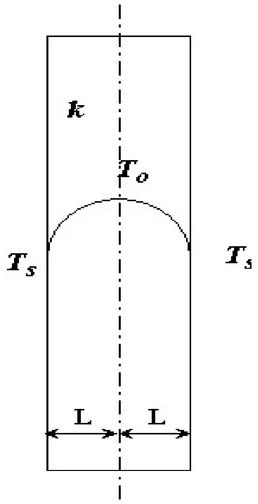

Integrating and applying the boundary conditions described in figure we get

$$T = -\frac{q'''}{2k}x^2 + C_1 x + C_2$$

$C_1 = 0$ and $C_2 = T_s + (q''' L^2/2k)$
Then we get

$$T = -\frac{q'''}{2k}(L^2 - x^2) + T_s$$

The above equation differs for different wall construction and condition for an example if there is an outer cladding the temperature distribution through the wall will differ.

$q = q''' \times A \times L = T_s - T_c/(L_c/k_c\, A_c)$

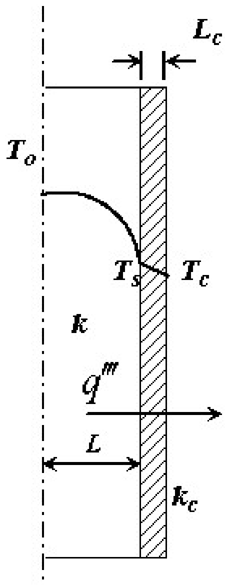

Temperature distribution through the wall will be

$T = T_c + q''' L \times L_c / k_c + q''' / 2k(L^2 - x^2)$

Similarly we can apply these cases on the other coordinate systems (cylindrical and spherical).

The boundary condition of each case affects the constants introduced in the equation of the temperature distribution leading to a change in the final formula.

Cylindrical Coordinates

The heat equation becomes

$$\frac{1}{r}\frac{\partial}{\partial r}\left(kr\frac{\partial T}{\partial r}\right)+q'''=0$$

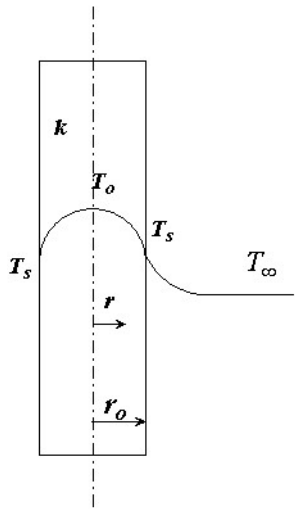

For the following boundary conditions
At $r = 0$ $dT/dr = 0$ where $C_1 = 0$
At $r = r_o$ $T = T_s$ where $C_2 = T_s + q''' r_o^2 / 4k$

We get the temperature distribution expression as follows
$T = T_s + q''' / 4k(r_o^2 - r^2)$

If the wall is subjected to a convective boundaries or it is cladded the same as in the plane wall the boundary conditions is to be applied and we are going to give the final form and the derivation is left to the student.

For a convective boundaries: $T = T_\infty + q''' / 4k (r_o^2 - r^2) + q''' r_o / 2h$

And if it is cladded: $T = T_\infty + \frac{q'''}{4k}(r_o^2 - r^2) + q'''\left[\frac{\ln(r_c / r_o)}{2k_c} + \frac{1}{2hr_c L}\right]r_o^2\ L$

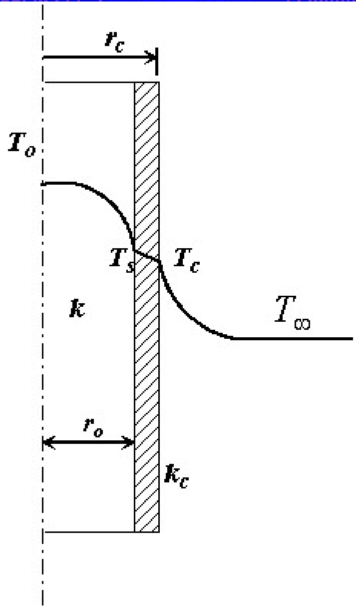

4.4 Extended Surfaces (Fins)

As clear from the rate equations that enhancing heat transfer could be done by several methods it could be by increasing the temperature difference or by increasing the heat transfer coefficient and also by increasing the surface area A, in this section we are going to deal with the last one, and this idea is done by adding a secondary surface to the primary surface and it is called extended surfaces, due to temperature gradient through the fins the heat transferred is decreased per unit area.

In electronic equipment cooling straight rectangular fins are mostly used and are done of good conducting material to attain the root temperature through the fins in order to increase the heat transferred.

Fins used in electronics cooling are usually used of aluminum and quite thin about 1.3 to 1.5 mm thick. Also in electronics cooling fins are usually considered of insulated tip. The heat transferred by fins are expressed in its effectiveness which is defined as

$\eta_f = q_f \,/\, q_{max}$

Where q_f is the heat actually transferred by the fin and q_{max} is the maximum heat could be dissipated by the fin and this happens when the fin has a uniform temperature equals to the root temperature t_r.

$\eta_f = (\tanh m l)/(m l)$

Where $m = \sqrt{2h(L+b)/k(b\ L)}$, l , L and b are defined on the fin sketch (Figure 4.11a).

Also the fin effectiveness could be considered as the fraction of the total surface area of the fin A_f that is effective for the heat transfer by convection maintained at root temperature t_r.

$\eta_f = A_{f,\,eff}/A_{f,tot}$

$$q = h\,[(A_{tot} - A_f) + \eta_f A_f]\,(t_r - t_a)$$
$$= \eta_o A_{tot}\, h\,(t_r - t_a)$$

Where $\eta_o = 1 - (A_f/A_{tot})\,(1 - \eta_f)$

If the fin is of convective tip a correction could be done as
$l_c = l + (b/2)$

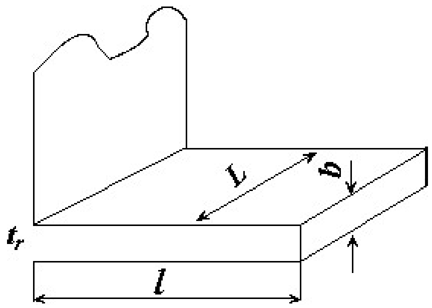

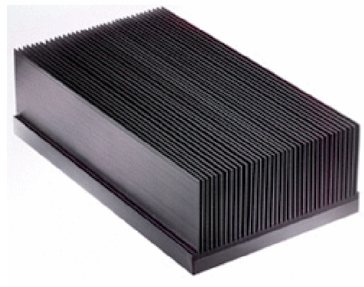

Figure 4.11a Straight rectangular fin dimensions	Figure 4.11b Typical heat sink with straight rectangular fins for electronic device

4.4.1 Fin Geometries

There are many types of plate-fin surfaces including plain fins, louvered fins, strip (or lanced offset) fins, wavy fins and pin fins. With 56 plate-fin surfaces tested, there is a wide range of fin geometries for which data is directly available. Figure 4.12 shows five common plate fin types and the critical fin dimensions.

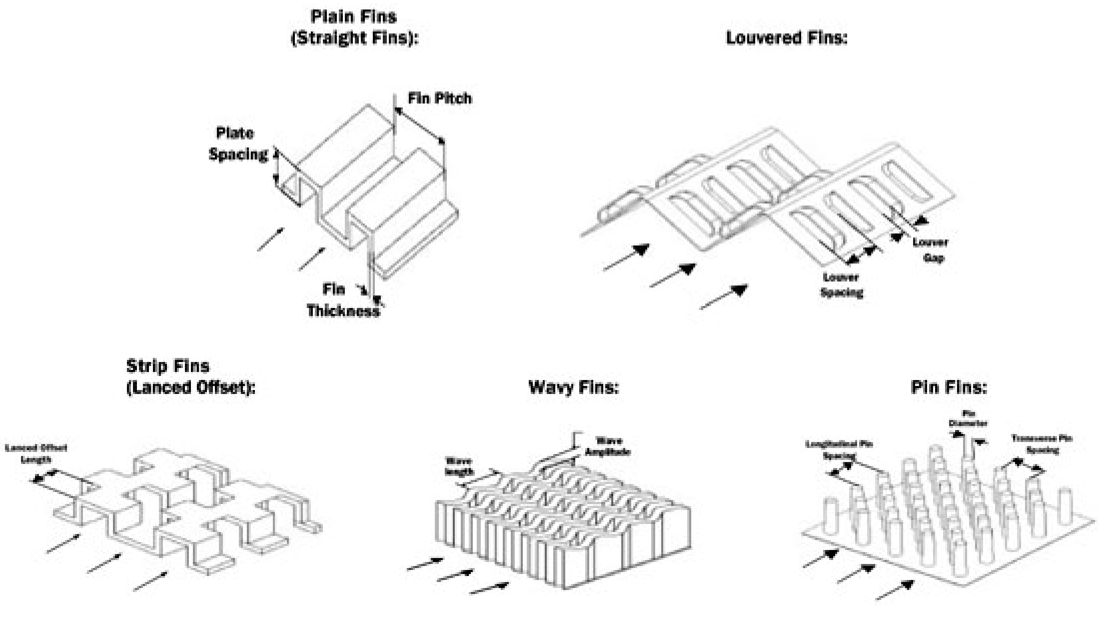

Figure 4.12 Fin descriptions

4.4.2 Factors Affected on the Fin Selection

With avionics power densities increasing, it becomes even more critical to design an optimum compact heat exchanger to remove the heat load most efficiently. There are many factors to consider in the selection of fin style and geometry. All of the parameters will discusses and should help the thermal engineer understand and trade these factors so that the best design may be obtained. There will always be some give and take among all these factors, but knowing and evaluating these factors is critical in obtaining an optimum design.

Using the Data

The data in Kays & London is presented as Fanning friction factor and Colburn factor vs Reynold's number. The Fanning friction factor also known as the skin friction coefficient, is defined as

$$f = \frac{\tau_o}{(1/2)\rho v^2} \tag{4.27}$$

It is related to the more common D'Arcy friction factor by

$$f_{D'Arcy} = 4f \tag{4.28}$$

The pressure drop, using the Fanning friction factor provided by Kays & London, is given by:

$$\Delta P = 4f\frac{L}{D_h}\left(\frac{\rho v^2}{2}\right) \tag{4.29}$$

The Colburn factor, j is defined by:

$$j = N_{St}\,N_{\text{Pr}}^{2/3} = \frac{N_{Nu}}{N_{\text{Re}}N_{\text{Pr}}^{1/3}} \tag{4.30}$$

The film coefficient, using the Colburn factor provided by Kays & London is given by:

$$h = \frac{k}{D_h}jN_{\text{Re}}N_{\text{Pr}}^{1/3} \tag{4.31}$$

Design Practices

Now that you have all this good information on heat transfer and pressure drop for the different extended surfaces, you need to find the best way to use it. In the past, the thermal engineer would open up the Kays & London text book and look for a certain type of fin, such as pin, straight, lanced offset, or wavy, that worked for the combination of heat transfer, required pressure drop, and size constraints. This approach produces a design that works, but is hardly optimized for any of the considerations involved in designing the compact heat exchanger. A typical heat transfer plot of straight fins, from Kays and London, is shown in Figure 4.13.

Figure 4.13 allows the thermal engineer to calculate the heat transfer and pressure drop by picking off the j-Colburn factor and friction factor at the proper Reynolds number for a certain configuration, but it is unknown whether the proper design was chosen from a size and efficiency standpoint. The first thing the thermal engineer needs to do is prioritize the design factors. Pressure drop, heat transfer, size, weight and cost must be placed in order of importance. Hence, figures of merit were developed in an effort to compare the different fin configurations.

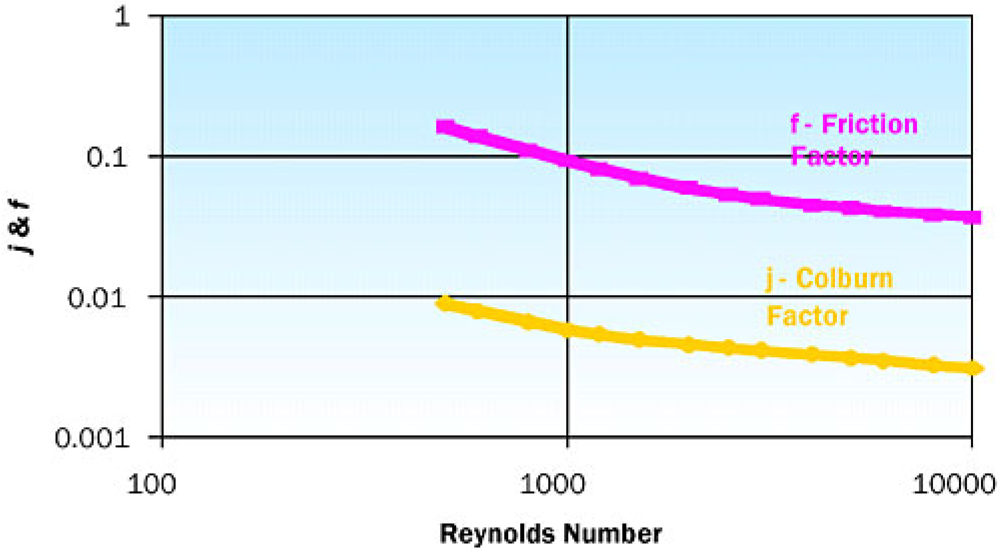

Figure 4.13 Finstock data # 14.77 from Kays & London (0.4 mm high, 0.15mm thick, 37.5 fins/mm, ST [0.330" high, 0.006" thick, 14.77 fpi, ST])

If pressure drop and heat transfer are the most critical factors in the compact heat exchanger design then a good figure of merit is heat transfer per unit of pressure drop, or in basic terms: j-Colburn factor divided by f-friction factor. Figure 4.14 shows a comparison of the different types of extended surfaces using heat transfer/pressure drop as the figure of merit.

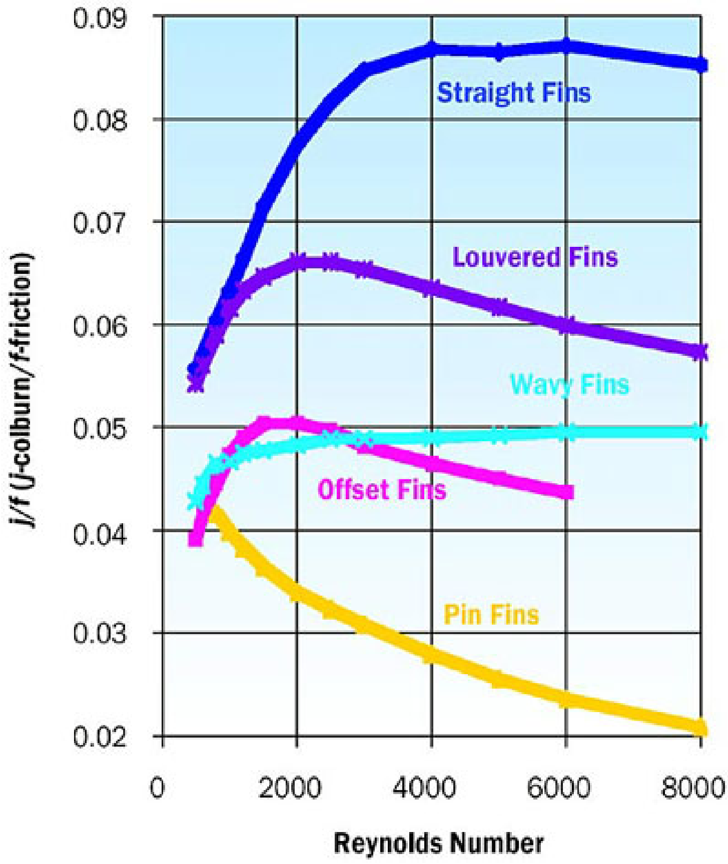

Figure 4.14 Heat transfer/pressure drop

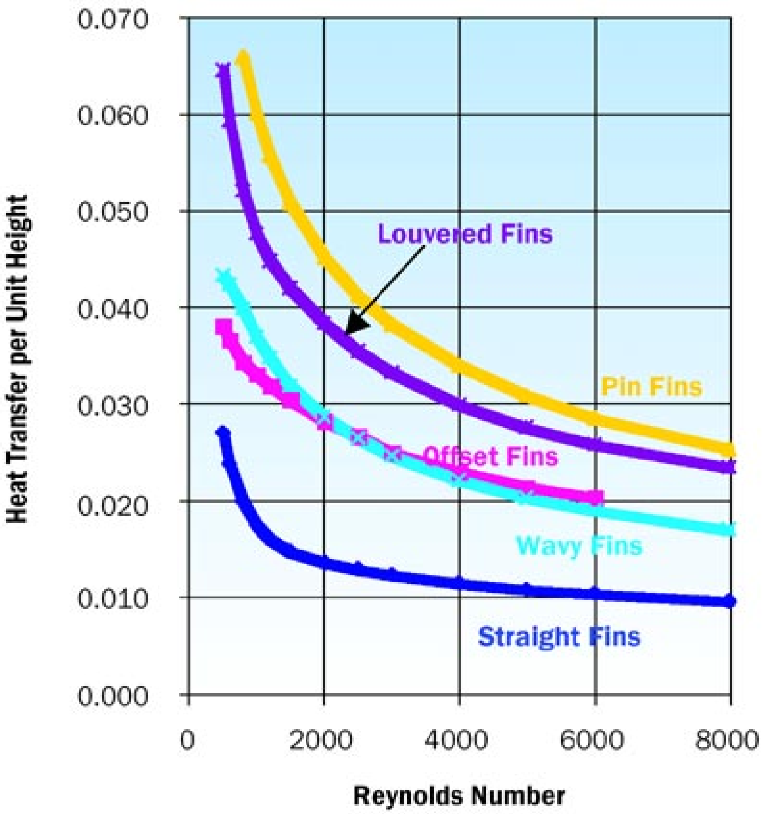

Figure 4.15 Size figure of merit

As can be seen from Figure 4.14, the efficiency of straight fins used in a heat exchanger is better than the other fin configurations over almost the whole range of typical Reynolds numbers. At a Reynolds number of 4000 the straight fin produces a three times better ratio of heat transfer per unit of pressure drop than the pin fin configuration. This figure of merit is based strictly on getting the best heat transfer for a given pressure drop.

Size is generally an important factor in the heat exchanger design. If size is the overall driving design factor then a good figure of merit is heat transfer per unit height. Figure 4.15 provides a comparison if size or height is the critical factor in the heat exchanger design. Figure 4.15 shows that, from a purely size standpoint, pin fins offer the smallest design for the best heat transfer while straight fins are the most inefficient from a heat transfer and smallest size constraint.

Weight is almost always an important factor in avionics cooling and designing a heat exchanger for an aircraft. A good figure of merit for weight is based on the heat transfer per weight unit. Figure 4.16 shows a comparison of fin configurations when weight is the critical factor in the design.

The last parameter that must be traded is cost, which is always an important factor in the design of a compact heat exchanger. It is also one of the more subjective areas. In general, pin fins, which are incorporated directly into the casting of the heat exchanger, are the least expensive. The other fin configurations, such as wavy, straight, offset louvered and cost about the same with some minor differences in set up costs.

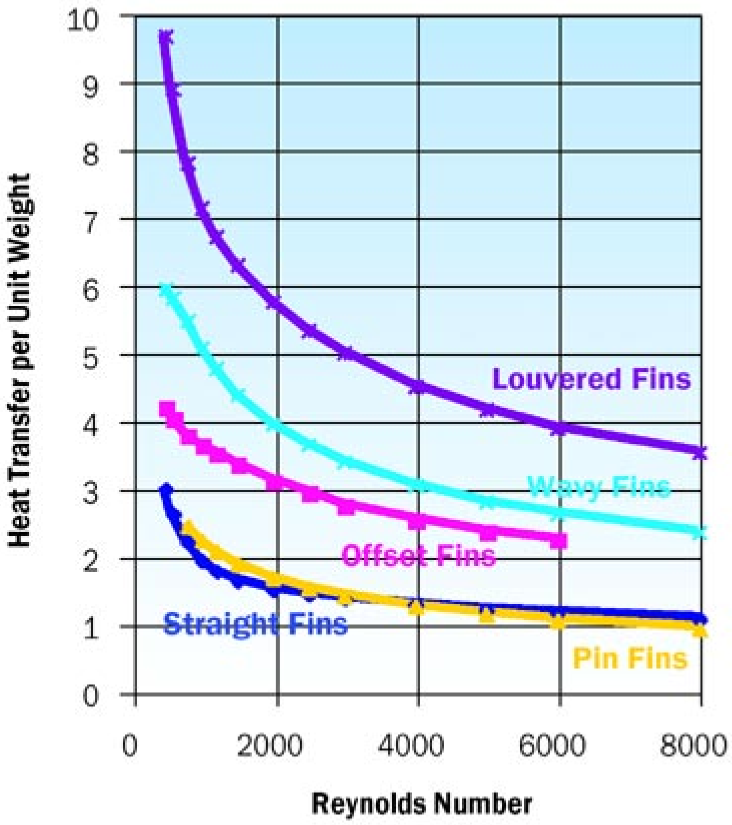

Figure 4.16 Weight figure of merit

A relative comparison of the fin configurations, based on all the factors discussed is critical in determining the proper design. All of the parameters are presented as individual design points, while the charts show the relative comparison for one parameter such as size, the assumption is made that pressure drop is unlimited as well as weight or cost. All of these parameters must be considered to obtain the proper design. The table above summarizes or ranks each factor so that the thermal engineer can get a relative view of all the parameters together. The rankings in Table 4.1 are from 1 to 5 with a ranking 1 being the most desirable and a ranking of 5 being the least desirable.

Table 4.1 Comparison of all parameters

Fin Configuration	ΔP	Size	Weight	Cost	Average
Straight	1	5	4	2	3
Offset	4	3	3	4	3.5
Pin	5	1	5	1	3
Wavy	3	4	2	3	3
Louver	2	2	1	5	2.5

With all of the parameters weighted equally the louvered fin configuration produces the best design for a compact heat exchanger. Another important factor is that even though the cost of the louvered fin is highest its cost is only slightly higher than the wavy, offset and straight fins. By contrast, the pin fin structure is an all or nothing configuration, with the highest figure of merits for cost and size, while performing extremely poorly in pressure drop and weight. So if cost and size are the number one priority without concern for pressure drop then the pin fins performs very well. Straight fins are also your best choice if pressure drop is the limiting factor in the design, which is usually a driving factor in avionics heat exchanger design. With all the parameters considered, all five fin configurations came out surprisingly equal, so a weighted average would be most appropriate in finding the proper design for a given set of prioritized factors.

5. Multi-Dimensional Conduction

In this lecture, we will deal with heat conduction problem significant in more than one-dimension. This approach should be used as the applications imply. First, several alternatives are developed to deal with two-dimensional, steady state conduction. Then as we reach the numerical approach, we can extend its use for a three-dimensional problem.

5.1 Two-Dimensional and Steady-State Conduction

Under the assumptions of two dimensional steady state conduction the general heat equation is reduced to

$$\frac{\partial^2 T}{\partial x^2} + \frac{\partial^2 T}{\partial y^2} = 0 \qquad (5.1)$$

Now we have two goals for solving the above equation, the first is to determine the temperature distribution across the flied which became a function in the two coordinates x and y T(x, y), then to determine the heat fluxes q_x'' and q_y'' in the two direction x and y respectively.

There are many techniques for solving the Equation 5.1 including: analytical, graphical and numerical solution (finite element and finite difference approaches).

The analytical solution is much more difficult than that of the one dimensional steady state conduction since the equations are partial differential equations, the mathematical solution is very difficult and is limited to a set of simple geometries, on the other hand the exact solution gives the dependent variable T as a continuous function in the independents (x, y) and the solution could be determined at any point of interest in the field of study.

On the other hand the graphical and the numerical solution gives an approximate solution at discrete points in the medium, as the graphical and numerical can solve complex geometries, they are more widely used for the multidimensional conduction problems.

5.1.1 The Method for Separation of Variables

Solving Equation 5.1 for a rectangular plate as shown in Figure 5.1, with three boundaries maintained at T_1, while the fourth side is maintained at T_2, where $T_2 \neq T_1$, the solution of this problem should give the temperature distribution T(x, y) at any point in the solution domain. For solution purpose, the following transformation is done.

$$\theta = \frac{T - T_1}{T_2 - T_1} \qquad (5.2)$$

And thus the heat equation yields

$$\frac{\partial^2\theta}{\partial x^2}+\frac{\partial^2\theta}{\partial y^2}=0 \qquad (5.3)$$

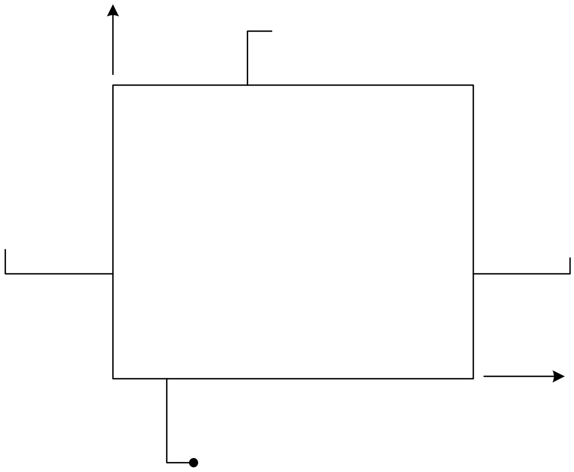

Figure5.1 Geometric configuration for the method of separation of variables

Since the equation is second order in both x and y, two boundary equations are required for each coordinate which are

$$\begin{aligned}&\theta(0,y)=0 \quad \text{and} \quad \theta(x,0)=0\\ &\theta(L,y)=0 \quad \text{and} \quad \theta(x,W)=1\end{aligned} \qquad (5.4)$$

The separation of variables technique is applied by assuming that the required function is the product of the two functions X (x) and Y (y)

$$\theta(x,y)=X(x)\cdot Y(y) \qquad (5.5)$$

Substituting in Equation 5.3 and dividing by XY

$$-\frac{1}{X}\frac{d^2X}{dx^2}=\frac{1}{Y}\frac{d^2Y}{dy^2} \qquad (5.6)$$

It is evident that Equation 5.6 is separable as the left-hand-side depends only on x, and the right-hand-side depends only on y. Therefore, the equality can only apply if both sides are equal to the same constant, λ^2, called the separation constant. Using this constant, Equation 5.6 can yield the following equations

$$\frac{d^2X}{dx^2}+\lambda^2X=0 \qquad (5.7)$$

$$\frac{d^2Y}{dy^2}-\lambda^2Y=0 \qquad (5.8)$$

Then the partial differential equation is converted to two second order ordinary differential equations. The value of λ^2 must not be negative nor zero in order that the solution satisfies the prescribed boundary equation.

The solutions equation of the above ODE gives

$$X = C_1 \cos \lambda x + C_2 \sin \lambda x \qquad (5.9)$$

$$Y = C_3 e^{-\lambda y} + C_4 e^{+\lambda y} \qquad (5.10)$$

The general solution of the heat equation is

$$\theta = \left(C_1 \cos \lambda x + C_2 \sin \lambda x\right)\left(C_3 e^{-\lambda y} + C_4 e^{+\lambda y}\right) \qquad (5.11)$$

Then applying the boundary condition that θ (0, y) = 0, we get that $C_1 = 0$,

Then the condition that θ (x, 0) = 0, we get

$$C_2 \sin \lambda x \,(C_3 + C_4) = 0 \qquad (5.12)$$

The above equation is satisfied by either $C_3 = -C_4$ or $C_2 = 0$, but if we consider the solution that $C_2 = 0$ this will eliminate the solution dependency on x coordinate, which is a refused solution, thus the first solution is chosen $C_3 = -C_4$, applying the condition that θ (L, y) = 0, we get:

$$C_2 C_4 \sin \lambda L \,(e^{\lambda y} - e^{-\lambda y}) = 0 \qquad (5.13)$$

The only acceptable solution is that sin (λ L) = 0, this is satisfied for the values of

$$\lambda = \frac{n\pi}{L} \qquad \text{where } n = 1, 2, 3, \ldots$$

$$\therefore \theta = C_2 C_4 \sin \frac{n\pi x}{L}\left(e^{n\pi y/L} - e^{-n\pi y/L}\right) \qquad (5.14)$$

Rearranging

$$\theta(x, y) = C_n \sin \frac{n\pi x}{L} \sinh \frac{n\pi y}{L} \qquad (5.15)$$

Where C_n is a combined constant Equation 5.16 has an infinite number of solutions depending on n, however it is a linear problem. Thus a more general solution may be obtained by superposing all the solutions as

$$\theta(x, y) = \sum_{n=1}^{\infty} C_n \sin \frac{n\pi x}{L} \sinh \frac{n\pi y}{L} \qquad (5.16)$$

Now in order to determine C_n the remaining boundary condition should be applied

$$\theta(x, W) = 1 = \sum_{n=1}^{\infty} C_n \sin \frac{n\pi x}{L} \sinh \frac{n\pi y}{L} \qquad (5.17)$$

An analogous infinite series expansion is used in order to evaluate the value of C_n resulting that

$$C_n = \frac{2[(-1)^{n+1} + 1]}{n\pi \sinh(n\pi W / L)}$$

Substituting in Equation 5.16 we get

$$\theta(x,y) = \frac{2}{\pi}\sum_{n=1}^{\infty}\frac{[(-1)^{n+1}+1]}{n}\sin\frac{n\pi x}{L}\,\frac{\sinh(n\pi y/L)}{\sinh(n\pi W/L)} \qquad (5.18)$$

Then we obtain the solution of the rectangular shape in terms of θ as represented in the Figure 5.2 in the form of Isotherms for the schematic of the rectangular plate.

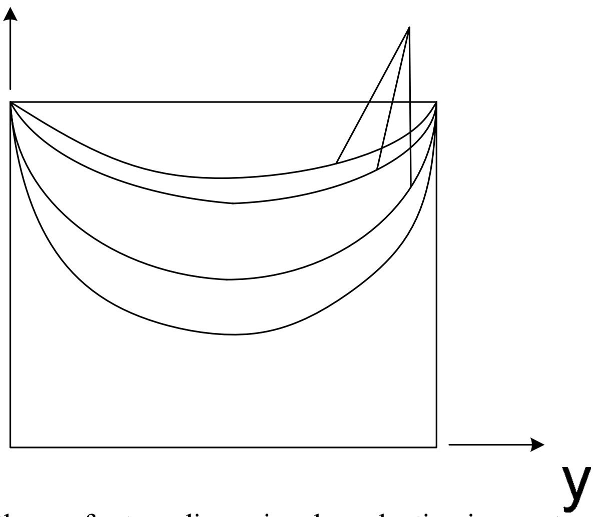

Figure 5.2 Isotherms for two-dimensional conduction in a rectangular plate

5.1.2 The Graphical Method

The graphical approach is applied for two dimensional conduction problems with adiabatic and isothermal boundaries, it has been used as a first estimate for the temperature distribution and to develop a guess for the physical nature of the temperature field and heat flux in the medium.

The idea of the graphical solution comes from the fact that the constant temperature lines must be perpendicular on the direction of heat flow, the objective in this method is to form a symmetrical network of isotherms and heat flow lines (adiabatic) which is called plot flux.

Consider a square, two-dimensional channel whose inner and outer surfaces are maintained at T_1 and T_2 respectively as shown in Figure 5.3(a). The plot flux and isothermal lines are shown in Figure 5.3(b).

The procedure for constructing the flux plot is enumerated as follows:

1. The first step in any flux plot should be to identify all relevant lines of symmetry. Such lines are determined by thermal, as well as geometrical, conditions. For the square channel of Figure 5.3(a), such lines include the designated vertical, horizontal, and diagonal lines. For this system it is therefore possible to consider only one-eighth of the configuration, as shown in Figure 5.3(b).

2. Lines of symmetry are adiabatic in the sense that there can be no heat transfer in a direction perpendicular to the lines. They are therefore heat flow lines and should be treated as such. Since there is no heat flow in a direction perpendicular to a heat flow line, such a line can be termed adiabatic.

3. After all known lines of constant temperature associated with the system boundaries have been identified, an attempt should be made to sketch lines of constant temperature within the system. Note that isotherms should always be perpendicular to adiabatic lines.

4. The heat flow lines should then be drawn with an eye toward creating a network of curvilinear squares. This is done by having the heat flow lines and isotherms intersect at right angles and by requiring that all sides of each square be of approximately the same length. It is often impossible satisfy this second requirement exactly, and it is more realistic to strive for equivalence between the sums of the opposite sides of each square. Assigning the x coordinate to the direction of the flow and the y coordinate to the direction normal to this flow, the requirement may be expressed as:

$$\Delta x \equiv \frac{ab+cd}{2} \approx \Delta y \equiv \frac{ac+bd}{2} \qquad (5.19)$$

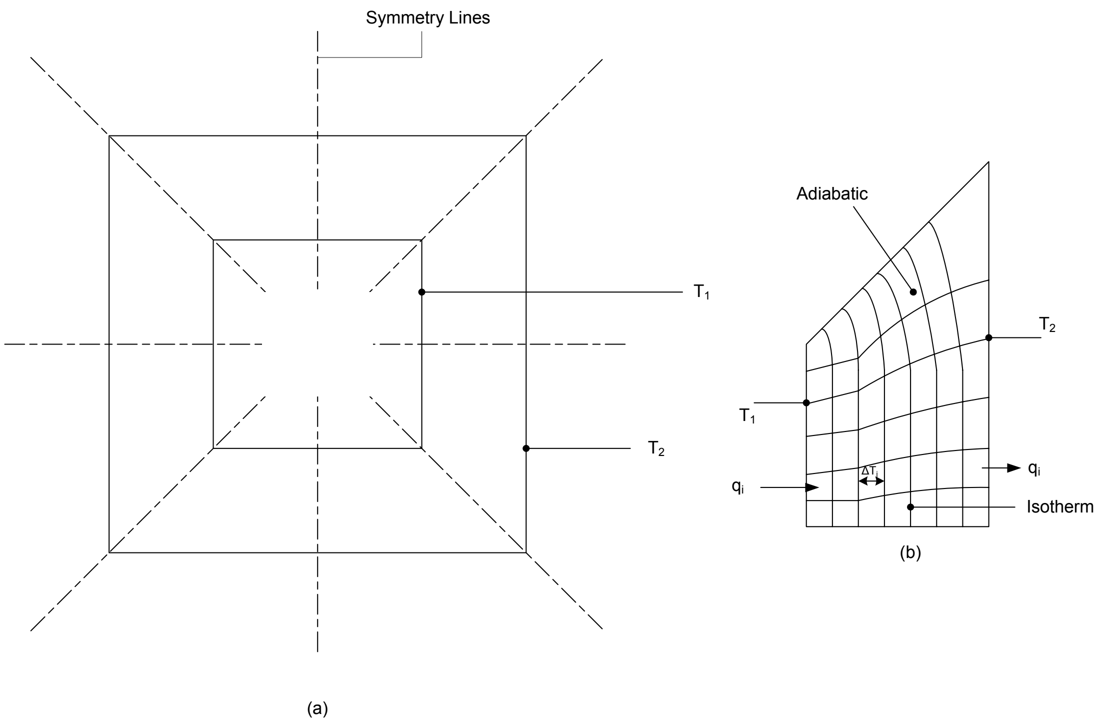

Figure 5.3 Graphical solution for Two-dimensional conduction in a square channel

The rate at which energy is conducted through a heat flow path, which is the region between adjoining adiabatic lines, is designated as q_i. If the flux plot is properly constructed, the value of q_i will be the same for all heat flow paths and the total heat transfer rate may be expressed as:

$$q = \sum_{i=1}^{M} q_i \qquad (5.20)$$

Where M is the number of heat flow paths associated with the plot. q_i may be expressed as:

$$q_i \approx kA_i \frac{\Delta T_j}{\Delta x} \approx k(\Delta y \cdot l)\frac{\Delta T_j}{\Delta x} \qquad (5.21)$$

Where ΔT_j is the temperature difference between successive isotherms, A, is the conduction heat transfer area for the heat flow path, and l is the length of the channel normal to the page. However, if the flux plot is properly constructed, the temperature increment is the same for all adjoining isotherms, and the overall temperature difference between boundaries, T_{1-2} may be expressed as

$$\Delta T_{1-2} = \sum_{j=1}^{N} \Delta T_j = N\Delta T_j \tag{5.22}$$

Where N is the total number of temperature increments. Combining Equations 5.20 to 5.22 and recognizing that Δx ≈ Δy for curvilinear squares, we obtain

$$q \approx \frac{Ml}{n} k\Delta T_{1-2} \tag{5.23}$$

The manner in which a flux plot may be used to obtain the heat transfer rate for a two-dimensional system is evident from Equation 5.23. The ratio of the number of heat flow paths to the number of temperature increments (the value of M/N) may be obtained from the plot. Recall that specification of N is based on step 3 of the foregoing procedure, and the value, which is an integer, may be made large or small depending on the desired accuracy. The value of M is then a consequence of following step 4. Note that M is not necessarily an integer, since a fractional lane may be needed to arrive at a satisfactory network of curvilinear squares. For the network of Figure 5.3(b), N = 7 and M = 6. Of course, as the network, or mesh, of curvilinear squares is made finer. N and 1W increase and the estimate of M/N becomes more accurate.

The above procedure is very time consuming, and can be done only for simple geometries. For this reasons, a simplification has been made by tabulating the shape factors for various two-dimensional problems in order to enable easier analysis of 2-D conductions.

Equation 5.23 may be used to define the shape factor, S, of a two-dimensional system as being the ratio (Ml / N). Hence, the heat transfer rate may be expressed as

$$q = Sk\Delta T_{1-2} \tag{5.24}$$

From Equation 5.24, it also follows that a two-dimensional conduction resistance may he expressed as

$$R_{t,2-D\ cond} = \frac{1}{Sk} \tag{5.25}$$

Shape factors for numerous two-dimensional systems and results are summarized in Table 5.1 for some common configurations. For each case, two-dimensional conduction is supposed to occur between boundaries that are maintained at uniform temperatures.

Table 5.1 Conduction shape factors for selected two-dimensional systems, $q = S\,k\,(T_1 - T_2)$

System	Schematic	Restrictions	Shape Factor
Case 1. Isothermal sphere buried in a semi-infinite medium	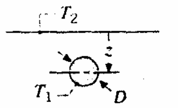	$z > D/2$	$\frac{2\pi D}{1 - D/4z}$
Case 2. Horizontal isothermal cylinder of length L buried in a semi-infinite medium	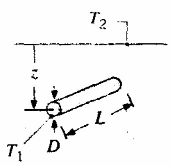	$L \gg D$ $L \gg D$ $z > 3D/2$	$\frac{2\pi L}{\cosh^{-1}(2z/D)}$ $\frac{2\pi L}{\ln(4z/D)}$
Case 3. Vertical cylinder in a semi-infinite medium	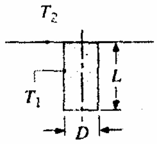	$L \gg D$	$\frac{2\pi L}{\ln(4L/D)}$
Case 4. Conduction between two cylinders of length L in infinite medium	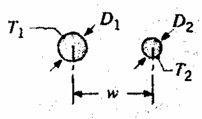	$L \gg D_1, D_2$ $L \gg w$	$\frac{2\pi L}{\cosh^{-1}\left(\frac{4w^2 - D_1^2 - D_2^2}{2D_1 D_2}\right)}$
Case 5. Horizontal circular cylinder of length L midway between parallel planes of equal length and infinite width	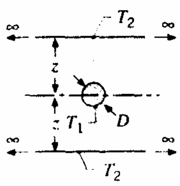	$z \gg D/2$ $L \gg z$	$\frac{2\pi L}{\ln(8z/\pi D)}$
Case 6. Circular cylinder of length L centred in a square solid of equal length	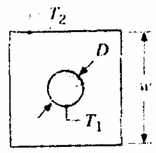		$\frac{2\pi L}{\ln(1.08\,w/D)}$
Case 7. Eccentric circular cylinder of length L in a cylinder of equal length	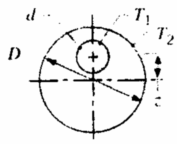	$D > d$ $L \gg D$	$\frac{2\pi L}{\cosh^{-1}\left(\frac{D^2 + d^2 - 4z^2}{2Dd}\right)}$
Case 8. Conduction through the edge of adjoining walls	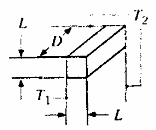	$D > L/5$	0.54 D
Case 9. Conduction through corner of three walls with a temperature difference ΔT_{1-2} across the walls	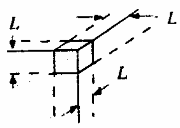	$L \ll$ length and width of wall	0.15 L
Case 10. Disk of diameter D and T_1 on a semi-infinite medium of thermal conductivity k and T_2	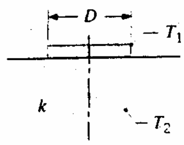	None	2 D

Example 5.1:
A hole of diameter D = 0.25 m is drilled through the centre of a solid block of square cross section with w = 1 m on a side. The hole is drilled along the length l = 2 m of the block, which has a thermal conductivity of k = 150 W/m K. A warm fluid passing through the hole maintains an inner surface temperature of T_1 75 °C, while the outer surface of the block is kept at T_2 = 25 °C.
1. Using the flux plot method, determine the shape factor for the system.
2. What is the rate of heat transfer through the block?

Solution:

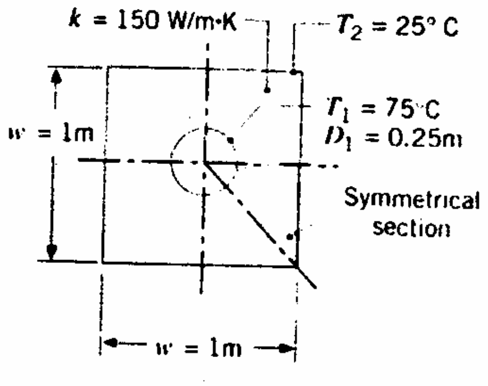

Assumptions:
1. Steady-state Conditions.
2. Two-dimensional conduction.
3. Constant properties.
4. Ends of block are well insulated.

Analysis:
1. The flux plot may be simplified by identifying lines of symmetry and reducing the system to the one-eighth section shown in the schematic. Using a fairly coarse grid involving N = 6 temperature increments, the flux plot was generated. The resulting network of curvilinear squares is as follows.

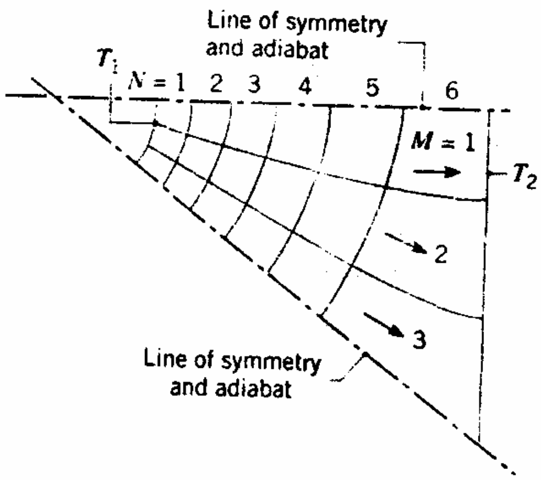

With the number of heat flow lanes for the section corresponding to
M = 3, it follows that the shape factor for the entire block is
S = 8× (M × l / N) = 8 × (3 × 2 / 6) = 8 m

Where the factor of 8 results from the number of symmetrical sections.

The accuracy of this result may be determined by referring to Table 5.1, where, for the prescribed system, it follows that

$$S = \frac{2\pi L}{\ln(1.08w/D)} = \frac{2\pi \times 2}{\ln(1.08 \times 1/0.25)} = 8.59 \text{ m}$$

Hence the result of the flux plot under predicts the shape factor by approximately 7%. Note that, although the requirement l >> w is not satisfied.

2. Using S = 8.59 m with Equation 5.24, the heat rate is

$q = S\,k\,(T_1 - T_2)$

$q = 8.59$ m × 150 W/m K (75 – 25) °C = 64.4 kW.

5.1.3 The Numerical Method

An alternative to the analytical and the graphical method is the numerical method, the numerical method involve different techniques such as finite difference, finite element and boundary –element method.

As stated in section 5.1.1 that the analytical solution gives the dependent variable T as a continuous function in the independent variables x and y. in contrast to the analytical solution the numerical solution converts the field or the system to discrete points at which the temperature is obtained. The domain is divided to small regions, referring to each region with a point at its centre as a reference point this point is termed nodal point or node, the network formed from these points is called nodal network, grid or mesh. Figure 5.4 presents a discritised domain along with the proper nomenclature.

The space or the difference between nodes is Δx in x direction and Δy in y direction, These nodes are numbered in both x and y direction and vary from 1 to m and n respectively and then conservation equation is applied to each point.

Using Taylor expansion the first and second derivatives are approximated to algebraic equations then we get number of simultaneous equations equal to number of nodes then this system of linear equations is solved either by a direct or indirect method to obtain the temperature value at each point.

Here are the algebraic equations expressing the derivatives in the conservation equation that is applied to each point.

$$\frac{\partial^2 T}{\partial x^2} = \frac{T_{m-1,n} - 2T_{m,n} + T_{m+1,n}}{(\Delta x)^2} \tag{5.27}$$

Similarly the derivative in the y direction is expressed as

$$\frac{\partial^2 T}{\partial y^2} = \frac{T_{m,n+1} - 2T_{m,n} + T_{m,n-1}}{(\Delta y)^2} \tag{5.28}$$

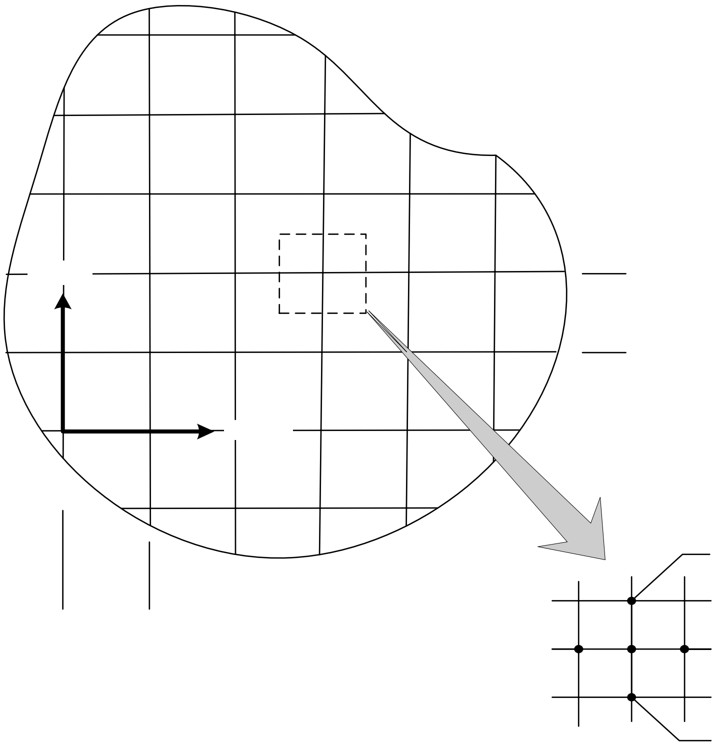

Figure 5.4 Discritised domains for a two-dimensional conduction problem

Substituting from Equations 5.27 and 5.28 into Equation 5.1 gives the discretised heat equation as

$$T_{m,n+1} + T_{m,n-1} + T_{m+1,n} + T_{m-1,n} - 4T_{m,n} = 0 \qquad (5.29)$$

Now Equation 5.29 can be applied at each grid point so that a set of n × m simultaneous equations is formed. This set of equations can be solved either directly by matrix inversion method or indirectly by iterative procedures. Special care must be taken for boundary nodes, for this energy conservation should be applied.

5.2 Three-Dimensional and Steady-State Conduction

The problem of three-dimensional, steady-state conduction is a very tricky one. The most widely approach for such problems is the numerical approach. For this a discretised equation is developed and similar solution procedure as described in section 5.1.3 is performed to get temperature values at nodal points inside the domain.

6. Transient Conduction

In this lecture we will deal with the conduction heat transfer problem as a time dependent problem in order to investigate the heat transfer behavior with time. Similarly as in the steady state conduction our aim is to obtain the temperature distribution and heat rate through our field of study and this could be obtained using the same procedure followed for the steady state conditions, we have to solve the appropriate form of heat equation and also for simplicity we may use some approach for simpler cases as we are going to discuss.

6.1 The Lumped Capacitance Method

The approach of the lumped capacitance method is based on the assumption that the temperature gradient across the media is small. For example, consider a spoon at initial temperature T_i then it is suddenly immersed in a cup of hot tea at temperature T_∞ which is higher than T_i, if the spoon immersion starts at time t = 0 the temperature of the solid will increase as t > 0 until at some time it reaches T_∞, this increase in temperature is due to convection heat transfer at the solid – liquid (spoon – Tea) interface. The lumped capacitance method is based on the assumption that the temperature is spatially uniform at any instant during the transient process so that the temperature gradient maybe considered negligible.

$$k \equiv -\frac{q''_x}{(\partial T / \partial x)} \tag{6.1}$$

The above form of Fourier's law implies that the thermal conductivity is infinite at approximately zero temperature gradient.

After the pervious assumption it is no longer possible to consider the problem from the framework of the heat equation, therefore to obtain the transient temperature response we should apply the overall energy balance on the solid (spoon) and this balance connect the heat gained by the increase in internal energy. Through the equation

$$\dot{E}_{in} = \dot{E}_{st} \tag{6.2}$$

The energy flowing into the solid (spoon) is due to convection as we mentioned before and it is expressed as

$$q_{conv} = hA_s(T - T_\infty) \tag{6.3}$$

$$E_{st} = \rho Vc\frac{dT}{dt} \tag{6.4}$$

Then by equating the last two equations we get

$$hA_s(T - T_\infty) = \rho Vc\frac{dT}{dt} \tag{6.5}$$

Introducing the temperature difference θ

$$\theta = T_\infty - T$$

Differentiating the above equation we get that dT/dt = - dθ/dt, Substituting in Equation 6.5 and rearranging the equation we obtain

$$\theta = \frac{\rho Vc}{hA_s}\frac{d\theta}{dt} \tag{6.6}$$

By separation of variables and integration from the initial condition at t = 0 and T (0) = T_i, we get

$$\frac{\rho Vc}{hA_s}\int_{\theta_i}^{\theta}\frac{d\theta}{\theta} = \int_0^t dt \tag{6.7}$$

$$\therefore \frac{\rho Vc}{hA_s}\ln\frac{\theta}{\theta_i} = t \tag{6.8}$$

Where $\theta_i = T_\infty - T_i$

The fraction θ/θ_i can be obtained by rearranging Equation 6.8 such as

$$\frac{\theta}{\theta_i} = \frac{T_\infty - T}{T_\infty - T_i} = \exp\left[\left(\frac{hA_s}{\rho Vc}\right)t\right] \tag{6.9}$$

Equation 6.9 could be easily used to determine the temperature T reached after a given time t or the time t needed to reach a certain temperature T. The coefficient of t inside the exponential function may be regarded as a thermal time constant. Hence, the thermal time constant can be defined as

$$\tau_t = \left(\frac{1}{hA_s}\right)(\rho Vc) = R_t C_t \tag{6.10}$$

Where R_t is the convection resistance to heat transfer and C_t is the lumped thermal capacitance of the solid. This new term is an indication to the material response to the change in thermal environment. As this constant increases the response time of the material to thermal changes decreases. An analogy between these types of heat conduction problem can be made. This analogy is shown in Figure 6.1 below.

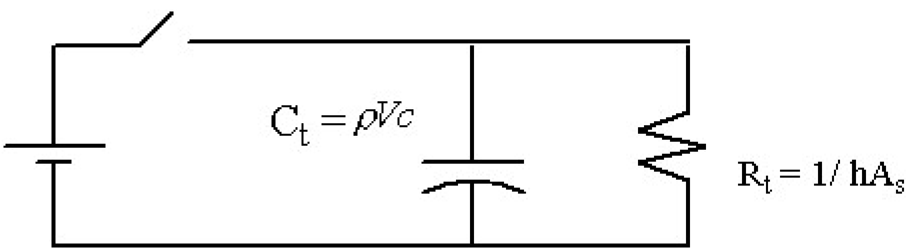

Figure 6.1 Analogous Electric circuit to a transient heat conduction problem

The amount of heat transferred from time t = 0 till a certain time t can be calculated by integrating the convection heat transferred from time t = 0 till a certain time t. this is simply shown in Equation 6.11 as

$$Q = \int_0^t q\,dt = hA\int_0^t \theta\,dt \qquad (6.11)$$

Substituting for θ from Equation 6.9 and performing the integrating Equation 6.11 yields

$$Q = (\rho Vc)\theta_i\left[1 - \exp\left(\frac{t}{\tau_t}\right)\right] \qquad (6.12)$$

The amount of heat transferred Q is that taken or gained by the internal energy. So that Q is positive when the solid is heated and there is a gain in the internal energy and Q is negative when the solid is cooled and there is a decrease in the internal energy.

6.2 Validity of the Lumped Capacitance Method

Lumped capacitance method is very desirable due to its simplicity and convenience. However, it is important to determine under what conditions it should be used in order to yield reasonable accuracy.

To develop a suitable criterion consider a steady state conduction through the plane wall of area A, as seen in Figure 6.2, where one surface is maintained at temperature $T_{s,1}$ and the other is exposed to a fluid of temperature T_∞ where $T_{s,1} > T_\infty$. The surface temperature, $T_{s,2}$, has a value between $T_{s,1}$ and T_∞ is called, thus under steady state conditions the surface energy balance will be

$$\frac{kA}{L}\left(T_{s,1} - T_{s,2}\right) = hA(T_{s,2} - T_\infty) \qquad (6.13)$$

Rearranging the Equation 6.13 we get

$$\frac{T_{s,1} - T_{s,2}}{T_{s,2} - T_\infty} = \frac{(L/kA)}{(1/hA)} = \frac{R_{cond}}{R_{conv}} = \frac{hL}{k} \equiv Bi \qquad (6.14)$$

The quantity (hL/k) appearing in Equation 6.14 is a dimensionless parameter called Biot number. This number plays a fundamental role in conduction problems involving surface convection effects. If Biot number is less than unity, then the conduction resistance within the solid is much less than the convection resistance across the boundary layer. Thus the assumption of a uniform temperature distribution is reasonable. Hence, the lumped capacitance method could only be used if:

$$Bi = \frac{hL_c}{k} < 0.1 \qquad (6.15)$$

Where L_c is the characteristic length of the solid shape and for more complicated shapes it can be defined as $L_c \equiv V/A_s$ for simplicity and the characteristic length L_c is reduced to L for a plane wall of thickness 2L and to $r_o/2$ for a long cylinder and $r_o/3$ for a sphere.

When substituting with the characteristics length $L_c \equiv V/A_s$ in the exponent of Equation 6.9 we get the following simplification

$$\frac{hA_s t}{\rho Vc} = \frac{h\,t}{\rho c\,L_c} = \frac{hL_c}{k}\frac{k}{\rho c}\frac{t}{L_c^2} = \frac{hL_c}{k}\frac{\alpha t}{L_c^2} \qquad (6.16)$$

Or

$$\frac{hA_s t}{\rho Vc} = Bi \cdot Fo \qquad (6.17)$$

Where a new parameter, called Fourier number, is introduced which is a dimensionless time

$$Fo \equiv \frac{\alpha t}{L_c^2} \qquad (6.18)$$

Substituting from Equation 6.17 into Equation 6.9 we get

$$\frac{\theta}{\theta_i} = \frac{T - T_\infty}{T_i - T_\infty} = \exp(-Bi \cdot Fo) \qquad (6.19)$$

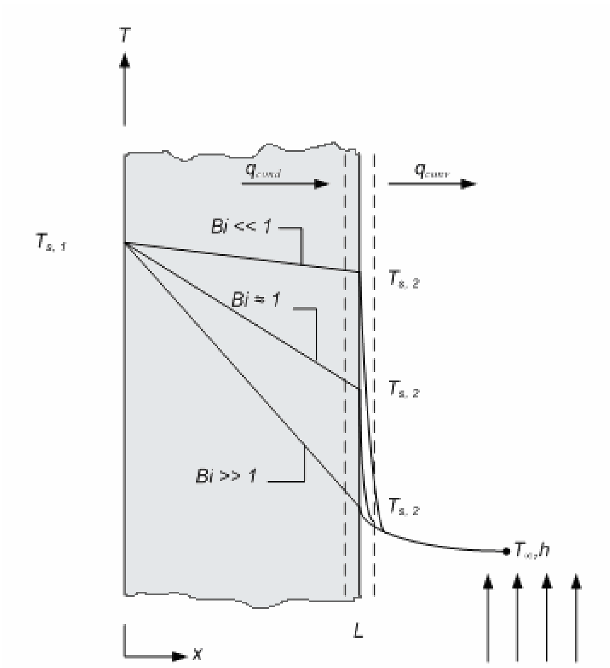

Figure 6.2 Biot number effect on steady state temperature distribution

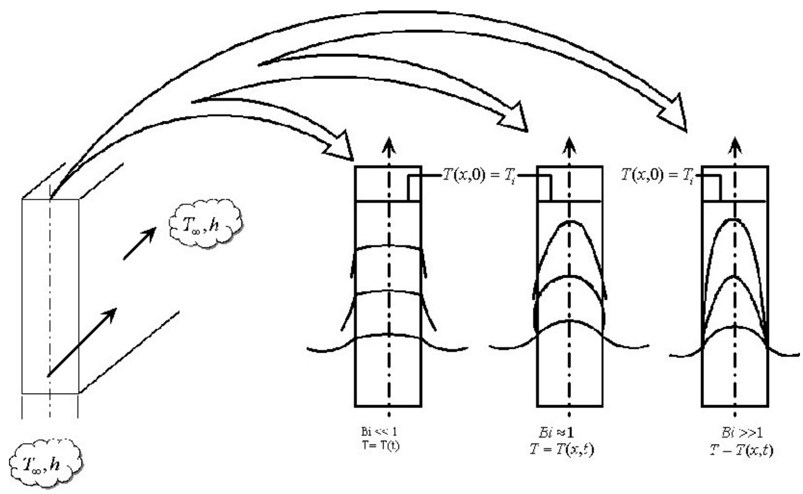

Figure 6.3 Transient temperature distribution for different Bi numbers in a plane symmetrically cooled from the two sides by convection

Exercise 6.1: A thermocouple junction, who may be approximated as a sphere, is to be used for temperature measurement of cooling air stream for electronic box. The convection coefficient between the junction and the air is known to be h = 400 W / m^2 K. The junction thermophysical properties are:

k = 20 W / m · K
c = 400 J / kg · K
ρ = 8500 kg / m^3

Determine the junction diameter needed for the thermocouple to have a time constant of 1 s.
If the junction is at 25 ºC and is placed in air at 15 ºC, how long would it take for the junction to reach 16 ºC?

6.3 Spatial Effect

The transient conduction problem in its general form is described by the heat equation either in Cartesian, cylindrical or spherical coordinates. Many problems such as plane wall needs only one spatial coordinate to describe the temperature distribution, with no internal generation and constant thermal conductivity the general heat equation has the following form

$$\frac{\partial^2 T}{\partial x^2} = \frac{1}{\alpha}\frac{\partial T}{\partial t} \qquad (6.20)$$

Equation 6.20 is a second order in displacement and first order in time; therefore we need an initial condition and two boundary conditions in order to solve it. Following are some graphical solutions for simple cases.

6.3.1 Large Plate of Finite Thickness Exposed to Convection

In this case the initial condition is:

$$T(x,0) = T_i$$

And the boundary conditions are

$$\left.\frac{\partial T}{\partial x}\right|_{x=0} = 0$$

And

$$-k\left.\frac{\partial T}{\partial x}\right|_{x=L} = h[T(L,t) - T_\infty]$$

Dimensional analysis is a very useful method when the problem involves many variables as it reduces the variables being involved into groups and provides mathematical relations between them

For this reason, two dimensional groups are used in the graphical solution of the one dimensional transient conduction, the two groups are the dimensionless temperature difference $\theta^* = \theta / \theta_i$ and the dimensionless time Fourier number $t^* = Fo = \alpha\, t / L_c^2$ and the dimensionless displacement $x^* = x / L$. Solutions are represented in graphical forms that illustrate the functional dependence of the transient temperature distribution on the Biot and Fourier numbers.

Figure 6.4 may be used to obtain the midplane temperature of the wall, T (0, t) ≡ T_a (t), at any time during the transient process.

If T_o is known for particular values of Fo and Bi, Figure 6.5 may be used to determine the corresponding temperature at any location off the midplane. Hence Figure 6.5 must be used in conjunction with Figure 6.4. For example, if one wishes to determine the surface temperature ($x^* = \pm 1$) at some time t, Figure 6.4 would first be used to determine T_o at t. Figure 6.5 would then be used to determine the surface temperature from the knowledge of T_o. The procedure would be rolled back if the problem involves determining the time required for the surface to reach a prescribed temperature.

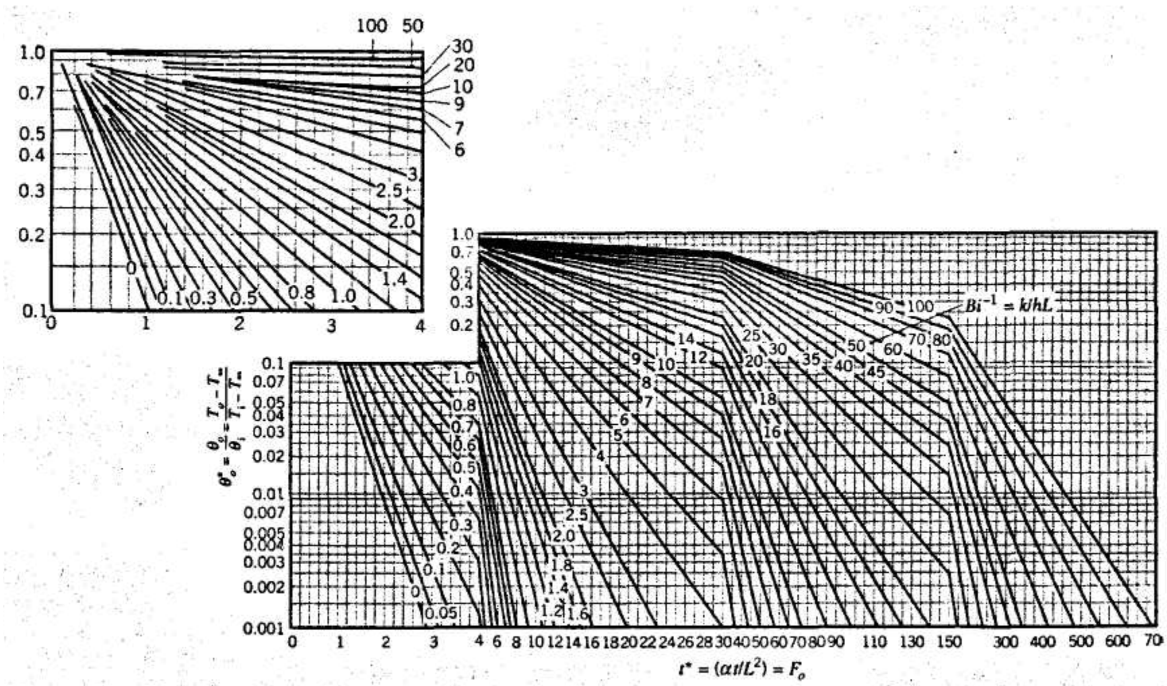

Figure 6.4 Midplane temperature as a function of time for a plane wall of thickness 2L

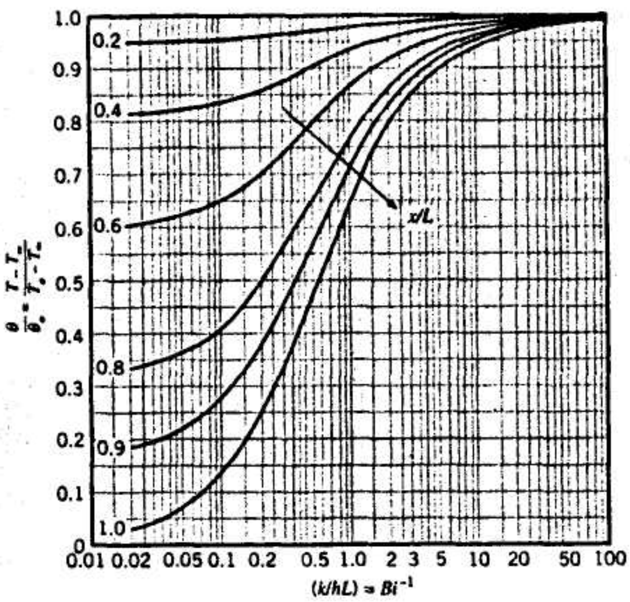

Figure 6.5 Temperature distribution in a plane wall of thickness 2L

Graphical results for the energy transferred from a plane wall over the time interval t are presented in Figure 6.6. The dimensionless energy transfer Q/Q_o is expressed exclusively in terms of Fo and Bi.

The foregoing charts may also be used to determine the transient response of a plane wall, an infinite cylinder, or a sphere subjected to a sudden change in surface temperature. For such a condition it is only necessary to replace T_∞ by the prescribed surface temperature T_s, and to set Bi^{-1} equal to zero. In so doing, the convection coefficient is tacitly assumed to be infinite, in which case $T_\infty = T_s$.

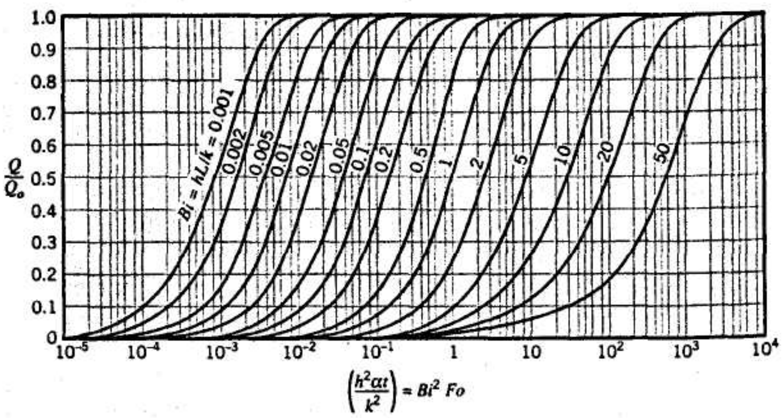

Figure 6.6 Internal energy change as a function of time for plane wall of thickness 2L

Similarly for the infinite cylinder the results are presented in Figures 6.6 to 6.8 only the L_c is replaced by r_o then $Bi^{-1} = k / h\, r_o$.

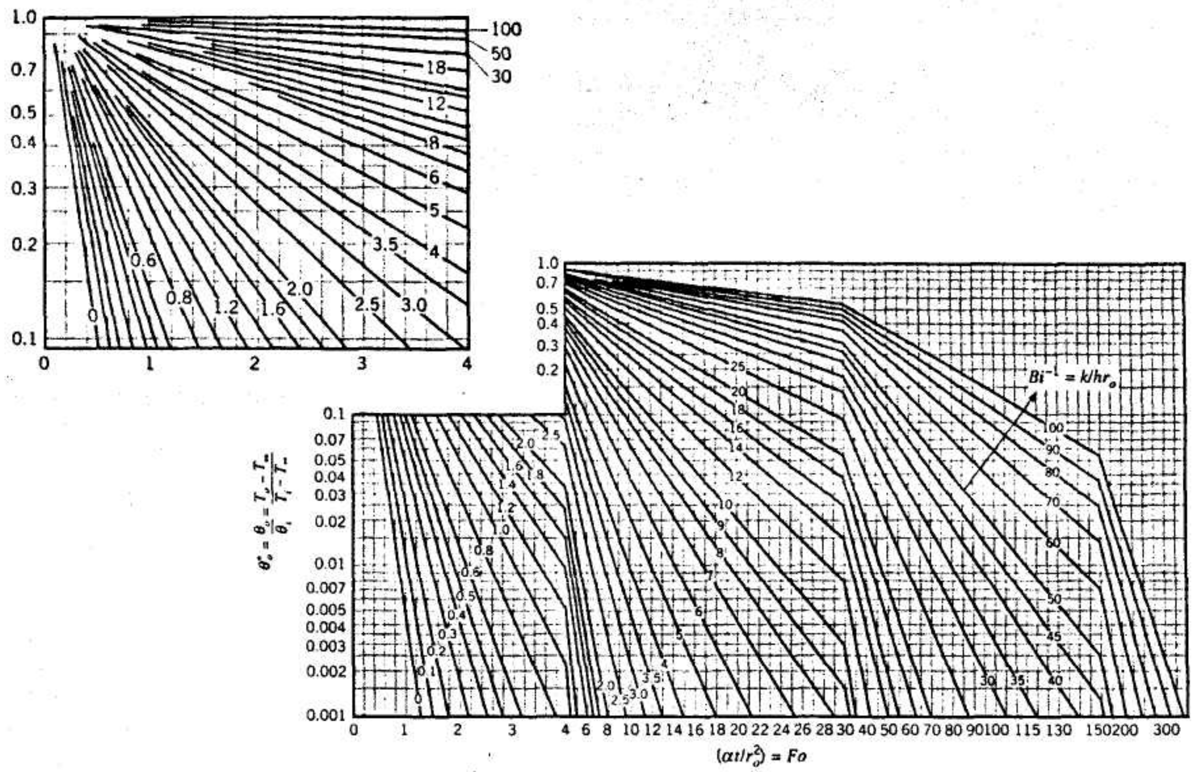

Figure 6.6 Centerline temperature as a function of time for an infinite cylinder of radius r_o

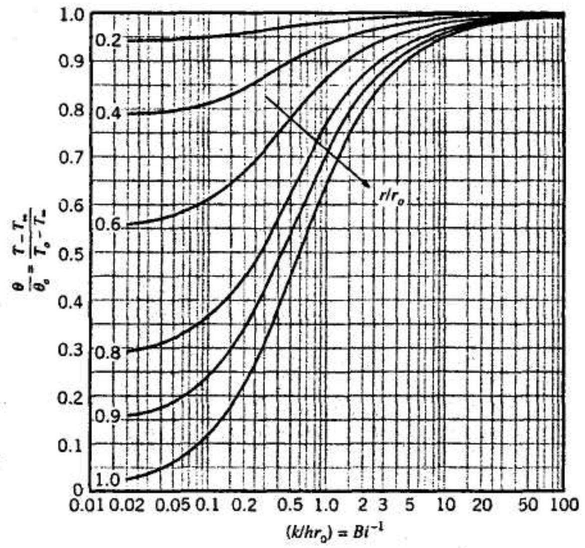

Figure 6.7 Temperature distribution in an infinite cylinder of radius r_o

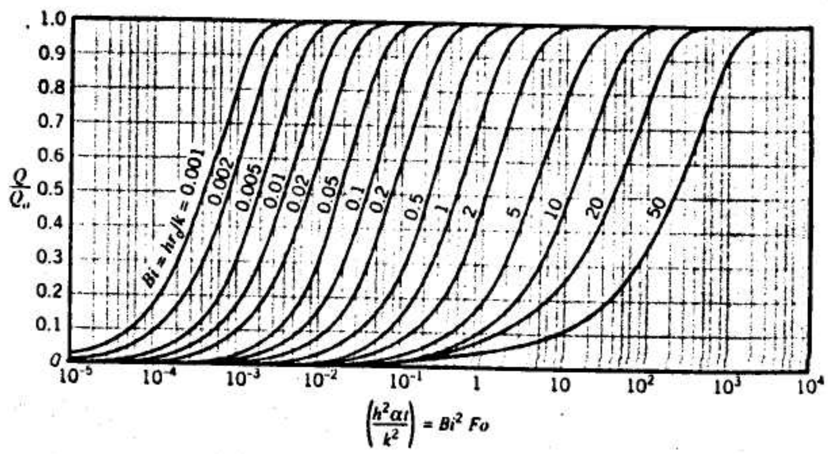

Figure 6.8 Internal energy change as a function of time for an infinite cylinder of radius r_o

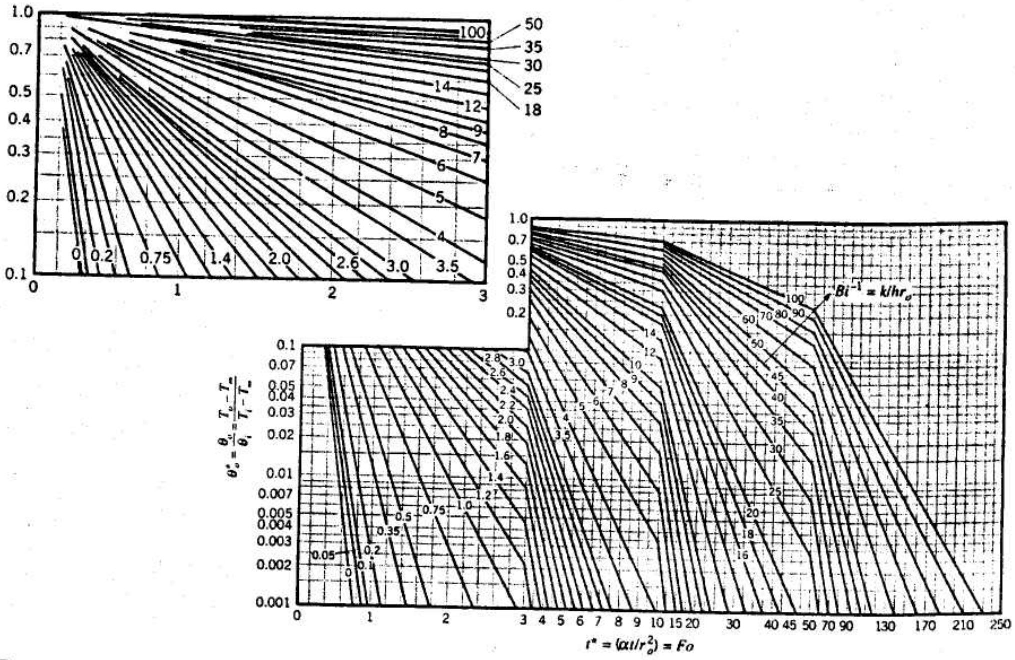

Figure 6.9 Center temperature as a function of time sphere of radius r_o

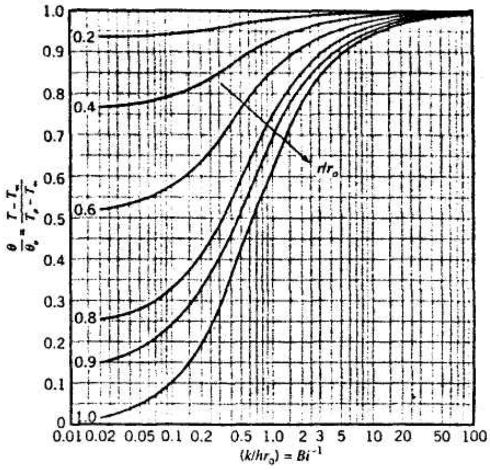

Figure 6.10 Temperature distribution in a sphere of radius r_o

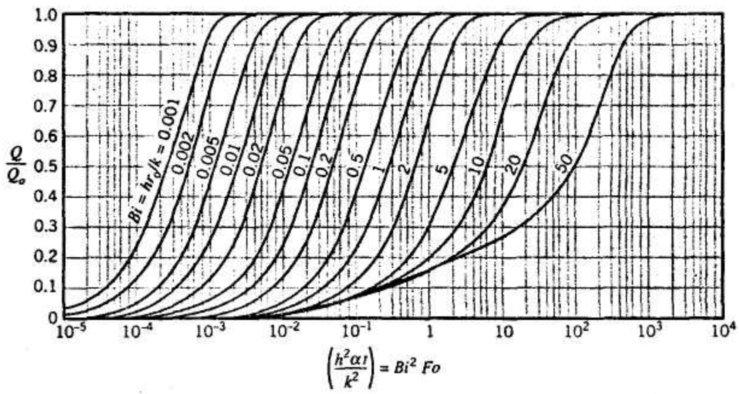

Figure 6.11 Internal energy change as a function of time for a sphere of radius r_o

6.4 Semi-Infinite Solids

Another simple geometry for which analytical solutions may be obtained is the semi-infinite solids it is characterized by a single defined surface since it extends to infinity in all directions except one. If a sudden change is imposed to this surface transient one dimensional conduction will occur within the solid.

Equation 6.20 still applies as a heat equation. Under the same assumptions which is one dimensional with no heat generation heat transfer.

The initial condition is

$$T(x,0) = T_i$$

While the interior boundary condition is

$$T(x \to \infty, t) = T_i$$

for the above initial and interior boundary conditions three closed form solutions have been obtained for the surface conditions, which are applied suddenly to the surface at t = 0. These conditions include application of constant surface temperature, constant heat flux and exposure of a surface to a fluid characterized by $T_\infty \neq T_i$ and the convection coefficient h, as shown in Figure 6.12.

For each case, an analytical solution can be obtained as:

Case (1) Constant surface temperature: $T(0,t) = T_i$

$$\frac{T(x,t) - T_i}{T_i - T_s} = erf\left(\frac{x}{2\sqrt{\alpha t}}\right) \tag{6.21}$$

$$q_s''(t) = \frac{k(T_s - T_i)}{\sqrt{\pi \alpha t}} \tag{6.22}$$

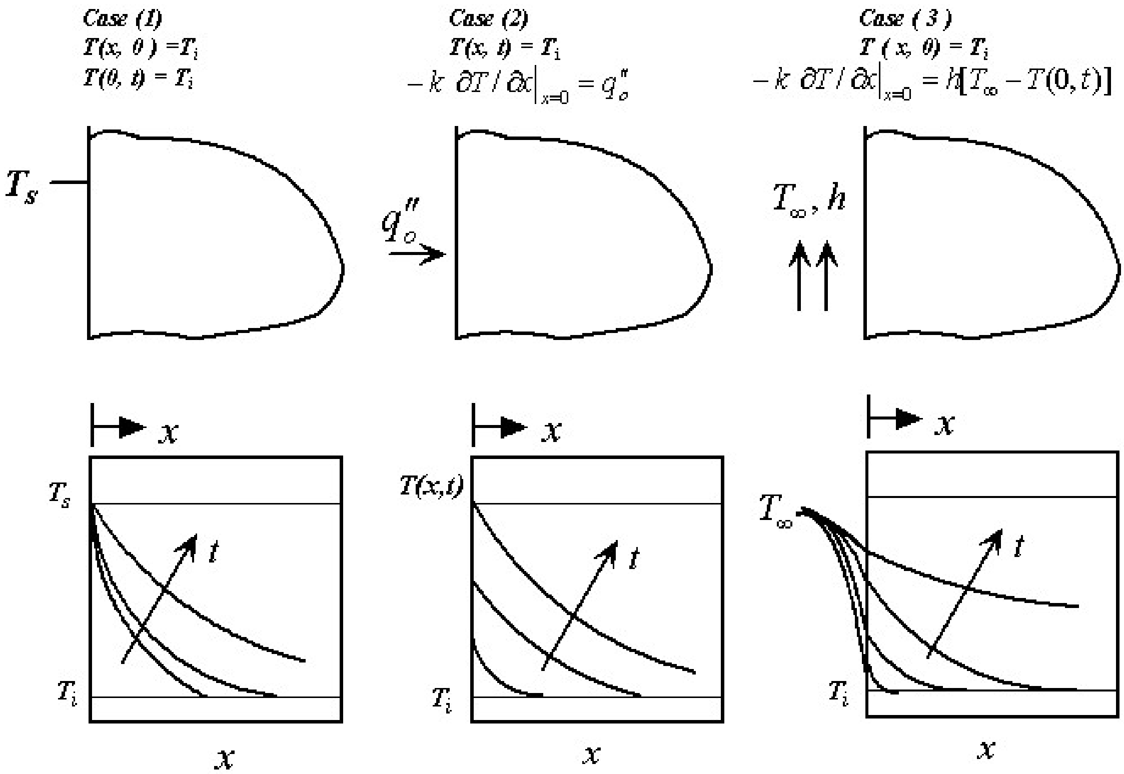

Figure 6.12 Transient Temperature distribution in a semi-infinite solid for three surface conditions: case (1) constant surface temperature, case (2) constant surface heat flux, and case (3) surface convection

Case (2) Constant surface heat flux: $q''_s = q''_o$

$$T(x,t) - Ti = \frac{2q''_o(\alpha t/\pi)^{1/2}}{k}\exp\left(\frac{-x^2}{4\alpha t}\right) - \frac{q''_o x}{k}\,erfc\left(\frac{x}{2\sqrt{\alpha t}}\right) \qquad (6.23)$$

Case (3) Surface convection: $-k\ \partial T/\partial x|_{x=0} = h[T_\infty - T(0,t)]$

$$\frac{T(x,t) - T_i}{T_\infty - T_i} = erfc\,(\frac{x}{2\sqrt{\alpha t}}) - \left[\exp\left(\frac{hx}{k} + \frac{h^2\alpha t}{k^2}\right)\right]\left[erfc\left(\frac{x}{2\sqrt{\alpha t}} + \frac{h\sqrt{\alpha t}}{k}\right)\right] \qquad (6.24)$$

Where the complementary error function erfc w is defined as erfc w = 1- erf w.

7. Natural Convection in Electronic Devices

7.1 Introduction

Natural or free convection occurs due to the change in density of the fluid caused by heating process. In a gravity field, the fluid, which has a lower density, is lighter and therefore rises, creating a movement in the fluid which is called convection. This movement permits the fluid to pick up heat and carry it away.

The natural convection is the common method used in electronics cooling; there is a large class of equipment that lends itself to natural convection .This category includes stand-alone packages such as modems and small computers having an array of printed circuit boards (PCB) mounted within an enclosure.

The general liquids coolant use in electronics cooling as in the case of air, and liquid cooled radar transmitter and test equipment fluorinert liquid (FC-77).

The general equation to define the convective heat transfer either forced or free is given by the Newton's law of cooling:

$$q = hA(T_s - T_\infty) \tag{7.1}$$

The convection heat transfer coefficient (h) is expressed by the dimensionless Nusselt number (Nu) which is related to the dimensionless ratios Grashof (Gr) and Prandtl (Pr) numbers or the Rayleigh number (Ra) which is the product of the last two dimensionless groups.

$$Nu = Nu(\mathrm{Gr}, \mathrm{Pr}) = \frac{hL}{k} \tag{7.2}$$

Where:

$$\text{L = characteristic length (m)} = \frac{\text{Surface are area (A)}}{\text{perimeter of the surface (P)}}$$

k = Thermal conductivity of the fluid (W/m.^{o}C)

And

$$\mathrm{Gr} = \frac{g\beta(T_S - T_\infty)L^3}{\nu^2} \tag{7.3}$$

Where:
g = Gravitational acceleration = 9.81 m/s^2
β = Volume coefficient of expansion =1/T (for ideal gas), T is the absolute temperature
L = Characteristic length (m)
ν = Kinematics viscosity (m^2/s)
and

$$\mathrm{Pr} = \frac{\mu C}{k} \tag{7.4}$$

Where:
μ = Dynamic viscosity (kg/m.s)
C = Specific heat (J/kg.^{o}C)

k =Thermal conductivity of the fluid (W/m.°C)

7.2 Empirical Correlations for Free Convection

All the average free-convection heat-transfer coefficients for external flow can be summarized in the following expression

$$\overline{Nu} = \frac{\bar{h}L}{k} = c(\mathrm{Gr\,Pr})^m \qquad (7.5)$$
$$= c(Ra)^m$$

The constants c, m are given in Table 7.1 for the uniform surface temperature case .The fluid properties are evaluated at mean film temperature (T_f) where $T_f = (T_s + T_\infty)/2$.

Table 7.1 Constants for Equation 7.5 for isothermal surfaces

Geometry	Ra	c	m
Vertical planes and cylinders	10^{-1}-10^4	use Figure 7.4	use Figure 7.4
	10^4-10^9	0.59	0.25
	10^9-10^{13}	0.1	1/3
Horizontal cylinder	0-10^{-5}	0.4	0
	10^{-5}-10^4	use Figure 7.5	use Figure 7.5
	10^4-10^9	0.53	0.25
	10^9-10^{12}	0.13	1/3
	10^{-10}-10^{-2}	0.675	0.058
	10^{-2}-10^2	1.02	0.148
	10^2-10^4	0.85	0.188
	10^4-10^7	0.48	0.25
	10^7-10^{12}	0.125	1/3
Upper surface of heated plates or lower surface of cooled plates	2×10^4-8×10^6	0.54	0.25
Upper surface of heated plates or lower surface of cooled plates	8×10^6-8×10^{11}	0.15	1/3
Lower surface of heated plates or upper surface of cooled plates	10^5-10^{11}	0.27	0.25
Vertical cylinder, height = diameter Characteristic length = diameter	10^4-10^6	0.775	0.21
Irregular solids Characteristic length = distance Of fluid particle travels in boundary layer	10^4-10^9	0.52	0.25

The characteristic length for different geometries is:

- vertical plate L = height
- Horizontal plate L = W/2 ,W = width
- Spheres L = D
- Horizontal tube L = D
- Vertical tube

If:

$$\frac{D}{L} \geq \frac{35}{\sqrt[4]{Gr_L}} \qquad \therefore L = \text{length (L)}$$

If not;

$$\therefore \ L = D$$

7.2.1 Free Convection over Vertical Plates and Cylinders

Natural heat transfer from a vertical plate is shown in Figure 7.1.

At Uniform Surface Temperature (T_S = constant)
For wide ranges of the Rayleigh number we can use the correlations given by Churchill and Chu

$$\overline{Nu}_L = 0.825 + \frac{0.387 Ra_L^{1/6}}{\left[1 + \left(0.492/\Pr\right)^{9/16}\right]^{8/27}} \qquad \text{For } 10^{-1} < Ra_L < 10^{2} \qquad (7.6)$$

This equation has better accuracy for laminar flow and the subscript L indicates the characteristic length based on plate height.

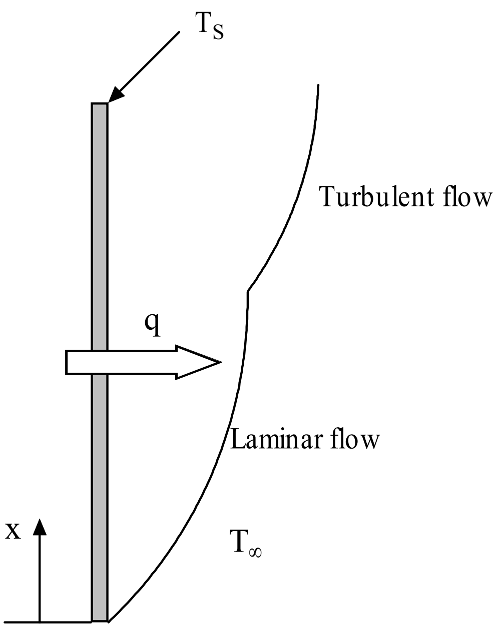

Figure 7.1 Flow over vertical plate

$$\overline{Nu}_L = 0.68 + \frac{0.67 Ra^{1/4}}{\left[1 + \left(0.492/\Pr\right)^{9/16}\right]^{4/9}} \qquad \text{For } Ra_L < 10^{9} \qquad (7.7)$$

Fluid properties for both Equation 7.6 and 7.7 are evaluated at mean film temperature.

For Uniform Surface Heat Flux ($q^{//}$ = constant)

If the plate surface has a constant heat flux; the Grashof number is modified as Gr^* based on x-direction as following:

$$\mathrm{Gr}_x^* = \mathrm{Gr}_x Nu_x = \frac{g\beta q^{//} x^4}{k\nu^2} \tag{7.8}$$

The local heat transfer coefficients given as follow

$$Nu_x = \frac{hx}{k} = 0.6(\mathrm{Gr}_x^* \, \mathrm{Pr})^{1/5} \qquad 10^5 < \mathrm{Gr}_x^* < 10^{11} \tag{7.9}$$

$$Nu_x = \frac{hx}{k} = 0.17(\mathrm{Gr}_x^* \, \mathrm{Pr})^{1/4} \qquad 2\mathrm{X}10^{13} < \mathrm{Gr}_x^* \, \mathrm{Pr} < 10^{16} \tag{7.10}$$

Fluid properties for both Equations 7.9 and 7.10 are evaluated at local film temperature.

To get the average heat transfer coefficient for the constant heat flux integration along the plate height is performed.

$$\bar{h} = \frac{1}{L}\int_0^x h_x \, dx$$

Applying this integration to Equation 7.9 we get the average heat transfer coefficient in the form

$$\bar{h} = \frac{5}{4} h_{x=L}$$

7.2.2 Free Convection from Horizontal Cylinder

For flow over a horizontal cylinder with uniform surface temperature for wide ranges of Ra the following expressions are given by Churchill and Chu

$$\overline{Nu}_D^{1/2} = 0.6 + 0.387\left(\frac{\mathrm{Gr}\,\mathrm{Pr}}{\left[1 + (0.559/\mathrm{Pr})^{9/16}\right]^{16/9}}\right)^{1/6} \qquad 10^{-5} < \mathrm{Gr}\,\mathrm{Pr} < 10^{12} \tag{7.11}$$

Again fluid properties for Equation 7.11 are evaluated at mean film temperature.

For horizontal cylinder with liquid metals following equation may be applied.

$$Nu_D = 0.53\left(Gr\,\mathrm{Pr}^2\right)^{1/4} \tag{7.12}$$

7.2.3 Free Convection over Horizontal Plates

For Uniform Surface Temperature (T_S = constant)

We have many cases for horizontal plates with constant surface temperature as shown in Figure 7.2

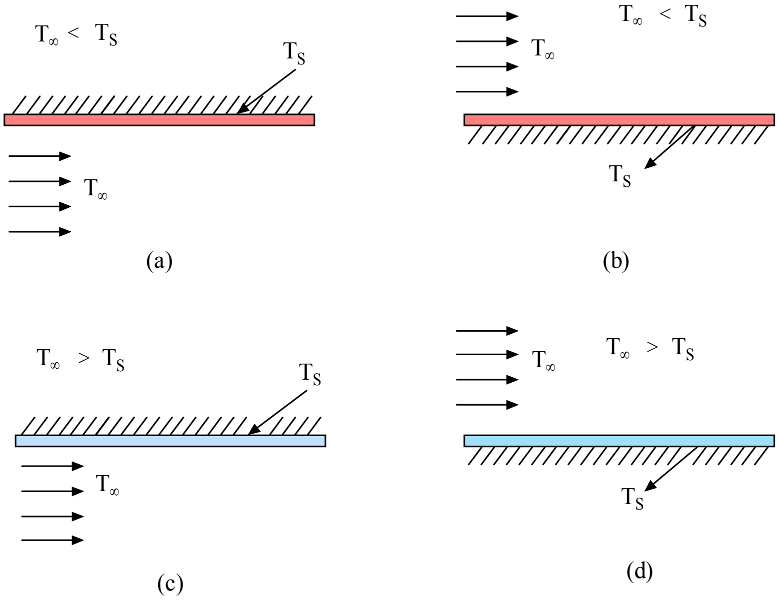

Figure7.2 (a) Lower surface of heated plates, (b) Upper surface of heated plates

(c) Lower surface of cooled plates, (d) Upper surface of cooled plates

For lower surface of heated plates or upper surface of cooled plates

$$\overline{Nu}_L = 0.27(\mathrm{Gr}_L\ \mathrm{Pr})^{1/4} \qquad 10^5 \le \mathrm{Gr}_L\ \mathrm{Pr} \le 10^{11} \qquad (7.13)$$

For upper surface of heated plates or Lower surface of cooled plates the average heat transfer coefficient is expressed by:

$$\overline{Nu}_L = 0.54(\mathrm{Gr}_L\ \mathrm{Pr})^{1/4} \qquad 2x10^4 \le \mathrm{Gr}_L\ \mathrm{Pr} \le 8x10^6 \qquad (7.14)$$

$$\overline{Nu}_L = 0.15(\mathrm{Gr}_L\ \mathrm{Pr})^{1/3} \qquad 8x10^6 \le \mathrm{Gr}_L\ \mathrm{Pr} \le 10^{11} \qquad (7.18)$$

Where fluid properties are evaluated at mean film temperature $T_f = (T_s + T_\infty)/2$

For Uniform Surface Heat Flux ($q^{//}$ = constant)

For hot surface facing upward (Upper surface of heated plate)

$$\overline{Nu}_L = 0.13(\mathrm{Gr}_L\ \mathrm{Pr})^{1/3} \qquad \mathrm{Gr}_L\ \mathrm{Pr} < 2x10^8 \qquad (7.19)$$

$$\overline{Nu}_L = 0.16(\mathrm{Gr}_L\ \mathrm{Pr})^{1/3} \qquad 2x10^8 < \mathrm{Gr}_L\ \mathrm{Pr} < 10^{11} \qquad (7.20)$$

For hot surface facing downward (Lower surface of heated plates)

$$\overline{Nu}_L = 0.58(\mathrm{Gr}_L\ \mathrm{Pr})^{1/3} \qquad 10^6 < \mathrm{Gr}_L\ \mathrm{Pr} < 10^{11} \qquad (7.21)$$

For the Equations 7.19, 7.20, and 7.21 the fluid properties are evaluated at the equivalent temperature (T_e) which is defined as

$$T_e = T_s - 0.25\ (T_s - T_\infty)$$

Where:

T_s= the average surface temperature

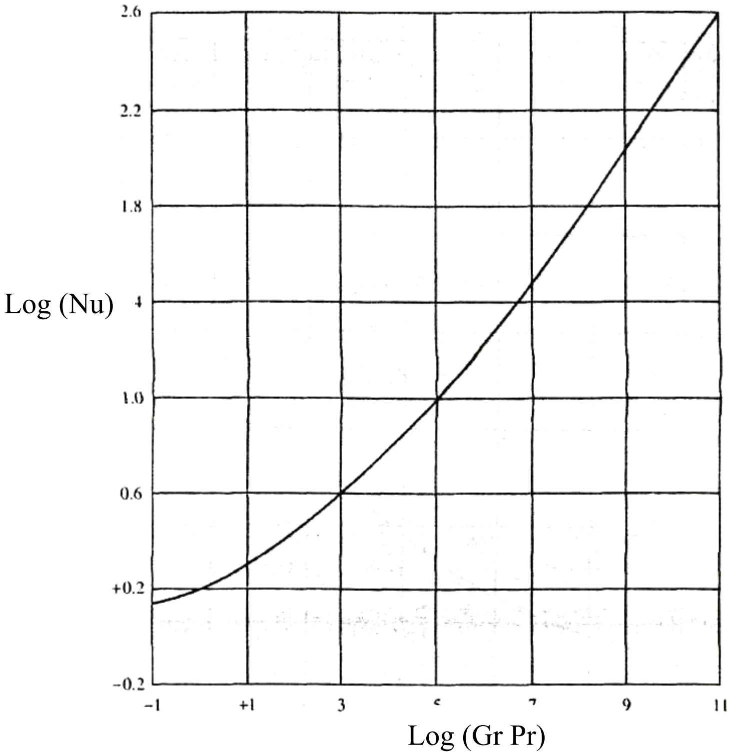

Figure 7.4 Heat transfer correlation for vertical planes and cylinders at (Ra = 10^{-1} - 10^{4})

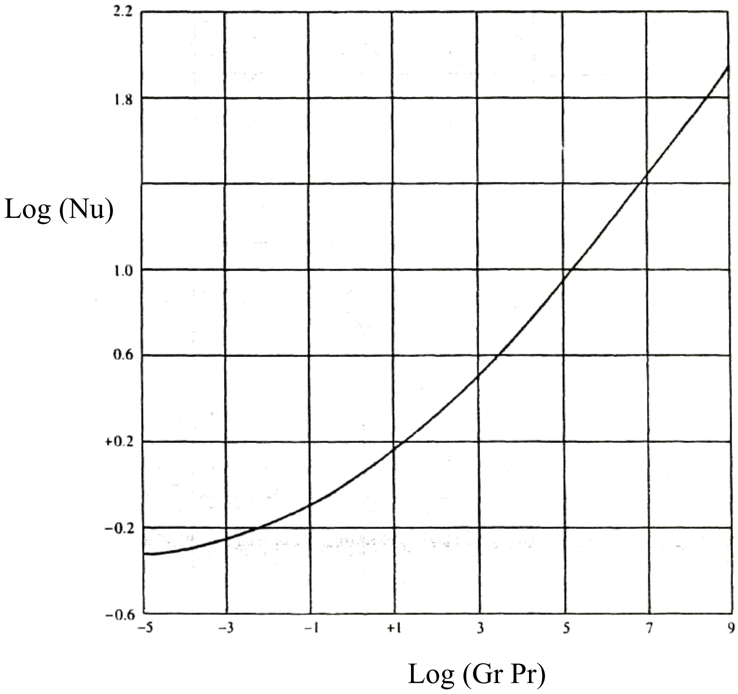

Figure 7.5 Heat transfer correlation for horizontal cylinder (Ra = 10^{-5} -10^{4})

7.2.4 Free Convection over Irregular Surfaces

For irregular surfaces the average heat transfer coefficient is given by Lienhard formula

$$\overline{Nu} = 0.52(Gr\,\mathrm{Pr})^{0.25} \tag{7.22}$$

Where fluid properties are evaluated at mean film temperature $T_f = (T_s + T_\infty)/2$. The characteristic length is the distance of a fluid particle travels in the boundary layer, for example, see figure 7.3, the characteristic length (L) = H+ (w/2)

.

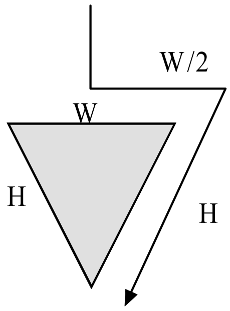

Figure 7.3 Travel distance of a particle along an irregular surface

7.2.5 Free Convection over Spheres

When the flow occurs on sphere the recommended correlation is provided by Churchill for $Ra_D<10^{11}$ and Pr >0.5

$$\overline{Nu}_D = 2 + \frac{0.589(Gr_D\,\mathrm{Pr})^{1/4}}{[1+(0.469/\mathrm{Pr})^{9/16}]^{4/9}} \tag{7.23}$$

Where fluid properties are evaluated at mean film temperature $T_f = (T_s + T_\infty)/2$

Example7.1: Air flow across an electronic box used in a spacecraft that is 0.2 m high and 0.3 m wide to maintain the outer box surface at 45 ^{o}C. If the box is not insulated and exposed to air at 25 ^{o}C, Calculate is the heat loss from the duct per unit length.

Schematic:

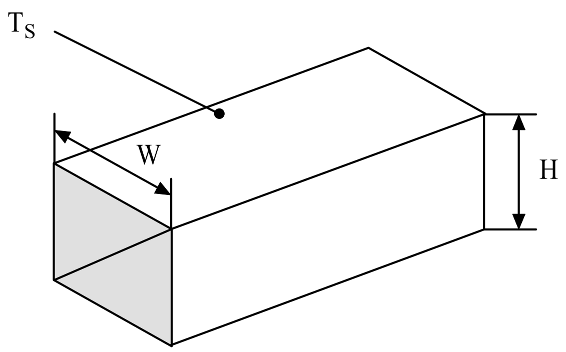

Solution:

The properties of air evaluated at mean film temperature:

$$T_f = (45+25)/2 = 35\,^oC$$

Air properties are:

$\nu = 16.7x10^{-6}\ m^2/s.$
$k = 0.0269 W/m.\,^oC$
$Pr = 0.706$
$\beta = 1/308 = 3.247\ x10^{-3}\ K^{-1}$

For the two vertical sides:
The characteristic length is the height H = 0.2 m.
The Gr Pr product is:

$$Gr\,Pr = \frac{9.81x3.247x10^{-3}x20(0.2)^3}{(16.7x10^{-6})^2} 0.706 = 12.9x10^6$$

By using the Equation 7.7

$$\overline{Nu}_S = 0.68 + \frac{0.67(12.9x10^6)^{1/4}}{\left[1+(0.492/0.706)^{9/16}\right]^{4/9}} = 31.47$$

The average heat transfer coefficient is

$$\bar{h}_S = \frac{\overline{Nu}_S k}{L} = \frac{31.47x0.0269}{0.2} = 4.234\ W/m^2.^oC$$

For the top surface (Upper surface of heated plates):
The characteristic length is half the width W/2 = 0.15 m.
The Gr Pr product is:

$$Gr\,Pr = \frac{9.81x3.247x10^{-3}x20(0.15)^3}{(16.7x10^{-6})^2} 0.706 = 5.443x10^6$$

By using the Equation 7.18: upper surface of heated plate case

$$\overline{Nu}_t = 0.15(5.443x10^6)^{1/3} = 26.38$$

The average heat transfer coefficient is

$$\bar{h}_t = \frac{\overline{Nu}_t k}{L} = \frac{26.38x0.0269}{0.15} = 4.732\ W/m^2.^oC$$

For the bottom (Lower surface of heated plates): The characteristic length half the width W/2 = 0.15 m, same Gr Pr product

By using the Equation 7.13 lower surface of heated plate case

$$\overline{Nu}_b = 0.27(5.443x10^6)^{1/4} = 13.04$$

The average heat transfer coefficient is

$$\bar{h}_b = \frac{\overline{Nu}_b k}{L} = \frac{13.04x0.0269}{0.15} = 2.34\ W/m^2.^oC$$

The heat loss from the electronic box per unit length is

$$q' = (T_S - T_\infty)\,[2 \text{ x } \bar{h}_S \text{ x } H + \bar{h}_t \text{ x } w + \bar{h}_b \text{ x } w]$$

$$= (45 - 25)\,[2 \text{ x } 4.234 \text{ x } 0.2 + 4.732 \text{ x } 0.3 + 2.34 \text{ x } 0.3] = 76.3 \text{ W/m}$$

Example 7.2: A cube of 10cm side length is left to cool in air. It is considered as irregular surface. The cube surface is maintained at 60 °C and exposed to atmospheric air at 10 °C.
Calculate the heat transfer rate.

Schematic: to show the travel distance of a particle from the fluid along the surface

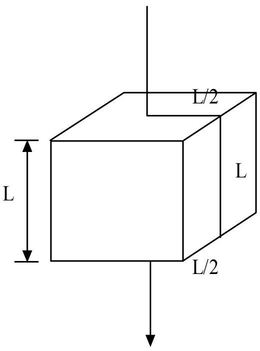

Solution:

The mean film temperature is:

$$T_f = (60+10)/2 = 35\,^oC$$

Thus air properties are

$\nu = 17.47 \times 10^{-6}$ m^2/s.
k = 0.0268W/m. °C
Pr= 0.7
$\beta = 1/308 = 3.247 \times 10^{-3}$ K^{-1}

From the schematic shown the characteristic length is

$$L = (L/2) + L + (L/2) = 2L = 20 \text{ cm}$$

The Gr Pr product is

$$Gr\,\Pr = \frac{9.81x3.247x10^{-3}x50(0.2)^3}{(17.47x10^{-6})^2}0.7 = 29.223x10^6$$

By using the Equation 7.22

$$\overline{Nu} = 0.52(29.223x10^6)^{0.25}$$
$$= 38.23$$

The average heat transfer coefficient is

$$\bar{h} = \frac{\overline{Nu}k}{L} = \frac{38.23x0.0268}{0.4} = 2.56 \text{ W/m}^2.^oC$$

The total heat transfer surface area is

$$A = 6x\ (0.1x0.1) = 0.06\ m^2$$

The total heat transfer is

$$q = 2.56 \times 0.06 \times 50 = 7.68\ W$$

7.3 Natural Convection from Finned Surfaces

The amount of heat that can be removed from an electronic component that is cooled by natural convection will be substantially increased if the surface area of the component can be substantially increased. One convenient method for increasing the surface area is to add fins as shown in Figure 7.6 with a low thermal resistance. The temperature of the fins will then be nearly equal to the surface temperature of the electronic component. The additional heat transfer to the atmosphere will be proportional to the increase in the surface area.

Fins will increase the size and weight of the electronic component. This may be a small penalty to pay if the cost is reduced and the reliability is increased by eliminating the need for a cooling fan.

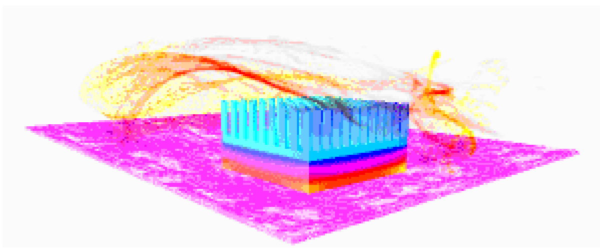

Figure 7.6 Fined surface over PCB to increase the heat transfer rate

The effectiveness of the finned surface will depend upon the temperature gradient along the fin as it extends from the surface of the electronic component. When the fin has a small temperature gradient, the temperature at the tip of the fin will be nearly equal to the temperature at the base of the fin or the chassis surface, and the fin will have a high efficiency.

Then the total heat transfer divided into two components due to the heat transferred from the free exposed surface of the electronic component and the heat transferred from fins surface as explained before is

$$\begin{aligned} q &= h\,[(A_{tot} - A_f) + \eta_f\, A_f]\,(t_s - t_\infty) \qquad (7.24) \\ &= \eta_o\, A_{tot}\, h\,(t_s - t_\infty) \end{aligned}$$

Where:

$A_{tot} - A_f$ = free exposed surface area of the electronic component

A_f = fins area

7.3.1 Natural Convection over PCBs

The natural convection cooling for PCBs are usually used when the heat loads are not too high. Where the PCBs are usually mounted within electronic chassis that are completely open at the top and bottom as shown in the Figure 7.7, and the minimum space between the components and the adjacent is 0.75 in to prevent chocking of the natural convection flow.

Where the air enters at the bottom to remove the heating load from the PCBs, The warmer air has a reduced density, so that it starts to rise to finally exit at the top of the chassis. We must be neglect the radiation effect because the PCBs see each other. The heat flow through the PCB more easily than it flow over the external boundary layer due to a very low conduction thermal resistance through the PCB, compared with the convection thermal resistance over the external boundary layer on one face of the PCB.

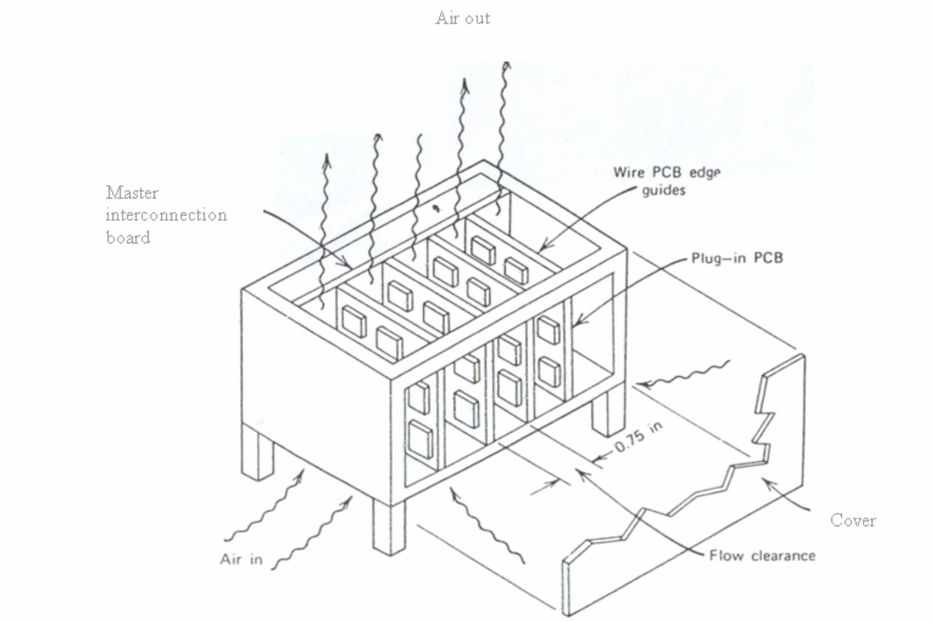

Figure 7.7 Example of natural convection heat transfer over PCBs

Example 7.3: a PCB inside electronic chassis in vertically position with 15 x 23 x 0.15 cm, the thermal conductivity for the PCB with ignoring lead wires is 2.25 W/m ^oC, and the convective heat transfer coefficient is 5 W/m^2 ^oC. Calculate the ratio between the convection thermal resistance to conduction thermal resistance.

Solution:
The convection thermal resistance is

$$R_{convection} = \frac{1}{hA} = \frac{1}{(5)(1.5 \, x \, 2.3)} = 0.058 \ ^oC/W$$

The conduction thermal resistance is

$$R_{condution} = \frac{L}{KA} = \frac{0.015}{(2.25)(1.5 \, x \, 2.3)} = 0.00193 \ ^oC/W$$

The resistances ratio is

$$\frac{R_{\text{convection}}}{R_{\text{conduction}}} = 30$$

Comment: This example shows the convection thermal resistance is 30 times of the conduction thermal resistance through the PCB. So that the heat flow through the PCB more easily than it flow over the external boundary layer.

7.4 Natural Convection inside Enclosure

The free-convection flow phenomenon inside an enclosed space is one of the interesting examples of very complex fluid systems that may yield to analytical, empirical, and numerical solutions. Consider the system shown in Figure 7.8, where a fluid is contained between two vertical plates separated by the distance δ. As a temperature difference $\Delta T = T_1 - T_2$ is impressed on the fluid, a heat transfer will be experienced with the approximate flow regions shown in Figure 7.9, according to MacGregor and Emery. In this figure, the Grashof number is calculated as

$$\mathrm{Gr}_{\delta} = \frac{g\,\beta\,\Delta T \delta^{3}}{v^{2}} \tag{7.25}$$

At very low Grashof number the heat transfer occurs mainly by conduction across the fluid layer. As the Grashof number is increased, different flow regimes are encountered, as shown, with a progressively increasing heat transfer as expressed through the Nusselt number

$$Nu_{\delta} = \frac{h\delta}{k} \tag{7.26}$$

The empirical correlations obtained were:

$$Nu_{\delta} = 0.42(\mathrm{Gr}_{\delta}\,\mathrm{Pr})^{1/4}\,\mathrm{Pr}^{0.012}\left(\frac{L}{\delta}\right)^{-0.3} \qquad q_W = cons\tan t \tag{7.27}$$

$$10^{4} < \mathrm{Gr\,Pr} < 10^{7}$$
$$1 < \mathrm{Pr} < 20000$$
$$10 < L/\delta < 40$$

$$Nu_{\delta} = 0.46(\mathrm{Gr}_{\delta}\,\mathrm{Pr})^{1/3} \qquad q_W = cons\tan t \tag{7.28}$$

$$10^{6} < \mathrm{Gr\,Pr} < 10^{9}$$
$$1 < \mathrm{Pr} < 20$$
$$1 < L/\delta < 40$$

The heat flux is calculated as

$$\frac{q}{A} = q_w^{//} = h\Delta T \tag{7.29}$$

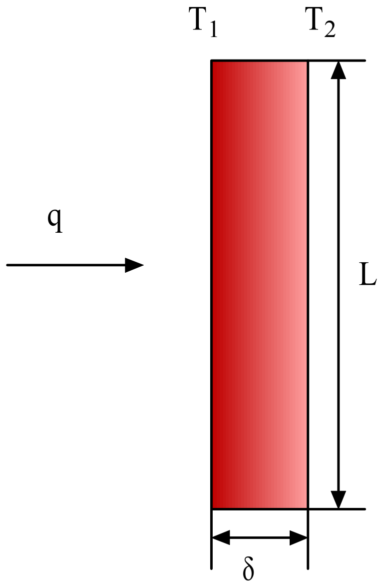

Figure 7.8 free convection inside vertical enclosure space

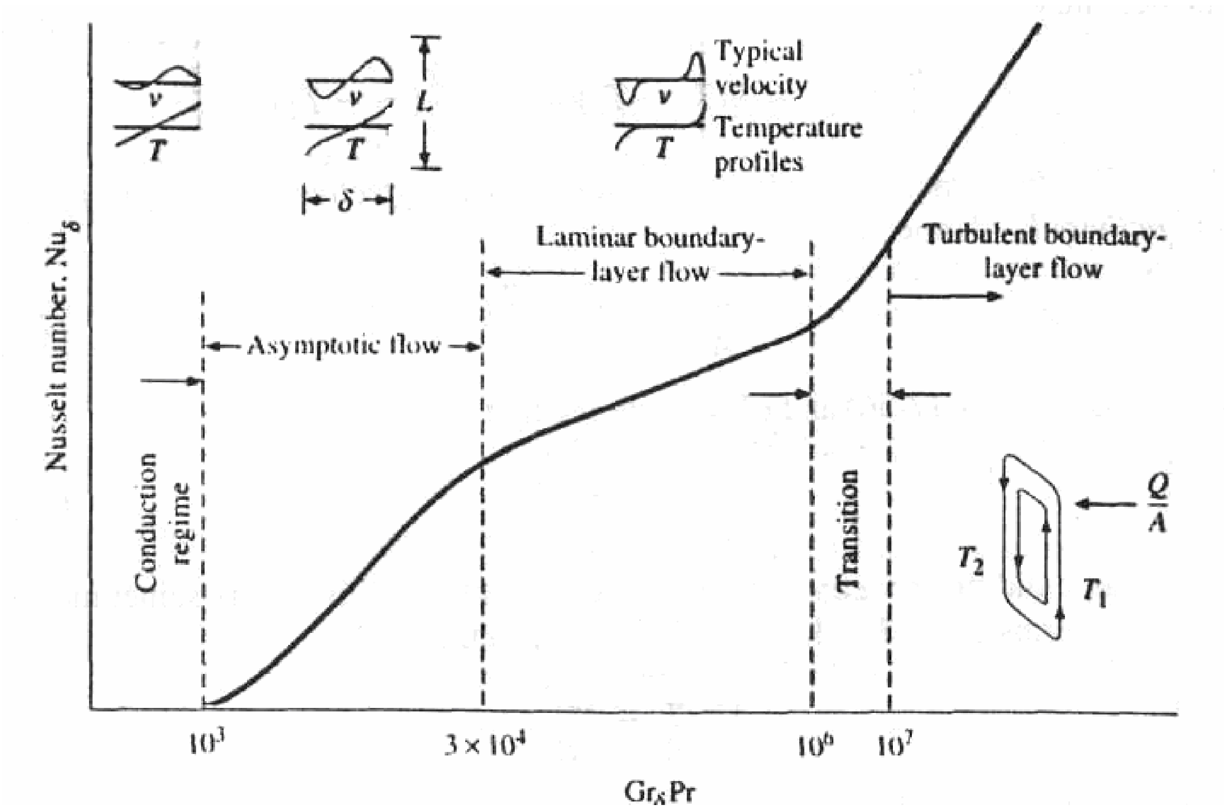

Figure 7.9 Flow regimes for the vertical convection layer inside enclosure

8. Forced Convection Heat Transfer

8.1 Introduction

The general definition for convection may be summarized to this definition "energy transfer between the surface and fluid due to temperature difference" and this energy transfer by either forced (external, internal flow) or natural convection.

Heat transfer by forced convection generally makes use of a fan, blower, or pump to provide high-velocity fluid (gas or liquid). The high-velocity fluid results in a decreased thermal resistance across the boundary layer from the fluid to the heated surface. This, in turn, increases the amount of heat that is carried away by the fluid

To understand the convection heat transfer we must know some of the simple relations in fluid dynamics and boundary layer analysis. Firstly we study boundary layer with forced convection flow systems.

8.2 Boundary Layer over Flat Plate

We consider the (x) direction along the wall with (y) direction normal to the wall as in Figure8.1. Where the laminar boundary layer begins at leading edge (x= 0), and followed by transition region and finally to the turbulent region to the trailing edge (x= L). The velocity and temperature of the fluid far away from the surface (out side the boundary layer thickness δ) are the free-stream velocity u_∞ and free-stream temperature T_∞.

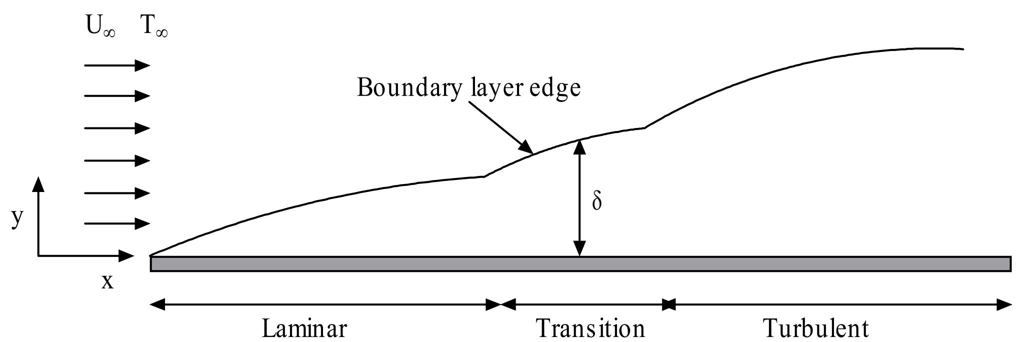

Figure 8.1 Fluid flow over flat plate with laminar, transition, and turbulent boundary layers

8.2.1 Laminar Boundary Layer Equations over Flat Plate ($Re_x \leq 5x10^5$)

The assumptions made to give the simplicity on the analysis are:

1- Steady flow
2- Two-dimensional incompressible viscous flow
3- No pressure variation in the y direction
4- No shear force in the y direction
5- Neglect body force due to gravity

All the basic differential equations can be derived by considering an element control volume inside the laminar region as shown in Figure 8.2.

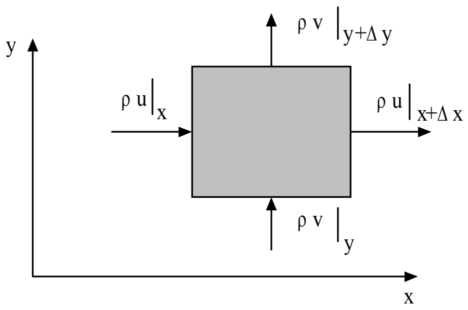

Figure 8.2 Element control volume on laminar region

Continuity equation:

{Rate of mass accumulation within control volume}+

{Net rate of mass flux out of control volume}= 0

Rate of mass accumulation within control volume = $\dfrac{\partial(\rho \Delta x \Delta y)}{\partial t} = 0$ (steady state assumption)

Net rate of mass flux in x- direction per unit depth = $(\rho u]_{x+\Delta x} - \rho u]_x)\Delta y = \dfrac{\partial(\rho u)}{\partial x}\Delta y \Delta x$

Net rate of mass flux in y- direction per unit depth = $(\rho v]_{y+\Delta y} - \rho v]_y)\Delta x = \dfrac{\partial(\rho \upsilon)}{\partial x}\Delta x \Delta y$

Substitute in continuity equation expression it produce:

$$\frac{\partial(\rho u)}{\partial x}\Delta x \Delta y + \frac{\partial(\rho \upsilon)}{\partial y}\Delta x \Delta y = 0$$

$$\frac{\partial(\rho u)}{\partial x} + \frac{\partial(\rho \upsilon)}{\partial y} = 0$$

$$\frac{\partial(u)}{\partial x} + \frac{\partial(\upsilon)}{\partial y} = 0 \qquad (8.1)$$

Momentum equation:

By applying Newton's 2nd low on the same element control volume as in Figure 8.2

Time rate of change of linear momentum within the control volume	+	Net rate of linear momentum flux out of the control volume	=	Net rate of linear momentum flux out of the control volume summation of external force acting in the control volume

... mom... ...ume =

Net rate of linear momentum out of the control unit

$$= (\rho uu]_{x+\Delta x} - \rho uu]_x)\Delta y + (\rho vu]_{y+\Delta y} - \rho vu]_y)\Delta x$$

$$= \frac{\partial(\rho uu)}{\partial x}\Delta x\Delta y + \frac{\partial(\rho \upsilon u)}{\partial y}\Delta x\Delta y$$

External forces divided into:

- Pressure force = $-\dfrac{\partial P}{\partial x}\Delta x\Delta y$
- Viscous force = $\mu\dfrac{\partial^2 u}{\partial y^2}\Delta x\Delta y$

Substituting in the Newton's 2nd low equation it yeilds

$$\frac{\partial(\rho uu)}{\partial x}\Delta x\Delta y + \frac{\partial(\rho \upsilon u)}{\partial y}\Delta x\Delta y = -\frac{\partial P}{\partial x}\Delta x\Delta y + \mu\frac{\partial^2 u}{\partial y^2}\Delta x\Delta y$$

Or,

$$u\frac{\partial(\rho u)}{\partial x} + \rho u\frac{\partial(u)}{\partial x} + u\frac{\partial(\rho \upsilon)}{\partial y} + \rho\upsilon\frac{\partial(u)}{\partial y} = -\frac{\partial P}{\partial x} + \mu\frac{\partial^2 u}{\partial y^2}$$

From continuity equation we have:

$$\frac{\partial(\rho u)}{\partial x} + \frac{\partial(\rho \upsilon)}{\partial y} = 0$$

Then the momentum equation for laminar boundary layer is

$$\rho u\frac{\partial(u)}{\partial x} + \rho\upsilon\frac{\partial(u)}{\partial y} = \mu\frac{\partial^2 u}{\partial y^2} - \frac{\partial P}{\partial x} \qquad (8.2)$$

Energy equation:

For the shown element control volume as in Figure 8.3.with neglected heat conduction in x-direction and applying energy balance, the energy equation may be written as follows:

Energy convected in left face + Energy convected in bottom face + heat conduction in bottom face + net viscous work done on element = energy convected out right face + energy convected out top face + heat conduction out top face

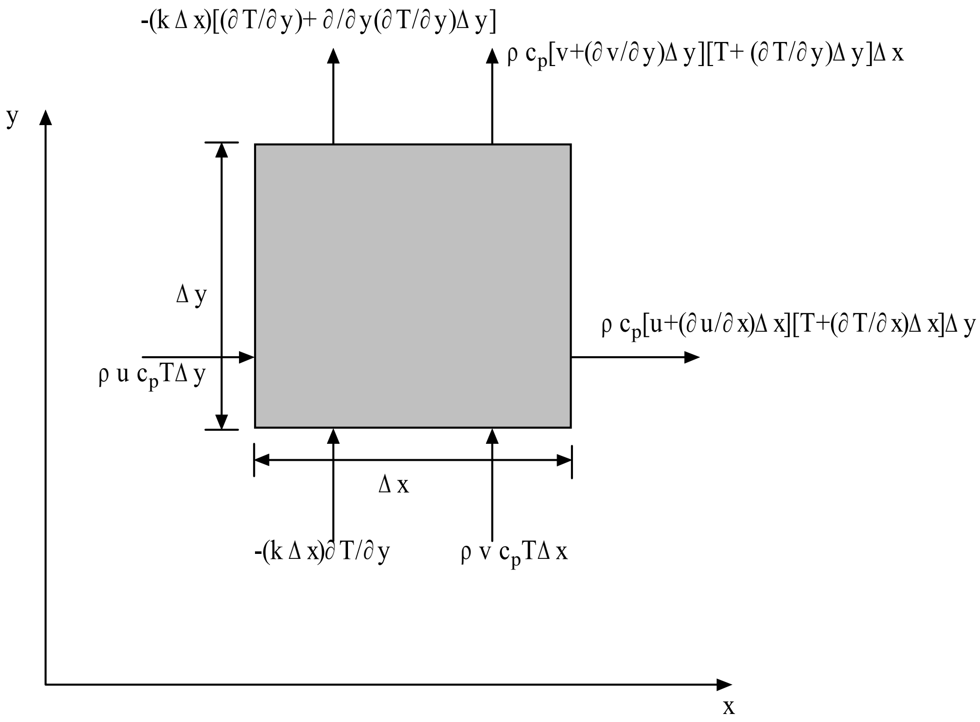

Figure 8.3 Element control volume for energy balance

The viscous shear force is the product of the shear stress and the area per unit depth Δx

$$\mu \frac{\partial u}{\partial y} \Delta x$$

And the distance through which it moves per unit time in respect to the element control volume Δx Δy is

$$\frac{\partial u}{\partial y} \Delta y$$

The net viscous energy delivered to the element control volume

$$\mu \left(\frac{\partial u}{\partial y} \right)^2 \Delta x \Delta y$$

By applying energy balance on the element control volume shown in Figure8.3 neglecting the second order differentials yields to

$$\rho c_p \left[u \frac{\partial T}{\partial x} + \upsilon \frac{\partial T}{\partial y} + T \left(\frac{\partial u}{\partial x} + \frac{\partial \upsilon}{\partial y} \right) \right] \Delta x \Delta y = k \frac{\partial^2 T}{\partial y^2} \Delta x \Delta y + \mu \left(\frac{\partial u}{\partial y} \right)^2 \Delta x \Delta y$$

From continuity Equation 8.1 the energy equation can be written as follow

$$\rho c_p\left[u\frac{\partial T}{\partial x}+\upsilon\frac{\partial T}{\partial y}\right]=k\frac{\partial^2 T}{\partial y^2}+\mu\left(\frac{\partial u}{\partial y}\right)^2$$

Dividing by ρC_p

$$u\frac{\partial T}{\partial x}+\upsilon\frac{\partial T}{\partial y}=\alpha\frac{\partial^2 T}{\partial y^2}+\frac{\mu}{\rho c_p}\left(\frac{\partial u}{\partial y}\right)^2 \tag{8.3}$$

The viscous work term is important only at high velocities since its magnitude will be small compared with other terms when low velocity flow is studied. This may be shown with an order-of-magnitude analysis of the two terms on the right side of energy equation. For this order-of-magnitude analysis we might consider the velocity as having order of the free stream velocity u_∞ and the y dimension of the order of velocity boundary layer thickness δ.

$u \approx u_\infty$ and $y \approx \delta$

So that

$$\alpha\frac{\partial^2 T}{\partial y^2} \approx \alpha\frac{T}{\delta^2} \tag{8.4}$$

And

$$\frac{\mu}{\rho c_p}\left(\frac{\partial u}{\partial y}\right)^2 \approx \frac{\mu}{\rho c_p}\frac{u_\infty^2}{\delta^2} \tag{8.5}$$

Now if the ratio between Equations 8.5 and 8.4 is

$$\frac{\mu}{\rho c_p \alpha}\frac{u_\infty^2}{T}=\Pr\frac{u_\infty^2}{c_p T}\langle\langle 1$$

Then we can neglect this term compared to other terms and we can write the energy equation in this simple form.

$$u\frac{\partial T}{\partial x}+\upsilon\frac{\partial T}{\partial y}=\alpha\frac{\partial^2 T}{\partial y^2} \tag{8.6}$$

The solution of these equations (continuity, momentum and energy) is simplified by the fact that, for conditions in the velocity (hydrodynamic) boundary layer fluid properties are independent of temperature.

We may begin by solving the Equations 8.1 and 8.2 (continuity, momentum) to get u and v. Then the energy equation can be solved which depending on calculated results.

The solution of Equations 8.1 and 8.2 can be solved by Blausis exact (analytic) solution for:

- $\frac{\partial P}{\partial x}=0$
- Laminar flow.

In Blausis exact solution, the velocity components are defined in terms of a stream function $\Psi(x,y)$ where

$$u = \frac{\partial \Psi}{\partial y} \qquad (8.7)$$

And

$$\upsilon = -\frac{\partial \Psi}{\partial x} \qquad (8.8)$$

So that the continuity equation may be intrinsically satisfied

Considering the partial differential equation describing the momentum equation (Equation 8.2), we may use the similarity method in order to convert it into an ordinary differential equation.

Defining the dependent and independent dimensionless variables f and η, will help us in this analytical approach.

$$f(\eta) = \frac{\Psi}{u_\infty \sqrt{vx/u_\infty}} \qquad (8.9)$$

$$\eta = y\sqrt{u_\infty / vx} \qquad (8.10)$$

The Blausis exact solution is termed a similarity solution, and η is the similarity variable.

This terminology is used because, despite growth of the boundary layer with distance x from the leading edge, the velocity profile u/u_∞, remains geometrically similar as shown in Figure 8.4.

$$\frac{u}{u_\infty} = fun.(\frac{y}{\delta})$$

Where δ is the boundary layer thickness and usually difficult to measure

Assuming this thickness to vary as $(\nu\, x / u_\infty)^{1/2}$, its follows that

$$\frac{u}{u_\infty} = fun.(\eta)$$

Hence the velocity profile is assumed to be uniquely determined by the similarity variable η which depends on x and y directions.

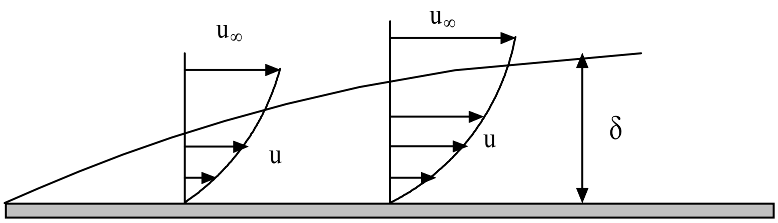

Figure 8.4 the profile u/u_∞ geometrically similar

From Equations 8.7 and 8.8

$$u = \frac{\partial \Psi}{\partial y} = \frac{\partial \Psi}{\partial \eta}\frac{\partial \eta}{\partial y} = u_\infty \sqrt{\frac{vx}{u_\infty}}\frac{df}{d\eta}\sqrt{\frac{u_\infty}{vx}} = u_\infty \frac{df}{d\eta} \qquad (8.11)$$

And

$$\upsilon = -\frac{\partial \Psi}{\partial x} = -(u_\infty \sqrt{\frac{\nu x}{u_\infty}} \frac{\partial f}{\partial x} + \frac{u_\infty}{2} \sqrt{\frac{\nu}{u_\infty x}} f)$$

$$\upsilon = \frac{1}{2}\sqrt{\frac{\nu u_\infty}{x}}\left(\eta \frac{df}{d\eta} - f\right) \tag{8.12}$$

By differentiating the velocity components, it may also be shown that

$$\frac{\partial u}{\partial x} = -\frac{u_\infty}{2x}\eta \frac{d^2 f}{d\eta^2} \tag{8.13}$$

$$\frac{\partial u}{\partial y} = u_\infty \sqrt{\frac{u_\infty}{\nu x}} \frac{d^2 f}{d\eta^2} \tag{8.14}$$

$$\frac{\partial^2 u}{\partial y^2} = \frac{u_\infty^2}{\nu x} \frac{d^3 f}{d\eta^3} \tag{8.15}$$

Substituting these equations in the momentum equation, then we obtain

$$2\frac{d^3 f}{d\eta^3} + f\frac{d^2 f}{d\eta^2} = 0 \tag{8.16}$$

This is non linear, third-order differential equation, so that we need three boundary conditions to get a solution, these boundary conditions are:

At $\eta = 0$

$$f'(\eta) = f(\eta) = 0$$

At $\eta = \infty$

$$f'(\eta) = u/u_\infty = 1$$

The solution of Equation 8.16 by numerical integration and the results are given in Table 8.1.

At $u/u_\infty = 0.99$ for $\eta = 5$, substitute in Equation 8.10

$$\frac{\delta}{x} = \frac{5}{\sqrt{\mathrm{Re}_x}} \tag{8.17}$$

The shear stress can be expressed as

$$\tau_s = \left(\mu \frac{\partial u}{\partial y}\right)_{y=0} = \left(\mu u_\infty \sqrt{\frac{u_\infty}{\nu x}} \frac{d^2 f}{d\eta^2}\right)_{\eta=0}$$

From the Table 8.1

$$\tau_s = 0.332 u_\infty \sqrt{\frac{\rho \mu u_\infty}{x}}$$

And the wall local shear stress coefficient C_f,is given by

$$C_f = \frac{\tau_s}{\frac{1}{2}\rho u_\infty^2} = \frac{0.664}{\sqrt{\mathrm{Re}_x}} \tag{8.18}$$

Table 8.1: The function *f* (η) for laminar boundary layer over flat plate

$\eta = y\sqrt{\frac{u_\infty}{\nu x}}$	$f(\eta)$	$\frac{df}{d\eta} = \frac{u}{u_\infty}$	$\frac{d^2 f}{d\eta^2}$
0	0	0	0.332
0.4	0.027	0.133	0.331
0.8	0.106	0.265	0.327
1.2	0.238	0.394	0.317
1.6	0.42	0.517	0.297
2	0.65	0.63	0.267
2.4	0.922	0.729	0.228
2.8	1.231	0.812	0.184
3.2	1.569	0.876	0.139
3.6	1.93	0.923	0.098
4	2.306	0.956	0.064
4.4	2.692	0.976	0.039
4.8	3.085	0.988	0.022
5.2	3.482	0.994	0.011
5.6	3.88	0.997	0.005
6	4.28	0.999	0.002
6.4	4.679	1	0.001
6.8	5.079	1	0

Example 8.1: Consider fluid flow at u_∞=0.3 m/s past a flat plate 0.3 m long. Compute the boundary layer thickness at the trailing edge for (a) air and (b) water at 20 °C.

Solution:

Part (a)

From air properties table at 20 °C

ν =15.267x10^{-6} m^2/s.

The trailing edge Reynolds number is

$$\mathrm{Re}_L = \frac{u_\infty L}{\nu} = \frac{(0.3)(0.3)}{15.267\mathrm{x}10^{-6}} = 5895$$

The flow is laminar, from Equation 8.17 the predicted laminar thickness is

$$\frac{\delta}{x} = \frac{5}{\sqrt{5895}} = 0.065$$

At x = 0.3 m

$$\delta = 0.0195 \text{ m}$$

Part (b)

From saturated water properties table at 20°C:

$\nu_{water} = 1.0437\text{x}10^{-6}\ \text{m}^2/\text{s}$.

The trailing edge Reynolds number is

$$\text{Re}_L = \frac{u_\infty L}{\nu} = \frac{(0.3)(0.3)}{1.0437\text{X}10^{-6}} = 86231.67$$

This again satisfies the laminar condition the laminar thickness is

$$\frac{\delta}{x} = \frac{5}{\sqrt{86231.67}} = 0.017$$

At x = 0.3 m

$$\delta = 0.0051\ \text{m}$$

Solving the energy equation (Equation 8.6):

Let the dimensionless temperature $T^* = \dfrac{T - T_s}{T_\infty - T_s}$ and assume similarity solution of the form $T^* = T^*(\eta)$, and substitute in energy equation to give this form.

$$\frac{d^2T^*}{d\eta^2} + \frac{\text{Pr}}{2} f \frac{dT^*}{d\eta} = 0 \qquad (8.19)$$

Where the variable f depend on the Prandtl number values

The appropriate boundary conditions are

$T^*(0) = 0$ And $T^*(\infty) = 1$

The solution may be achieved by numerical integration method for $0.6 \le \text{Pr} < 50$

It will produce the surface temperature gradient $\left(\dfrac{dT^*}{d\eta}\right)_{\eta=0}$ as the following relation.

$$\left(\frac{dT^*}{d\eta}\right)_{\eta=0} = 0.332\ \text{Pr}^{1/3}$$

If $T_s > T_\infty$

Expression for the local heat convection coefficient determined as follow.

$$q_x^{//} = h_x(T_s - T_\infty) = -k\frac{\partial T}{\partial y}$$

$$h_x = \frac{-k}{(T_s - T_\infty)}\frac{\partial T}{\partial y} = -k\frac{T_\infty - T_s}{T_s - T_\infty}\left(\frac{\partial T^*}{\partial y}\right)_{y=0}$$

$$h_x = k\left(\frac{u_\infty}{\nu x}\right)^{1/2}\left(\frac{\partial T^*}{\partial \eta}\right)_{\eta=0}$$

It follows that the local Nusselt number in this form

$$Nu_x = \frac{h_x x}{k} = 0.332\,\mathrm{Re}_x^{1/2}\,\mathrm{Pr}^{1/3} \tag{8.20}$$

And the average heat transfer coefficient can be obtained by integration $\therefore \overline{h_x} = 2h_x$

$$\overline{h_x} = \frac{1}{x}\int_0^x h_x \tag{8.21}$$

$$\overline{Nu_x} = \frac{\overline{h_x}\,x}{k} = 0.664\,\mathrm{Re}_x^{1/2}\,\mathrm{Re}^{1/3}$$

8.3 The Thermal Boundary Layer

Analogous to the velocity boundary layer there is a thermal boundary layer adjacent to a heated (or cooled) plate. The temperature of the fluid changes from the surface temperature at the surface to the free-stream temperature at the edge of the thermal boundary layer as shown in Figure 8.5.

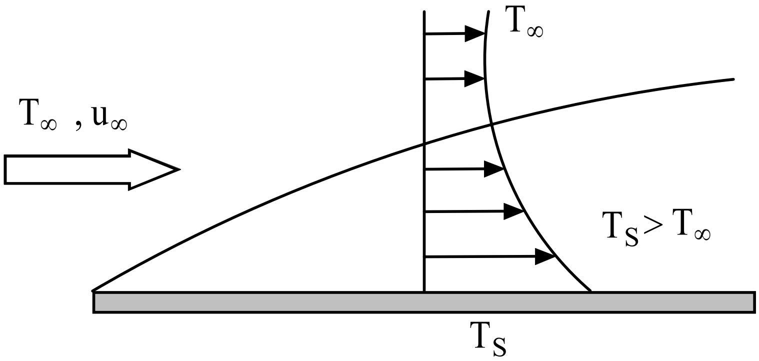

Figure 8.5.Fluid temperature variations inside the thermal boundary layer

The velocity boundary layer thickness depends on the Reynolds number Re_X. But the thermal boundary layer thickness depends both on Re_X and Pr as shown in Figure8.6.

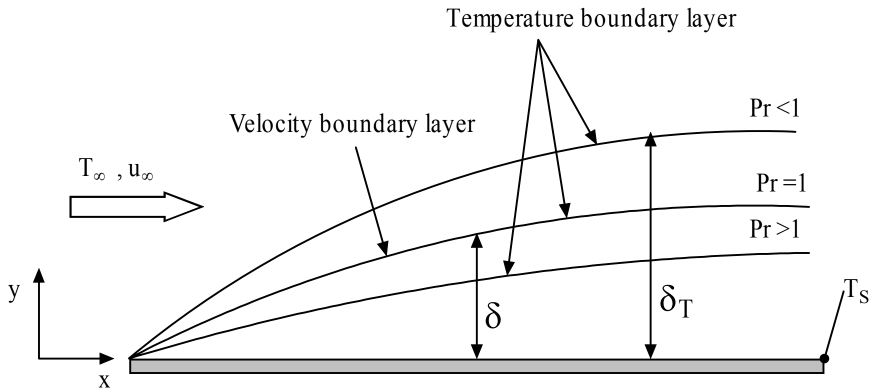

Figure 8.6 thermal boundary layer thicknesses relative to velocity boundary layer thickness at different Prandtle number

For laminar flow ($Re_x < Re_{cr}$):

$$\frac{\delta}{x} = \frac{5}{\sqrt{\mathrm{Re}_x}} \qquad \text{At Pr} \geq 0.7 \qquad \frac{\delta}{\delta_T} = \mathrm{Pr}^{1/3}$$

$$\text{At Pr} \ll 1 \qquad \frac{\delta}{\delta_T} = \mathrm{Pr}^{1/2} \tag{8.22}$$

For turbulent flow ($Re_x > Re_{cr}$):

$$\frac{\delta}{x} = \frac{0.37}{\mathrm{Re}_X^{0.2}} \qquad \delta \approx \delta_T \tag{8.23}$$

8.4 Cooling Air Fans for Electronic Equipment

Air is the most commonly used medium for heat transfer. It is available everywhere on the surface of the planet .Air is usually taken directly from the surrounding atmosphere and returned to it. Many different types of fans are available for cooling electronic equipment. These can generally be divided into two major types: axial and centrifugal fans. These fans can be driven by various types of electric motors, single phase, three phase, 60 cycles, 400 cycles, 800 cycle ac/dc, constant speed, variable speed. The flow rates also vary from 1 cfm to several thousand cfm. When a fan is used for cooling electronic equipment, the airflow direction can be quite important. The fan can be used to draw air through a box or to blow air through a box. A blowing fan system will raise the internal air pressure within the box, which will help to keep dust and dirt out of a box that is not well sealed. A blowing system will also produce slightly more turbulence, which will improve the heat transfer characteristics within the box. However, when an axial flow fan is used in a blowing system, the air may be forced to pass over the hot fan motor, which will tend to heat the air as it enters the electronic box, as shown in Figure 8.7.

An exhaust fan system, which draws air through an electronic box, will reduce the internal air pressure within the box. If the box is located in a dusty or dirty area, the dust and dirt will be pulled into the box through all of the small air gaps if the box is not sealed. In an exhaust system, the cooling air passes through an axial flow fan as the air exits from the box, as shown in Figure 8.8. The cooling air entering the electronic box is therefore cooler.

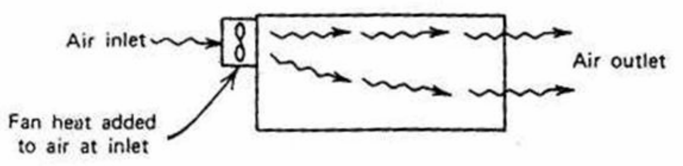

Figure 8.7 Axial flow fan blowing cooling air through a box

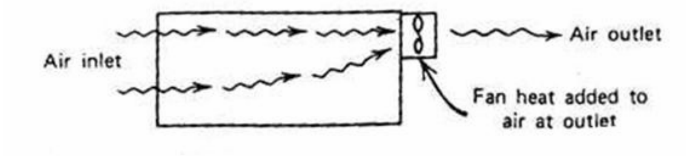

Figure 8.8 Axial flow fan drawing cooling air through a box

8.5 Static Pressure and Velocity Pressure

Airflow through an electronic box is due to a pressure difference between two points in the box, with the air flowing from the high-pressure side to the low-pressure side. The flow of air will result in a static pressure and a velocity pressure. Static pressure is the pressure that is exerted on the walls of the container or electronic box, even when there is no flow of air; it is independent of the air velocity. Static pressure can be positive or negative, depending upon whether it is greater or less than the outside ambient pressure.

Velocity pressure is the pressure that forces the air to move through the electronic box at a certain velocity. The velocity pressure depends upon the velocity of the air and always acts in the direction of the airflow. The amount of cooling air flowing through an electronic box will usually determine the amount of heat removed from the box. The higher the air flow rate through the box the higher heat will be removed. As the airflow through the box increases, however, it requires an even greater pressure to force the air through the box.

Static and velocity pressures can be expressed in lb/in^2 and g/cm^2. However, these values are usually very small, so that it is often more convenient to express these pressures in terms of the height of a column of water. The velocity head (H_v) is a convenient reference that is often used to determine pressure drops through electronic boxes. The velocity head can be related to the air flow velocity as follow

$$V = \sqrt{2 g H_v} \tag{8.24}$$

Where:

V = Velocity of the air
g = gravitational acceleration
H_v = velocity head in centimeter of water

The Equation 8.24 can be modified using standard air with a density of 0.0012 g/cm^3 at 20.5 °C and 1 bar, this is shown in Equation 8.25.

$$V = \sqrt{\frac{2(979.6\, cm/\sec^2)(1\, g/cm^3 water)(H_V\ cm\, water)}{0.0012\ \ g/cm^3 air}}$$

$$V = 1277\sqrt{H_v (cm\, water)} = cm/\sec. \tag{8.25}$$

The total head will be the sum of the velocity head and the static head as follow

$$H_t = H_v + H_s \tag{8.26}$$

We have many cases for measurement of the total heads inside the electronic box as shown in the Figures 8.9, 8.10, and 8.11. In case of a pressurized electronic box with no air flows the total pressure equal to the static pressure as shown in Figure 8.9. While in case of a fan blows air through the electronic box, the pressure within the box will be slightly higher than the outside air pressure. A velocity head will now be developed, as shown in Figure 8.10. But, in case of a fan draws the air through the box, the pressure within the box will be slightly lower than the outside air pressure, and the pressure head characteristics will appear as shown in Figure 8.11. And the total head is still constant as shown by Equation. 8.26.

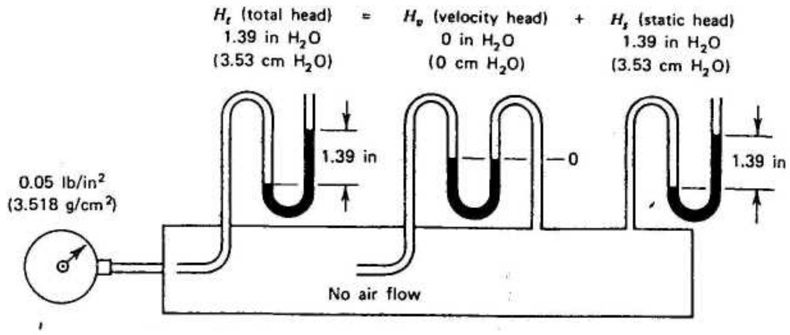

Figure 8.9 a pressurized electronic box with no air flow

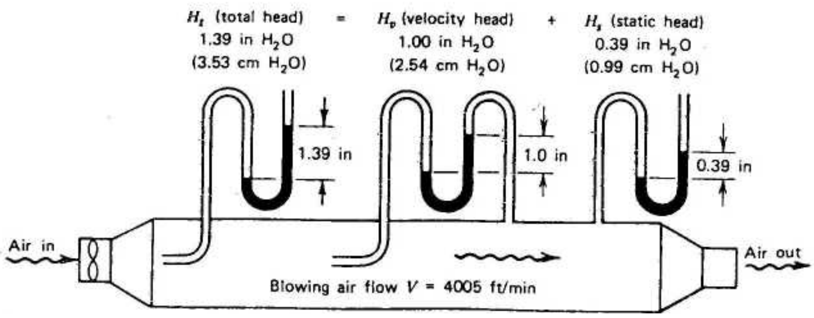

Figure 8.10 pressure head characteristics when the fan blows air through an electronic box

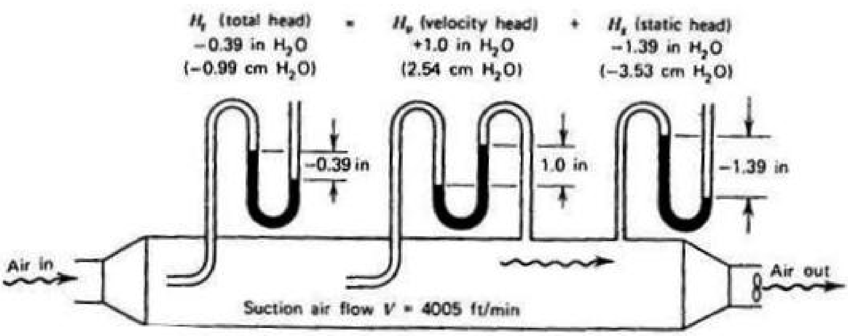

Figure 8.11 pressure head characteristics when the fan draws air through an electronic box

8.6 Fan Performance Curve

Electronic boxes that are cooled with the use of fans must be carefully evaluated to make sure the fan will provide the proper cooling. If the fan is too small for the box, the electronic system may over heat and fail. If the fan is too big for the box, the cooling will be adequate, but the larger fan will be more expensive, heavier, and will draw more power.

Air flowing through the electronic box will encounter resistance as it enters the different chambers and is forced to make many turns. The flow resistance is approximately proportional to the square of the velocity, so that it is approximately proportional to the square of the flow rate in cubic feet per minute (cfm). When the static pressure of the air flow through a box is plotted against the air flow rate, the result will be a parabolic curve. This curve can be generated by considering the various flow resistances the airflow will encounter as it flows through the box. The method of analysis is to assume several different flow rates through the box and then to calculate a static pressure drop though the box for each flow rate. This curve is called impedance curve for the electronic box as shown in Figure 8.12.

Once the box flow impedance curve has been developed, it is necessary to examine different fan performance curves to see how well the fans will match the box. A typical fan performance curve is shown in Figure 8.13.

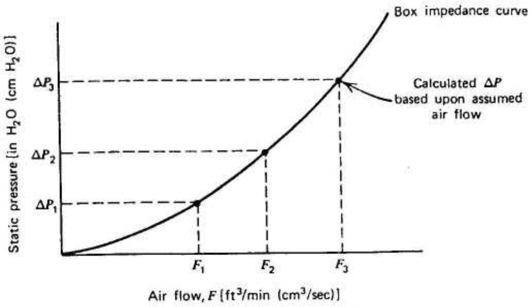

Figure 8.12 air flow impedance curve for the electronic box

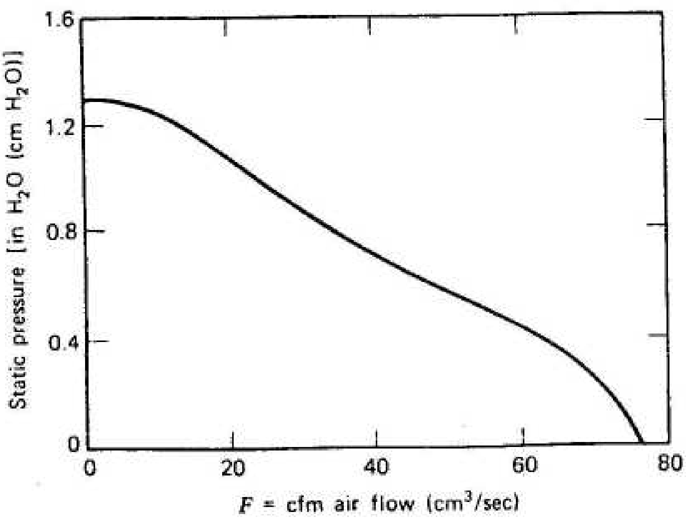

Figure 8.13 fan impedance curve

If the impedance curve for the box is superimposed on the impedance curve for the fan, they will intersect. The point of intersection represents the actual operating point for the system, as shown in Figure 8.14.

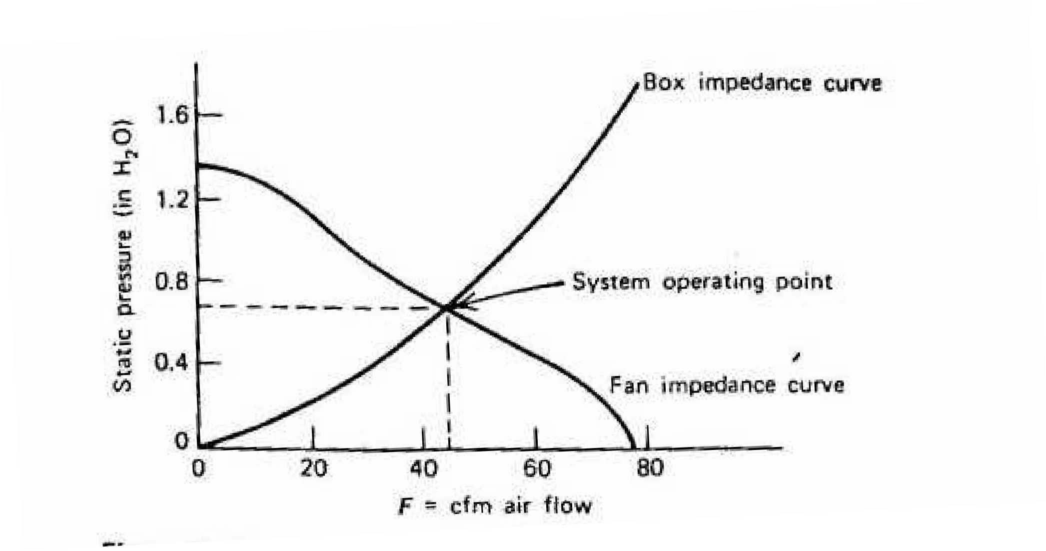

Figure 8.14 intersection of fan and box impedance curves

8.7 Cabinet Cooling Hints

In addition to selecting a fan, there may be some choice in the location of the fan or fans, and in this regard, the illustration in Figure 8.15 may prove useful. The following comments should also be kept in mind with regard to fan location:

1) Locate components with highest heat dissipation near the enclosure air exits
2) Size the enclosure air inlet and exit vents at least as large as the venturi opening of the fan used
3) Allow enough free area for air to pass with velocity less than 7 meters/sec
4) Avoid hot spots by spot cooling with a small fan
5) Locate components with the most critical temperature sensitivity nearest to inlet air to provide the coolest air flow
6) Blow air into cabinet to keep dust out, i.e. pressurize the cabinet
7) Use the largest filter possible, in order to reduce pressure drop and keep the system from the dust

8.8 Design Steps for Fan-Cooled Electronic Box Systems

The system as shown in Figure 8.16 must be capable of continuous operation in a 55 °C (131 °F) ambient at sea level condition. The maximum allowable hot spot component surface temperature is limited to 100 °C (212 °F). The system contains seven PCBs, each dissipating 20 watts, for a total power dissipation of 140 watts. This does not include fan power dissipation.

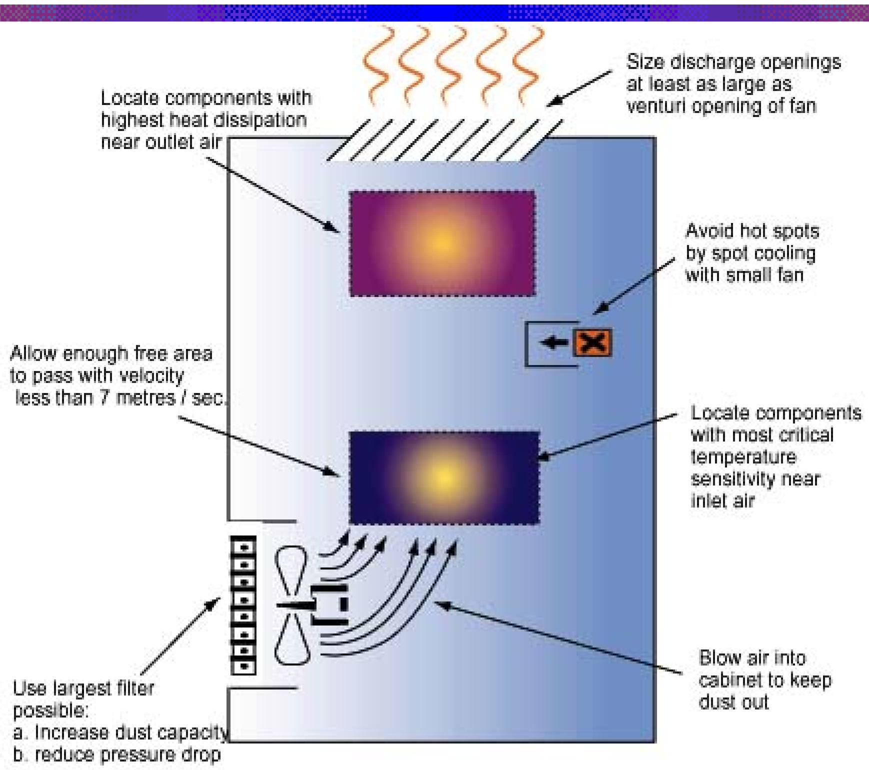

Figure 8.15 Cabinet cooling hints

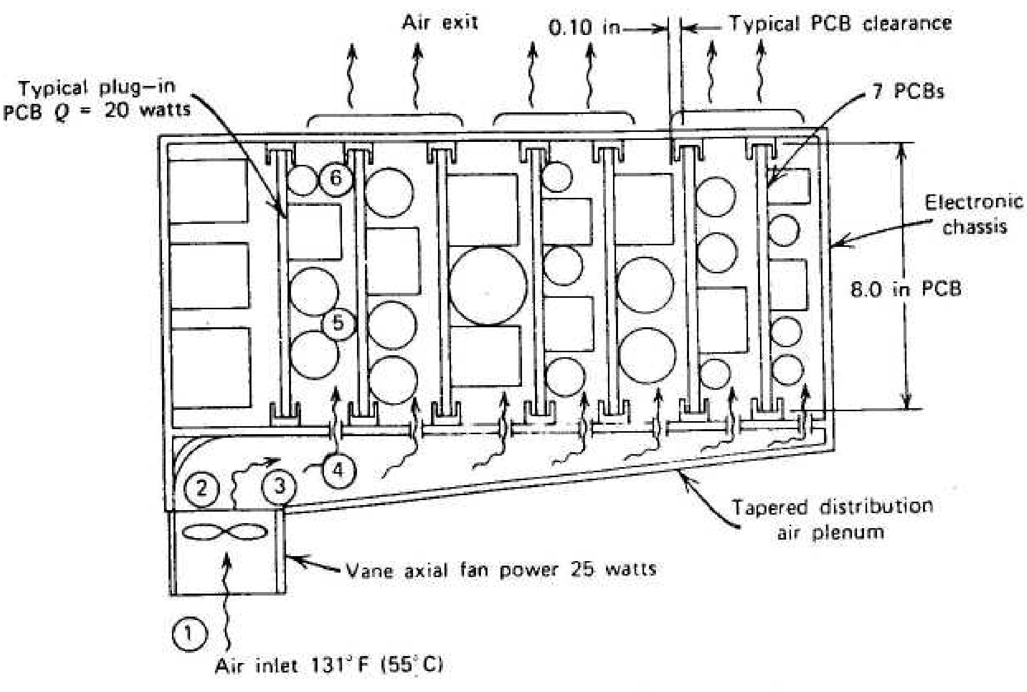

Figure 8.16 plan view of fan-cooled electronic box

The flow area at the partitions designed on the drawing are as follows

Inlet to fan is an annuals (dimensions are in mm)

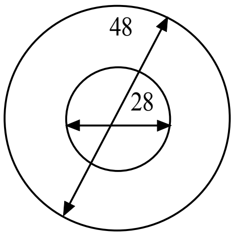

90^o turn and transition from a round section at the fan to an oval section

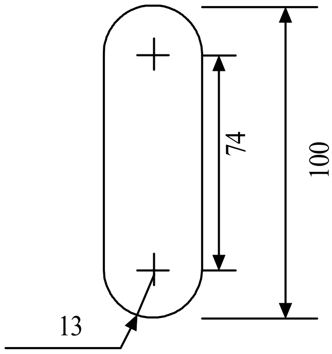

Contraction and transition to rectangular section a rectangle 8 x 125 mm2

Plenum entrance to a PCB duct rectangle each 1.5 x 155 mm2

PCB channel duct as shown in the following drawing

Rectangle each 2.5 x 230 mm^2 (0.1 x 9 in^2)

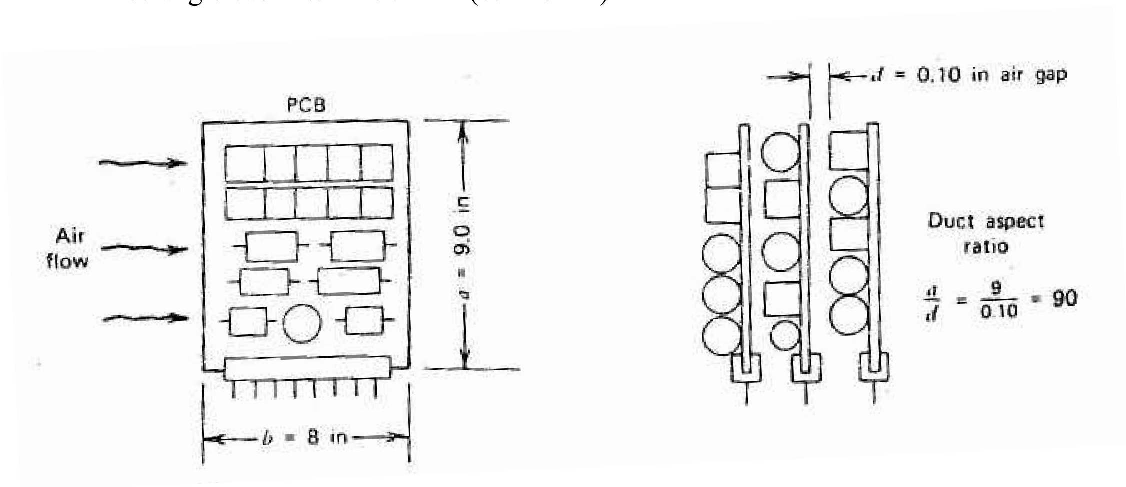

Design procedures:

Two fans are available for cooling the box: Fan A is three phase 15500 rpm that has a 25 Watts motor. Fan B is single phase, with an 18 Watts motor that operates at 11000 rpm at sea level. The box must be examined in two phases to ensure the integrity of the complete design. In phase 1, the thermal design of the box is examined, with the proposed fan, to make sure the component hot spot temperature of 100°C (212°F) is not exceeded. In phase 2, the electronic chassis airflow impedance curve is developed and matched with several fans, to make sure there is sufficient cooling air available for the system.

Phase 1: Electronic box thermal design:
To be on the safe side, base the calculation on the use of larger, 25 W motor, Fan A
The total energy to be dissipated would then be
$q = 140 + 25 = 165\ \text{W}$
Air required for cooling is

$$m^{\bullet} = \frac{q}{c_p (t_{a,o} - t_{a,i})}$$

Past experience with air-cooled electronic systems has shown that satisfactory thermal performance can be obtained if the cooling air exit temperature from the electronic chassis does not exceed 70 °C (160 °F), so that assume exit air temperature $t_{a,o}$= 70 °C

From the air property table at mean temperature t_m= (70+55)/2 = 62.5 °C
$\rho = 1.052\ \text{kg/m}^3$
$\nu = 19.23\ \text{x}10^{-6}\ \text{m}^2\text{/s}$
Pr = 0.7
$C_p = 1008$ J/kg.K
k = 0.0289 W/m..°C

Air required for cooling is

$$m^{\bullet} = \frac{165}{1008(70 - 55)} = 0.01091\,\text{kg/s}$$

By calculating the heat transfer coefficient between the air and PCB's and, hence, the temperature rise of the PCB's above the ambient air. For this purpose we calculate the Reynolds' number

$$\text{Re} = \frac{\text{V}D_H}{\nu}$$

$$\because D_H = \frac{4A}{P} = \frac{4\ x\ 9\ x0.1}{2(9 + 0.1)} = 0.197\ in = 0.005\ m$$

$$and\quad \text{V} = \frac{m^{\bullet}}{\rho\ A} = \frac{0.01091}{1.052\ (7x9x0.1)x(0.0254)^2} = 2.55\ m/s$$

$$\therefore \text{Re} = \frac{2.55\ x\ 0.005}{19.23\ \text{x}10^{-6}} = 663$$

The heat transfer coefficient for laminar flow through ducts is shown in the following relation

$$\frac{\bar{h}\ D_H}{k} = \overline{Nu}_D = 1.86\left(\frac{\text{Re}\ \ \text{Pr}}{L/D_H}\right)^{1/3}$$

$$= 1.86\left(\frac{663\ x0.7\ x0.005}{8\ x\ 0.0254}\right)^{1/3} = 4.19$$

$$\bar{h} = 24.2\ \text{W/m}^2\text{.K}$$

The total heat transfer is

$$q = h\ S_{eff}\ \Delta t_h$$

Actually, the back surface of a PCB is not available for heat transfer; the practice is to assume 30 percent only available for this purpose

$$S_{eff} = 7\ x1.3\ x8\ x\ 9\ (0.0254)^2 = 0.423\ m^2$$

$$\Delta t_h = 165/24.2\ x0.423 = 16.1\ ^oC$$

Therefore, maximum component surface temperature

$t_{max} = t_{a,o} + \Delta t_h = 70 + 16.1 = 86.1\ ^oC$

This is acceptable surface temperature since it is less than 100 °C

Phase 2: Electronic chassis air flow impedance curve:

The air flow conditions are examined at six different points in the chaises, where the maximum static pressure losses are expected to occur, as shown in Figure 8.16. These static pressure losses are itemized as follow:

1- Air inlet to fan
2- 90^o turn and transition to an oval section
3- Concentration and transition to a rectangular section
4- Plenum entrance to PCB duct
5- Flow through PCB channel duct
6- Exhaust from PCB duct and chaises

The following table gives the ratio between static head loss to velocity head at the different positions

Position number	H_s / H_v
1	1
2	0.9
3	0.4
4	2
5	1
6	1

The flow areas at each position are:

Position 1: $A_1 = \frac{\pi}{4}\left(d_o^2 - d_i^2\right) = \frac{\pi}{4}\left(0.048^2 - 0.028^2\right) = 1.194\ x10^{-3}\ m^2$

Position 2: $A_2 = 0.026\ x0.074 + \pi\ x0.013^2 = 2.455\ m^2$

Position 3: $A_3 = 0.008\ x0.125 = 1\ x10^{-3}\ m^2$

Position 4: $A_4 = 0.0015\ x0.155\ x7\text{slots} = 1.628\ x10^{-3}\ m^2$

Position 5: $A_5 = 0.0025\ x0.23\ x7 = 4.025\ x10^{-3}\ m^2$

Position 6: $A_5 = A_6 = 4.025\ x10^{-3}\ m^2$

The following table gives velocity, velocity heads at each position at 10 cfm (0.283 m^3/min)

Position	V (cm/s.)	H_v(cm H_2O)
1	400	0.098
2	376	0.087
3	488	0.146
4	290	0.0516
5	116	0.0082
6	116	0.0082

Performing the test under different cfm air flow: let the flow rate also at 20 cfm, and 30 cfm
The losses for each another flow calculated from

$$H = (H_s / H_v)\, H_{v,10} \left(\frac{V^{\bullet}}{10}\right)$$

The following table gives the static pressure loss in (cm H_2O) at 10 cfm, 20 cfm, and 30 cfm

Position	10 cfm	20 cfm	30 cfm
1	0.098	0.392	0.882
2	0.086	0.345	0.777
3	0.0729	0.292	0.657
4	0.103	0.411	0.927
5	0.0082	0.0325	0.0731
6	0.0082	0.0325	0.0731
Total	0.3761	1.5	3.3892

Then drawing the chassis air flow impedance curve at different fan curves as shown below

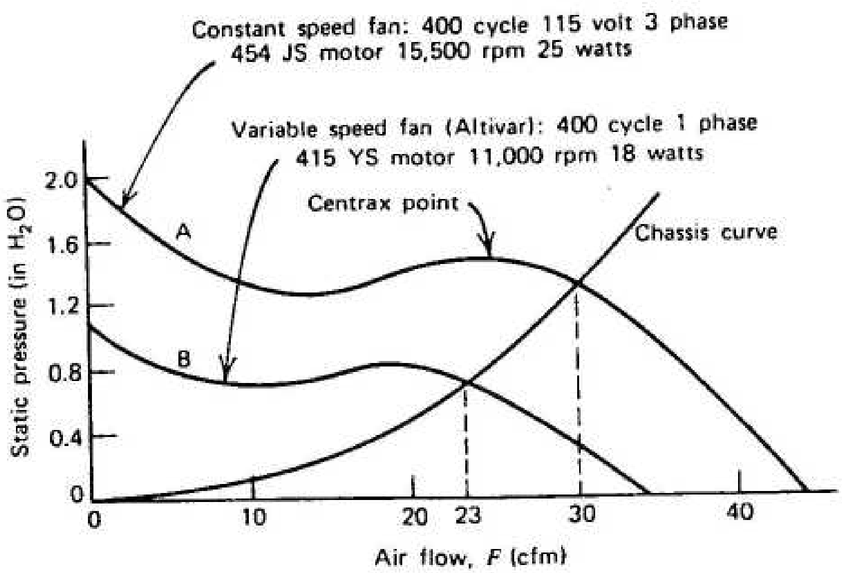

The minimum flow rate required for this system is

$$V^{\bullet} = \frac{m^{\bullet}}{\rho} = \frac{0.01091}{1.052} = 0.01\, m^3/s = 10370.7\, cm^3/s$$

From the impedance curve it shows:

The flow rate supplied by fans A is

$$V^{\bullet} = 30\text{cfm} = 14157\ cm^3 / s$$

The flow rate supplied by fans B is

$$V^{\bullet} = 23\text{cfm} = 10854\ cm^3 / s$$

So that both fans A and B can supply more than the minimum required flow rate, either fan will be acceptable.

9. Forced Convection Correlations

Our primary objective is to determine heat transfer coefficients (local and average) for different flow geometries and this heat transfer coefficient (h) may be obtained by experimental or theoretical methods. Theoretical methods involve solution of the boundary layer equations to get the Nusselt number such as explained before in the previous lecture. On the other hand the experimental methods involve performing heat transfer measurement under controlled laboratory conditions and correlating data in dimensionless parameters. Many correlations for finding the convective heat transfer coefficient are based on experimental data which needs uncertainty analysis, although the experiments are performed under carefully controlled conditions. The causes of the uncertainty are many. Actual situations rarely conform completely to the experimental situations for which the correlations are applicable. Hence, one should not expect the actual value of the heat transfer coefficient to be within better than □10%of the predicted value.

9.1 Flow over Flat Plate

With a fluid flowing parallel to a flat plate we have several cases arise:

- Flows with or without pressure gradient
- Laminar or turbulent boundary layer
- Negligible or significant viscous dissipation (effect of frictional heating)

9.1.1 Flow with Zero Pressure Gradient and Negligible Viscous Dissipation

When the free-stream pressure is uniform, the free-stream velocity is also uniform. Whether the boundary layer is laminar or turbulent depends on the Reynolds number Re_X $(\rho u_\infty x/\mu)$ and the shape of the solid at entrance. With a sharp edge at the leading edge the boundary layer is initially laminar but at some distance downstream there is a transition region and downstream of the transition region the boundary layer becomes turbulent. For engineering applications the transition region is usually neglected and it is assumed that the boundary layer becomes turbulent if the Reynolds number, Re_X, is greater than the critical Reynolds number, Re_{cr}.   A typical value of 5×10^5 for the critical Reynolds number is generally accepted.

The viscous dissipation and high-speed effects can be neglected if $Pr^{1/2}\,Ec<1$. The Eckert number Ec is defined as $Ec = u^2_\infty/C_p\,(T_S-T_\infty)$ with a rectangular plate of length L in the direction of the fluid flow.

9.1.1.1 Laminar Boundary Layer ($Re_x \leq 5x10^5$)

With heating or cooling starting from the leading edge the following correlations are recommended. Note: in all equations evaluate fluid properties at the film temperature (T_f) defined as the arithmetic mean of the surface and free-stream temperatures unless otherwise stated.

$$T_f = (T_S + T_\infty)/2$$

Flow with uniform surface temperature (T_S = constant)

- Local heat transfer coefficient

The Nusselt number based on the local convective heat transfer coefficient is expressed as

$$Nu_X = f_{\Pr} \operatorname{Re}_X^{1/2} \qquad (9.1)$$

The expression of $f_{\Pr}$ depend on the fluid Prandtl number

For liquid metals with very low Prandtl number liquid metals ($\Pr \le 0.05$)

$$f_{\Pr} = 0.564 \Pr^{1/2}$$

For $0.6 < \Pr < 50$

$$f_{\Pr} = 0.332 \Pr^{1/3}$$

For very large Prandtl number

$$f_{\Pr} = 0.339 \Pr^{1/3}$$

For all Prandtl numbers; Correlations valid developed by Churchill (1976) and Rose (1979) are

$$Nu_x = \frac{0.3387 \operatorname{Re}_x^{1/2} \Pr^{1/3}}{\left[1 + \left(\frac{0.0468}{\Pr}\right)^{2/3}\right]^{1/4}} \qquad (9.2)$$

- Average heat transfer coefficient

The average heat transfer coefficient can be evaluated by performing integration along the flat plate length, if Prandtl number is assumed constant along the plate, the integration yields to the following result:

$$\overline{Nu}_x = 2 Nu_x \qquad (9.3)$$

Flow with uniform heat flux ($q^{//}$ = constant)

- Local heat transfer coefficient

Churchill and Ozoe (1973) recommend the following single correlation for all Prandtl numbers

$$Nu_X = \frac{0.886 \operatorname{Re}_X^{1/2} \Pr^{1/2}}{\left[1 + \left(\frac{\Pr}{0.0207}\right)^{2/3}\right]^{1/4}} \qquad (9.4)$$

9.1.1.2 Turbulent Boundary Layer ($Re_x > 5x10^5$)

With heating or cooling starting from the leading edge the following correlations are recommended.

- Local heat transfer coefficient

$Re_{cr} < Re_x \leq 10^7$ $$Nu_x = 0.0296 \, Re_x^{4/5} \, Pr^{1/3} \qquad (9.5)$$

$Re_x > 10^7$ $$Nu_x = 1.596 \, Re_x (\ln Re_x)^{-2.584} \, Pr^{1/3} \qquad (9.6)$$

Equation 9.6 is obtained by applying Colburn's j factor in conjunction with the friction factor suggested by Schlichting (1979).

With turbulent boundary layers the correlations for the local convective heat transfer coefficient can be used for both uniform surface temperature and uniform heat flux.

- Average heat transfer coefficient

If the boundary layer is initially laminar followed by a turbulent boundary layer some times called mixed boundary layer the Following correlations for $0.6 < Pr < 60$ are suggested:

$Re_{cr} < Re_x \leq 10^7$ $$\overline{Nu}_x = (0.037 \, Re_x^{4/5} - 871) \, Pr^{1/3} \qquad (9.7)$$

$Re_x > 10^7$ $$\overline{Nu}_x = [1.963 \, Re_x (\ln Re_x)^{-2.584} - 871] \, Pr^{1/3} \qquad (9.8)$$

9.1.1.3 Unheated Starting Length

Uniform Surface Temperature & Pr > 0.6

If the plate is not heated or (cooled) from the leading edge where the boundary layer develops from the leading edge until being heated at $x = x_o$ as shown in Figure 9.1, the correlations have to be modified.

.

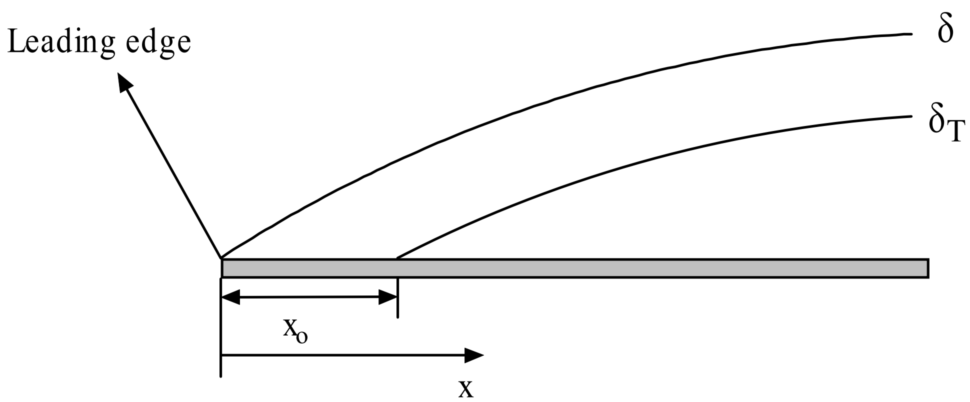

Figure 9.1 Heating starts at $x = x_o$

- Local heat transfer coefficient

Laminar flow ($Re_x < Re_{cr}$)

$$Nu_x = \frac{0.332\, Re_x^{1/2}\, Pr^{1/3}}{\left[1-\left(\frac{x_o}{x}\right)^{3/4}\right]^{1/3}} \tag{9.9}$$

Turbulent flow ($Re_x > Re_{cr}$)

$$Nu_x = \frac{0.0296\, Re_x^{4/5}\, Pr^{3/5}}{\left[1-\left(\frac{x_o}{x}\right)^{9/10}\right]^{1/9}} \tag{9.10}$$

- Average heat transfer coefficient over the Length (L – xo)

Laminar flow ($Re_L < Re_{cr}$)

$$\bar{h}_{L-x_o} = \left(\frac{k}{L-x_o}\right) 0.664\, Re_L^{1/2}\, Pr^{1/3} \left[1-\left(\frac{x_o}{L}\right)^{3/4}\right]^{2/3} \tag{9.11}$$

$$= 2\left(\frac{h_{x=L}}{1-(x_o/L)}\right)\left(1-\left(\frac{x_o}{L}\right)^{3/4}\right)$$

Evaluate $h_{x=L}$ from Equation 9.9.

Turbulent flow ($Re_L > Re_{cr}$)

$$\bar{h}_{L-x_o} = \frac{0.037\, Re_L^{4/5}\, Pr^{3/5}\left[1-\left(\frac{x_o}{L}\right)^{9/10}\right]^{8/9} k}{L-x_o} \tag{9.12}$$

$$= 1.25 \frac{1-\left(\frac{x_o}{L}\right)^{9/10}}{1-\left(\frac{x_o}{L}\right)} h_{x=L}$$

Evaluate $h_{x=L}$ from Equation 9.10.

Example 9.1: Experimental results obtained for heat transfer over a flat plate with zero pressure gradients yields

$$Nu_x = 0.04\, Re_x^{0.9}\, Pr^{1/3}$$

Where this correlation is based on x (the distance measured from the leading edge). Calculate the ratio of the average heat transfer coefficient to the local heat transfer coefficient.
Schematic:

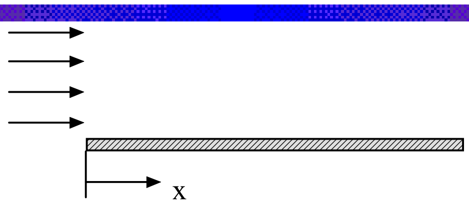

Solution:
It is known that

$$Nu_x = \frac{h_x x}{k}$$

Local heat transfer coefficient

$$h_x = 0.04\frac{k}{x}\mathrm{Re}_x^{0.9}\ \mathrm{Pr}^{1/3}$$

The average heat transfer coefficient is:

$$\bar{h}_x = \frac{1}{x}\int_0^x h_x dx = \frac{0.04k\,\mathrm{Pr}^{1/3}}{x}\int_0^x\left(\frac{u_\infty x}{v}\right)^{0.9}\frac{1}{x}dx$$

$$= \frac{0.04k\,\mathrm{Pr}^{1/3}}{x}\left(\frac{u_\infty}{v}\right)^{0.9}\int_0^x x^{-0.1}dx$$

$$= \frac{0.04k\,\mathrm{Pr}^{1/3}}{0.9x}\left(\frac{u_\infty}{v}\right)^{0.9}x^{0.9}$$

$$= \frac{0.04k}{0.9x}\mathrm{Re}_x^{0.9}\ \mathrm{Pr}^{1/3}$$

$$= \frac{h_x}{0.9}$$

The ratio of the average heat transfer coefficient to the local heat transfer coefficient is:

$$\frac{\bar{h}_x}{h_x} = \frac{1}{0.9}$$

Example 9.2: Air at a temperature of 30 ºC and 6 kPa pressure flow with a velocity of 10 m/s over a flat plate 0.5 m long. Estimate the heat transferred per unit width of the plate needed to maintain its surface at a temperature of 45 ºC.
Schematic:

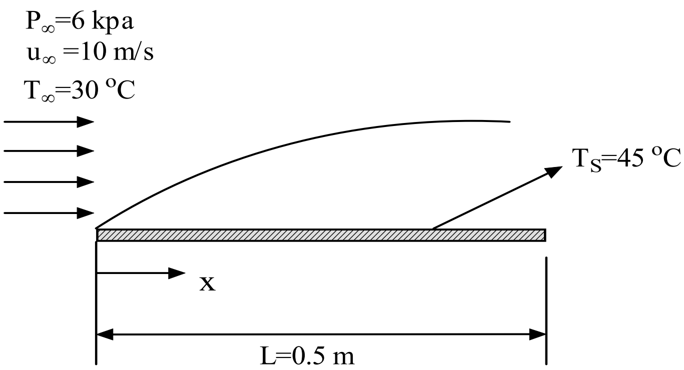

Solution:

Properties of the air evaluated at the film temperature

$T_f = 75/2 = 37.5$ ºC

From air properties table at 37.5 ºC:

$\nu = 16.95 \times 10^{-6}$ m²/s.

$k = 0.027$ W/m. ºC

$Pr = 0.7055$

$C_p = 1007.4$ J/kg. ºC

Note: These properties are evaluated at atmospheric pressure, thus we must perform correction for the kinematic viscosity

$$\nu)_{act.} = \nu)_{atm.} \times (1.0135/0.06) = 2.863 \times 10^{-4} \text{ m}^2/\text{s}.$$

Viscous effect check,

$$Ec = u^2_\infty / C_p(T_S - T_\infty) = (10)^2/(1007.4 \times 15) = 6.6177 \times 10^{-3}$$

It produce $Pr^{1/2}\, Ec < 1$ so that we neglect the viscous effect

Reynolds number check

$$Re_L = u_\infty L / \nu = 10 \times 0.5 / (2.863 \times 10^{-4}) = 17464.2$$

The flow is Laminar because $Re_L \leq 5 \times 10^5$

Using the Equation 9.3

$$\overline{Nu}_L = 0.664\, Re_L^{1/2}\, Pr^{1/3}$$
$$= 0.664\, (17464.2)^{1/2}(0.7055)^{1/3}$$
$$= 78.12$$

Now the average heat transfer coefficient is

$$\overline{Nu}_L = \frac{\bar{h}L}{k}$$

$$\bar{h} = 78.12 \times 0.027 / 0.5 = 4.22 \text{ W/m}^2.\ ºC$$

Then the total heat transfer per unit width equals

$$q = \bar{h}\, L\, (T_S - T_\infty) = 4.22 \times 0.5\, (45 - 30) = 31.64 \text{ W/m}$$

Example 9.3: Water at 25 ºC is in parallel flow over an isothermal, 1-m long flat plate with velocity of 2 m/s. Calculate the value of average heat transfer coefficient.

Schematic:

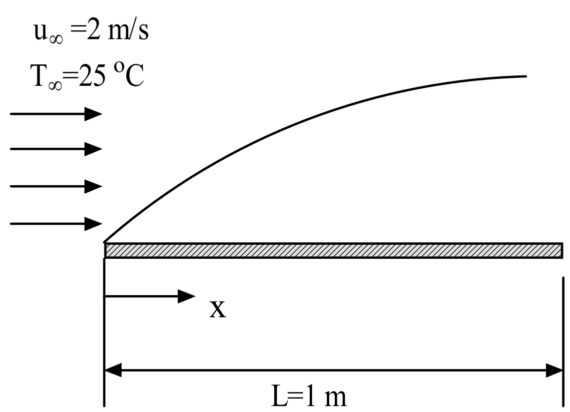

Solution:

Assumptions

- neglect the viscous effect
- The properties of water are evaluated at free stream temperature

From water properties table at 25 ºC:

ν =8.57x10^{-7} m/s.

k = 0.613W/m. ºC

Pr= 5.83

C_p= 4180 J/kg. ºC

Reynolds number check,

$$Re_L = u_\infty L / \nu = 2 \text{ x } 1 / (8.57\text{x}10^{-7}) = 2.33\text{x}10^6$$

The flow is mixed because $Re_L \geq 5\text{x}10^5$

By using the Equation 9.7

$$\overline{Nu}_x = (0.037\,\mathrm{Re}_x^{4/5} - 871)\,\mathrm{Pr}^{1/3}$$
$$= [0.037x(2.33x10^6)^{4/5} - 871](5.83)^{1/3}$$
$$= 6704.78$$
$$= \frac{\overline{h}_L L}{k}$$

The average heat transfer coefficient is

$$\overline{h}_L = 4110 \ \ \mathrm{W/m^2 \cdot K}$$

9.3 Flow over Cylinders, Spheres, and other Geometries

The flow over cylinders and spheres is of equal importance to the flow over flat plate, they are more complex due to boundary layer effect along the surface where the free stream velocity u_∞ brought to the rest at the forward stagnation point (u = 0 and maximum pressure) the pressure decrease with increasing x is a favorable pressure gradient (dp/dx<0) bring the pressure to minimum, then the pressure begin to increase with increasing x by adverse pressure gradient (dp/dx>0) on the rear of the cylinder. In general, the flow over cylinders and spheres may have a laminar boundary layer followed by a turbulent boundary layer.

The laminar flow is very weak to the adverse pressure gradient on the rear of cylinder so that the separation occurs at θ = 80º and caused wide wakes as show in Figure9.2.a.

The turbulent flow is more resistant so that the separation occurs at θ = 120º and caused narrow wakes as show in Figure9.2.b.

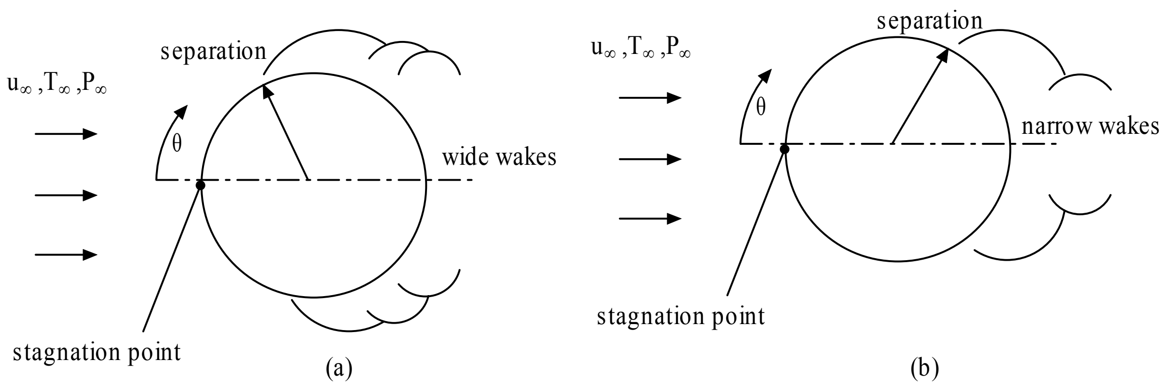

Figure 9.2 Flow over cylinder

Because of the complexity of the flow patterns, only correlations for the average heat transfer coefficients have been developed.

9.3.1 Cylinders

The empirical relation represented by Hilpert given below in Equation 9.13 is widely used, where the constants c, m is given in Table 9.1, all properties are evaluated at film temperature T_f.

$$\overline{Nu}_D = c\,\mathrm{Re}_D^m\,\mathrm{Pr}^{1/3} \tag{9.13}$$

Table 9.1 Constants of Equation 9.13 at different Reynolds numbers

Re_D	c	m
0.4-4	0.989	0.33
4-40	0.911	0.385
40-4000	0.683	0.466
4000-40,000	0.193	0.618
40,000-400,000	0.027	0.805

Other correlation has been suggested for circular cylinder. This correlation is represented by Zhukauskas given below in Equation 9.14 , where the constants c ,m are given in Table 9.2 , all properties are evaluated at Free stream temperature T_∞, except Pr_S which is evaluated at T_S which is used in limited Prandtl number $0.7 < Pr < 500$

$$\overline{Nu}_D = c\,\mathrm{Re}_D^m\,\mathrm{Pr}^n\left(\frac{\mathrm{Pr}}{\mathrm{Pr}_S}\right)^{1/4} \tag{9.14}$$

If $Pr \leq 10$, n= 0.37
If $Pr > 10$, n= 0.36

Table 9.2 Constants of Equation 9.14 at different Reynolds numbers

Re_D	c	m
1-40	0.75	0.4
40-1000	0.51	0.5
$1000\text{-}2\times10^5$	0.26	0.6
$2\times10^5\text{-}10^6$	0.076	0.7

For entire ranges of Re_D as well as the wide ranges of Prandtl numbers, the following correlations proposed by Churchill and Bernstein (1977): $Re_D\,Pr > 0.2$. Evaluate properties at film temperature T_f:

Re □400, 000

$$\overline{Nu}_D = 0.3 + \frac{0.62\,\mathrm{Re}_D^{1/2}\,\mathrm{Pr}^{1/3}}{\left[1+\left(\frac{0.4}{\mathrm{Pr}}\right)^{2/3}\right]^{1/4}}\left[1+\left(\frac{\mathrm{Re}_D}{282{,}000}\right)^{5/8}\right]^{4/5} \tag{9.15}$$

10, 000□Re□ 400, 000

$$\overline{Nu}_D = 0.3 + \frac{0.62\,Re_D^{1/2}\,Pr^{1/3}}{\left[1+\left(\frac{0.4}{Pr}\right)^{2/3}\right]^{1/4}}\left[1+\left(\frac{Re_D}{282{,}000}\right)^{1/2}\right] \qquad (9.16)$$

$Re \le 10{,}000$

$$\overline{Nu}_D = 0.3 + \frac{0.62\,Re_D^{1/2}\,Pr^{1/3}}{\left[1+\left(\frac{0.4}{Pr}\right)^{2/3}\right]^{1/4}} \qquad (9.17)$$

For flow of liquid metals, use the following correlation suggested by Ishiguro et al. (1979):
$1 \le Re_d\,Pr \le 100$

$$\overline{Nu}_d = 1.125(Re_D\,Pr)^{0.413} \qquad (9.18)$$

9.3.2 Spheres

Boundary layer effects with flow over circular cylinders are much like the flow over spheres. The following two correlations are explicitly used for flows over spheres,

1. Whitaker (1972): All properties at T_∞ except μ_s at T_s

$3.5 \le Re_d \le 76{,}000$ $\quad 0.71 \le Pr \le 380$ $\quad 1 \le \mu/\mu_s \le 3.2$

$$\overline{Nu}_D = 2 + \left(0.4\,Re_D^{1/2} + 0.06\,Re_D^{2/3}\right)Pr^{2/5}\left(\frac{\mu}{\mu_s}\right)^{1/4} \qquad (9.20)$$

2. Achenbach (1978): All properties at film temperature

$100 \le Re_d \le 2\text{ x}10^5$ $\quad Pr = 0.71$

$$\overline{Nu}_D = 2 + \left(0.25\,Re_D + 3x10^{-4}\,Re_D^{8/5}\right)^{1/2} \qquad (9.21)$$

$4\text{ x}10^5 \le Re_d \le 5\text{ x}10^6$ $\quad Pr = 0.71$

$$\overline{Nu}_D = 430 + 5x10^{-3}\,Re_D + 0.25x10^{-9}\,Re_D^2 - 3.1x10^{-17}\,Re_D^3 \qquad (9.22)$$

For Liquid Metals convective flow, experimental results for liquid sodium, Witte (1968) proposed,

$3.6\text{ x}10^4 \le Re_d \le 1.5\text{ x}10^5$

$$\overline{Nu}_D = 2 + 0.386(Re_D\,Pr)^{1/2} \qquad (9.23)$$

9.3.3 Other Geometries

For geometries other than cylinders and spheres, use Equation 9.24 with the characteristic dimensions and values of the constants given in the Table 9.3 for different geometries, all properties are evaluated at film temperature T_f.

$$\overline{Nu}_D = c\,Re_D^m\,Pr^{1/3} \qquad (9.24)$$

Equation 9.24 is based on experimental data done for gases.
Its use can be extended to fluids with moderate Prandtl numbers by multiplying Equation 9.24 by 1.11.

Table 9.3 Constants for Equation 9.24 for non circular cylinders external flow

Geometry	Re_D	C	m
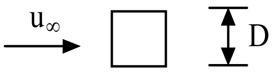	5×10^3-10^5	0.102	0.675
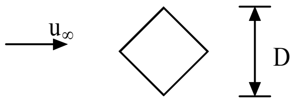	5×10^3-10^5	0.246	0.588
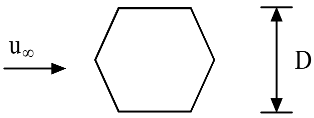	5×10^3-10^5	0.153	0.638
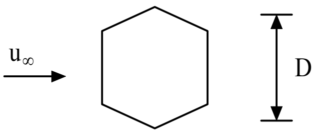	5×10^3-1.95×10^4 1.95×10^4-10^5	0.16 0.0385	0.638 0.782
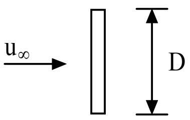	4×10^3-1.5×10^4	0.228	0.731

Example 9.4: Atmospheric air at 25 °C flowing at velocity of 15 m/s. over the following surfaces, each at 75 °C. Calculate the rate of heat transfer per unit length for each arrangement.

a) A circular cylinder of 20 mm diameter ,
b) A square cylinder of 20 mm length on a side
c) A vertical plate of 20 mm height

Schematic:

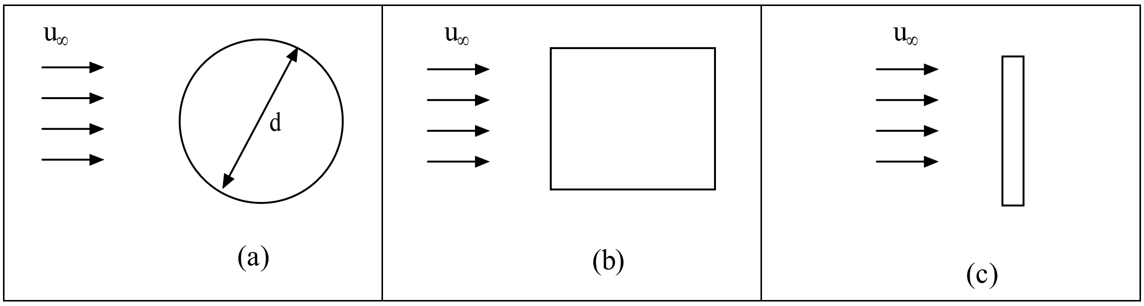

Solution:
From the film temperature

$$T_f = (25+75)/2 = 50\ ^\circ C$$

Air properties are:
$\nu = 1.8\times10^{-5}$ m/s.
k = 0.028W/m. °C
Pr= 0.70378

Calculation of Reynolds number for all cases have the same characteristic length=20mm

$$Re_D = u_\infty L / \nu = 15 \times 0.02 / 1.8\times10^{-5} = 16666.667$$

By using Equation 9.13 for all cases

$$\overline{Nu}_D = c\,Re_D^m\,Pr^{1/3}$$

Case (a) a circular cylinder
From Table 9.1
C = 0.193 and m= 0.618

$$\overline{Nu}_D = 0.193(16666.667)^{0.618}(0.70378)^{1/3}$$
$$= 69.79$$

The average heat transfer coefficient is

$$\bar{h}_D = \frac{\overline{Nu}_D k}{D} = \frac{69.79x0.028}{0.02} = 97.7 \quad \text{W/m}^2.^\circ\text{C}$$

The total heat transfer per unit length is

$$q^/ = 97.7\ (\pi \text{ x } 0.02)50 = 306.9 \text{ W/m}$$

Case (b) a square cylinder
From Table 9.3
C = 0.102 and m= 0.675

$$\overline{Nu}_D = 0.102(16666.667)^{0.675}(0.70378)^{1/3}$$
$$= 64.19$$

The average heat transfer coefficient is

$$\bar{h}_D = \frac{\overline{Nu}_D k}{D} = \frac{64.19x0.028}{0.02} = 89.87 \quad \text{W/m}^2.^\circ\text{C}$$

The total heat transfer per unit length is

$$q^/ = 89.87\ (4 \text{ x } 0.02)50 = 359.48 \text{ W/m}$$

Case (c) a vertical plate
From Table 9.3
C = 0.228 and m= 0.731

$$\overline{Nu}_D = 0.228(16666.667)^{0.731}(0.70378)^{1/3}$$
$$= 247.316$$

The average heat transfer coefficient is

$$\bar{h}_D = \frac{\overline{Nu}_D k}{D} = \frac{247.316x0.028}{0.02} = 346.24 \quad \text{W/m}^2.^\circ\text{C}$$

The total heat transfer per unit length is

$$q^/ = 346.24 \text{ x } (2 \text{ x } 0.02) \text{ x } 50 = 692.48 \text{ W/m}$$

9.4 Heat Transfer across Tube Banks (Heat Exchangers)

Heat transfer through a bank (or bundle) of tubes has several applications in industry as heat exchanger which can be used in many applications.

When tube banks are used in heat exchangers, two arrangements of the tubes are considered aligned and staggered as shown in Figure 9.3.

If the spacing between the tubes is very much greater than the diameter of the tubes, correlations for single tubes can be used. Correlations for flow over tube banks when the spacing between tubes in a row and a column are not much greater than the diameter of the tubes have been developed for use in heat-exchanger applications will be discussed as follows.

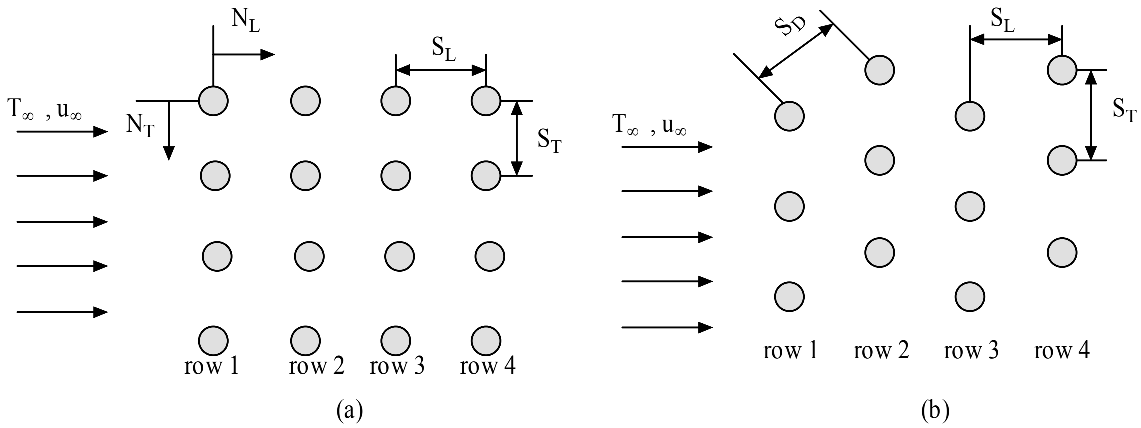

Figure 9.3 Arrangements of the tubes (a) In-line arrangement, (b) staggered arrangement

For the average convective heat transfer coefficient with tubes at uniform surface temperature, experimental results carried by Zukauskas (1987) recommended the following correlation:

$$\overline{Nu}_D = c(a/b)^P \, \mathrm{Re}_D^m \, \mathrm{Pr}^n (\mathrm{Pr}/\mathrm{Pr}_s)^{0.25} \qquad (9.25)$$

$a = S_T/D$; $b = S_L/D$.
S_T = Transverse pitch
S_L = Lateral pitch
D = tube diameter

All properties are evaluated at the arithmetic mean of the inlet and exit temperatures of the fluid ($T_{\infty i}$ + $T_{\infty o}$)/2, except Pr_S which is evaluated at the surface temperature T_S. The values of the constants c, p, m, and n are given in Table 9.4 for in-line arrangement and in Table 9.5 for staggered arrangement.
The maximum average velocity between tubes is used to calculate Re_D. The maximum velocity can be calculated as follows:

For in-line arrangement: $$u_{max} = u_\infty \left(\frac{S_T}{S_T - D} \right)$$

For Staggered arrangement: If $$S_D > \frac{S_T + D}{2}$$ $$\therefore u_{max} = \frac{S_T}{S_T - D} u_\infty$$

If not $$\therefore u_{max} = \frac{0.5 S_T}{(S_D - D)} u_\infty$$

Where $$S_D = \left[S_L^2 + \left(\frac{S_T}{2} \right)^2 \right]^{1/2}$$

Table 9.4 In-Line arrangement values of constants in Equation 9.25 (p = 0 in all cases)

Re_D	C	m	n
1-100	0.9	0.4	0.36
100-1000	0.52	0.5	0.36
1000-2x10^5	0.27	0.63	0.36
2x10^5-2x10^6	0.033	0.8	0.4

Table 9.5 Staggered arrangement values of constants in Equation 9.25

Re_D	c	P	m	n
1-500	1.04	0	0.4	0.36
500-1000	0.71	0	0.5	0.36
1000-$2x10^5$	0.35	0.2	0.6	0.36
$2x10^5$-$2x10^6$	0.031	0.2	0.8	0.36

The temperature of the fluid varies in the direction of flow, and, therefore, the value of the convective heat transfer coefficient (which depends on the temperature-dependent properties of the fluid) also varies in the direction of flow.
It is a common practice to compute the total heat transfer rate with the assumption of uniform convective heat transfer coefficient. With such an assumption of uniform convective heat transfer coefficient, uniform surface temperature and constant specific heat, the heat transfer rate to the fluid is related by the heat balance.

$$q = m^{\bullet} C_P (T_{\infty o} - T_{\infty i}) = \bar{h} A \left[T_S - \left(\frac{T_{\infty o} + T_{\infty i}}{2} \right) \right] \quad (9.26)$$

$T_{\infty i}$ = inlet free stream temperature
$T_{\infty o}$= outlet free stream temperature
$m^{\bullet}$ = out side tubes gaseous flow rate
= $\rho_{\infty i}(N_T S_T L)u_{\infty}$
A = Total heat transfer area
= $N_T N_L \pi DL$
N_T = number of tubes in transverse direction
N_L = number of tubes in lateral direction
L = length of tube per pass.

Pressure drop across tube banks:
Pressure drop is a significant factor, as it determines the power required to move the fluid across bank. The pressure drop for flow gases over a bank may be calculated with Equation 9.27.

$$\Delta p = \frac{2 f^{/} G_{\max}^2 N_T}{\rho} \left(\frac{\mu_S}{\mu} \right)^{0.14} \quad (9.27)$$

Δp = pressure drop in pascals.
$f^{/}$ = friction factor is given by Jacob
G_{max}= mass velocity at minimum flow rate, $kg/m^2.s$
ρ = density evaluated at free stream conditions, kg/m^3
N_T = number of transverse rows.
μ_S = fluid viscosity evaluated at surface temperature.
μ = average free stream viscosity.

For in-line:

$$f' = \left[0.044 + \frac{0.08 S_L / D}{\left(\frac{S_T - D}{D} \right)^{0.43 + 1.13 D / S_L}} \right] \mathrm{Re}_{\max}^{-0.15} \tag{9.28}$$

For staggered:

$$f' = \left[0.25 + \frac{0.118}{\left(\frac{S_T - D}{D} \right)^{1.08}} \right] \mathrm{Re}_{\max}^{-0.16} \tag{9.29}$$

Example 9.5: A heat exchanger with aligned tubes is used to heat 40 kg/sec of atmospheric air from 10 to 50 °C with the tube surfaces maintained at 100 °C. Details of the heat exchanger are
Diameter of tubes 25 mm
Number of columns (N_T) 20
Length of each tube 3 m
$S_L = S_T$ 75 mm
-Determine the number of rows (N_L) required

Solution:
Properties of atmospheric air at average air temperature = $(T_{\infty i} + T_{\infty o})/2 = 30$ °C.
$\rho = 1.151$ kg/ m^3
C_P= 1007 J/ kg.°C
k = 0.0265 W/ m.°C
$\mu = 186\text{x}10^{-7}$ N.s/ m^2
Pr = 0.7066

At surface temperature T_s=100 °C
$Pr_s = 0.6954$

At inlet free stream temperature $T_{\infty i}$=10 °C
$\rho_{\infty i} = 1.24$ kg/ m^3

To find u_∞

$$\dot{m} = \rho_{\infty i}(N_T S_T L) u_\infty$$
$$40 = 1.24(20\text{x}0.075\text{x}3)\, u_\infty$$
$$u_\infty = 7.168 \text{ m/s}$$

For in-line arrangement:

$$u_{\max} = u_\infty \left(\frac{S_T}{S_T - D} \right)$$
$$= 7.168 \times 0.075\ (0.075 - 0.025)$$

$$= 10.752 \text{ m/ s}$$

Reynolds number based on maximum velocity

$$Re_D = \rho u_{max} D/\mu = 1.151\times10.752\times0.025/(186\times10^{-7})$$
$$= 16633.8$$

From Table 9.4

$$p = 0$$
$$C = 0.27$$
$$m = 0.63$$
$$n = 0.36$$

From Equation 9.25

$$\overline{Nu}_D = 0.27\ (16633.8)^{0.63}\ (0.7066)^{0.36}(0.7066/0.6954)^{0.25} = 109.15$$
$$= \bar{h}\ D/\ k$$

The average heat transfer coefficient is

$$\bar{h} = 109.15\text{x}0.0265/0.025 = 115.699 \text{ W/m}^2.\text{k}$$

From Equation 9.26.The Total heat transfer is

$$q = m^{\bullet} C_P (T_{\infty o} - T_{\infty i}) = \bar{h}A\left[T_S - \left(\frac{T_{\infty o} + T_{\infty i}}{2}\right)\right]$$

$$40\text{x}1007\ (50 - 10) = 115.699\text{A}\ [100\text{-}30]$$

Total heat transfer area

$$A = 198.94 \text{ m}^2$$

Number of rows (N_L)

$$A = N_T N_L \pi D L$$
$$198.94 = 20 N_L\ (\pi \text{ x } 0.025 \text{ x } 3)$$
$$N_L = 43 \text{ rows}$$

9.5 Heat Transfer with Jet Impingement

The heat transfer with jet impingement on a heated (or cooled) surface results in high heat transfer rates, and is used in a wide range of applications such as cooling of electronic equipments. Usually, the jets are circular with round nozzle of diameter d, or rectangular with width w. They may be used individually or in an array. The jets may impinge normally to the heated surface as shown in Figure 9.4 or at an angle.

The liquid coolant under pressure inside a chamber is allowed to pass through a jet and directly into the heated surface, there are two modes of operation possible with liquid jet impingement, namely single phase cooling, and two phases cooling. And the jet may be free or submerged.

If there is no parallel solid surface close to the heated surface, the jet is said to be free as shown in Figure 9.4, while Jets may be submerged if the cavity is completely filled with the fluid (from the nozzle into a heated surface). In this lecture only single, free jets (round or rectangular) impinging normally to the heated surface are considered.

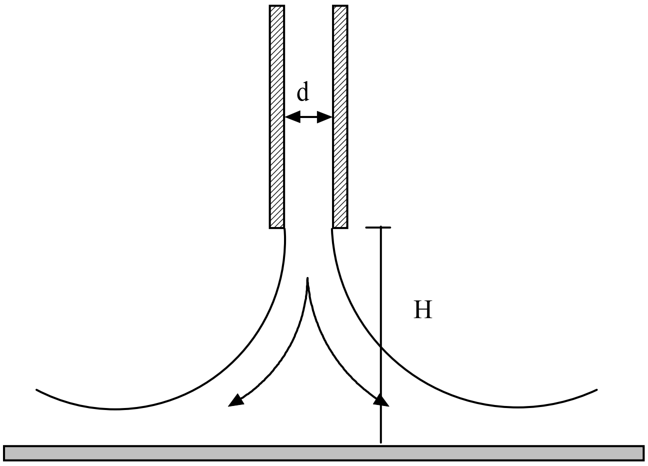

Figure 9.4 Jet impinge normally to the heated surface

Cooling analysis:

Free single phase jet impingement cooling is affected with many variables such as:

- Jet diameter (d)
- Fluid velocity (v)
- Jet to heated surface distance (H)
- Size of heated surface area (L x L)
- Coolant properties

The average heat transfer coefficient correlation is given by Jigi and Dagn

$$\overline{Nu}_L = 3.84\,\mathrm{Re}_d^{0.5}\,\mathrm{Pr}^{0.33}\left(0.008\frac{L}{d}+1\right) \qquad (9.30)$$

The properties are evaluated at mean film temperature $(T_S + T_\infty)/2$

This correlation is experimented for FC-77 and water and also valid for 3< H/d <15

- 3< H/d <15
- d = 0.508 to 1.016 mm
- v < 15 m/s
- small surface dimensions L<12.7 mm (microelectronic devices)

Example 9.6: A single phase free jet impingement nozzle is placed in the center of an electronic heated surface 12x12 mm^2 and the heated surface is placed at 4 mm from the jet.

The working medium is FC-77 passing through 1mm tube diameter at a rate of 0.015 kg/s.

To cool the plate, if the supply coolant is at 25 ºC and the heat load is 20 W

Determine the average heat transfer coefficient and the surface temperature of the heated surface.

Solution:

To get the properties of the FC-77 we need to assume the surface temperature: let the surface temperature equal 45 ºC as a first approximation.

$$T_f = (45 + 25)/2 = 35\,^{o}C$$

From FC-77 property tables at 35 ºC:

$\rho = 1746\ kg/m^3$

$\mu = 1.198\times10^{-3}\ N.s/m^2$

$k = 0.0623\ W/m.^{o}C$

$Pr = 20.3$

We must check on H/d ratio:

$$H/d = 4/1$$

Calculation of Reynolds number

$$Re = \rho vd / \mu = 4m' / \pi d\mu$$
$$= 4\times0.015 / \pi \times1\times10^{-3}\times1.198\times10^{-3}$$
$$= 15942$$

From Equation 9.30

$$\overline{Nu}_L = 3.84\,Re_d^{0.5}\,Pr^{0.33}\left(0.008\frac{L}{d}+1\right)$$
$$= 3.84\,(15942)^{0.5}\,(20.3)^{0.33}(0.008\times12/1+1)$$
$$= 1435.12$$

Knowing that $\overline{Nu}_l = \dfrac{\bar{h}L}{k}$

And so the average heat transfer coefficient is:

$$\bar{h} = (1435.12\times0.0623)/\,(12\times10^{-3})$$
$$= 7450.656\ W/m^2.k$$

But since $q = \bar{h}\,A\,\Delta T$

Then the temperature difference is:

$$\Delta T = 20/\,(7450.656\times12\times12\times10^{-6})$$
$$= 18.64\ ^{o}C$$

Therefore the surface temperature is:

$$T_S = 43.64\ ^{o}C$$

For more accuracy we may make another trial at new film temperature and reach more accurate results.

9.5.1 Case Study

The use of impinging air jets is proposed as a means of effectively cooling high-power logic chips in a computer. However, before the technique can be implemented, the convection coefficient associated with jet impingement on a chip surface must be known. Design an experiment that could be used to determine convection coefficients associated with air jet impingement on a chip measuring approximately 10 mm by 10 mm on a side.

9.6 Internal Flows (Inside Tubes or Ducts)

The heat transfer to (or from) a fluid flowing inside a tube or duct used in a modern instrument and equipment such as laser coolant lines ,compact heat exchanger , and electronics cooling(heat pipe method). Only heat transfer to or from a single-phase fluid is considered.

The fluid flow may be laminar or turbulent, the flow is laminar if the Reynolds number ($\square u_m D_H/\square$) is less than 2300 ($Re \le 2300$), based on the tube hydraulic diameter ($D_H = 4A / P$) where A, P is the cross sectional area and wetted perimeter respectively and u_m is average velocity over the tube cross section. Also the hydraulic diameter should be used in calculating Nusselt number. And If the Reynolds number is greater than 2300 the flow is turbulent ($Re > 2300$).

9.6.1 Fully Developed Velocity Profiles

When a fluid enters a tube from a large reservoir, the velocity profile at the entrance is almost uniform because the flow at the entrance is almost inviscid while the effect of the viscosity increase with the length of tube (in x-direction) which have an effect on the shape of the velocity profile as shown in Figure 9.5.

At some location downstream of the pipe inlet, the boundary layer thickness (δ) reaches its maximum possible value, which is equal to the radius of the tube at this point and the velocity profile does not change.
The distance from the entrance to this point is called fully developed region or entrance region, and it is expressed as the fully developing length (L_D), this length depends on the flow which may be laminar or turbulent.
Through the developing length (L_D) the heat transfer coefficient is not constant and after the developing length the heat transfer coefficient is nearly constant as shown in Figure 9.5.

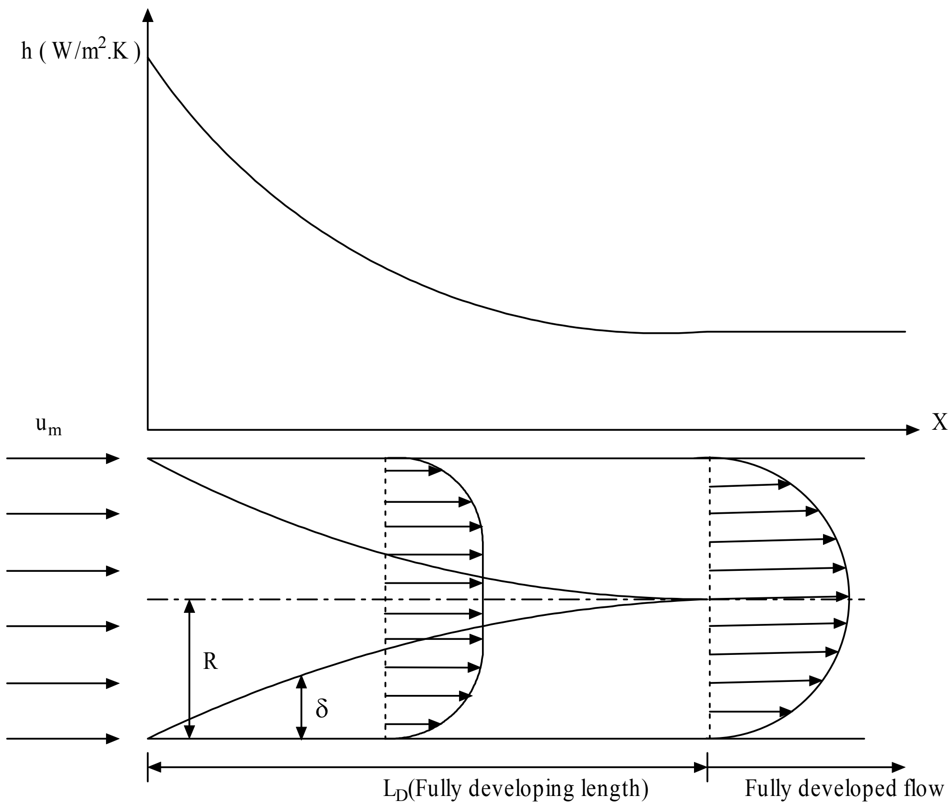

Figure 9.5 Flow inside the pipe

The fully developing length is given by:

$L_D/D = 0.05Re\ Pr$ -For laminar flow

And

$L_D/D = 10$ -For turbulent flow

9.6.2 Heat Transfer Correlations

Through the entrance region and after this region (fully developed flow) both regions have different heat transfer correlations, given in Table 9.6.

Table 9.6 Summery for forced convection heat transfer correlations - internal flow

Correlations		Conditions
Sieder and Tate (1936) $\overline{Nu}_D = 1.86\left(\frac{Re_D \Pr}{L/D}\right)^{1/3}\left(\frac{\mu}{\mu_S}\right)^{0.14}$	(9.31)	- Laminar , entrance region - uniform surface temperature - L/D < $\frac{Re_D \Pr}{8}\left(\frac{\mu}{\mu_S}\right)^{0.42}$ - 0.48 < Pr <16,700 - 0.0044 < μ/μ_S < 9.75
Nu_D =3.66	(9.32)	- Laminar , fully developed - Uniform surface temperature - Pr ≥ 0.6
Nu_D = 4.36	(9.33)	- Laminar , fully developed - Uniform Heat Flux - Pr ≥ 0.6
Dittus–Boelter (1930) $Nu_D = 0.023 Re_d^{4/5} \Pr^n$	(9.34)	- Turbulent flow, fully developed - 0.7 ≤ Pr≤ 160 , L/D ≥10 - n = 0.4 for heating ($T_s > T_m$) and - n = 0.3 for cooling ($T_s < T_m$).
Sleicher and Rouse (1976) $Nu_{D,m} = 4.8 + 0.0156 Re_{D,f}^{0.85} \Pr_S^{0.93}$ $Nu_{D,m} = 6.3 + 0.0167 Re_{D,f}^{0.85} \Pr_S^{0.93}$	(9.35) (9.36)	- For liquid metals , Pr «1 - Uniform surface temperature - For liquid metals , Pr «1 - Uniform heat flux

Properties of the fluid for each equation:
For Equation 9.31 at the arithmetic mean of the inlet and exit temperatures $(T_{mi}+T_{mo})/2$
For Equation 9.32, Equation 9.33 Equation 9.34 and at the mean temperature T_m
For Equation 9.35 and Equation 9.36 the subscripts m, f, and s indicate that the variables are to be evaluated at the mean temperature T_m, film temperature T_f (arithmetic mean of the mean temperature and surface temperatures $(T_S + T_m)/2$, and surface temperature, respectively.

9.6.3 Variation of Fluid Temperature(T_m) in a Tube

By taking a differential control volume as shown in Figure 9.6 considering that the fluid enters the tube at T_{mi} and exits at T_{mo} with constant flow rate m', convection heat transfer occurring at the inner surface (h), heat addition by convection q, neglecting the conduction in the axial direction, and assuming no work done by the fluid. Then applying heat balance on the control volume we can obtain an equation relating the surface temperature at any point.

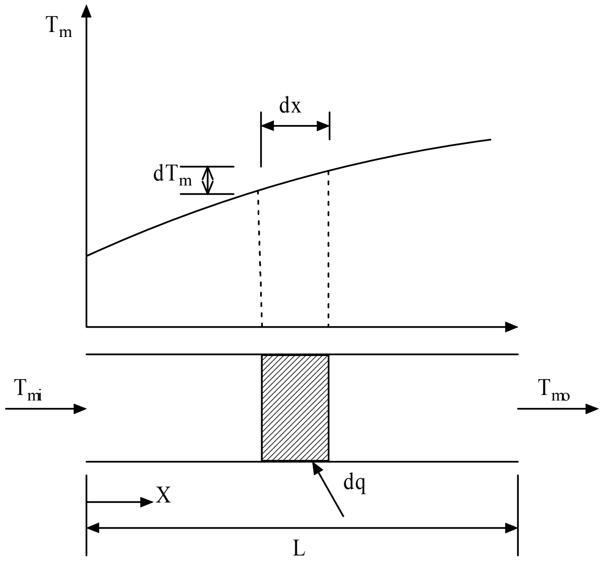

Figure9.6 differential control volume inside tube

Case 1:

- At uniform surface temperature T_S = constant

$$dq = m' C_p \, dT_m \tag{9.37}$$
$$= h\,(P_w dx)\,(T_S - T_m) \tag{9.38}$$

Where P_w = out side tube perimeter

By equating the both Equations 9.37, 9.38

$$\frac{dT_m}{dx} = \frac{hP_w}{m' C_p}(T_S - T_m) \tag{9.39}$$

$$T_S - T_m = \Delta T$$

$$\frac{dT_m}{dx} = -\frac{d\Delta T}{dx}$$

$$-\frac{d\Delta T}{dx} = \frac{hP_w}{m' C_p}(\Delta T)$$

$$-\frac{d\Delta T}{\Delta T} = \frac{hP_w}{m' C_p}dx \tag{9.40}$$

By integration of Equation 9.40 as shown bellow:

$$\int_{\Delta T_i}^{\Delta T_X} \frac{d\Delta T}{\Delta T} = \int_0^x \frac{hP_w}{m' C_p}dx$$

$$\int_{\Delta T_i}^{\Delta T_X} \frac{d\Delta T}{\Delta T} = \frac{xP_w}{m' C_p}\left(\frac{1}{x}\int_0^x h\,dx\right)$$

$$-\ln\left(\frac{\Delta T_x}{\Delta T_i}\right)=\frac{P_w \bar{h}}{m^{\cdot} C_p}x$$

$$\frac{\Delta T_x}{\Delta T_i}=e^{-\left(\frac{P_w \bar{h}}{m^{\cdot} C_p}x\right)}$$

At x = L

$$\frac{\Delta T_o}{\Delta T_i} = e^{-\left(\frac{p_w \bar{h}}{m^{\cdot} C_p} L\right)} \tag{9.41}$$

So that the temperature distribution along the tube is as shown in Figure 9.7

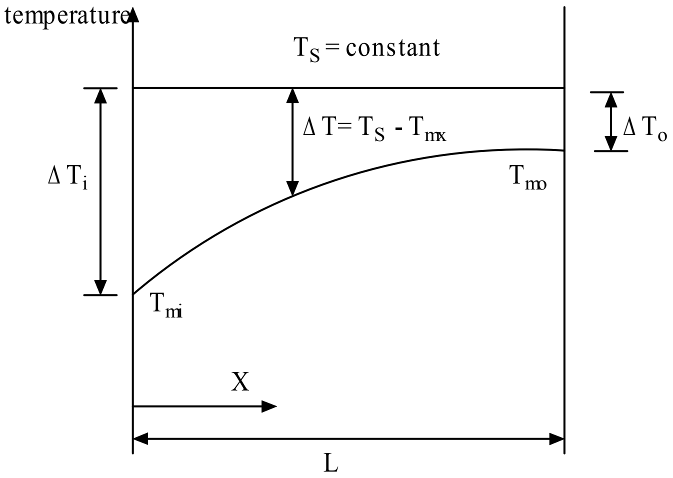

Figure 9.7 Temperature distributions along the tube at uniform surface temperature

The total heat transfer is:

$$q_t = m^{\cdot} C_p (T_{mo} - T_{mi}) \tag{9.42}$$

But also

$T_{mo} - T_{mi} = \Delta T_i - \Delta T_o$

So that the Equation 9.42 can be written as follows

$$q_t = m^{\cdot} C_p (\Delta T_i - \Delta T_o) \tag{9.43}$$

Also for total heat transfer by average heat transfer coefficient

$$q_t = \bar{h} L P_w (T_S - T_m)_{average} \tag{9.44}$$

From Equations 9.43, 9.44 produce:

$$m^{\cdot} C_p (\Delta T_i - \Delta T_o) = \bar{h} L P_w (\Delta T)_{average}$$

$$\Delta T_{average} = (\Delta T_i - \Delta T_o) \frac{m^{\cdot} C_p}{\bar{h} L P_w} \tag{9.45}$$

Where $\Delta T_{average} = (T_S - T_m)_{average}$

Substitute the Equation 9.41 in Equation 9.45 produces:

$$\Delta T_{average} = \frac{\Delta T_i - \Delta T_o}{\ln\left(\frac{\Delta T_i}{\Delta T_o}\right)} \tag{9.46}$$

$\Delta T_{average}$ called logarithmic mean temperature difference (LMTD)

Case 2:

- At uniform heat flux $q^{//}$ = constant

From Equation 9.37

$$dq = m^{'} C_p \, dT_m$$

And

$$dq = q^{//} P_w dx \qquad (9.47)$$

Combining both Equations 9.37, 9.47 produces:

$$\frac{dT_m}{dx} = \frac{q^{//} P_w}{m^{'} C_p} \qquad (9.48)$$

By integration:

$$\int_{T_{mi}}^{T_{mx}} dT_m = \frac{q^{//} P_w}{m^{'} C_p} \int_0^x dx$$

$$T_{mx} - T_{mi} = \frac{q^{//} P_w}{m^{'} C_p} x \qquad (9.49)$$

And

$$q^{//} = h\,(T_S - T_m)$$

$$T_S - T_m = q^{//} / h \approx \text{constant along the tube length} \qquad (9.50)$$

From the Equations 9.49, 9.50 the temperature distribution as shown in Figure 9.8.

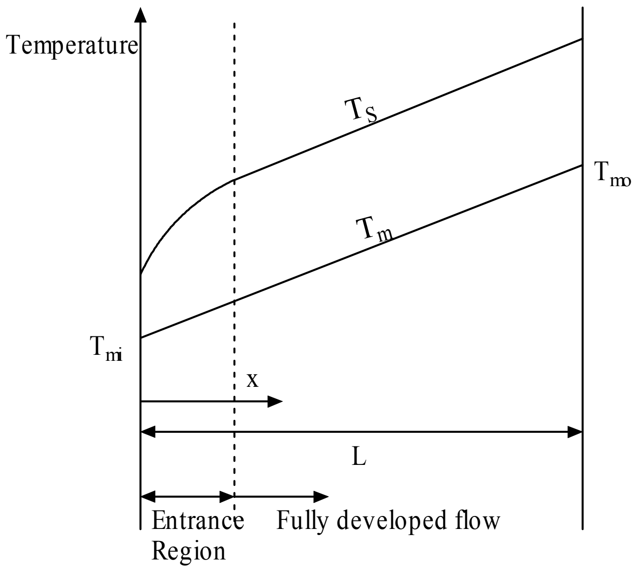

Figure 9.8 Temperature distributions along the tube at uniform heat flux

For along the tube length

$$T_{mo} = T_{mi} + \frac{q^{//} P_w}{m^{'} C_p} L$$

10. Radiation Heat Transfer

10.1 Introduction

Radiation heat transfer plays a major role in the cooling of electronics. As well as conduction and convection heat transfer, radiation is an equally important mode.
Also the thermal radiation has many applications such as engine cooling, furnaces, boilers, piping and solar radiation.
The thermal radiation transferred by electromagnetic waves, called photons, is emitted by bodies due to temperature differences. All surfaces continuously emit and absorb radiative energy by lowering or raising their molecular energy levels.
The electromagnetic waves travel through any medium or in vacuum at the speed of light (c), which equals 3×10^8 m/s. this speed equal to the product of the wave length λ and frequency ν

$$c = \lambda \nu$$

The metric unit for the wave length λ is centimeters or angstroms (1 angstrom = 10^{-8} centimeter). A portion of the electromagnetic spectrum is shown in Figure 10.1.

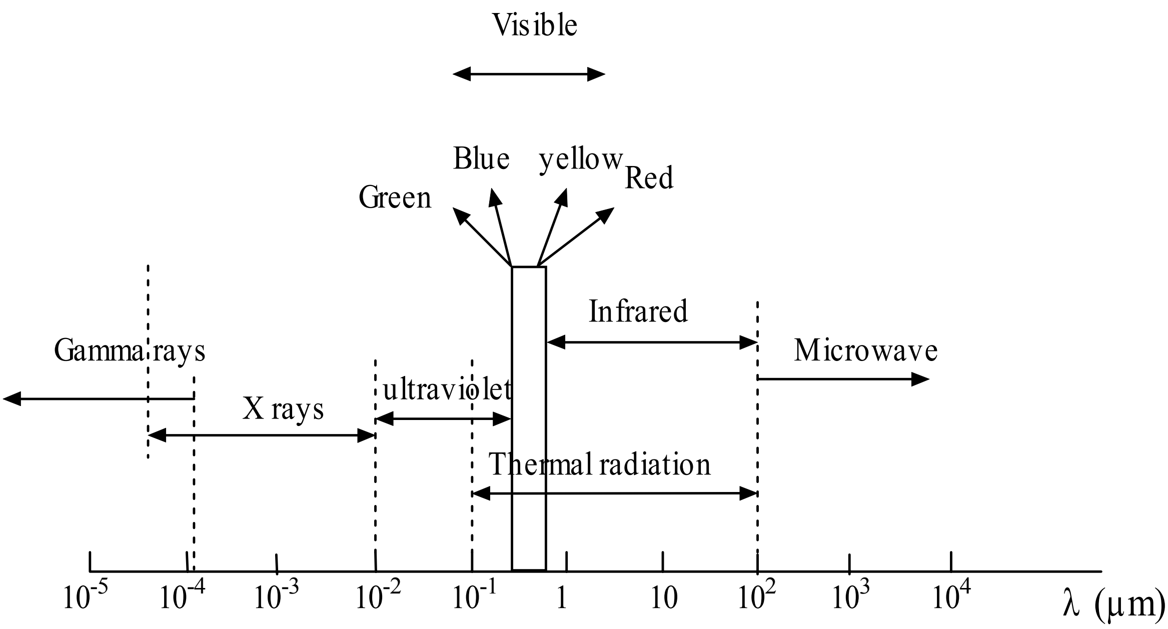

Figure 10.1 Electromagnetic spectrum

10.2 Blackbody Radiation

Materials used in electronic hard ware may be classified as black or gray surfaces.
The ideal surface is known as a "blackbody" or "black surface," since it absorbs or emits 100% of the all incoming radiation.
A rough surface has higher emittance than the same surface when it is smooth. Also, a finned surface has a higher emittance than does the same surface without fins. In both cases the emittance increases because the surfaces have many small cavities. These cavities act as many small partial black bodies.

For example a small hole in a hollow sphere is often used to represent a black body. The energy enters the small opening and strikes the opposite wall, where part of the energy is absorbed and part is reflected. The reflected energy again strikes the opposite wall, where part of the energy is absorbed and part is

reflected. This process continues until all of the energy is absorbed, as shown in Figure10.2.
The total amount of radiative energy emitted from a surface into all directions above it is termed emissive power; we distinguish between spectral (at a given wavelength λ, per unit wavelength and per unit surface area) and total (encompassing all wavelengths) emissive power. The magnitude of emissive power depends on wavelength λ, temperature T, and a surface property, called emissivity ε, which relates the ability of a surface to emit radiative energy to that of an ideal surface, which emits the maximum possible energy (at a given wavelength and temperature).
The spectral distribution of the emissive power $E_{\lambda,b}$ of a black surface is given by Planck's law is of the form

$$E_{\lambda,b} = \frac{C_1}{\lambda^5[e^{(C_2/\lambda T)} - 1]} \qquad (10.1)$$

Where the radiation constants or some times called Planck function constants are $C_1 = 3.742 \times 10^8$ W.µm^4/m^2 and $C_2 = 1.439 \times 10^4$ µm.k.

The total emissive power E_b of a blackbody is given by Stefan-Boltzmann law. Expressed as

$$E_b = \int_0^\infty E_{b,\lambda} d\lambda$$

Integration yields;

$$E_b = \sigma T^4 \qquad (10.2)$$

Where the temperatures in the Kelvin's and the Stefan-Boltzmann constant (σ) has the numerical value

$$\sigma = 5.67 \times 10^{-8} \text{ W/m}^2.\text{K}$$

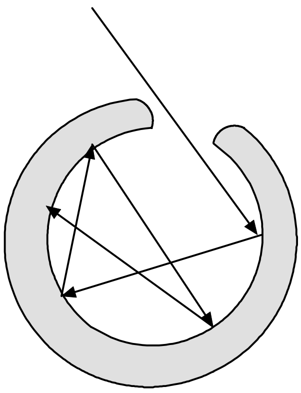

Figure 10.2 Constructing a black body enclosure

Figure 10.3 shows the spectral emissive power $E_{\lambda,b}$ as a function of temperature and wavelength, the maximum $E_{\lambda,b}$ is corresponding to wave length λ_{max} which depends on surface temperature.
The nature of this dependence may be obtained by differentiating the Equation 10.1 with respect to λ and setting the result equal to zero, we obtain

$$\lambda_{max} T = 2897.6 \text{ µm.K} \qquad (10.3)$$

The Equation 10.3 is known as Wien's displacement law.

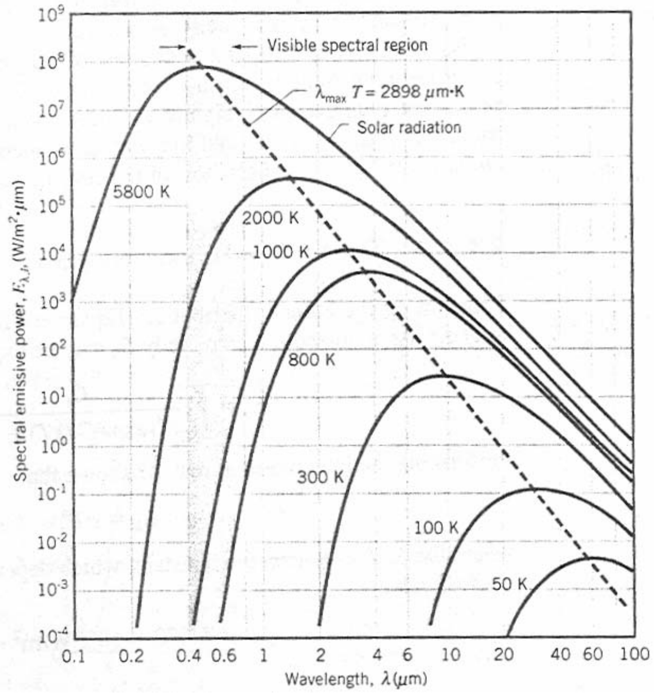

Figure 10.3 Spectral emissive power $E_{\lambda,b}$ as a function of temperature and wavelength

10.3 Radiation Properties of Surfaces

When radiant energy strikes a material surface as shown in Figure 10.4, part of this radiation is reflected, part is absorbed, and part is transmitted. So that radiation properties are defined:

Reflectivity $\rho = \dfrac{\text{reflected part of incoming radiation}}{\text{total incoming radiation}}$

Absorptivity $\alpha = \dfrac{\text{absorbed part of incoming radiation}}{\text{total incoming radiation}}$

Transmissivity $\tau = \dfrac{\text{transmitted part of incoming radiation}}{\text{total incoming radiation}}$

Emissivity $\varepsilon = \dfrac{\text{energy emitted from a surface}}{\text{energy emitted by a black surface at same temperature}}$

The emissivities of clean metallic materials are generally very low while the emissivities of nonmetallic materials are much higher. Typical emissivity values for various materials are shown in Table 10.1. That emissivity is a surface phenomenon can be demonstrated by placing a thin coat of paint on a highly polished metal surface. Before painting a polished copper surface, the emissivity will be about 0.03. However, with just a thin coat of lacquer, 0.00127 cm thick, the emissivity of the same surface will increase sharply to about 0.8.

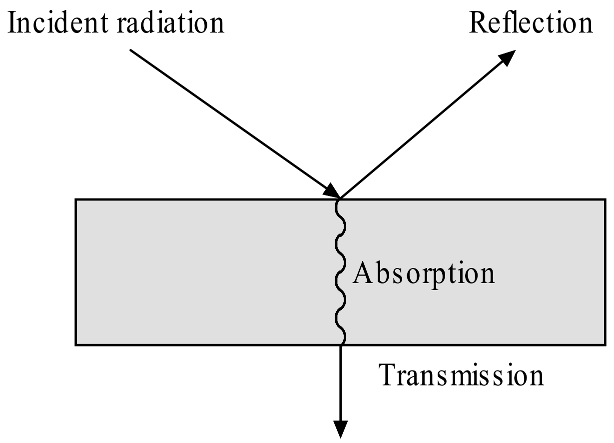

Figure 10.4 Reflection, absorption, and transmission

Since all radiation striking a body must be reflected, absorbed, or transmitted, it follows that

$$\rho + \alpha + \tau = 1 \qquad (10.4)$$

In some practical applications surface layers are thick enough to be opaque then the transmissivity may be taken as zero.

All four properties may be functions of wavelength, temperature, incoming direction (except emissivity), and outgoing direction (except absorptivity).

Table 10.1 Typical emissivities at 100 ^{o}C

Material	Emissivity
Aluminum	
Commercial sheet	0.09
Rough polish	0.07
Gold, highly polished	0.018-0.035
Steel, polished	0.06
Iron, polished	0. 14-0.38
Cast iron, machine cut	0.44
Brass, polished	0.06
Copper, polished	0.023-0.052
Polished steel casting	0.52-0.56
Glass, smooth	0.85-0.95
Aluminum oxide	0.33
Anodized aluminum	0.81
Black shiny lacquer on iron	0.8
Black or white lacquer	0.8-0.95
Aluminum paint and lacquer	0.52
Rubber, hard or soft	0.86-0.94

Two types of reflection phenomena may be observed when radiation strikes a surface. The reflection is called specular if the angle of incidence is equal to the angle of reflection as shown in Figure 10.5(a), the reflection is called diffuse when the incident beam is distributed uniformly in all directions after reflection as shown in Figure 10.5(b).No real surface is either specular or diffuse. An ordinary mirror is quite specular for visible light, but would not necessarily be specular over the entire wave length range of thermal radiation. Ordinarily, a rough surface exhibits diffuse behavior better than polished surface. Similarly, a polished surface is more specular than a rough surface.

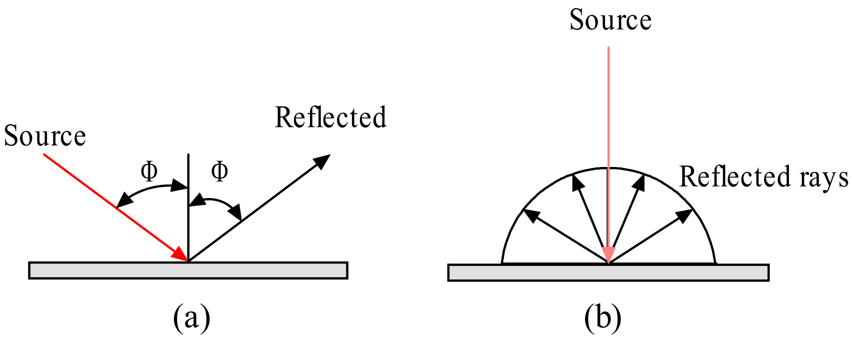

Figure 10.5 (a) Specular reflection (b) Diffuse reflection

10.4 Kirchhoff's Law

Assume that a perfectly black enclosure is available, i.e., one which absorbs all the incident radiation falling upon it, as shown in Figure10.6.

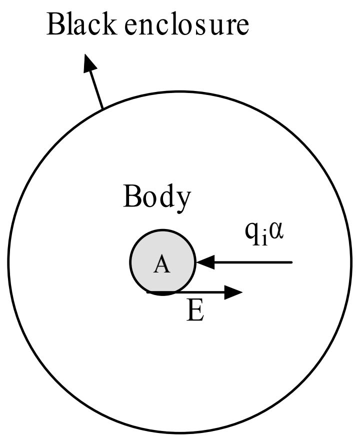

Figure10.6 Model used for deriving Kirchhoff's law

This enclosure will also emit radiation according to the T^4 law. The radiant flux arriving at a given area inside the enclosure is q_i W/m^2.

Now suppose that a body is placed inside the enclosure until it reaches equilibrium. At equilibrium the energy absorbed must be equal to the energy emitted.

The radiation absorbed by the body = $q_i\alpha$ A

The radiation emitted from the body = EA

At equilibrium

$$EA = q_i \alpha A \qquad (10.5)$$

If the body is replaced by a black body (α =1) with the same area and shape and allowed to equilibrium at the same temperature.

$$E_b A = q_i A \qquad (10.6)$$

If the Equation 10.5 is divided by Equation 10.6 it yields

$$\alpha = E / E_b$$

This ratio is the emissive power of a body to the emissive power of a black body at same temperature. It is also defined before as the emissivity(ε) of the body.
So that, for any surface inside enclosure

$$\alpha = E / E_b = \varepsilon \qquad (10.7)$$

The Equation 10.7 is called Kirchhoff's law.

10.5 Radiation between Black Surfaces and Shape Factors

The shape factor F_{ij} is the fraction of radiant energy leaving one surface that is intercepted by another surface; other names for the shape factor are view factor, angle factor, and geometrical factor. To develop a general expression for F_{ij}, consider two black surfaces has A_1 and A_2 as shown in Figure 10.7.When the two surfaces are maintained at different temperature we want to determine the amount of energy which leaves one surface to another. Firstly we define the shape factor as
F_{1-2} = Fraction of radiation leaving A_1 arriving at A_2
F_{2-1} = Fraction of radiation leaving A_2 arriving at A_1

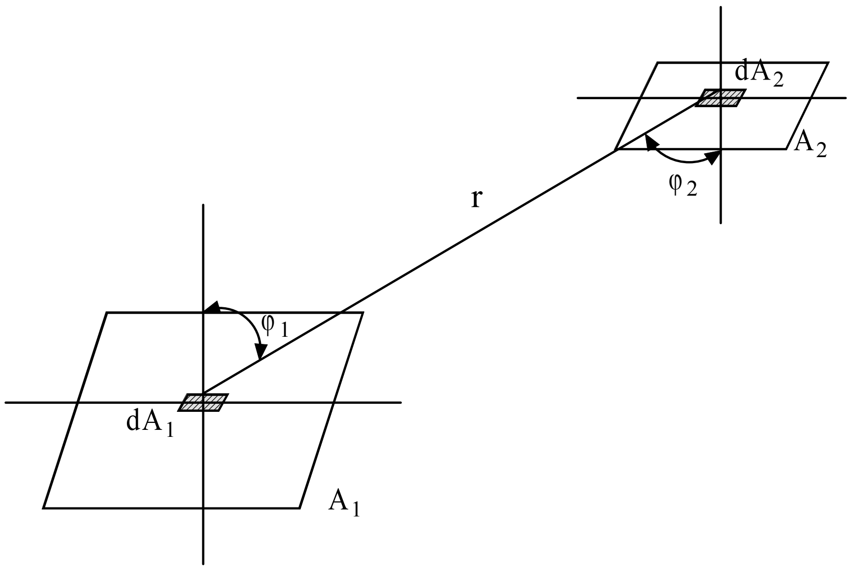

Figure 10.7 Model for deriving radiation shape factor

The energy leaving surface 1 and arriving at surface2 is

$$q_{1-2} = A_1F_{12}\, E_{b1}$$

The energy leaving surface 2 and arriving at surface1 is

$$q_{2-1} = A_2F_{21}\, E_{b2}$$

The net energy exchange is

$$q_{net} = A_1F_{12}\, E_{b1} - A_2F_{21}\, E_{b2} \qquad (10.8)$$

If the two surfaces are at same temperatures, there would not be heat exchange between them so that q_{net} equals to zero. In this case Equation10.8 will be

$$A_1F_{12}\, E_{b1} = A_2F_{21}E_{b2} \qquad (10.9)$$

Also at same temperatures: $E_{b1} = E_{b2}$ which simplify Equation10.9 to

$$A_1F_{12} = A_2F_{21} \qquad (10.10)$$

For general expression for any two surfaces i and j:

(10.11)

$$A_iF_{ij} = A_jF_{ji}$$

Equation 10.11 is known as the reciprocity relation

Considering the elements dA_1 and dA_2 as shown in Figure 10.7, the energy leaving surface dA_1 and arriving at surface dA_2 is

$$dq_{1-2} = \frac{E_{b1}}{\pi} dA_1 \cos\varphi_1 \, dw \tag{10.12}$$

Where dw is the solid angle subtended by dA_2 when viewed from dA_1, its mathematical expression is:

$$dw = \frac{\text{Projection of } dA_2 \text{ on the line between centers}}{r^2} = \frac{dA_2 \cos\varphi_2}{r^2}$$

Substituting in Equation 10.12 gives

$$dq_{1-2} = \frac{E_{b1} \cos\varphi_1 \cos\varphi_2}{\pi r^2} dA_1 dA_2$$

Similarly the energy leaving surface dA_2 and arriving at surface dA_1 is

$$dq_{2-1} = \frac{E_{b2} \cos\varphi_2 \cos\varphi_1}{\pi r^2} dA_1 dA_2 \tag{10.13}$$

The net energy exchange between dA_1 and dA_2 is

$$\begin{aligned} dq_{net} &= dq_{1-2} - dq_{2-1} \\ &= \frac{(E_{b1} - E_{b2})}{\pi r^2} \cos\varphi_2 \cos\varphi_1 dA_1 dA_2 \end{aligned} \tag{10.14}$$

Performing double integration on Equation 10.14 with respect to A_1 and A_2 yields

$$q_{net} = (E_{b1} - E_{b2}) \iint_{A_2 \, A_1} \frac{\cos\varphi_2 \cos\varphi_1 dA_1 dA_2}{\pi r^2} \tag{10.15}$$

But

$$A_1 F_{12} = A_2 F_{21} = \iint_{A_2 \, A_1} \frac{\cos\varphi_2 \cos\varphi_1 dA_1 dA_2}{\pi r^2} \tag{10.16}$$

This gives

$$\begin{aligned} q_{net} &= (E_{b1} - E_{b2}) A_1 F_{12} \\ &= (E_{b1} - E_{b2}) A_2 F_{21} \\ &= \sigma (T_1^4 - T_2^4) A_2 F_{21} \end{aligned} \tag{10.17}$$

A few graphical results that present the shape factor for important geometries are shown in Appendix A.
But For nontrivial geometries shape factors must be calculated by double integration of Equation10.16.

10.6 Shape Factor Relations

Some important shape factor relations are suggested below.

10.6.1 Reciprocity Relation

As explained before during previous derivations, this relation is useful in determining one shape factor from knowledge of the other.

$$A_iF_{ij} = A_jF_{ji}$$

10.6.2 Summation Rule

$$\sum_{j=1}^{N} F_{ij} = 1 \tag{10.18}$$

Note that the term F_{ii} is non zero if the surface is concave because it sees it self and equal zero for a plane or convex surface.
This role is applied on enclosures surfaces.

Example 10.1: Determine the view factor F_{12} for the Figure shown below knowing that $D_1 = D_2 = 5$ cm and a = 8 cm.

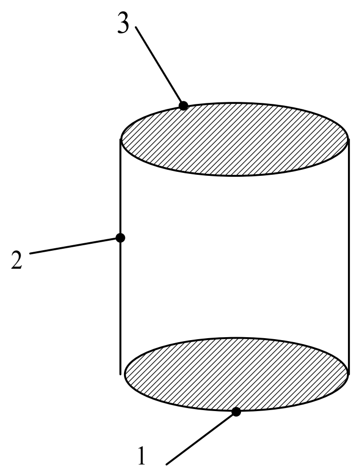

Solution:

For an enclosure
$$\sum_{j=1}^{N} F_{ij} = F_{11} + F_{12} + F_{13} = 1$$

Where $F_{11} = 0$

From Figure A.1 at $r_1/a = r_2/a = 5/8 = 0.625$

$$\therefore\ F_{13} = 0.22$$

Then

$$F_{12} = 1 - F_{13} = 1 - 0.22 = 0.78$$

Example 10.2: Determine the view factor F_{12} and F_{13} for the figure shown below knowing that the angles $\alpha_1 = \alpha_2$.

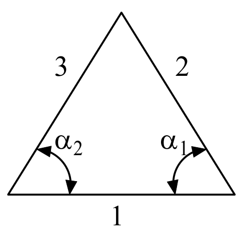

Solution:
It is an enclosure rectangle so that

$$F_{11} + F_{12} + F_{13} = 1$$

Where $F_{11} = 0$
Because $\alpha_1 = \alpha_2$ then

$$F_{12} = F_{13} = 0.5$$

10.6.3 Division of Receiving Surface

$$F_{ij} = \sum_{k=1}^{n} F_{ik} \tag{10.19}$$

I.e. chip exposed to several heat sinks as shown below

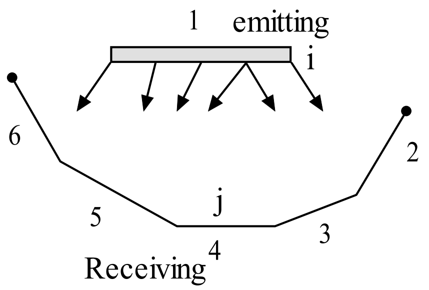

The fraction of heat radiates from chip 1 arrived to the another surfaces2, 3,4,5,6 is

$$F_{1-2,\,3,4,5,6} = F_{12} + F_{13} + F_{14} + F_{15} + F_{16}$$

10.6.4 Division of Emitting Surface

$$A_j F_{ji} = \sum_{k=1}^{n} A_k F_{ki} \tag{10.20}$$

The schematic shown below is a typical example for Division of emitting surface.

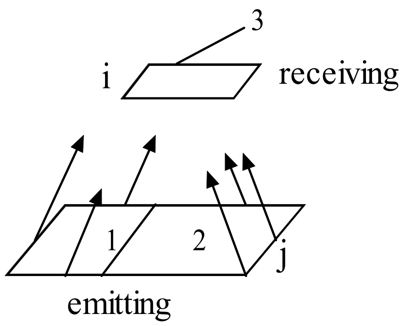

$$A_j = \sum_{k=1}^{n} A_k$$

Where $\qquad A_{1,2} F_{1,\,2\text{-}3} = A_1 F_{13} + A_2 F_{23}$

Example 10.3: Determine the view factor F_{13} for the Figure shown below knowing that it's dimensions $L = h = w = 1$ cm.

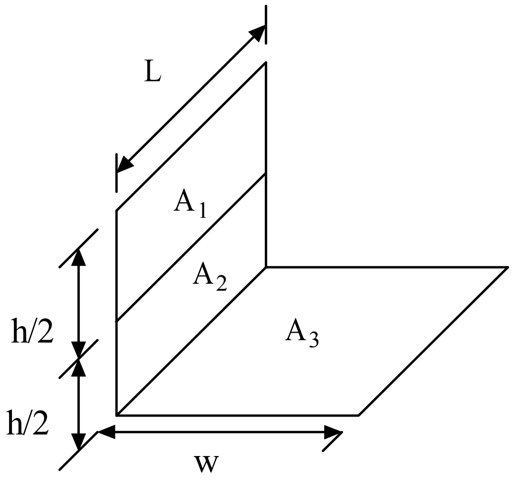

Solution:
By taking the areas $A_1$and A_2 with A_3 and using Equation 10.19 to gives

$$F_{3\text{-}1,\,2} = F_{31} + F_{32}$$

From Figure A.3 at
W = 1   and   H = 1

$$\therefore F_{3\text{-}1,\,2} = 0.2$$

By taking the areas A_2 with A_3 and from Figure A.3 at
H = 0.5   and W = 1

$$\therefore F_{32} = 0.15$$

Substitute in main equation to gives

$$F_{31} = 0.2 - 0.15 = 0.05$$

By using reciprocity relation
$A_3F_{31}=A_1F_{13}$
Then $\therefore F_{13} = 0.1$

Appendix A

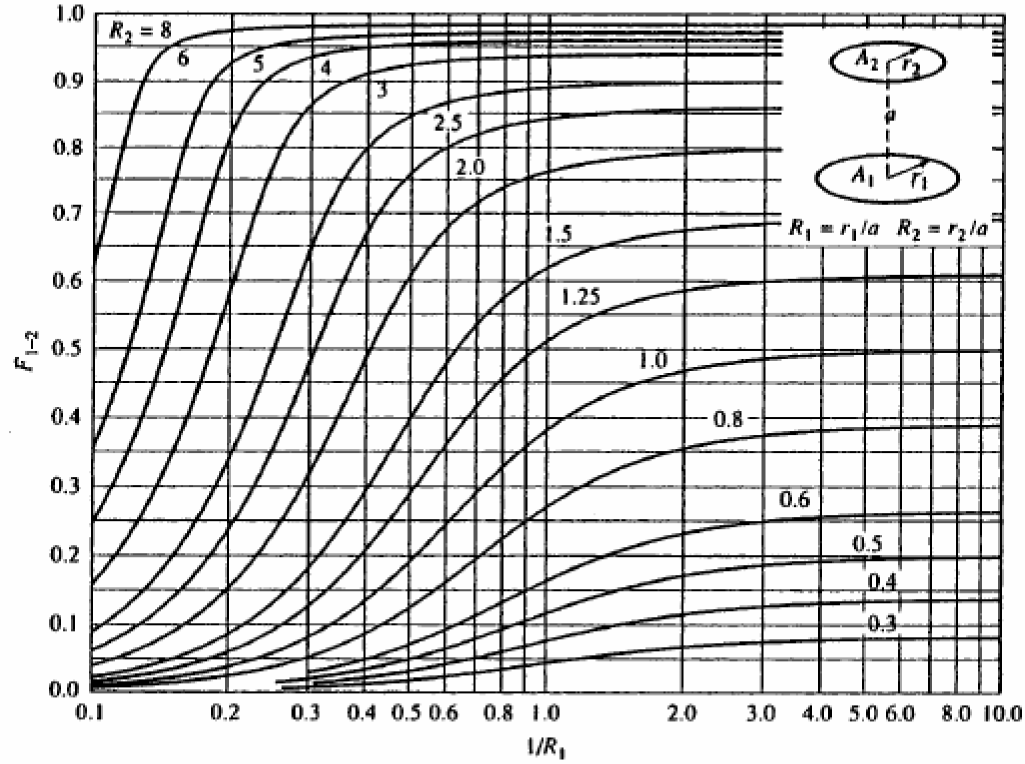

Figure A.1 View factor between parallel, coaxial disks of unequal radius

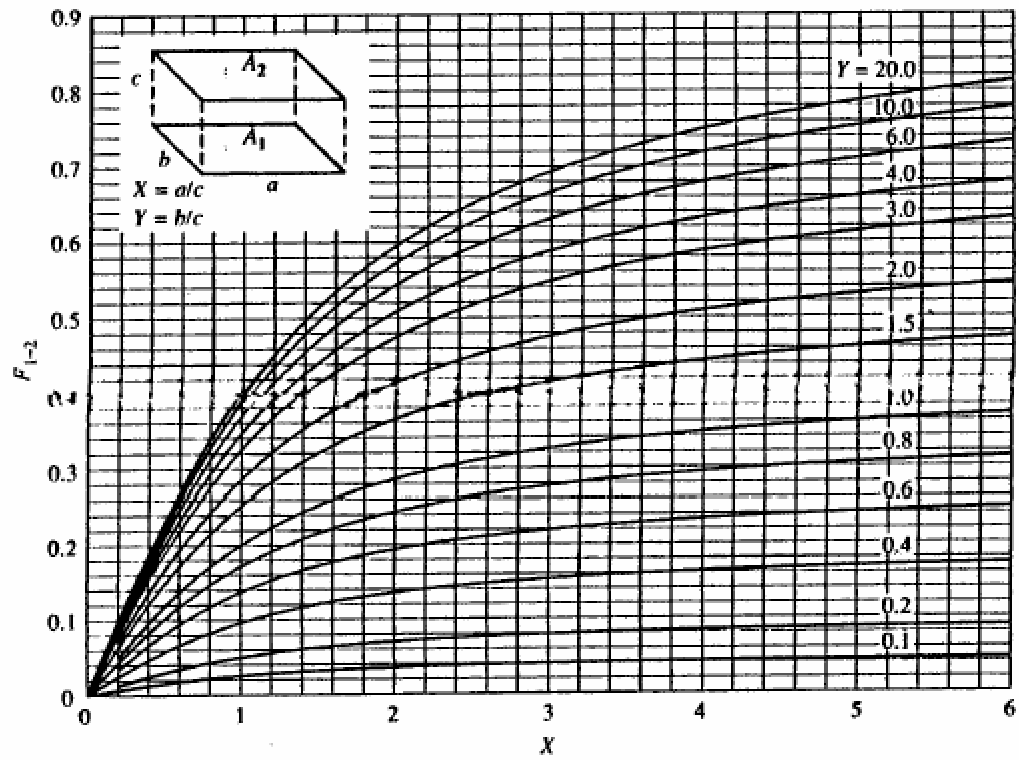

Figure A.2 View factor between identical, parallel, directly opposed rectangles

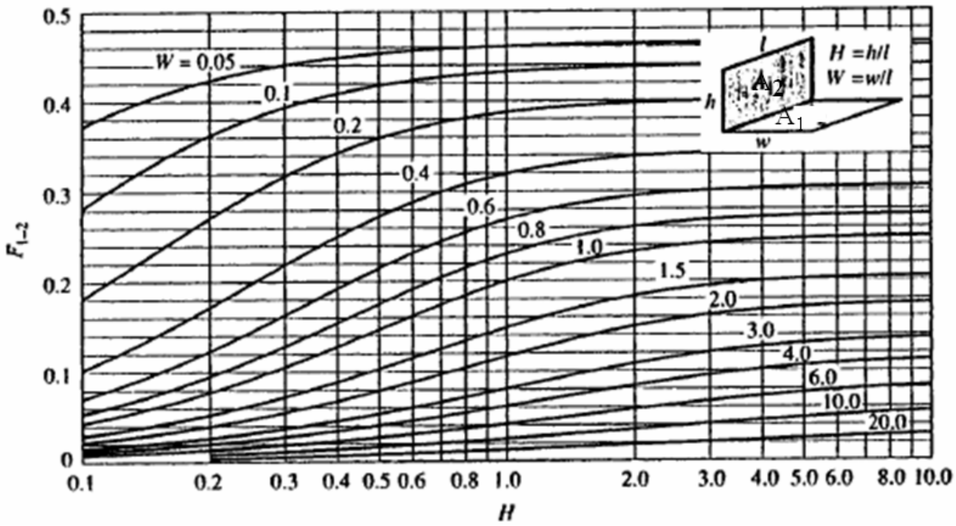

Figure A.3 View factor between perpendicular rectangles with common edge

11. Advanced Radiation

11.1 Gray Surfaces

The gray surface is a medium whose monochromatic emissivity (ε_λ) does not vary with wavelength. The monochromatic emissivity is defined as the ratio of the monochromatic emissive power of the body to monochromatic emissive power of a black body at same wave length and temperature.

$$\varepsilon_\lambda = E_\lambda / E_{\lambda,b} \qquad (11.1)$$

But

$$E = \int_0^\infty \varepsilon_\lambda E_{\lambda,b} d\lambda$$

And

$$E_b = \int_0^\infty E_{\lambda,b} d\lambda = \sigma T^4$$

So that

$$\varepsilon = \frac{\int_0^\infty \varepsilon_\lambda E_{\lambda,b} d\lambda}{\sigma T^4} \qquad (11.2)$$

Where: $E_{\lambda,b}$ is the emissive power of a black body per unit wave length.

If the gray body condition is imposed, that is, ε_λ = constant, so that:

$$\varepsilon = \varepsilon_\lambda = \text{constant} \qquad (11.3)$$

11.2 Radiation Exchange between Gray Surfaces (ε = Constant)

The calculation of the radiation heat transfer between black bodies is relatively easy because all the radiant energy which strikes a surface is absorbed (reflectivity = 0). For non black bodies (such as gray bodies) the situation is much more complex, because all the radiant energy which strikes a surface will not be absorbed, part will be reflected back to another surface, and part will be reflected out of the system entirely. Thus, we need to define two new terms:

G = irradiation or total incident radiation (W/m^2)

J = radiosity or total radiation leaving the surface (W/m^2)

Our assumptions are that all surfaces considered in our analysis are diffuse, isothermal and that the radiations properties are constant over all surfaces as well as the irradiation and radiosity. Now the objective is to determine the net radiation heat transfer (q) from each surface.

From Figure 11.1 (a) and the definition of the radiosity we can mathematically define the radiosity as:

$$J = \varepsilon E_b + \rho G \qquad (11.4)$$

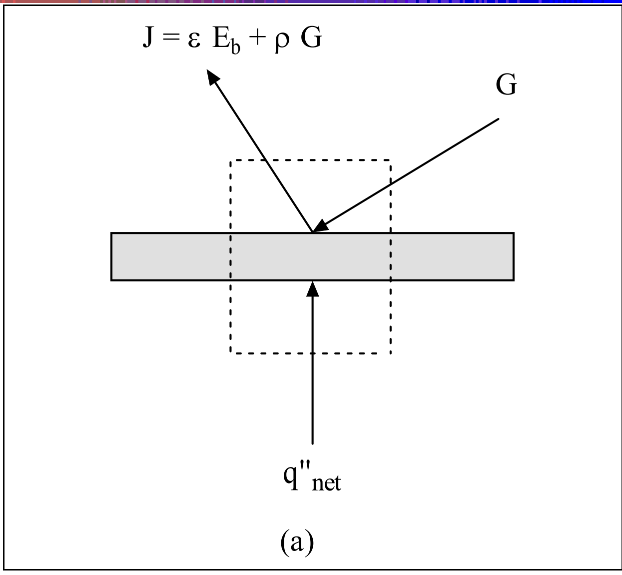

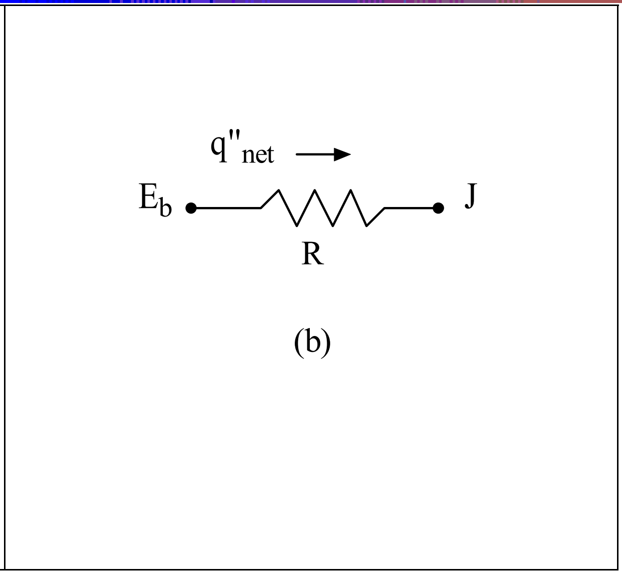

Figure 11.1(a) surface energy balance, (b) surface resistance in the radiation network method

Since the transimissivity is assumed to be zero then the reflectivity may be expressed as

$$\rho = 1- \alpha$$

Knowing that for a gray surface $\alpha = \varepsilon$, then

$$\rho = 1- \varepsilon$$

An enhanced mathematical formula for the radiosity will be:

$$J = \varepsilon E_b + (1-\varepsilon) G$$

Or,

$$G = \frac{J - \varepsilon E_b}{(1-\varepsilon)}$$

From the energy balance shown in Figure11.1 (a) the net radiation flux leaving the surface is

$$q''_{net} = J - G = J - \frac{J - \varepsilon E_b}{(1-\varepsilon)} = \frac{\varepsilon (E_b - J)}{(1-\varepsilon)} \qquad (11.5)$$

The general equation for net radiation heat transfer leaving the surface is

$$q_{net} = \frac{(E_b - J)}{\left(\dfrac{1-\varepsilon}{\varepsilon A}\right)} = \frac{(E_b - J)}{R} = \frac{\text{Potential difference}}{\text{Surface resistance}} \qquad (11.6)$$

The analogy between radiation heat transfer and electric circuit is shown in Figure 11.1 (b). The heat flows as the current through a resistance.

Now consider the exchange of radiant energy between two surfaces 1, 2 as shown in Figure 11.2.

The total radiation which leaves A_1, reaching A_2 is

$$J_1 A_1 F_{12}$$

Similarly the total radiation which leaves A_2, reaching A_1 is

$$J_2 A_2 F_{21}$$

The net radiation between the two surfaces is

$$q_{1-2} = J_1 A_1 F_{12} - J_2 A_2 F_{21}$$

Recalling the reciprocity relation

$$A_1 F_{12} = A_2 F_{21}$$

Then,

$$q_{1-2} = (J_1 - J_2) A_1 F_{12}$$

$$q_{1-2} = q_{net} = \frac{J_1 - J_2}{\left(\frac{1}{A_1 F_{12}}\right)} = \frac{J_1 - J_2}{R} = \frac{\text{Potential difference}}{\text{Space resistance}} \qquad (11.7)$$

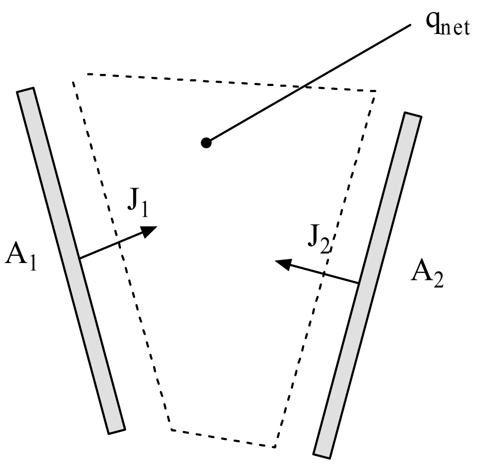

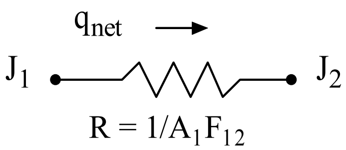

Figure 11.2 Radiation exchange between two surfaces

Now we can write the general equation which connect between the surface and space resistance between two surfaces as

$$q_{1-2} = \frac{E_{b1} - E_{b2}}{\left(\frac{1-\varepsilon_1}{\varepsilon_1 A_1}\right) + \left(\frac{1}{A_1 F_{12}}\right) + \left(\frac{1-\varepsilon_2}{\varepsilon_2 A_2}\right)} = \frac{\sigma(T_1^4 - T_2^4)}{\left(\frac{1-\varepsilon_1}{\varepsilon_1 A_1}\right) + \left(\frac{1}{A_1 F_{12}}\right) + \left(\frac{1-\varepsilon_2}{\varepsilon_2 A_2}\right)} \qquad (11.8)$$

The resistances of Equation 11.8 are shown in Figure 11.3 below.

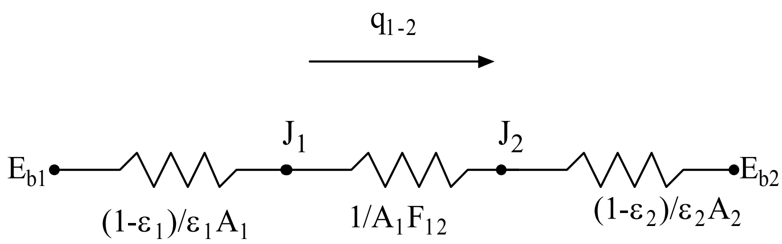

Figure 11.3 Radiation network for two surfaces

11.2.1 Special Cases for Two Gray Surfaces

(a) Long (infinite) concentric cylinders:

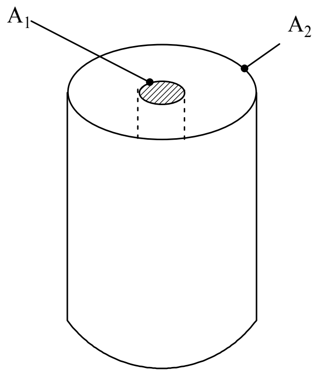

By applying summation rule

$$F_{11} + F_{12} = 1$$

$$F_{11} = 0 \quad \text{so that} \quad F_{12} = 1$$

$$q_{1-2} = \frac{\sigma A_1 (T_1^4 - T_2^4)}{\frac{1}{\varepsilon_1} + (\frac{1}{\varepsilon_2} - 1)\frac{A_1}{A_2}}$$

(b) Two long (infinite) parallel planes:

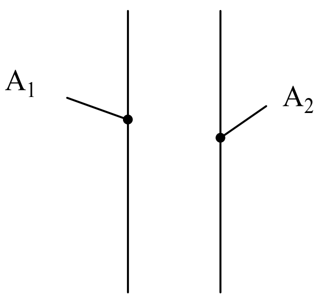

By applying summation rule

$$F_{11} + F_{12} = 1$$

$$F_{11} = 0 \quad \text{so that} \quad F_{12} = 1 \text{ and } A_1 = A_2$$

$$q_{1-2} = \frac{\sigma A\ (T_1^4 - T_2^4)}{(\frac{1}{\varepsilon_1} + \frac{1}{\varepsilon_2} - 1)}$$

(c) Two concentric spheres:

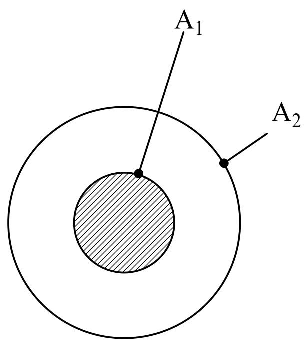

By applying summation rule to gives $F_{12} = 1$ and knowing that $A_1/A_2 = (r_1/r_2)^2$

$$q_{1-2} = \frac{\sigma A_1 (T_1^4 - T_2^4)}{\frac{1}{\varepsilon_1} + (\frac{1}{\varepsilon_2} - 1)\left(\frac{r_1}{r_2}\right)^2}$$

(d) Small body in large enclosure:

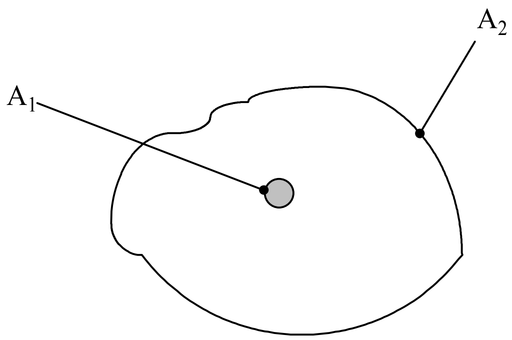

$A_1/A_2 \approx 0$

By applying summation rule to gives $F_{12} = 1$

$$q_{1-2} = \sigma \varepsilon_1 A_1 (T_1^4 - T_2^4)$$

11.3 Radiation Exchange between Three Gray Surfaces

If we have three surfaces the network for this system is shown in Figure 11.4.

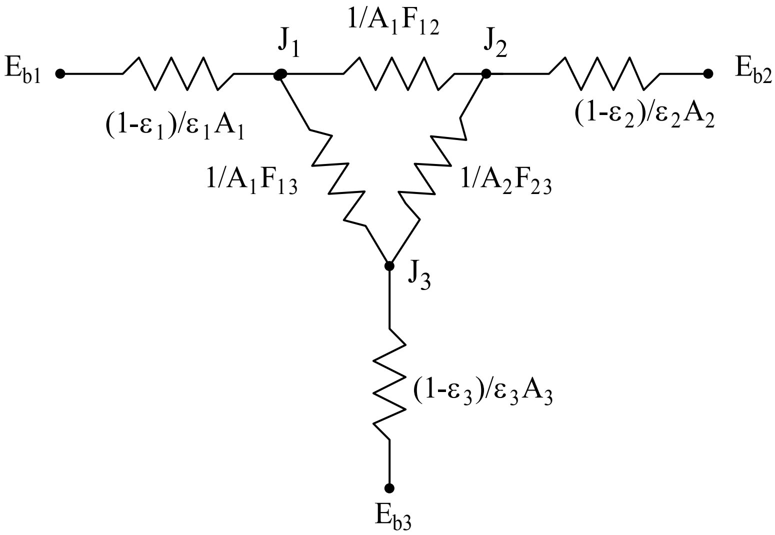

Figure 11.4 Network for three surfaces

By applying the Kirchhoff's law: "Summation of currents entering each node equals to zero"

At node J_1:

$$\frac{E_{b1}-J_1}{\left(\frac{1-\varepsilon_1}{\varepsilon_1 A_1}\right)}+\frac{J_2-J_1}{\left(\frac{1}{A_1F_{12}}\right)}+\frac{J_3-J_1}{\left(\frac{1}{A_1F_{13}}\right)}=0$$

At node J_2:

$$\frac{E_{b2}-J_2}{\left(\frac{1-\varepsilon_2}{\varepsilon_2 A_2}\right)}+\frac{J_3-J_2}{\left(\frac{1}{A_2F_{23}}\right)}+\frac{J_1-J_2}{\left(\frac{1}{A_1F_{12}}\right)}=0$$

At node J_3:

$$\frac{E_{b3}-J_3}{\left(\frac{1-\varepsilon_3}{\varepsilon_3 A_3}\right)}+\frac{J_2-J_3}{\left(\frac{1}{A_2F_{23}}\right)}+\frac{J_1-J_3}{\left(\frac{1}{A_1F_{13}}\right)}=0$$

Solving the above three equations for the radiosity yield the values of them, thus we could calculate the energy exchange between different surfaces.

11.3.1 Special Cases for Three Gray Surfaces

(a) Two surfaces inside very large enclosure:

Due to a very large area ($A \longrightarrow \infty$) the surface resistance approaches zero, which makes it behave like a black body with $\varepsilon = 1$, and will have $J = E_b$ because of the zero surface resistance.

An example network for this case may be as shown in Figure 11.5.

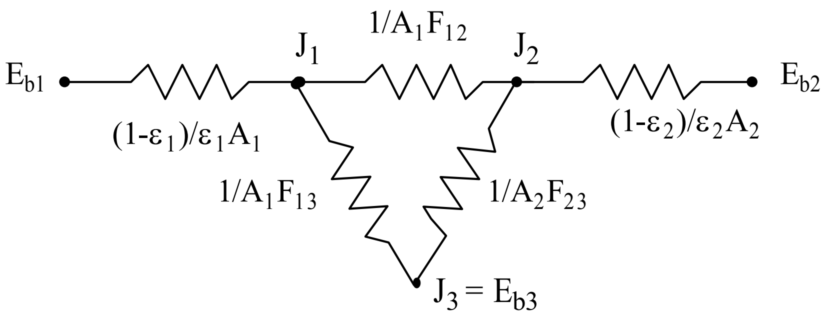

Figure 11.5 Network for surfaces inside enclosure

(b) Insulated surfaces:

If a surface is perfectly insulated, or re-radiates the entire energy incident upon it, it has zero heat flow and the potential across the surface resistance is zero surface resistance. In effect, the J node in the network is floating, i.e., it does not draw any current. An example network for this case may be as shown in Figure 11.6(a) and may be simplified to Figure 11.6(b).

The total circuit resistance of the circuit is

$$R_{total} = R_1 + \frac{1}{\left(\frac{1}{R_2}\right) + \left(\frac{1}{R_3 + R_4}\right)} + R_5$$

So that the net radiation heat exchange is

$$q_{net} = \frac{E_{b1} - E_{b2}}{R_{total}} = \frac{\sigma (T_1^4 - T_2^4)}{R_{total}} \qquad (11.9)$$

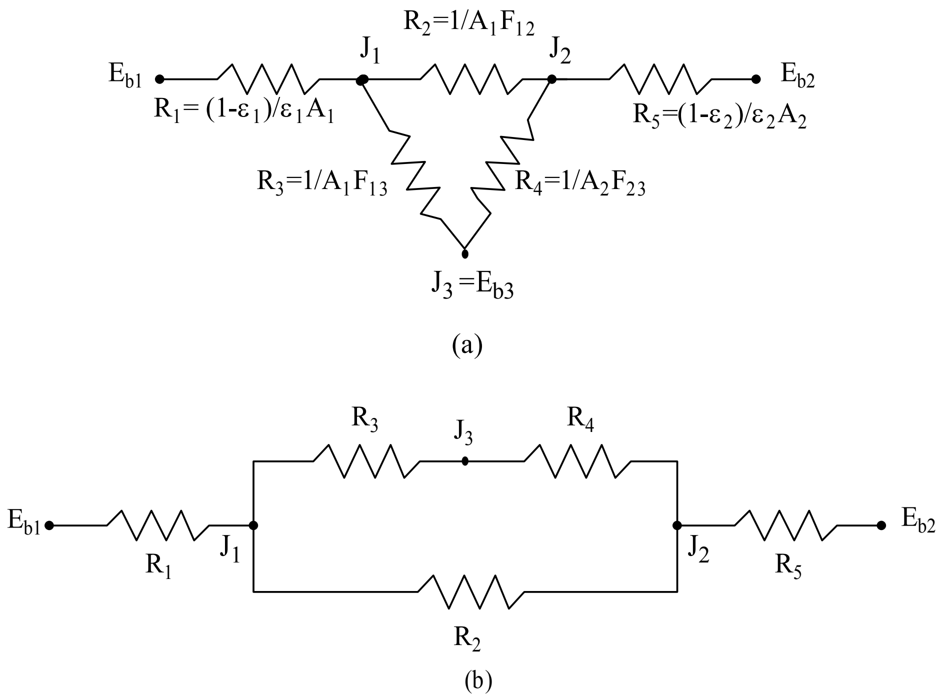

Figure 11.6 (a) Network for two surfaces with another insulated surface.
(b) Simplification for this network.

11.4 Radiation Shields

If it is desired to minimize radiation heat transfer between two surfaces, it is a common practice to place one or more radiation shields between them as shown in Figure 11.7. These shields do not deliver or remove any heat from the overall system; they only place another resistance in the heat flow path so that the overall heat transfer is retarded.

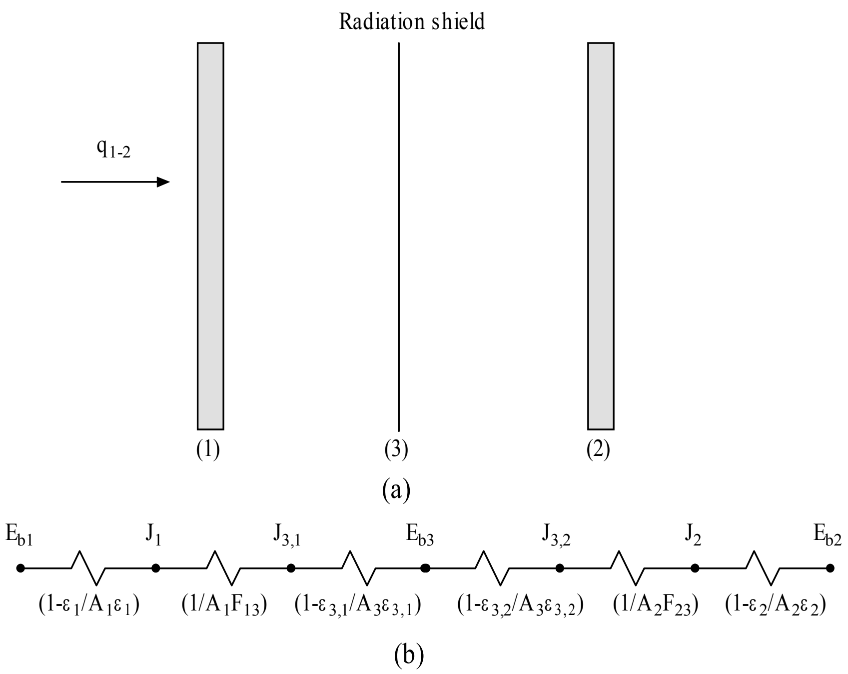

Figure 11.7 (a) Radiation between parallel planes with radiation shield,
(b) Network representation.

The general equation for the net radiation heat transfer is

$$q_{1-2} = \frac{E_{b1} - E_{b2}}{\left(\frac{1-\varepsilon_1}{A_1\varepsilon_1}\right) + \left(\frac{1}{A_1F_{13}}\right) + \left(\frac{1-\varepsilon_{3,1}}{A_3\varepsilon_{3,1}}\right) + \left(\frac{1-\varepsilon_{3,2}}{A_3\varepsilon_{3,2}}\right) + \left(\frac{1}{A_2F_{23}}\right) + \left(\frac{1-\varepsilon_2}{A_2\varepsilon_2}\right)}$$

$$= \frac{\sigma(T_1^4 - T_2^4)}{\left(\frac{1-\varepsilon_1}{A_1\varepsilon_1}\right) + \left(\frac{1}{A_1F_{13}}\right) + \left(\frac{1-\varepsilon_{3,1}}{A_3\varepsilon_{3,1}}\right) + \left(\frac{1-\varepsilon_{3,2}}{A_3\varepsilon_{3,2}}\right) + \left(\frac{1}{A_2F_{23}}\right) + \left(\frac{1-\varepsilon_2}{A_2\varepsilon_2}\right)} \qquad (11.10)$$

If surfaces are large (Infinite) and close together, so that $A_1 \approx A_2 \approx A_3 = A$, and $F_{13} = F_{23} = 1$
Then the net radiation heat transfer is.

$$q_{1-2} = \frac{\sigma A(T_1^4 - T_2^4)}{2 + \left(\frac{1-\varepsilon_1}{\varepsilon_1}\right) + \left(\frac{1-\varepsilon_{3,1}}{\varepsilon_{3,1}}\right) + \left(\frac{1-\varepsilon_{3,2}}{\varepsilon_{3,2}}\right) + \left(\frac{1-\varepsilon_2}{\varepsilon_2}\right)} \qquad (11.11)$$

Example 11.1: A PCB maintained at 45 ºC is exposed to a parallel cold plate which is maintained at 10 ºC. Each plate is 0.2 × 0.15 m, the plates are placed 0.04 m apart. Consider the PCB and Cold plate as black bodies. What is the net radiant heat exchange between the PCB and the Cold plate?

Solution:

From the Figure A.2 with the ratios

X = 0.2 / 0.04 = 5 and Y = 0.15 / 0.04 = 3.75

We can read F_{12} = 0.64

Using Equation 10.17 the net radiant heat transfer is

$$\begin{aligned} q_{net} &= \sigma\, A_1 F_{12}(T_1^4 - T_2^4) \\ &= (5.67x10^{-8})(0.2x0.15)(0.64)(318^4 - 283^4) \\ &= 4.15 \text{ W} \end{aligned}$$

Example 11.2: The vertical side of an electronics box is 40 × 30 cm with the 40 cm side vertical. What is the maximum heat transfer that could be dissipated by this side if its temperature is not to exceed 60 ºC in an environment and surrounding of 40 ºC, if its emissivity is 0.8?

Solution:

The total heat transfer is due to natural convection and radiation heat transfer so that

$$q_{tot} = q_{conv.} + q_{rad.}$$

(a) Convection heat transfer calculation:

$$q_{conv.} = \bar{h}A(T_S - T_\infty)$$

Evaluate the properties of the air at the film temperature (T_f = 100/2 = 50 °C)
ν = 18.2 x 10^{-6} m^2/s.
k = 0.028 W/m. °C
Pr= 0.7038
C_p= 1008 J/kg. °C
β = 1/323 = 3.096 x10^{-3}
The characteristic length (L) = 0.4 m

The Gr Pr product is

$$Gr\,\mathrm{Pr} = \frac{9.81 \times 3.096 \times 10^{-3} \times 20(0.4)^3}{(18.2 \times 10^{-6})^2} 0.7038 = 82.6 \times 10^6$$

From the Nusselt number

$$\overline{Nu} = \frac{\bar{h}L}{k} = c(Gr\,\mathrm{Pr})^m$$

With the constants

$$c = 0.59 \quad \text{and} \quad m = 0.25$$

Then;

$$\overline{Nu} = 0.59(82.6 \times 10^6)^{0.25}$$
$$= 56.25$$

So that the average heat transfer coefficient is

$$\bar{h} = \frac{\overline{Nu}\,k}{L} = \frac{56.25 \times 0.028}{0.4} = 3.94 \text{ W/m}^2.^\circ\text{C}$$

The convection heat transfer is

$$q_{conv.} = 3.94 \times (0.3 \times 0.4)(60 - 40) = 9.456 \text{ W}$$

(b) Radiation heat transfer calculation: (Small body in large enclosure)

$$q_{rad.} = \sigma\varepsilon\ A\ (T_S^4 - T_{surrounding}^4)$$
$$= 5.67 \times 10^{-8}(0.8)(0.3 \times 0.4)(333^4 - 313^4)$$
$$= 14.688 \text{ W}$$

The maximum heat transfer that could be dissipated by this side is

$$q_{tot.} = 9.456 + 14.688 = 24.144 \text{ W}$$

Example 11.3: Two parallel PCBs 0.2 × 0.2 are spaced 0.1 m apart. One PCB is maintained at 55 ºC and the other at 40 ºC. The emissivities of the PCBs are 0.2 and 0.5, respectively. The PCBs are located inside a large chassis, the inside walls of chassis are maintained at 30 ºC. The PCBs exchange heat with each other and with the chassis, but only the PCBs surfaces facing each other are to be considered in the analysis. Calculate the net transfer to PCBs and to the chassis.

Schematic:

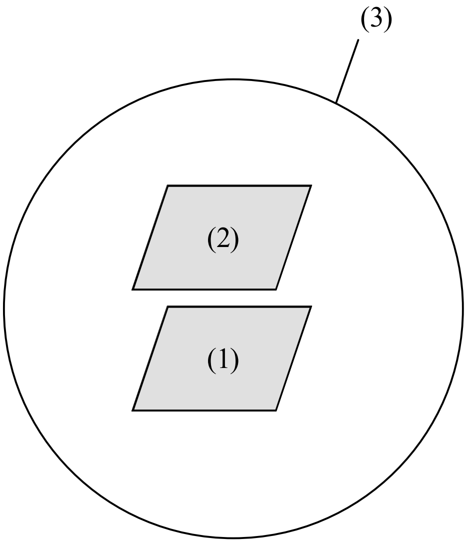

Solution:

This case resembles two surfaces inside a large enclosure case.

$T_1 = 328$ K $\quad A_1 = 0.04\ m^2 \quad \varepsilon_1 = 0.2$
$T_2 = 313$ K $\quad A_1 = A_2 = 0.04\ m^2 \quad \varepsilon_1 = 0.5$
$T_3 = 303$ K

From Figure A.2 with the ratios

$X = 0.2/0.1 = 2$ and $Y = 0.2/0.1 = 2$

So that $F_{12} = F_{21} = 0.42$

$F_{13} = 1 - F_{12} = 0.58$
$F_{23} = 1 - F_{21} = 0.58$

The network for this case is typically as that of Figure 11.5, and then the resistances in the network are:

$$\frac{1-\varepsilon_1}{\varepsilon_1 A_1} = \frac{1-0.2}{(0.2)(0.04)} = 100$$

$$\frac{1-\varepsilon_2}{\varepsilon_2 A_2} = \frac{1-0.5}{(0.5)(0.04)} = 25$$

$$\frac{1}{A_1 F_{12}} = \frac{1}{(0.04)(0.42)} = 59.5$$

$$\frac{1}{A_1 F_{13}} = \frac{1}{A_2 F_{23}} = \frac{1}{(0.04)(0.58)} = 43.1$$

At node J_1:
$$\frac{E_{b1}-J_1}{100}+\frac{J_2-J_1}{59.5}+\frac{E_{b3}-J_1}{43.1}=0 \qquad (1)$$

At node J_2:
$$\frac{E_{b2}-J_2}{25}+\frac{E_{b3}-J_2}{43.1}+\frac{J_1-J_2}{59.5}=0 \qquad (2)$$

But,

$$E_{b1}=\sigma T_1^4=656.26\ \text{W/m}^2$$
$$E_{b2}=\sigma T_2^4=544.2\ \text{W/m}^2$$
$$E_{b3}=J_3=\sigma T_3^4=477.92\ \text{W/m}^2$$

Now both Equations (1) and (2) have two unknowns J_1 and J_2 which may be solved simultaneously to give

$J_1 = 528.27$ W/m^2
$J_2 = 521.63$ W/m^2

The total heat lost by PCB number 1 is

$$q_1=\frac{E_{b1}-J_1}{\left(\dfrac{1-\varepsilon_1}{\varepsilon_1 A_1}\right)}=\frac{656.26-528.27}{100}=1.28\,\text{W}$$

The total heat lost by PCB number 2 is

$$q_2=\frac{E_{b2}-J_2}{\left(\dfrac{1-\varepsilon_2}{\varepsilon_2 A_2}\right)}=\frac{544.2-521.63}{25}=0.903\,\text{W}$$

From an overall-balance we must have

$$q_3=q_1+q_2=2.183\,\text{W}$$

Example 11.4: A square flat pack hybrid 2.54 cm side, 0.457cm high have a maximum allowable temperature of 100 ºC mounted on the end of a PCB so that it faces the end wall of an electronic chassis, which has a temperature of 50 ºC, as shown in the following figure. The hybrid is about 1.02 cm from the wall, so that natural convection and conduction heat transfer will be negligible. Determine the maximum allowable power dissipation for the hybrid with ($\varepsilon = 0.8$) and without ($\varepsilon = 0.066$) a conformal coating.

Schematic:

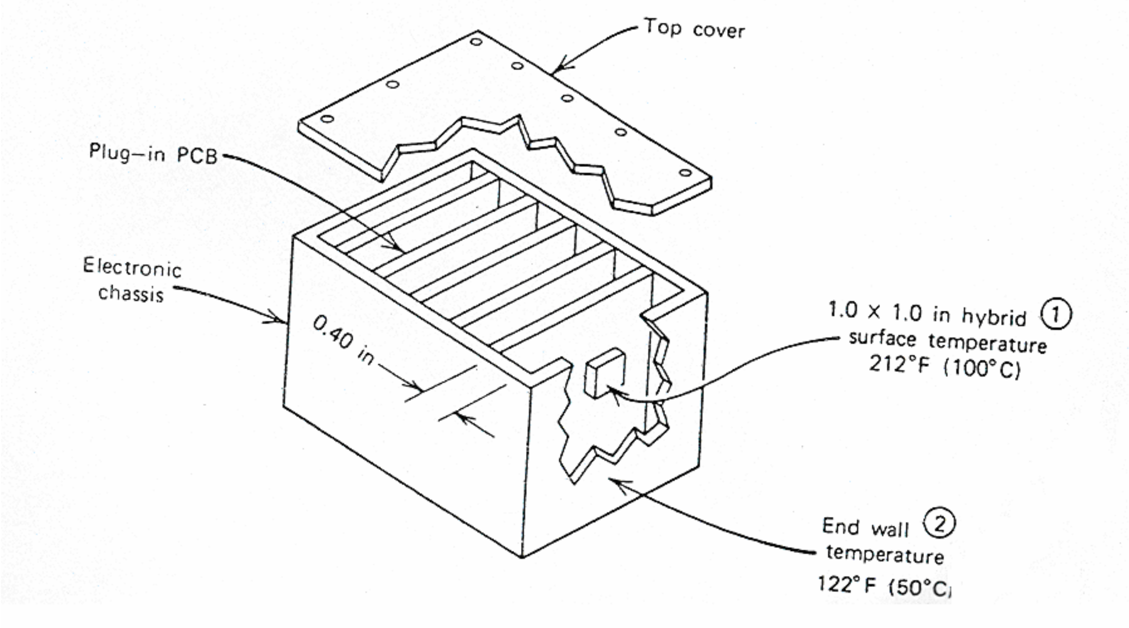

Solution:

The hybrid flat pack may be assumed as a small body in large enclosure case.

(a) The heat transfer from the hybrid without coating is:

$$q = \sigma \varepsilon_1 A_1 (T_1^{\,4} - T_2^{\,4})$$

$$q = 5.67 \times 10^{-8} \times 0.066 \times (0.0254)^2 \left(373^4 - 323^4\right) = 0.02 \text{ W}$$

(b) The heat transfer from the hybrid with coating.

$$q_{coat} = \frac{0.8}{0.066} q_{without\ coat} = \frac{0.8}{0.066} \times 0.02 = 0.242 \text{ W}$$

Comment:
Adding a conformal coating to the hybrid will increase its heat transfer capability, thus allowing for extra heat dissipation. This might be regarded as a plus as it allows extra packing of electronic components inside this hybrid.

12. Case Study: Using EES in Electronics Cooling

What is EES?

EES (pronounced 'ease') stands for Engineering Equation Solver. The basic function provided by EES is the solution of a set of algebraic equations. EES can solve differential equations, equations with complex variables, do optimization, provide linear and non-linear regression and generate plots.

There are two major differences between EES and existing numerical equation-solving programs. First, EES automatically identifies and groups equations that must be solved simultaneously. This feature simplifies the process the user and ensures that the solver will always operate at optimum efficiency.
Second. EES provides many built-in mathematical and thermophysical property functions useful for engineering calculations. So that we can use EES for solving many electronics cooling problems

EES Features List

- Flexible for any engineer to use it
- Solves up to 6000 simultaneous non-linear equations
- Extremely fast computational speed
- SI and English units
- Parametric studies with spreadsheet-like table
- Single and multi-variable optimization capability
- Multi-dimensional optimization
- Uncertainty analysis
- Linear and non-linear regression
- Professional plotting (2-D, contour, and 3-D) with automatic updating
- Graphical user input/output capabilities with Diagram window

EES Applications in Electronics Cooling Problems

Problem 1:
A cable 10 mm diameter at 80 ^{o}C surface temperature is to be insulated to maximize its current carrying capacity. The heat transfer coefficient for the outer surface is estimated to be 10 W /m^2 .K. and 25 ^{o}C outside air temperature.
What should be the radius of the chosen insulation at 0.15 W /m .K. insulation thermal conductivity? By what percentage would the insulation increase the energy carrying capacity of the bare cable?

Objective: (1) modeling any problems (2) Optimization (3) Plot results

Solution:

1- Governing equations or the equation window.

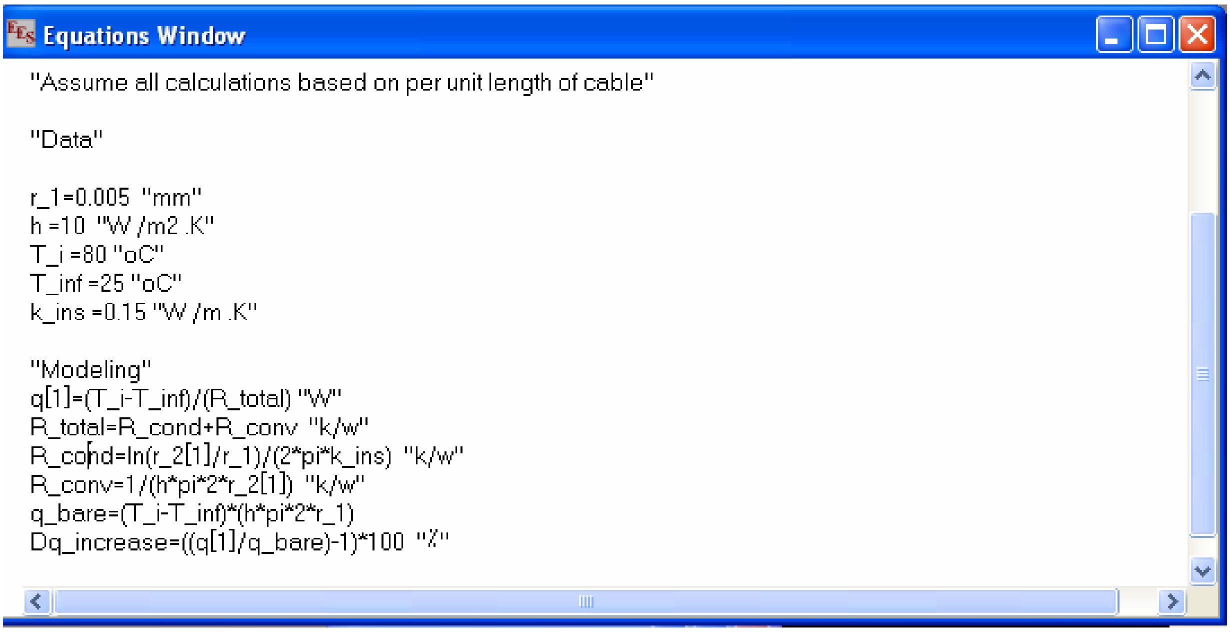

2- Press the following

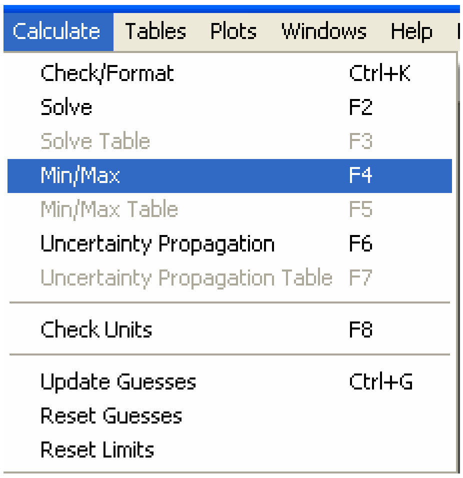

3- Change the dialog box to appear as the following one

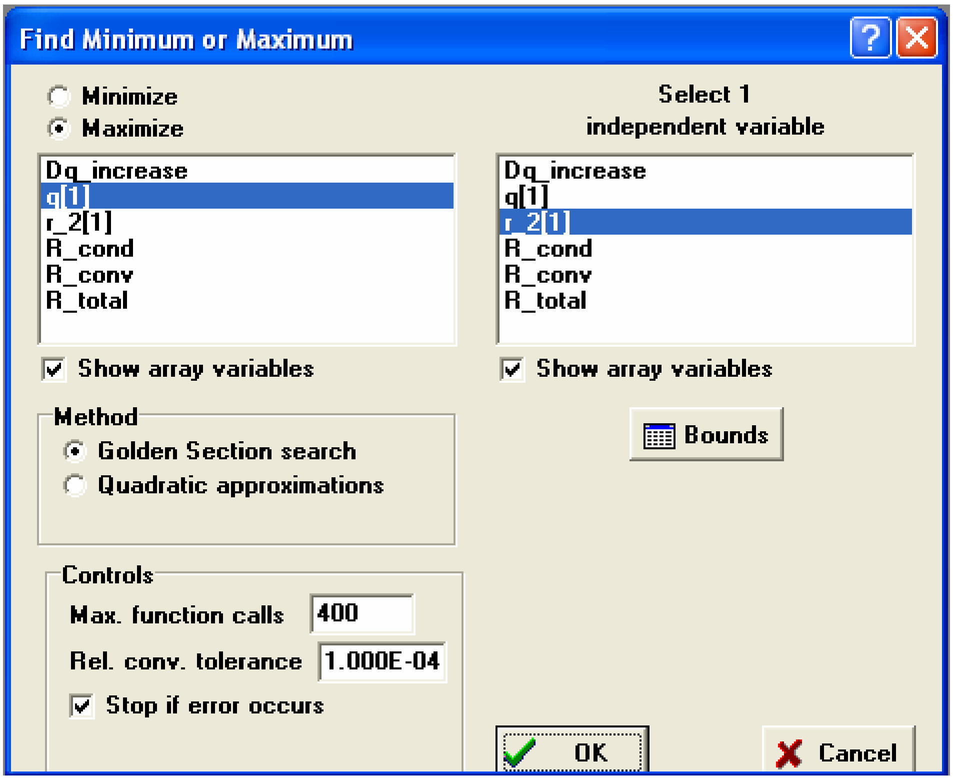

4- Press OK, the following window appears with the solution

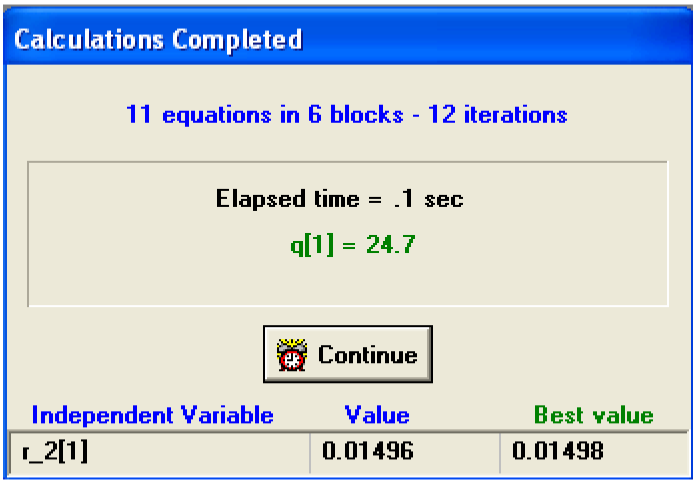

5- Press continue, the following window appears (out put window)

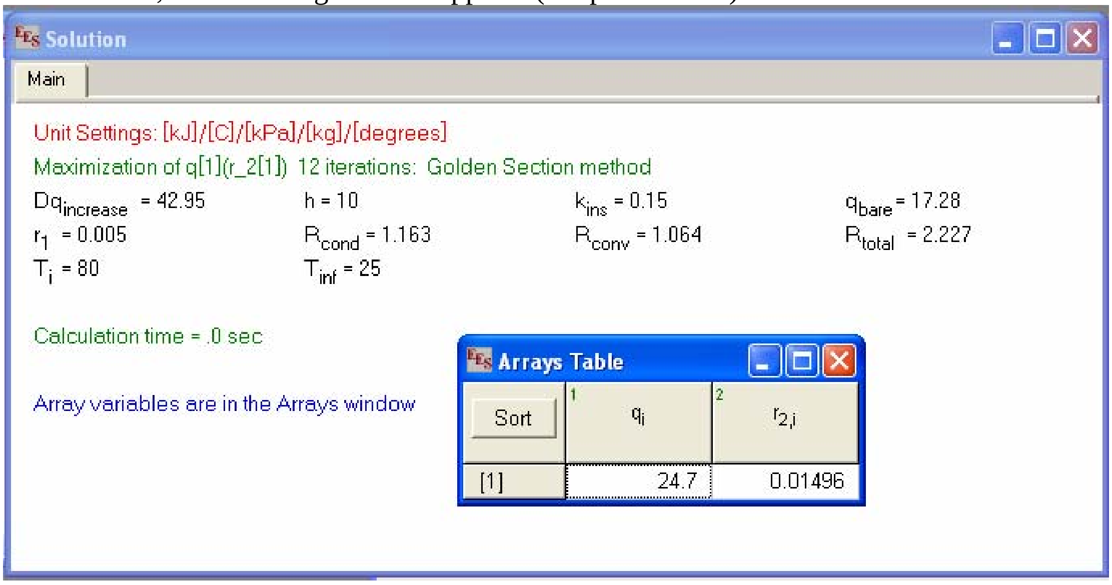

6- Out put graphical representations

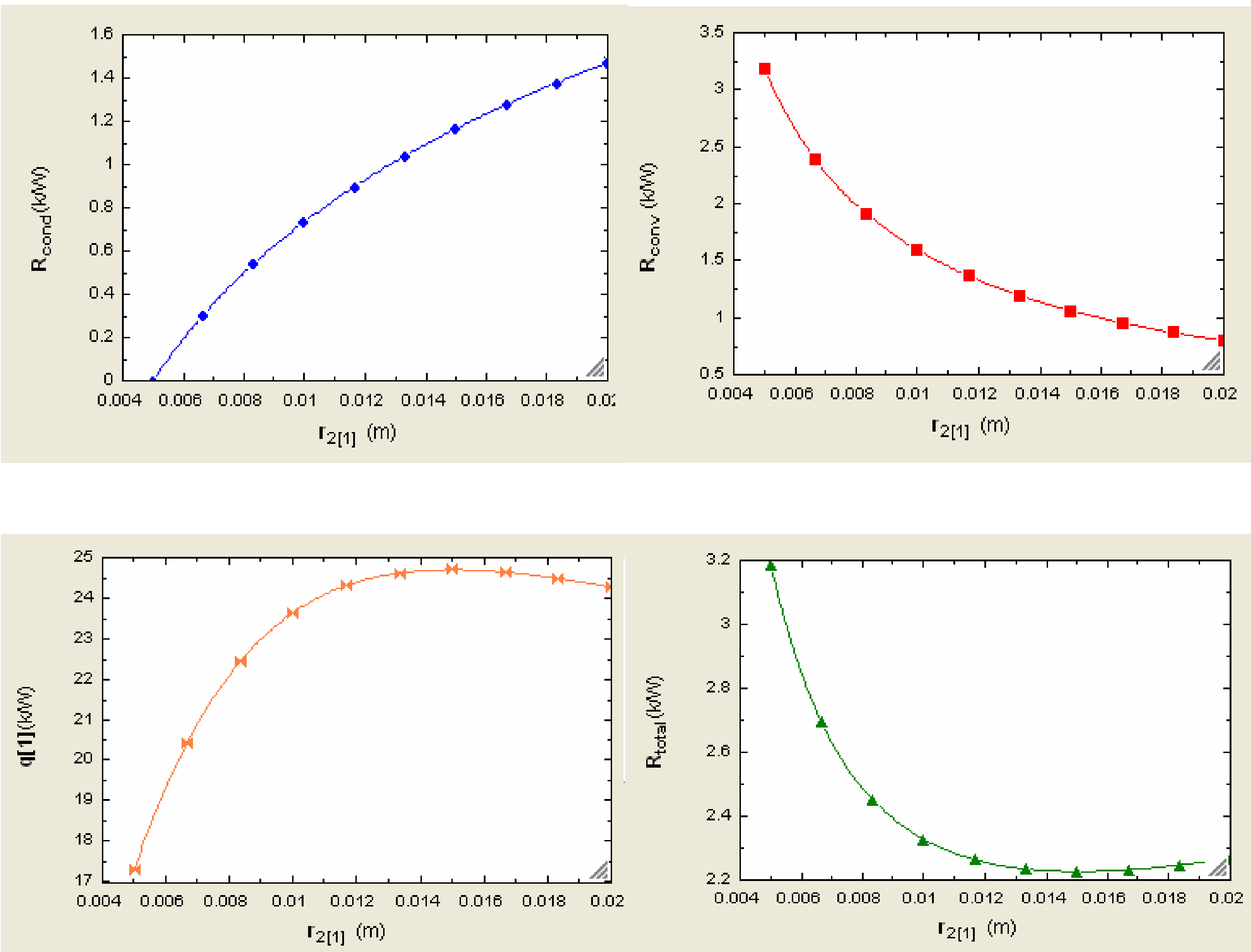

Part C: Electronics Cooling Methods in Industry

Indicative Contents

13. Heat Sinks

13.1 Definition

Heat sinks are devices that enhance the heat dissipation from hot surfaces. It is high thermal conductivity materials that makes low impedance, are often used on circuit boards to reduce component operating temperatures by minimizing the component-to-sink temperature difference.
The heat sink also provides an effective path for transferring the generated heat to an adjoining assembly or to the environment.

13.2 Components of Heat Sinks

13.2.1 Heat Sinks (Without using Fins)

Conductively cooled circuit boards use either strips or plates fabricated from copper or aluminum to transfer the generated heat to the card interface. These heat sinks could be found in different methods:

1. Bonded to the board surface either beneath rows of similarly shaped components Figure 13.1 (a)
2. On the unpopulated opposite surface, Figure 13.1 (b)
3. Printed wiring boards with high generated thermal power densities may be fabricated using an aluminum plate integrally bonded between thin layers of copper clad circuit board material, Figure 13.1 (c). Components can be attached to this assembly using the techniques developed for any two-sided circuit boards. Higher packaging densities are achieved by bonding assembled component boards to each side of an aluminum plate. In this case, the heat sink must transfer the heat generated by both assemblies

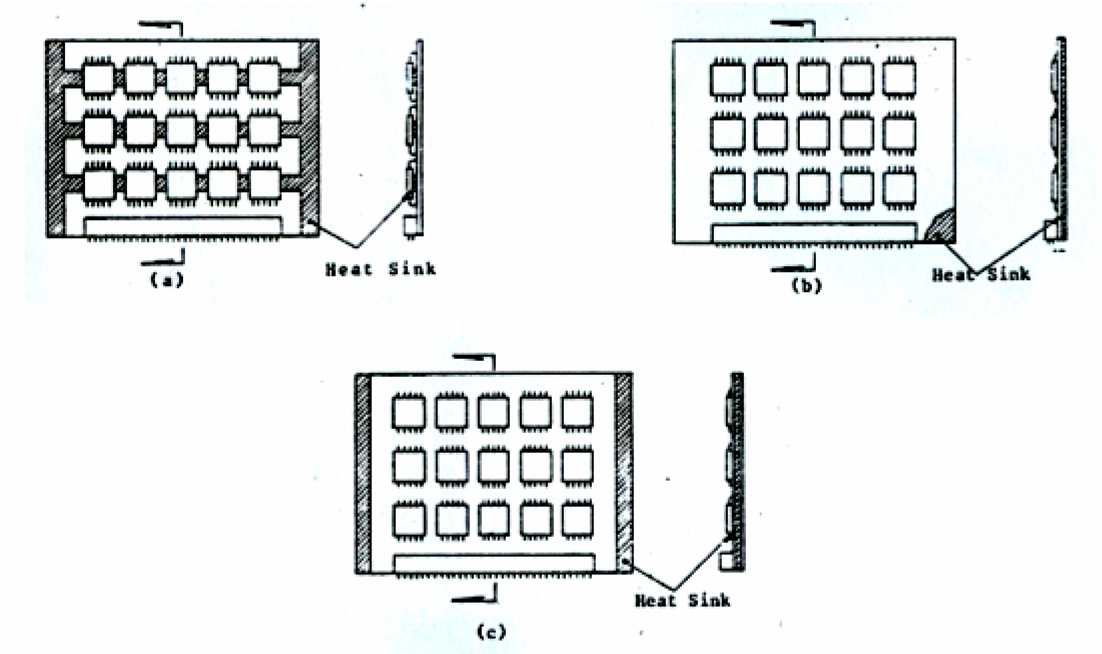

Figure 13.1 Different methods of low impendence material "heat sinks"

Built-up assemblies consisting of copper or aluminum and epoxy glass fiberboard may distort or warp when the equipment is operated. Changes in temperature may cause severe stresses in the attaching media because copper and aluminum experience about twice the expansion of the epoxy glass material. These effects can be reduced by the use of symmetrical sections with equal thicknesses of epoxy glass on each side of the metal center. Thermally induced distortion of nonsymmetrical assemblies can be minimized by fabricating them at a temperature approximately midway between their expected high (operating) and low (storage or transport) service temperatures.

13.2.2 Heat Sinks (With Extended Surfaces "Fins")

We can more increase the effectiveness of the heat sink by installed local heat transfer enhancement devices "extended surfaces or fins" to increasing the convective surface area of the heat sink.

Principle of operation

For a given Q, A_s, V, and T_a, the convective heat transfer rate on the fluid side of the surface determines T_s

Increase the effective area for convection by adding fins.

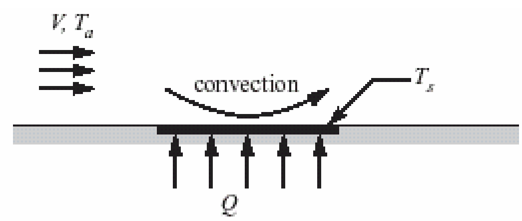

$$T_s = T_a + \frac{Q}{hA_s}$$

Where h_{eff} is the effective heat transfer coefficient for the fin and exposed surface, and A_{eff} is the effective area.

From two pervious cases, we can deduce:

- Adding a single fin increases A_{eff}, and thereby decreases T_s.
- Increasing the number of fins will change the heat transfer coefficient.

Besides adding fins the effective heat transfer coefficient could be increased by using fans mounted to extended surfaces as shown in Figure13.2 and hence the surface temperature could be more reduced and the rate of heat dissipation also increased.

Figure13.2 Fans using with heat sinks

Fin Performance

The performance of the fin affected by fin configuration, the air velocity, number of fins and fin materials but the most important parameter is the air velocity, Figure 13.3 show the heat sink (fins) performance of the pin fins attached by thermal tape.

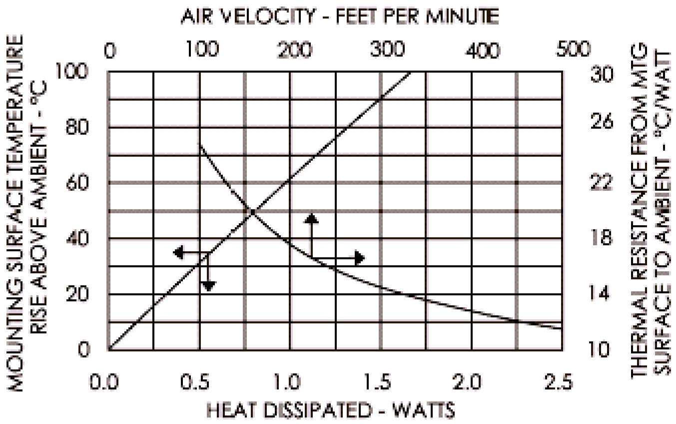

Figure 13.3 Fins performance of pin fins attached by thermal tape

Case study

1. Show that various shapes of extended surfaces (Fins) using in electronic cooling.
2. Find experimentally the relation between the thermal resistance and both heat input and number of fins.
3. Show the effect of fan speed on the heat sink's (Fins) heat input, base temperature and finally the thermal resistance.

13.3 Cold Plates

High power electronic components or high heat density assemblies that result from miniaturization often require a more effective heat removal system than is offered by conductive heat sinks. The cold plate combines the effects of a conductive heat sink with convection heat transfer to reduce the impedances between the generating heat sources and the thermal sink. Because of the availability of air from either the surrounding environment or conditioned sources, so that it is commonly used. The cold plate isolates the cooling air from the circuits and components being cooled, avoiding difficulties attributed to entrained moisture and airborne contaminants.
The configuration and design of the cold plate may take on different forms and sizes depending on equipment packaging and thermal requirements. Specific flow paths depend on the nature and distribution of the assemblies requiring cooling, intermediate conductive paths between the thermal sources and the cold plate interface, and equipment structural, and maintenance consideration.
Cold plates are usually fabricated from aluminum as welded or brazed assemblies. These assemblies can be used as chassis walls, Figure 13.4 (a) or for the indirect cooling of high powered electronic assemblies such as that illustrated in Figure 13.4 (b).Cold plates can also be integrated into the chassis design via the use of formed finned stock assembled into a prepared cavity, as shown in Figure 13.4 (c) Adhesives retain the finned stock, preventing flow short circuiting. The wall-to-air temperature difference along the flow path can be minimized by the selection of a suitable fin density. Higher fin densities also increase the resistance to flow which may impact on the selection of increase the resistance to flow which may impact on the selection of a fan or otherwise constrain the application of the equipment.

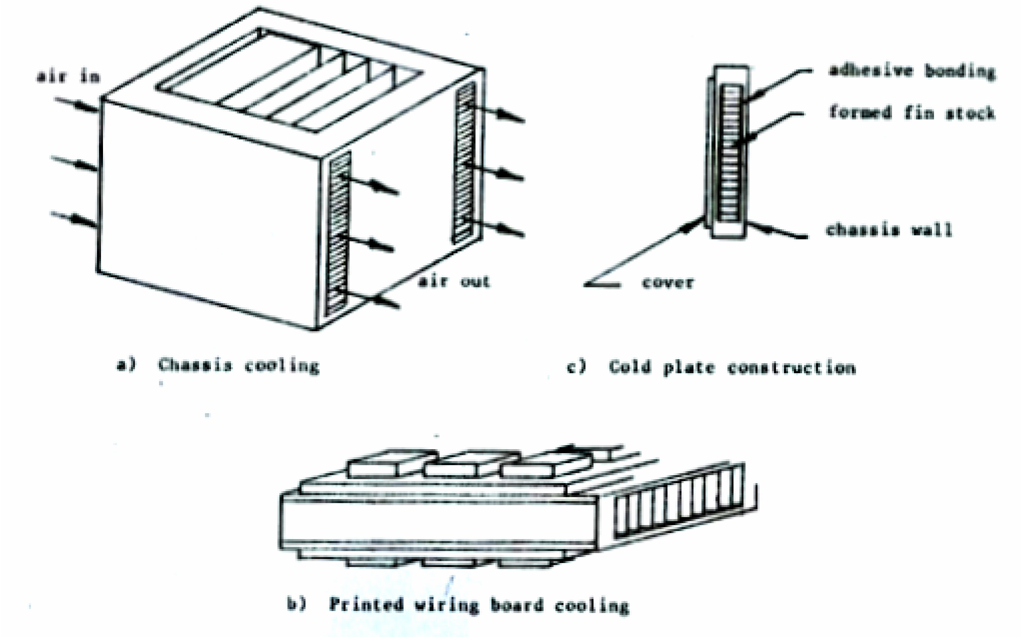

Figure 13.4 Cold plate configurations

Cold plates equipped with heat pipes as possible which will also reduce temperature gradients within the cold plate, developing a uniform temperature sink for attached assemblies.
Hardware design using cold plate techniques achieves an orderly arrangement of conductive heat transfer paths and air flow paths. Components or assemblies with high heat generation should be located either close to the cold plate wall or the coolant inlet.

13.4 Heat Sink attachment and Thermal Interface Effects on Production Assembly and Repair

Today's market offers many heat sink attachment and thermal interface options. Your design decisions usually aim to optimize product performance at minimum cost. Secondary effects not always sufficiently considered, significantly impact production cost, delivery performance, and reliability. These effects stem from the impact of the heat sink attachment design on the product assembly and disassembly processes. A product designed for easy assembly will have more consistent quality, reliability, and delivery performance. The ability to remove and replace the heat sink without damaging the device, the heat sink, or neighboring devices can also improve production parameters. To optimize assembly and repair processes consider these questions:

- Is the heat sink easily removable for repair?
- How many different parts and materials are needed to install the heat sink onto the board?
- Will personnel be exposed to any chemicals during installation or cleanup?
- Are specialized tools or equipment required?
- How sensitive is the assembly process to surface flatness or contamination?
- Will waste material for disposal be generated by the process or during cleanup?
- Will removal cause damage?
- Are attachment reliability and thermal performance sensitive to assembly techniques that may be inconsistent among assemblers?

13.4.1 Mechanical Attachment

Mechanical attachment generally consists of screws or clips that affix the heat sink directly to the device or to the PCB. The issues to consider here are the interface between the heat sink and the device, the number and type of parts needed, and the stresses imparted to the PCB and the device. A thermal interface material is often needed to reduce contact resistance at the interface. This interface material may be applied during board assembly (usually the case with thermal grease) or it may be pre-applied by the heat sink vendor as a dry material. Assembly and repair operations will usually benefit from a dry pre-applied interface material. This reduces assembly time and eliminates cleanup and re-application of grease and exposure to chemicals in case of repairs. The pre-applied material will usually give more predictable and consistent thermal performance because the application thickness and coverage area are well controlled.

When designing the fastening system, consider the number and type of fasteners as well as the effect on the device and the PCB of the forces imparted by the hardware. Screws and clips generally permit the heat sink to be installed and removed without damage. Clips also generally accomplish the installation with the fewest parts. When designing for adequate contact pressure, consider the effect of the hardware on the devices and the PCB. High contact pressure designs can impart substantial camber to the PCB. Depending on the complexity of the design, a mechanically attached heat sink is often the easiest type to remove and replace for repair. In particular, designs that clip the heat sink directly to the device are simpler to replace without damage to the device, the board, or the heat sink.

13.4.2 Adhesive Attachment

Adhesive attachment is accomplished with double-sided tapes or dispensed adhesives such as epoxies. The advantages can be significant in the assembly process; however there are some drawbacks to repair. Adhesive tapes offer many design and assembly advantages. Tapes can be pre-applied to the heat sink for simple "peel and stick" assembly with little waste generation or chemical exposure. The attachment and thermal interface are combined in a single material. Also camber-inducing stress on the PCB is minimized.

One concern with adhesive tape attachment is that interface resistance and attachment reliability may be affected by surface flatness or contamination. Special tooling may be required to ensure proper bonding time and pressure is attained at assembly, particularly with delicate heat sinks. If the heat sink must be removed for repair, damage may occur and personnel may need chemicals or heat to remove adhesive residues.

The "wetness" of dispensed adhesives offers some advantages and disadvantages as compared with tapes. Employees will likely be exposed to the adhesive and cleanup chemicals when working with the dispensed material. Thermal performance may vary with adhesive thickness and coverage, thus tight process control may be required to ensure consistent results. Waste for disposal may be created from dispensing equipment cleanup. However, these materials tend to be more forgiving of surface flatness and roughness.

13.4.3 Repair

The cost and anticipated quality level of the components requiring heat sinks and the production volume and expected yield of the complete assemblies should influence the weight you place on repairability. A custom high power ASIC (application specific integrated circuit) may prompt a repair-friendly design. Such devices may be subject to running design changes requiring component replacements on the fly or on recalled or upgraded products. If a costly device is incorrectly installed it can be cost effective to remove, rework, and re-install that component provided the repair process is not too burdensome. An additional point is that quality improvement processes usually require FMA (failure mode analysis) of certain defective components. This analysis is sometimes difficult or impossible if the component is damaged during removal.

13.5 Specifying Filters for Air Forced Convection Cooling

Introduction

The importance and utility of air filters is often underestimated since it is typically an after-thought in the design cycle. Different filter designs and the selection process are reviewed to assist the design engineers in selecting a suitable filter for their specific application.

13.5.1 Filter Purpose

The two main reasons air filters are used in forced convection cooling systems are:

1. To remove particulate contaminants from the air
2. To create a laminar air flow

13.5.1.1 Particulate Contaminants

The importance of the removal of corrosive materials is well appreciated, but the reason for removing more benign ones (dust and dirt) may not be as obvious. These particles can accumulate on and in between electronic components, resulting in an electrical short and shrouding. The latter can alter air flow distribution and thus adversely affect thermal performance.

13.5.1.2 Laminar Air Flow

Flows with less turbulence are better in many applications because they have less friction and subsequently require less fan work. The latter is very desirable since fan generated acoustic noise is a point of contention in the forced convection cooling of electronic systems.

13.5.2 Operating Characteristics

There are a variety of materials used as filter media. These include coarse glass fibers, metallic wools, expanded metals and synthetic open cell foams. Each type of filter will have its own filter efficiency and pressure drop at a given air flow.

13.5.3 Filter Efficiency

Filter efficiency is the percentage measure of the air borne particulates that a filter is able to remove from the flow at a given velocity.

Hence, filters with higher efficiency have a larger pressure drop for a given air velocity. Also, the smaller particle a filter can collect, the greater the pressure drop across the filter for a given air velocity.

13.5.4 Pressure Drop

Filter pressure drop is a measure of the force required to move air through the filter at a given velocity. Each component in the system contributes a resistance to the air flow, which results in a pressure drop across itself. The total system resistance is the sum of all the pressure drops along the air flow path (including the filter).

The air filter pressure drop is a function of the velocity of the air and the filter type. Each filter will have a unique pressure versus air velocity characteristics. Performance curves showing these characteristics are used by designers during the filter selection process.

13.5.5 Filter Selection

Several specifications are required before an appropriate filter can be selected. A minimum list of specifications would be:

1. The available area for the filter
2. The system's volumetric flow rate
3. The maximum pressure drop allowed for the filter
4. Filter efficiency
5. Ability to create laminar air flow
6. Type of contaminants to be filtered

a). size of particles
b). corrosive or non-corrosive

Even more important than the filter selection is the orientation of the filter with respect to the fan or blower. The filter should be placed several inches away from the blower or fans via a mixing plenum. The filter should also be oriented perpendicular to the desired air flow direction, for example; as shown in the following Figure 13.5.

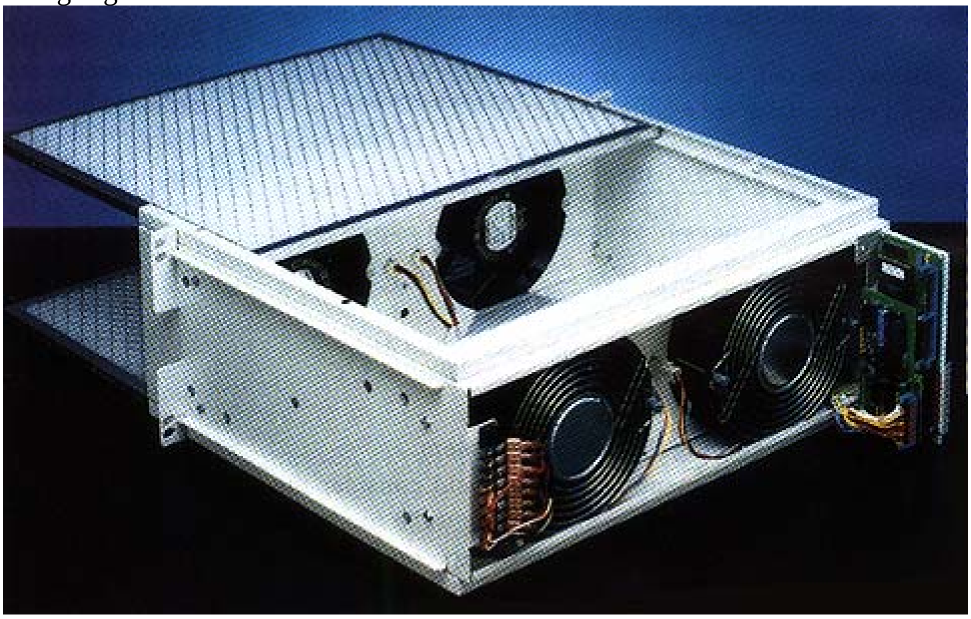

Figure 13.5 a custom cooling system for the telecommunications application, showing an example of air filters used to create a laminar air flow

14. Heat Pipes

Gaugler proposed the principle of heat pipe in 1942 for refrigeration engineering applications. However, his principle was not effectively applied and was not widely known until 1963, when Grover and his colleagues developed heat pipes for space applications and described the concept with the name of "Heat Pipe". Since then, heat pipe has been undergone considerable research and development for a wide range of applications, including the cooling of electronic systems.

- Definition

Heat pipe is a high performance heat transmission device with an extremely high thermal conductivity. It utilizes latent heat of evaporation of the working fluid to transmit heat from one point to another along the length of the heat pipe with a very small temperature gradient. Due to the heat pipe technique depends on two phase flow heat transfer, so that we should devote apart to the concept of Boiling and Condensation heat transfer.

- Boiling and Condensation Heat Transfer

Boiling and condensation heat transfer in two-phase flow (Liquid-vapor phase) is important in many engineering processes and systems. Due to increased heat transfer rates compared to single-phase heat transfer.

The virtually isothermal heat transfer associated with boiling and condensation processes makes their inclusion in power and refrigeration processes highly advantageous from a thermodynamic efficiency point of view.

The convection coefficient for both boiling and condensation could depend on the difference between the surface and saturation temperatures, $\Delta T = T_s - T_{sat}$, the body force arising from the liquid – vapor density difference, $(\rho_L - \rho_v)g$, the surface tension σ, the latent heat h_{fg}, characteristic length, and the thermophysical properties of the liquid or vapor (ρ, cp, μ, k), so that.

$$h = h\{\Delta T, (\rho_L - \rho_\upsilon)g, \sigma, h_{fg}, L, \rho, c_p, \mu, k\} \tag{14.1}$$

Applications of this type of heat transfer include boiling and condensation heat transfer to cool electronic components in computers such as in heat pipe method which mainly depend on both phenomena as shown in Figure14.1, the use of compact evaporators and condensers for thermal control of aircraft avionics and spacecraft environments and immersion cooling for electronics.

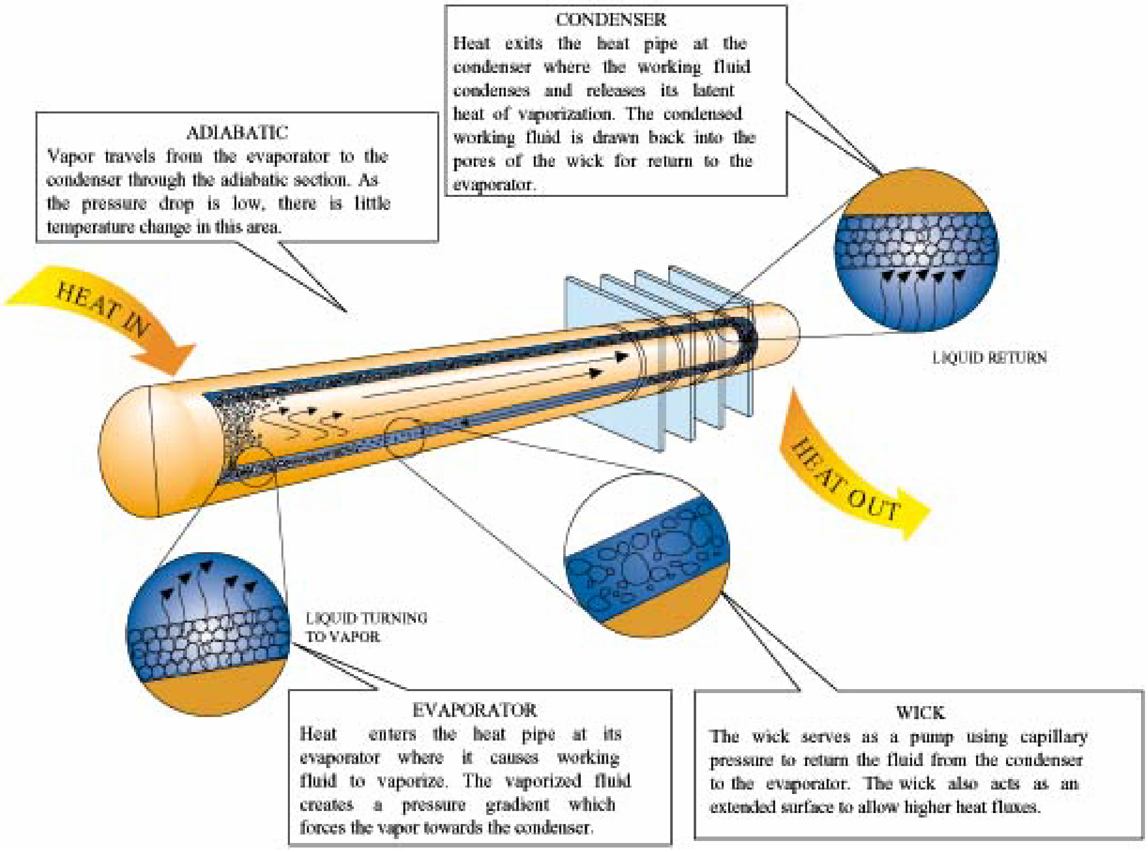

Figure14.1 Heat pipe configuration in horizontal position

14.1 Boiling Heat Transfer

When a surface maintained at a temperature above the saturation temperature of the liquid is exposed to a liquid as shown in Figure 14.2. This liquid starts to evaporate; this phenomenon is known as boiling. Heat transferred from the solid surface to the liquid is

$$q^{//} = \bar{h}(T_S - T_{sat}) = \bar{h}\Delta T \tag{14.2}$$

The total evaporation rate may be then determined from the relation

$$m^{\bullet} = \frac{q}{h_{fg}} \tag{14.3}$$

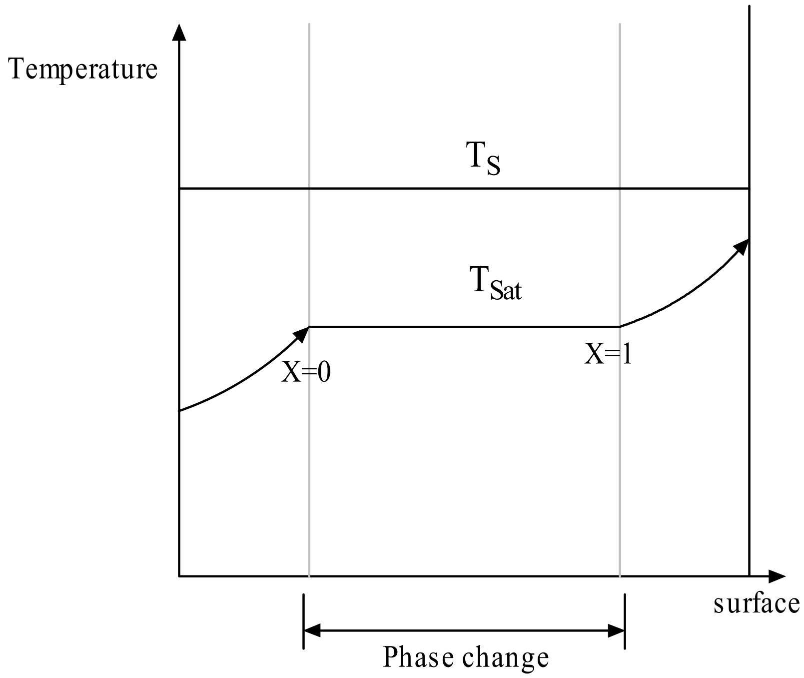

Figure 14.2 Surface –Temperature diagram for boiling heat transfer

The boiling may be divided into pool or flow boiling. If the heated surface is submerged below a free surface of liquid, this process is referred to as pool boiling. While if the fluid is moving by external means through duct or external flow over heated surfaces, this process is referred to as flow boiling. Also the boiling may be classified into subcooled or saturated boiling. In subcooled boiling, the temperature of the liquid is below the saturation temperature and the bubbles formed at the surface are condensed back when they travel up through the liquid (no liquid evaporation). While in saturated boiling the temperature of the liquid nearly equal the saturation temperature and the bubbles formed at the surface are then propelled by buoyancy forces, eventually escaping from a free surface(liquid is evaporated). In the foregoing lecture, we will consider saturated boiling only due to its importance.

14.1.1 Pool Boiling

The nature of the pool boiling process varies considerably depending on the conditions at which boiling occurs. The level of heat flux, the thermophysical properties of the liquid and vapor, the surface material and finish, and the physical size of the heated surface all may have an effect on the boiling process. The regimes of pool boiling are most easily understood by the boiling curve.

14.1.1.1 Pool Boiling Curve

In 1943, Nukiyama was the first to identify different regimes of pool boiling. He boiled saturated water on a horizontal wire. Then drew the heat flux versus temperature difference developing the so called pool boiling curve as shown in Figure14.3,

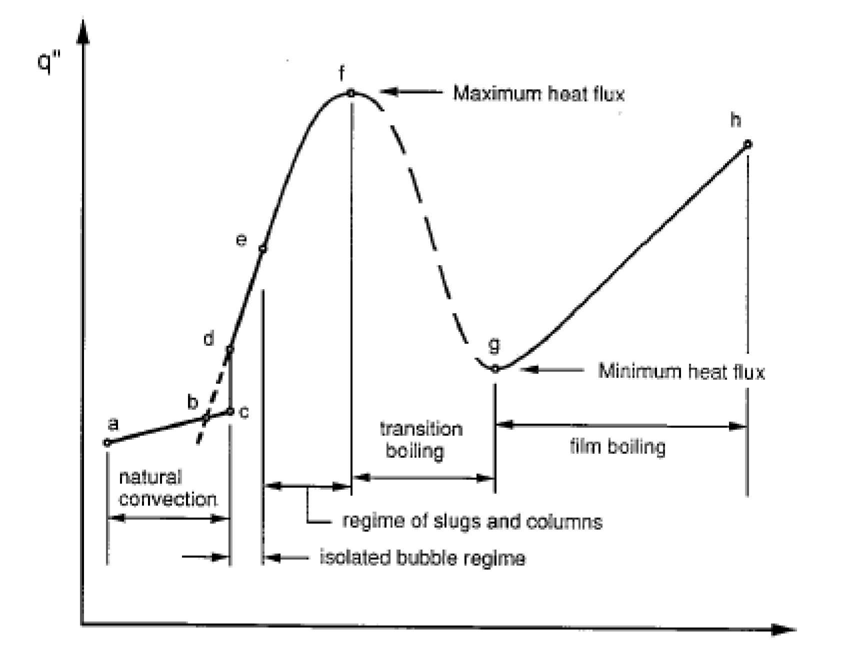

$(\Delta T = T_S - T_{sat})$

Figure14.3 Pool boiling curve: heat flux versus Temperature difference

14.1.1.2 Modes of Pool Boiling

The boiling curve in Figure14.3.has been divided into five regimes. Different boiling regimes are:

- Natural convection boiling:

When the surface temperature is a few degrees above the saturation temperature (T_{sat}), no nucleation sites may be active and heat may be transferred from the surface to the ambient liquid by natural convection alone as shown in Figure14.4. And q'' increases slowly with $T_s - T_{sat}$.

- Nucleate boiling:

The superheat becomes large enough to start nucleation at some of the cavities on the surface. This onset of nucleate boiling (ONB) condition occurs at point *c*. Once nucleate boiling is started as shown in Figure14.4. Any further increase in surface temperature causes the system operating point to move upward along section *d - f* of the boiling curve. This portion of the curve corresponds to the nucleate boiling regime. The nucleate boiling regime is divided into two distinct regimes namely:

1. Isolated bubble regime: it is the segment *d-e* of the boiling curve, where the flow becomes bubbly.

2. Slugs and columns regime: it is the segment *e-f* of the curve, where vapor is being produced so rapidly that bubbles merging together form columns of vapor slugs that rise upward in the liquid pool toward its free surface.

A peak heat flux is reached if the surface temperature within the nucleate boiling regime is increased to a certain value. The peak value of heat flux is called the critical heat flux (CHF), designated as point *f* in the pool boiling curve.

- Transition boiling:

It is the segment *f-g* of the boiling curve, where bubble formation is now so rapid that a vapor film or blanket begins to form on the surface as shown in Figure14.4. At any point on the surface, conditions may oscillate between film and nucleate pool boiling.

- Film boiling:

It start from point *g* this point also known as the Leidenfrost point (minimum heat flux); where the surface is hot enough to sustain a stable vapor film on the surface for an indefinite period of time. The entire surface then becomes blanketed with a vapor film as shown in Figure14.4. Within the film boiling regime; the heat flux increases as the superheat increases. This trend is a consequence of the increased conduction and/or convection transport due to the increased driving temperature difference across the vapor film. Radiation transport across the vapor layer may also become important at higher wall temperatures.

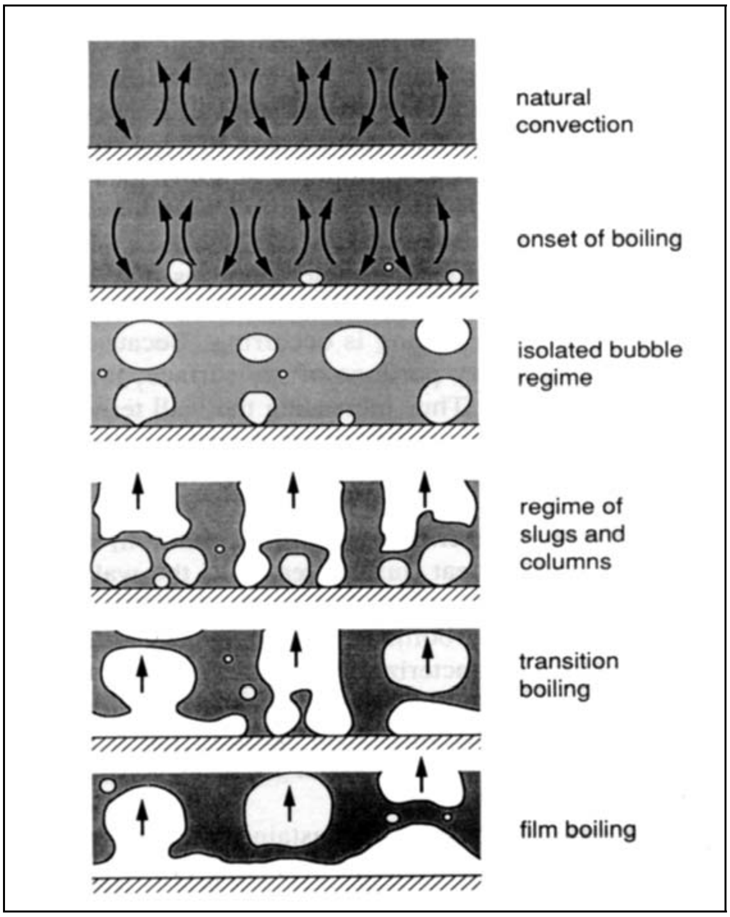

Figure14.4 Pool boiling regimes

14.1.1.3 Correlations of Pool Boiling

- nucleate pool boiling:

Commonly used correlation for nucleate boiling heat transfer developed by Rohsenow (1962) is

$$q'' = \mu_L h_{fg} \left[\frac{g(\rho_L - \rho_\upsilon)}{\sigma} \right]^{1/2} \left[\frac{c_{p,L} \Delta T}{C_{sf} h_{fg} \Pr_L^s} \right]^3 \tag{14.4}$$

All properties are evaluated at saturated temperature (T_{sat})
Where the exponent $s = 1$ for water
$= 1.7$ for other liquids
And the values of C_{sf} in this correlation vary with the type of solid surface and the fluid type in the system and these values are shown in table 14.1.

Table14.1 Selected values for C_{sf} for use with Equation14.4

Fluid-Surfaces combination	C_{sf}
Water-copper	
Scored	0.0068
Polished	0.013
Water-stainless steel	
Chemically etched	0.013
Mechanically polished	0.013
Ground and polished	0.006
Water-brass	0.006
Water-nickel	0.006
Water-platinum	0.013
n-Pentane-copper	
Polished	0.0154
Lapped	0.0049
Benzene-chromium	0.0101
Ethyl alcohol- chromium	0.0027

- Critical heat flux $q''_{\max}$:

According to Zuber (1959) for flat horizontal surfaces, the predicted maximum heat flux $q''_{\max}$ is

$$q''_{\max} = \frac{\pi}{24} h_{fg} \rho_\upsilon \left[\frac{\sigma g(\rho_L - \rho_\upsilon)}{\rho_\upsilon^2} \right]^{1/4} \left[\frac{\rho_L + \rho_\upsilon}{\rho_L} \right]^{1/2} \tag{14.5}$$

All properties are evaluated at saturated temperature (T_{sat})
Other geometries are treated by Lienhard et al. (1973) and Lienhard and Dhir (1973b). An alternative model has been proposed by Haramura and Katto (1983).

- Minimum heat flux $q''_{\min}$:

The transition regime is of small practical interest, as it may be obtained only by controlling the surface heater temperature so that no suitable theory has been obtained for this regime.
The minimum heat flux corresponds approximately to the lowest heat flux which will sustain stable film boiling. The following relation for the minimum heat flux $q''_{\min}$ derived by Zuber (1959) and Berenson (1961), from a large horizontal heated surface plate

$$q''_{\min} = 0.09\rho_{\upsilon}h_{fg}\left[\frac{g\sigma(\rho_L-\rho_{\upsilon})}{(\rho_L+\rho_{\upsilon})^2}\right]^{1/4} \tag{14.6}$$

Properties of vapor are evaluated at $T_f = (T_{sat} + T_s)/2$, while ρ_L and h_{fg} at T_{sat}

This correlation is accurate to approximately 50% for most fluids at moderate pressures but poorer at higher pressures. Similar result has been obtained for horizontal cylinders.

- Film pool boiling:

In film boiling, transport of heat across the vapor film from the wall to the interface may occur by boiling and radiation heat transfer. So that the total heat transfer coefficient may be calculated from the empirical relation

$$h = h_b\left(\frac{h_b}{h}\right)^{1/3} + h_r \tag{14.7}$$

Where Bromley, suggests the following relation for calculation of heat transfer coefficient in the stable film boiling region h_b on horizontal tube is

$$h_b = 0.62\left[\frac{k_{\upsilon}^3\rho_{\upsilon}g(\rho_L-\rho_{\upsilon})(h_{fg}+0.4c_{p\upsilon}\Delta T)}{d\mu_{\upsilon}\Delta T}\right]^{1/4} \tag{14.8}$$

All properties evaluated as for the minimum heat flux calculation.

And the radiation heat transfer h_r is expressed as:

$$h_r = \frac{q''_{rad}}{T_s - T_{sat}} = \frac{5.67x10^{-8}\,\varepsilon\,(T_s^4 - T_{sat}^4)}{T_s - T_{sat}} \tag{14.9}$$

Where: ε is the emissivity of the solid surface.

Note that at low surface temperatures, radiation effects are negligible. At higher temperatures radiation effects must also be included. If the working fluid is water the radiation effect becomes significant at elevated surface temperature $T_s \geq 250$ ºC (arbitrary).

Table14.2 Approximate temperature difference for different regimes in water boiling curve

Pool boiling regime	$\Delta T = T_s - T_{sat}$
Natural convection boiling	0 ºC< $\Delta T \leq 5$ ºC
Nucleate boiling	5 ºC $\leq \Delta T \leq \Delta T_{CHF}$
Transition boiling	$\Delta T_{CHF} \leq \Delta T \leq 120$ ºC
Film boiling	120 ºC $\leq \Delta T$

The critical temperature difference ΔT_{CHF} for various surface metals with water as working fluid at different pressures is shown in Figure 14.5.

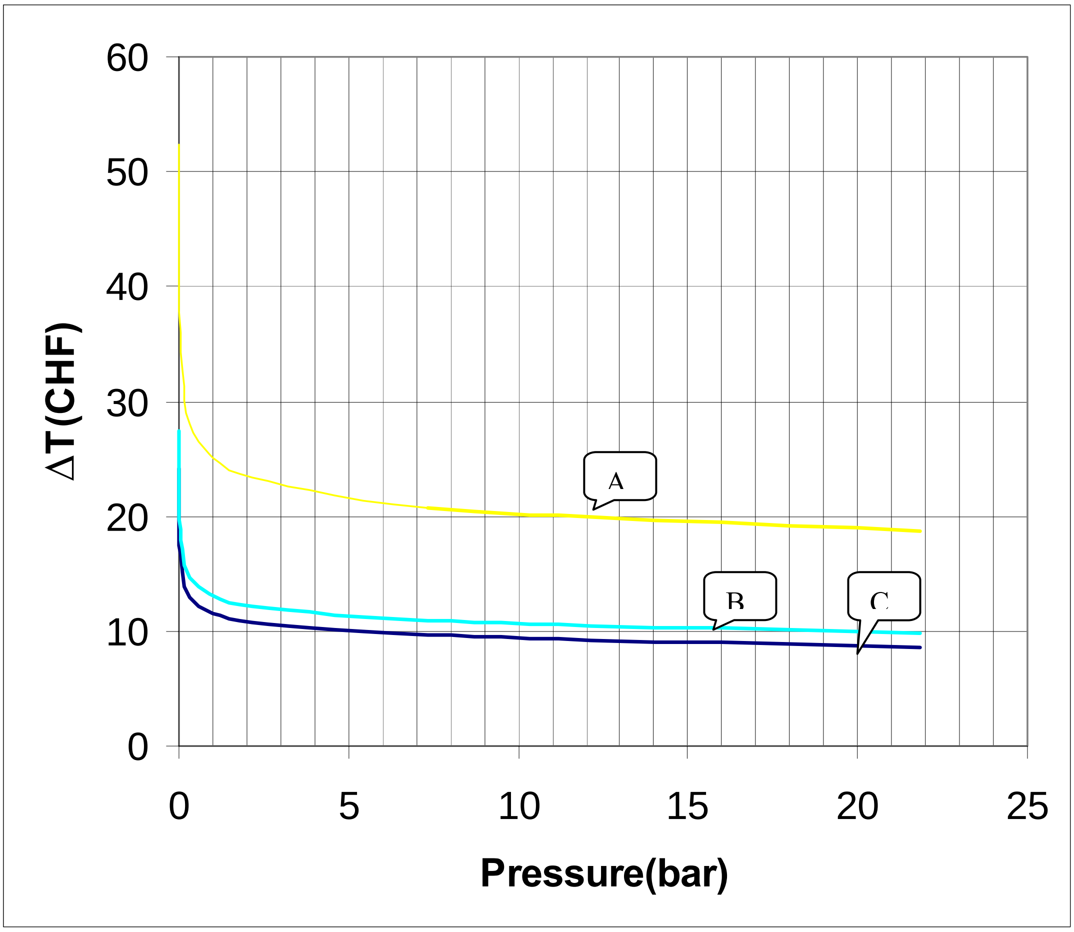

A	**Copper polished-water**
B	**Copper scored-water**
C	**Brass-water**

Figure 14.5 Pressure versus critical temperature difference ΔT_{CHF} for water

Example 14.1: An electronic box 0.02 m^2 upper surface area is immersed in bottom of a copper pan which contains water. The surface temperature of the box is 105 ^{o}C under steady state boiling condition. Estimate

1- The boiling heat transfer to boil water in this pan.
2- evaporation rate

Schematic:

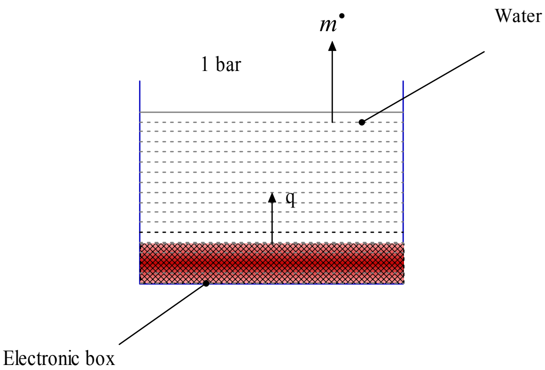

Assumptions
1- Steady state conditions
2- Water at uniform temperature T_{sat}=100 ^{o}C due to the water exposed to atmospheric pressure
3- Pan surface of copper Polished
4- Negligible losses from heater to surrounding

Solution

$$\Delta T = T_S - T_{sat} = 105 - 100 = 5\,°\mathrm{C}$$

According to the boiling curve of Figure 14.5: For water-copper surface at nearly 1 bar it shows that ΔT_{CHF} = 25 ºC which is greater the temperature difference in our problem, thus nucleate boiling will occur.

Recall Equation 14.4

$$q^{//} = \mu_L h_{fg}\left[\frac{g(\rho_L - \rho_\upsilon)}{\sigma}\right]^{1/2}\left[\frac{c_{p,L}\Delta T}{C_{sf} h_{fg}\,\mathrm{Pr}_L^s}\right]^3$$

s =1 for water, C_{sf} = 0.013 for surface of copper Polished and The properties of the water are evaluated at T_{sat} = 100 ºC.

The boiling heat flux is:

$$q^{//} = 279\times10^{-6}\times 2557\times10^3\left[\frac{9.8(957.3)}{58.9\times10^{-3}}\right]^{1/2}\left[\frac{4.217\times10^3\times5}{0.013\times2557\times10^3\times1.76}\right]^3 = 17.1\ \mathrm{kW/m^2}$$

The boiling heat transfer is

$$q = q^{//}\times A = 17.1\times10^3\times0.02 = 342\ \mathrm{W}$$

Under steady state conditions the evaporation rate is:

$$m^{\bullet} = \frac{q}{h_{fg}} = \frac{342}{2557\ \mathrm{X}\ 10^3} = 0.1337\times10^{-3}\ kg/s$$

14.1.2 Flow Boiling

Flow boiling may be experienced for either external or internal flows. Flow boiling in tubes is the most complex convective process encountered in applications such as evaporators; the flow is either horizontal or vertically upward, bubble growth and separation are strongly influenced by the flow velocity. Figure 14.6 schematically depicts a typical low-flux vaporization process in a horizontal tube. In this example liquid enters as subcooled liquid and leaves as superheated vapor. As indicated in Figure 14.6, the flow undergoes transitions in the boiling regime and the two-phase flow regime as it proceeds down the tubes. The regimes encountered depend on the entrance conditions and the thermal boundary conditions at the tube wall.

At low quality(x) the vaporization process is dominated by nucleate boiling, with convective effects being relatively weak. As the quality increases, the flow quickly enters the annular film flow regime in which convective evaporation of the annular liquid film is the dominant heat transfer mechanism. Often the conditions are such that liquid droplets are often entrained in the core vapor flow during annular flow evaporation. Eventually, the annular film evaporates away, leaving the wall dry. Mist-flow evaporation of entrained liquid droplets continues in the post-dry out regime until only vapor remains.

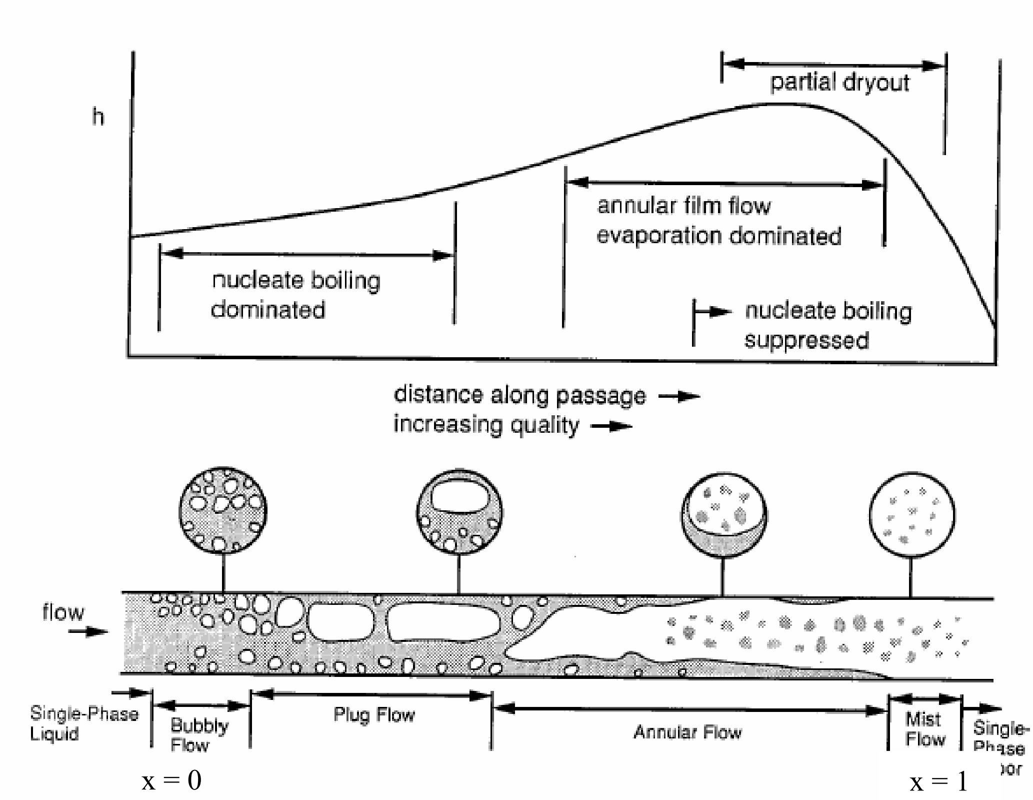

Figure 14.6 Qualitative variation of the heat transfer coefficient *h* and flow regime with quality for internal convective boiling in a horizontal tube at moderate wall superheat

The heat flux in the subcooled region is due to both forced convection and boiling heat transfer mechanisms, hence:

$$q''_{total} = q''_{boiling} + q''_{forced\,convection} \tag{14.10}$$

Where

$$q''_{boiling} = \mu_L h_{fg} \left[\frac{g(\rho_L - \rho_v)}{\sigma} \right]^{1/2} \left[\frac{c_{p,L} \Delta T}{C_{sf} h_{fg} \Pr_L^s} \right]^3 \tag{14.10 a}$$

And

$$q''_{forced\,convection} = 0.019 \operatorname{Re}_d^{0.8} \Pr^{0.4} \tag{14.10 b}$$

Once saturation boiling conditions are reached, A fully developed boiling is eventually encountered which is independent of the flow velocity or forced convection effects, and the following relation for boiling water inside tubes can be used

$$q'' = 2.253(\Delta T)^{3.96} \text{ W/m}^2 \qquad \text{for } 0.2 < \text{P} \le 0.7 \text{ MN/m}^2 \tag{14.11}$$

$$q'' = 283.2(P)^{4/3}(\Delta T)^3 \text{ W/m}^2 \qquad \text{for} \quad 0.7 < \text{P} \le 14 \text{ MN/m}^2 \tag{14.12}$$

Where P is the pressure in MN/ m^2

14.2 Condensation

Condensation occurs when a surface is exposed to a liquid if it is maintained at a temperature below the saturation temperature of the liquid as shown in Figure 14.7. Also the heat transferred from the fluid to solid surface is

$$q'' = \bar{h}(T_S - T_{sat}) = \bar{h}\Delta T \tag{14.13}$$

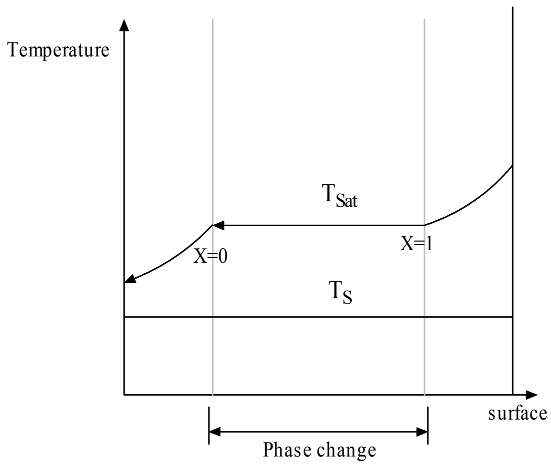

Figure 14.7 Surface –Temperature diagram for condensation heat transfer

As in the case of boiling, surface tension effects, surface wetting characteristics, and phase stability also play important roles in condensation processes.
Condensation on external surfaces may occur either as dropwise condensation or as film condensation, depending on the surface conditions. In fact, heat transfer rates in dropwise condensation are as much as 10 times higher than in film condensation.

14.2.1 Dropwise Condensation

Dropwise condensation occurs on new surfaces but it is extremely difficult to be maintained since most surfaces become wetted after exposure to a condensing vapor over an extended period of time. More than 90% of the surface is covered by drops, ranging from a few micrometers in diameter to agglomerations visible to the naked eye as shown in Figure14.8. When droplets become large enough, they are generally removed from the surface by the action of gravity or drag forces resulting from the motion of the surrounding gas. As the drops roll or fall from the surface they merge with droplets in their path as shown in Figure14.9.

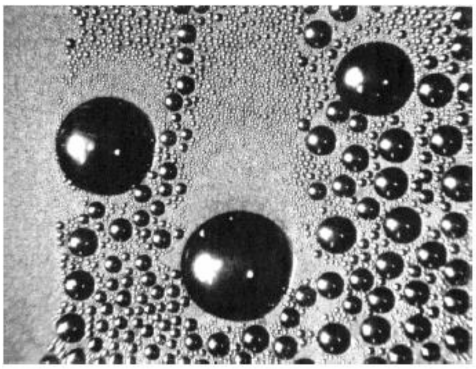

Figure 14.8 Typical photograph of dropwise condensation provided by Professor Borivoje B. Mikic

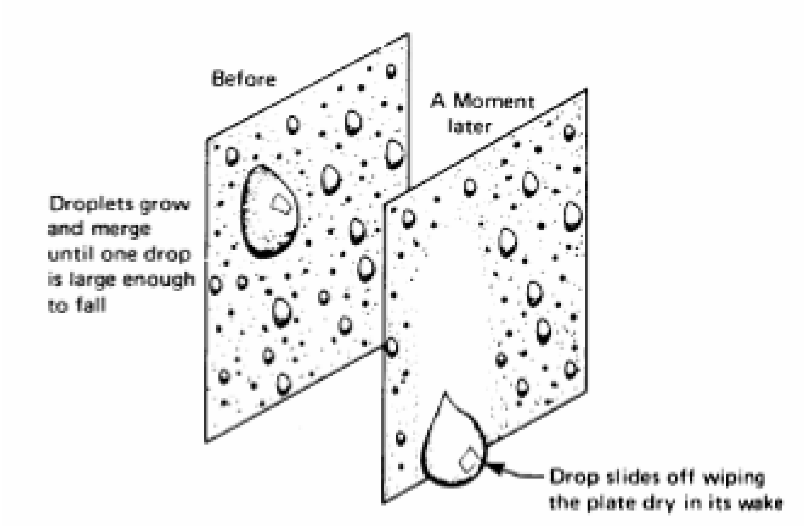

Figure 14.9 Process of liquid removal during dropwise condensation

14.2.2 External Film Condensation

In film condensation the liquid phase fully wets a cold surface in contact with a vapor near saturation conditions; the conversion of vapor to liquid will take the form of film condensation. As the name implies, the condensation takes place at the interface of a liquid film covering the solid surface as shown in Figure14.10.

Because the latent heat of vaporization must be removed at the interface to sustain the process, the rate of condensation is directly linked to the rate at which heat is transported across the liquid film from the interface to the surface

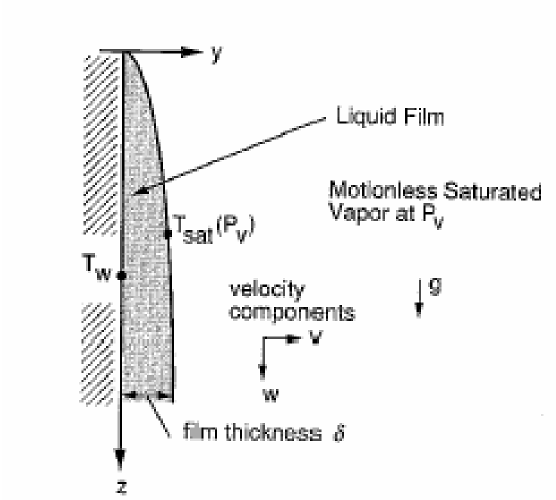

Figure14.10 System model for falling-film condensation

Because the liquid film flows down the surface by gravity, this situation is sometimes referred to as falling-film condensation. Although it is desirable to achieve drop wise condensation in industrial application, it is often difficult to maintain this condition. Thus most of the common designs are based on film condensation.

14.2.2.1 Laminar Film Condensation on a Vertical Plate (Re < 1800)

The Reynolds number defined as

$$\mathrm{Re} = \frac{4m^{\bullet}}{\mu_L p_w} \tag{14.14}$$

Where $m^{\bullet}$ is the condensation rate and p_w is the wetted perimeter (width for vertical plate and πd for vertical tube)

In its simplest form, the classic Nusselt analysis incorporates the following idealizations:

(1) Laminar flow,
(2) Constant thermophysical properties,
(3) That subcooling of liquid is negligible in the energy balance,
(4) That inertia effects are negligible in the momentum balance,
(5) The vapor is stationary and exerts no drag,
(6) The liquid-vapor interface is smooth, and
(7) The heat transfer across film is only by conduction (convection is neglected).

Under the above assumptions, the following relation for the local heat transfer coefficient h_x can be obtained

$$h_x = \left[\frac{g\rho_L(\rho_L - \rho_\upsilon)k_L^3 h_{fg}}{4(T_{sat} - T_s)\mu_L x}\right]^{1/4} \tag{14.15}$$

From

$$\bar{h}_L = \frac{1}{L}\int_0^L h_x dx$$

Then the average heat transfer coefficient over the entire length is then:

$$\bar{h}_L = 0.943\left[\frac{g\rho_L(\rho_L - \rho_v)k_L^3 h_{fg}}{(T_{sat} - T_s)\mu_L L}\right]^{1/4} \tag{14.16}$$

Liquid properties are evaluated at $T_f = (T_s + T_{sat})/2$ while ρ_υ and h_{fg} at T_{sat}

The analysis is identical for an inclined surface, except that the gravitational acceleration g is replaced by $g\cos\theta$ where θ is the angle between the vertical and the surface.

The total heat transfer to the surface may be obtained from the Newton's law of cooling:

$$q = \bar{h}_L A(T_{sat} - T_s) \tag{14.17}$$

The total condensation rate may be then determined from the relation

$$m^{\bullet} = \frac{q}{h_{fg}} \tag{14.18}$$

14.2.2.2 Turbulent Film Condensation on a Vertical and Inclined Plates and Cylinders (Re > 1800)

The suggested relation for turbulent film condensation on a vertical and inclined plates and cylinders is

$$\bar{h} = 0.0077\left[\frac{g\rho_L(\rho_L-\rho_\upsilon)k_L^3}{\mu_L^2}\right]^{1/3}\mathrm{Re}^{0.4} \qquad (14.19)$$

14.2.2.3 Film Condensation on Radial Systems

The average heat transfer coefficient for laminar film condensation on the outer surface of a sphere and horizontal tubes (Re < 1800) is

$$\bar{h}_d = C\left[\frac{g\rho_L(\rho_L-\rho_\upsilon)k_L^3\,h'_{fg}}{\mu_L(T_{sat}-T_s)d}\right]^{1/4} \qquad (14.20)$$

The properties are evaluated as in Equation 14.16.

Where C = 0.826 for the sphere and 0.729 for the tube and h'_{fg} is the modified latent heat of the form $h'_{fg} = h_{fg} + 0.68C_{p,L}(T_{sat}-T_s)$

For tube bank: put d = N_Td where N_T is the number of tube in vertical direction and C = 0.729

14.2.2.4 Film Condensation inside Horizontal Tubes

Schematically in Figure 14.11 depicts a typical condensation process in a horizontal round tube. Superheated vapor enters the tube and at the exit end the liquid is subcooled. At a point some distance downstream of the entrance, vapor begins to condense on the interior walls of the tube. The location at which this occurs is at or slightly before the bulk flow reaches the equilibrium saturation condition.

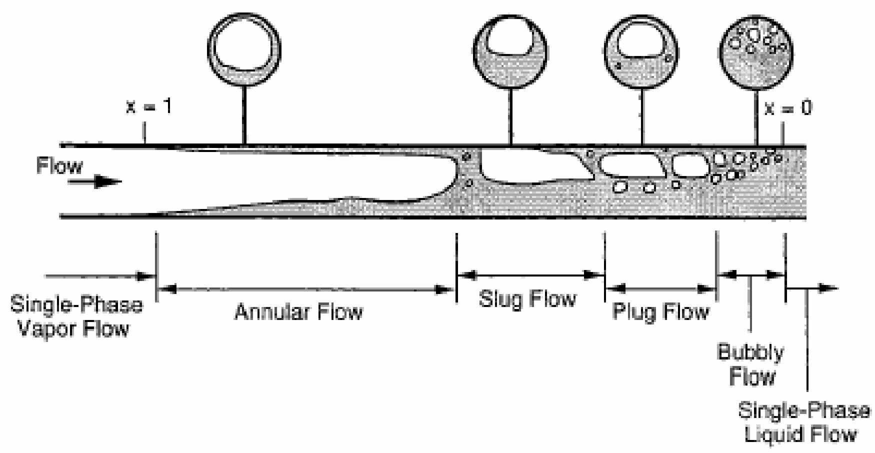

Figure14.11 Typical condensation process in a horizontal tube

Condensation of refrigerants at low vapor velocities inside horizontal tubes can be modeled using the following equation:

$$\bar{h}_d = 0.555\left[\frac{g\rho_L(\rho_L-\rho_\upsilon)k_L^3\,h'_{fg}}{\mu_L(T_{sat}-T_s)d_i}\right]^{1/4} \qquad (14.21)$$

For this case

$$h'_{fg} = h_{fg} + \frac{3}{8} C_{p,L} (T_{sat} - T_s)$$

15. Heat Pipes in Electronics (1)

15.1 Components of a Heat Pipe

The three basic components of a heat pipe are:

15.1.1 The Container

The function of the container is to isolate the working fluid from the outside environment. It has to therefore be leak-proof, maintain the pressure differential across its walls, and enable transfer of heat to take place from and into the working fluid.

15.1.2 The Working Fluid

A first consideration in the identification of a suitable working fluid is the operating vapor temperature range. Within the approximate temperature band, several possible working fluids may exist, and a variety of characteristics must be examined in order to determine the most acceptable of these fluids for the application considered. The prime requirements are:

- compatibility with wick and wall materials
- good thermal stability
- wettability of wick and wall materials
- vapor pressure not too high or low over the operating temperature range
- high latent heat
- high thermal conductivity
- low liquid and vapor viscosities
- high surface tension
- acceptable freezing or pour point

The selection of the working fluid must also be based on thermodynamic considerations which are concerned with the various limitations to heat flow occurring within the heat pipe like, viscous, sonic, capillary, entrainment and nucleate boiling levels.

In heat pipe design, a high value of surface tension is desirable in order to enable the heat pipe to operate against gravity and to generate a high capillary driving force. In addition to high surface tension, it is necessary for the working fluid to wet the wick and the container material i.e. contact angle should be zero or very small. The vapor pressure over the operating temperature range must be sufficiently great to avoid high vapor velocities, which tend to setup large temperature gradient and cause flow instabilities.

A high latent heat of vaporization is desirable in order to transfer large amounts of heat with minimum fluid flow, and hence to maintain low pressure drops within the heat pipe. The thermal conductivity of the working fluid should preferably be high in order to minimize the radial temperature gradient and to reduce the possibility of nucleate boiling at the wick or wall surface. The resistance to fluid flow will be minimized by choosing fluids with low values of vapor and liquid viscosities.

15.1.3 The Wick or Capillary Structure

It is a porous structure made of materials like steel, aluminum, nickel or copper in various ranges of pore sizes. The prime purpose of the wick is to generate capillary pressure to transport the working fluid from the condenser to the evaporator. It must also be able to distribute the liquid around the evaporator section to any area where heat is likely to be received by the heat pipe. Often these two functions require wicks of different forms. The selection of the wick for a heat pipe depends on many factors, several of

which are closely linked to the properties of the working fluid.
The maximum capillary head generated by a wick increases with decrease in pore size. The wick permeability increases with increasing pore size. Another feature of the wick, which must be optimized, is its thickness. The heat transport capability of the heat pipe is raised by increasing the wick thickness. The overall thermal resistance at the evaporator also depends on the conductivity of the working fluid in the wick. Other necessary properties of the wick are compatibility with the working fluid and wettability.

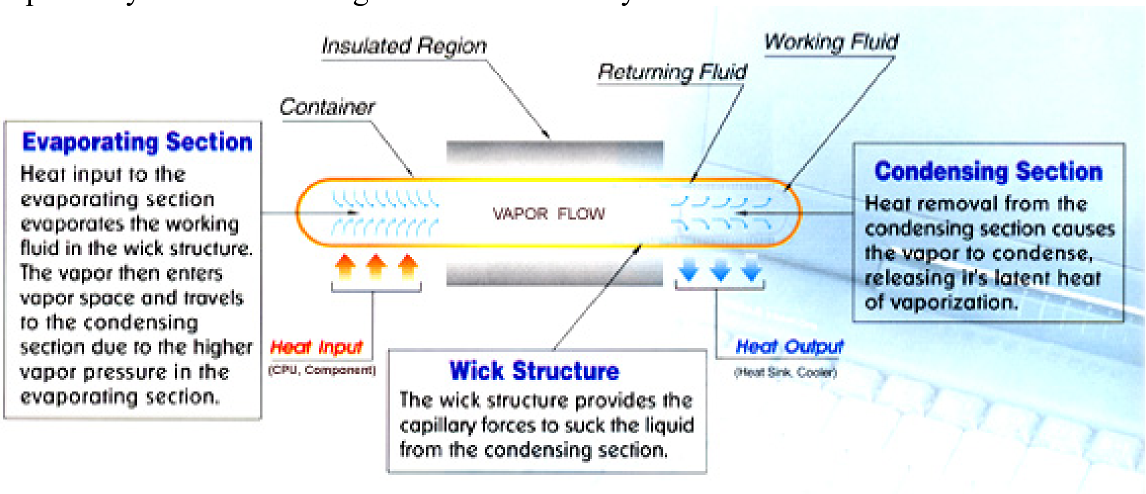

Figure 15.1 Components of the heat pipe

Figure15.2 Wick structures

15.2 Principle of Operation

As shown in Figure15.3, the heat pipe in its simplest configuration is a closed, evacuated cylindrical vessel with the internal walls lined with a capillary structure or wick that is saturated with a working fluid. Since the heat pipe is evacuated and then charged with the working fluid prior to being sealed, the internal pressure is set by the vapor pressure of the fluid.
As the heat input to the evaporator, liquid in the wick structure is vaporized, creating a pressure gradient in the vapor core. Such pressure gradient forces the vapor to flow along the pipe to the cooling region where it condenses releasing its latent heat of evaporation, which is rejected to the surrounding by a heat sink.
The liquid then returns to the evaporator region through the pores in the wick structure by the action of capillary pressure produced by the small pores of the wick structure. As a result, heat is absorbed at one end of the heat pipe and rejected to the other. The working fluid serves as the heat transport medium. The heat input region of the heat pipe is called evaporator, the cooling region is called condenser, and this is because the working fluid is being vaporized or condensed. In between the evaporator and condenser regions, there may be an adiabatic region.

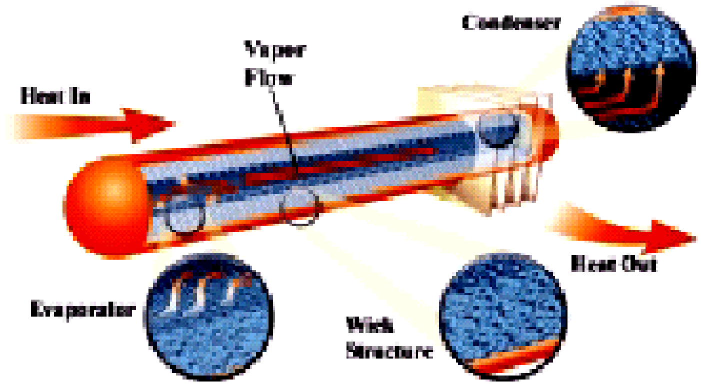

Figure 15.3 Principle of operation of heat pipe

15.3 The Special Features of Heat Pipes

The heat pipe has its special features:

15.3.1 Very High Thermal Conductivity

Heat pipe utilizes latent heat of evaporation of the working fluid to transfer heat from the evaporator to condenser of the heat pipe. This mode results a very high thermal conductivity. The effective thermal conductivity is several orders of magnitudes greater than that of the best solid conductor. Figure 15.4 shows the comparison of the effective thermal conductivity of heat pipe with that of solid copper and solid aluminum rods. The length and diameter of the three devices are, respectively, equal to 0.5m and 1.27cm. The rate of heat flow from one end to another of the devices was 20 W. The temperature differences for the three devices are indicated in Figure 15.4 for copper and aluminum rods, the temperature differences are 260 ^{o}C and 400 ^{o}C, respectively. However, the temperature difference for heat pipe is only 6 ^{o}C. This indicates that the effective thermal conductivity of the heat pipe is about 43 times larger than that of copper and 66 times larger than that of aluminum.

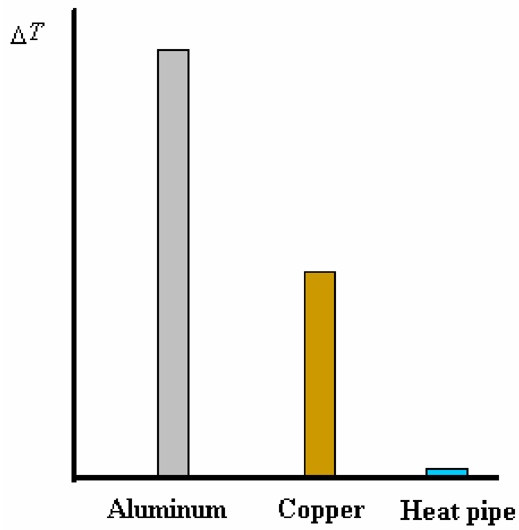

Figure 15.4 Comparison of the devices temperature difference "effective thermal Conductivity"

15.3.2 Low Relative Weight

The heat pipe is not a solid metal piece. The weight can be significantly reduced. In the previous example, it was found that the weight of the solid copper and solid aluminum rods are about 13.7 and 4.2 times greater than that of the copper-water heat pipe.

15.3.3 Reliable in Operation

Heat pipes do not have moving parts; they are extremely reliable. The main cause of failure is non-condensable gas generation in the heat pipe. By proper chosen of container and working fluid combination, this problem can be eliminated.

15.3.4 Flexible

The heat pipes can be made in various forms. Circular heat pipe is the most popular from, since it is easy fabrication and low cost. There exist flat plate and double casing heat pipes, rigid and flexible heat pipes, as well as large and micro heat pipes.

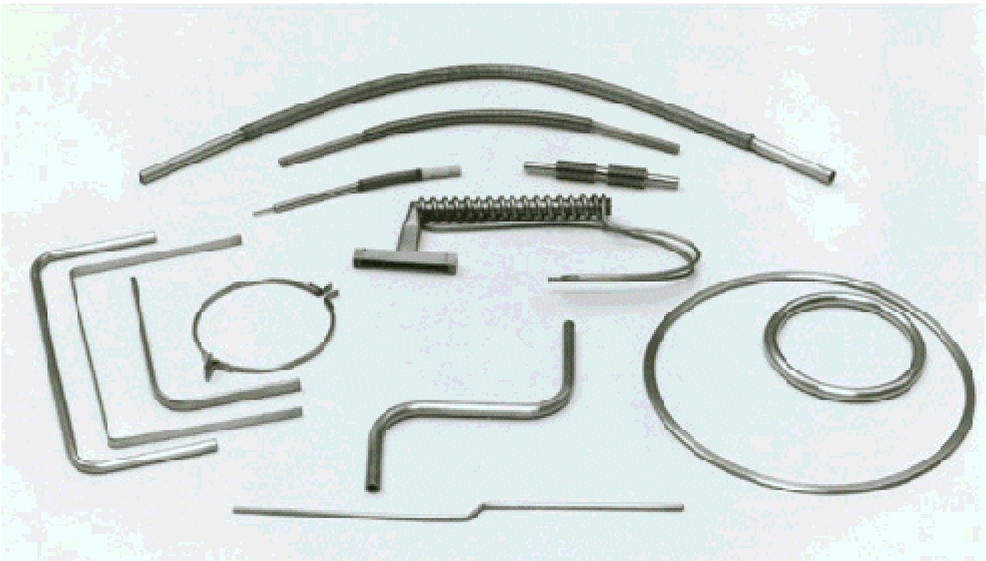

Figure 15.5 Various forms of flexible heat pipes

15.3.5 The Temperature Operating Range

Heat pipe can be designed to operate over a wide range of temperature from cryogenic applications using helium or nitrogen as the working fluid to high temperature applications using silver. The type of working fluid and the operating pressure inside the heat pipe depend on the operating temperature. The operating temperature, in general, should be above the triple point temperature and below the critical temperature of the working fluid. For example the triple point and the critical of water are, respectively, 0.01 ^oC and 374.1 ^oC. This is the reason that the recommended working temperature of water heat pipe is set between the two temperatures, as shown in Table 15.1. One more factor should be considered is high saturation pressure at high operating temperature. For high saturation pressure, the thickness of the container must be large. This will result a large transverse thermal resistance due to large conduction thermal resistance across the container walls. In electronic cooling applications it is desirable to maintain junction temperature below 80 to 150 ^oC, copper-water heat pipe are typically used. Table 15.1 shows the range of working temperature for some working fluids.

Table 15.1 shows the range of working temperature for some working fluids

Fluids	**Temperature Range °C**
Helium	-271 ---- -269
Nitrogen	-203 ---- -160
Ammonia	-78 ---- 100
Acetone	0 ---- 120
Methanol	10 ---- 130
Water	30 ---- 200
Mercury	250 ---- 650
Sodium	600 ---- 1200
Silver	1800 ---- 2300

15.4 The Limitation of Operation with Heat Pipe

The maximum heat transport capacity of a heat pipe is governed by five primary heat transport limitations, which must be addressed when designing a heat pipe as a function of the heat pipe operating temperature. These heat transport limits include: viscous, sonic, capillary pumping, entrainment or flooding, and boiling. Each heat transport limitation is summarized in Table 15.2 with description and its cause and suggested solution.

Table 15.2 Heat transportation limitation and its potential solution

Heat Transport Limitation	Description	Cause	Potential Solution
Viscous	Viscous forces prevent vapor flow in the heat pipe	Heat pipe operating below recommended operating temperature	Increase heat pipe operating temperature or find alternative working fluid
Sonic	Vapor flow reaches sonic velocity when exiting heat pipe evaporator resulting in a constant heat pipe transport power and large temperature gradients	Power/temperature combination, too much power at low operating temperature	This is typically only a problem at start-up. The heat pipe will carry a set power and the large ^T will self correct as the heat pipe warms up
Entrainment (Flooding)	High velocity vapor flow prevents condensate from returning to evaporator	Heat pipe operating above designed power input or at too low an operating temperature	Increase vapor space diameter or operating temperature
Capillary	Sum of gravitational, liquid and vapor flow pressure drops exceed the capillary pumping head of the heat pipe wick structure	Heat pipe input power exceeds the design heat transport capacity of the heat pipe	Modify heat pipe wick structure design or reduce power input
Boiling	Film boiling in heat pipe evaporator typically initiates at 5-10 W/cm^2 for screen wicks and 20-30 W/cm^2 for powder metal wicks	High radial heat flux causes film boiling resulting in heat pipe dry out and large thermal resistances	Use a wick with a higher heat flux capacity or spread out the heat load

15.5 Applications of Heat Pipe for Cooling of Electronic Systems

Heat pipe heat sink has been frequently used to remove the heat from power transistors, Thyristors, and individual chips. Currently, a popular application to use heat pipes is cooling Intel's Pentium processors in notebook computers.
Perhaps the best way to demonstrate the heat pipes application to electronics cooling is to present a few of the more common examples.

1- Cooling of Laptop Computer

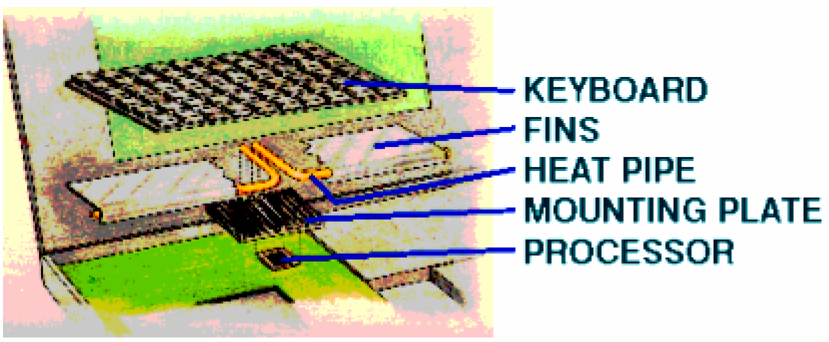

Figure 15.6 Heat pipe technology used in a laptop computer

2- Cooling of High Power Electronics

In addition, other high power electronics including Silicon Controlled Rectifiers (SCR's), Insulated Gate Bipolar Transistors (IGBT's) and Thyristors, often utilize heat pipe heat sinks. Heat pipe heat sinks similar to the one shown in Figure 15.7, are capable of cooling several devices with total heat loads up to 5 kW. These heat sinks are also available in electrically isolated versions where the fin stack can be at ground potential with the evaporator operating at the device potentials of up to 10 kV. Typical thermal resistances for the high power heat sinks range from 0.05 to 0.1°C/watt. Again, the resistance is predominately controlled by the available fin volume and air flow.

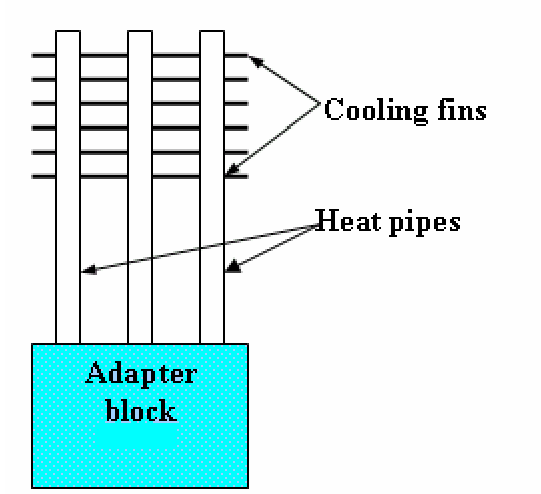

Figure 15.7 High power heat pipe heat sink assembly

Figure 15.8 Heat pipe heat sink cools four IGBT's used as motor controllers in heavy industry

Figure 15.9 shows a large heat pipe unit that has several IGBTs mounted on it. The IGBTs are attached to a mounting plate and heat pipes embedded in the plate transports the heat to an air-cooled fin section. There are several different sized units like this being used in the field. Heat rejection from units like these is from 500 W to 8.3 kW with thermal resistance values from 0.004^{o}C/W to 0.062^{o}C/W. another example of some multi-kilowatt heat pipe units installed in a motor drive cabinet as shown in Figure 15.10.

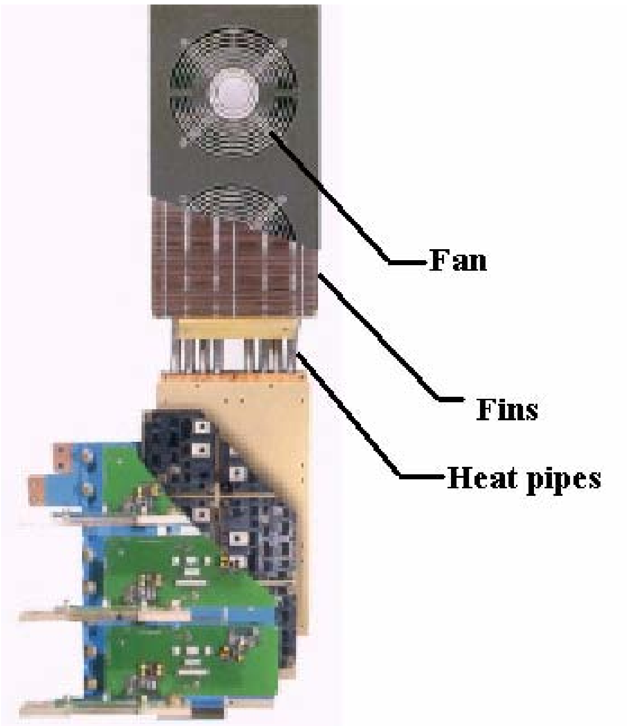

Figure 15.9 Multi-Kilowatt heat pipe assembly

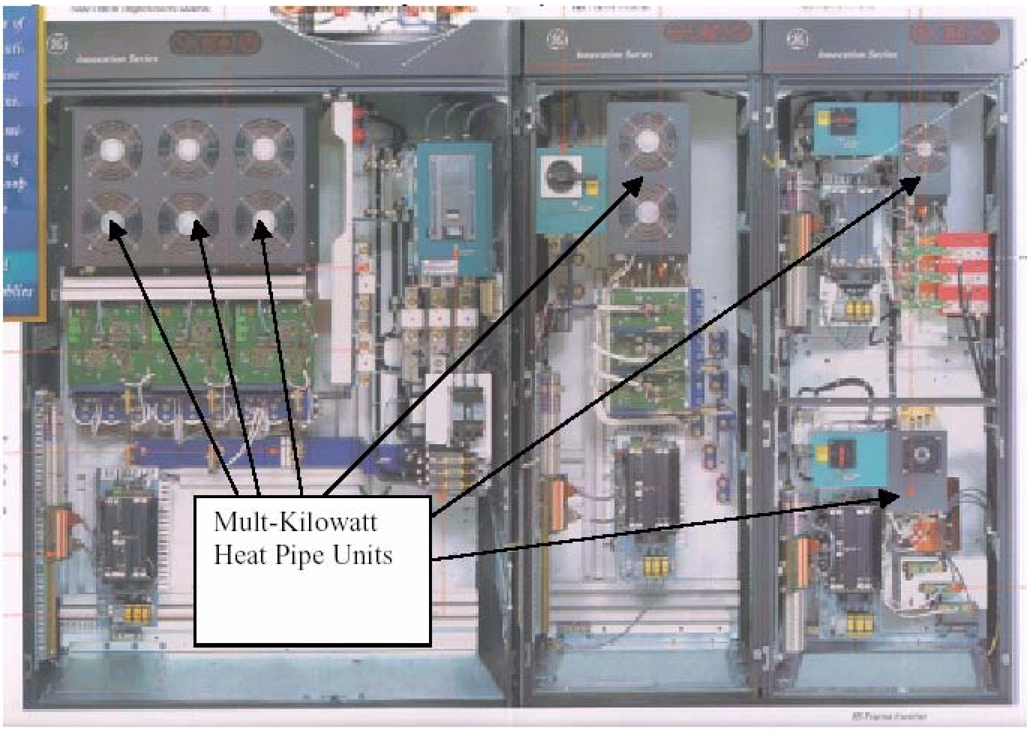

Figure 15.10 Multi-Kilowatt heat pipe units mounted in a motor drive cabinet

15.6 Heat Pipe Performance

Heat pipe performance is a function of the size of the evaporator and condenser areas, wick construction, fluid media and pipe orientation.

The operating temperature and energy transfer performance of a heat pipe is a function of its working fluid. Fluids that have a high latent heat of vaporization λ, high surface tension σ and a low viscosity are considered viable candidates. The relative performance of a fluid in terms of its ability to optimize flow can be assessed using the relation ship

$$\mathrm{Pr}\, ormance\ \ (Pf) = \frac{\lambda\, \sigma}{\nu}$$

Table 15.3 Characteristics of a few common fluids

Property	Ammonia	Water	Freon 21	Sulfur Dioxide	Mercury
Operating Range (°F)	−50 to 125	40 to 450	−20 to 200	15 to 110	400 to 820
Surface Tension σ, lb/ft	0.00124	0.005	0.00062	0.001	0.0322
Heat of Vaporization λ, BTU/lb	508.	980.	62	149	128
Kinematic Viscosity ν, ft^2/hr	0.014	0.038	0.0076	0.011	0.00414
Performance Factor p_f, $\frac{\text{BTU hr}}{\text{ft}^3}$	45.	129.	5.	13.	996.

The energy transferred at the evaporator in terms of the wick flow rate $\dot{m}_{wick}$ is

$$Q_{evap} = \lambda\, \dot{m}_{wick}$$

The flow rate depends upon the cross-sectional wick area and porosity in addition to the density and capillary diffusion rate of the fluid. Porosity also influences pipe performance at different orientations. A variety of wick structures may be used, including screen or woven wire meshes, sintered powders extruded grooves along the inside length of the pipe wall. Designs that increase the flow rate experience an attendant increased capability for thermal energy transfer.

15.7 Case Studies

- Show the effect of fluid media on heat pipe performance.
- Show the effect of orientation of heat pipe on its performance.

16. Heat Pipes in Electronics Cooling (2)

16.1 Pulsating Heat Pipes

16.1.1Introduction

Conventional heat pipe technology has been successfully applied in the last thirty years for the thermal management of a variety of applications like heat exchangers, economizers, space applications, and electronics cooling, to cite a few .

Although a plethora of designs of classical heat pipes are available, recent industry trends have frequently shown the limitations of these conventional designs. This has led to the evolution of novel concepts fitting the needs of present industry demands. A relatively new and emerging technology, Pulsating or Loop-type Heat Pipes (PHP), as proposed by Akachi, represent one such field of investigation. This range of devices is projected to meet all present and possibly future specific requirements of the electronics cooling industry, owing to favorable operational characteristics coupled with relatively cheaper costs.

Although grouped as a subclass of the overall family of heat pipes, the subtle complexity of internal thermo-fluidic transport phenomena is quite unique, justifying the need for a completely different research outlook. A comprehensive theory of operation and a reliable database or tools for the design of PHPs according to a given microelectronics-cooling requirement still remain unrealized. Nevertheless, the prospects are too promising to be ignored.

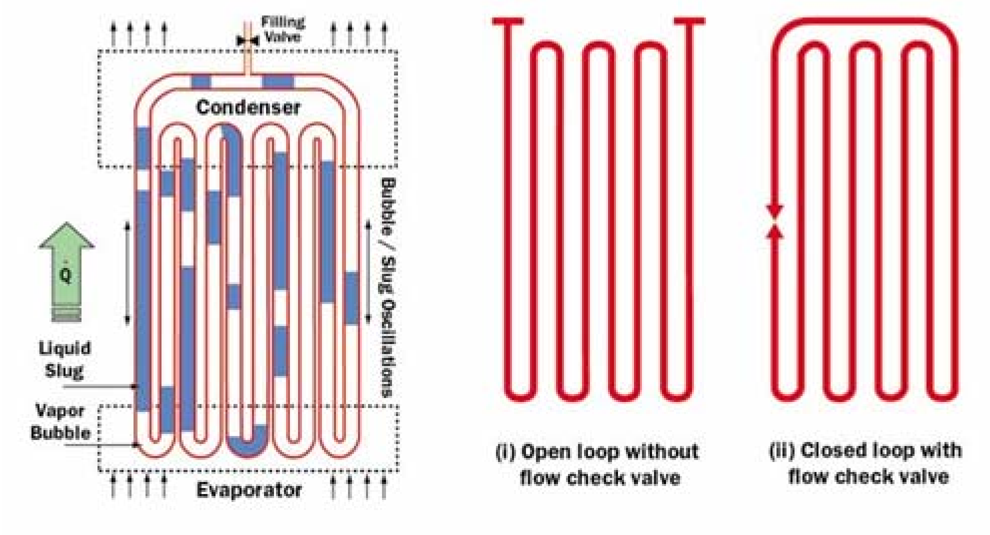

(a) (b)

Figure 16.1:
(a) Schematic of a closed loop pulsating heat pipe without check valve
(b) Two types of possible layouts (i) Open loop (ii) Closed loop

16.1.2 Construction Details

A PHP consists of a plain meandering tube of capillary dimensions with many U-turns (Figure 16.1a). In contrast to a conventional heat pipe, there is no additional capillary structure inside the tube. There are two ways to arrange the tube: open loop and closed loop. As the names suggest, in a closed loop structure, the tube is joined end-to-end (Figure 16.1b). The tube is first evacuated and then filled partially with a working fluid, which distributes itself naturally in the form of liquid-vapor plugs and slugs inside the capillary tube. One end of this tube bundle receives heat, transferring it to the other end by a pulsating action of the liquid-vapor/bubble-slug system. There may exist an optional adiabatic zone in between. Also, one or more flow-direction control check valves may be introduced at suitable locations to augment the performance. Figure 16.2 represents some practical design variations as proposed in.

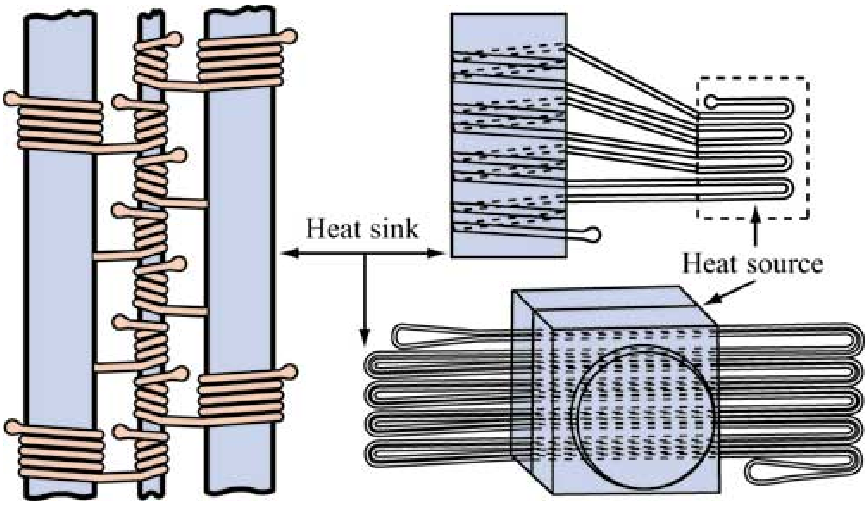

Figure 16.2: Some practical design variations of pulsating heat pipes.

16.1.3 Operational Features

A PHP is a complex heat transfer device with a strong thermo-hydraulic coupling governing its performance. It is essentially a non-equilibrium heat transfer device. The performance success of the device primarily depends on the continuous maintenance or sustenance of these non-equilibrium conditions within the system. The liquid and vapor slug transport results because of the pressure pulsations caused in the system. Since these pressure pulsations are fully thermally driven, because of the inherent constructions of the device, there is no external mechanical power source required for the fluid transport.

Consider a case when a PHP is kept isothermal throughout, say at room temperature. In this case, the liquid and vapor phases inside the device must exist in equilibrium at the saturated pressure corresponding to the fixed isothermal temperature. Referring to the pressure-enthalpy diagram, Figure 16.3, the thermodynamic state of all the liquid plugs, irrespective of their size and position, can be represented by point A. Similarly point B represents the thermodynamic state of all the vapor bubbles present in the PHP.

Suppose the temperature of the entire PHP structure is now quasi-statically increased to a new constant value. Then the system will again come to a new equilibrium temperature and corresponding saturation pressure, point A' and point B', in Figure 16.3. In doing so, there will be some evaporation mass transfer from the liquid until equilibrium is reached again. A similar phenomenon will be observed if the system is quasi-statically cooled to a new equilibrium condition A" and B".

In an actual working PHP, there exists a temperature gradient between the evaporator and the condenser section. Further, inherent perturbations are always present in real systems as a result of:

- Pressure fluctuations within the evaporator and condenser sections due to the local non uniform heat transfer always expected in real systems.
- Unsymmetrical liquid-vapor distributions causing uneven void fraction in the tubes.
- The presence of an approximately triangular or saw-tooth alternating component of pressure drop superimposed on the average pressure gradient in a capillary slug flow due to the presence of vapor bubbles.

The net effect of all these temperature gradients within the system is to cause non-equilibrium pressure condition which, as stated earlier, is the primary driving force for thermo-fluidic transport. As shown in

Figure 16.3, heating at the evaporator continuously tries to push point A upwards on the liquid saturation line of the pressure-enthalpy diagram. Simultaneously, point B is forced to move downwards on the vapor line at the other end.

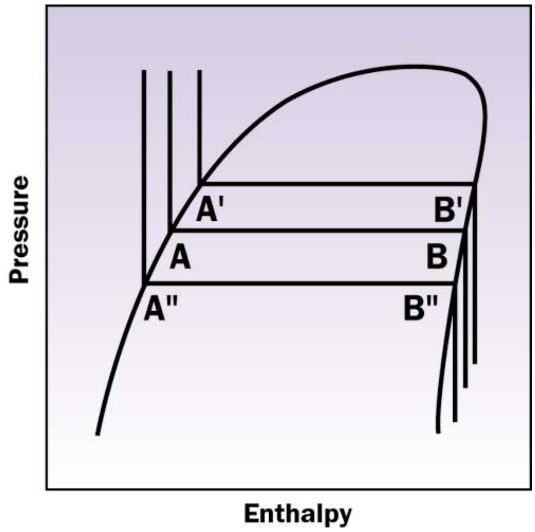

Figure 16.3: Typical pressure-enthalpy diagram

In this way a sustained non-equilibrium state exists between the driving thermal potentials and the natural causality, which tries to equalize the pressure in the system. Thus, a self-sustained thermally driven oscillating flow is obtained in a PHP. Note that no "classical steady state" occurs in PHP operation. Instead pressure waves and pulsations are generated in each of the individual tubes which interact with each other possibly generating secondary and ternary reflections with perturbations. From a force balance of gravity and surface tension leading to the definition of the Eötvös number, the theoretical maximum tolerable inner diameter (d_{crit}) of a PHP capillary tube can be calculated as:

$$d_{crit} = 2\sqrt{\sigma / g\left(\rho_{liq} - \rho_{vap}\right)} \quad or \quad E\ddot{o} = (Bo)^2 = 4$$

Where:

Bo	Bond number = d • (g(ρ liq - ρ vap)/ σ)$^{0.5}$
D	Tube internal diameter (m)
Eö	Eötvös number = $(Bo)^2$
G	Acceleration due to gravity (m/s^2)
σ	Surface tension (N/m)
ρ	Liquid density ($kg/m^{3)}$

At diameters below this value, there is a tendency for surface tension forces to predominate, and this assists in formation of stable liquid slugs, an essential prerequisite for PHP operation. In vertical orientation, slug flow is known to exist even at bigger diameters in devices such as a standard bubble pump, depending on the heat flux. In horizontal flow, there exists a greater possibility of flow stratification as the diameter of the tube increases. In the light of these facts, the PHP critical diameter, as suggested above, requires further investigation to be established as a design rule.

13.1.4 Design Parameters

Various experimental investigations have been done with the aim of making a parametric study of a PHP. These studies indicate the following main variables affecting PHP performance:

- **Geometric Variables**: Overall length of the PHP, diameter/size and shape of the tube, length and number of turns of evaporator/condenser/adiabatic section.
- **Physical Variables:** Quantity of the working fluid (filling ratio), physical properties of the working fluid, tube material.

- **Operational Variables:** Open loop or closed loop operation, heating and cooling methodology, orientation of the PHP during operation, use of check valves.

It is evident that there are multiple variables which simultaneously affect the operation and performance of PHPs. Further, so far as capillary slug flow exists inside the entire device, it has been demonstrated that latent heat will not play a significant role in the device performance. Nevertheless, bubbles are certainly needed for self-sustained thermally driven oscillations.

On the other hand, under certain operating conditions, flow pattern transition to annular flow may occur. The probability of such an event is high with a combination of a high Eötvös number, high heat flux, and comparatively low liquid filling ratio (≈ 50% or lower). Note that if a flow regime changes from slug to annular, the respective roles of the latent and sensible heat transport mechanism may change considerably. This aspect requires further investigation.

So, the performance not only depends on a large number of parameters described above, but also on the flow pattern. This makes it all the more difficult to undertake mathematical modeling using conventional techniques.

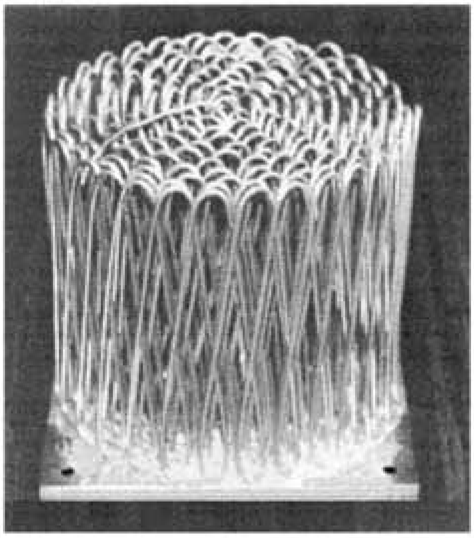

Base plate = 80mm x 80mm x 2mm

Heat thoughput capacity = 450W

At a temperature difference = 40 °C

Air velocity = 3 m/s

Thermal resistance = 0.089 °C/W

Tube outside diameter = 1.6 mm

Tube inter nal diameter = 1.2 mm

Number of capillary turns = 500

Figure16. 4: A typical 'Kenzan Fin' and its performance data.

16.1.5 Typical Performance Data

Figure 16.4 shows a typical pulsating heat pipe, also referred to as "Kenzan Fin" which has been applied for cooling multi-chip modules. The thermal performance data is also included. The advantages of such systems can be summarized as follows:

- Compared to solid metal fins, this type of fin structure is certainly light weight.
- If optimal operation is achieved, this fin structure is thermally an order of magnitude better than equivalent solid fins even with an air cooling option.
- As the tube diameter is reduced, thermal performance of wicked conventional heat pipes is drastically reduced, while there is a parallel increase in manufacturing complexity and cost.

The latter fact is clear from Figure 16.5, which shows the maximum thermal performance of conventional wicked copper-water heat pipes of internal diameters 3 mm, 2.5 mm and 2.0 mm respectively in vertical orientation. In addition, PHPs have an edge over conventional wicked heat pipes as they are not limited by capillary or entrainment performance limits encountered in conventional heat pipes.

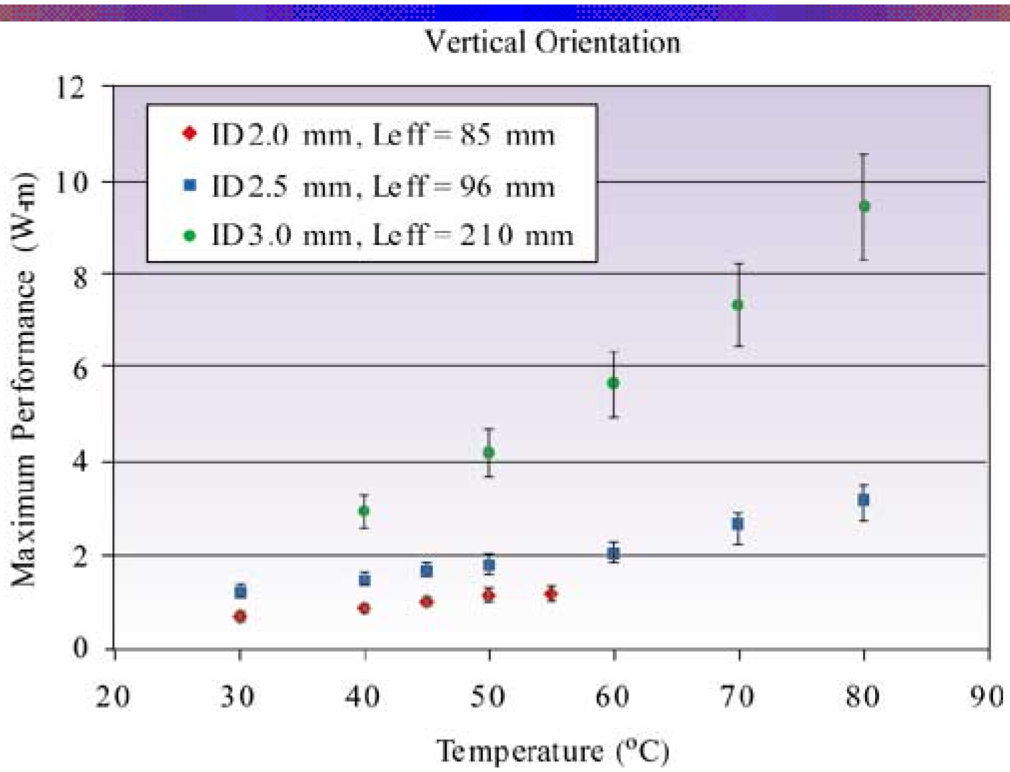

Figure 16.5: Maximum performance of miniature cylindrical copper-water conventional wicked heat pipes.

16.1.6 Conclusions

Pulsating Heat Pipes, apparently simple and very promising cooling devices, are very intriguing for theoretical and experimental investigations alike. They are attractive heat transfer elements, which due to their simple design, cost effectiveness, and excellent thermal performance may find wide applications. Since their invention in the early nineties, they have so far found market niches in electronics equipment cooling. Their complex operational behavior, which is not yet fully understood, has raised an ever growing academic interest. Until now, it has not been possible to simulate the PHP performances and there exists no complete engineering design tools.

16.2 Thermosyphons

16.2.1 Historical Development

The Thermosyphons was known as the Perkins tube was introduced by the Perkins family from the mid-nineteenth to the twentieth century through a series of patents in the United Kingdom. Most of the Perkins tubes were wickless gravity-assisted Thermosyphons, in which heat transfer was achieved by evaporation. The design of the Perkins tube, which is closest to the present heat pipe, was described in a patent by Jacob Perkins [1836]. A schematic drawing of the Perkins tube is shown in Figure 16.6 This design was a closed tube containing a small quantity of water operating in either a single- or two-phase cycle to transfer heat from a furnace to a boiler.

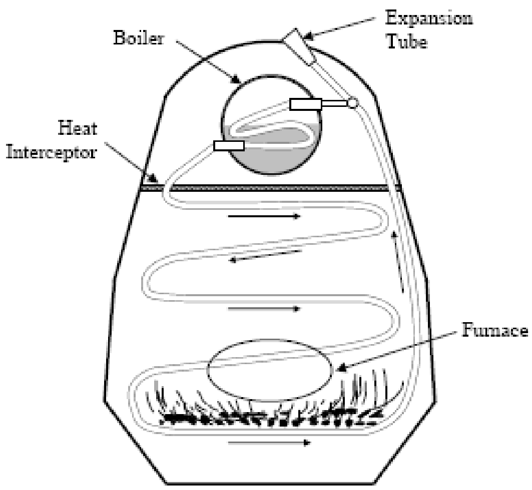

Figure 16.6: A schematic diagram of Perkins tube.

16.2.2 Principle of Operation

These are heat "transport" systems that use gravity to transfer heat (always gravity driven) from the source to sink or Thermosyphone refers to a heat transfer device in which the working fluid is circulated by the density difference between a cold temperature and a hot temperature fluid or between vapor and liquid, they can be put into a category of a cooling solution.
Thermosyphons transfer heat in exactly the same way as the Heat Pipe by evaporation followed by condensation. However no capillary structure is present to aid liquid transport from the condenser back to the evaporator, and thus the evaporator must be located vertically below the condenser, gravity will then ensure that the condensate returns to the evaporator.
To avoid the confusion because the term "Heat Pipe" is commonly used to describe both the Heat Pipe and Thermosyphone the term "Gravity Assisted Heat Pipe" has been used to describe Thermosyphons.

<u>The features of the system can be summarized as follows:</u>
- Requires no pump and reservoir/expansion tank, compared to closed loop cooling solutions.
- Can be made compact, so that the evaporator is the size of the module.
- Sensitive to orientation and internal fouling.
- Plumbed system, subject to shock/vibration, leakage, and potential dry-out

<u>The most common industrial Thermosyphon applications include:</u>
- Gas turbine blade cooling
- Electrical machine rotor cooling
- Transformer cooling
- Nuclear reactor cooling
- Steam tubes for baker’s oven
- Cooling for internal combustion engines
- Electronic cooling.

16.2.3 Different Structure of Modern Thermosyphons

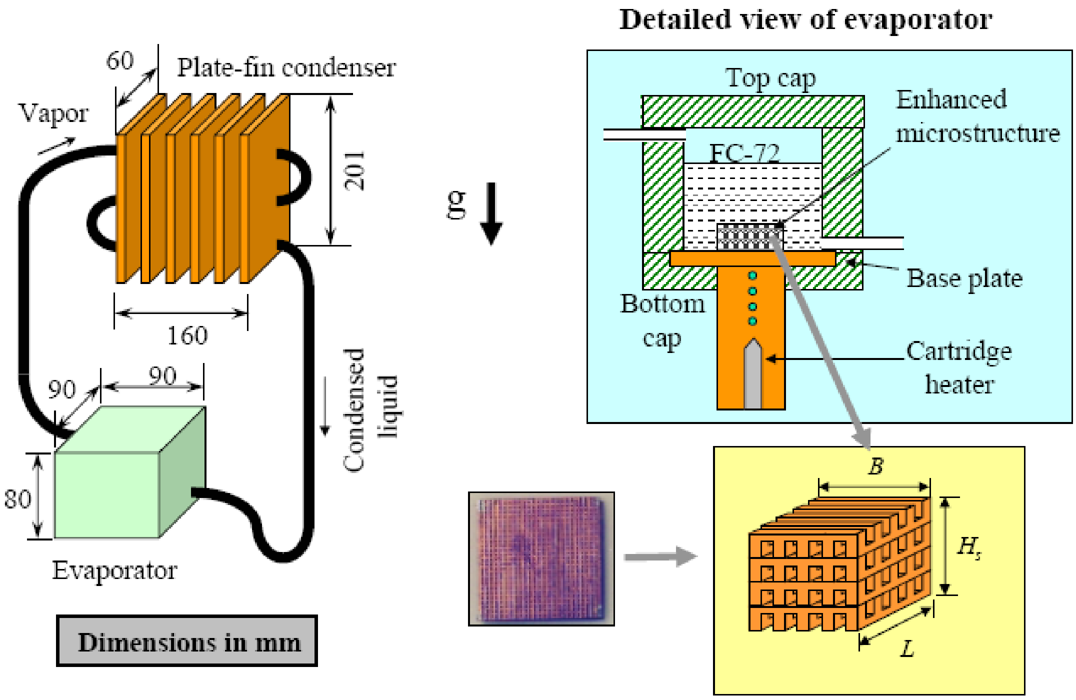

Figure 16.7: Thermosyphone incorporating enhanced structure.

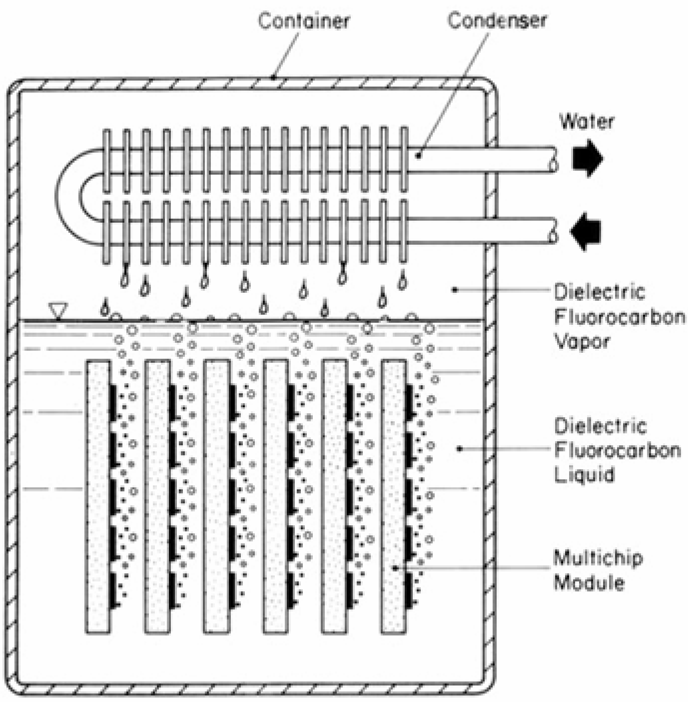

Figure 16.8: Water-Cooled multi chip module

16.2.4 Effect of Working Fluids

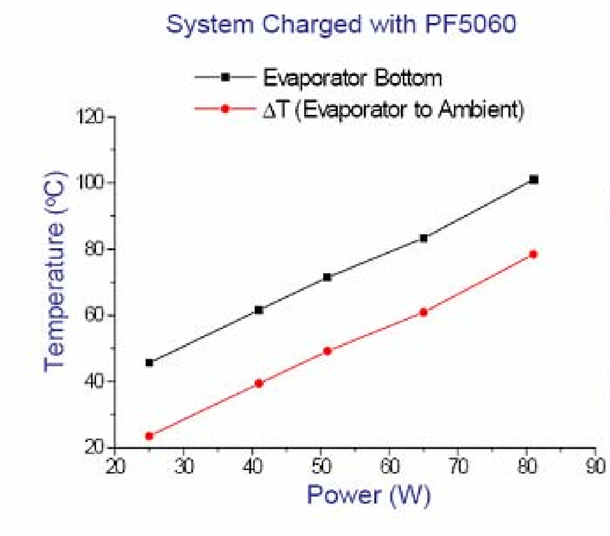

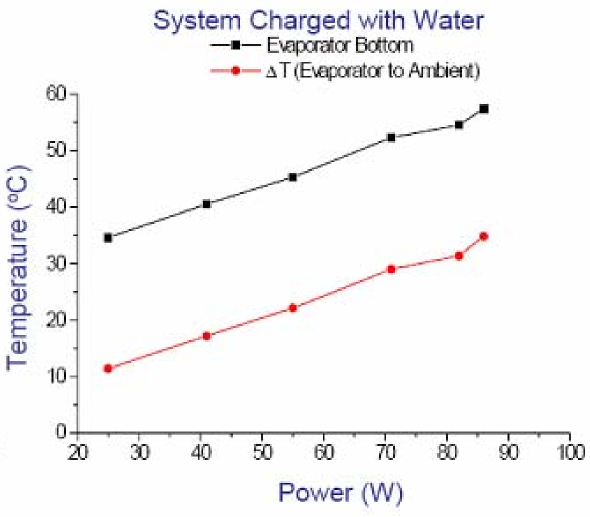

16.2.5 Effect of Inclination on the Thermosyphone

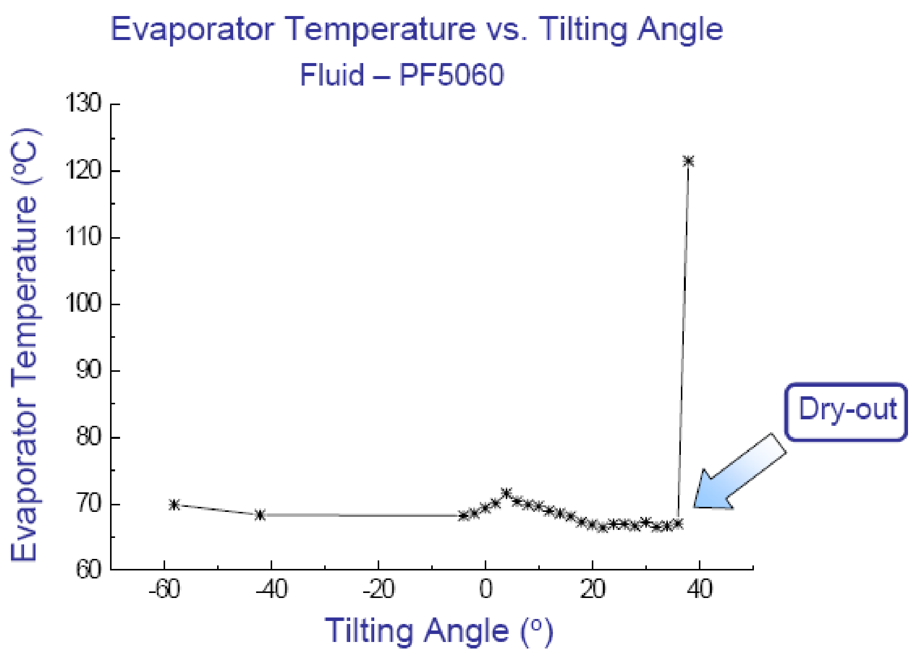

16.2.6 Comparison: Heat pipe and Thermosyphon

- Thermosyphon and heat pipe cooling both rely on evaporation and condensation. The difference between the two types is that in a heat pipe the liquid is returned from the condenser to the evaporator by surface tension acting in a wick, but Thermosyphon rely on gravity for the liquid return to the evaporator.
- However the cooling capacity of heat pipes is lower in general compared to the Thermosyphon with the same tube diameter.

16.2.7 Classification and Application of Thermosyphon System

- Open Thermosyphon
- Closed Thermosyphon
- Pipe Thermosyphon
  - Single-phase flow
  - Two-phase flow
- Simple loop Thermosyphon
  - Single-phase flow
  - Two-phase flow
- Closed advanced two-phase flow Thermosyphon loop

17. Thermoelectric Cooling

17.1 Historical Background

Although commercial thermoelectric modules were not available until almost 1960, the physical principles upon which modern thermoelectric coolers are based actually date back to the early 1800s.

The first important discovery relating to thermoelectricity occurred in 1821 when German scientist Thomas Seebeck found that an electric current would flow continuously in a closed circuit made up of two dissimilar metals, provided that the junctions of the metals were maintained at two different temperatures. Seebeck did not actually comprehend the scientific basis for his discovery, however, and falsely assumed that flowing heat produced the same effect as flowing electric current.

In 1834, a French watchmaker and part-time physicist, Jean Peltier, while investigating the Seebeck Effect, found that there was an opposite phenomenon where by thermal energy could be absorbed at one dissimilar metal junction and discharged at the other junction when an electric current flowed within the closed circuit. Twenty years later, William Thomson (eventually known as Lord Kelvin) issued a comprehensive explanation of the Seebeck and Peltier Effects and described their relationship. At the time, however, these phenomena were still considered to be mere laboratory curiosities and were without practical application.

In the 1930s, Russian scientists began studying some of the earlier thermoelectric work in an effort to construct power generators for use at remote locations throughout their country. This Russian interest in thermoelectricity eventually caught the attention of the rest of the world and inspired the development of practical thermoelectric modules. Today's thermoelectric coolers make use of modern semiconductor technology in which doped semiconductor material takes the place of the dissimilar metals used in early thermoelectric experiments.
The Seebeck, Peltier and Thomson effects, together with several other phenomena, form the basis of functional thermoelectric modules.

17.2 Introduction

Thermoelectric are based on the Peltier Effect, The Peltier Effect is one of the three thermoelectric effects; the other two are known as the Seebeck Effect and Thomson Effect. Whereas the last two effects act on a single conductor, the Peltier Effect is a typical junction phenomenon.

Thermoelectric coolers are solid state heat pumps used in applications where temperature stabilization, temperature cycling, or cooling below ambient are required. There are many products using thermoelectric coolers, including CCD cameras (charge coupled device), laser diodes, microprocessors, blood analyzers and portable picnic coolers. This article discusses the theory behind the thermoelectric cooler, along with the thermal and electrical parameters involved.

Seebeck Effect

The conductors are two dissimilar metals denoted as material A and material B. The junction temperature at A is used as a reference and is maintained at a relatively cool temperature (T_C). The junction temperature at B is used as temperature higher than temperature T_C. With heat applied to junction B, a voltage (E_{out}) will appear across terminals T_1 and T_2 and hence an electric current would flow continuously in this closed circuit. This voltage as shown in Figure 17.1, known as the Seebeck EMF, can be expressed as

$$E_{out} = \alpha\,(T_H - T_C) \qquad (17.1)$$

Where:

- $\alpha = dE / dT = \alpha_A - \alpha_B$
- α is the differential Seebeck coefficient or (thermo electric power coefficient) between the two materials, A and B, positive when the direction of electric current is same as the direction of thermal current, in volts per ^oK.
- E_{out} is the output voltage in volts.
- T_H and T_C are the hot and cold thermocouple temperatures, respectively, in ^oK.

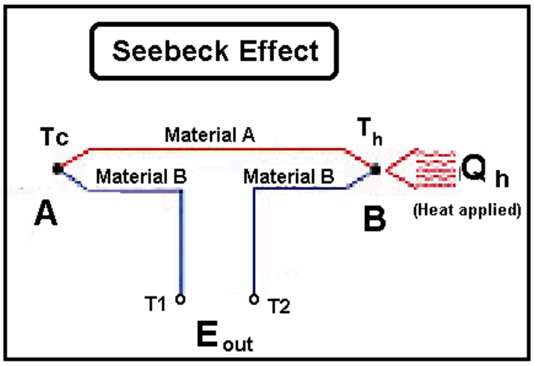

Figure 17.1 Seebeck effect

Peltier Effect

Peltier found there was an opposite phenomenon to the Seebeck Effect, whereby thermal energy could be absorbed at one dissimilar metal junction and discharged at the other junction when an electric current flowed within the closed circuit.

In Figure 17.2, the thermocouple circuit is modified to obtain a different configuration that illustrates the Peltier Effect, a phenomenon opposite that of the Seebeck Effect. If a voltage (Ei_n) is applied to terminals T_1 and T_2, an electrical current (I) will flow in the circuit. As a result of the current flow, a slight cooling effect (Q_C) will occur at thermocouple junction A (where heat is absorbed), and a heating effect (Q_H) will occur at junction B (where heat is expelled). Note that this effect may be reversed whereby a change in the direction of electric current flow will reverse the direction of heat flow. Joule heating, having a magnitude of $I^2 \times R$ (where R is the electrical resistance), also occurs in the conductors as a result of current flow. This Joule heating effect acts in opposition to the Peltier Effect and causes a net reduction of the available cooling. The Peltier effect can be expressed mathematically as

$$\begin{aligned} Q_C \text{ or } Q_H &= \beta \times I \qquad (17.2) \\ &= (\alpha\, T) \times I \end{aligned}$$

Where:

- β is the differential Peltier coefficient between the two materials A and B in volts.
- I is the electric current flow in amperes.
- Q_C and Q_H are the rates of cooling and heating, respectively, in watts.

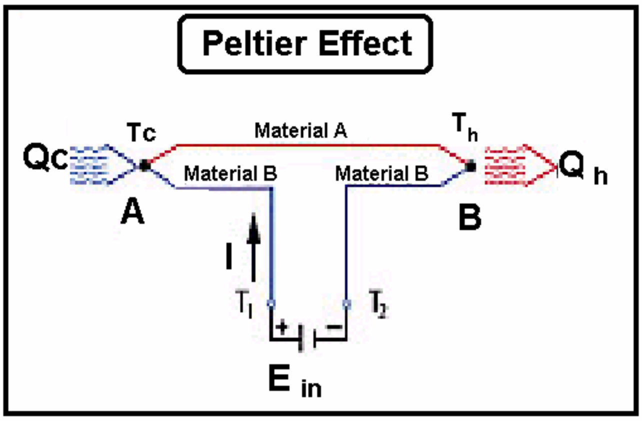

Figure 17.2 Peltier effect

Peltier coefficient β has important effect on Thermoelectric cooling as following:

a) β <0 ; Negative Peltier coefficient

High energy electrons move from right to left.

Thermal current and electric current flow in opposite directions

b) β >0 ; Positive Peltier coefficient

High energy holes move from left to right.

Thermal current and electric current flow in same direction

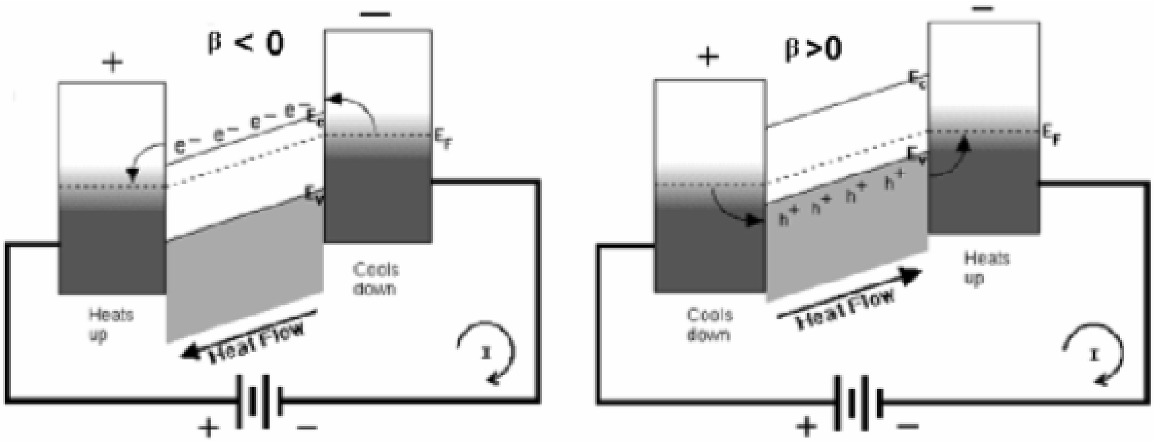

a) -ve Peltier coefficient b)+ve Peltier coefficient

Figure 17.3 Effect of Peltier coefficient on cooling Process

Thomson Effect

William Thomson, who described the relationship between the two phenomena, later issued a more comprehensive explanation of the Seebeck and Peltier effects. When an electric current is passed through a conductor having a temperature gradient over its length, heat will be either absorbed by or expelled from the conductor. Whether heat is absorbed or expelled depends on the direction of both the electric current and temperature gradient. This phenomenon is known as the Thomson Effect.

17.3 Thermoelectric Principle of Operation

The typical thermoelectric module is manufactured using two thin ceramic wafers with a series of P and N doped bismuth-telluride semiconductor material sandwiched between them as shown in Figure 17.4. The ceramic material on both sides of the thermoelectric adds rigidity and the necessary electrical insulation. The N type material has an excess of electrons, while the P type material has a deficit of electrons. One P and one N make up a couple, as shown in Figure 17.5. The thermoelectric couples are electrically in series and thermally in parallel. A thermoelectric module can contain one to several hundred couples.

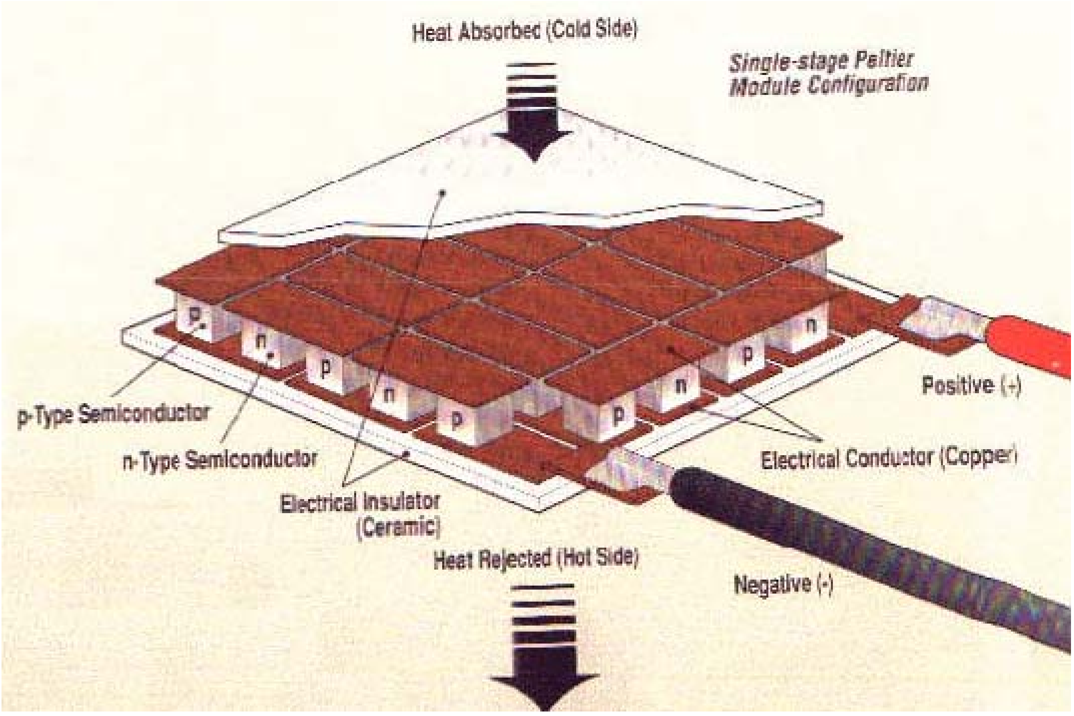

Figure17. 4 TEC Principle of operation

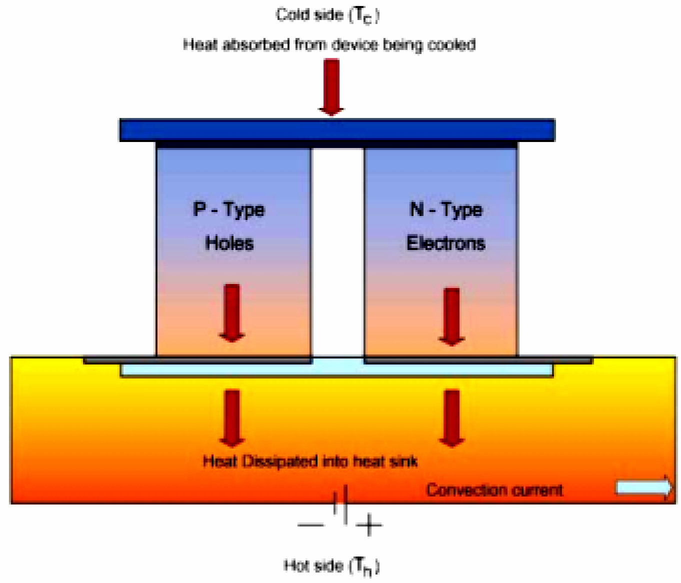

Figure 17.5 Cross section of a thermoelectric cooler

As the electrons move from the P type material to the N type material through an electrical connector, the electrons jump to a higher energy state absorbing thermal energy (cold side). Continuing through the lattice of material; the electrons flow from the N type material to the P type material through an electrical connector dropping to a lower energy state and releasing energy as heat to the heat sink (hot side).

Thermoelectric can be used to heat and to cool, depending on the direction of the current. In an application requiring both heating and cooling, the design should focus on the cooling mode. Using a thermoelectric in the heating mode is very efficient because all the internal heating (Joulian heat) and the load from the cold side is pumped to the hot side. This reduces the power needed to achieve the desired heating.

17.4 Thermal Analysis and Parameters Needed

The appropriate thermoelectric for an application, depends on at least three parameters. These parameters are the hot surface temperature (T_h), the cold surface temperature (T_c), and the heat load to be absorbed at the cold surface (Q_C).

The hot side of the thermoelectric is the side where heat is released when DC power is applied. This side is attached to the heat sink. When using an air cooled heat sink (natural or forced convection) the hot side temperature and its heat transferred can be found by using Equations 17.3 and 17.4.

$$T_h = T_{amb} + \theta\, Q_h \qquad (17.3)$$

Where:

- T_h = the hot side temperature (°C).
- T_{amb} = the ambient temperature (°C).
- θ = Thermal resistance of heat exchanger (°C/watt).

And

$$Q_h = Q_C + P_{in} \qquad (17.4)$$

$$COP = Q_C / P_{in} \qquad (17.5)$$

Where:

- Q_h = the heat released to the hot side of the thermoelectric (watts).
- Q_C = the heat absorbed from the cold side (watts).
- P_{in} = the electrical input power to the thermoelectric (watts).
- COP = coefficient of performance of the thermoelectric device, typically is between 0.4 and 0.7 for single stage applications.

Estimating Q_C, the heat load in watts absorbed from the cold side is difficult, because all thermal loads in the design must be considered. Among these thermal loads are:

1. <u>Active:</u>

i. I^2R heat load from the electronic devices

ii. Any load generated by a chemical reaction

2. <u>Passive:</u>

i. Radiation (heat loss between two close objects with different temperatures)

ii. Convection (heat loss through the air, where the air has a different temperature than the object)

iii. Insulation losses

iv. Conduction losses (heat loss through leads, screws, etc.)

v. Transient load (time required to change the temperature of an object)

By energy balance across the hot and cold junction it produces

$$Q_h = (\alpha\, T_h) \times I - C\,(T_h - T_c) + I^2 R/2 \qquad (17.6)$$

$$Q_C = (\alpha\, T_c) \times I - C\,(T_h - T_c) - I^2 R/2 \qquad (17.7)$$

$R = R_A + R_B$
$C = (k_A + k_B)\,(A/L)$

To get the max the heat absorbed from the cold side (Q_C); by differentiate the Q_c to the electric current I,

$$d\,Q_c / d\,I = 0$$

Then it produces

$$I_{opt.} = \alpha\, T_c / R$$

Substitute for $I_{opt.}$ In Equation 17.7 to get the max the heat absorbed from the cold side

$$Q_C\,(\max) = [(Z\, T_c^{\,2})/2 - (T_h - T_c)]\, C \qquad (17.8)$$

Where:

Z = Figure of merit for the material A and B
$= \alpha^2 / R\,C$

The cold side of the thermoelectric is the side that gets cold when DC power is applied. This side may need to be colder than the desired temperature of the cooled object. This is especially true when the cold side is not in direct contact with the object, such as when cooling an enclosure.

The temperature difference across the thermoelectric (ΔT) relates to T_h and T_c according to Equation 17.9.

$$\Delta T = T_h - T_c \qquad (17.9)$$

The thermoelectric performance curves in Figures 17.6 and 17.7 show the relationship between ΔT and the other parameters.

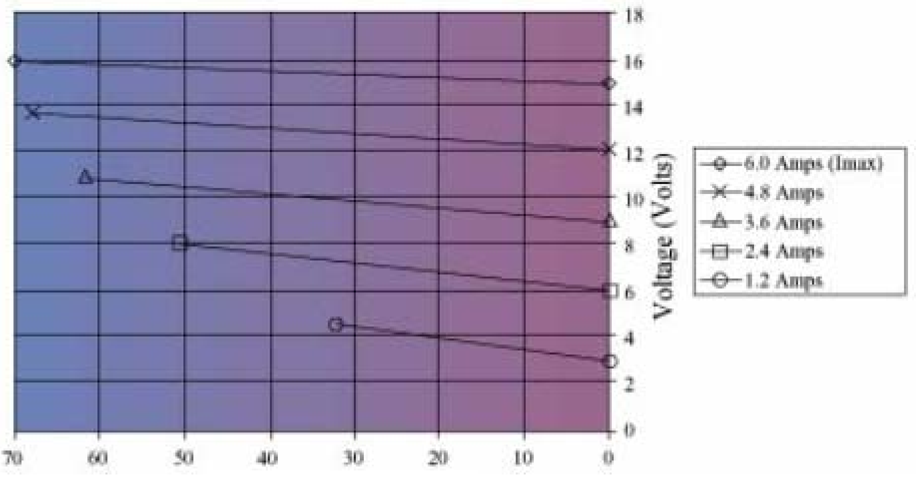

ΔT (^{O}C)

Figures 17.6 Performance curve (ΔT vs. Voltage)

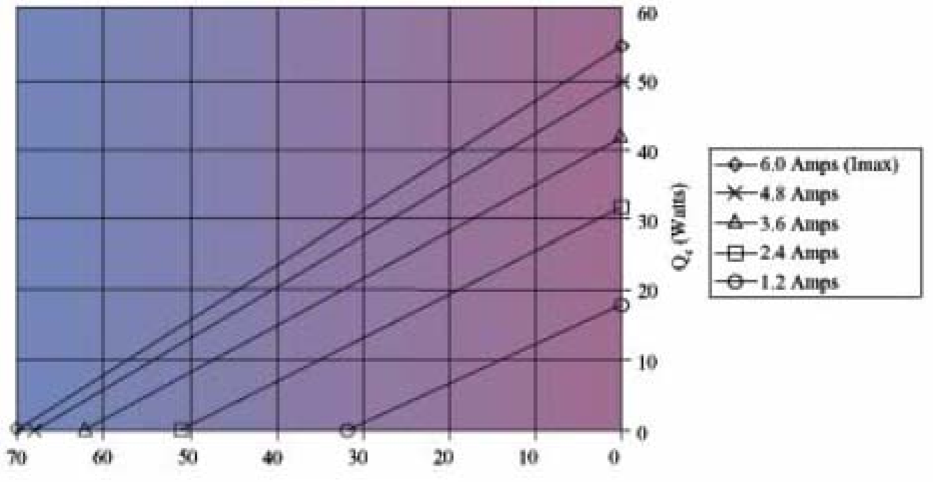

Figures 17.7 Performance curve (ΔT vs. Q_C)

Example:
A thermoelectric cooling system is to be designed to cool a PCB through cooling a conductive plate mounted on the back surface of the PCB. The thermoelectric cooler is aimed to maintain the external surface of the plate at 40 °C, when the environment is 48 °C. Each thermoelectric element will be cylindrical with a length of 0.125 cm and a diameter of 0.1 cm. The thermoelectric properties are:

	p	n
α (V/K)	170×10^{-6}	-190×10^{-6}
ρ (Ω.cm)	0.001	0.0008
k (W/cm K)	0.02	0.02

Assume the cold junction at 38 °C and the warm junction at 52 °C, and the electrical resistance of the leads and junctions = 10 % of the element resistance and design for maximum refrigeration capacity. If 10 W are being dissipated through the plate and steady-state conditions then

Determine:
1- Number of couples required.
2- Rate of heat rejection to the ambient.
3- The COP.
4- The voltage drop across the d.c. power source.

Solution:
$T_h = 52\ ^oC = 325$ K
$T_c = 38\ ^oC = 311$ K
d = 0.1 cm
L = 0.125 cm
$A = (\pi/4)(0.1)^2 = 7.854 \times 10^{-3}$ cm^2

Overall electric resistance (R) $= R_{element} + R_{junction}$
$= 1.1\ R_{element}$
$= 1.1(\rho_p + \rho_n)\ (L/A)$
$= 1.1\ (0.001 + 0.0008)\ (0.125 / 7.854 \times 10^{-3})$
$= 0.0315\ \Omega$

Conduction coefficient (C) = $(k_p + k_n)$ (A/L)
$= (0.02 + 0.02)\ (7.854 \times 10^{-3} / 0.125)$
$= 2.513 \times 10^{-3}$ W/K

Figure of merit (Z) = $(\alpha_p - \alpha_n)^2 / RC$
$= (360 \times 10^{-6})^2 / (0.0315 \times 2.513 \times 10^{-3})$
$= 1.636 \times 10^{-3}\ K^{-1}$

1- Number of couples required.

$Q_C = Q_C\ (max) = N\ C\ [(Z\ T_c^2)/2 - (T_h - T_c)]$
$10 = N\ (2.513 \times 10^{-3})\ [0.5\ (1.636 \times 10^{-3} \times (311)^2) - (14)]$
$N \approx 62$ couples

2- Rate of heat rejection to the ambient (Q_h).

$I_{opt.} = (\alpha_p - \alpha_n)\ T_c / R$
$= (360 \times 10^{-6}) \times 311 / 0.0315$
$= 3.55$ A

Then

$Q_h = N\ [(\alpha_p - \alpha_n)\ T_h \times I_{opt} - C\ (T_h - T_c) + I^2_{opt}\ R/2]$
$= 62\ [(360 \times 10^{-6})\ 325 \times 3.55 - 2.513 \times 10^{-3}\ (14) + (3.55)^2\ 0.0315/2]$
$= 35.8$ W

3- The COP.

$COP = Q_C / P_{in}$
P_{in} (Power input by power source to the thermoelectric) = $Q_h - Q_C$
$= 35.8 - 10 = 25.8$ W

$COP = 10 / 25.8$
$= 0.386$

4- The voltage drop across the d.c. power source.

The voltage drop (ΔV) = P_{in} / I
$= 25.8 / 3.55$
$= 7.27$ volt

17.5 Powering the Thermoelectric

All thermoelectric are rated for I_{max}, V_{max}, Q_{max}, and ΔT_{max}, at a specific value of T_h. Operating at or near the maximum power is relatively inefficient due to internal heating (Joulian heat) at high power. Therefore, thermoelectric generally operate within 25% to 80% of the maximum current. The input power to the thermoelectric determines the hot side temperature and cooling capability at a given load.

As the thermoelectric operates, the current flowing through it has two effects:

i. the Peltier Effect (cooling)

ii. The Joulian Effect (heating). The Joulian Effect is proportional to the square of the current. Therefore, as the current increases, the Joule heating dominates the Peltier cooling and causes a loss in net cooling. This cut-off defines I_{max} for the thermoelectric.

For each device, Q_{max} is the maximum heat load that can be absorbed by the cold side of the thermoelectric. This maximum occurs at I_{max}, V_{max}, and with $\Delta T = 0°C$. The ΔT_{max} value is the maximum temperature difference across the thermoelectric. This maximum occurs at I_{max}, V_{max} and with no load ($Q_c = 0$ watts). These values of Q_{max} and ΔT_{max} are shown on the performance curve (Figures 17.7) as the end points of the I_{max} line.

17.6 Other Parameters to Consider

The material used for the assembly components deserves careful thought. The heat sink and cold side mounting surface should be made out of materials that have a high thermal conductivity (i.e., copper or aluminum) to promote heat transfer. However, insulation and assembly hardware should be made of materials that have low thermal conductivity (i.e., polyurethane foam and stainless steel) to reduce heat loss.

Environmental concerns such as humidity and condensation on the cold side can be alleviated by using proper sealing methods. A perimeter seal (Figure 17.8) protects the couples from contact with water or gases, eliminating corrosion and thermal and electrical shorts that can damage the thermoelectric module

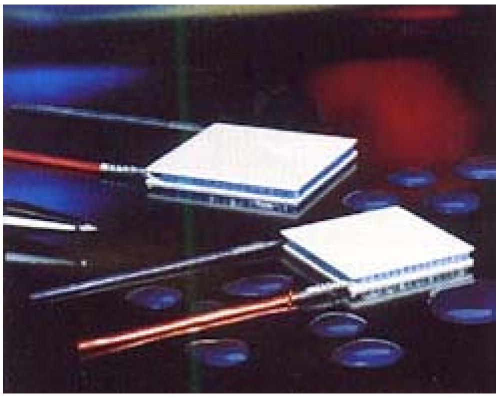

Figure 17.8 Typical thermoelectric with a perimeter seal

The importance of other factors, such as the Thermoelectric's footprint, its height, its cost, the available power supply and type of heat sink, vary according to the application.

17.7 Advantages of Thermoelectric Coolers

Thermoelectric modules offer many advantages including:

- No moving parts
- Small and lightweight
- Maintenance-free
- Acoustically silent and electrically “quiet”
- Heat or cool by changing direction of current flow
- Wide operating temperature range
- Highly precise temperature control (to within 0.1°C)
- Operation in any orientation, zero gravity and high G- levels
- Environmentally friendly
- Sub-ambient cooling

- Cooling to very low temperatures (-80 °C)

17.8 Reliability & Mean Time between Failures (MTBF)

Thermoelectric devices are highly reliable due to their solid state construction. MTBF calculated as a result of tests performed by various customers are on the order of 200,000 to 300,000 hours at room temperature. Elevated temperature (80 °C) MTBF is conservatively reported to be on the order of 100,000 hours.

17.9 Moisture and Vibration Effect

Moisture:

Moisture must not penetrate into the thermoelectric module area. The presence of moisture will cause an electro-corrosion that will degrade the thermoelectric material, conductors and solders. Moisture can also provide an electrical path to ground causing an electrical short or hot side to cold side thermal short. A proper sealing method or dry atmosphere can eliminate these problems.

Shock and Vibration:

Thermoelectric modules in various types of assemblies have for years been used in different Military/Aerospace applications. Thermoelectric devices have been successfully subjected to shock and vibration requirements for aircraft, ordinance, space vehicles, shipboard use and most other such systems. While a thermoelectric device is quite strong in both tension and compression, it tends to be relatively weak in shear. When in a sever shock or vibration environment, care should be taken in the design of the assembly to insure "compressive loading" of thermoelectric devices.

17.10 Comparison: Conventional Refrigeration

Because thermoelectric cooling is a form of solid-state refrigeration, it has the advantage of being compact and durable. A thermoelectric cooler uses no moving parts (except for some fans), and employs no fluids, eliminating the need for bulky piping and mechanical compressors used in vapor-cycle cooling systems.
Such sturdiness allows thermoelectric cooling to be used where conventional refrigeration would fail. In a current application, a thermoelectric cold plate cools radio equipment mounted in a fighter jet wingtip. The exacting size and weight requirements, as well as the extreme g forces in this unusual environment, rule out the use of conventional refrigeration.
Thermoelectric devices also have the advantage of being able to maintain a much narrower temperature range than conventional refrigeration. They can maintain a target temperature to within ±1° or better, while conventional refrigeration varies over several degrees.
Unfortunately, modules tend to be expensive, limiting their use in applications that call for more than 1 kW/h of cooling power. Owing to their small size, if nothing else, there are also limits to the maximum temperature differential that can be achieved between one side of a thermoelectric module and the other.
However, in applications requiring a higher ΔT, modules can be cascaded by stacking one module on top of another. When one module's cold side is another's hot side, some unusually cold temperatures can be achieved

17.11 Thermoelectric Multistage (Cascaded) Devices

A multistage thermoelectric device should be used only where a single stage device does not fill the need.

Given the hot side temperature, the cold side temperature and the heat load, a suitable thermoelectric can be chosen. If ΔT across the thermoelectric is less than 55 °C, then a single stage thermoelectric is sufficient. The theoretical maximum temperature difference for a single stage thermoelectric is between 65 °C and 70 °C.

If ΔT is greater than 55 °C, then a multistage thermoelectric should be considered. A multistage thermoelectric achieves a high ΔT by stacking as many as six or seven single stage thermoelectric on top of each other.

The two important factors are ΔT and C.O.P. should affect on selection of the number of stages. The following Figure 17.9 depicts ΔT, vs. C.O.P.max, vs. Number of stages at $T_h = 35\ ^oC$.

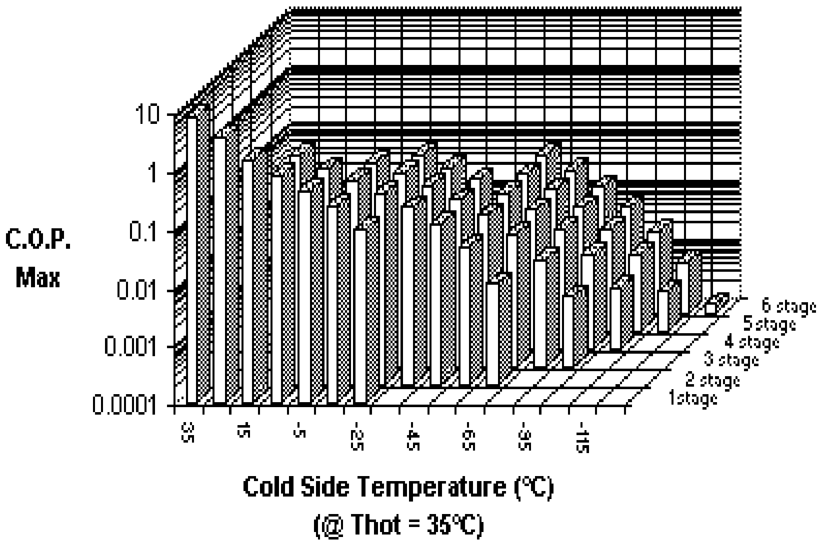

Figure 17.9 ΔT vs. C.O.P. Max as a function of stages

There is another very significant factor that must always be considered and that is the cost. Usually, as the number of stages increase, so does the cost. Certain applications require a trade-off between C.O.P. and cost.

17.12 Summary

Although there are a variety of applications that use thermoelectric devices, all of them are based on the same principle. When designing a thermoelectric application, it is important that all of the relevant electrical and thermal parameters be incorporated into the design process. Once these factors are considered, a suitable thermoelectric device can be selected based on the guidelines presented in this article.

18. Immersion Cooling

18.1 Passive Immersion Cooling

18.1.1 Introduction

This section presents an overview and guidelines far the packaging engineer and the subject of liquid immersion heal transfer of electronics. Power supplies, both law- and high-voltage, fall into this category, as do microcircuits having high heal density. The efficient heat transfer provided by nucleate and pool boiling has long been recognized as a superior cooling technique, but only recently base applications developed as a result of increased packaging flux densities.

Heat removal from electronic components has become a problem of significant interest due to the continuing reduction in feature size and increase in functional performance. A number of direct liquid immersion cooling techniques have recently been examined for removal of very high heat fluxes. For example, heat flux handling capabilities on the order of 200 W/cm^2 have been demonstrated with micro-channel heat sinks under flow boiling conditions. These high heat flux removal immersion cooling methods require an intimate contact between the coolant liquid and electronic components. Also, the use of forced convection, employed in many cases, increases design complexity and costs. These constraints are often unacceptable during product design and a strong need exists for the development of passive cooling techniques for removal of moderately high heat fluxes (up to 50 W/in^2).

Recent advances in material technology have resulted in several new materials with extremely high thermal conductivity. Fibers with unidirectional thermal conductivity of almost 1100W/m.K have been developed and used to produce composite materials in sheet form as potential substrate materials for electronic thermal management. In parallel to these advances in high thermal conductivity materials, efforts have been made to adapt several high performance thermal technologies to electronics cooling. An in-depth review of the saturated boiling process and the characteristic of common modes of boiling appear in foregoing sections.

18.1.2 Passive Immersion Module (PIM) Concept

Passive in that the module is a self-contained, sealed enclosure with no moving parts, where Electronic component(s) are immersed in the fluid contained within and the liquid acts as heat spreader to module cold plate, aided by vigorous boiling process.

The question now that why it is called "Passive immersion", and not "full immersion" or active immersion or whatever, Due to The passive cooler that doesn't use any pumps to move the fluid around, this system depend on free convection to work. Passive immersion cooling where there is physical walls separating the microelectronic chips and the surface of the substrate from the liquid coolant, Note that the electronics module to the customer can appear as an externally air-cooled “black box.” and no moving parts = increased reliability over pumped liquid systems.

The entire system components (except mechanical parts such as disk drives are submerged in specialized dielectric, non-corrosive, flouro-carbon based liquid. The liquid is cooled by a copper or aluminum cold plate. Heat is dissipated from the components directly into the liquid, and convection causes the heated liquid to move towards the colder liquid near the cold plate. Cooled liquid in turn flows down towards the components.

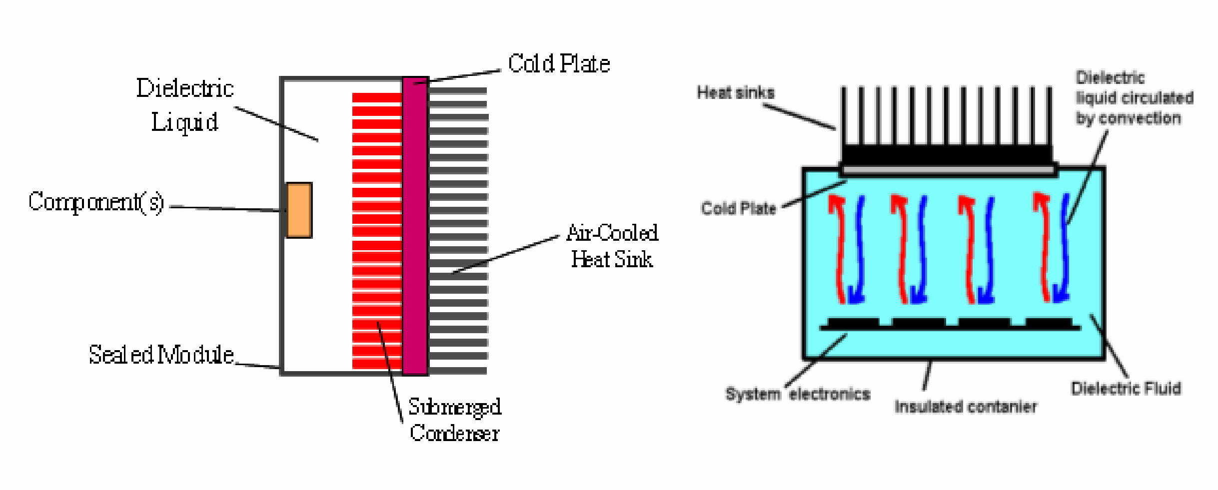

Figure 18.1 Passive immersion concepts

18.1.3 Types of Passive Immersion Cooling

Figure 18.2 illustrates the general types of liquid-filled packages; those basing vapor space above the components as in Figure 18.2a and b, and those that ate completely filled, as in Figure 18.2d and e. In same high voltage power supplies, as in Figure 18.2e, the space abuse the component is filled with a gas such as SF_6, which provide increased ace suppression at law temperature where the vapor dielectric properties are mush reduced. Packages that are completely fitted require an expansion device to account for volumetric changes of the fluid over temperature, whereas units with vapor space usually are designed to withstand both positive and negative pressure differentials caused by temperature and altitude changes in airborne applications. A completely filled unit in best foe heat transfer and voltage ace suppression, but it is heavy and requires a bellow: partially filled units on the other hand eliminate the need for bellows and may have poorer heat transfer and voltage suppression, especially when the components arc in the vapor space.

For all of the units depicted in Figure 18.2, the existence of some no condensable gas will degrade the thermal performance by impeding the heat transfer at the interfaces. It is good practice, therefore to pump the air from the package prior to filling and to degas the coolant since in many cases the liquid can absorb as much as 50 percent of its volume on gas at room temperature. Note that the condensers shown in Figure 18.2 are located either internal or external the package. In all eases the operating temperature of the liquid in related to the heat-sink or condenser temperature under steady-state conditions.

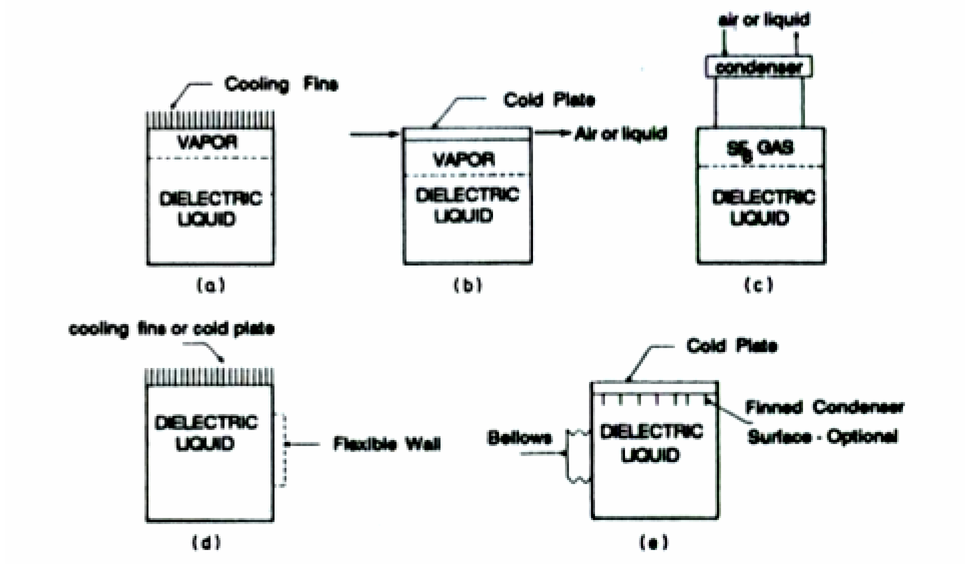

Figure 18.2 Types of liquid-filled enclosures. (a)Ambient cooled. (b) Forced convection cooled. (c) Forced convection cooled. (d) External condenser and (e) Filled enclosure

18.1.4 Passive Immersion Cooling Curve

The heat transfer process for immersion-canted components is explained by meant of Figure 18.3 (Liquid boiling curve), which illustrates the classical hailing curse with only alight modification. A heated microelectronics component immersed in liquid exhibits a superheat or temperature rise $\Delta T_{w\text{-}sat}$ from the wall to the liquid saturation temperature to a degree depending on the surface heat flux. At low flux levels, A to B, the heat transfer is by free convection with out phase change, and the natural convection film coefficient equations are applicable. Between B and C, an increase in flux level results in the formation of vapor bubbles and boiling occurs. Along this portion of the curve, higher heat flux rates produce activation of more nucleation sites with only small increase in temperature difference. The nucleate boiling regime from B to C in Figure 18.3 is characterized by a continuous stream of babbles, which travel from the component surface to the vapor interface in a partially filled enclosure or to the condenser surface in a filled unit. At C, the critical heat flux, or “burnout", is reached, and the component is completely blanketed with vapor. The babbles form so rapidly at the surface that a large increase in temperature results from C to D and beyond to the unstable region. Upon a reduction in heat flux rate, the operating point moves along to F and G and then along the nucleate boiling line to B.

Although the general shape of the curve in Figure 18.3 is common for the coolants used in immersion applications, the relative position of the curves are dependent on the coolant and the surface in contact. A surface treatment such as selective enchants and the depositions of alumina on silicon surface as well as the devotement of “dendridic” heat sinks are recent innovations introduced to increase the number of nucleation sites for improved heat transfer. Another phenomenon to be dealt with in boiling heat transfer is the hysteresis carve in Figure 18.3, identified as line BHI. This portion of the curve is less defined and shows a delay in nucleate boiling and an extension of the free-convection curve *AB.* Repeated test runs often result in lowering the incipience of boiling (paint H), as does surface treatment, and other means are used to promote nucleation at the surface.

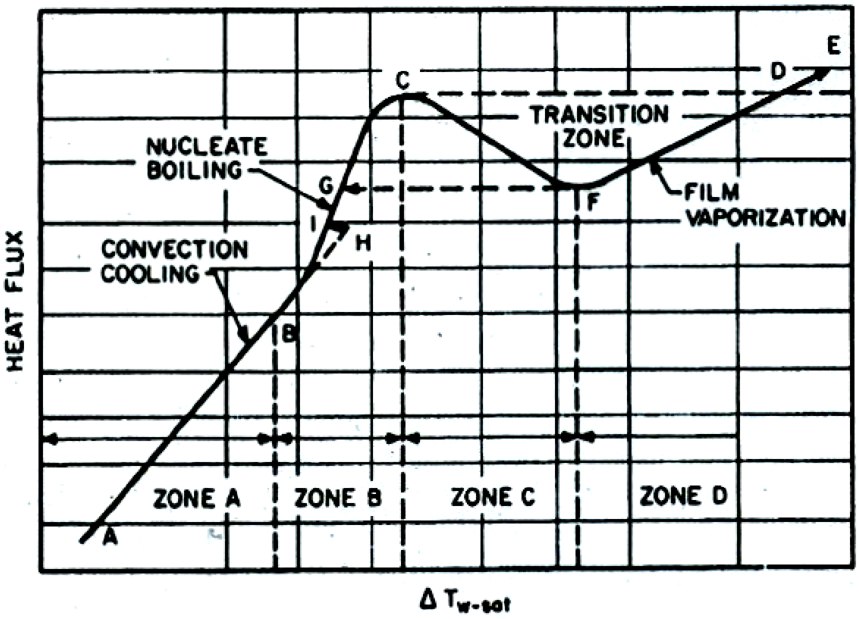

Figure 18.3 Liquid boiling curve

18.1.5 Advantage and Limitation

Advantages:

- Very wide operating temperature range
- Able to handle much larger heat loads than other methods
- Condensation on components is ruled out (they're submerged in a liquid)
- Absolutely silent

Disadvantages:

- Suitable dielectric fluid may be expensive
- Hardware upgrades are made difficult, since the module must be opened and drained to access the components.

Possible problems:

- If liquid on the component surfaces reaches boiling point (Many dielectric liquids have a low boiling point), gaseous bubbles could result, which although in theory would vastly increase heat transfer from the components due to the phase change, can lead to decreased efficiency if they accumulate on the surface of the cold plate. If it proves impossible to avoid bubbles then a means must be devised of condensing the bubbles back into liquid. One way of delaying the appearance of bubbles is to slightly increase pressure inside the module.
- It is possible that over time, the dielectric liquid will begin to lose its insulating properties, due to the introduction of impurities.

- If the liquid is to be super-cooled, then steps must be taken to prevent condensation on the outside of the module. The module must be well insulated to achieve this.

18.1.6 Design Guidelines

Free single-phase immersion cooling using a dielectric coolant such as Freon R-113, or a fluorocarbon such as FC-77, generally produces acceptable temperature rises for flux rates of under 5 W/cm^2 (32 W/in^2) higher flux rates results in nucleate boiling with mach smaller rates of temperature rise, that is, surface-to-liquid ΔT values, as the flux is increased compared in free-convection temperature rises.
The design of immersion cooling systems must include an examination of all of the internal heat

producing surfaces for maximum flux rates is order so maintain an adequate margin of safety with respect so the critical heal flux. Dielectric coolants suitable for immersion are typically those that exhibit large superheats of 10 to 30 ^{o}C; hence one mast sake account of this in designing liquid systems.

Fins used on component surfaces to enhance cooling efficiency as in pin grid array packages are best oriented in the horizontal or vertical planes for unrestricted heat transfer, as opposed to downward-facing surfaces, in which case bubble entrapment may lead to serious overheating, particularly in the case of high flux surfaces. Bubble escape is a necessary requirement in nucleate boiling in order to achieve free flow and liquid replacement near the boiling surface. The testing of enclosures using Plexiglas or glass windows can often reveal these trouble spots, which are correctable in the design phase. Surface treatment of cooled surfaces such as silicon to enhance nucleation can produce up to 50 percent increases in film coefficients us compared so smooth surfaces. Some common treatment methods include the following:

- Mechanical surface treatment. such us “vapor blasting’
- Etching techniques to roughen the surface
- Dendritic surface treatment to increase area-forming a brush of nickel powder with a magnet and plating the needles in place
- Laser treatment
- Machining microchannels or grooves into the surface

18.2 Active Immersion liquid cooling for High Power Density Microelectronics

18.2.1 Introduction

Since the development of the first electronic computers in the 1940s, the development of faster and denser circuit technologies and packages has been accompanied by increasing heat fluxes at the chip and package levels. Over the years, significant advances have been made in the application of air cooling techniques to manage increased heat fluxes. Although air cooling continues to be the most widely used method for cooling electronic packages, it has long been recognized that significantly higher heat fluxes can be accommodated through the use of liquid cooling as in active immersion liquid cooling. Applications of active immersion liquid cooling for microelectronics may be categorized as either indirect or direct.

Indirect liquid cooling is one in which the liquid does not contact the microelectronic chips, nor the substrate upon which the chips are mounted. In such cases a good thermal conduction path is provided from the microelectronic heat sources to a liquid cooled cold-plate attached to the module surface, as shown in Figure 18.4. Since there is no contact with the electronics, water can be used as the liquid coolant, taking advantage of its superior thermophysical properties.

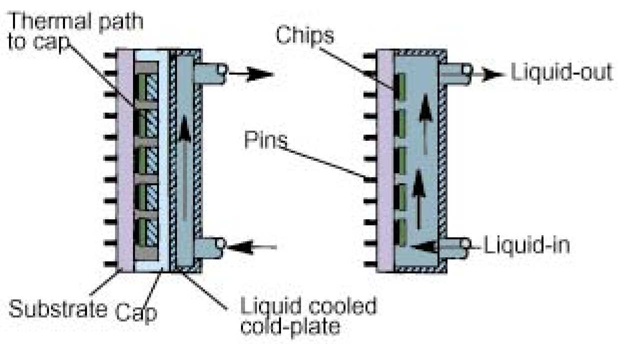

Figure 18.4 Example of indirect and direct liquid immersion cooling for a multi-chip module package

Direct liquid cooling, the focus of this article, may also be termed direct liquid immersion cooling, since there are no physical walls separating the microelectronic chips and the surface of the substrate from the liquid coolant. This form of cooling offers the opportunity to remove heat directly from the chip(s) with no intervening thermal conduction resistance, other than that between the device heat sources and the chip surfaces in contact with the liquid. Interest in direct liquid immersion as a method for cooling integrated circuit chips may be traced back as early as the 1960s.

Direct liquid immersion cooling offers a high heat transfer coefficient which reduces the temperature rise of the chip surface above the liquid coolant temperature. As shown in Figure 18.5, the relative magnitude of a heat transfer coefficient is affected by both the coolant and the mode of convective heat transfer (i.e. natural convection, forced convection, or boiling). Water is the most effective coolant and the boiling mode offers the highest heat transfer coefficient. Direct liquid immersion cooling also offers greater uniformity of chip temperatures than is provided by air cooling.

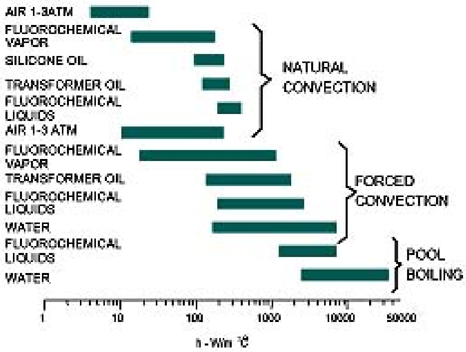

Figure 18.5 Relative magnitude of heat transfer coefficients for various coolants and modes of convection

18.2.2 Coolant Considerations

The selection of a liquid for direct immersion cooling cannot be made on the basis of heat transfer characteristics alone. Chemical compatibility of the coolant with the chips and other packaging materials exposed to the liquid must be a primary consideration.

There may be several coolants which can provide adequate cooling, but only a few will be chemically compatible. Water is an example of a liquid which has very desirable heat transfer characteristics, but which is generally unsuitable for direct immersion cooling on account of its chemical characteristics. Fluorocarbon liquids (e.g. FC-72, FC-86, FC-77, etc.) are generally considered to be the most suitable liquids for direct immersion cooling, in spite of their poorer thermo-physical properties.

As shown in Table 18.1, the thermal conductivity, specific heat, and heat of vaporization of fluorocarbon coolants are lower than water. These coolants are clear, colorless per-fluorinated liquids with a relatively high density and low viscosity. They also exhibit a high dielectric strength and a high volume resistivity. The boiling points for the commercially available "Fluorinert" liquids manufactured by the 3M Company, range from 30 to 253 °C.

Table18. 1 Comparison of thermophysical properties of fluorocarbon coolants and water

PROPERTY	FC-87	FC-72	FC-77	H_2O
Boiling Point @ 1 Atm (°C)	30	56	97	100
Density x 10^{-3} (kg/m^3)	1.633	1.680	1.780	0.997
Specific Heat x 10^{-3} (w-s/kg-K)	1.088	1.088	1.172	4.179
Thermal Conductivity (w/m-K)	0.0551	0.0545	0.057	0.613
Dynamic Viscosity x10^4 (kg/m-s)	4.20	4.50	4.50	8.55
Heat of Vaporization x10_L^{-4} (w-s/kg)	8.79	8.79	8.37	243.8
Surface Tension x10^3 (N/m)	8.90	8.50	8.00	58.9
Thermal Coefficient of Expansion x 10^3 (K^{-1})	1.60	1.60	1.40	0.20
Dielectric Constant	1.71	1.72	1.75	78.0

These liquids should not be confused with the "Freon" coolants which are chlorofluorocarbons (CFCs). Although some of the "Freons" (e.g. R-113) exhibit similar cooling characteristics, concern over their environmental effect on the ozone layer preclude their use.

18.2.3 Other Considerations

Although this discussion has concentrated on the merits of immersion cooling, coolant selection, and possible modes of heat transfer; several other considerations should be kept in mind when considering direct liquid immersion for cooling electronics.

- Since fluorocarbon liquids are expensive they should only be considered for use in closed systems. Whether the application is in a self-contained module like the LEM (Liquid Encapsulated Module package) or a forced flow scheme, care must be taken to ensure that the seal materials chosen are compatible with the liquid. Information or guidance in this regard may sometimes be obtained from the manufacturer of the coolant. If boiling is to take place, then the design must incorporate a means to condense the resulting vapors.
- A finned surface may be designed for this purpose as in the LEM example, or a remote finned condenser surface cooled by air or water might be used. In flow systems, care must be taken in selecting a pump.
- The relatively high vapor pressure of the low boiling point fluorocarbons generally requires that a higher suction head be provided to prevent cavitation in the pump. Whether using a self-contained boiling module or a circulating flow system, care should be taken to make sure all internal surfaces in contact with the coolant are clean. This will ensure that manufacturing process residues or unclean surfaces do not introduce a contaminant into the liquid which could be carried to the heated chip surfaces and interfere with the boiling process.
- In forced circulating liquid systems, it may be desirable to add a particulate and a chemical filter to ensure the long-term purity of the coolant. By selecting the appropriate liquid coolant and the mode of heat transfer, and by giving appropriate attention to these other considerations; direct liquid immersion cooling can be used successfully to provide an effective solution for cooling high heat flux chips and packages.

18.2.4 Application (Examples)

In spite of prolonged interest in direct immersion liquid cooling as a means to cool high heat flux micro-electronics, there have been only a limited number of applications. As with indirect liquid cooling, these applications have been almost exclusively in the large mainframe and supercomputer arena. This is not surprising, since this has been the microelectronics technology sector with the highest packaging densities and concentration of heat.

The Liquid Encapsulated Module (LEM) developed at IBM in the 1970s provides an example of a package utilizing pool boiling. As shown in Figure 18.6, a substrate with integrated circuit chips (100) was mounted within a sealed module-cooling assembly containing a fluorocarbon coolant (FC-72). Boiling at the exposed chip surfaces provided high heat transfer coefficients (1700 to 5700 w/m^2-K) to meet chip cooling requirements. Internal fins provided a means to condense the vapors and remove heat from the liquid. Either an air-cooled or water cooled cold-plate could be used to cool the module. Using this approach, it was possible to cool 4 W chips (4.6 mm x 4.6 mm) and module powers up to 300 W. Direct liquid immersion cooling has been used within IBM for over 20 years, as a means to cool high powered chips on multi-chip substrates during electrical testing prior to final module assembly.

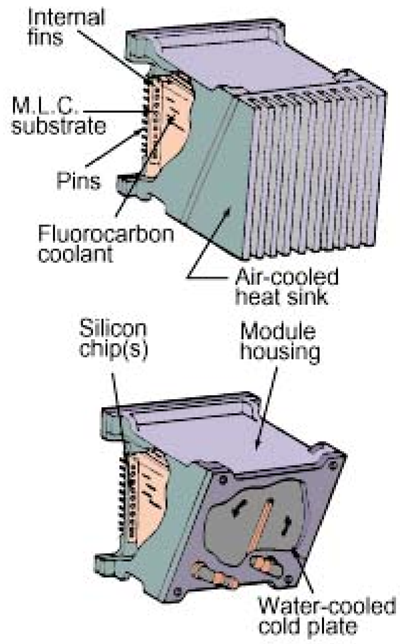

Figure 18.6 Air or water-cooled Liquid Encapsulated Module (LEM) packages

An example of a large scale forced convection fluorocarbon cooling system is provided by the CRAY-2 supercomputer. As shown schematically in Figure 18.7, stacks of electronic module assemblies were cooled by a forced flow of FC-77 in parallel across each module assembly. Each module assembly consisted of 8 printed circuit boards on which were mounted arrays of single chip carriers. A total flow rate of 70 gpm was used to cool 14 stacks containing 24 module assemblies each. The power dissipated by a module assembly was reported to be 600 to 700 watts. Coolant was supplied to the electronics frame by two separate frames containing the required pumps and water-cooled heat exchangers to reject the total system heat load to customer supplied chilled water.

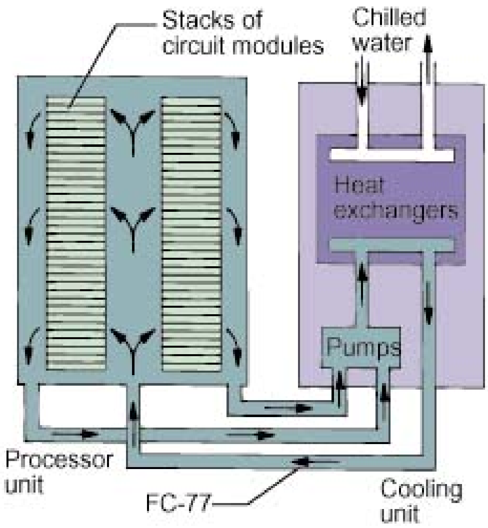

Figure 18.7 CRAY-2 liquid immersion cooling system

19. Cooling Techniques for High Density Electronics (1)

Cold Plate Technology for High Density Server

19-1 Introduction

Most cold plates based on water cooling for computers was introduced more than twenty years ago, but had disappeared from the mainstream by the mid 1990s. The conversion of chip technology from bipolar to CMOS (complementary metal oxide semiconductor) was the main reason. As chip powers continue to increase, water cooling appears likely to become main stream again. In the current market, the major benefits of changing from air to water cooling are increased packaging density and lower power noise. Among the systems most likely to benefit are rackmount servers, both 1 unit (1U = 44.45 mm) and blade configurations with even more severe space requirements.

In the near future, water cooling of processors and air cooling of other components may be introduced. The water (or refrigerant) used to cool the processors would transfer heat to the outside environment, probably through the building water supply, avoiding the CRAC (computer room air conditioner) units. The capital cost, energy consumption and floor space required by the CRAC units would be significantly reduced. In a case study by Prechtl and Kurtz, a total (server plus cooling) power reduction of 23% and CRAC power reduction of 50% were found.

19-2 Parameters affected on Cold Plate Performances

Nomenclature

A	Wetted surface area	m^2
C	Thermal conductance	W/K
C_p	Thermal capacity	J/kgK
ε	Effectiveness	-
h	Heat transfer coefficient	W/m^2K
$\dot{m}$	Mass flow rate	kg/s
NTU	Number of transfer units	-

The volume of water required per hour will be slightly lower than the volume of air required per second to provide the same thermal capacity. The convective resistance of a cold plate or heat sink and the thermal capacity of the coolant are related by:

$$NTU = hA/(\dot{m}\,C_p) \qquad (19.1)$$

The effectiveness of a cold plate or heat sink is the ratio of heat transferred to the ideal case in which all fluid achieves the surface temperature:

$$\varepsilon = 1 - \exp(-NTU) \qquad (19.2)$$

The resulting thermal conductance is given by:

$$C = \varepsilon\,\dot{m}\,Cp \qquad (19.3)$$

For a fixed pressure drop, thermal conductance is maximized at NTU = 1, resulting in ε = 0.63. For a fixed pumping power (the product of volume flow rate and pressure drop), thermal conductance is maximized at NTU = 1.9, resulting in ε = 0.85. Cold plates with effectiveness lower than optimum require excessive flow; those with effectiveness higher than optimum require excessive pressure drop.

Achieving such high values of effectiveness in a small form factor has historically been a manufacturing challenge. Even large cold plates for multichip modules, over 100 mm square, required only a few flow channels making several passes back and forth across the cold plate. CNC (computer numerically controlled) machining has practical limits of about 0.5 mm channel width and 0.5 mm fin thickness. Inserted folded fins also have limits of about 0.5 mm in channel width, but can use finstock to about 0.2 mm thickness. Even 0.5 mm channels result in small values of effectiveness for typical single-chip size cold plates, and smaller dimensions are required to achieve optimum effectiveness.

For the purposes of this article, a conventional cold plate is defined as one in which coolant channels are parallel and run from one side of the cold plate to the other. This can also include cases in which coolant channels turn back and forth across the face of the heat source(s).An experiment simulated 60 x 64 mm cold plates with channels 1 to 3 mm wide. Figure 19.1 shows velocity and temperature distributions at 1 m/s. With 20 channels 3 mm wide, variations in velocity and temperature are much greater than with 60 channels 1 mm wide.

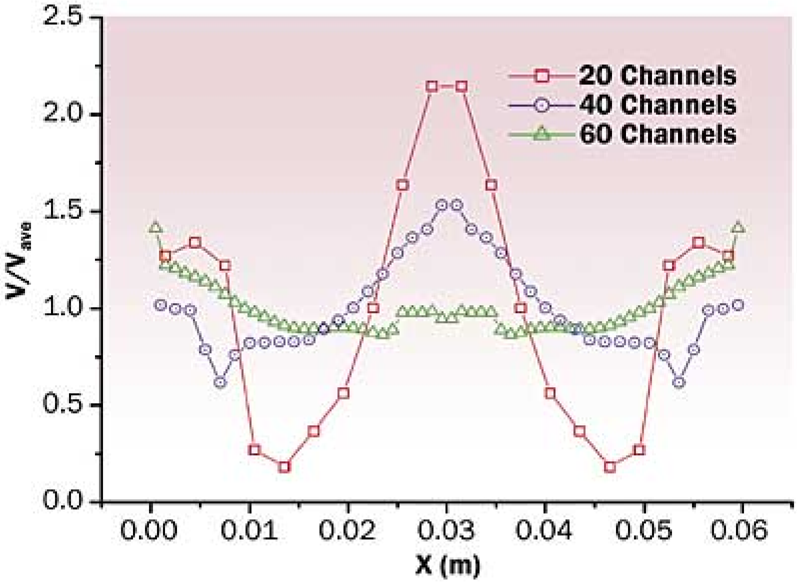

Figure 19.1a Velocity distribution

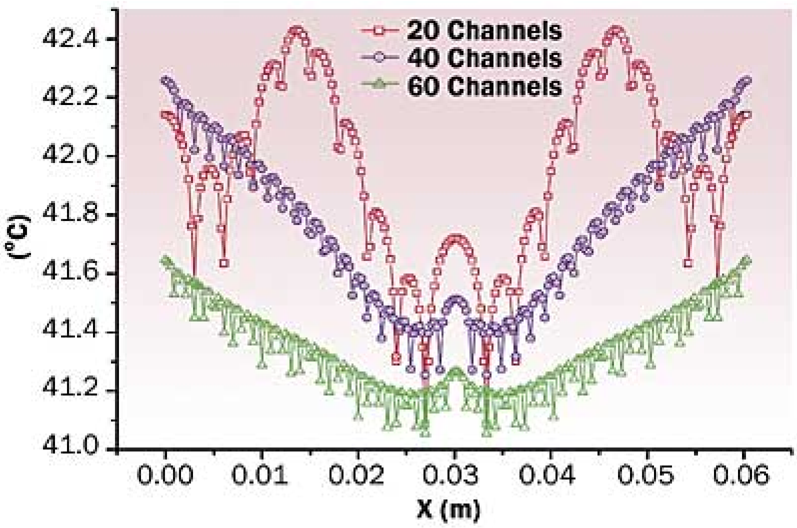

Figure 19.1b Temperature distribution at 1.0 m/s

19-3 Manifold Flow Distribution

Improvement of the conductance of cold plates has been studied but new designs have seldom been implemented. Harpole and Eninger proposed a manifold microchannel in which alternate inlet and outlet channels guided flow in and out of parallel channels. In their case, the optimum dimensions were quite small. Manifold channel spacing was 333 µm, fin height 167 µm and channel width 7 to 14 µm, with the ratio of fin thickness to channel width from 0.5 to 1.0, significantly smaller than dimensions considered practical for fabrication in copper.

Manifolding has appeared in recent commercial products. Valenzuela and Jasinski describe a normal flow cold plate (NCP) with alternating inlet and outlet manifold channels approximately 1 mm wide. Figure 19.2 shows a cutaway view of the NCP. The heat transfer matrix is quite thin but not described in detail. Effectiveness values of 0.8 at low flow rates and 0.6 at high flow rates were demonstrated. North and Cho tested an assembly with a multistage manifold, as shown in Figure 19.3. Coolant enters the inlet port (1), is distributed to a manifold inlet channel (2), then flows the short path through the heat transfer matrix (3) into the adjacent outlet channel (4) and finally through the outlet port (5).

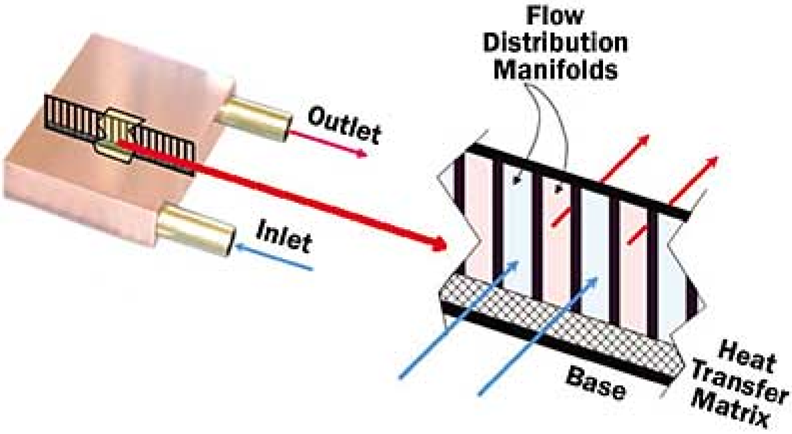

Figure 19.2 Normal flow cold plate (NCP) and manifold structure

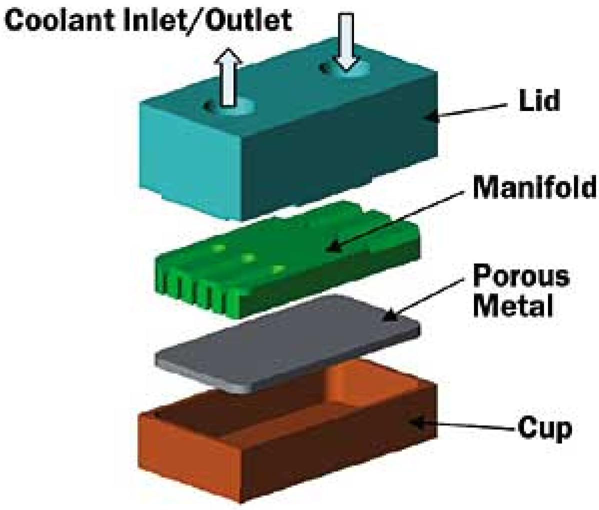

Figure 19.3a Powdered metal cold plate (PCMP) assembly

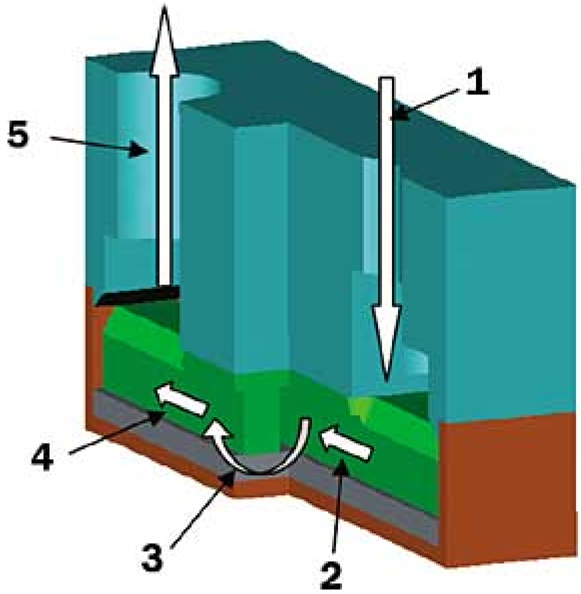

Figure 19.3b Coolant flow path

Patterson et al. Considered four possible arrangements for multilevel flow: single level flow (1F), parallel flow (PF), counter flow (CF) and series flow (SF), shown in Figure 19.4. Their goals were reduction of both average wall temperature and wall temperature variation. Results with silicon and water at an inlet velocity of 1 m/s are shown in Figure 19.5. While series flow achieves good uniformity, the wall temperature rise is high. The counter flow arrangement provides low and uniform values of wall temperature rise.

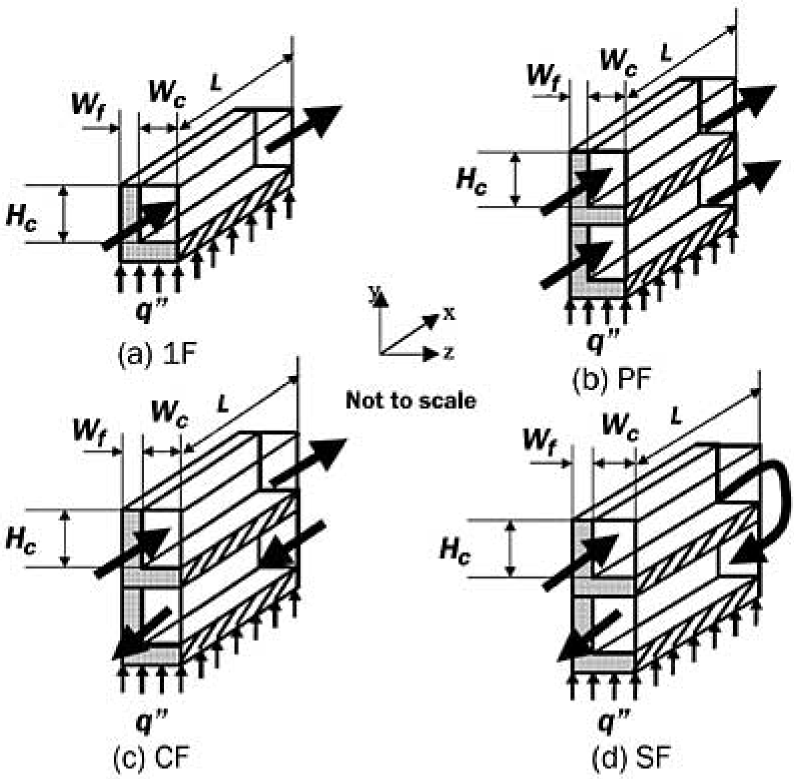

Figure 19.4 Flow arrangements

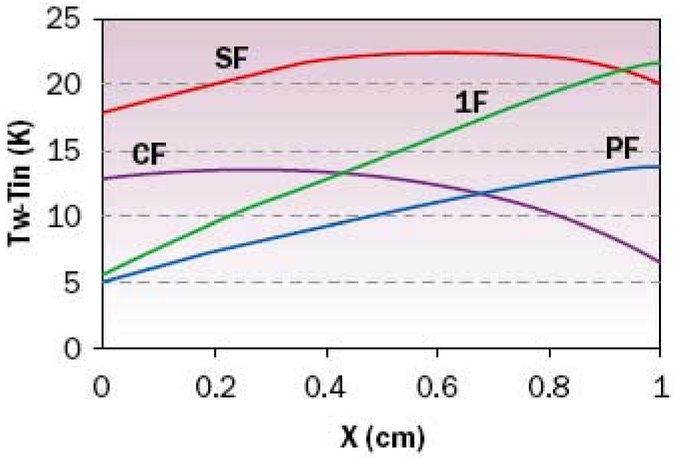

Figure 19.5 Wall temperature distributions

19-4 Nontraditional Heat Transfer Surfaces

Heat transfer surfaces other than parallel plate fins have also emerged. North and Cho described a porous metal heat sink in which spheroid particles are bonded together, shown in Figure 19.6. Nominal particle diameters were 274, 325 and 537 µm. Prechtl and Kurtz presented a microstructured fabrication process in which etched layers were joined together to form a multilayer heat sink, as shown in Figure 19.7. The resulting channels were 400 x 600, 200 x 300 and 100 x 200 µm.

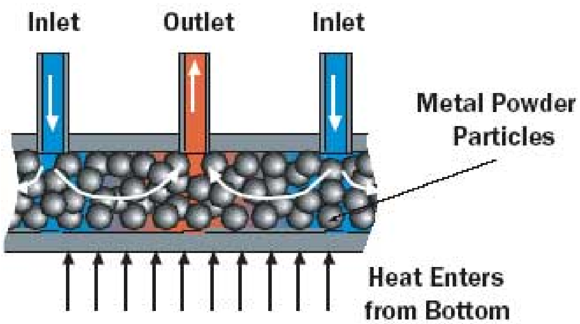

Figure 19.6 Powdered metal cold plate (PCMP) heat transfer matrix

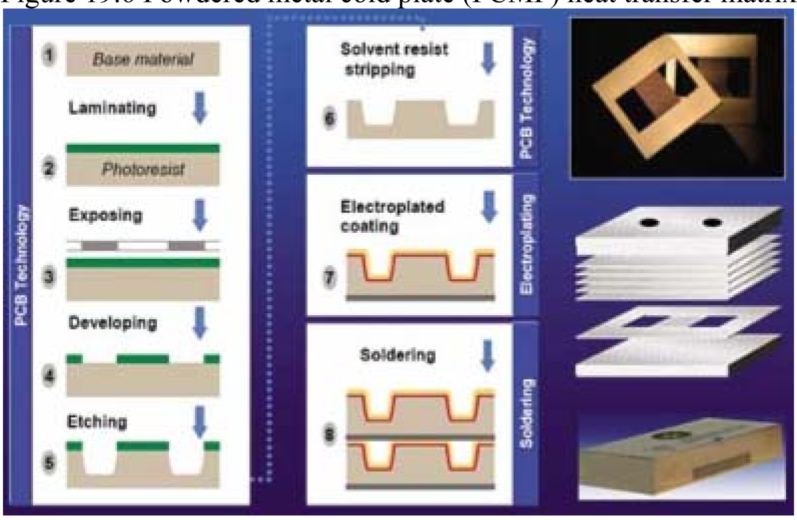

Figure 19.7 Microstructure cold plate fabrication process

Muller and Frechette presented a comprehensive numerical study of manifold microchannel heat sinks. With copper and water, using 1 cm^2 as the reference area, a thermal conductance of 15.5 W/K could be achieved with 0.005 W pumping power, significantly higher performance than achieved to date. A zigzag fin configuration was introduced, which could lead to even further improvement in performance.

19-5 Conclusions

A complete evaluation of cold plate performance requires measurement of flow rate, thermal resistance and pressure drop. Flow rate and thermal resistance for cold plates of different size must be normalized to a unit surface area, traditionally 1 cm^2. Figure 19.8 shows normalized thermal resistance and pressure drop as functions of volume flow rate per unit area for a normal flow cold plate. At the lowest flow rate, effectiveness is about 63%, corresponding to NTU = 1, the optimum value for fixed pressure drop. Small differences in pressure drop at different values of heat flux reflect changes in fluid properties with temperature.

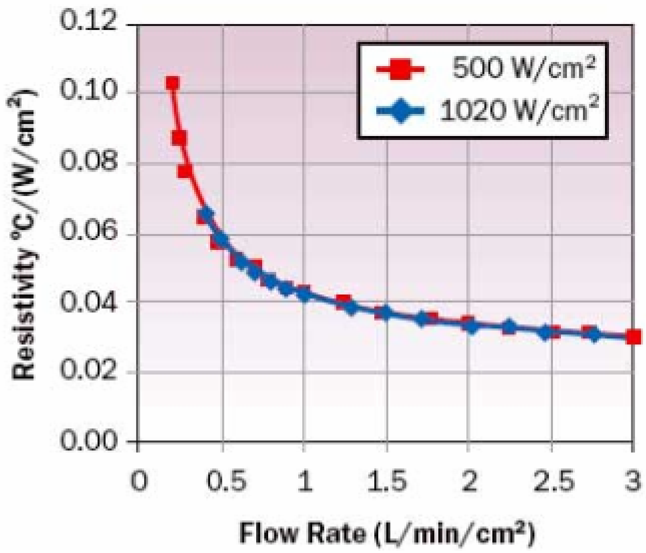

Figure 19.8a Ultra high flux NCP thermal performance

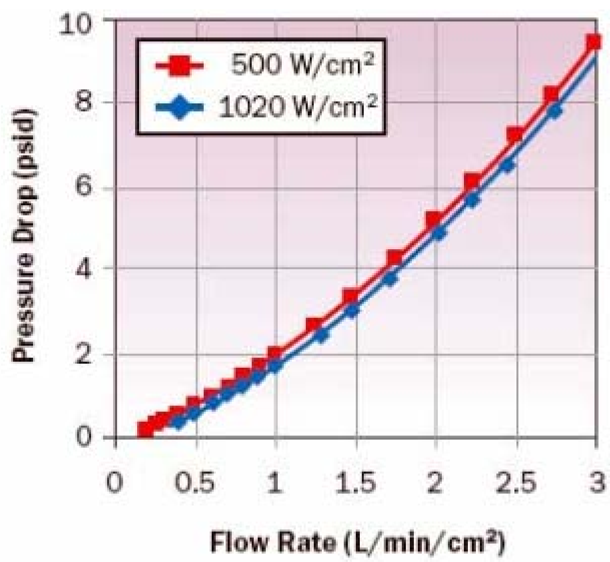

Figure 19.8b Ultra high flux NCP hydraulic performance

In air cooling, nonoptimized heat sinks were adequate until quite recently. The current need for minimization of noise, fan power, heat sink volume and weight have forced optimized designs into production. As a result of volume production, manufacturing techniques such as soldered stacked fins have seen significant reductions in cost. Manufacturing techniques, which allow variation of both the manifold and coolant channel dimensions, will permit the effectiveness of the cold plate to be optimized. Once water cooling becomes mainstream, the dual expectations of designs moving closer to optimized values and reduction of manufacturing cost through volume are reasonable.

20. Cooling Techniques for High Density Electronics (2)

20.1 Direct Impingement Cooling

In this method, components are cooled directly by blowing the coolant (such air). Flow channels are developed in the equipment design exposing heat generated components to the moving cooling air mass, Figure 20.1 This heat removal method develops low component-to-air temperature differences since the components are directly exposed to the thermal sink.

Component spacing and distribution become a prime design factor in order to assure proper cooling of all components in the flow channel. Coolant routing and the flow channel configuration must asst that sufficient cooling is directed and distributed over high heat generating devices. A flow system of this nature usually develops large flow losses due to viscous drag, and turbulence. This condition necessitates balancing of the pressure losses in different flow branches to assure adequate cooling throughout the equipment.

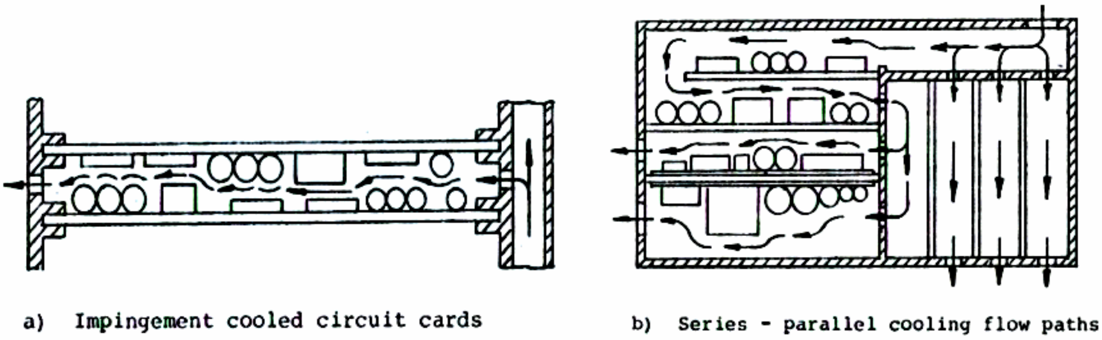

Figure 20.1 Direct impingement cooling

Hot spots on component boards or other assemblies due to concentrations of heat generating sources result in an uneven distribution of heat which increases the difficulty of obtaining effective cooling. Variations in component size and shape add an additional degree of complexity; Figure 20.1 In general, smaller parts experience lower case-to-coolant temperature differences due to end effects which increase its conductance. When determining on conductance as a result of flow directly over components, one should include the actual surface area of the parts.

Coolant temperature must also be accounted for. Variations in coolant temperature along surfaces of heat producing parts are a consequence of the duct configuration and component spacing at the location of interest. For this reason, hot spots within a given flow configuration determine the flow requirements for that branch. This approach generally results in conservative operating temperatures for low-heat generating components on the same assembly.

Airborne applications require consideration of varying air densities and flow losses due to changes in altitude. Air that cools airborne equipment can become moisture laden and m transport vehicle-associated contaminants which can cause intermittent performance or short-circuit printed circuit boards and connector interfaces. Exposed surfaces and components should be protectively coated to minimize the effects of moisture and other airborne contaminants.

<u>The process of developing impingement cooled equipment requires</u>

- Determination and description of heat generating components.
- Definition of the allowable maximum temperature for different classes of circuits or components used.
- Selection of candidate flow paths accounting for equipment configuration, interfaces and assembly arrangement in terms of generated heat distribution, coolant temperature rise and allowable component temperatures.
- Determination of low rates and pressure losses along each flow path
- Determination of component operating temperatures and equipment cooling requirements, e.g. inlet air temperature, flow rate and flow loss.

20.2 Jet Impingement Cooling

Jet impingement and microchannel cooling are two methods presently under investigation. Jet impingement cooling of microelectronic chips is accomplished by passing a coolant through a capillary tube or orifice aimed at the surface to be cooled. A typical arrangement is shown in Figure 20.2. A liquid under pressure in the chamber is allowed to pass through an orifice plate and directly onto the microchip component. Shown in the figure is a leadless chip carrier attached to a substrate through a series of solder bump joints. The dielectric coolant strikes the chip and absorbs its heat dissipation. The development model shown is not representative of a system in production. However, in addition to microchip cooling, there are applications in electronics which utilize spray cooling or direct impingement cooling of component surfaces. One such application is a variable- speed constant-frequency (VSCF) generator for use aboard commercial and military air craft. The dielectric coolant in this case passes through small-orifice jets aimed directly at high heat dissipators, mostly diodes, and power transistor assemblies located within a partially filled liquid reservoir. Since these units are exposed to wide temperature extremes, the coolant flow at low temperature through the nozzles is much reduced, and this reduction must be taken into account in the thermal design. The oil that cools the electronic components also cools the generator and stator. There are two modes of operation possible with liquid jet impingement single-phase and two-phase cooling. In addition, the jet can be free or submerged.

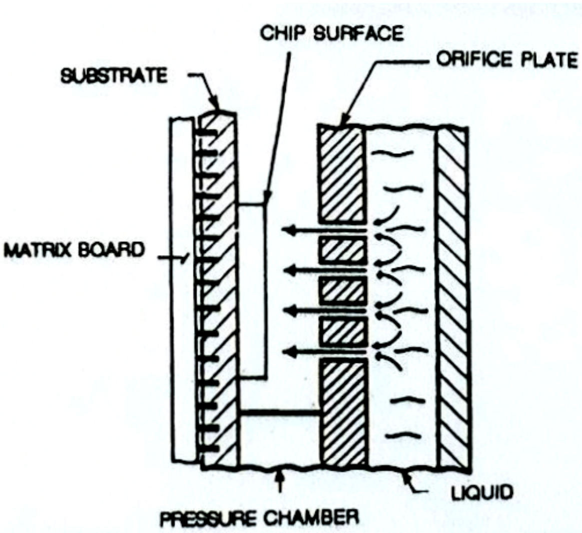

Figure 20.2 Jet impingement configurations

In the submerged case the cavity is filled with the coolant while in the free mode, as shown in Figure 20.2, the liquid jet is exposed to a gaseous environment. The most efficient heat transfer takes place in the free liquid impingement case when the cooling mode is a combination of boiling and free convection. Ma and Berg have reported experiments with Freon R- 113 where up to 100 W/cm^2 over a small chip surface (0.2 by 0.2 in) was cooled using jet impingement boiling.

These experiments and others have found that significant improvements in heat transfer are possible with jet impingement above that normally encountered in the boiling mode alone for immersed components. The combination of loca1 boiling and forced convection leads to an extension of the critical heat flux for Freon R-l 13 beyond the 20- to 40-W/cm^2 free zone to 70 W/cm^2 with jet impingement under saturated liquid conditions, to as high as 100 W/cm^2 when the liquid is subcooled. As in boiling alone, the surface condition and coolant in contact are important parameters in determining the heat transfer. The advancement of wafer scale integration (WSI) with its packaging and electrical advantages may well result in the initial development of novel jet impingement techniques for IC cooling implementation into hardware.

The design of this type of system must take into account the ultimate heat- sink or boiling-point temperature of the jet coolant and the heat-path resistance from chip to sink. Goodling et al. report on the use of Freon-12 and Freon-22 operating below room temperature with jet impingement on the backside of 4.0-in water. Their tests reveal flux densities of 100 W/cm^2 and higher as the critical heat flux. However, despite this and other reported progress, future implementation into a production system using ICs will require compatibility tests to verify the coolant stability in contact with the electronic enclosure and the chip surface overlong periods. These same experimenters found that th temperature overshoot in boiling could be much reduced using jet impingement as com pared to the normal free saturation boiling mode. In the jet impingement experiments reported to date small high-velocity jets of fewer than 50 ft/s are directed to the backside of chip surfaces for local heat removal; present experimentation has been done mostly with dielectric liquid fluorocarbons and with freons and water. The options in this type of cooling include free jet versus submerged jet, type of coolant, spacing of the jets, and the distribution of liquid to large array surfaces.

20.3 Impingement Cooling Thermal Analysis

Single-phase free jet impingement cooling is influenced by many variables, such as jet diameter d, velocity V, number of jets n ,per source, jet-to-source distance x, jet configuration, size of heat source area $\ell \times \ell$ and coolant properties. Based on the single-phase free jet tests, the correlation data for FC-77 and water were found to agree well with following Equation 20.1, for jet distances to the heat source falling within the limits of 3 <x/d<15.

$$\bar{N}_u = 3.84 R_e^{0.5} P_r^{0.33}\left(0.008\frac{\ell}{d_h} + 1\right) \tag{20.1}$$

Their tests were for nozzle diameters d_h of 0.020 to 0.040 in and jet velocities of under 50 ft/s. The foregoing Equation 20.1 holds true for small surface dimensions of $\ell < 0.5$ in, which in most cases is typical of microelectronic devices. Larger surfaces with multijet impingement can also be analyzed provided the number of jets per unit heat source area is comparable with the test conditions specified.

A large increase in heat transfer is possible with jet impingement boiling where the dependence on surface condition and fluid in contact is most important. In the case of submerged jet cooling on small surfaces, Ma and Bergles report significant increases in the critical heat flux or burnout as compared to the same surfaces when exposed to immersion boiling alone. They found that the pool boiling curve is coincident with the jet boiling curve and can in fact be extrapolated to values of critical heat flux for jet impingement boiling on the order of five times the pool boiling values. Not all experimenters report similar results. At the present time there are no generalized equations defining jet boiling for either submerged or free conditions. In the case of non boiling jet impingement in a submerged liquid, the stagnation-point Nusselt number within the potential core correlatable to within 10 percent is in accordance with the following equation

$$N_u = 1.29 R_e^{0.5} P_r^{0.4} \tag{20.2}$$

A comparison of the submerged Nusselt number at stagnation (Equation 20.2) with the free jet Nusselt number (Equation 20.1) for average conditions on small areas indicates a 3:1 improvement in these single-phase heat transfer cases.

20.4 Hybrid Cooling

This simply implies a combination of liquid and air cooling for high power dissipation electronics, while minimizing contact resistance throughout the system. In this process, the avionics industry has made great strides and produced cooling systems capable of removing high heat fluxes. Figure 20.3 shows one such system.

Figure 20.3a, on the lift shows a rack/card guide system where the liquid is flowing through the card rack. The heat that is generated within the PCB is conduction through the solid core to the rack where the liquid is used as the transport vehicle to remove it from the system. The illustration on the right in Figure 20.3a shows a thru-card scheme where the PCB core is chambered for fluid passage. Thus the conduction heat transfer from the PCB to the rack, as shown in the figure on the right, is eliminated.

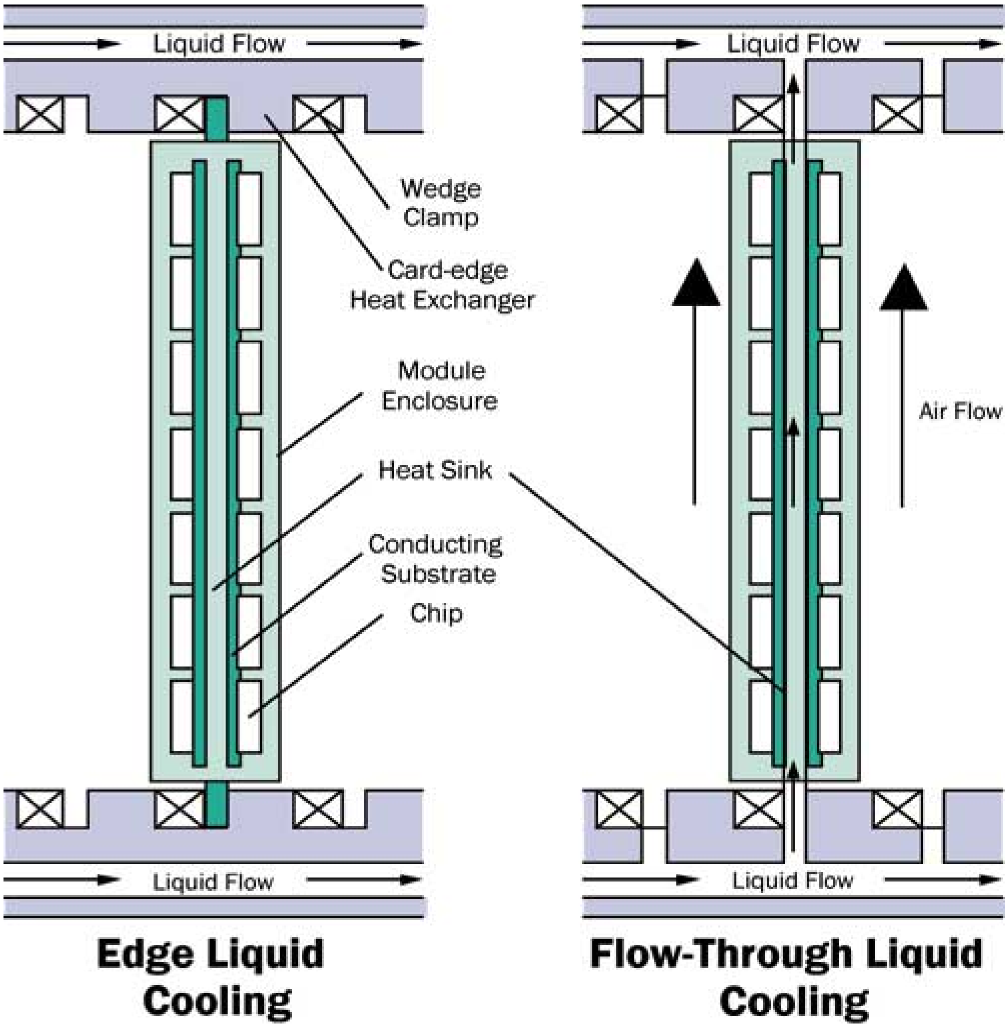

Figure 20.3a.Two hybrid systems for an avionics application: On the left, edge liquid cooling; on the right, thru-card liquid cooling

Figure 20.3b shows the extensive packaging required to make such systems happen. Tightly sealed joints and mechanical contacts with least resistance are required to attain the level of thermal performance required for such a cooling option.

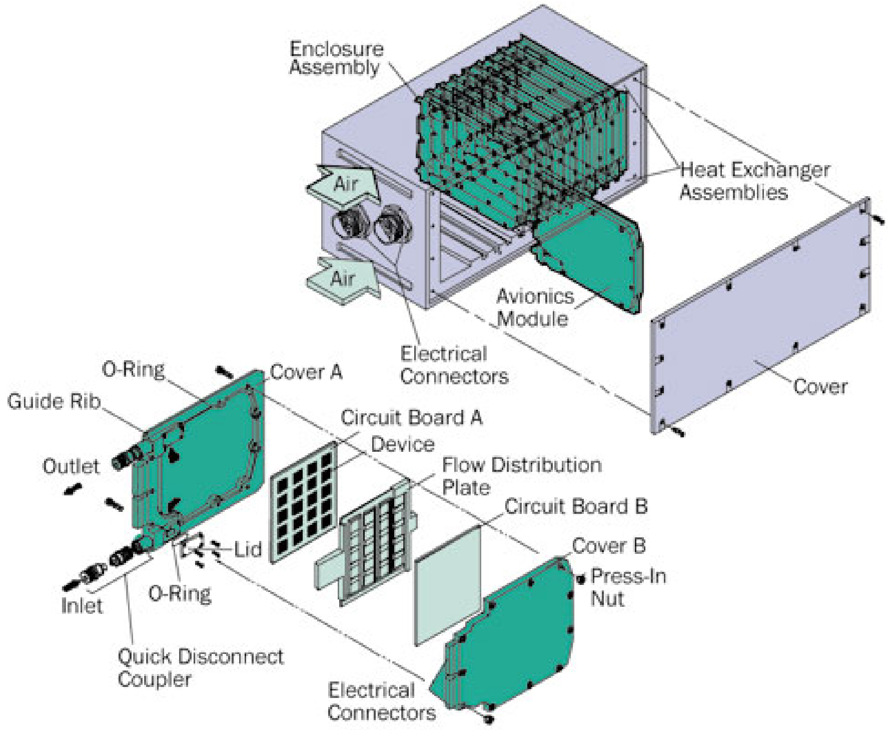

Figure20.3b Card and rack level packaging required for hybrid cooling

Although I have purposefully avoided the discussion of cooling capacity, the exception to the path may be merited here since these systems are not commonly encountered nor discussed in the open literature. Therefore, Figure 20.4 shows the removal capabilities of the hybrid systems for different cooling arrangements.

The data depicted in Figure 20.4 clearly show the advantage of, say, subcooled jet impingement and a conventional cooled system, approximately a factor of 13 However, one cannot overlook the packaging requirements to deliver such a cooling solution, as shown in Figure 20.3b. The cost of these requirements and the attainment of a high reliability cooling system may not make these systems suitable for typical commercially available electronics.

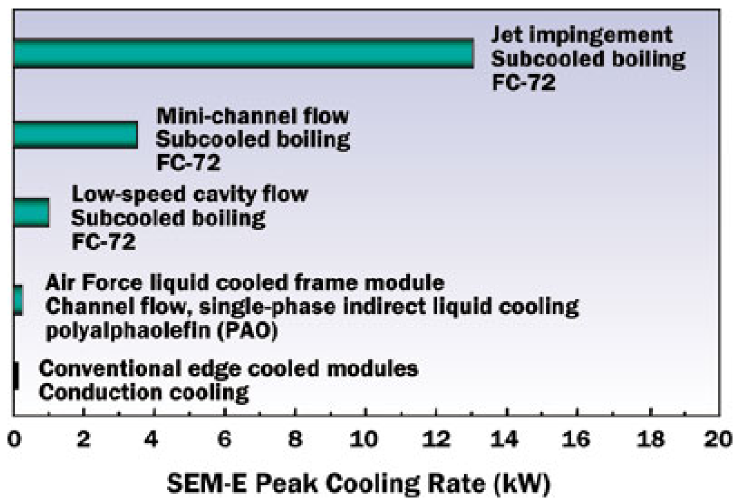

Figure 20.4 Heat removal capacity for different hybrid system as compared with a convection cooled system

20.5 Vapor Compression Cooling for High Performance Applications

Introduction

This is a relative newcomer to the electronics industry. Vapor compression refrigeration is being adapted to cool computer and telecommunications equipment in a limited number of high performance applications. Vapor compression can lift large heat loads and can heat sink at below ambient temperatures. Cold plates can offset high case-to-junction temperature gradients to keep high power integrated circuits from overheating and/or can lower junction temperatures for enhanced integrated circuit performance.

As a method of enhancing computer performance, below ambient cooling has been actively researched since the 1960's. Today's mainstream semiconductor technology, CMOS, has been repeatedly characterized at low temperatures. Multiple performance enhancing reasons exist to cool CMOS (complementary metal oxide semiconductor) devices to very low temperatures. The challenge is to do so reliably and cost-effectively.

Although early (1960-1980) cold electronics development programs targeted 77K or lower temperatures, a moderate approach to low temperature computing has gained momentum in recent years. Vapor compression cooling technology is employed to chill components to a minimum temperature of 233K (-40 ^{o}C) for two good reasons.

First, reliable, relatively inexpensive vapor compression systems can lift high heat loads at this temperature. Second, 233K presents less significant electronic packaging problems to be overcome than does operation at 77K.

Mechanically Assisted Cooling Benefits

High power electronic systems are testing the limits of traditional cooling methods. Effective heat removal is required to keep silicon junction temperatures below critical temperatures at which devices will fail to operate correctly. Natural convection or forced air cooling is proving to be insufficient in an increasing number of applications. Mechanically assisted cooling can meet these needs, but must do so at acceptable costs. Vapor compression cooling of specific, high performance applications can provide favorable cost/benefit ratios.

Mechanically assisted cooling subsystems are said to provide "active cooling" since they require energy. Some mechanically assisted cooling subsystems reduce the heat sink surface temperature below ambient air temperature. It is convenient to refer to a heat sink that operates at below ambient temperatures as a cold plate.

Key attributes of the cooling subsystem include its efficiency, its operating temperature and its cooling capacity. The subsystem's efficiency can be specified as its Coefficient of Performance (COP), or the amount of heat it can move divided by the power the subsystem consumes to move that heat.

The most common cold plate technologies for high performance cooling are currently thermoelectric devices, chilled fluid loops and vapor compression refrigeration.

Vapor Compression Refrigeration

Vapor compression refrigeration offers several important advantages. These include low mass flow rate, high COP, low cold plate temperatures and the ability to transport heat away from its source. The following is a more detailed look at vapor compression refrigeration of high performance electronics.

Figure 20.5 is a schematic representation of the vapor compression cycle. At the top of the loop, heat is introduced to the system by the device being cooled. This heat vaporizes liquid refrigerant in the evaporative cold plate. This vapor is subsequently carried through the suction tube to the compressor. Work is supplied to compress the warm vapor into a hot, high-pressure vapor that is passed to the condenser.

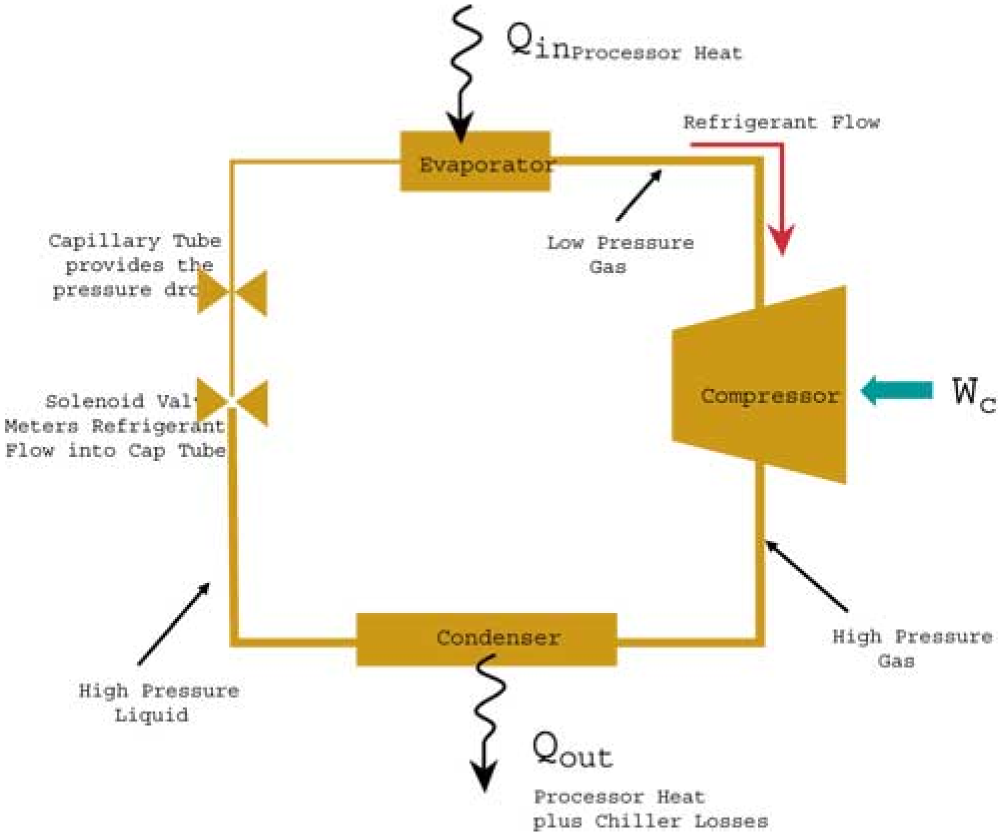

Figure 20.5 Refrigeration cycle schematic

The hot high-pressure vapor releases its heat to the air stream across the condenser fins as it condenses into a warm liquid. Warm liquid is pumped from the bottom of the condenser through an expansion device where its pressure and temperature drop significantly, creating the refrigeration effect. The cycle completes as the cold fluid passes to the cold plate.

The cycle depicted in Figure 20.5 offers several advantages for electronic cooling applications. Vapor compression systems can reject heat far from the source by separating the evaporator and condenser in a so-called "split system". Vapor compression refrigeration transports large quantities of heat with a small mass of circulating fluid.

Vapor compression operates at a COP approximately three times that of thermoelectric devices in a similar application. Vapor compression can produce -40 ^{o}C cold plate temperatures using common food storage and cooling refrigerants.

Refrigerant Fluids

The refrigerant physical properties and operating pressures determine its evaporating temperature and its capacity to transport heat. A wide variety of vapor compression refrigerant fluids are commercially available. Water, alcohol, butane, and ammonia are among the list of well studied refrigerant fluids.

Operating pressure range, heat capacity, atmospheric disruption potential, explosion hazard and corrosion potential make some fluids inappropriate for some applications. R-134a and R-404a are common refrigerants currently in use in high power electronics cooling applications.

Heat Capacity and Heat of Vaporization

When bounded systems of gases, liquids or solids absorb heat they must either increase in temperature or change their physical state. For example, the temperature of a gram of water will increase one degree centigrade when it absorbs one calorie of heat. Similarly, at a given pressure and temperature, one gram of water will absorb nearly 540 calories of heat without temperature increase as it changes from a liquid to a gaseous state.

This characteristic amount of heat absorbed during a state change is referred to as a material's heat of vaporization. Vapor compression refrigeration employs the refrigerating fluid's heat of vaporization. Practically this allows a small fluid mass to transport a relatively large amount of heat.

Temperature of Vaporization

Just as water turns to steam (water vapor) at 100 ^{o}C at atmospheric pressure, a given refrigerant will vaporize at a specific temperature at a given pressure. The pressure vs. temperature characteristic curve determines the lowest practical operating limit of a particular refrigerant. Figure 20.6 shows the pressure-temperature characteristic curves for the commercial refrigerant R-404a. Low cold plate temperatures can be used to offset the temperature rise that occurs at the interface between a cold plate and its load device or to lower the operating temperature of the load device.

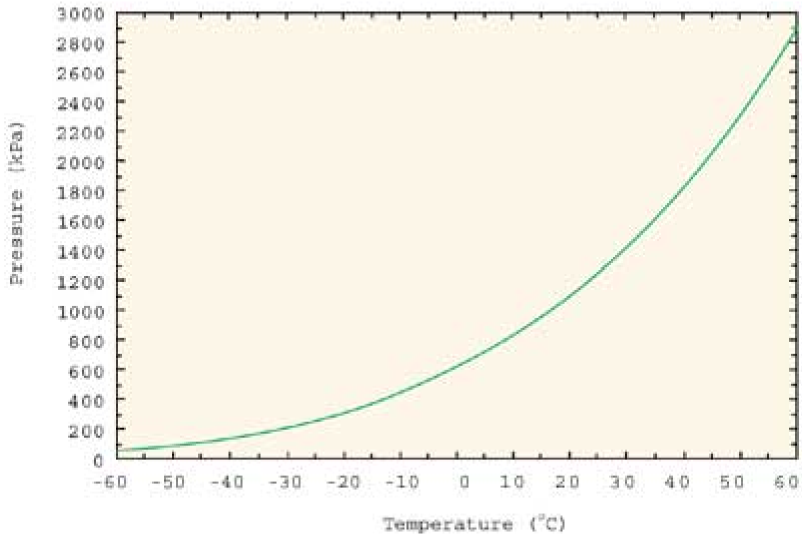

Figure 20.6 PT curve for R-404a

Benefits of Sub-Ambient Cooling

CMOS technology has scaled predictably since the early 1970's. Smaller features allow more circuit elements, such as transistors, to be interconnected on a single silicon chip. Smaller transistors switch on and off faster. As CMOS scales from generation to generation, faster and more functionally rich chips are produced.

Continued improvement in wafer and device fabrication has encouraged development of physically larger chips. Larger chips containing more transistors operating at higher frequencies dissipate more power. Large quantities of heat must be removed from the integrated circuit surface to ensure that junction temperatures remain below critical temperatures. High power chips may require below ambient cold plate temperatures to ensure that device junctions be maintained at below their critical temperatures. Sub-ambient cooling can also allow CMOS transistors to switch on and off faster.

Vapor Compression Application Issues

Application of vapor compression to electronic cooling requires careful engineering. The cold plate must efficiently lift heat from the device being cooled. Cold surfaces cannot be allowed to collect condensate from the surrounding air. Refrigerant tubing must be incorporated into the physical design to supply and remove refrigerant. The compressor and condenser unit must be integrated into the physical design. The entire solution must be cost effective and reliable.

Cold plate design must assure efficient thermal transfer from the device being cooled to the refrigerant stream inside the cold plate. Flat and smooth interface surfaces are generally required. The cold plate is fabricated from a thermally conductive material with thin wall design to shorten the thermal path from the target to the refrigerant. The cold plate internal design optimizes heat transfer. Surface texture and refrigerant path length are increased within the limits of an acceptable pressure drop between the inlet and outlet of the evaporative cold plate.

Water, a hazard to electronic assemblies, condenses on exposed surfaces at or below dew point temperatures. This issue extends to all exposed cold area of the refrigerant path. Cold surfaces must be insulated from and sealed against moisture-laden air to avoid hazardous condensation.

Vapor compression applications are typically closed loop. Refrigerant is recirculated around the loop indefinitely. This requires that refrigerant tubing be routed within the electronic assembly to connect the evaporative cold plate to the compressor/condenser assembly. Clever design is required to minimize the impact of this particular "issue".

The "cooling engine" must be integrated into or otherwise accommodated in the physical design. Vapor compressors have not been designed for aesthetics. They are typically hidden in the bottom of refrigerators and water fountains. Industrial design or styling must be considered. Compressors are heavy, consume power and radiate noise. Table 20.1 provides size, weight and capacity information for typical modern compressors A and B along with parameters for a technically feasible but unavailable mini-compressor.

All of the application issues discussed must be considered during the physical design stage of a system if vapor compression cooling is to be effectively integrated. An example of such a system is shown in Figure 20.7.

Figure20.7 Vapor compression cooling for Super G™ Computer

Reliability at 233K

Low temperature operation results in a blend of hazards and benefits. Hazards include electro-mechanical failure due to material or thermal coefficient of expansion mismatches or electronic failure due to hot carrier effects. Only materials and components that are known to maintain their physical integrity at -40 °C can be chilled.

Table20.1 Specifications for Typical Compressors

Compressor	Size	Weight	Capacity
A	6" x 6" x 8"	16 lbs	30 W @ -40°C
B	8" x 10" x 9"	25 lbs	150 W @ -40°C
Mini-Compressor	1.5" x 4"	2 lbs	200 W @ -40°C

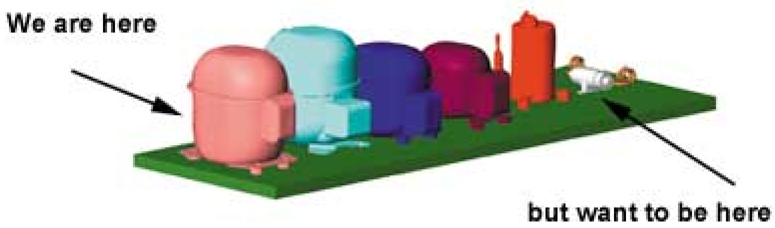

Conclusion

Reliable vapor compression driven cooling subsystems can be designed and manufactured for use in high performance electronic applications. Vapor compression cooling can be used for thermal management and/or performance enhancement.

Today a small fraction of all computers are equipped with vapor compression coolers. Broader use of this powerful cooling technology depends on several factors. First, the cooling technology will evolve to become a better fit for computing and telecommunication applications. Programs are underway to reduce the size and weight of vapor compressors and to build-in capacity control features that can interface seamlessly with computing. The lower temperature limit of the commodity vapor compression technology of 233K is also being addressed. Vapor compression systems are operating at much lower temperatures in the laboratory now.

Mechanically assisted cooling is emerging as a practical solution to high performance electronic cooling problems. The adoption and refinement of vapor compression cooling to address these problems can unlock a new era of electronics. One in which electronic cooling-specific compressors allow the use of ultra-high performance semiconductor devices designed specifically for low temperature operation. Microprocessor frequencies will be both scaled up and cooled up.

Part D: Packaging of Electronic Equipments

Indicative Contents

21. Components of Electronic Systems

21.1 Introduction

Electronic packaging is the art and science of connecting circuitry to perform some desired function in some applications. Packaging also provides ease of handling and protection for assembly operations. We will devote this partition for engineering technologies include mechanical, thermal, materials, and components for electronic systems.

In mechanical design concerns the supports, frames, etc. to withstand the mechanical stresses due to vibration, shocks, etc to which the electronic package may be subjected.

While the thermal design to ensure that the electronic systems are amply cooled and would not over heat to a point where they become unable to function properly.

21.2 Components for Electronic Systems and its Cooling Solution

21.2.1 Electronic Components for Airplanes, Missiles, Satellites, and Spacecraft

Electronic boxes used in airplanes, missiles, satellites, and spacecraft often have odd shapes that permit them to make maximum use volume available as shown in Figure 21.1. An odd-shaped box may require more time to design, because it is usually more difficult to provide the circuit cards with an efficient heat flow path, regardless of the cooling method used.

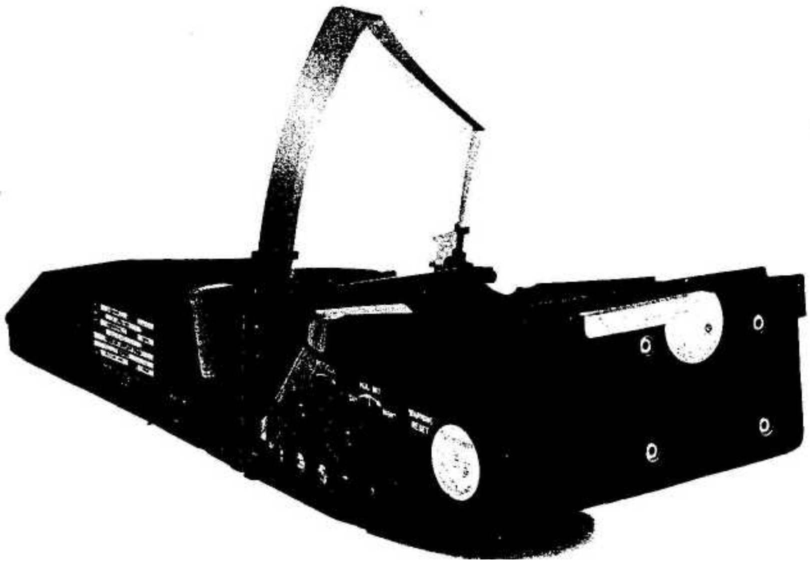

Figure 21.1 Ahead-up-display (HUD) electronic box for fighter air craft

Many of the electronic boxes are cooled by forced convection with bleed air from the jet engine compressor section. Since this air is at a high and pressure, it is throttled (passed through the cooling turbine), cooled, and dried with a water separator before it is used.

Sometimes the conditioned cooling air is not completely dry because of excessive moisture in the air from humidity or rainstorm so that small drops of water will often be carried into the electronics section together with the cooling air. If this water accumulates on PCBs or their plug-in connectors, electrical problems may develop. Therefore, many specifications do not permit external cooling air to come into direct contact with electronic components or circuits. Air-cooled heat exchangers, commonly called air-cooled plates, which are being used more in airplanes, provide conditioned air for cooling the electronics. Theses heat exchangers are usually dip-brazed when many thin (0.006 to 0.008 in) aluminum plate fins are used. Pin fin aluminum castings are becoming very popular because of their low cost but performing extremely poorly in pressure drop and weight.

Electronic systems for missiles have two cooling conditions to consider, captive and free flight.

If the missiles flight duration is relatively short, the electronics can be precooled during captive phase so that the system can function with no additional cooling during the flight phase. The electronic support structure would act as the heat sink.

Some missiles, such as the Cruise missiles, have a very long free flight phase, so that the cooling system must be capable of cooling the electronics for several hours. If ram air is used at speed near Mach 1, the ram temperature rise of the cooling air may exceed 100 ^{o}F. Since Cruise missiles fly at low altitudes, where the surrounding ambient air temperatures can be as high as100 ^{o}F, the cooling air temperature could reach values of 200 ^{o}F (93 ^{o}C) even before the cooling process begins. Since the maximum desirable component mounting surface temperature is about 212 ^{o}F(100 ^{o}C), the out- side air cannot be used directly for cooling.

Electronic systems for satellite and spacecraft generally rely upon radiation to deep space for all their cooling. Deep space has a temperature of absolute zero, -460 ^{o}F (-273 ^{o}C). This low temperature can provide excellent cooling.

Special surfaces finishes and treatments may be required for satellite and spacecraft to prevent them from absorbing large quantities of heat from the sun. This heat may be direct solar radiation plus solar radiation reflected from the various planets and their moons.

Natural convection cannot be used to transfer heat in satellite and spacecraft electronics. Natural convection requires field to permit the heated air to rise, because of its reduced density. In satellite and spacecraft, the effects of gravity are neutralized by velocity and the continuous free-fall characteristics of the flight path. Therefore, only radiation, conduction, and forced convection (in sealed boxes) should be considered for cooling electronic systems in space.

21.2.2 Electronic Components for Ships and Submarines

Large cabinets, consoles, or enclosures are normally used to support the electronic equipments used on ships and submarines as shown in Figure 21.2. These cabinets are usually heavy and rugged, to provide protection for the electronics during storms and rough seas. Some cabinets may dissipate more than 2 kilowatts of heat. The electronic components are often mounted on panels and sliding drawer. Panels are used to support displays, and drawers are used to support the heavy power supply units.

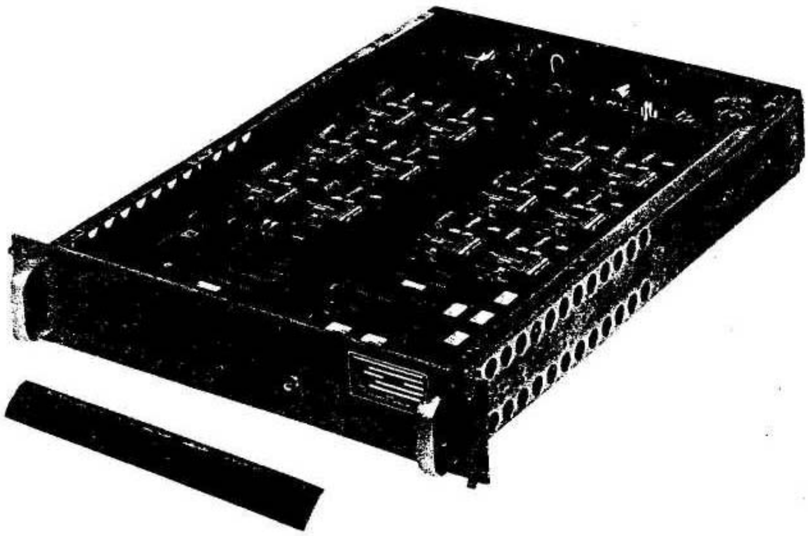

Figure 21.2 Plug-in drawer type of chassis for use in a cabinet

Water is usually available on ships and submarines, so that it is natural to utilize it for cooling. Water-cooled heat exchangers are often used, with external fins to permit cooling with forced air. Fans are used to force the air through heat exchanger fins to cool the air, which is then circulated through the consoles. This type of forced convection cooling can be used with both closed-loop and open-loop systems.

With closed-loop system, a cooling air supply plenum and a return plenum may be established within the sidewalls of the consoles. The sidewalls are often several inches deep, with ribs to provide rigidity from high shock loads, so that they can easily carry the cooling air to and from the electronic equipment. For an open-loop system the air entering the consoles would be forced through the Water-cooled heat exchangers, which is usually at the base of the console. The conditioned air would be circulated through the electronic equipments and then exhausted at the top of the console.

When the heat loads are not too high, natural convection techniques can often be used to cool the electronic equipments. This works well on tall cabinets, which can use chimney effects to force the air through the system without the use of fans. Air enters the bottom of the cabinet, where it first picks up heat from the electronic equipments. The warmer air has a reduced density, so that it starts to rise through the chassis, picking up more heat as it rises. The air finally exits at the top of the cabinet.

21.2.3 Electronic Components for Communication Systems and Ground Support Systems

Both communication systems and ground support systems must capable of continuous operation for extended periods of time at hot desert areas, arctic area, and in rain, sleet, and snow. Large systems have their electronics completely enclosed within shelter that similar to small barns and can hold several people for along periods of time. While small systems usually enclosed in transit cases and may be carried on the back seat of vehicle for rapid mobility.

The communication shelters are used all over the world by military personnel and by commercial television networks to transmit and receive all forms of data.

The shelters are usually lined from wall to wall with large electronic control consoles that can easily dissipate many kilowatts of heat. Such shelters are insulated to protect them from both heat and cold. In hot climates the shelters are often equipped with exhaust fans to flush out hot air that has been trapped. This is important because the electronic consoles within the shelters use the local ambient air for cooling. This is done using forced or natural convection, depending on the power dissipation and the location of the console. If the internal ambient temperatures within the shelter become too hot, refrigeration units may be provided, with auxiliary power units, to keep the shelters cool.

Ground support systems usually used to perform functional checks of the electronic equipment such as airplanes, missiles, ships, submarines, trains, trucks, and automobiles to ensure that they are operating properly

Ground support equipments are also used to supply auxiliary power or auxiliary cooling for electronic equipment.

21.2.4 Personal Computers, Microcomputers, and Microprocessors

The computer industry has been changing very rapidly. Since the first chip were introduced in about 1962 which made from semiconductor silicon and contained only about 15 to 20 diodes, transistors, and resistors on a substrate that measured about 0.15 by 0.2 in. Component densities have since increased sharply, so that the same size chip can now incorporate several million components, and the costs have dropped just as fast.

Personal computers have found exciting new applications in many areas. Their small size, flexibility, reduced costs, and improved memory storage have permitted more small business to make use of them.

Microcomputers are even smaller than personal computers. A typical personal computer will occupy one drawer of a filing cabinet. While microcomputer will fit on one plug –in PCB a bout 5 x 7 in. Microcomputers are not as fast as personal computers and are generally used where flexibility, size, and cost are more important than speed.

Both personal computers and microcomputers requires some type of central processing unit(CPU) to control input an out put, to perform mathematical operations, to decode, and move information in and out the memory. This CPU, which would normally require the mounting surface area of one plug-in PCB, can now be placed on a single small chip. This chip is called microprocessors, and it is the most expensive part of the microcomputer.

Microprocessors are available in rectangular cases about 2.5 x 0.75 x 0.2 in with about 40 external wires, which perform all of the CPU functions. Microprocessors must be used with memory systems, which can also be expensive.

21.3 Surface Mount Technology (SMT)

SMT allows production of more reliable assemblies with higher I/O, increased board density, and reduced weight, volume, and cost. The weight of printed board assemblies (PBAs) using SMT is reduced because surface mount components (SMCs) can weigh up to 10 times less than their conventional counterparts and occupy about one-half to one-third the space on the printed board (PB) surface. SMT also provides improved shock and vibration resistance due to the lower mass of components.

The smaller size of SMCs and the option of mounting them on either or both sides of the PB can reduce board cost by four times. A cost savings of 30% or better can also be realized through a reduction in material and labor costs associated with automated assembly.

21.3.1 SMT Process Flow

Surface mount components are placed directly on the substrate surface. To create a metal-lurgical connection between the SMC and the substrate, solder paste is first deposited on the component lands. The SMCs are then mounted on the lands using a suitable placement method. The printed wiring boards (PWBs) plus SMCs are then reflow soldered, forming a surface mount PWA.

The PWAs are then cleaned and tested. In a nutshell, these are the major steps for producing surface mount PWAs:

- Solder paste application on the lands of a suitable substrate (e.g., a PWB)
- Adhesive deposition {not always required)
- Component preparation (if required)
- Component placement
- Soldering
- Cleaning
- Inspection
- Clean prior to conformal coat (if required)
- Conformal coat (if required).
- Test

21.3.2 Surface Mount Classification

There are two widely used classification schemes for surface mount PWAs. These assemblies are often simply called surface mount assemblies (SMAs). The first classification is the most classification follows IPC-CM-770, Component Mounting Guidelines for Printed Boards. This classification utilizes two categories: assembly types and assembly classes. According to this classification, there are two assembly types:

1. Type 1 assembly: The components only on its top side.
2. Type 2 assembly: The components on both its top side and its bottom side.

According to the IPC classification, there are three assembly classes:
1. Class A assembly is entirely through hole technology (THT). A Type 1 Class A assembly as shown in Figure 21.3.
2. Class B assembly is entirely surface mount technology (SMT).
3. Class C assembly is a combined THT and SMT assembly (mixed technology).

Based on the IPC classification, the types of SMT assemblies are:

- Type 1B (single-sided pure SMT assembly). As shown in Figure 21.4.
- Type 2B (double-sided pure SMT assembly-no adhesive). As shown in Figure 21.5.
- Type 2B (double-sided pure SMT assembly-adhesive). As shown in Figure 21.5.
- Type 1C (single-sided with a mixture of THCs and SMCs). As shown in Figure 21.6.
- Type 2C (S) (simple) (double-sided with THCs only on top; small, discrete SMCs on the bottom). As shown in Figure 21.7.
- Type 2C (C) (complex) (double-sided with large SMCs and THCs on the top; small, discrete SMCs on the bottom) As shown in Figure 21.8
- Type 2C (VC) (very complex) (double-sided with large SMCs and THCs on the top; large and small SMCs on the bottom) As shown in Figure 21.9

The second classification for surface mount PWAs is the oldest classification based on the soldering technology employed.

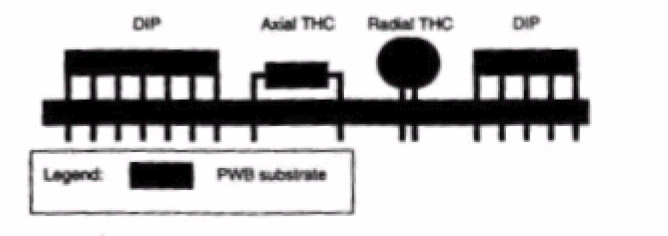

Figure 21.3 Type 1A assembly (all through hole)

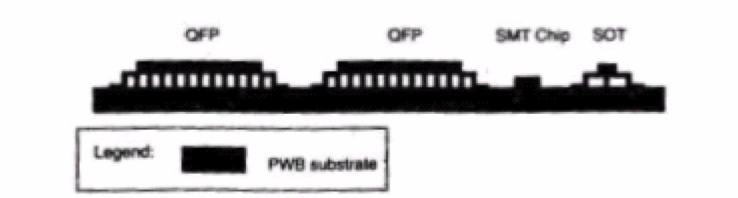

Figure 21.4 Type 1B assembly (single-sided pure SMT)

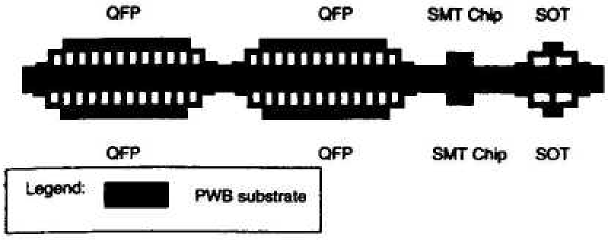

Figure 21.5 Type 2B assembly (double-sided pure SMT)

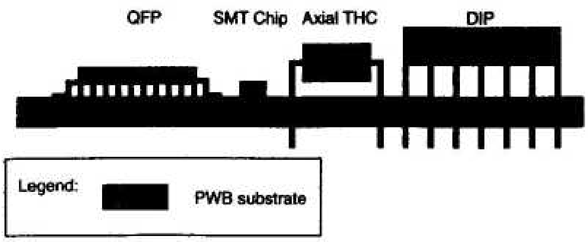

Figure 21.6 Type 1C assembly (single- sided mixed technology SMT)

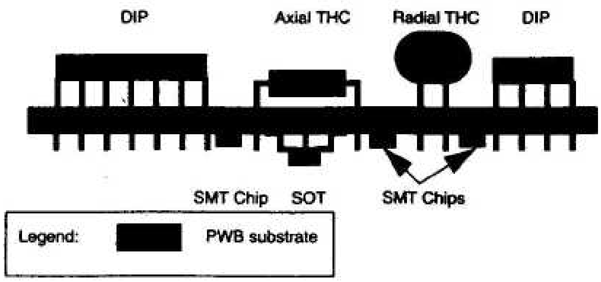

Figure 21.7 Type 2C (S) assembly

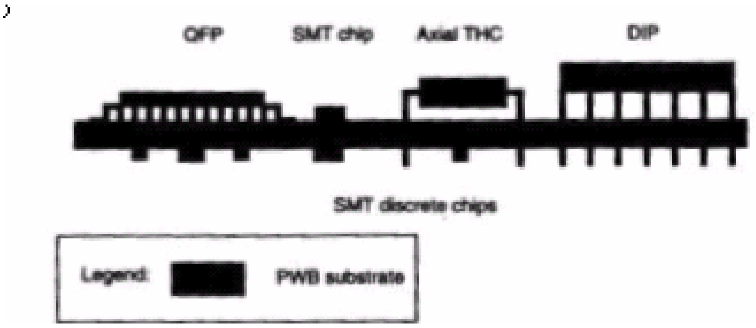

Figure 21.8 Type 2C (C) assembly

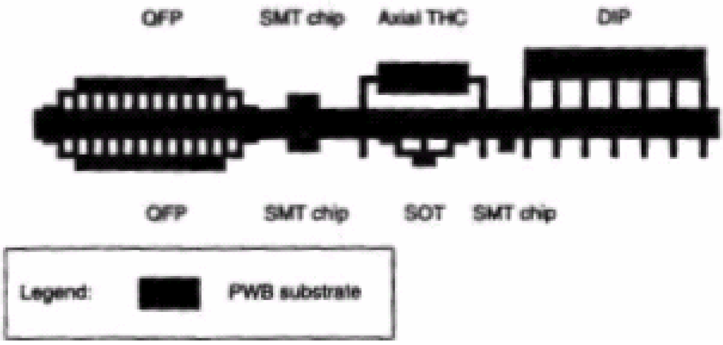

Figure 21.9 Type 2C (VC) assembly

21.3.3 Component Placement Machines

Requirements for accuracy make it necessary to use auto-placement machines for placing surface mount components on the PB. The type of parts to be placed and their volume dictate selection of the appropriate auto-placement machine. There are different types of auto-placement machines available on the market today: (A) in-line, (B) simultaneous, (C) sequential, and (D) sequential/ simultaneous.

In-line placement equipment employs a series of fixed-position placement stations. Each station places its respective component as the PB moves down the line. These machines can be very fast by ganging several in sequence. Simultaneous placement equipment places an entire array of components onto the PC board at the same time. Sequential placement equipment typically utilizes a software-controlled X- Y moving table system. Components are individually placed on the PC board in succession. These are currently the most common high speed machines used in the industry. Sequential/simultaneous placement equipment features a software- controlled X-Y moving table system. Components are individually placed on the PC board from multiple heads in succession. Simultaneous firing of heads is possible. Many models of auto-placement equipment are available in each of the four categories. Selection criteria should consider such issues as the kind of parts are to be handled, whether they come in tube, trays, or tape and reel, and whether the machine can accommodate future changes in other shipping media.

21.3.4 Soldering

Like the selection of auto-placement machines, the type of soldering process required depends upon the type of components to be soldered and whether surface mount and through-hole parts will be combined. For example, if all components are surface mount types, the reflow method will be used. However, for a combination of through-hole and surface mount components, reflow soldering for surface mount components followed by wave soldering for through-hole mount components is optimum.

21.3.4.1 Infrared/Convective Reflow Soldering

There are basically two types of infrared reflow processes: focused (radiant) and non-focused (convective). Focused IR, also known as Lamp IR, uses quartz lamps that produce radiant energy to heat the product. In non- focused or diffused IR, the heat energy is transferred from heaters by convection. A gradual heating of the assembly is necessary to drive off volatiles from the solder paste. This is accomplished by various top and bottom heating zones that are independently controlled. After an appropriate time in preheat, the assembly is raised to the reflow temperature for soldering and then cooled.

The most widely accepted reflow is now "forced convection" reflow. It is considered more suitable for SMT packages and has become the industry standard. The advantage of forced convection reflow is better heat transfer from hot air that is constantly being replenished in large volume thus supplying more consistent heating, and While large mass devices on the PB will heat more slowly than low mass devices.

21.3.5 Conduction Cooling for Components Mounted on PCBs

The electronic components are usually the major heat source in electronic systems. For effective cooling of these components, it is necessary to plan in advance the heat flow mechanism and heat flow path from the component to the sink.

In many cases, it is sufficient to dissipate the heat generated by the components to the PCB. This heat is then conducted through the PCB to a highly conducting plate, usually aluminum, in a good contact with it. The heat is then dissipated laterally to a heat sink cooled by flow of air or sometimes water for highly heat dissipated. This arrange as shown in Figure21.10.

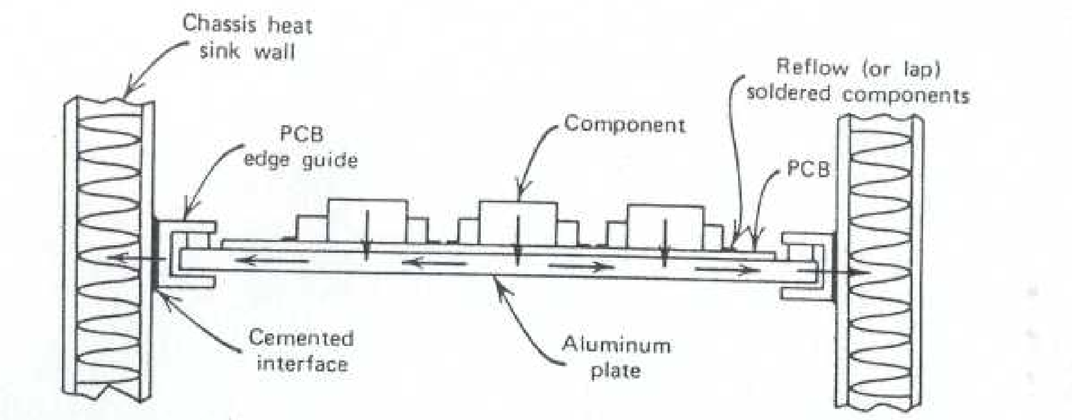

Figure21.10 Conduction heat flow path from component to heat sink

Example 21.1 Several power transistors, which dissipate 5 watts each, are mounted on a power supply circuit board that has a 0.093 in (0.236 cm) thick 5052 aluminum heat sink plate, as shown in Figure 21.11. Determine how much lower the case temperatures will be when these components are mounted close to the edge of the PCB, as shown in Figure 21.11b, instead of the center, as shown in Figure 21.11a.

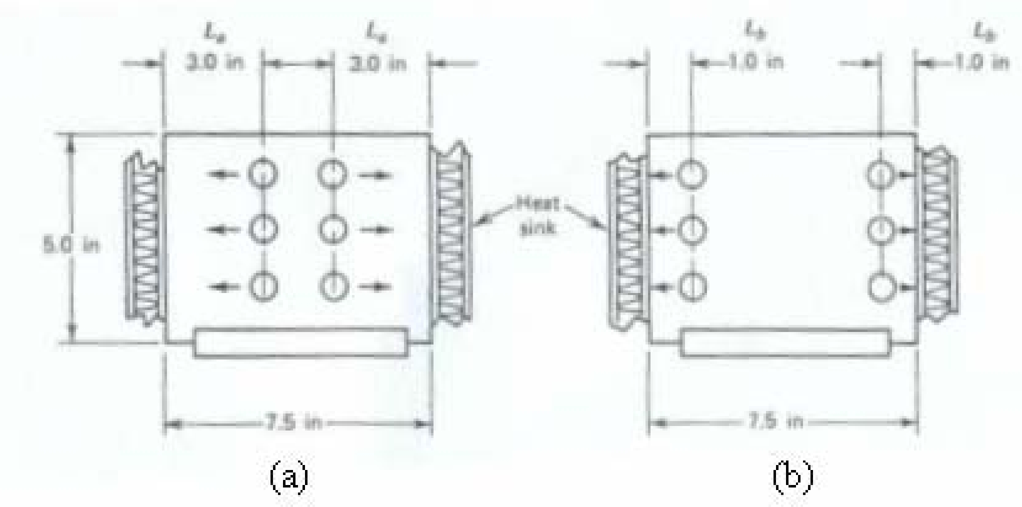

Figure 21.11 Power transistors mounted on an aluminum heat sink plate. (a) Old design (b) new design.

Solution:
Since both plug-in PCBs are Symmetrical about the center, consider each half of the board for the analysis.
Q = 3 x 5 = 15 watts
L_a = 3.0 in = 7.62 cm (length of old design)
L_b= 1.0 in = 2.54 cm (length of new design)
k = 143.8 W/m.K (5052 aluminum)
A = (5.0) (0.093) = 0.465 in^2 = 3.0 cm^2 (area)

The temperature rise at the old design locations:

$$\Delta t_a = \frac{(15)(0.0762)}{(3/10000)(143.8)} = 26.5\ ^oC$$

The temperature rise for the mounting position near the edge of the PCB, new design:

$$\Delta t_b = \frac{(15)(0.0254)}{(3/10000)(143.8)} = 8.83\ ^oC$$

This shows that moving the transistors closer to the edge of the PCB can reduce the component surface mounting temperature by 26.5 – 8.83 = 17.7 °C.

21.4 Electronics Chassis Design Procedures

Electronic systems normally consist of many different electronic component parts, such as resistors, capacitors, diodes, transistors, microprocessors, and transformers, which are enclosed within a support structure called the chassis, such as a chassis used in a space craft as shown in Figure21.12.

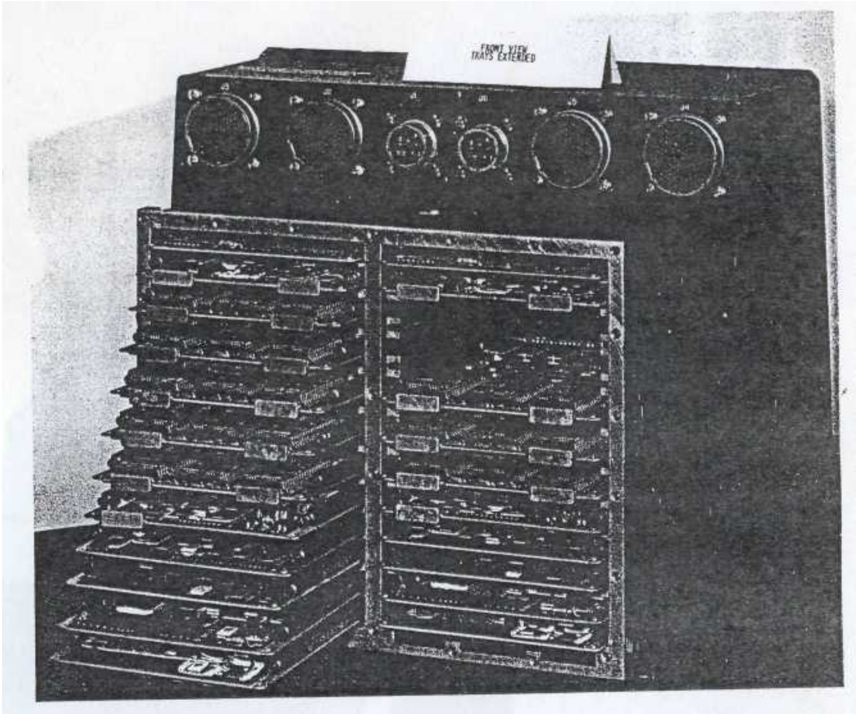

Figure21.12 Electronic box uses in a space craft

The purpose of the electronic chassis is to support the components while providing a low thermal resistance path to a heat sink, which will absorb this waste heat with a minimum rise in the temperature of the components. The heat sink may be the ambient air surrounding the chassis or a liquid-cooled cold plate is an integral part of the chassis wall.

Whatever method of heat transfer is selected, the technique should be as simple and as cost effective as possible. Many factors will have to be considered, such as space available, the power requirements of the cooling system, the maximum allowable component temperatures, component sizes, power densities, and the heat sink temperature. Other factors, such as shock and vibration, may have to be considered together with the thermal environment to ensure an adequate chassis design.

21.4.1 Formed Sheet Metal Electronic Assemblies

Sheet metal structures are often used for many different types of electronic boxes because the manufacturing costs are so low. Thin-gauge aluminum or steel sheets can be blanked and formed into a lightweight chassis with the use of rivets, spot welding or arc welding. The final assembly is usually painted for protection and appearance. This type of construction can be used for 7 or 70 in high.

Light-gauge steel sheet metal structures are usually not suitable for cooling high power electronic systems by means of conduction. The cross-sectional areas are small because the metal is thin and the thermal conductance is low. This increases the thermal resistance, which also increases the component hot spot temperatures. Also light-gauge steel sheet metal structures are not generally capable of withstand high vibration and shock levels, so that their use in theses environments is very limited.

Lightweight sheet metal structures may tend to amplify any acoustic noise generated by cooling fans or pumps. If large, thin flat panels are used on electronic box that is to be fan-cooled, make sure that it is not too close to workers, who may object to the acoustic noise that is generated.

Structural epoxies are being used very successfully for assembling small electronic boxes. These epoxies have high shear strength, with a short cure time at 100 ^{o}C, which makes them very cost effective.

21.4.2 Dip-Brazed Boxes with Integral Cold Plates

Dip-brazed aluminum boxes as shown in Figure 21.13 are convenient to use for small, light weight systems when quantities are small, usually less than about 8 or 10 boxes. Most electronic boxes will require shelves and brackets for mounting electronic components, ribs for stiffening the chassis to resist vibration, and cutouts for the cables and electrical harness. A dip-brazed electronic chassis can often provide these features at a relatively low cost.

The size of the dip-brazed assembly is usually limited by the size of the dip-brazed tank, or salt bath, which is used to completely submerge the structure that is to be brazed. The individual parts of the chassis are joined together like a three-dimensional jigsaw puzzle. Sometimes, a stainless steel fixture is used to hold the individual parts together during the dip-brazing process. Sometimes the parts are tack welded, riveted, or screwed together with aluminum screws. Aluminum slurry or a brazing strip, with a melting temperature slightly lower than the temperature of the salt bath, is used to join the individual structural members, which have a melting temperature slightly higher than that of the salt bath. As the slurry melts, capillary action draws the molten aluminum into the small voids between the individual parts and joins them rigidly.

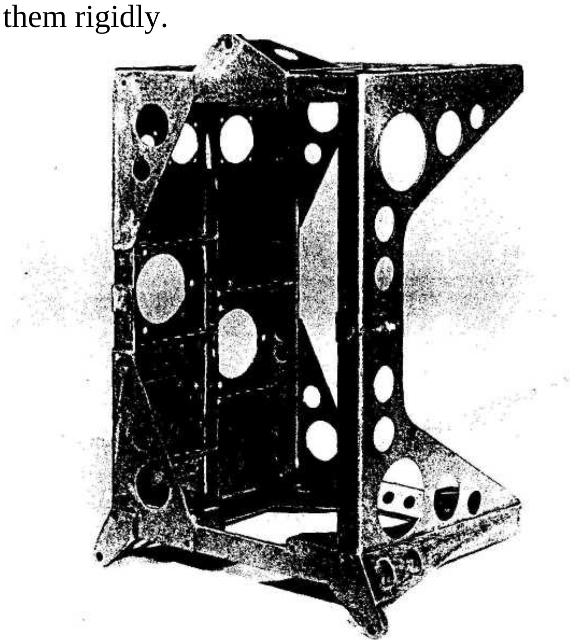

Figure21.13 Dip-brazed electronic chassis with tack welds for positioning piece parts

Thin-plate fin types of heat exchangers are often used for the side walls of chassis. The heat exchangers (or cold plates) are often dip-brazed first as a subassembly and then cemented together to form a chassis. Sometimes the heat exchangers can be dip-brazed as an integral part of the chassis without first forming a subassembly. The multiple fins provide a large surface area, which sharply in creases the amount of heat that can be removed from the chassis with air or with liquids. A typical cross section through a chassis with finned sidewall heat exchangers as shown in Figure 21.14.

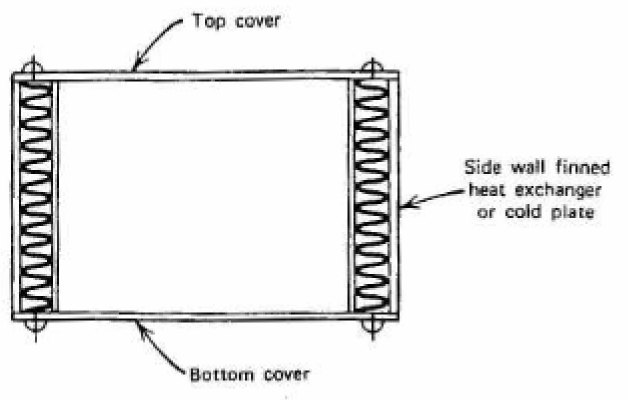

Figure 21.14 Chassis with side wall heat exchanger

The plate fin material is usually about 0.006 in (0.0152 cm) or 0.008 in (0.0203 cm) thick so that many fins can be spaced close together. The typical spacing is about 14 to 18 fins per inch. Some companies can dip-braze as many as 23 to 25 fins per inch.

When the fins get very close together, it becomes very difficult to clean out the salts left from the dip-brazed tank, so that they may become trapped. This can block the fin passages and reduce the cooling effectiveness. Also, trapped salts can corrode the metal and weaken the structure.

It is desirable to have some method for checking the dip-brazed heat exchangers to make sure that the fins are not blocked. A visual check is very valuable. If it is possible to look down the heat exchanger, blocked fins can be spotted and either rejected or cleaned. If a visual check is not possible, a pressure drop check should be made with a known flow passing through the fins. If a blockage occurs, the pressure drop across the fins will be very high.

The fin material is generally very soft, so that it can be deformed easily. If fins in an air-cooled cold plate are allowed to extend to extend to the end of the chassis opening, they can become bent or deformed by foreign objects, such as bolts, nuts, screw drivers, and even pencils. Therefore, for added protection, the ends of the fins should be recessed at least 1/4 in.

21.4.3 Plaster Mold and Investment Casting with Cooling Fins

Plaster mold castings and investment castings are very popular for small electronic support structures or small electronic enclosures. Plaster mold castings and investment castings use plaster for the mold, into which a molten metal is poured. Typical metals are usually aluminum, magnesium, zinc, bronzes, and some steels. Wall thicknesses of 0.040 to 0.060 in (0.102 to 0.152 cm) can be readily obtained with both methods.

Investment piece part castings are generally slightly more expensive than plaster mold castings because an intermediate wax core is required. This core is made up in the exact detail required by the finished product. It is coated with several thin coats of plaster or refractory material and thoroughly dried. The coated core is heated to melt the wax, which is then drained, leaving the hollow mold. The mold is filled with molten metal while a vacuum is applied to remove tiny air pockets from the porous plaster or refractory outer shell. This permits the molten metal to fill in every small corner in the mold for excellent detail, surface finish, and accuracy. The outer shell must be broken away and destroyed to obtain the finished product.

Investment castings are somewhat limited in their size, depending upon the complexity. Intricate chassis castings 15 x 8 x 10 in (38.10 x 20.32 x 25.40 cm), with wall thicknesses of 0.070 in (0.178 cm), can be readily obtained.

Plaster mold casted piece parts are normally less expensive than investment castings because the process does not require the use of an intermediate disposable wax pattern. However, tooling costs for the plaster mold casting will be higher if permanent molds are used, because of the extra machining required.

Very large plaster mold castings can be made, up to 100 in (254 cm) in length if required, with considerable detail. However, plaster castings usually cannot produce small details as well as can investment castings.

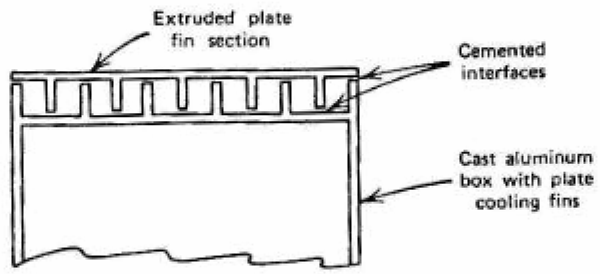

Figure 21.15 Plate fin extrusion cemented to a cast plate fin to form a multiple-fin heat exchanger

Investment castings and plaster castings methods can be used to make very efficient, lightweight heat exchangers and cold plates with integrally cast pin fins. Typical pin fins are about 0.062 in (0.157 cm) in diameter, 0.50 in (1.27 cm) long, and spaced on 0.200 in (0.508 cm) centers. Plate fin types of heat exchangers and cold plates are much more difficult to cast. Continuous plate fins require cores that must be supported as the molten metal is poured. These cores can shift and crack if the ribs are very long. If plate fins are desired, it might be better to cast them in short lengths instead of in a continuous length, to provide a means for supporting the cores.

Cemented construction techniques can often be combined with castings to provide a plate fin heat exchanger or cold plate. Extruded plate fin sections can be cemented to cast plate fin sections to provide a plate fin heat exchanger, as shown in Figure 21.15.

21.4.4 Die Cast Housing

The die casting process is capable of providing the lowest cost piece parts, with high quality and excellent appearance. However, tooling costs are very high, tools take a long time to fabricate, and modifications or design changes are very expensive. Die castings should therefore not be considered for production runs of less than about 1000 piece parts. This requires long range planning, scheduling, and coordinating to ensure a satisfactory product. For large production runs it may even be possible to use investment castings or plaster mold castings as a buffer until the die casting tools have been fabricated, installed, and proven out.

21.4.5 Extruded Sections for Large Cabinet

Weight is often a problem with large cabinets that must be designed to withstand the Navy shock and vibration. Thick cast walls can provide the required rigidity, but with a high-weight penalty. Under these circumstances extruded sections, with ribs or hollow cores, are capable of providing a rigid but relatively lightweight electronic enclosure. This type of structure can be welded, bolted, or riveted together to form a very rugged console. The hollow core type of extrusion is very convenient for ducting cooling air to various parts of the cabinet with fans or blowers. Large hollow core cross sections can carry large quantities of cooling air with a small pressure drop. Openings can be placed at various points in the extruded wall sections to direct the cooling air to hot spot areas. These openings can be blocked or reduced in size with plugs if the power distribution is changed at a later date.

Extruded sidewall sections are convenient to use with closed forced-air cooling systems, where a water-cooled heat exchanger or a refrigeration unit cools the recirculated air. One vertical sidewall can be used as the supply plenum, and the opposite sidewall can be used as the return plenum, as shown in Figure 21.16.

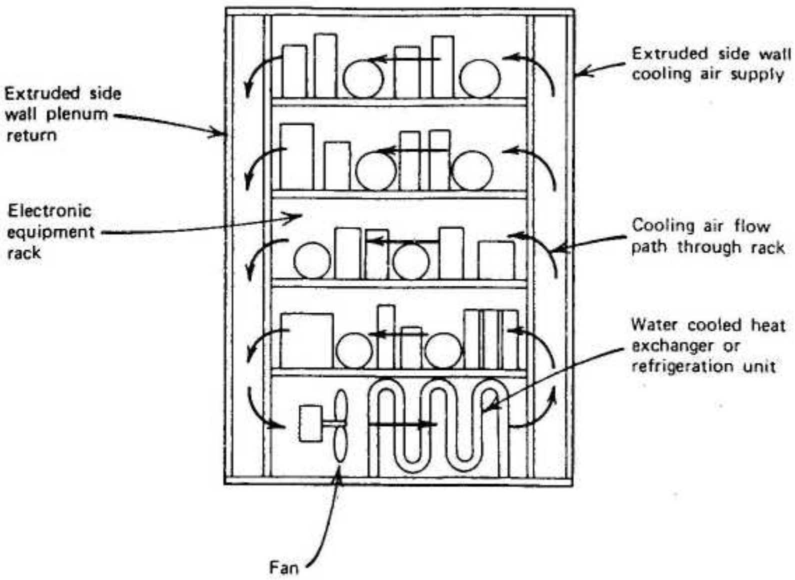

Figure 21.16 Closed-cooling air recirculating systems for electronic equipment rack

21.4.6 Humidity Considerations in Electronic Boxes

Electronic equipment must often be capable of operating in very humid environments, where condensation will produce large amounts of water over a long period of time.

When high-humidity environments are encountered, equipment designers must make a choice. They can seal the box against moisture or let the box breathe. Past experience with moisture problems shows that it is better to let the box breathe, because it is extremely difficult to seal an electronic box against moisture.

Humidity can cause serious problems in the electronic equipment when the internal circulating air is cooler than the outside ambient air. Moisture can condense on the electronic components, connectors, and circuit boards, producing short circuits or radical changes in the resistance between electronic components.

A moisture drainage path should be provided that permits the condensation to drain from the console walls, circuit boards, connectors, and wire harness to a drip pan at the bottom of the unit, where the moisture can evaporate or drain out of the system. Avoid moisture traps where the condensate can settle and cause corrosion. Drill holes, with a minimum diameter of 0.25 in, in the corners of horizontal bulkheads, away from the electronic components, to provide a moisture drainage path through the cabinet.

Use vertically oriented circuit boards and connectors, if possible, to provide a natural moisture drainage path away from the boards to the bottom of the chassis.

Offset drain holes may be required in the base of the chassis to prevent foreign objects, such as screwdrivers, from being poked into these holes and causing internal damage. Drain holes similar to the one shown in Figure 21.17 will reduce the possibility of foreign objects entering the chassis.

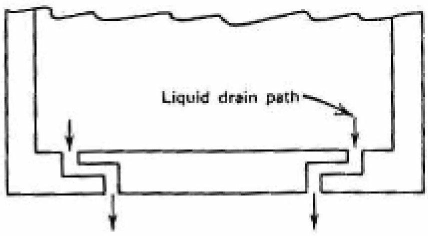

Figure 21.17 Offset drain holes in bottom of chassis

21.4.7 Conformal Coatings

There are five popular types of conformal coatings: acrylic, epoxy, polyurethane, silicone, and parylene. A thin conformal coating 0.0003 to 0.005 in (0.00076 to 0.0127 cm) thick may be required to protect the circuit boards from moisture. However, these coatings should be applied only if they are absolutely necessary In general, coatings are expensive to apply. They require special cleaning processes, special tools to apply the coatings, and the circuit boards are difficult to rework. In addition, many coatings tend to crack, chip, and peel, and they will contaminate the connector contacts unless they are masked during the application. Also, water vapor tends to creep under the coatings and condense, so that coatings can change the electrical resistance between the circuits they are supposed to help. Therefore, if it becomes necessary to apply a conformal coating for moisture protection, make sure that the cleaning and application procedures are carefully followed, or the coatings may create more problems than they solve.

The conformal coat should not be applied so that it bridges the strain relief on the component lead wires. The purpose of the strain relief is to reduce stresses in the wire and in the solder joints. If the strain relief is bridged (completely filled), it will act like a short circuit and will not provide strain relief during vibration as the PCB flexes. Also, a filled strain relief will restrict the relative motion that results during temperature cycling tests. This will increase the stresses in the solder joints, which will increase the chance of failure.

21.4.8 Sealed Electronic Boxes

Electronic systems with high-impedance circuits are usually very sensitive to humidity and moisture in the ambient air. Slight amounts of condensation on sensitive components, printed circuits, or electrical connectors can often produce large changes in the operating characteristics of the system. Therefore, to minimize potential problems resulting from humidity, moisture, and condensation, sensitive electronic systems are often packaged in sealed electronic boxes.

Sealed electronic boxes are also used for some air-cooled electronic systems, which must be capable of operating in the hard-vacuum environment of outer space. The sealed box is used to prevent the loss of air, which is required to cool the electronic components.

Many different types of seals can be used, depending upon the size of the unit, the cost, and the ease of repair. Solder seals are very effective for small covers on boxes, but repairs are inconvenient. O-ring seals are popular and easy to use for large or small boxes.

A large, stiff, machined mounting flange with many high-strength screws is required for the box and the cover, to provide an effective seal. A typical O-ring seal is shown in Figure 21.18.

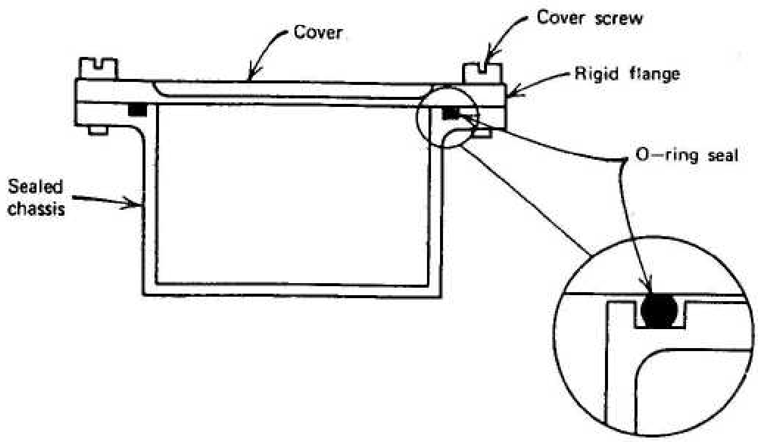

Figure 21.18 O-ring for electronic box

21.4.9 Standard Electronic Box Sizes

Electronic boxes can come in a wide variety of sizes and shapes, depending upon the application and environment. One organization, however, has made an attempt to standardize the size, shape, and mounting for electronic boxes used in air transport equipment. This has become the standard known as ARINC, which is an acronym for Aeronautical Radio Inc. This specification, ARINC 404, Air Transport Equipment Cases and Racking (ATR), December 31, 1970, defines a group of rectangular plug-in types of electronic equipment cases, which have the outer dimensions listed in Table 21.1.

Table 21.1 ARINC standard rectangular box sizes

Description	Width (in)	Length (in)	Height (in)
Short one quarter ATR	2.250	12.5625	7.625
Long one quarter ATR	2.250	19.5625	7.625
Short three eights ATR	3.5625	12.5625	7.625
Long three eights ATR	3.5625	19.5625	7.625
Short half ATR	4.875	12.5625	7.625
Long half ATR	4.875	19.5625	7.625
Short three quarters ATR	7.50	12.5625	7.625
Long three quarters ATR	7.50	19.5625	7.625
One ATR	10.125	19.5625	7.625
One and one half ATR	15.375	19.5625	7.625

22. Packaging of Electronic Equipments (1)

22.1Printed Wiring Boards (PWBs)

Introduction

Printed-wiring boards, commonly called PWBs, are sometimes referred to as the baseline in electronic packaging. Electronic packaging is fundamentally an interconnection technology and the PWB is the baseline building block of this technology. It serves a wide variety of functions. Foremost, it contains the wiring required to interconnect the component electrically and acts as the primary structure to support those components. In some instances it is also used to conduct away heat generated by the components.

22.2 Printed Wiring Board Types

PWBs can be classified into several categories based on their dielectric material or their fabrication technique. This section describes PWBs fabricated using organic dielectric, ceramic dielectric, and discrete wire techniques.

22.2.1 Organic PWBs

These PWBs are fabricated using an organic dielectric material with copper usually forming the conductive paths. The organic-based boards can be subdivided into the following classifications: rigid, flexible, rigid-flex combining the attributes of both rigid and flexible boards in one unit, and molded. Each of these classifications, except for molded, can be further subdivided into single-sided, double-sided, or multilayer PWBs.

The circuit interconnection pattern, except for molded PWBs, is created by imaging the conductor pattern on copper sheets using a photoresist material and one of two image-transfer techniques—screen printing or photo imaging. The resist acts as a protective cover defining the conductor patterns while unwanted copper is etched away. Molded PWBs are usually nonplanar (three-dimensional) and consist of conductive materials selectively applied through printing conductive pastes or additively plating conductors to either extruded or injection molded thermoplastic resins.

These techniques can be used with a variety of dielectric materials to achieve various mechanical and electrical characteristics in the final product. Among the most common dielectric materials are epoxy/e-glass (electronic-grade glass) laminates used in the fabrication of rigid PWBs and polyimide film used in the fabrication of flexible printed wiring. The rigid-flex boards use a combination of these two materials.

22.2.1.1 Rigid PWB

The rigid PWB is fabricated from copper-clad dielectric materials. The dielectric consists of an organic resin reinforced with fibers. The most commonly used fiber materials are paper and e-glass. The organic media can be of a wide formulation and include flame-retardant phenolic, epoxy, polyfunctional epoxy, or polyimide resins.

As the name implies, rigid PWBs consist of layers of the organic laminates that are laminated through heat and pressure into a rigid interconnection structure. This structure is usually sufficiently rigid in nature to be able to support the components that are mounted to it. Specialized applications may require the PWB to be mounted to a support structure. The support structure may be used to remove heat generated by the components, decrease the movement of the PWB under extreme vibration.

The rigid PWB interconnection structure may be further subdivided by the number of wiring layers contained within the structure into the following three categories—single-sided, double-sided, or multilayered. Figure 22.1 shows a cross-sectional view of each type.

Single-Sided PWBs: A single-sided PWB consists of a single layer of copper inter-connection (usually on the component side of the PWB). The rigid dielectric material is fabricated from multiple layers of unclad laminate material pressed to the final end-use thickness. A single layer of copper cladding is applied to one of the outside layers during this process. In some instances double-sided copper cladding may be used, with the copper on one face being completely etched away during the processing.

The base laminate of single-sided boards can be of woven or paper (unwoven) materials with copper foil, usually of 1- or 2-oz weight, clad to one side. It should be noted here that copper cladding is most often referred to by its weight (1 oz/ft^2 equals 0.00137 in thick) rather than by its thickness. The raw clad laminate is first cut into working panels suited to the equipment, which will handle the subsequent operations. The panel is then drilled or punched to provide a registration system. Laminate flatness is important in achieving a good registration baseline. These are critical in an automated print and etch system because the panel tends to warp after the copper is removed during etching. This warping allows stresses built into the material during its fabrication to be relieved. Excessively warped panels may not register properly for subsequent operations.

The individual artworks which define the conductor patterns are then arranged or panelized so that one or more PWBs will be produced from a single panel. This is accomplished by stepping and repeating the patterns into a panel phototool. Once the panel layout is established, the panel can be drilled or punched to produce the final hole pattern. Holes required are either drilled in glass-reinforced products or punched in paper-reinforced products. Registration of the conductor pattern to holes is accomplished through either the right-angle edge of the panel or on pilot holes contained in opposite comers of the panel. Drilling of holes is usually done after the panels are first cut; punching of holes is done as the last operation.

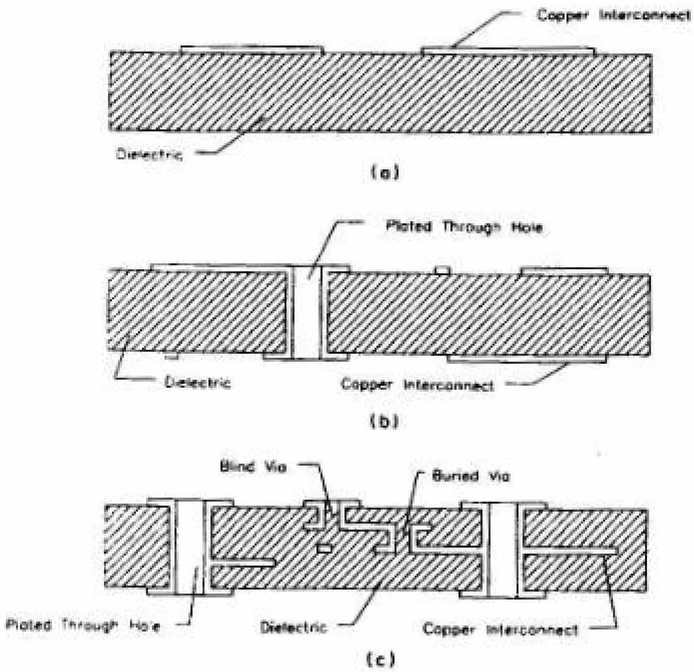

Figure 22.1 Organic PWBs (a) single-sided, (b) double-sided, and (c) multilayer

Following the drilling operation, the etch resist is applied and the circuit pattern formed. This pattern can be made by printing a liquid resist or photo imaging of a film or liquid. The next step is to etch away the unwanted copper from the laminate, leaving only the desired circuit pattern. Finally the resist is stripped and the single-sided board is complete in panel form.

At this point additional processes such as platings or solder masks may be performed, or the individual boards may be sheared or routed from the panel.

While single-sided boards with their simplicity might seem doomed due to the emergence of modern complex electronics, they continue to have a substantial market, especially where cost is a strong driver. Their use with fairly complex IC devices can be seen in many places, such as watches, cameras, and automobiles. This will probably continue to be the case for the foreseeable future.

Double-Sided PWBs: From a historical perspective the double-sided board is probably the most often designed type of all PWBs. It retains much of the production simplicity of the single-sided board but allows circuit complexities far in excess of 2:1 over its simpler cousin. This is the case because it allows basic x and y routing of the circuit on its two outer faces, thus improving the routing efficiency and the circuit density. Interconnection of the two conductor patterns is accomplished through drilling and subsequent plating or filling the interconnection holes, called vias. The most widely used method is to plate the vias with copper. Silver-conductive ink is another process used in low-cost consumer products.

Double-sided boards are fabricated from laminates with copper (usually 1 oz) clad to both outside layers. The copper may be clad to a variety of materials. Here, as with the single-sided board, the material is purchased from a laminator who specializes in providing laminates to the electronic industry.

Once the raw laminate is cut into panels, the fabrication operation begins with the inter-connection hole drilling. The via holes may also serve as mounting holes for the components to be soldered into. After the via hole pattern has been drilled, the holes may be filled with the conductive ink or the panel is copper plated by an electroless technique in preparation for subsequent plating by either of two methods—pattern plating or panel plating.
The conductor image is formed in a similar way as with single-sided boards, except that the photoresist application and imaging take place on both sides of the panel. Obviously, the registration of the photo images from one side of the panel to the other is critical. The circuit pattern on one side must be properly registered to the pattern on the other side, or the plated-through holes will not properly connect between the two sides.

The next step is to etch away the copper laminate, leaving only the desired circuit pattern. At this point additional processes such as resist stripping, platings, or solder masks may be performed and the individual PWBs then sheared or routed from the panel (see Fig. 22.1).

Multilayered PWBs. Multilayer boards are those PWBs having three or more conductive layers, including any pads-only layers. The typical modern multilayer board will have from 4 to 10 layers of circuitry, with some high-density applications requiring upward of 50 layers. Most multilayer boards are fabricated by laminating single- or double-clad, pre-etched, patterned sheets of thin (<0.005-in) laminate together using partially cured resin in a carrier fabric. The materials commonly used for this purpose are discussed at length in Section22.3.

The single- or double-clad laminate material is processed similarly to the single- or double-sided PWB, except that the via or component holes are usually not drilled until after lamination. It should be noted here that the importance of registration is amplified as the layer count increases. Increased pad sizes may be required to minimize via hole breakout due to misregistration. The same requirement may limit the size of panels due to run out of the circuit features.

Following the fabrication of the individual layers or layer pair, a "book" of layers and their interposed bonding layers are stacked together in a particular sequence to achieve the required lay-up. This book is then laminated under heat and pressure to the appropriate thickness for the final board. The outer layers are not pre-etched so that the laminated book appears the same as a double-sided copper-clad laminate of comparable thickness. After lamination, the book is processed the same as a thick double-sided board. The book is drilled to add the via holes and then processed as if it were a double-sided board using plated-through holes. A cross-section of a typical multilayer board is shown in Fig. 22.1.

In some cases standardized layers, such as power or ground distribution can be "mass"-laminated into the raw laminate. This is a very cost-effective means of achieving multilayer density at near double-sided board cost since the outer layer processing and via drilling is identical to that for double-sided PWB processing. As a result, four-layer boards are the most prevalent multilayer boards.

Where circuit density requirements override cost considerations, techniques such as blind or buried vias are used to increase the interconnection wiring density on a given layer. Where these techniques are used, the inner layer pairs are fabricated as double-sided boards, complete with plated vias, and then assembled into books for processing into multilayer boards. Thus the inner layers may be interconnected without a via hole through the entire board. Similarly, blind vias may connect to the first or subsequent buried layer on each side of the board without penetrating the entire board (see Figure 22.1).

The multilayer board has now achieved a cost and reliability level that allows its use in any level of electronics. It is no longer the exclusive tool of the mainframe computer, telecommunications, or military electronics. It is often seen even in toys.

22.2.1.2 Flexible PWB

As defined by the Institute for Interconnection and Packaging Electronic Circuits (IPC), flexible printed wiring is a random arrangement of printed wiring, Utilizing flexible base material with or without cover layers. Interconnection systems consisting of flat cables, collated cable, ribbon cable and sometimes wiring harnesses are sometimes confused with flexible printed wiring. Flexible printed wiring is used in applications requiring continuous or periodic movement of the circuit as part of the end product function and those applications where the wiring cannot be planar and is moved only for servicing. Flexible wiring can be used as interconnect cabling harnesses between various systems circuit card assemblies and or connectors as well as to interconnect individual electrical components. Figure 22.2 shows a typical flexible printed wiring interconnect.

Visually, flexible printed wiring looks similar to rigid printed wiring. The main difference in the products is the base or dielectric material. Flexible printed wiring is manufactured using ductile copper foil bonded to thin, flexible dielectrics. The dielectric materials include polyimide (Kapton), polyester terephthalate (Mylar), random fiber aramid (Nomex), polyamide-imide TFE Teflon and FEP Teflon and polyvinyl chloride (PVC).

As with their rigid printed wiring, the flexible printed wiring may be manufactured in single-sided, double-sided or multilayer configurations as shown in Figure 22.3. The conductor patterns are formed in a similar manner to rigid PWBs using either a screen printing or photo-imaging of a resist to form the conductor pattern and then etching of the unwanted copper. A variety of adhesive materials are used in their manufacture to bond the various layers together. These including acrylics, epoxies, phenolic butyrals, polyesters, and polytetrafluoroethylene (PTFE). In addition, newer processes have been developed to laminate the conductor directly to the dielectric film without the use of an adhesive layer.

On single- and double-sided flexible wiring, cover layers are often used to protect the etched copper circuitry. When a film cover layer is employed, the access holes to the circuitry are either punched or drilled in the adhesive-coated film. The cover layer is then mechanically aligned to the wiring and laminated in a platen press under heat and pressure. The adhesive systems must be of a "no" or "low" flow formulation to keep from contaminating the interconnection pads. Screen printable cover coats may also be used. These are usually ultraviolet curable and give a moderately pinhole-free insulating surface.

Unlike their rigid counterparts, the outline features of flexible wiring are not routed but cut using either soft or hard tooling. Soft tooling involves a rule die. In its simplest form, this can be a steel die and Exact to knife to cut the outline pattern. More complex dies may consist of steel strips imbedded in plywood. When pressed against the flexible wiring they act as cookie cutters to form the outline. Rule dies are dimensionally less accurate and less expensive than hard tools. Hard tools are punches, die plates and strippers manufactured from hardened steel. They can hold tolerances within the die of ±0.001 in.

Figure 22.2 Typical flexible printed wiring interconnect in connector assembly

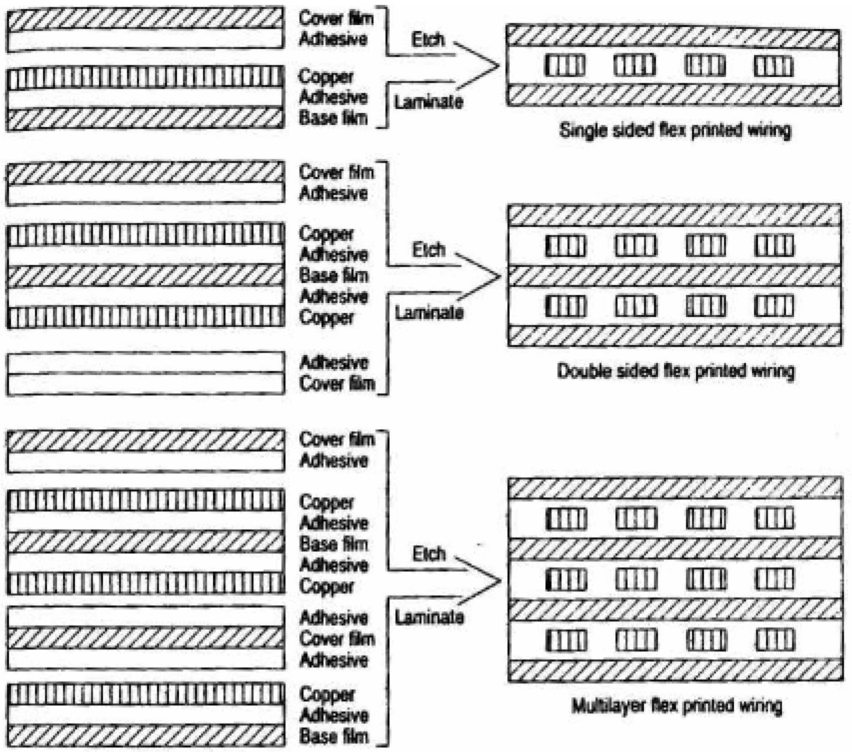

Figure 22.3 Flexible PWB types

Due to the extreme flimsiness of flexible wiring, when components are to be mounted, adequate reinforcement must be added to the flexible wiring to eliminate stress points at the component circuit interfaces. Reinforcements typically used are simple pieces of unclad rigid laminates or complex formed, cast or machined metals or plastics to which the flexible wiring is laminated.

22.2.1.3 Rigid-Flexible

Rigid-flex circuitry consists of single or multiple flexible wiring layers selectively bonded together using cither a modified acrylic adhesive or an epoxy bond film. Cap layers of rigid core copper clad laminate may be bonded to the top and bottom surfaces of the circuit to add further stability to the bonded areas as shown in Figure 22.4(a).

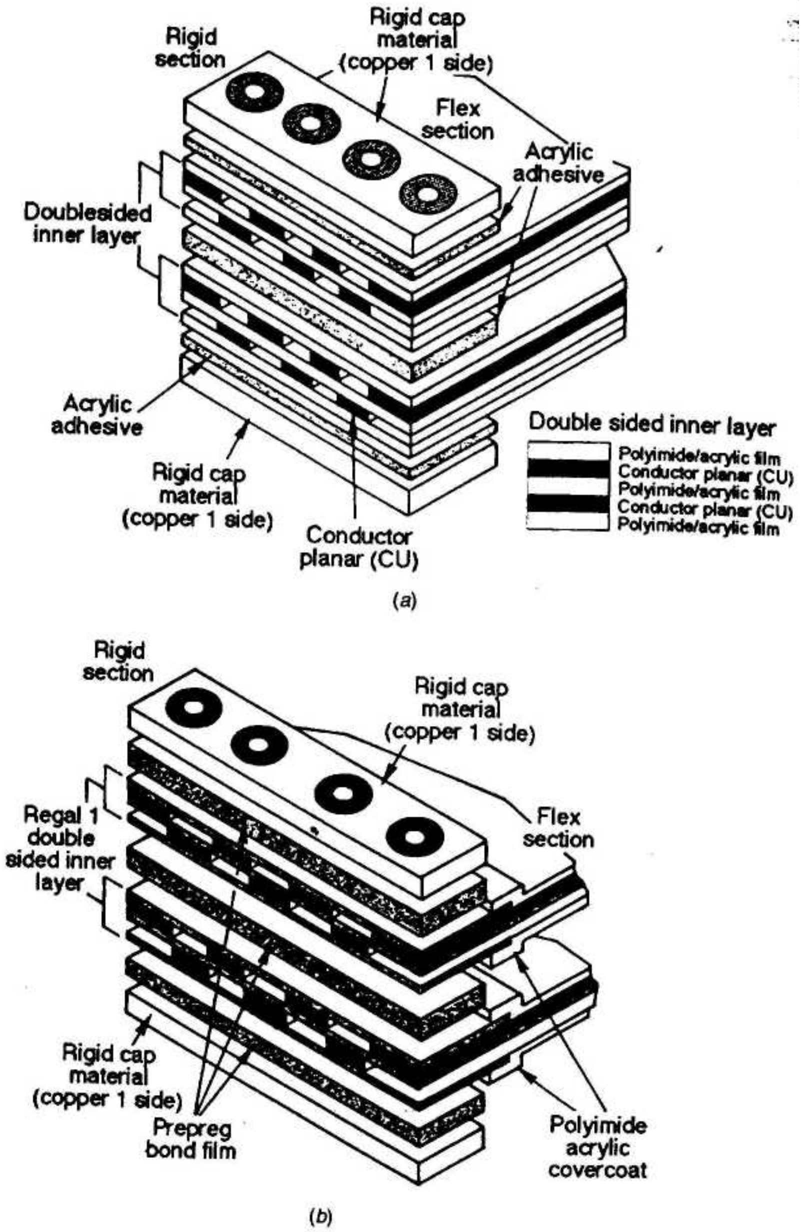

Figure 22.4(a) Rigid-flexible multilayer, (b) REGAL flexible multilayer

To allow for increased reliability in multilayer applications, the amount of acrylic adhesive in the rigidized area must be limited. There are a couple of methods in use in the IP industry today to accomplish this. One method involves using a polyimide/acrylic base with a cover coat in the rigid area and a polyimide acrylic selective cover coat in the flexible areas. This technique does force the manufacturer to develop tooling techniques to overlap the separate dielectrics.

A second technique that was developed is called a Rigid Epoxy Glass Acrylic Laminate (REGAL) Flex as shown in Figure 22.4(b). In this technique, the manufacturer starts with a base stock of Epoxy prepreg clad with copper. The traces are etched in the copper. The base-stock epoxy prepreg is then encapsulated in the flex area with flexible dielectric to allow the circuit to bend. The traces in the rigid section are encapsulated with epoxy prepreg which has been windowed to remove the prepreg from the flex section. Each cover coated flex layer can be selectively bonded together with pre-windowed epoxy prepreg to form a rigidized area for subsequent through hole processing.

The benefits of rigid-flexible wiring are apparent in the design, manufacturing, installation and assembly, quality control and product enhancement of the end item.

The designer has increased conceptual freedom in the end item design. Conformability, three dimensional interconnects and a space saving form factor are benefits. In many cases reduced interconnect length lead to optimal electrical performance. Mechanical and electrical interfaces are reduced and mechanical, thermal and electrical characteristics are more repeatable than with conventionally wired systems.

In manufacturing their use leads to reduced assembly costs within a totally unitized interconnect system. There are increased opportunities for automation. In addition, reduced system interconnect errors and improved system interconnect yields occur.

Installation and assembly benefits include elimination of miswiring and indexing errors encountered in discrete wired systems. A reduction in the installer skill and training, increased speed of installation and mounting simplification leading to reduced hardware requirements are other benefits.

Quality control benefits by the adaptability of the product to automated inspection, a simplification of error cause analysis and more effective error cause correction.

Products are enhanced through a reduced weight, volume and cost. Fewer interconnections are usually required leading to increased system reliability. Reduction in product inventory, maintenance and field service time and expense are also realized.

22.2.2 Ceramic PWBs

These PWBs are classified by their method of manufacture and type of metallization. There are four distinct types. Thick film uses alumina, beryllia, and similar materials as the substrate base material and fired thick-film dielectric paste (a glass-frit paste) as the dielectric. Conductors are formed from fired conductive noble metal pastes. Thin film uses ceramic, glass, quartz, silicon, or sapphire as the substrate base and deposits various metals by plating, sputtering, or vapor deposition. Cofired substrates can be broken into two distinct groupings. Cofired ceramic uses ceramic tape as the dielectric that is cofired with refractory metal pastes which form the conductors; cofired low-temperature tape uses a glass/ceramic tape dielectric that is cofired with noble metal pastes which form the conductors. Direct-bond copper directly bonds copper conductors to a ceramic substrate. All of these ceramic-based PWBs are most often referred to as substrates.

Ceramic boards do offer advantages, compared to organic boards. The ceramic dielectric is inherently much more rigid than organic material dielectrics. Component soldering (183 to 240 °C) is usually performed above or near the glass transition temperature T_g of organic materials (100 to 240 °C) and can lead to damaged PWBs when the process is controlled improperly. The 1600 °C needed to fire ceramic is well above this soldering temperature.

Higher thermal conductivities available with ceramic materials offer improved thermal management over organic boards. When thermal vias are required, the smaller buried vias available with ceramic boards provides a low thermal resistance while sacrificing less routing area.

Increased costs and design time are disadvantages to the use of ceramic boards. A weight penalty is usually paid when ceramic boards are used. The ceramic and noble metal materials used in ceramic boards are also more costly than their organic counterparts. The demand for these boards has usually been in low-volume military and avionics applications. This has led to a limited number of ceramic PWB facilities, which has also helped to maintain higher costs. The following sections describe in detail each of the four different ceramic substrate types.

22.2.2.1 Thick Film

This class of ceramic PWBs is manufactured by building up alternating layers of conductors and dielectric on a ceramic substrate. A thick-film substrate may be called a true printed circuit in that resistive elements may also be built into the substrate. Thick-film substrates have dielectric thicknesses of 0.0015 to 0.0025 in, metallization thicknesses of 0.0005 to 0.001 in, and resistor thicknesses of 0.001 to 0.0015 in. Each layer is pattern-printed onto the substrate using screen or stencil printing processes.

Several different ceramic materials can be used as the substrate base. These include alumina, beryllia, aluminum nitride, boron nitride, silicon carbide, and silicon nit depending on the end item requirements. Dielectric, conductor, and resistive inks (pastes) are printed and fired to build the interconnect structure.

The manufacture of a thick-film ceramic PWB begins with the generation of artwork defining the following: conductor patterns, dielectric layers including via openings in multilayer applications, via fill patterns, and resistor networks when required. From this artwork a screen or stencil for each wiring, via, resistor, and dielectric layer is developed. When a screen is to be used, its manufacturing begins with stainless-steel wire mesh stretched over a metal frame. Nylon and polyester mesh are sometimes used due to their lower costs. They can stretch and be affected by temperature and humidity and are not as durable as the stainless-steel screens. The mesh count (number of wires per linear in screen) and wire diameter determine the obtainable print resolution of the various layers. In general, mesh counts vary from 200 to 400 and wire diameters from 0.9 to 1.1 mil, with the lower mesh counts (200) and greater wire diameters (1.1 mil) being used for gross conductor patterns (>0.010-in line widths and spaces).

A photosensitive polyvinyl or polyimide emulsion is next applied to the screen, and the conductor, dielectric, via, or resistor pattern is photo-imaged on the emulsion under ultraviolet light using the artwork. Uncured resin is then washed away, leaving the final conductor pattern. The emulsion thickness determines the final wet print thickness of the various layers for a given mesh and wire diameter.

Stencil printing involves etching the patterns to be printed in a thin metal foil, usually nickel or brass. This once again uses photoresistive materials in a photpimaging operation to define the pattern and then etching away the unwanted metal similar to etching copper on a PWB laminate. The metal stencil is then mounted in a metal frame. The advantages of stencils over screen meshes are many. They offer more uniform print thicknesses, greater print resolution, reduced dimensioning capabilities, and easier process control.

The ceramic substrate is prepared by cutting to size using laser drilling, diamond scribing, or ultrasonic milling. The laser is by far the most prevalent method. Overlapping of the laser drill hole pattern can yield a smooth cut surface. Spacing of the holes yields a perforated surface, which can be used to define a number of substrates on a single ceramic panel. This "snapstrate" can be processed, and after the processing is completed, the individual substrates can be snapped along the perforation.

Cleaning of the ceramic to remove the melted ceramic or glass residue (slag) left after laser drill is called deslagging. A variety of methods may be used, including sandblasting with alumina slurry followed by a cleaning in hot isopropyl alcohol. Subsequent heating in a furnace at 800 to 925 °C is usually done to burn off any organic contaminants left during the previous processes.

Following substrate preparation, the metallization process begins. Conductive, dielectric, or resistive inks (pastes) contain the desired metals or conductors. These are combined with glass frits to allow bonding during firing and needed solvents to accomplish a definable print. Each layer is printed, dried to volatilize the solvents, and then fired in a furnace. This print, dry, fire sequence continues until the multilayer structure is complete. Resistor layers are the last high-temperature firing (800 to 900 °C) performed and are done together. Subsequent high firings can cause an oxidation of the resistive material and an unacceptable rise in resistance of the material. A low-temperature (425 to 525 °C) glass encapsulant can be printed and fired over selective resistors and conductors as a protective overcoat or solder mask. Resistors are usually trimmed to a final value using a laser-trimming process. This requires the overcoat encapsulant to be composed of a glass that allows the laser to penetrate to the resistor.

Thick-film ceramic boards are used mainly as interconnect substrates in multichip modules. Their use as interconnection substrates for applications similar to rigid organic PWBs is usually limited to a maximum PWB size of 8 in.

22.2.2.2 Thin Film

Thin-film ceramic boards are normally limited to specialized designs or single-layer applications. They are more expensive and difficult to multilayer when compared to their thick-film counterparts. Their use requires the substrate surface to be very flat and smooth and causes higher-purity ceramics to be used. These include alumina, glass, quartz, silicon, or sapphire. Thin-film metallizations use noble metals (such as gold) and are used most often in microwave applications due to their improved electrical performance over thick-film substrates at higher frequencies.

Thin-film interconnections in multilayer applications are through buried vias, as is the case with all ceramic PWBs. The top and bottom metallization on a double-sided substrate can be connected using plated-through holes for electrical interconnection or improved thermal performance. Metallization patterning of thin-film ceramics is accomplished through the use of photo lithography, plating, etching, vapor deposition, and sputtering methods.

22.2.2.3 Cofired

This type of ceramic PWB requires the printing of pastes containing conductor metallization onto unfired tape (dielectric) materials. These layers are then stacked and cofired together in a furnace to form the interconnect structure. The unfired tape materials can be either ceramic or a low-temperature dielectric.

The ceramic tape system requires higher firing temperatures. This results in refractory metals such as tungsten, molybdenum, or tungsten copper to be used as the conductor within the paste. These metals have higher vaporization temperatures to withstand the firing, but lower thermal and electrical conductivities than the noble metals (gold, silver, or copper). Their lower conductivities typically limit the use of these substrates to digital applications.

The conductor paste is applied to the tape using a screen or stencil similar to the thick-film process. For multilayer applications, holes are punched in the dielectric prior to printing. The conductive paste fills the hole and later forms a buried via during the firing operation. After all layers have been printed, they are stacked in the proper sequence, laminated together under heat and pressure, and fired to solidify the ceramic.

Upon completion of the cofiring operation, the exposed refractory metals are electroplated with typically 0.000080 to 0.000350 in of nickel and 0.000050 to 0.000100 in of gold. The nickel acts as a barrier to intermetallic formations between the gold and tungsten and as a corrosion barrier. The gold serves as a wire-bondable or solderable surface for component attachment.

The dielectric tape systems are composed of lower-temperature reflow glasses similar to those found in thick-film pastes. The printing, stacking, and laminating operations fare the same as those used for the ceramic materials. The firing, however, occurs at a lower firing temperature, which allows the use of noble metal pastes. These tapes allow the substrates to be used in microwave applications. In addition, no additional platings are required upon postfiring.

Cofired PWBs offer distinct advantages over thin- or thick-film processed PWBs. Multilayering is limited only by the thickness limitation of the overall package. Each fired layer is 0.003 to 0.012 in thick, depending on the tape thickness used. Thermal vias may be more readily incorporated into the design using an array of vias punched in the dielectric and filled with conductive pastes. Cutting of the tape prior to stacking and firing can allow cavities to be formed in the final product to allow component mounting. Cofired substrates are the main manufacturing method used to produce leadless chip carrier and multichip module component bodies. The patterning of the conductor layers prior to firing allows for easier inspection and rework.

The main disadvantages are in the longer life-cycle time needed to develop the tooling required to produce the item.

22.2.2.4 Direct-Bond Copper

As the name implies, a direct-bond copper (DBCu) board uses copper directly bonded to a ceramic dielectric. The most commonly used ceramic is alumina, although beryllia and aluminum nitride (which offer improved thermal performance) have been used successfully in the process. The DBCu structure offers improved thermal and structural performance compared with conventional thick- or thin-film technologies using alumina dielectrics.

The process involves oxidation of the surface of a copper foil, which is then placed against a ceramic substrate. The pieces are placed in a furnace which reflows the copper oxide and fuses it with the surface ceramic oxides. This directly bonds the two materials together.

Any currently available ceramic material thicknesses can be used (0.005 to 0.125 in). Copper foils of 0.001- to 0.080-in thickness have been used successfully. To prevent the substrate from warping or cracking, it is recommended that the copper foil thickness be less than or equal to the ceramic thickness.

The bonding process occurs at approximately 1000 °C. During cooling, the copper contracts at a much higher rate than the ceramic. The cooling increases the tensile strength of the ceramic by an order of magnitude by placing it in compression. This allows thinner ceramic materials to be used and will decrease the overall assembly height and reduce the thermal resistance of the board. Coupling the reduction in thickness with the heat-spreading capabilities of copper allows a DBCu board to offer reductions in thermal resistance.

The copper interconnect features can be formed by punching the copper sheet prior to attachment to the ceramic or by photo-imaging techniques similar to those used in rigid PWBs after bonding to the ceramic. The latter process allows finer line features. Typically, 0.015-in minimum line widths and spacings are used.

Alternately stacking layers of copper and ceramic can create multilayer interconnect structures. Three conductor layers are the limits achieved to date. Buried vias consisting of windows in the ceramic filled with copper spheres or particles are used to interconnect from layer to layer.

DBCu boards offer the advantages of improved structural strength, thermal management, and high thermal conductivity. In addition, the copper offers bondability when nickel- or gold-plated and is capable of excellent solderability. Limitations in dimensioning and multilayering are its disadvantages.

22.2.3 Developmental PWBs

Advances in the state of the art of integrated circuitry are leading to systems applications requiring higher packaging densities and improved thermal and electrical performance. In many instances this has led to the requirement for multichip modules to be designed to meet system electrical throughput and volumetric requirements. This has placed increasing emphasis on the interconnection substrate design within the module. Ceramic materials with their high dielectric constant impart unacceptable losses in throughput due to propagation delay for high-speed applications. In addition, limitations in wiring density on the substrate due to the printing techniques used cause unacceptably thick substrates because of the need for more wiring layers. New combinations of standard materials and processes have been combined to address these requirements. These are mainly in the form of a thin-film dielectric on silicon or ceramic.

The dielectric used by most companies is polyimide. A thin-film polyimide layer is applied through screen printing or spinning onto a silicon or ceramic substrate. In some instances the silicon or ceramic may have wiring routed within. The polyimide is then metallized with aluminum or copper and patterned using standard thin-film photo-imaging techniques. Via interconnects from layer to layer are done in an additive "pillar" process. The polyimide dielectric layers provide a thin, low-dielectric-constant material (<4.0), and the thin-film metallization allows very-high-density routing (0.001- to 0.002-in lines and spaces).

A second interconnection technique involving a thin-film polyimide process involves the "growing" of a circuit on top of the die in a multichip module. This technique, called high-density interconnect (HDI), was developed by General Electric. Here, die are mounted into wells inside a multichip package (MCP) such that the top of the die forms a planar surface with the inside surface of the module. Polyimide dielectric and thin-film metal layers are then fabricated on top of the die to perform the interconnection.

Another developing technology for multichip module applications is the silicon circuit board (as shown in Figures. 22.5and 22.6). This board uses silicon as a base substrate. The difference in this board over similar silicon interconnection techniques is the use of silicon dioxide as the dielectric material instead of polyimide. The manufacturer reports that material costs less as a base material and requires fewer processing steps than polyimide. It offers a second advantage in that a thin silicon dioxide layer between power and ground planes in the substrate gives an integral decoupling capacitor between the planes not obtainable with other technologies.

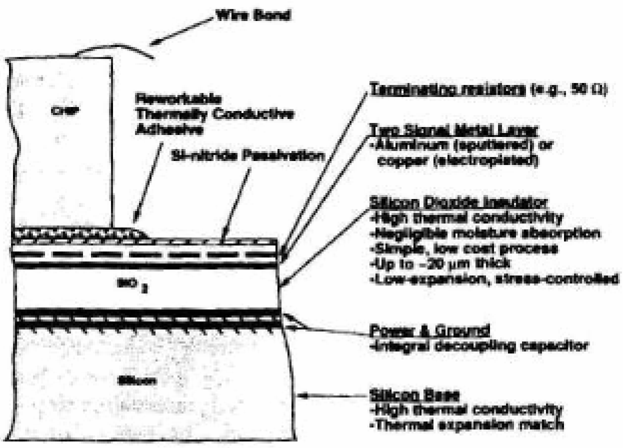

Figure 22.5 Cross-sectional view of silicon circuit board

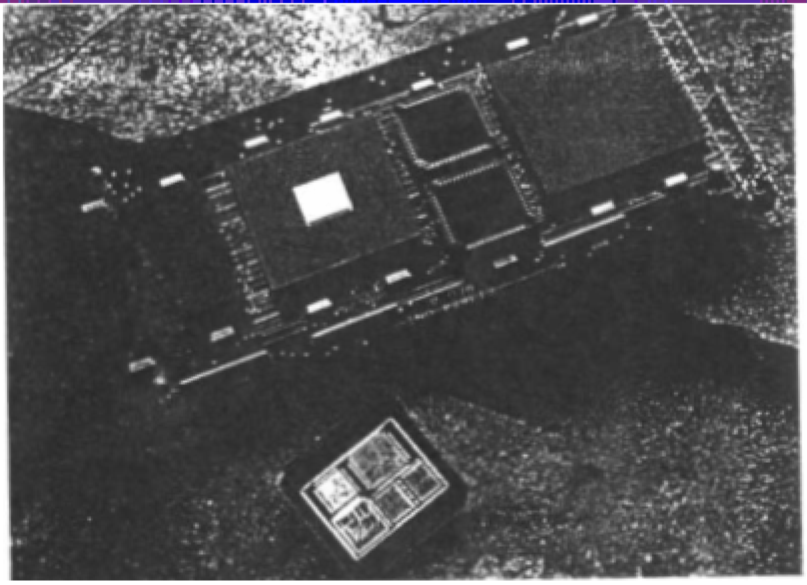

Figure 22.6.High-speed RISC/SPARC processor using multichip design with silicon circuit board

22.2.4 Discrete-Wired PWBs

Most discrete-wired boards use an organic rigid PWB as a base substrate, their primary difference being that the circuit is wired using discrete or individual wires. Several varieties of theses boards are in use today. Such as the multiwire board, the Microwire board, the stitch –welded board and the wire-wrap technique. Lets to discuss the multiwire board only into considered.

22.2.4.1 Multiwire

Multiwire technology was developed as an alternative PWB method to conventional multilayer PWBs. The invention of Multiwire addressed a variety of concerns of multilayer PWB designers and fabricators. The time and cost required to produce the artwork films (especially for existing designs, which need to be quickly modified), layer-to-layer registration requirements of a large number of layers, and the inability to inspect or repair inner layers in a finished product are reduced or eliminated using this technology.

Multiwire most commonly uses a rigid epoxy/e-glass laminate as a base, although any base material (polyimide, metal core, or flexible material) used in the printed-circuit industry can be used.

The design of the wiring is done on a computer-assisted design (CAD) system. The CAD system generates the necessary instructions to drive a numerically controlled wiring machine. Wiring can be done in an x-y orthogonal grid as well as at a 45° angle to intersect the component locations as shown in Figure. 22.7.

After all wires have been routed, they are pressed more deeply into the adhesive and then encapsulated with an epoxy cover and copper foil. The board at this stage resembles a conventional multilayer PWB prior to the drilling step.

A via pattern is drilled at the component locations using conventional drilling processes, which cut into the wiring. The holes are cleaned using high-pressure water and prepared for copper plating in a proprietary alkaline permanganate solution.

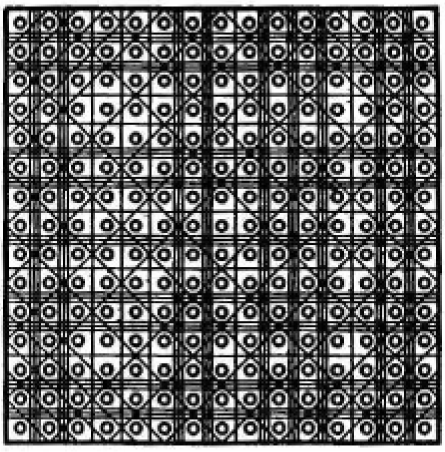

Figure 22.7 Multiwire typical wired circuit pattern using x-y and 45° geometry

This solution removes resin smear and microetches the hole wall to promote plating adhesion. In addition, it chemically removes some of the wire insulation at the point of wire entry into the drilled hole.

Hole plating to complete the interconnect is accomplished in a way similar to conventional PWB processing. The boards are catalyzed and plated using an appropriate electro-less copper bath. Application of a dry-film photoresist defines the surface features. Exposed holes and surface features are then electroplated with copper and then tin-lead plated. The photoresist is stripped and the tin-lead plate acts as the resist for etching the background copper and completing the termination process. Figure 22.8 describes the final structure of a Multiwire board.

It should be noted that the Multiwire board use is aimed toward through-hole component (such as DIP and PGA) designs and low-density SMT designs. To address ultra-high-density SMT designs another product, called Microwire.

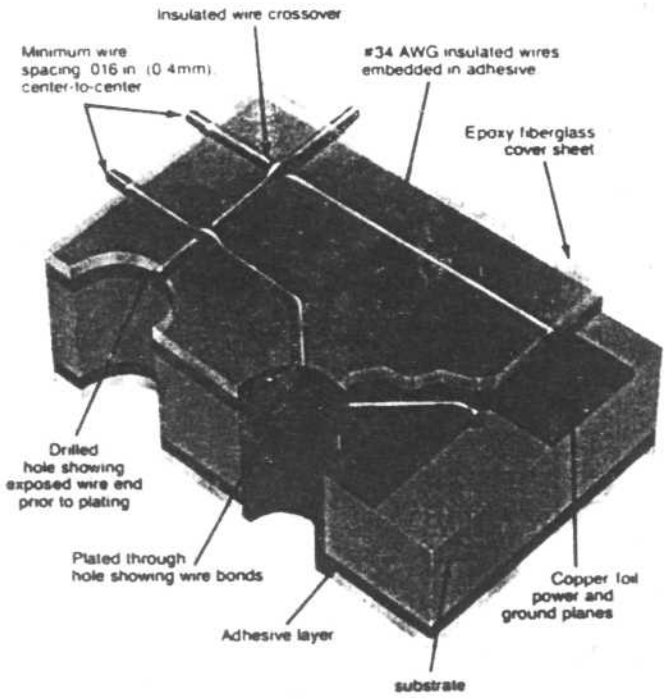

Figure 22.8 Cross-sectional view of typical multiwire board

22.3 Conformal Coatings for PWB Assemblies

Conformal coatings have been used for many years. Their main functions have been to protect circuit boards from dust, dirt, and moisture.

In the past due to the cost of the coating itself as well as the cost of applying the coating to the board, only the most expensive boards or those with especially demanding needs for reliability were coated (mainly military). With advances in application technology and process ability the economics of using conformal coatings have improved favorably.

Additionally as circuit size has diminished and components have become more delicate the need for a protective coating has become a necessity in many cases.
The different Conformal Coatings for PWB are described as follow.

22.3.1 Acrylic Coatings

Acrylics are excellent coating systems from a production standpoint because they are relatively easy to apply. Furthermore, application mistakes can be corrected readily, because the cured film can be removed by soaking the printed circuit assembly in a chlorinated solvent such as trichloroethane or methylene chloride. Spot removal of the coating from isolated areas to replace a component can also be accomplished easily by saturating a cloth with a chlorinated solvent and gently soaking the area until the cured film is dissolved.

Since most acrylic films are formed by solvent evaporation, their application is simple and is easily adaptable to manufacturing processes. Also, they reach optimum physical characteristics during cure in minutes instead of hours.

Acrylic films have desirable electrical and physical properties, and they are fungus-resistant. Further advantages include long pot life, which permits a wide choice of application procedures; low or no exotherm during cure, which avoids damage to heat-sensitive components; and no shrinkage during cure. The most obvious disadvantage of the acrylics is poor solvent resistance, especially to chlorinated solvents.

22.3.2 Polyurethane Coatings

Polyurethane coatings are available as either single- or two-component systems. They offer excellent humidity and chemical resistance and good dielectric properties for extended periods of time.

In some instances the chemical resistance property is a major drawback because rework becomes more costly and difficult. To repair or replace a component, a stripper compound must be used to remove effectively all traces of the film. Extreme caution must be exercised when the strippers are used, because any residue from the stripper may corrode metallic surfaces.

In addition to the rework problem, possible instability or reversion of the cured film to a liquid state under high humidity and temperature is another phenomenon which might be a consideration. However, polyurethane compounds are available to eliminate that problem.

Although polyurethane coatings systems can be soldered through, the end result usually involves a slightly brownish residue which could affect the aesthetics of the board. Care in surface preparation is most important, because a minute quantity of moisture on the substrate could produce severe blistering under humid conditions. Blisters, in turn, lead to electrical failures and make costly rework mandatory.

Single-component polyurethanes, although fairly easy to apply, require anywhere from 3 to 10 days at room temperature to reach optimum properties. Two-component polyurethanes, on the other hand, provide optimum cure at elevated temperatures within 1 to 3 h and usually have working pot lives of 30 min to 3 h.

22.3.3 Epoxy Coatings

Epoxy systems are available, as two-component compounds only, for coating electronic systems. Epoxy coatings provide good humidity resistance and high abrasive and chemical resistance. They are virtually impossible to remove chemically for rework, because any stripper that will attack the coating will also attack epoxy-coating or potted components and the epoxy-glass printed board as well. That means that the only effective way to repair a board or replace a component is to burn through the epoxy coating with a knife or soldering iron.

When epoxy is applied, a buffer material must be used around fragile components to prevent fracturing from shrinkage during the polymerization process. Curing of epoxy systems can be accomplished either in 1 to 3 h at elevated temperature or in 4 to 7 days at room temperature. Since epoxies are two-component materials, a short pot life creates an additional limitation in their use.

22.3.4 Silicone Coatings

Silicone coatings are especially useful for high-temperature service (approximately 200°C). The coatings provide high humidity and corrosion resistance along with good thermal endurance, which makes them highly desirable for PWAs that contain high heat-dissipating components such as power resistors.

Repairability, which is a prime prerequisite in conformal coating, is difficult with silicones. Because silicone resins are not soluble and do not vaporize with the heat of a soldering iron, mechanical removal is the only effective way to approach spot repair. That means the cured film must be cut away to remove or rework a component or assembly. In spite of some limitations, silicone coatings fill a real need because they are among the few coating systems capable of withstanding temperatures of 200 °C.

22.3.5 Polyimide Coatings

Polyimide coating compounds provide high-temperature resistance and also excellent humidity and chemical resistance over extended periods of time. Their superior humidity resistance and thermal range qualities are offset by the need for high-temperature cure (from 1 to 3 h at 200 to 250 °C). High cure temperatures limit the use of these coating systems on most printed circuit assemblies. Because the polyimides were designed for high-temperature and chemical resistance, chemical removal and burn-through soldering cannot be successful.

22.3.6 Silicon Nitride Coating

Silicon Nitride has been in use as a passivation coating on integrated circuits since the early 1970s. With the advent of chip on board (COB) packaging for use in both military and harsh consumer environments, this coating has begun to be looked at as a conformal coating for board level COB applications. A room temperature plasma deposition system has been developed by Ionic Systems that allows a low stress silicon nitride coating to be applied over components on a circuit assembly. The silicon nitride coating thickness is approximately 0.5 μm.

23. Packaging of Electronic Equipments (2)

23.1 Packaging and Interconnection Techniques

Introduction

Electronic packaging, which for many years was only an afterthought in the design and manufacture of electronic systems, increasingly is being recognized as the critical factor in both cost and performance.

Current electronic systems employ a packaging technology which limits system performance because of a number of factors. As the circuit density on a chip goes up, the speed of functions it performs increases, Retention of signal integrity is another consideration, the power needed to run the chips generates significant amounts of heat which must necessarily be removed an important requirement. The selection of packaging and interconnection techniques is a very complex task for the designer and manufacturing engineer where the selection depends on a number of driving forces: mechanical, electrical, and thermal force.

23.1.1 Mechanical requirements

The mechanical diving force strives to attain technology advancements to keep pace with the considerable improvements being made by the continued reduction (per function) in the integrated circuit package size.

23.1.2 Electrical requirements

The electrical driving force is bringing new technology to the fabricator of conventional PWBs, with expressions such as controlled impedance, dielectric constant, insulation resistance. Improvements in dimensional stability and registration accuracy and use of new (more expensive) materials are the result of attempting to satisfy these needs.

23.1.3 Thermal requirements

Thermal driving forces are threefold. In one case, it is giving credence to the use of materials and processes that can satisfy the higher assembly processing temperatures to which the PWBs must be subjected, that is, materials with a higher glass transition temperature (Tg). Another instance concerns coefficient of thermal expansion which has resulted in some applications using reinforced metal planes or constraining metal cores. In third instance, the printed board becomes an active element in the thermal management of the assemblies cooling systems.

The different advanced packaging and interconnection techniques as shown in the Figure 23.1.

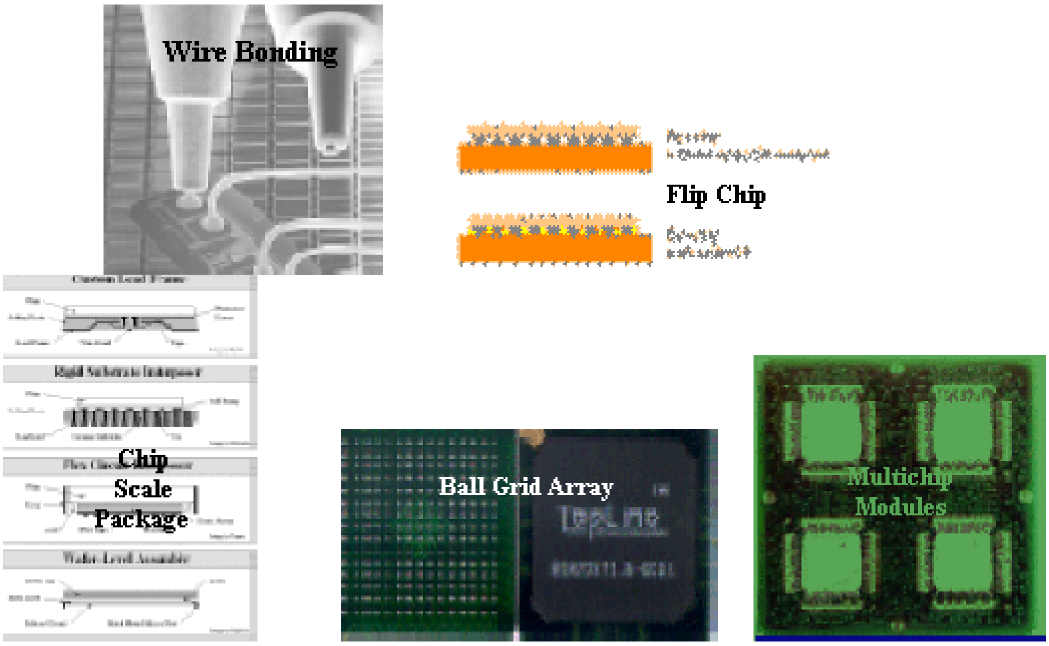

Figure23.1 Different packaging and interconnection techniques used in manufacturing

23.2 Electronics Packaging Levels

There are six generally recognized levels of electronic packaging. Figure 23.2 shows the general packaging levels. The six levels are:

- **Level 0:** Bare semiconductor (unpackaged).
- **Level 1:** Packaged semiconductor or packaged electronic functional device. There are two cases to be distinguished regarding packaged IC devices. The first case entails a single semiconductor microcircuit within a suitable package.. The second case entails several semiconductor microcircuits plus discrete chips on a suitable substrate. This entire package is generally referred to as a multichip module (MCM).
- **Level 2:** Printed wiring assembly (PWA).This level involves joining the packaged electronic devices to a suitable substrate material. The substrate is most often an organic material such as FR-4 epoxy-fiberglass board, or ceramic such as alumina. Level 2 is sometimes referred to as the circuit card assembly (CCA) or, more simply, the card assembly.
- **Level 3:** Electronic subassembly. This level refers to several printed wiring assemblies (PWAs), normally two, bonded to a suitable backing functioning both as a mechanical support frame and a thermal heat sink. Sometimes this backing, or support frame, is called a subchassis. In some packaging hierarchies, e.g., computer packaging, Level 3 is the electronic assembly, also called the electronic box. As shown in Figure23.3.
- **Level 4:** Electronic assembly. This level consists of a number of electronic subassemblies mounted in a suitable frame. An electronic assembly, then, is a mechanically and thermally complete system of electronic subassemblies. This level is sometimes referred to as the electronic box or simply box level.
- **Level 5:** System. This refers to the completed product.

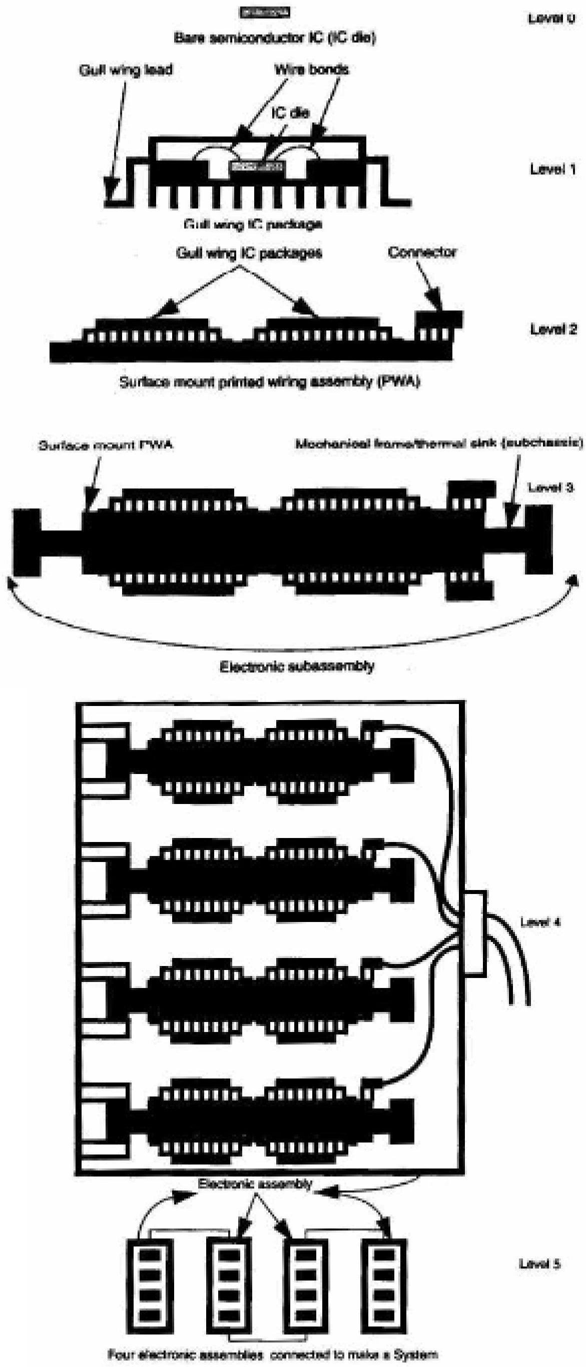

Figure 23.2 Packaging levels

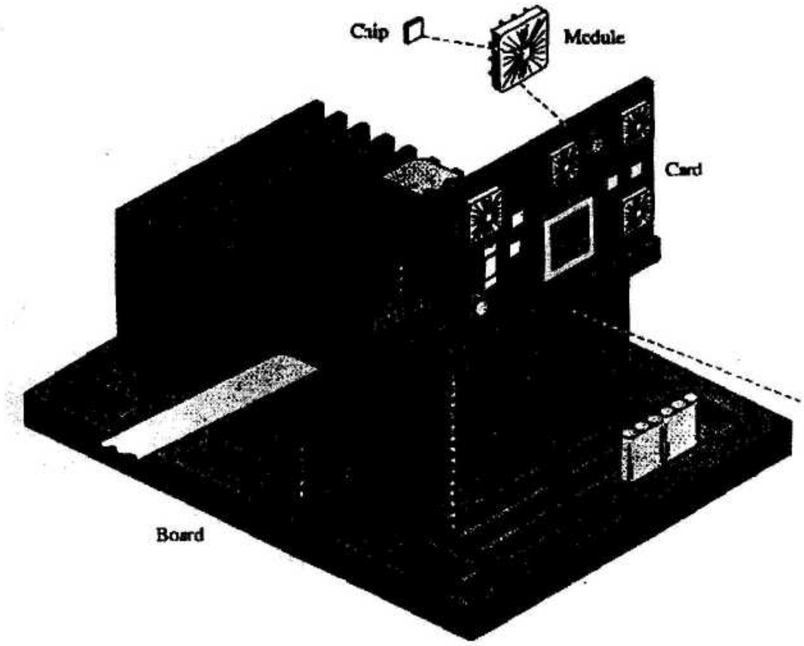

Figure23.3 Level 3 packaging

23.3 Wire Bonding Packaging

Wire bonding packaging also called chip-on-board packaging is the earliest technique of device assembly, whose first result was published by Bell Laboratories in 1957. Sine then, the technique has been extremely developed. Wire bonding, as the dominant chip-connection technology, has been used with all styles of microelectronic packages, from small individual chip packages to large, high-density multichip modules.
Virtually all dynamic random access memory (DRAM) chips and most commodity chips in plastic packages are assembled by wire bonding. About 1.2-1.4 trillion wire interconnections are produced annually.

In wire bonding (chip-and-wire) packaging, the IC chip is bonded directly on an interconnecting substrate either a printed wiring board or hybrid-and protected with a top encapsulant against moisture as shown in Figure23.4.

The encapsulants are materials such as silicone or epoxy which does provide very good moisture sealing in applications where high reliability is required.

Wire bonding is an electrical interconnection technique using thin wire and a combination of heat, pressure and/or ultrasonic energy. Wire bonding is a solid phase welding process, where the two metallic materials (wire and pad surface) are brought into intimate contact. Once the surfaces are in intimate contact, electron sharing or interdiffusion of atoms takes place.

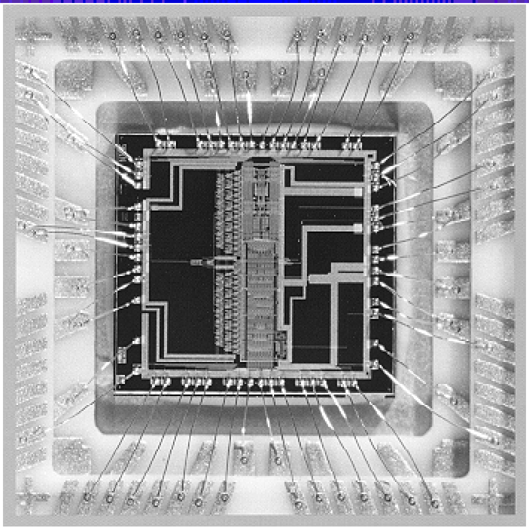

Figure 23.4 Chip interconnection using wire bonding technology

23.3.1 Wire Bonding Process

There are three types of wire bonding processes: thermocompression, ultrasonic, and thermosonic bonding.

Thermocompression wire bonding:

Thermocompression wire bonding is the most frequently used in wire bonding process .The principle is to join two metals using heat and pressure but without melting. The elevated temperature maintains the metals in annealing state as they join in molecular metallurgical bond (e.g. heating up to 300 ^{o}C for gold bonding). In order to avoid pre-damaging the material, the bonding force must be applied with a gradient, the process of bonding as shown in Figure 23.5.

Ultrasonic wire bonding:

Ultrasonic bonding is a different concept of bonding that uses pressure in addition to rapid scrubbing or wiping to achieve a molecular bond. The scrubbing action effectively removes any oxide films that may be present. Extreme care must be taken so that the chip is not damaged during the ultrasonic wire-bonding action. Since ultrasonic energy softens the bonding material and makes it easy to plastic deformation, ultrasonic bonding can create bonds between wide varieties of materials.

Thermosonic wire bonding:

Ultrasonic energy is used with thermocompression wire bonding methods, resulting in a technique known as Thermosonic wire bonding**.** The process depends on vibrations created by ultrasonic action to scrub the bond area to remove any oxide layers and create the heat necessary for wire bonding.

The main benefit of the method compared to thermocompression is lower bonding temperature and shorter processing time.

The comparison between the three bonding processes as shown in Table 23.1.

Table 23.1 Three wire bonding processes

Wire bonding	Pressure	Temperature	Ultrasonic energy
Thermocompression	High	300-500 ^oC	No
Ultrasonic	Low	25 ^oC	Yes
Thermosonic	Low	100-150 ^oC	Yes

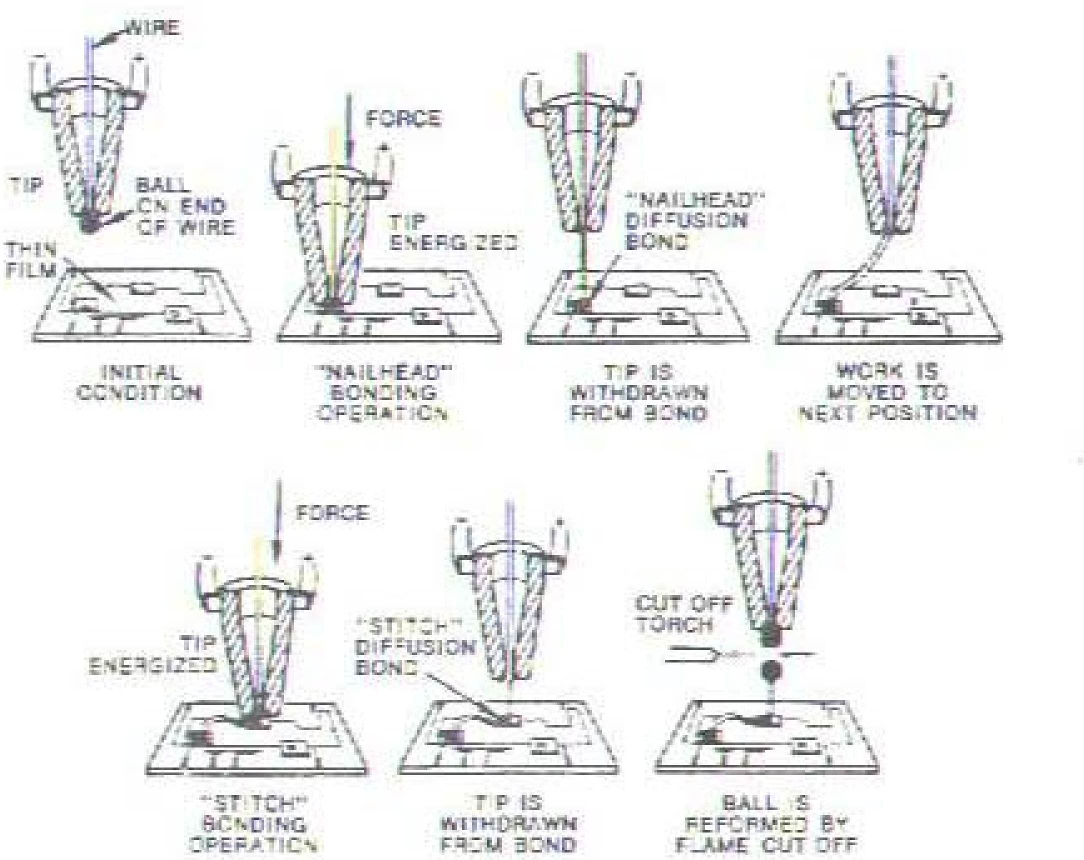

Figure 23.5 Wire bonding steps with thermocompression bonding

23.3.2 Wire Bonding Techniques

The basic method actually includes two different bonding techniques: wedge, and ball bonding.

Approximately 93% of all semiconductor packages are manufactured using ball bonding method, while wedge bonding is used to produce about 5% of all assembled packages.

23.3.2.1 Ball Bonding

In this technique, wire is passed through a hollow capillary, and an electronic-flame-off system (EFO) is used to melt a small portion of the wire extending beneath the capillary. The surface tension of the molten metal forms a spherical shape or ball. The ball is pressed to the bonding pad on the die with sufficient force to cause plastic deformation and atomic interdiffusion of the wire and the underlying metallization, which ensure the intimate contact between the two metal surfaces and form the first bond (ball bond). The capillary is then raised and repositioned over the second bond site on the substrate as shown in Figure 23.6; a precisely shaped wire connection called a wire loop is thus created as the wire goes. Deforming the wire against the bonding pad makes the second bond (wedge bond or stitch bond), having a crescent shape (as shown in Figure23.7) made by the imprint of the capillary's outer geometry. Then the wire clamp is closed, and the capillary ascends once again, breaking the wire just above the wedge, an exact wire length is left for EFO to form a new ball to begin bonding the next wire. This technique requires a high temperature raging from 100^{o}C to 500^{o}C depending on bonding process. Heat is generated during the manufacturing process either by a heated capillary feeding the wire or by a heated pedestal on which the assembly is placed or by both depending on the bonding purpose and materials.

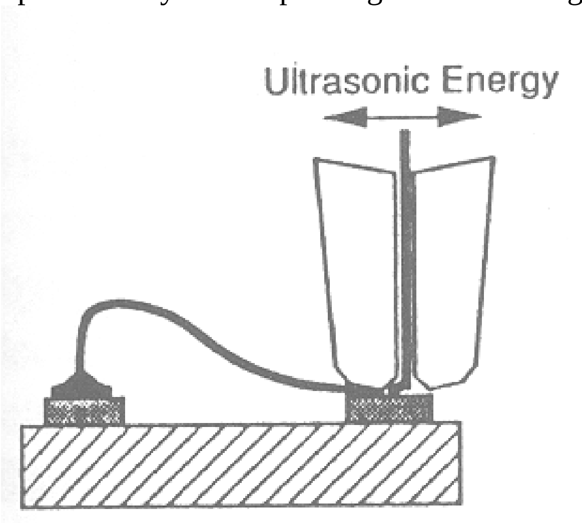

Figure 23.6 Ball bonding technique

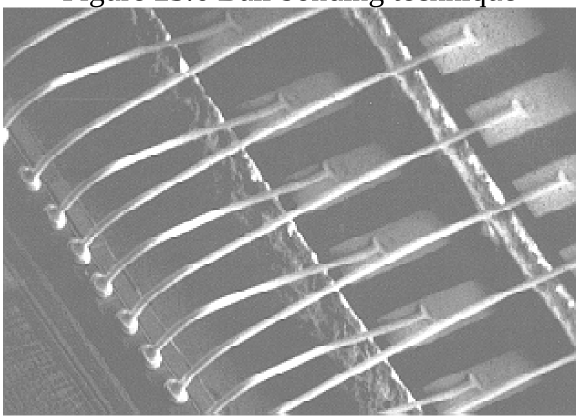

Figure 23.7 Application of ball bonding

23.3.2.2 Wedge Bonding

Wedge bonding is named based on the shape of its bonding tool. In this technique, the wire is fed at an angle usually 30-60^{o} from the horizontal bonding surface through a hole in the back of a bonding wedge. By descending the wedge onto the IC bond pad, the wire is pinned against the pad surface and an Ultrasonic or thermosonic is performed. Next, the wedge rises and executes a motion to create a desired loop shape. At the second bond location, the wedge descends, making a second bond.

Wedge bonding technique can be used for both aluminum wire and gold wire bonding applications. The principle difference between the two processes is that the aluminum wire is bonded in an ultrasonic bonding process at room temperature as shown in Figure 23.8, whereas gold wire wedge bonding is performed through a thermosonic bonding process with heating up to 150 ^{o}C. A considerable advantage of the wedge bonding is that it can be designed and manufactured to very small dimensions. Aluminum ultrasonic bonding is the most common wedge bonding process because of the low cost and the low working temperature. The main advantage for gold wire wedge bonding is the possibility to avoid the need of hermetic packaging after bonding due to the inert properties of the gold. In addition, a wedge bond will give a smaller footprint than a ball bond as shown in Figure 23.9, which specially benefits the microwave devices with small pads that require a gold wire junction.

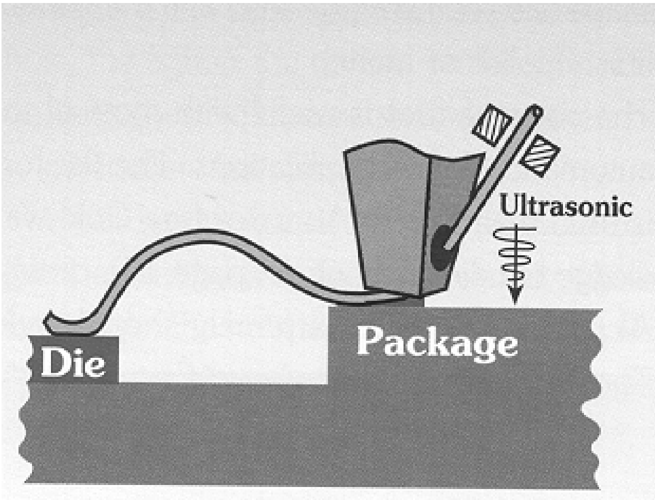

Figure 23.8 Ultrasonic wedge bonding

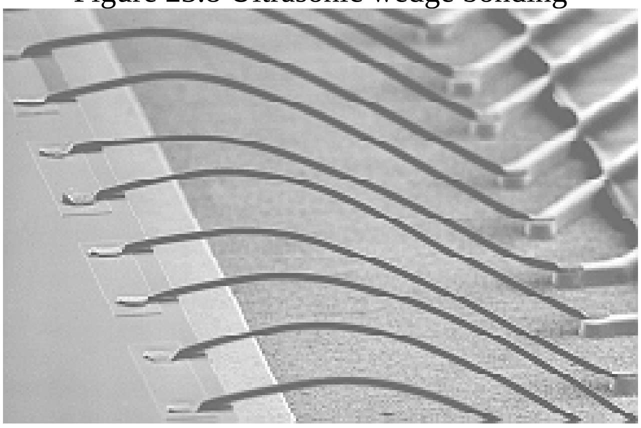

Figure 23.9 Application of wedge bonding

23.3.3 Cost

The main cost of wire bonding method includes:

- Wire bonder
- Die attach equipment.
- Support equipment
- Materials including tool, wire, die attach materials.
- Engineering.

Cost analysis should include volume and individual process cycle time predictions.

23.4 Flip-Chip Packaging

In the development of packaging of electronics the aim is to lower cost, increase the packaging density, and improve the performance while still maintaining or even improving the reliability of the circuits. The concept of flip-chip process where the semiconductor chip is assembled directly face down onto circuit board.

Flip-chip joining is not a new technology. The technology has been driven by IBM for mainframe computer applications. Many millions of flip-chips have been processed by IBM on ceramic substrates since the end of 60`s. At the beginning of 70`s the automotive industry also began to use flip-chips on ceramics. Today flip-chips are widely used for watches, mobile phones, portable communicators, disk drives, hearing aids, LCD displays, automotive engine controllers as well as the main frame computers. The number of flip-chips assembled was over 500 million in year 1995 and close to 600 million flip chips were consumed 1997.

23.4.1 Flip-Chip Process by Solder Joining

The flip-chip concept process employed small, solder-coated copper balls (electrically conducting bumps) sandwiched between the chip and the substrate, and may the flip-chip joints without or with underfill material are shown in Figure23.10.

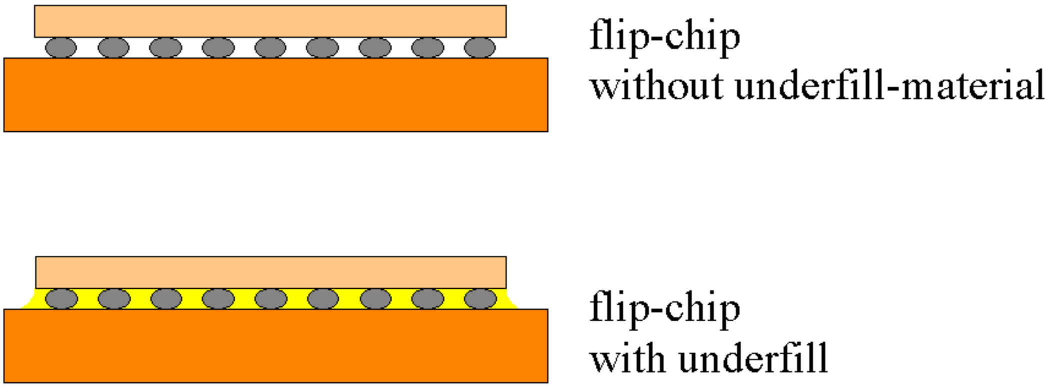

Figure 23.10.Cross sections of flip-chip joints without and with underfill material.

Tacky flux is applied to the solder contact areas by dipping the chip into a flux reservoir or by dispensing flux onto the substrate. The bumps of chips are placed into the tacky paste and they are reflowed in an oven to drive off any flux residues. After the reflow process cleaning of the flux is preferred. If the solder reflow has been accomplished correctly the flip-chip solder joints will be smooth, and shiny. The underfill material is applied by dispensing along one or two sides of the chip, from where the low viscosity epoxy is drawn by capillary forces into the space between the chip and substrate as shown in Figure23.11. Finally the underfill is cured by heat. Repairing of the flip-chip joint is usually impossible after the underfill process. Therefore testing must be done after reflow and before the underfill application.

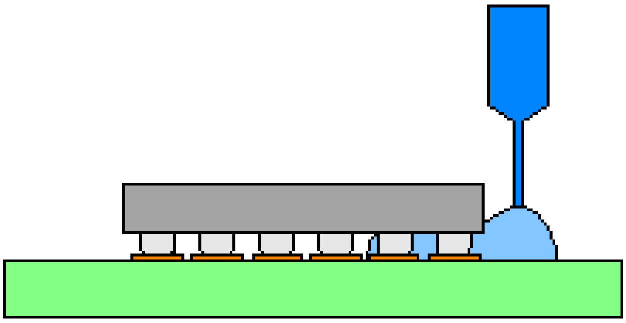

Figure 23.11.the underfill application by dispensing.

23.4.2 Flip-Chip Joining

The flip-chip joining mainly by thermocompression or thermosonic processes as shown in Figure 23.12. In the thermocompression bonding process, the bumps of the chip are bonded to the pads on the substrate by force and heat applied from an end effector. The bonding temperature is usually high, e.g. 300 ^{o}C for gold bonding, to soften the material and increase the diffusion bonding process. The bonding force can be up to 1 N for an 80µm diameter bump. Due to the required high bonding force and temperature, the process is limited to rigid substrates such as alumina or silicon. A bonder with high accuracy in the parallelism alignment is required. In order to avoid pre-damaging of the semiconductor material, the bonding force must be applied with a gradient.

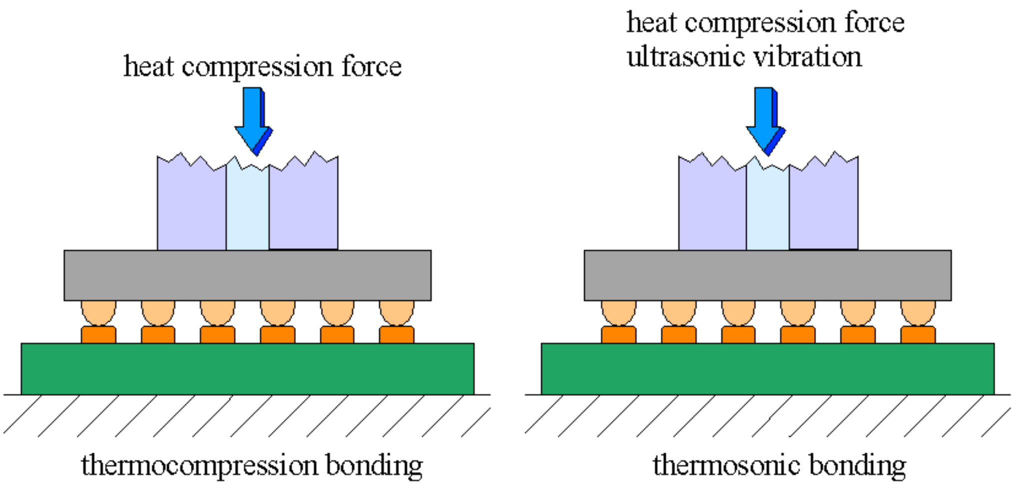

Figure 23.12 Principles of flip-chip joining by thermocompression and thermosonic processes

The thermocompression bonding process can be made more efficient by using ultrasonic power to speed up the welding process. Ultrasonic energy is transferred to the bonding area from the pick-up tool through the back surface of the chip. The thermosonic bonding introduces ultrasonic energy that softens the bonding material and makes it easy to plastic deformation.

23.4.3 General Advantages and Disadvantages using Flip-Chip Technology

Advantages:

- Improved thermal capabilities: Because flip-chips are not encapsulated, the back side of the chip can be used for efficient cooling.
- The chip is capable of handling a high number of I /Os because solder bumps can be arranged in an area array rather than being restricted to the chip's periphery.
- Due to surface tension factors related to the solder, this technique has a self-aligning during bonding.
- Improved performance due to short interconnect distance: delivers low inductance, resistance and capacitance, and small electrical delays.

Disadvantages:

- Difficult testing the joints. For inspection of hidden joints X-ray equipment is needed.
- Flux removal is difficult.
- High assembly accuracy needed.
- Low reliability for some substrates.
- Repairing is difficult or impossible.

23.4.4 Relative Cost Comparison

Cost of flip-chip process is less than half of the corresponding cost for wire bonding technology and the floor space needed is also only about one half of that for wire bonding technology.

The cost of flip-chip technology can be divided into bumping cost and assembly process cost. The assembly processes for the most common flip-chip technology include pick and place together with flux application, reflow and cleaning as well as underfill process. The cost of the necessary equipment and floor space, the capacity of the equipment and its compatibility with other manufacturing processes are also important factors having influence on the economy of the technology for particular product. The substrate has also an important impact on the packaging costs. The cost of substrate depends e.g. on via sizes, layer count, line width and spaces, die pad pitch, flatness requirements, material type and the fabrication process.

23.5 Chip Scale Packaging

Chip Scale Packaging combines the best of flip chip assembly and surface mount technology. The Chip Scale Packaging Task Force carried out between 1996 and 1997 and a project work carried out by two students at Chalmers University of Technology.

23.5.1 Description of Various Types of CSPs

CSPs are often classified based on their structure. At least four major categories have been proposed. These are: Flex circuit interposer, rigid substrate interposer, custom lead frame, and wafer-level assembly. Examples of packages of these categories are given in Figure 23.13.

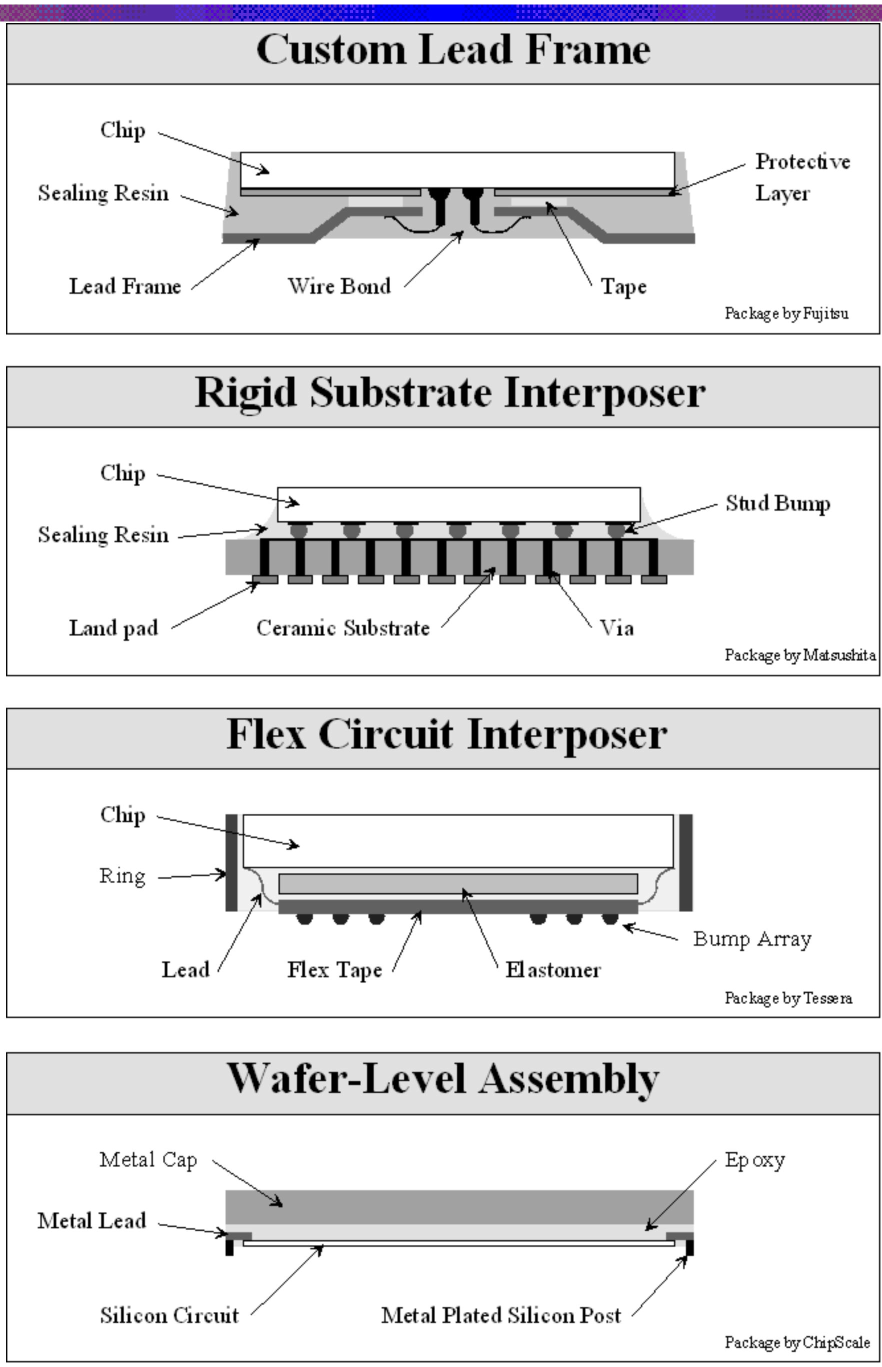

Figure23.13 Main CSP categories

The main driving forces for using CSPs are:

- Improvement in performance
- Size and weight reduction
- Easier assembly process

Of these, reduction of size and weight are probably the most important factors for selection of CSP technology. Consequently, consumer products like camcorders, mobile phones, and laptops gare among the products that have been first to utilise CSPs.

23.5.2 Production Issues

23.5.2.1 Assembly Issues

Most CSPs can be mounted using current fine pitch SMT assembly materials and processes. Vision systems may have problem recognising the structure of some CSPs. In addition, some packages are moisture sensitive. That is, they must be stored in dry conditions and used within a specified time frame after they have been exposed to humid environments. If the time frame is surpassed, or if a package needs to be reworked, it should be baked before any work is performed.

23.5.2.2 Tools and Investments

As pitches for CSP may get smaller conventional pick & placement machines may not suffer for mounting of the components which then will necessitate investments in new advanced machines. Also, X-ray equipment may be necessary for inspection for verification of solder joints. In cases when underfills must be used of reliability reasons, material and equipment for the underfilling process will add to the total cost.

23.5.3 Price

Only a few CSPs are in production today and then in low volume production. Therefore, it is difficult to get information of what the price will be for various CSPs. Furthermore, the large variations in construction of the various package types will also affect the production costs for the various packages. Many company forecast that the cost initially will be 10 to 50 % higher than conventional packages and that cost equality will be reached when they are produced in high volumes.

23.6Ball Grid Array Packaging

The information presented in this technique has been collected from a number of sources describing BGA activities, the most important of the former being the Swedish National Research Programme "BGA Modules for Automotive Electronics in Harsh Environments", and carried out between 1994 and 1997.

The Quad Flat Pack (QFP) and the Ball Grid Array (BGA) packages today both offer a large number of I/Os, as required by modern IC technology. The peripheral QFP technology is fragile leads around the periphery-all four sides. The BGA taking advantage of the area under the package for the solder sphere interconnections in an array to increase both the numbers of I/Os and pitch.

Figure 23.14 below illustrates the difference between QFP and BGA packages, showing an ultra fine-pitch 160 lead QFP (pitch 0.3 mm) on a background consisting of the bottom side of a 1.5 mm pitch PBGA with 225 interconnection solder balls. From this picture it is easy to understand the popularity this BGA package has received among the people in the assembly business. Note that there are five QFP leads for every BGA solder sphere period.

Figure 23.14 A 160-lead 0.3 mm pitch QFP placed on a grid of 1.5 mm pitch spheres (bottom side of a PBGAS225)

A BGA package can typically be characterized by the following general statements:

- It is an IC package for active devices intended for surface mount applications.
- It is an area array package, i.e. utilizing whole or part of the device footprint for interconnections.
- The interconnections are made of balls (spheres) of most often a solder alloy or sometimes other metals. The length of the package body (most often square) ranges from 7 to 50 mm.
- The pitch, i.e. center-to-center distance, of the balls is generally between 1.0 and 1.5 mm.

23.6.1 Types of BGA Packages

The PBGA is one of the most types in BGA and another types of BGA packages such as the TBGA (Tape BGA), presented. Also outside the scope of this text is the multichip moudule - or MCM-BGAs, which are similar in construction to ordinary BGAs, but contain two or more chips inside the package.

23.6.1.1 PBGA (Plastic Ball Grid Array)

In plastic ball grid array (PBGA), a die is mounted to the top side of substrate, double-sided PWB as shown in Figure 23.15.

The silicon chip containing the integrated circuit is die bonded to the top surface of the substrate.

The over-molded or glop-top encapsulation is then preformed to completely cover the chip, wires and substrate bond pads. Interconnection of signal and power lines between the die and the PW-board contact points is through thermosonic gold wire bonding. From there, copper traces are routed to an array of metal pads on the bottom of the printed wiring board. . Most often a two sided substrate metallization is sufficient to provide electrical contacts from wire-bonds through plated through-holes are usually around the periphery of the board to solder ball pads. The substrate is generally is made of 0.25 mm thick BT (bismaleimide-triazine) epoxy glass laminate with 18 µm copper thickness. In addition, thermal balls under the center of the package are often used to remove heat from the device through thermal vias.

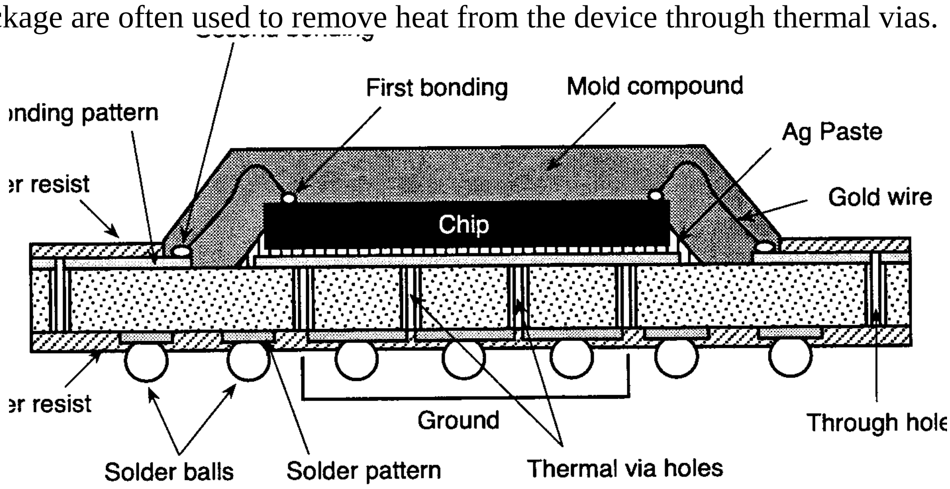

Figure 23.15.Across-section of a typical PBGA

23.6.1.1 TBGA (Tape or Tab Ball Grid Array)

Another interesting, but not yet so common type of BGA package, is the Tape or Tab BGA gets their name from the tape (a flexible polyimide conductor film with copper metallization) automated bonding (Tab) type frame that connects the chip with the next level board (Card).

Solder attachment balls of high temperature 10Sn90Pb alloy are used with diameter is usually 0.63 mm for a package pitch of 1.27 mm. The back of the chip can be put in direct contact with a thermally conductive adhesive to provide efficient transport of heat to the metal cover or heat sink to easily dissipate 10 to 15 W, as shown in Figure 23.16.

Current TBGA packages ranges from 21 to 40mm body size with 192 to 736 I/O connections.

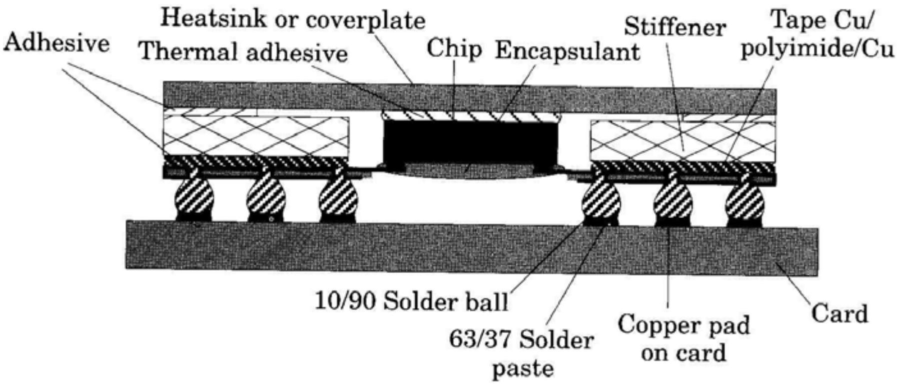

Figure 23.16 Cross-section of a Tape (or TAB) BGA – TBGA

23.5.2 Advantages and Disadvantages using BGAs

Advantages:

- BGAs are less fragile and easier to handle both before and during assembly.
- A much higher assembly yield is generally expected using BGAs.
- The smaller package size with higher I/O devices.
- Reduced manufacturing cycle time.
- The package can be hermetically sealed.

Disadvantages:

- Cost is high.
- Inspection of the solder joints is impossible without costly x-ray equipment.
- Board level rework potentially more difficult.

24. Conduction Cooling for Chassis and Circuit Boards

24.1 Introduction

Conduction cooling is important method used in many practical electronic systems such as spacecraft system as shown in Figure 24.1.

The heat is generated in active components whenever the electronic system is in operation. As the heat is generated, the temperature of the component increases and heat attempts to flow through any path it can find. If the heat source is constant, the temperature within the component continues to rise until the rate of the heat being generated is equal to the rate of the heat flowing away from the component. Steady state heat transfer then exists the heat flowing into the component is equal to the heat flowing away from the component.

Heat always flows from high temperature areas to low temperature areas. When the electronic system is operating, the electronic components are its hottest parts.

To control the hot spot component temperatures, the heat flow path must be controlled. If this is not done properly, the component temperatures are forced to rise in an attempt to balance the heat flow. Eventually, the temperatures may become so high that the component is destroyed if a protective circuit or a thermal cutoff switch is not used.

Conduction heat transfer in an electronic system is generally a slow process. Heat flow will not occur until a temperature difference has been established. This means that each member along the heat flow path must experience a temperature rise before the heat will flow to the next point along the path. This process continues until the final heat sink is reached, which is often the outside ambient air. This process may take many hours, perhaps even many days for a very large system, depending upon its size.

The materials along the heat flow path sharply influence the temperature gradients developed along the path. Heat can be conducted through any material: solid, liquid, or gas. The ability of the heat to flow through any material is determined by the physical properties of the material and by the geometry of the structure. The basic heat flow relation for steady state conduction from a single concentrated heat load is shown below in Equation.24.1.

$$Q = \mathrm{k}A\frac{\Delta \mathrm{t}}{\mathrm{L}} \tag{24.1}$$

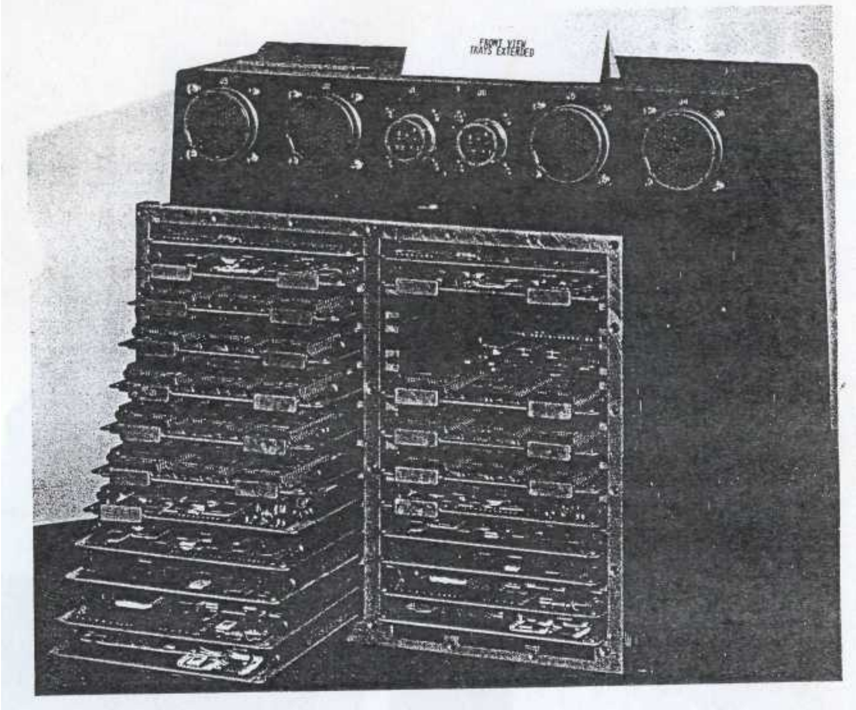

Figure 24.1 Conduction-cooled electronic box designed to carry the heat down the vertical walls to a base plate, for mounting in a spacecraft

24.2 Uniformly Distributed Heat Sources, Steady State Conduction

Identical electronic components are often placed next to one another, on circuit boards, as shown in Figure 24.2. When each component dissipates approximately the same amount of power, the result will be a uniformly distributed heat load.

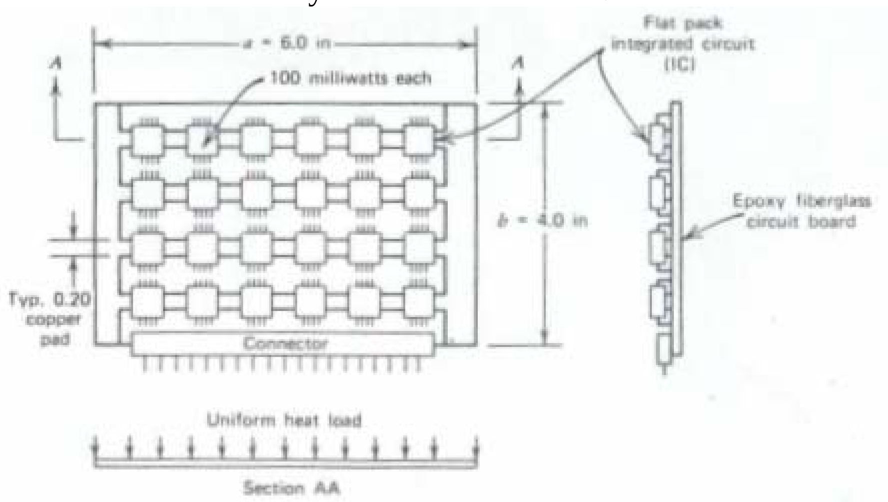

Figure 24.2 Printed circuit board with flat pack integrated circuits

When any one strip of electronic components is considered, as shown in section AA, the heat input can be evaluated as a uniformly distributed heat load. On a typical printed circuit board (PCB), the heat will flow from the component to the heat sink strip under the component, and then to the outer edges of the PCB, where it is removed. The heat sink strip is usually made of copper or aluminum, which have high thermal conductivity. The maximum temperature will occur at the center of the PCB and the minimum temperature will occur at the edges. This produces a parabolic temperature distribution, as shown in Figure 24.3.

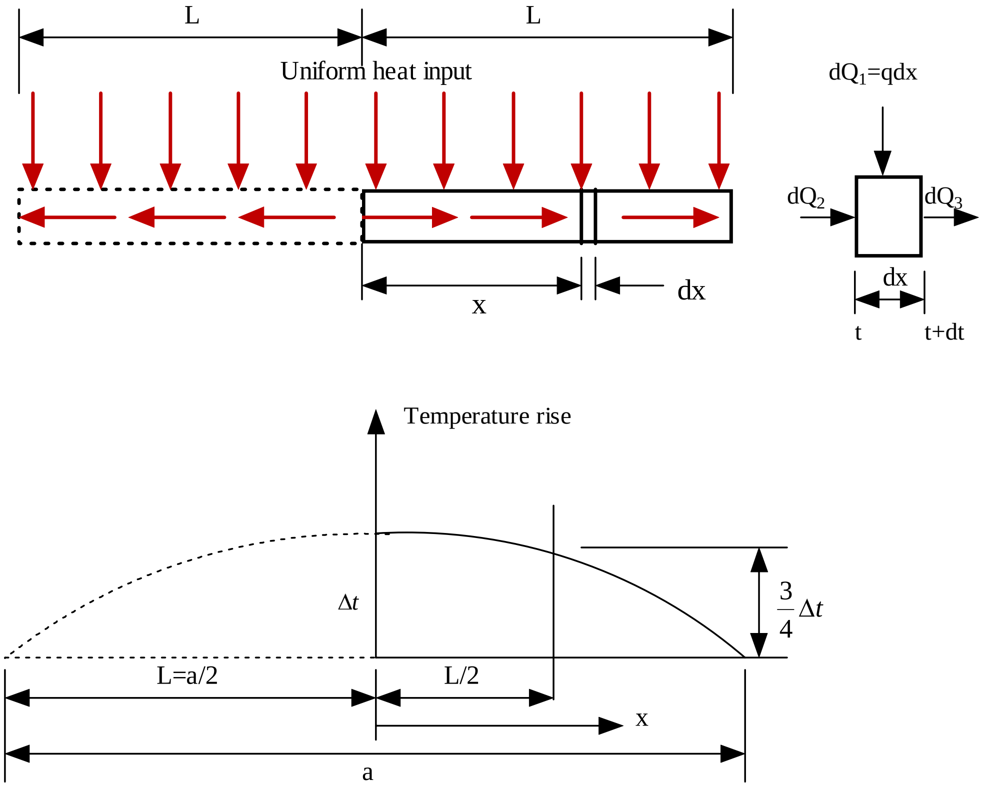

Figure 24.3 Parabolic temperature distributions for uniform heat load on a circuit board

When only one side of one strip is considered, a heat balance equation can be obtained by considering a small element dx of the strip, along the span with a length of L. Then

$$dQ_1 + dQ_2 = dQ_3$$

Where:

$$dQ_1 = \text{qdx} = \text{heat input}$$

$$dQ_2 = -\,kA\frac{dt}{dx} = \text{heat flow}$$

$$dQ_3 = -\,kA\frac{d(t+dt)}{dx} = \text{total heat}$$

Then

$$qdx - kA\frac{dt}{dx} = -kA\frac{dt}{dx} - kA\frac{d}{dx}(dt)$$

Then

$$\frac{d^2t}{dx^2} = -\frac{q}{kA}$$

This is a second-order differential equation, which can be solved by double integration. Integrating once yields to

$$\frac{dt}{dx} = -\frac{qx}{kA} + C_1$$

The second integrating yields to

$$t = -\frac{qx^2}{2kA} + C_1 x + C_2$$

The constant C_1 is zero because at x = 0, the plate is adiabatic, and no heat is lost. The slope of the temperature gradient is therefore zero.

The constant C_2 is determined by letting the temperature at the end of the plate be t_e;
Then

$$\frac{qL^2}{2kA} + t_e = C_2$$

The temperature at any point along the plate (or strip) is

$$\begin{aligned} t &= -\frac{qx^2}{2kA} + \frac{qL^2}{2kA} + t_e \\ &= \frac{q}{2kA}(L^2 - x^2) + t_e \end{aligned} \qquad (24.2)$$

This equation produces the parabolic shape for the temperature distribution; which is shown in Figure 24.3.

When x = 0. This results in the equation for the maximum temperature rise in a strip with a uniformly distributed heat load.

$$\Delta t = \frac{qL^2}{2kA}$$

The total heat input along the length L is

$$Q = qL$$

Then

$$\Delta t = \frac{QL}{2kA} \qquad (24.3)$$

When the temperature rise at the midpoint along the heat sink strip of length L is desired, then x = L/2 Substituting this value into Equation.24.2.Will result in the temperature rise at the midpoint of the strip.

$$\text{midpoint}\ \Delta t = \frac{3qL^2}{8kA}$$

Considering only the strip with a length of L, the ratio of the strip midpoint temperature rise to the maximum temperature rise is shown in the following relation:

$$\frac{\text{midpoint}\,\Delta t}{\text{maximum}\,\Delta t} = \frac{3qL^2}{8kA} / \frac{qL^2}{2kA} = \frac{3}{4}$$

Example 24.1: A series of flat pack integrated circuits are to be mounted on a multilayer printed circuit board (PCB) as shown in Figure 24.2. Each flat pack dissipates 100 milliwatts of power. Heat from the, components is to be removed by conduction through the printed circuit copper pads, which have 2 ounces of copper [thickness is 0.0028 in (0.0071 cm)]. The heat must be conducted to the edges of the PCB, where it flows into a heat sink. Determine the temperature rise from the center of the PCB to the edge to see if the design will be satisfactory.

Note that the typical maximum allowable case temperature is about 212 °F.

Solution:
The flat packs generate a uniformly distributed heat load, which results in the parabolic temperature distribution shown in Figure 24.4. Because of symmetry, only one half of the system is evaluated. Equation 24.3 is used to determine the temperature rise from the center of the PCB to the edge for one strip of components.

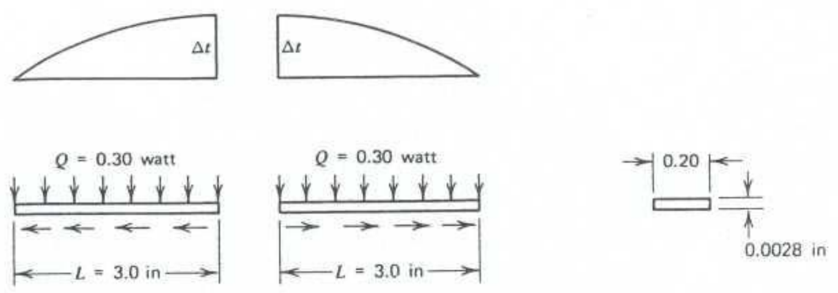

Figure 24.4 Uniformly distributed heat load on one copper strip

Q= 3(0.1) =0.3 Watt heat input, one half strip
L= 3 in = 7.62 cm (length)
k= 345 W/m.K
A= (0.2) (0.0028) =0.00056 in^2 =0.00361 cm^2 (cross-sectional area)

Substitute into Equation 24.3 to obtain the temperature rise from the center of the PCB to the edge.

$$\Delta t = \frac{(0.3)(0.0762)10000}{2(345)(0.00361)} = 91.7\ ^{O}C = 197\ °F$$

The amount of heat that can be removed by radiation or convection for this type of system is very small. The temperature rise is therefore too high. By the time the sink temperature is added, assuming that it is 80°F, the case temperature on the component will be 277 °F. Since the typical maximum allowable case temperature is about 212 °F, the design is not acceptable.

If the copper thickness is doubled to 4 ounces, which has a thickness of 0.0056 in (0.014 cm), the temperature rise will be 114.5 °F (45.85 °C) then the case temperature on the component will be about 195 °F so that the system can be operated safely.
For high-temperature applications, the copper thickness will have to be increased to about 0.0112 in (0.0284 cm) for a good design.

24.3 Chassis with Nonuniform Wall Sections

Electronic chassis always seem to require cutouts, notches, and clearance holes for assembly access, wire harnesses, or maintenance. These openings will generally cut through a bulkhead or other structural member, which is required to carry heat away from some critical high-power electronic component. The cutouts result in nonuniform wall sections, which must be analyzed to determine their heat flow capability.

One convenient method for analyzing nonuniform wall sections is to subdivide them into smaller units that have relatively uniform sections. The heat flow path through each of the smaller, relatively uniform sections can then be defined in terms of a thermal resistance. This will result in a thermal analog resistor network, or mathematical model, which describes the thermal characteristics of that structural section of the electronic system.

The basic conduction heat flow relation shown by Equation. 24.1 can be modified slightly to utilize the thermal resistance concept. The thermal resistance for conduction heat flow is then defined by Equation. 24.4.

$$R = \frac{L}{kA} \tag{24.4}$$

Substituting this value into Equation 24.1 results in the temperature rise relation when the thermal resistance concept is used as shown in Equation 24.5

$$Q = \frac{\Delta t}{R} \tag{24.5}$$

The thermal resistance concept is very convenient for developing mathematical models of simple or complex electronic boxes. Analog resistor networks can be established for heat flow in one, two, and three dimensions with little effort. Complex shapes can often be modeled with many simple thermal resistors to provide an effective means for determining the temperature profile for almost any type of system.

Two basic resistance patterns, series and parallel, are used to generate analog resistor networks. A simple series pattern network is shown in Figure 24.5.

The total effective resistance (R_t) for the series flow network is determined by adding all the individual resistances, as shown in Equation. 24.6.

Figure 24.5 Series flow resistor network.

$$R_t = R_1 + R_2 + R_3 \quad \ldots\ldots\ldots\ldots\ldots\ldots \tag{24.6}$$

A simple parallel flow resistor network is shown in Figure 24.6.

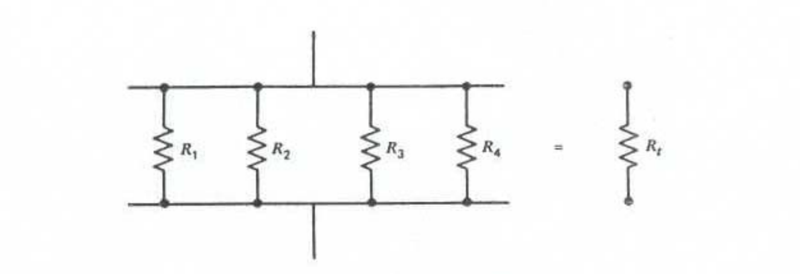

Figure 24.6 Parallel flow resistor network.

The total effective resistance for the parallel flow network is determined by combining the individual resistances as shown in Equation. 24.7.

$$\frac{1}{R_t} = \frac{1}{R_1} + \frac{1}{R_2} + \frac{1}{R_3} + \ldots\ldots\ldots \tag{24.7}$$

A typical electronic system will normally consist of many different combinations of series and parallel flow resistor networks.

Example 24.2: An aluminum (5052) plate is used to support a row of six power resistors. Each resistor dissipates 1.5 watts, for a total power dissipation of 9 watts. The bulkhead conducts the heat to the opposite wall of the chassis, which is cooled by a multiple fin heat exchanger. The bulkhead has two cutouts for connectors to pass through, as shown in Figure 24.7. Determine the temperature rise across the length of the bulkhead.

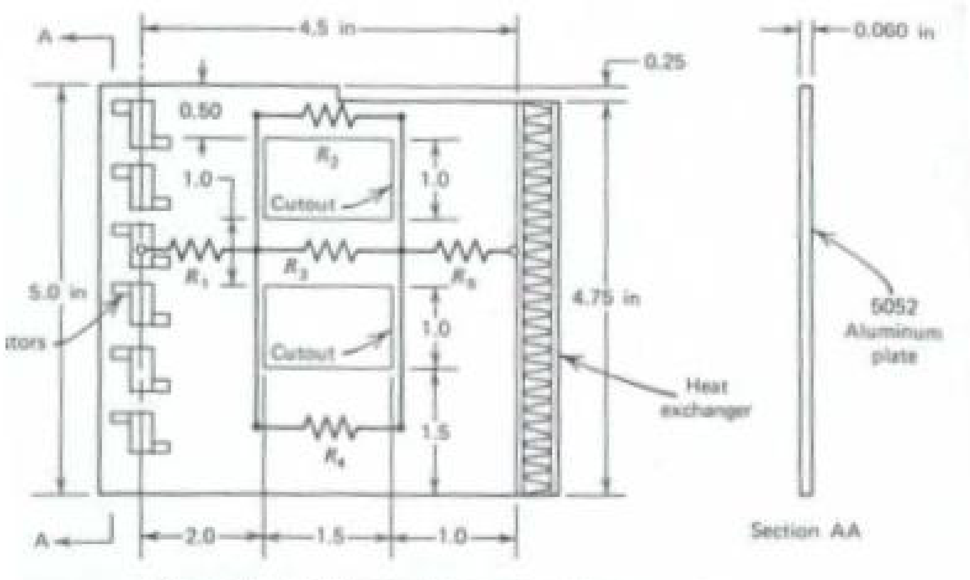

Figure 24.7 Bulkheads with two cutouts for connectors

Solution:
A mathematical model with series and parallel thermal resistor networks can be established to represent the heat flow path, as shown in Figure 24.8a.

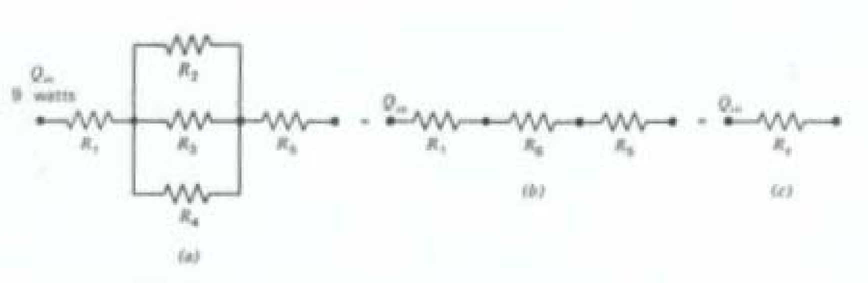

Figure 24.8 Bulkhead thermal models using a series and a parallel resistor network.

Firstly must determine the values of each resistor.
Determine resistor R_1:
L_1= 2 in = 5.08 cm
k_1= 158 W/m.K
A_1= (5) (0.06) = 0.3 in^2 = 1.935 cm^2

$$R_1 = \frac{(0.0508)10000}{(1.935)(158)} = 1.6616\ ^{o}C/W$$

Determine resistor R_2:
L_2= 1.5 in = 3.81 cm
K_2= 158 W/m.K
A_2= (0.375) (0.06) = 0.0225 in^2 = 0.145 cm^2 (average area)

$$R_2 = \frac{(0.0381)10000}{(0.145)(158)} = 16.63\ ^{o}C/W$$

Determine resistor R_3:
L_3= 1.5 in = 3.81 cm
K_3= 158 W/m.K
A_3= (1) (0.06) = 0.06 in^2 = 0.387 cm^2

$$R_3 = \frac{(0.0381)10000}{(0.387)(158)} = 6.23\ ^{o}C/W$$

Determine resistor R_4:
L_4= 1.5 in = 3.81 cm
K_4= 158 W/m.K
A_4= (1.5) (0.06) = 0.09 in^2 = 0.581 cm^2

$$R_4 = \frac{(0.0381)10000}{(0.581)(158)} = 4.15\ ^{o}C/W$$

Determine resistor R_5:
L_5= 1 in = 2.54 cm
K_5= 237 W/m.K
A_5= (4.75) (0.06) = 0.285 in^2 = 1.839 cm^2

$$R_5 = \frac{(0.0254)10000}{(1.839)(158)} = 0.874\ ^{o}C/W$$

After getting all resistors we can simplify the network from Figure24.8a to as shown in Figure24.8b.Where resistors R_2, R_3 and R_4 are in parallel, which results in resistor R_6.

$$\frac{1}{R_6} = \frac{1}{R_2} + \frac{1}{R_3} + \frac{1}{R_4}$$

$$R_6 = 2.166\ ^{o}C/W$$

The total thermal resistance is.

$$R_t = R_1 + R_6 + R_5 = 4.7\ ^{o}C/W$$

The temperature rise across the length of the bulkhead is then determined from Equation 24.5.

$$\Delta t = (9)(4.7) = 42.3^{o}C$$

24.4 Circuit Board Edge Guides

Plug-in PCBs are often used with guides, which help to align the PCB connector with the chassis connector. These guides, which are usually fastened to the side walls of a chassis, grip the edges of the PCB as it is inserted and removed. If there is enough contact pressure and surface area at the interface between the edge guide and the PCB, the edge guide can be used to conduct heat away from the PCB. A typical installation is shown in Figure 24.9.

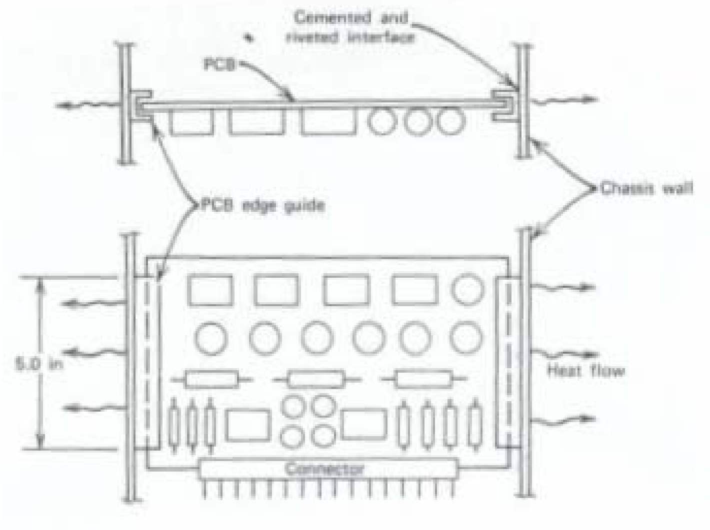

Figure 24.9 Plug-in PCB assembly with board edge guides

Plug-in PCBs must engage a blind connector, which is usually fastened to the chassis. If the chassis connector is rigid, with no floating provisions, the edge guide must provide that float, or many connector pins will be bent and broken. Rigid chassis connectors are generally used for electrical connections because wire-wrap harnesses, flex tape harnesses, and multilayer master interconnecting mother boards are being used for production systems. These interconnections cannot withstand the excessive motion required for a floating connector system. Therefore, the floating mechanism is often built into the circuit board edge guides.

Many different types of circuit board edge guides are used by the electronics industry. The thermal resistance across a typical guide is rather difficult to calculate accurately, so that tests are used to establish these values. The units used to express the thermal resistance across an edge guide are °C in/watt. When the length of the guide is expressed in inches and the heat flow is in watts, the temperature rise is in degrees Celsius. Figure 24.10 shows four different types of edge guides, with the thermal resistance across each guide.

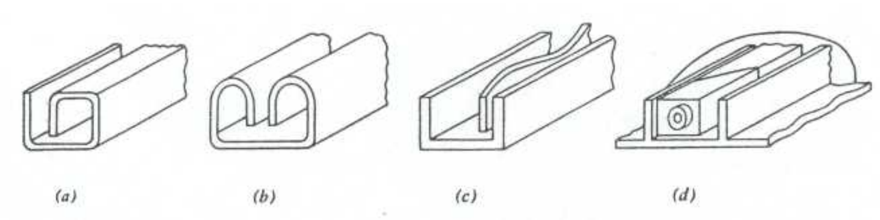

Figure 24.10 Board edge guides with typical thermal resistance, (a) G guide, 12°C in/watt; (b) B guide, 8°C in/watt; (c) U guide, 6°C in/watt; (d) wedge clamp, 2°C in/watt.

These board edge guides are generally satisfactory for applications at sea level or medium altitudes up to about 50,000 ft. At altitudes of 100,000 ft, test data show that the resistance values for the guides in Figure 24.10a-c will increase about 30%. The wedge clamp shown in Figure 24.10d will have about a 5% increase.

For hard-vacuum conditions, where the pressure is less than 10^{-6} torr (mm hg), as normally experienced in outer space work, some of these edge guides may not be satisfactory, except for very low power dissipations. Outer space environments generally require very high pressure interfaces, with fiat and smooth surfaces, to conduct heat effectively. Wedge clamps are very effective here because they can produce high interface pressures.

Example 24.3: Determine the temperature rise across the PCB edge guide (from the edge of the PCB to the chassis wall) for the assembly shown in Figure 24.9. The edge guide is 5.0 in long, type c, as shown in Figure 24.10. The total power dissipation of the PCB is 10 watts, uniformly distributed, and the equipment must operate at 100,000 ft.

Solution:
Since there are two edge guides, half of the total power will be conducted through each guide. The temperature rise at sea level conditions can be determined from Equation 24.8.

$$\Delta t = \frac{RQ}{L} \tag{24.8}$$

R= 6 °C in/watt (U guide)
Q=10/2 =5 watt
L= 5 in

$$\Delta t = \frac{(6)(5)}{5} = 6\ ^{o}C$$

At altitude of 100,000 ft, the resistance across the edge guide will increase about 30%. The temperature rise at this altitude will then be.

$$\Delta t = 1.3(6) = 9\ ^{o}C$$

24.5 Heat Conduction through Sheet Metal Covers

Lightweight electronic boxes often use sheet metal covers to enclose the chassis. Sometimes these covers are expected to conduct the heat away from the chassis for additional cooling. To effectively conduct heat from the chassis to the cover, a flat, smooth, high-pressure interface must be provided. The normal surface contact obtained at the interfaces of sheet metal members will not provide an effective heat conduction path. However, if a lip can be formed in the cover or on the sidewalls of the chassis, the heat conduction path can be substantially improved. Figure 24.11 shows how lips may be formed in the chassis and cover to improve the heat transfer across the interface.

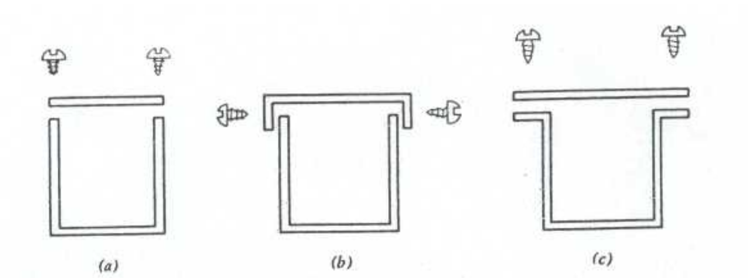

Figure 24.11 Different types of sheet metal covers on electronic boxes, (a) Poor; (b) good; (c) good.

24.6 Radial Heat Flow

Electronic support structures are not always rectangular in shape. If an electronic system is enclosed within a cylindrical structure, such as a small missile, it would be a waste of space to use a rectangular box for the electronics. The packaging form factor would probably conform to the natural cylindrical shape. Electronic components mounted on the inside surface of a cylindrical chassis would require a radial heat flow path to remove the heat when the heat sink is on the outer surface of the structure. The temperature rise from the inside surface to the outside surface of the cylindrical structure can be determined from Fourier's law as follow.

$$Q = -kA\frac{dt}{dr} = \text{constant}$$

$$= -k(2\pi Ra)\frac{dt}{dr} \qquad (24.9)$$

However, in a radial heat flow system, the cross-sectional area is constantly changing as the radius changes, as shown in Figure 24.12. So that we integrate the Equation 24.9, yields to

$$Q\int_{R_{in}}^{R_{out}}\frac{dR}{R} = -2\pi ka\int_{t_{in}}^{t_{out}} dt$$

$$Q = \frac{2\pi ka(t_{in} - t_{out})}{\ln(R_{out}/R_{in})}$$

$$= \frac{\Delta t}{\dfrac{\ln(R_{out}/R_{in})}{2\pi ka}} \qquad (24.10)$$

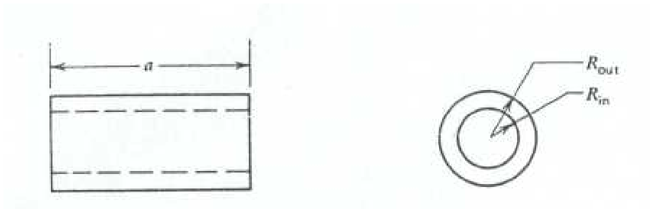

Figure 24.12 Hollow cylinder

Example 24.4: A hollow steel cylindrical shell has a group of resistors mounted on the inside surface, as shown in Figure 42.13. Heat is removed from the outside surface of the cylinder, so that the heat flow path is radial through the wall of the cylinder. Determine the temperature rise through the steel cylinder when the power dissipation is 10 watts.

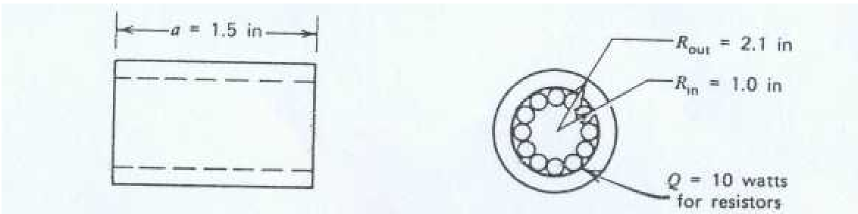

Figure 42.13 Resistors mounted on the inside wall of a hollow cylinder

Solution:
R_{out}= 2.1 in= 5.334 cm
R_{in}= 1 in=2.54 cm
a= 1.5 in=3.81 cm
Q=10 W
k= 60.5 W/m.K

Substitute into Equation 24.10 for the temperature rise through the steel cylindrical wall.

$$10 = \frac{\Delta t}{\dfrac{\ln(2.1/1)}{2\pi(60.5)(0.0381)}}$$

Then

$\Delta t = 0.51\ ^{o}C$

Part E: Analysis of Thermal Failure of Electronic Components

Indicative Contents

Analysis of Thermal Stresses and Strain
Effect of PCB Bending Stiffness on Wire Stresses
Vibration Fatigue in Lead Wires and Solder Joints

25. Analysis of Thermal Stresses and Strain

25.1 Introduction

For many years the reliability of an electronic system was based, to a great extent, upon the junction temperatures of the semiconductor devices. Substantial efforts were made in the fabrication methods, mounting methods, and cooling techniques of the electronic devices to reduce these hot spot temperatures below 100 °C. This has produced a significant improvement in the reliability and effective operating life of the equipment. However, the electronic failure rates are still too high. Additional reductions in the failure rates must be achieved to further improve the reliability of our electronic equipment.

Some of the failure mechanisms that can cause malfunctions in electronic systems are examined in this chapter. Experience has shown that most of these failures are produced by a mismatch in the thermal coefficients of expansion (TCE) of the different types of materials typically used in electronic assemblies. The mismatch often generates high forces and stresses, which produce fractures and cracks in the electronic components and assemblies.

An examination of a large number of avionics failures has shown that most of them are mechanical in nature. They typically involve fractures in solder joints, electrical lead wires, plated throughholes (PTH), electrical cables, connectors, adhesive bonded joints, and hermetic seals. These failures are often produced by various combinations of thermal, vibration, shock, humidity, and salt environments, combined with poor manufacturing processes and poor design practices. These failures must be reduced in order to achieve a substantial improvement in the system reliability.

25.2 Thermal Expansion Effects in Electronic Equipments

Electronic assemblies utilize a wide variety of plastics and metals in the fabrication and manufacturing of their products. These materials can have significant differences in their thermal TCE, which may result in high strains and stresses in the lead wires, solder joints, and PTH if these factors are not understood or if they are ignored. Temperature changes will produce dimensional changes in almost all materials normally used in the assembly of electronic chassis and PCBs. Dimensional changes can occur due to power cycling where the power is turned on and off, which induces temperature changes within the electronic assembly. This can also be caused by thermal cycling, where the outside ambient temperature changes and the thermal lag within the chassis forces thermal gradients to develop because of different mass effects. These dimensional changes, which can occur along the X, Y, or Z axes of the electronic assemblies, can produce a wide variety of failures in the structural elements of these assemblies.

Consider a surface mounted transformer on a PCB, as shown in Figure 25.1. Thermal expansion differences between the component and the PCB along the X and Y axes (in the plane of the PCB) can produce failures in this subassembly after 12 thermal cycles from -55 to +95 °C. The failures will not be in the lead wires or in the solder joints. Instead, the failures will occur in the solder pads, which will be lifted off the surface of the PCB by overturning moments in the lead wires. These moments are caused by the expansion differences between the transformer and the PCB because each material has a different TCE.

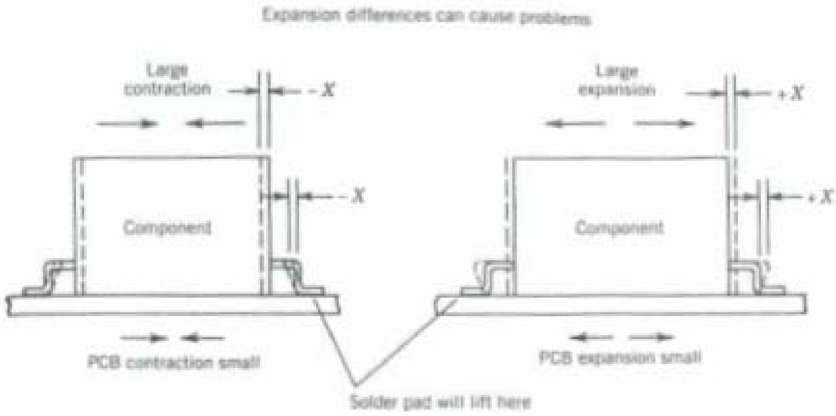

Figure 25.1 Surface mounted transformer where differences in expansion produce bending in the lead wires

Although epoxy is used in the PCB and for potting the transformer, the PCB contains glass fibers which have a low TCE. This reduces the TCE of the PCB in the X and Y planes, so the PCB expands and shrinks less than the transformer. This expansion difference produces the high forces in the lead wires. The wires transfer the load to the solder pads, lifting the pads, which are only cemented to the surface of the PCB.

Plated throughholes can be added to anchor the pads to prevent the pads from lifting off the PCB. The fatigue life of the assembly will now be increased to about 150 thermal cycles from -55 to +95 °C, where solder joint shear failures can now be expected.

Example: Determine the deflections and thermal stresses expected in the lead wires and solder joints of the surface mounted transformer shown in Figure 25.2, when it is mounted on an aluminum composite PCB which experiences in plane (X and Y) thermal expansion during rapid temperature cycling tests over a temperature range from -55 to +95 °C, with no electrical operation.

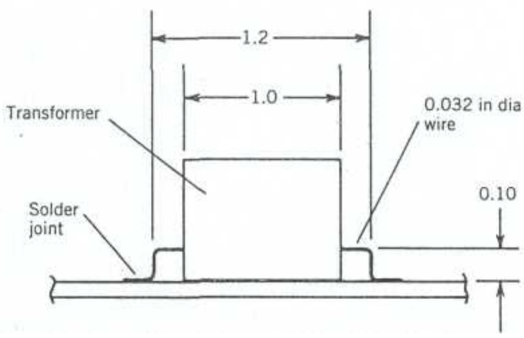

Figure 25.2 Dimensions of a surface mounted transformer

Solution:

Thermal expansion differences between the transformer and the PCB in the X-Y plane will produce a force on the lead wires and cause them to bend. This same force will produce a shear stress in the solder joint at the junction of the lead wire and the PCB. Since all masses tend to expand with respect to their centroid (or center of mass) and the proper length must be used in the expansion calculations. For a symmetrical structure, the effective length is simply half of the total length. Average physical properties must be used for the TCE of the transformer, which has an epoxy potting outer shell around a copper-iron core. This is also true for the PCB, which has an aluminum heat sink laminated between two epoxy fiberglass circuit boards, so an average TCE must be used for this subassembly.

The temperature is cycled over a range from -55 to +95 °C, for a total difference of 150 °C in this sample problem. However, the stresses are determined for a temperature range of only 75 °C, which is half of the total temperature range experienced. The 75 °C temperature range is used because it represents the stresses that will be developed during cycling from a neutral stress point to the maximum positive stresses, and from a neutral stress point to the maximum negative stress.

In this case the neutral stress point would be at 20 °C. Increasing the temperature 75 °C would bring the temperature to +95 °C. Decreasing the temperature 75 °C from the neutral point of 20 °C would bring the temperature down to -55 °C.

The solution divided into three parts:

1) Determine the expansion differences between the transformer and the PCB in X-Y planes is

$$X= (a_T - a_P)\, b\, \Delta t \qquad (25.1)$$

Where:

a_T = average TCE of transformer, considering a mixture of epoxy potting copper, and iron core

in and PCB in X-Y plane (Z axis expansion are ignored here)

= 35×10^{-6} in/in/°C or 35 parts per million/°C (35 ppm/°C)

a_P = average TCE of composite PCB with epoxy fiberglass and aluminum heat sink core in X-Y

planes

= 20×10^{-6} in/in/°C or 20 parts per million/°C (20 ppm/°C)

b = 1.2/2 = 0.6 in (effective length of transformer, including wire length with the transformer)

Δt = 95-(-55) = 150 °C (peak to peak temperature range)

Δt = 150/2 = 75 °C (neutral point to high and low temperature)

Substituting in Equation 25.1 yields to

$$X= (35-20) \times 10^{-6} (0.6)\,(75) = 0.000675 \text{ in}$$

2) Determine the horizontal force induced in the wire as it is forced to bend through this deflection. The wire geometry is shown in the following Figure 25.3.

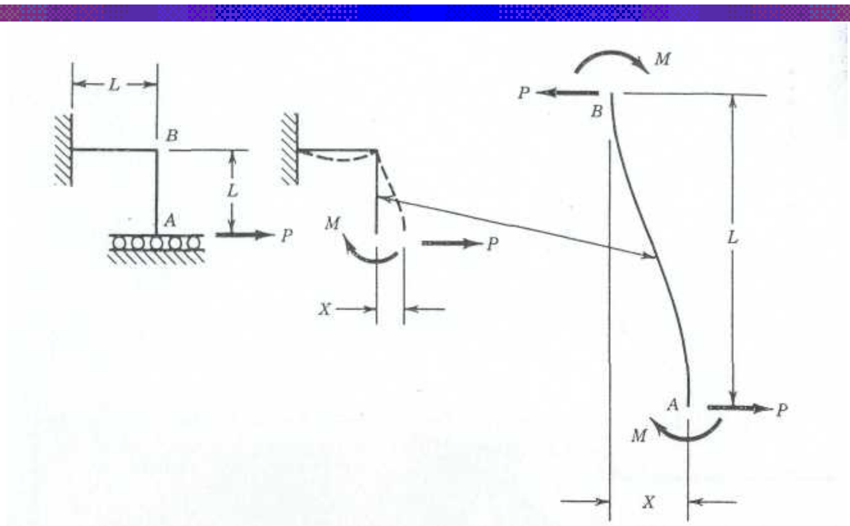

Figure 25.3 Deflection forces the lead wire to bend

The horizontal displacement of a square frame with clamped ends, with bending of both wire legs due to the action of the lateral force (P), can be determined from the following equation

$$X = \frac{PL_W^3}{7.5E_W I_W} \tag{25.2}$$

Where:
X = 0.000675 in (wire displacement in X-Y plane)
L_W = 0.1 in (vertical and horizontal wire length)
$I_W = \dfrac{\pi d^4}{64} = \dfrac{\pi(0.032)^4}{64} = 0.051\text{x}10^{-6}\text{in}^4$ (wire inertia)
$E_W = 16\text{x}10^6$ psi (modulus of elasticity, copper wire)

Substituting in Equation 25.2 yields to

$$P = \frac{7.5(0.000675)(16\text{x}10^6)(0.051\text{x}10^{-6})}{(0.1)^3} = 4.13 \text{ Ib}$$

3) Determine the bending stress in the lead wire and the shear stress in the solder joint.

The bending moment (P) in the wire at the solder joint can be determined from Figure 25.2, by summing up the bending moments for the wire frame.

$$\begin{aligned} M &= 1.2PL_W \quad \text{(wire bending moment)} \\ &= 1.2(4.13\text{x}0.10) = 0.495 \text{ lb in} \end{aligned} \tag{25.3}$$

Then the bending stress (S_b) in the wire can be obtained as in Equation 25.4

$$S_b = \frac{\text{KMC}}{\text{I}_\text{W}} \tag{25.4}$$

Where:
K = Stress concentration factor
 = 1 here
C = Wire radius to neutral axis
 = 0.032/2 = 0.016 in
Substituting in Equation 25.4 yields to

$$S_b = \frac{(0.459)(0.016)}{0.051\ \mathrm{x}10^{-6}} = 155294\ \mathrm{Ib/in}^2$$

This far exceeds the ultimate tensile stress of 45,000 psi for the copper lead wire, which means that the wire will be in the plastic bending range. However, testing experience with this condition shows that the probability of a wire failure is low (if there are no sharp cuts in the wire) due to the low number of stress cycles normally expected for this type of environment.

The direct shear stress (S_s) in the solder joint can be obtained from the solder pad area estimated to be about 0.09 in x 0.032 in. This direct shear stress does not include solder joint stresses produced by the overturning moment. Both stresses may be combined to obtain the maximum or the Von Mises stress. Only the shear stresses were used here to determine the approximate fatigue life of the solder joint. Stress concentrations are not considered here because the solder is so plastic.

$$\mathrm{S_s} = \frac{P}{A} \tag{25.5}$$

Where: P= 4.13 Ib
 A= 0.09 in x 0.032 in = 0.00288 in^2

Then the direct shear stress is

$$\mathrm{S_s} = \frac{4.13}{0.00288} = 1434\ \mathrm{Ib/in}^2$$

25.3 Reducing the Thermal Expansion Forces and Stresses

Lower forces and stresses in the electrical lead wires and solder joints will lead to a longer life with a higher reliability. The Equation 25.2 shows that the forces in the lead wires can be reduced by (a) decreasing the moment of inertia I, (b) decreasing the deflection of the wire X, or (c) increasing the length of the wire L.

(a) Decreasing the moment of inertia I

The moment of inertia of the component wire can be reduced by coining (squeezing or rolling) the round wire into a flat thin rectangular cross section. This will decrease the force in the wire, which will decrease the wire bending stress and the solder joint shear stress. Coining will also increase the width of the lead wire at the solder joint, which will increase the solder joint area and further reduce the solder joint stress. MIL-STD-2000 solder specification requires surface mounted components, with axial leads, to have their wires coined before they are soldered to the circuit boards.

Coining may be expensive since special machines are required for this operation. For a large manufacturing facility, where millions of components are involved, the coining costs for each component will be relatively small. However, for a small company the cost of the coining equipment can be too great, so other ways for mounting the components may have to be examined.

In the previous sample problem, if the lead wires are coined to a cross section that measures 0.010 in thick and 0.080 in wide (which maintains the same cross-sectional area), the forces and stresses will be reduced. The reduction will be directly related to the different moments of inertia for the wire cross sections, as shown in Equation 25.2. The new moment of inertia becomes.

$$I = \frac{(0.08)(0.01)^3}{12} = 6.667 \text{ x}10^{-9} \text{ in}^4$$

From Equation 25.2 the new shear force is

$$P = \frac{7.5(0.000675)(16\text{x}10^6)(6.667\text{x}10^{-9})}{(0.1)^3} = 0.54 \text{ Ib}$$

Substituting in Equation 25.5.With 0.09 in x 0.08 in estimated area yields to

$$S_s = \frac{0.54}{(0.09)(0.08)} = 75 \text{ Ib/in}^2$$

This low solder shear stress will provide a good fatigue life.

(b) Decreasing the deflection of the wire X

Wire deflections can be reduced by reducing the relative differences in the TCE between the component body and the PCB. In this application, the transformer has a TCE that is much greater than the TCE of the PCB, so the transformer expands and shrinks more than the PCB, producing high forces in the wires. Expansion differences can be reduced by increasing the TCE of the PCB or by reducing the TCE of the transformer, so the mismatch between them is reduced. It is a far easier task to reduce the TCE of the transformer by simply adding calcium carbonate or aluminum oxide powder to the epoxy solution before encapsulating the transformer. The reduction in the transformer TCE will be related to the amount of material added to the epoxy solution. An overall reduction in the transformer TCE of about 10% or 3.5 ppm/°C can be achieved. This will reduce the difference in the TCE as shown in Equation. 25.1. From 35 - 20 = 15, to 31.5 - 20 = 11.5 ppm/ °C. This ratio is 11.5/15 = 0.766.

This means that the forces and stresses will only be 76.6% of the levels previously shown, when the transformer TCE is reduced by 10%.

(c) Increasing the length of the wire L

Increasing the wire length will rapidly reduce the forces developed in the lead wires, because a cubic function is involved here. The wire length can be increased by using camel humps or loops as shown in Figure 25.4.

If the wire length increased 50% to a length of 0.15 in, the wire force will be reduced to 1.22 pounds. This will reduce the bending stress to 68900 psi and solder shear stress to 424 psi.

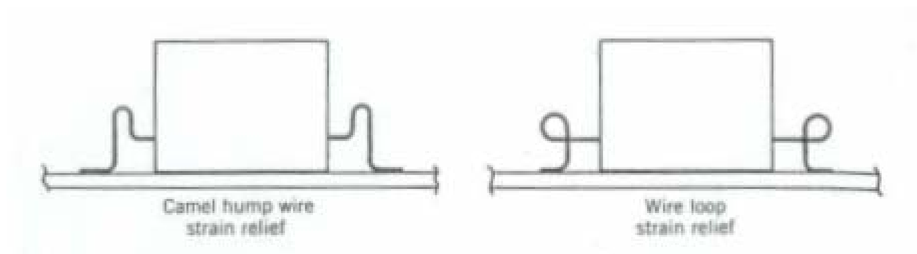

Figure 25.4 Methods for increasing the wire length to decrease the forces and stresses in the solder joints

25.4 X-Y Thermal Expansion Stresses for Throughhole Mounting

A large number of components such as resistors, capacitors, diodes, flat packs, and hybrids are fabricated with axial leads. Wire-forming tools are then used to bend the leads 90° for insertion in throughhole PCBs for flow soldering. During exposure to thermal cycling environments, the PCB typically ' has a higher TCE than the component in the X-Y plane, so the PCB will expand more than the component. Since the wire in an axially leaded component has a relatively low bending stiffness, virtually all of the deflection difference between the PCB and the component will be taken up by the bending in the wire, as shown in Figure 25.5.

A bending moment will be developed in the wire, at the PCB solder joint, which will produce a shear tear-out stress in the solder joint. This solder joint stress should be limited to a value of about 400 psi to ensure a long trouble-free operating life.

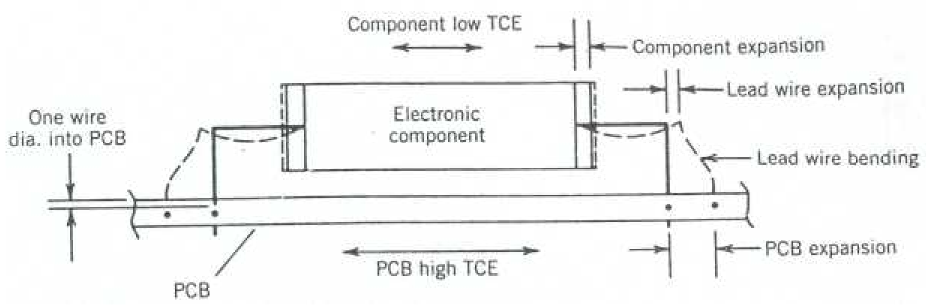

Figure 25.5 Deflection in throughhole technique

Example: Determine the stresses in the lead wires and solder joints of the axial leaded resistor, throughhole mounted as shown in Figure 25.6, due to a mismatch in the thermal expansion of the epoxy fiberglass PCB in the X-Y plane over a temperature cycling range from -40 to +80 °C.

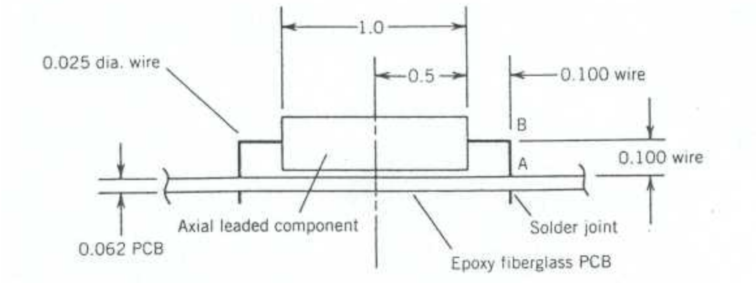

Figure 25.6 Dimensions of an axial leaded resistor throughhole mounted in a PCB

Solution:

The thermal expansion of the PCB will be greater than the expansion of the resistor because the TCE of the PCB is greater than the TCE of the resistor. The expansion differences will force the vertical leg of the resistor lead wire to bend. This action will produce bending and shear stresses in the lead wires, and shear tear-out stresses in the solder joints.

The expansion of the PCB must be equal to the expansions of the resistor body plus the horizontal expansion of the lead wire, plus the bending deflection of the vertical leg of the lead wire. This can be expressed in a simplified form as shown in the following equation.

$$X_p = X_R + X_H + X_W \tag{25.6}$$

Where:
X_p= Thermal expansion of PCB along X axis
X_R = Thermal expansion of resistor body along X axis
X_H = Thermal expansion of horizontal lead wire leg
X_W = Bending of vertical lead wire leg along X axis

The expansion differences force the wire legs to bend, which produces a horizontal force in the wire. The magnitude of this force can be obtained from the bending displacement produced in the vertical leg of the wire. This bending displacement can be obtained from Equation 25.7 as shown below.

$$X_W = a_P L_P \Delta t - a_R L_R \Delta t - a_H L_H \Delta t \tag{25.7}$$

Where:
a_P = 15 x 10-6 in/in/°C (TCE of PCB in X-Y plane)
L_P = 0.5 + 0.1 = 0.6 in (effective length of PCB)
Δt = 80-(-40) = 120 °C (total temperature range)
Δt = 120/2 = 60 °C (neutral to peak value for a rapid temperature cycle)
a_R = 6 x 10^{-6} in/in/°C (TCE of carbon composition resistor)
L_R = 0.5 in (half of resistor body length)
a_H = 16 x 10^{-6} in/in/°C (TCE of horizontal copper wire
L_H = 0.1 in (horizontal length of lead wire)

Substitute into Equation 25.7 yields to:

$$\begin{aligned} X_W &= (15x\,10^{-6})(0.6)(60) - (6x\,10^{-6})(0.5)(60) - (16x\,10^{-6})(0.1)(60) \\ &= 0.000264 \text{ in} \end{aligned}$$

This represents the bending displacement of the lead wire. The force produced in the wire due to this bending deflection can be determined from the following Equation 25.8, for a square frame, where the lengths of both legs are equal.

$$P = \frac{7.5E_W I_W X_W}{L_W^3} \tag{25.8}$$

The wire extends into the PCB, and it also extends into the resistor body, which makes the effective wire length slightly longer than the exposed wire length. Test data on similar electronic subassemblies show that for wires in bending, the lead wire appears to extend about one wire diameter into the component body and one wire diameter into the PCB. This approximation is used in the sample problem to obtain the effective length of the lead wire.

L_W = effective wire length = exposed length plus one wire diameter
= 0.1 +0.025 = 0.125 in
$E_W = 16 \text{ x } 10^6$ Ib/in^2 (copper wire modulus elasticity)
$X_W = 0.000264$ in
$I_W = \pi\,(d^4)/4 = 1.917 \text{ x}10^{-8} \text{ in}^4$

Substitute into Equation 25.8 yields to:

$$P = \frac{7.5(16x\,10^6)(1.917x\,10^{-8})0.000264)}{(0.125)^3} = 0.311 \text{ Ib}$$

Then the bending moment in the lead wire, at the solder joint is

$$M = 1.2PL_W = 1.2(0.311)\,(0.125) = 0.0466 \text{ Ib in}$$

Then the bending stress in the lead wire can be obtained from equation 25.4. Since the number of stress cycles over this wide temperature range is expected to be low, so fatigue is not a factor. So that stress concentration factor is not used here.

Where:
C = Wire radius to neutral axis
= d/2 = 0.025/2 = 0.0125 in

Substitute into Equation 25.4 yields to:

$$S_b = \frac{(0.0466)(0.0125)}{1.917 \text{ x}10^{-8}} = 30386 \text{ Ib/in}^2$$

Since this stress is well below the ultimate stress of 45,000 psi for copper wire, the condition is acceptable.

The overturning moment developed in the lead wire may lead to shear tear-out failures in the solder joint, as shown in Figure 25.7. Test data show that these failures do not always occur at the surface of the lead wire, where the shear area is minimum.

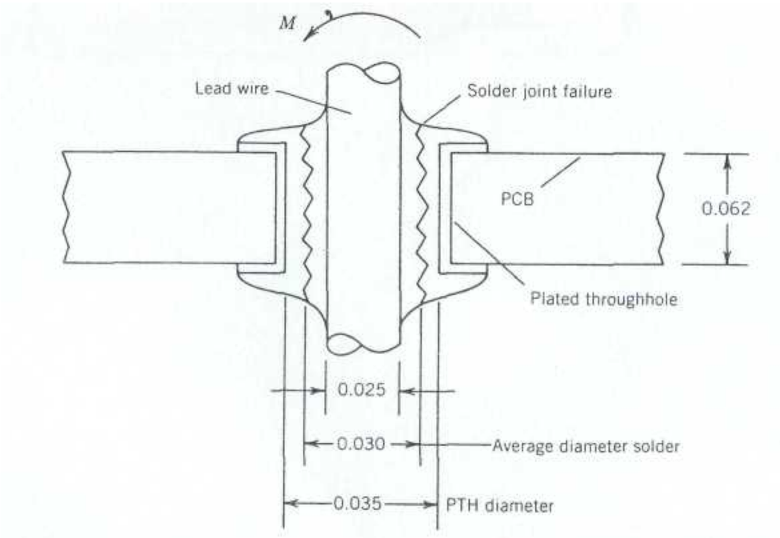

Figure 25.7 Typical solder joint failure in a throughhole PCB mounting

Many of the solder joint failures seem to occur in an area between the wire and the PTH in the PCB as shown in Figure 25.8. An average area based upon the diameter of the wire and the diameter of the PTH can be used to find the average area of the solder joint for this condition.

The magnitude of the shear tear-out stress can be obtained from Equation 25.9.

$$S_{ST} = \frac{M}{A_S h} \tag{25.9}$$

Where:
M = 0.0466 Ib in (overturning moment in solder joint)
h = 0.062 in (solder joint height, use PCB thickness)
$d_{av.}$= (0.025+0.035)/2 = 0.03 in
$A_S = \pi\ (0.03)^2/4 = 0.000707\ in^2$
Then the shear stress is:

$$S_{ST} = \frac{0.0466}{(0.000707)(0.062)} = 1063.3\ \frac{Ib}{in^2}$$

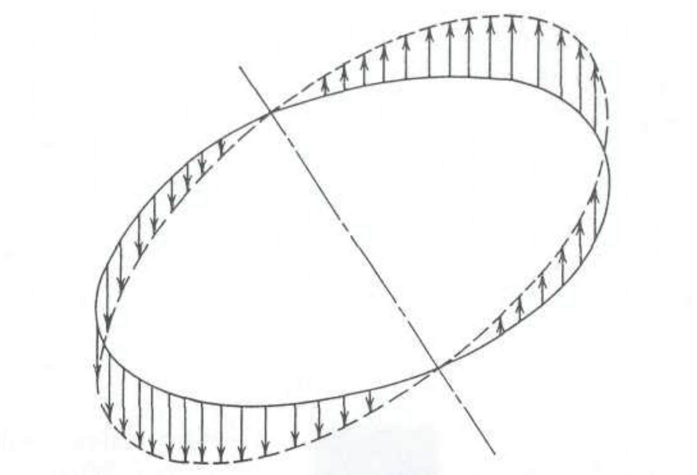

Figure 25.8 Shear tear-out stress pattern in the solder joint of a throughhole lead wire

26. Effect of PCB Bending Stiffness on Wire Stresses

26.1 Introduction

When axial leaded devices on a PCB are exposed to thermal cycling environments, overturning moments can occur which may force the PCB to bend as shown in Figure 26.1.

In the previous sample problems, the bending effects of the PCBs were not included in the force and displacement relations. Since bending in the PCB can occur during temperature cycling, the magnitude of these effects should be evaluated.

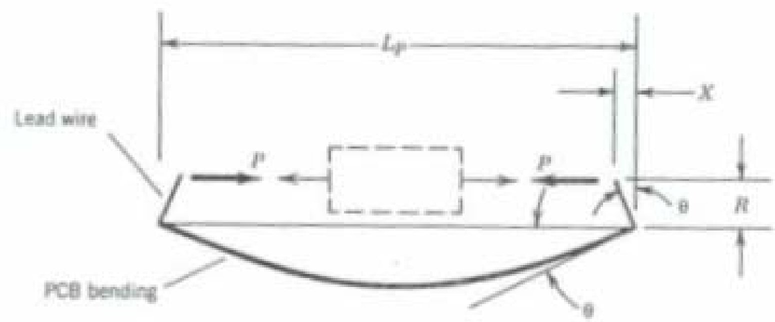

Figure 26.1 High axial loads in lead wires can force the PCS to bend

The Figure 26.1 shows that when the PCB bends, the magnitude of the horizontal load will be reduced. These relations can be obtained from Equation 25.2 by considering bending in the vertical member of the lead wire, and rotation of the PCB which will produce rotation of the vertical lead wire. The horizontal displacement expected at the top of the wire will be the sum of the wire bending and the PCB rotation, as shown in Equation.26.1, when the horizontal and vertical legs of the wire are the same length.

$$X = \frac{PL_W^3}{7.5E_W I_W} + \mathrm{R}\theta \qquad (26.1)$$

Example: Determine the axial force in the lead wire for the resistor shown in Figure 25.6, when bending of the PCB is included in the analysis over a temperature cycling range from -40 to +80 °C. As defined in the example of section 25.4.

Solution:

The axial load in the lead wire induced by the different TCE will produce an overturning moment in the PCB and force it to bend, as shown in Figure 26.1. Considering the pivot point to be at the lead wire solder joint, the angular rotation of the lead wire (for small angles) must be the same as the angular rotation of the PCB. The PCB angular rotation will be as shown in Equation 26.2.

$$\theta = \frac{ML_P}{2E_P I_P} \tag{26.2}$$

Substitute Equation 26.2 into Equation 26.1 to obtain the combined deflection of the bending wire and the rotating PCB.

$$X = \frac{PL_W^3}{7.5E_W I_W} + \frac{RML_P}{2E_P I_P} \tag{26.3}$$

Reference subscripts W and P are added for the wire and PCB respectively.

Where:
$X = 0.000264$ in
$E_W = 16 \times 10^6$ Ib/in^2 (copper wire modulus elasticity)
$I_W = \pi (d^4)/4 = 1.917 \times 10^{-8}$ in^4
$d = 0.025$ in
R = height of wire plus one wire diameter into the PCB for wire in bending
$= 0.1 + 0.025 = 0.125$ in (moment arm length)
L_W = effective wire length = length of wire plus one wire diameter
$= 0.1 + 0.025 = 0.125$ in
$E_P = 1.95 \times 10^6$ Ib/in^2 (PCB modulus of elasticity)
L_P = length of PCB between component lead wires
$= 1 + 2(0.1) = 1.2$ in (PCB length)
$h = 0.062$ in (PCB thickness)
b = effective width of PCB for bending = 30 x h = (30) (0.062) = 1.86 in (effective width of PCB assuming no other similar components on PCB)
$I_P = bh^3/12 = (1.86)(0.062)^3/12 = 3.694 \times 10^{-5}$ in^4
M = RP = 0.125 P (bending moment on PCB)
Substitute into Equation 26.3 to get the wire load when PCB bends:

$$0.000264 = \frac{P(0.125)^3}{7.5(16\text{x}10^6)(1.917\text{x}10^{-8})} + \frac{(0.125)(0.125P)(1.2)}{2(1.95\text{x}10^6)(3.69\text{x}10^{-5})}$$

$$P = 0.269 \text{ Ib}$$

When compare the results with the previous example of section 25.4. When neglect the bending of the PCB in the analysis, the wire force of 0.311 pound will be developed.

When the bending of the PCB is included in the analysis, the wire force of 0.269 pound will be developed. This means that the bending action of the PCB will reduce the wire load by about 13%.

26.2 Fatigue Life and Vibration Environments

26.2.1 Introduction to Fatigue Generation

Electronic assemblies are used in many commercial, industrial, and military applications worldwide. The common element in the vast majority of these systems is that power is turned on to perform a function and then turned off after the function has been completed. This turn-on and turn-off process introduces alternating stresses in the structural elements as the assembly heats up and then cools down. Every stress cycle experienced by the electronic system will use up a small part of its total life. When enough stress cycles have been experienced, the fatigue life will be used up and cracks will develop in structural elements such as solder joints, plated through holes, and electrical lead wires, resulting in failures.

Materials can fracture when they are subjected to repeated stresses that are considerably less than their ultimate static strength. The failure appears to be due to submicroscopic cracks that grow into visible cracks, which then leads to a complete rupture under repeated loadings.

The appearance of a small crack does not always mean that a failure will occur. Sometimes a small crack will just stop growing, or grow so slowly that a failure does not occur. When a crack is observed, it is best to be safe and to assume that the crack will eventually result in a fatigue failure. If the crack is in a major structural element, then the element should be repaired or replaced.

Fatigue can also be generated in electronic systems by shock and vibration. It is probably safe to say that all electronic equipment will be subjected to some type of vibration at some time in its life. If the vibration is not associated with the end use of the product, then the vibration will probably be due to the transportation of the product from the manufacturer to the consumer.

Thermal stresses can develop in an electronic assembly while it is stored or sitting on a shelf, with no electrical operation. Temperature changes can still occur within the assembly, as the local ambient temperature changes from day to night.

When electronic systems are associated with moving vehicles or machinery such as automobiles, airplanes, washing machines, or blenders, then vibration cycling fatigue can develop as well as thermal cycling fatigue. These two fatigue effects can combine to produce-more rapid fatigue failures. Small fractures may be initiated during the thermal cycling environment, but they do not propagate rapidly since the thermal cycling rate is very low (1 to 10 cycles per day). Vibration environments, on the other hand, often produce several hundred cycles per second, so small cracks can grow more rapidly in vibration until a full fracture occurs.

When structural failures are experienced during vibration, it is natural to assume that vibration caused the failures. The corrective action would then be based upon structural dynamics. This may not be true, however, if there is a previous history of exposure to any thermal cycling environments. An examination of the various failures experienced in military electronic equipment shows that about 80% of the failures are due to thermal cycling, while the remaining 20% are due to vibration and shock. Any structural changes made to correct a deficiency involving vibration may not stop crack initiation in a thermal cycling environment. It is therefore important to understand the difference between thermal cycling failures and vibration cycling failures, to ensure the reliability of an electronic system that is required to operate in both environments.

Field experience with military types of electronic equipment shows that the greatest number of failures typically occur in the electrical interconnect system. About 30% of all failures occur in the connectors, master interconnecting boards, cables, and harnesses. These failures are produced by a combination of relative motion resulting from thermal cycling, vibration, shock, and rough handling.

26.2.2 Slow Cycle Fatigue and Rapid Cycle Fatigue

Fatigue properties are typically obtained from controlled stress cycle tests, using precision-machined and polished test specimens that are tested to failure over a wide stress range. The data points obtained are plotted on log-log paper with stress on the vertical axis and the number of cycles to fail on the horizontal axis. A straight line that represents the best average fatigue properties for that specimen is then drawn through the various scattered points, as shown in Figure 26.2.

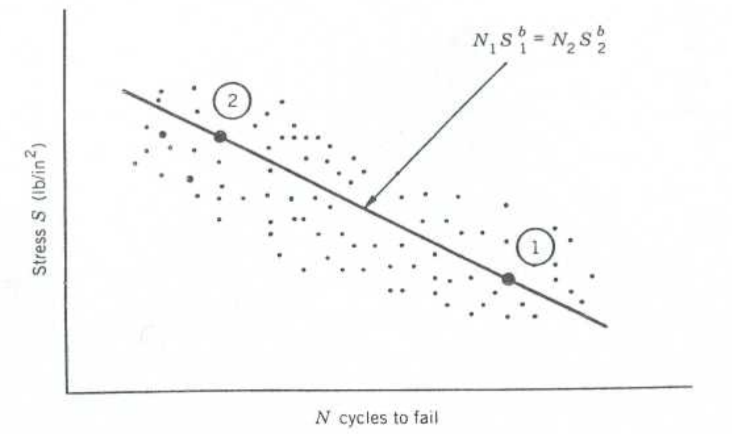

Figure 26.2 Typical S-N fatigue curves

The fatigue life can be estimated from the sloped portion of the curved based on the relation.

$$N_1 S_1^b = N_2 S_2^b \tag{26.4}$$

Where:
N= number of stress cycles to produce a fatigue failure
S = stress level at which these failures will occur
b = fatigue exponent related to the slope of the line

The b exponent shows the fatigue properties of each material, so it is useful in predicting the fatigue life of other members fabricated of the same material when exposed to similar environments. The slope of the fatigue curve must reflect the condition of the structure at critical areas such as holes, notches, and sharp changes in the cross section, which are defined as stress concentration areas. These stress concentration factors are not usually considered unless 5000 or more stress cycles are involved. Stress concentrations are not usually considered for very ductile materials, since these materials can often strain relieve themselves by plastically deforming.

Test data on solders shows that the frequency of the applied alternating load has a significant affect on the fatigue life, as shown in Figure 26.3. Where the effects of slow cycle fatigue and rapid cycle fatigue appears. The solder joint is significantly weaker for stresses that alternate at 0.06 cycle per minute compared with stresses that alternate at 5 cycles per minute under the same temperature conditions.

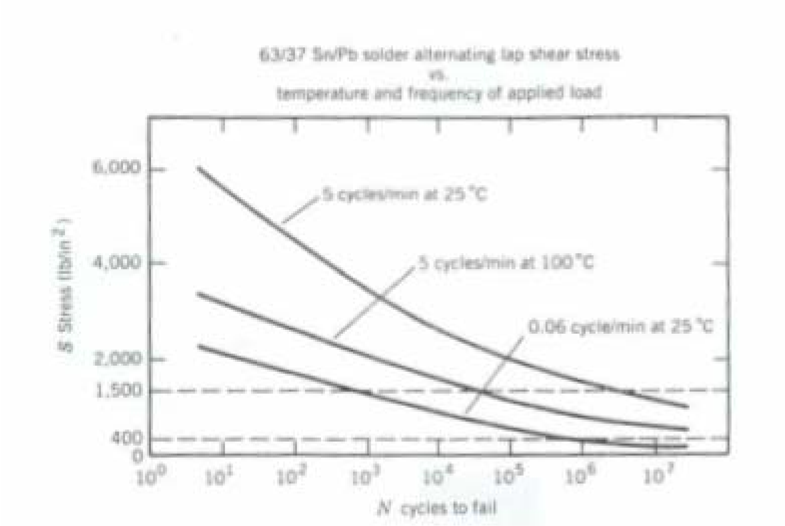

Figure 26.3 Solder subjected to slow cycle fatigue is weaker than solder in rapid cycle fatigue, especially at high temperatures.

Instead of a single-solder-joint fatigue curve, a dual curve is recommended, which shows the average properties for slow cycle fatigue and the average properties for rapid cycle fatigue. This dual-curve-concept recommendation is shown in Figure 26.4.

The slow cycle fatigue data portion of the solder curve was based upon a wide variety of temperature cycling tests, from -55 to +95 °C, and in some cases to + 125 °C, on a broad range of electronic circuit boards and chassis assemblies. The rapid cycle fatigue data portion of the solder curve was based upon random vibration and sinusoidal vibration tests, plus field exposure on many electronic boxes.

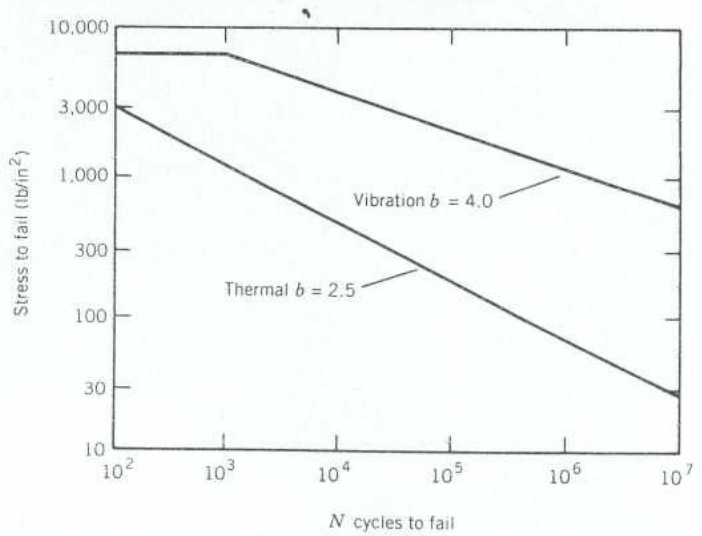

Figure 26.4 Vibration and thermal cycle fatigue, 63/37 solder, (vibration at room temperature)

Example: Determine the approximate fatigue life expected for the solder joints on the surface mounted transformer shown in sample solved example in section 25.2. For two different conditions as follows:

A) Original rapid temperature cycling from -55 to +95 °C, which resulted in a solder joint shear stress of 1434 psi.
B) Revised rapid temperature cycling from -25 to +75 °C.

Solution:

PART (A)
An examination of the solder joint fatigue curve has shown in Figure 26.4 for thermal cycling conditions with 1434 psi solder shear stress.

Approximate solder fatigue life = 650 cycles

At 650 the cracks may be expected in some of the solder joints when the solder shear stress level is about 1434 psi.

This does not mean that electrical failures will occur instantly. It means that visible cracks may have developed and that these cracks can continue to grow in this environment, so a catastrophic failure is not far away.

PART (B)
When the temperature cycling range is changed, the fatigue life of the solder joint can be approximated by assuming a linear system, so the stress is directly proportional to the temperature change. The high and low temperatures to the neutral points are:

Condition (A) $\frac{95-(-55)}{2} = 75\ °C$

Condition (B) $\frac{75-(-25)}{2} = 50\ °C$

Using a linear ratio of the temperature change, the solder joint shear stress for the 50 °C temperature change will be:

$$S_S = \frac{50}{75}(1434) = 956\ \ \text{Ib/in}^2$$

By Figure26.4 the approximate fatigue life is

Life = 1600 cycles to fail

Another method can be used to obtain the approximate fatigue life of the solder joint using Equation 26.4, along with the exponent b of 2.5, which represents the slope of the thermal fatigue curve for solder. A reference point must be obtained from Figure 26.4 to start the process. Any convenient starting point can be selected, such as 200 psi, where the fatigue life is 80,000 cycles to fail. This will be selected as point 2 on the fatigue curve.

Changing Equation 26.4 slightly to solve for N_1 cycles to fail and using the slow cycle fatigue exponent b with a value of 2.5:

$$N_1 = N_2(S_2/S_1)^{2.5}$$

Where:
N_2 = 80,000 (cycles to fail at reference point 2)
S_2 = 200 lb/in^2 (stress to fail at reference point 2)
S_1 = 956 lb/in^2 (stress resulting from 50 °C temperature change from condition B)

Substitute into Equation 26.4, to get the fatigue life for condition B is:

$$N_1 = 80000(200/956)^{2.5} = 1601\ \ \text{cycles to fail}$$

27. Vibration Fatigue in Lead Wires and Solder Joints

27.1 Introduction

Electronic systems are often required to operate in severe vibration environments for commercial, industrial, and military applications for extended periods without failing. Some examples are in automobiles, airplanes, trucks, trains, ships, submarines, farm tractors, atomic and fossil fuel power plants, communication systems, petroleum refineries, oil drilling equipment, blenders, elevators, machine tools, foundries, light and heavy manufacturing, washing machines, garage door openers, missiles, rockets, and others. Electronic assemblies, such as television sets and radios, may not have to operate in vibration environments, but they have to survive vibration when they are being transported from the manufacturer to the consumer in various types of shipping crates.

There are two basic types of vibration: sinusoidal (or sine) and random excitation. Sine vibration, or simple harmonic motion, repeats itself, but random motion does not.

Vibration-induced failures are often caused by the relative motion that develops between the electrical lead wires and the PCB, when the PCB is excited at its resonant frequency, as shown in Figure 27.1. The resonant frequency of the PCB must be determined in order to obtain the approximate fatigue life relations.

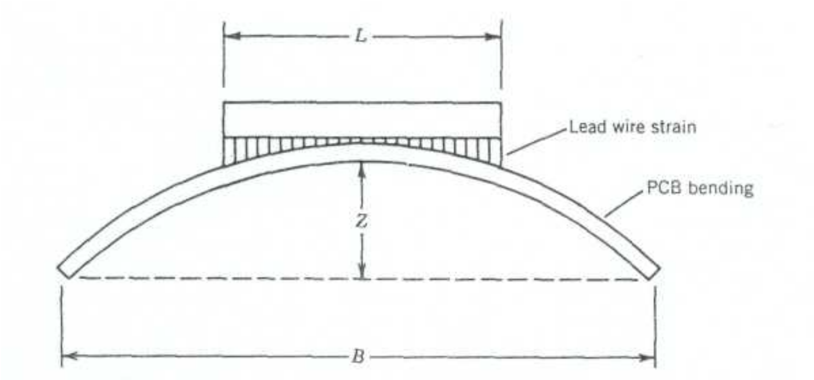

Figure 27.1 Relative motion in the lead wires of a large component due to the flexing of the PCB at its resonant frequency

26.4 PCB resonant Frequency

The resonant frequency of a plug-in type of PCB can be determined by considering it to be similar to a flat rectangular plate with four sides which can be clamped, or simply supported, or free, or any combination of these conditions. When a uniform load is distributed across the surface, and all four sides are assumed to be simply supported (or hinged), the resonant frequency can be obtained from Equation 27.1.

$$f_n = \frac{\pi}{2}\sqrt{\frac{D}{\rho}}\left(\frac{1}{a^2}+\frac{1}{b^2}\right) \quad \text{expected PCB resonant frequency} \tag{27.1}$$

$$D = \frac{Eh^3}{12(1-\mu^2)} \quad \left(\frac{\text{flexural stiffness}}{\text{in}}\right) \tag{27.2}$$

$$\rho = \frac{W}{gab} \quad \text{(mass per unit are)} \tag{27.3}$$

Where:
E = modulus of elasticity, Ib/in^2
h = thickness of PCB, in
μ = Poisson's ratio, dimensionless
W = Weight of assembly, Ib
g = 386 in/sec^2, acceleration of gravity
a = PCB length, in
b = PCB width, in

Example: Determine the resonant frequency of a rectangular plug-in epoxy fiberglass PCB simply supported (or hinged) on all four sides, 0.080 in thick, with a total weight of 1.2 pounds, as shown in Figure 27.2.

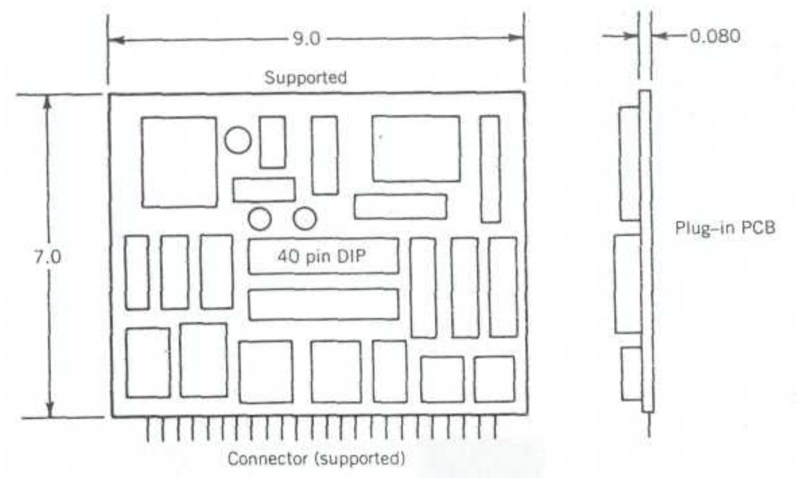

Figure 27.2 Plug-in PCB supported (hinged) on all four sides

Solution:
The following information is required for a solution:
E = 2 x 10^6 Ib/in^2 (epoxy fiberglass modulus of elasticity)
h = 0.080 in (PCB thickness)
μ = 0.12 (Poisson's ratio, dimensionless)
W = 1.2 Ib (weight)
a = 9.0 in (PCB length)
b = 7.0 in (PCB width)
g = 386 in/sec^2 (acceleration of gravity)

Substitute in Equations 27.2 and 27.3 yields to

$$D = \frac{(2 \text{ x } 10^6)(0.08)^3 h^3}{12(1-(0.12)^2)} = 86.6 \quad \text{Ib in} \quad \text{(stiffness)}$$

$$\rho = \frac{1.2}{(386)(9)(7)} = 0.493 \text{ x}10^{-4} \quad \frac{\text{Ibsec}^2}{\text{in}^3}$$

Substitute in Equations 27.1 to get the resonant frequency of PCB.

$$f_n = \frac{\pi}{2}\sqrt{\frac{86.6}{0.493 \text{ x } 10^{-4}}}\left(\frac{1}{(9)^2} + \frac{1}{(7)^2}\right)$$
$$= 68.2 \text{ HZ}$$

27.2 Desired PCB Resonant Frequency for Sinusoidal Vibration

Extensive electronic vibration testing data and analysis techniques, using finite element methods (FEM), have shown that the fatigue life of many types of electronic components can be related to the dynamic displacements developed by the PCBs. These studies have shown that the component lead wires and solder joints will fail long before any failures occur in the printed circuit etched copper traces on the PCB. These studies also showed that the electronic components can achieve a fatigue life of about 10 million stress reversals in a sinusoidal vibration environment when the peak single-amplitude displacement of the PCB is limited to the value shown in Equation 27.4 for PCBs excited at their resonant condition, as shown in Figure 27.1, when the component is mounted at the center of the PCB.

$$Z = \frac{0.00022B}{Chr\sqrt{L}} \quad \text{(maximum desired PCB displacement)} \qquad (27.4)$$

Where:
B = length of PCB edge parallel to component, in
L = length of component body, in
h = height, or thickness of PCB, in
C = component type
 = 1.0 (for standard DIP or a standard pin grid array)
 = 1.26 (for a side-brazed DIP, hybrid, or pin grid array; two parallel rows of wires extending

 from the bottom surface of the component.)
 = 2.25 (for a leadless ceramic chip carrier (LCCC))
r = relative position factor = 1.0 at center of PCB
 = 0.5 at 1/4 point on X axis and 1/4 point on Y axis

The maximum single-amplitude displacement expected at the center of the PCB during the resonant condition can be obtained by assuming the PCB acts like a single-degree-of-freedom system, as shown in the following equation:

$$Z = \frac{9.8G}{f^2} = \frac{9.8G_{in}Q}{f_n^2} \tag{27.5}$$

Where:
Q = transmissibility (Q) of the PCB
G = Peak input acceleration level of vibration
The transmissibility (Q) of the PCB at its resonance can be approximated by the following relation:

$$Q = \sqrt{f_n} \tag{27.6}$$

The minimum desired PCB resonant frequency that will provide a component fatigue life of about 10 million stress cycles can be obtained by combining Equations. 27.4. through 27.6. Yields to:

$$f_d = \left[\frac{9.8G_{in}Chr\sqrt{L}}{0.00022B}\right]^{2/3} \quad \text{(mimimum desired PCB resonant frequency)} \tag{27.7}$$

Example: A 40 pin DIP (Dual inline package, electronic equipment) with standard lead wires, 2.0 in length will be installed at the center of a 9.0 x 7.0 x 0.080 in plug-in PCB. The DIP will be mounted parallel to the 9 in edge. The assembly must be capable of passing a 5.0G peak sine vibration qualification test with resonant dwell conditions. Determine the minimum desired PCB resonant frequency for a 10 million cycle fatigue life, and the approximate fatigue life.

Solution:
B = 9.0 in (length of PCB parallel to component)
h =0.080 in (PCB thickness)
L = 2.0 in (length of a 40 pin DIP)
C =1.0 (constant for standard DIP geometry)
G = 5.0 (peak input acceleration level)
r = 1.0 (for component at the center of the PCB)

Substitute into Equation 27.7 for the desired PCB frequency

$$f_d = \left[\frac{(9.8)(5.0)(1.0)(0.08)(1.0)(\sqrt{2.0})}{(0.00022)(9.0)}\right]^{2/3} = 198.6 \text{ Hz}$$

The approximate fatigue life for 10 million cycles will be

$$\text{Life} = \frac{10\text{x}10^6 \text{ cycles to fail}}{(198.6 \text{ cycles/sec})(3600 \text{ sec/hr})} = 14 \quad \text{hr}$$

27.3 Random Vibration Fatigue Life

Random vibrations are nonperiodic in nature. Knowledge of the past history cannot be used to predict the precise magnitude of displacement or acceleration, but it is adequate to predict the probability of occurrences of these parameters.

Displacements and accelerations are typically expressed in terms of root mean square (rms) values, which follow the Gaussian or normal distribution patterns.

The method for designing PCBs for random vibration is very similar to the method used for sine vibration. The same equation can be used for the maximum allowable displacement Equation. 27.4. The expected displacement of the PCB is shown by Equation 27.5, and the approximate transmissibility Q is shown by Equation 27.6. One other equation is required, which is the response of the PCB to the random vibration input. This is shown below.

$$G_{rms} = \sqrt{\frac{\pi}{2} PfQ} \quad \text{(PCB response)} \tag{27.8}$$

Where:
P = power spectral density input = G^2/Hz at the PCB resonant frequency
f = resonant frequency of the PCB = Hz
Q = transmissibility of PCB at its resonance

Combining Equations 27.4, 27.5, 27.6, and 27.8 results in the minimum desirable PCB resonant frequency to achieve a 20 million cycle fatigue life for the components mounted on the PCB.

$$f_d = \left[\frac{29.4Chr\sqrt{(\pi/2)PL}}{0.00022B}\right]^{0.8} \quad \text{(mimimum desired PCB resonant frequency)} \tag{27.9}$$

Example: A 40 pin DIP with side-brazed lead wires with 2.0 in length is to be soldered to an 8.0 x 10.0 x 0.10 in plug-in PCB. The DIP will be mounted at the center of the PCB, parallel to the 8.0 in edge. The PSD (power spectral density) random vibration input is expected to be fiat at 0.075 G^2/Hz in the area of the PCB resonance. Find the minimum desired PCB resonant frequency for a 20 million cycle fatigue life. Also determine the expected fatigue life of the DIP lead wires.

Solution:
C = 1.26 (component type for side-brazed DIP)
h = 0.100 in (thickness of PCB)
r = 1.0 (for component at the center of the PCB)
L = 2.0 in (body length of a 40 pin DIP)
P = 0.075 G /Hz (power spectral density input)
B = 8.0 in (length of PCB edge parallel to DIP)

Substitute into Equation. 27.9 to determine the minimum desired PCB resonant frequency

$$f_d = \left[\frac{(29.4)(1.26)(0.10)(1.0)(\sqrt{(\pi/2)(0.075)(2)})}{(0.00022)(8.0)} \right]^{0.8} = 255.5 \text{ Hz}$$

The approximate fatigue life for 20 million cycles will be

$$\text{Life} = \frac{20\text{x}10^6 \text{ cycles to fail}}{(255.5 \text{ cycles/sec})(3600 \text{ sec/hr})} = 21.8 \quad \text{hr}$$

27.4 Miner's Cumulative Damage Fatigue Ratio

Every time a structural element experiences a stress cycle, a small part of the fatigue life is used up. When all of the life is used up, the structure can be expected to fail. This simple theory is widely used to determine the approximate fatigue life of structures operating in environments that produce stress reversals. The damage that is accumulated is assumed to be linear, so the damage developed in several different environments can simply be added together to obtain the total damage to determine if the part will fail. This is known as Miner's rule, or Miner's cumulative damage ratio R, which is defined below.

$$R = \frac{n_1}{N_1} + \frac{n_2}{N_2} + \frac{n_3}{N_3} + \ldots\ldots\ldots\ldots = 1 \qquad (27.10)$$

Where:
n = actual number of fatigue stress cycles accumulated at stress levels 1, 2, 3...
N = number of fatigue stress cycles required to produce a failure at stress levels 1, 2, 3…

Different fatigue cycle ratios are often used for different applications, depending upon how the electronic product will be used. For commercial electronic systems that have no involvement with the public safety, an R value of 1.0 is suggested. Where the public safety is involved, as in an airplane, train, or automobile, then an R value of 0.7 is suggested. Where a critical life system, such as a space shuttle, is involved, a higher safety factor is recommended, so an R value of 0.3 is suggested.

Example: A communication system contains many throughhole mounted resistors similar to those shown in Figure 25.6, for the sample problem described in Section 25.4. Determine if the solder joints on these resistors are capable of reliable operation after exposure to the following temperature cycling conditions.

A) Five years of storage (nonoperating) where the average daily temperature change within the electronics system is expected to vary from a low of 10 °C to a high of 40 °C.

B) Four years of electrical operation where the system is turned on twice a day, once in the morning and once in the afternoon, for about 1 hr. The average temperature in the system is expected to vary from a low of 20 °C to a high of 80 °C.

Solution:
Miner's cumulative fatigue damage method will be used to obtain the fatigue cycle ratio R for the three conditions shown above. The method of solution is to assume the stresses in the solder joints follow linear laws, so the stresses determined in the sample problem of Section 25.4 can be modified by a direct ratio of the temperature variations.

The temperature changes that will be used to determine the stress levels in the solder joints are as follows:

Condition A $\Delta t = (40°C - 10°C)/2 = 15\ °C$
Condition C $\Delta t = (80°C - 20°C)/2 = 30\ °C$

The actual number of thermal cycles (n) accumulated at each stress level must be divided by the number of stress cycles that are required to produce a failure (N) at each stress level, to obtain Miner's cumulative fatigue damage ratio R shown in Equation 27.10.

Solution: Condition A

The solder joint stress can be determined by using a ratio of the temperature change for the solder joint stress level of 1063 psi and the 60 °C temperature rise shown in Equation 25.9. For the temperature rise of 15 °C for condition A, the solder join shear tear-out stress will be as follows:

$$S_{St} = \frac{15}{60}(1063) = 266 \text{ Ib/in}^2$$

The actual number of stress cycles that will be accumulated in the five years of storage is based upon one thermal cycle per day for five years.

$$n_A = (1 \text{ cycle/day})(365 \text{ days/year})(5 \text{ year}) = 1825 \text{ cycles}$$

The number of stress cycles required to produce a failure in the solder joint can be determined with the use of Equation 26.4 with b = 2.5 as follows:

$$N_A = (80000)\ (200/266)^{2.5} = 39216 \text{ cycles to fails}$$

Miner's cumulative fatigue damage ratio for condition A is:

$$R_A = n_A / N_A = 1825/39216 = 0.046$$

Solution: Condition B
The solder joint stress can be determined by using a ratio of the temperature change for the solder joint stress level of 1063 psi and the 60 °C temperature rise shown in Equation 25.9. For the temperature rise of 30 °C for condition B, the solder join shear tear-out stress will be as follows:

$$S_{St} = \frac{30}{60}(1063) = 531 \text{ Ib/in}^2$$

The actual number of stress cycles that will be accumulated in the four years of operation is based upon two thermal cycles per day for four years.

$$n_B = (2 \text{ cycle/day})(365 \text{ days/year})(4 \text{ year}) = 2920 \text{ cycles}$$

The number of stress cycles required to produce a failure in the solder joint can be determined with the use of Equation 26.4 with b = 2.5 as follows:

$$N_B = (80000)\ (200/531)^{2.5} = 6965 \text{ cycles to fails}$$

Miner's cumulative fatigue damage ratio for condition B is:

$$R_B = n_B / N_B = 2920 / 6965 = 0.419$$

Substitute into Equation 27.10 for Miner's system cumulative fatigue damage ratio. Yields to:

$$R = R_A + R_B = 0.046 + 0.419 = 0.465$$

Since Miner's ratio less than the maximum allowable value of 1.0 as defined in Equation 27.10, the design is acceptable.

27.5 Electronic Systems Operating in Combined Environments

Electronic assemblies are often required to operate in areas exposed to vibration and temperature cycling at the same time. Some typical industries include airplanes, automobiles, trucks, trains, missiles, atomic power plants, paper mills, steel mills, oil drilling, petroleum processing, washing machines, ships, submarines, communication systems, portable computers, and many others. Miner's cumulative damage indicates that anytime a structural element is subjected to a stress cycle, a small part of its life is used up. It does not matter if the stress is due to vibration or to thermal cycling, since they can both produce failures when the stress levels and the number of stress cycles reach a critical combination.

Miner's cumulative fatigue damage ratio is convenient to use for combining the damage generated in vibration and in thermal cycling environments. The use of this ratio is demonstrated with a sample problem.

Example: An electronic controlled brake unit on an overhead rail car delivery system must provide a 15 year operational life. The car operates on a track system for 6 hours a day, 5 days per week, and 52 weeks per year. Test data on the track show sinusoidal vibration is present with a peak acceleration input level of 0.7 G over a frequency band from 10 to 500 Hz. The rail car is also required to enter a paint drying hot room for about one hour, three times a day, and 5 days a week for the same 15 year period. The hot room is maintained at a temperature that is 60 °C above the factory floor temperature.

An examination of the various components on the various PCBs shows that the most critical component is a poke-through hybrid at the center of several PCBs, as shown in Figure 27.3. Determine if the proposed design will meet the operating requirements.

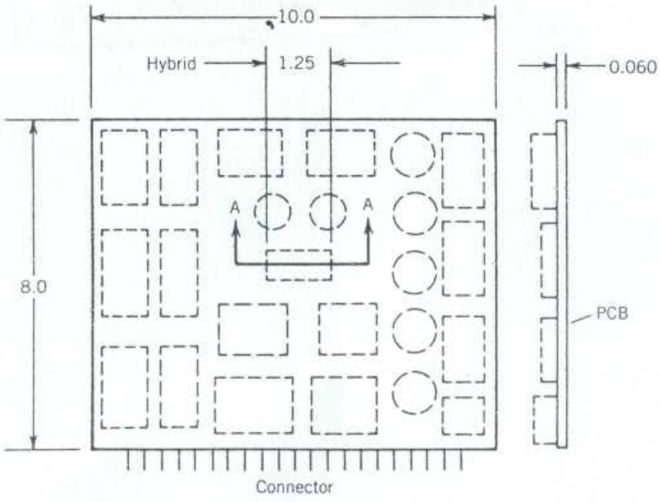

Figure 27.3 Throughhole mounted hybrid located at the center of the PCB

Solution:
Extensive testing of PCBs with throughhole mounted components shows that the electrical lead wires will fail more often than the solder joints during vibration. (For surface mounted components supported by electrical lead wires, vibration tests show that the numbers of wire failures are about the same as the number of solder joint failures.)

Thermal cycling test data for PCB expansions in the X-Y plane show that large throughhole mounted components will experience more solder joint failures than electrical lead wire failures.

In this sample problem the vibration fatigue life of the lead wires and solder joints were evaluated first. The thermal fatigue life of the wires and solder joints were determined next. Miner's cumulative damage index was then used to add up the total damage accumulated in the lead wires and solder joints. The worst-case conditions for the lead wires and the solder joints were combined to obtain a conservative estimate of the system fatigue life.

Solution: Track system vibration
The desired PCB resonant frequency necessary to achieve the approximate fatigue life of 10 million stress reversals in the sinusoidal vibration environment can be determined for the most critical hybrids by using Equation 27.7 when the hybrids are mounted at the center of the PCB.

Given:
C= 1.26 (component parameter for straight wires)
h = 0.060 in (PCB thickness)
r = 1.0 (relative position, component at center of PCB)
G = 0.7 G (peak sine vibration input acceleration)
L = 1.25 in (length of component)
B = 10 in (length of PCB parallel to component)

$$f_d = \left[\frac{(9.8)(0.7)(1.26)(0.06)(1.0)(\sqrt{1.25})}{(0.00022)(10)}\right]^{2/3} = 42 \text{ Hz}$$

The 42 Hz represents the desired resonant frequency the PCB must have to achieve an approximate fatigue life of 10 million fatigue cycles for the most critical electronic component. The minimum vibration life required for the electronic system can be determined from the duty cycle expected over the 15 year life span of the equipment on the rail car delivery system.

The minimum vibration life requirement for the electronic unit on the track system is as follows:

$$\text{Life} = (6 \text{ hr/day})\ (5 \text{ day/wk})\ (52 \text{ wk/year})\ (15 \text{ year}) = 23400 \text{ hr}$$

When the electronic unit has a resonant frequency of 42 Hz, and the most critical component has an approximate fatigue life of 10 million cycles, the lifetime is expected to be:

$$\text{Life} = \frac{10\text{x}10^6 \text{ cycles to fail}}{(42 \text{cycles/sec})(3600 \text{ sec/hr})} = 66.1 \quad \text{hr}$$

Since the 42 Hz PCB resonant frequency will only provide a component lead wire fatigue life of about 66.1 hr, and since the desired fatigue life must be greater than 23,400 hr, the 42 Hz PCB resonant frequency is not adequate. The PCB resonant frequency must be much higher, since a higher resonant frequency results in smaller dynamic displacements, which will rapidly increase the fatigue life.

The sinusoidal vibration acceleration response of the PCB for a 42 Hz resonant frequency is obtained using Equation 27.5.

Given:
G_{in} = 0.7 (peak acceleration input)
f_n = 42 Hz (PCB resonant frequency for 10 million cycle fatigue life)
$Q = \sqrt{42}$ = 6.5 (approximate PCB transmissibility)
$G_{out} = G_{in}Q = (0.70)\ (6.5) = 4.5$ (peak acceleration response of PCB)

The peak single-amplitude response displacement of the PCB for the 10 million cycle life and the 42 Hz resonant frequency can now be determined for the sinusoidal vibration as follows:

Given:
Gout = 4.5 (peak acceleration response of PCB)
f_n = 42 Hz (PCB resonant frequency)

$$Z = \frac{9.8(4.5)}{(42)^2} = 0.025 \text{ in} \qquad \text{(peak displacement)}$$

This provides a 10 million cycle life, which is equal to a life of 66.1 hr. This is not adequate. Therefore, a higher PCB resonant frequency is required to reduce the displacement.

Assumption of component fatigue life for a 95 HZ PCB resonant frequency
Since a 42 Hz PCB resonant frequency was shown to be too low, a higher value must be used. Assume a PCB resonant frequency of 95 Hz to start the revised analysis. If the results are not acceptable, another PCB resonant frequency can be assumed and the process repeated until an acceptable solution is obtained.

The peak acceleration response of the PCB can be determined for the sinusoidal vibration as follows:

$$G_{out} = G_{in}Q$$

Where:
$G_{in} = 0.7$ (peak acceleration input)
$f_n = 95$ Hz (PCB resonant frequency, assumed to start)
$Q = \sqrt{95} = 9.7$ (approximate PCB transmissibility)
$G_{out} = (0.7)\ (9.7) = 6.8$ (peak acceleration response)

The peak displacement of the PCB with the 95 Hz resonant frequency can be obtained from Equation 27.5 for the sine vibration.

Given:
$G_{out} = 6.8$ (peak acceleration response of PCB)
$f = 95$ Hz (PCB resonant frequency assumed to start)

$$Z = \frac{9.8(6.8)}{(95)^2} = 0.0074 \text{ in} \quad \text{(peak)}$$

The fatigue life of the component lead wire in the vibration environment can be determined with Equation 26.4. Assuming a linear system, the stress value S can be replaced with the displacement value Z. The b exponent includes a stress concentration of 2.0.

$$N_1 Z_1^b = N_2 Z_2^b$$

Where:
$N_2 = 10 \times 10^6$ (cycles for lead wire to fail when PCB resonant frequency is 42 Hz)
$Z_1 = 0.0074$ in (peak PCB displacement, for 95 Hz frequency)
$Z_2 = 0.025$ in (peak PCB displacement, for 42 Hz frequency)
$b = 6.4$ (fatigue exponent for electrical lead wires, which includes a stress concentration of 2.0)

$$N_1 = 10 \times 10^6\ (0.025/0.0074)^{6.4} = 2.42 \times 10^{10} \text{ cycles to fails}$$

The actual number of fatigue cycles that will be accumulated by the 95 Hz PCB resonant frequency during operation in the sine vibration environment for 23,400 hr, can be determined as follows:

$$n = (95 \text{ cycles/sec})\ (3600 \text{ sec/hr})\ (23400 \text{ hr})$$

$= 8 \times 10^9$ Actual cycles accumulated

The Miner's damage index for the sinusoidal vibration due to the rail car operation on the track system is:

$$R = n / N = (8 \times 10^9) / (2.42 \times 10^{10}) = 0.331 \text{ (vibration ratio)}$$

This vibration fatigue cycle ratio looks good at this time. Some parameters may have to be changed later, depending upon the value obtained from the thermal cycle fatigue environment.

Solution: Thermal cycle fatigue environments

Figure 27.3 shows a hybrid component in a kovar case, flow-soldered to a through-hole epoxy fiberglass PCB. Differences in the thermal coefficients of expansion (TCE) between the kovar and the PCB will produce expansion differences that will force the electrical lead wires in the component to bend as shown in Figure 27.4, at the high-temperature end of the cycle. This will induce bending stresses in the wires and shear tear-out stresses in the solder joints.

The temperature in the electronics section is not expected to stabilize for a long enough period to allow the solder joint stresses to completely relax to a strain-free condition. Under these circumstances, the neutral point to the high or low temperature will be half the peak-to-peak temperature.

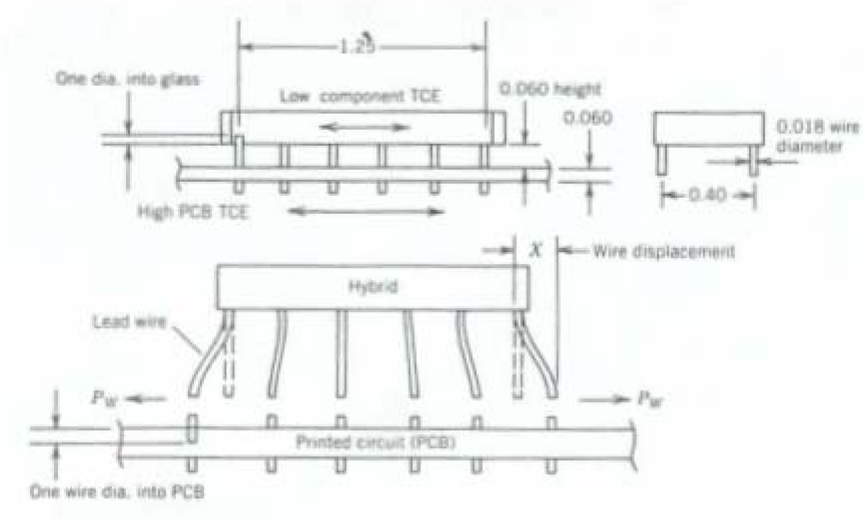

Figure 27.4 Cross section A-A of the hybrid shown in Figure 27.3, where the end lead wires are forced to bend due to differences in the expansions of the hybrid and the PCB

The difference in the thermal expansion between the hybrid and the PCB in the X-Y plane can be determined from Equation 25.1. The subscripts H and P now refer to the hybrid and the PCB.

$$X = (a_p - a_H) d_H \, \Delta t = \text{in} \quad \text{(expansion difference)}$$

Where:
a_P = TCE of epoxy fiberglass PCB in X-Y plane
= 15 x 10^{-6} in/in/°C
a_H = 6 x 10^{-6} in/in/°C (TCE of hybrid kovar case)
$d_H = \sqrt{\frac{(1.25)^2 + (0.4)^2}{2}}$ = 0.65 in (effective diagonal length of hybrid body)
Δt = 60°C (temperature of hot room above factory floor)

Δt =60 /2 = 30°C (neutral point to high and low value for a rapid temperature cycle)

$$X = (15\text{-}6) \times 10^{-6} (0.65)(30) = 0.000175 \text{ in}$$

The horizontal force developed in the electrical lead wires as they are forced to bend through this deflection can be determined from the wire geometry as shown in following equation.

$$P_W = \frac{12 E_W I_W X}{L_W^3} \quad \text{Ib} \tag{27.11}$$

Where:
Ew = 20 x 10^6 Ib/in^2 (modulus of elasticity, kovar wire)
d = 0.018 in (wire diameter)
$I_W = \frac{\pi (0.018)^4}{64} = 5.15 \times 10^{-9}$ in^4 (moment of inertia of lead wire)
L_W = 0.060 in (plus one diameter into PCB and hybrid)
Lw = 0.060 + 0.018 + 0.018 = 0.096 in (wire length)
X = 0.000175 in (wire deflection)

$$P_W = \frac{12(20 \times 10^6)(5.15 \times 10^{-9})(0.000175)}{(0.096)^3} = 0.244 \text{ Ib}$$

The bending moment in the wire and solder joint can be determined by taking the moments about either end of the wire.

$$M = P_W L_W / 2 \text{ (bending moment, Ib in)}$$

Where:
Pw = 0.244 lb
Lw = 0.096 in

$$M = (0.244)(0.096)/2 = 0.0117 \text{ Ib in}$$

Substitute into Equation 25.4 to obtain the lead wire bending stress. A stress concentration of 1.0 is used to start, since the number of thermal stress cycles accumulated is usually not enough to produce a fatigue failure unless there are sharp cuts in the wire at the high stress areas. A stress concentration of 2 will be used later for a conservative evaluation of the fatigue life.

Given:
M = 0.0117 lb in (bending moment in wire)
C = 0.018/2 = 0.009 in (wire radius)
$I_w = 5.15 \times 10^{-9}$ in4 (wire moment of inertia)

$$S_b = \frac{(1.0)(0.0117)(0.009)}{5.15 \times 10^{-9}} = 20447 \ \ \mathrm{Ib/in^2}$$

The number of stress cycles required to produce a failure in the electrical lead wire can be determined from the fatigue curve for kovar wire as shown in Figure 27.5. Considering a worst-case condition, where a stress concentration value of 2 exists at the highest stress point on the wire, the stress in the wire will be about 40,900 psi. The number of cycles (N) required producing a failure in the kovar lead wires will be as follows:

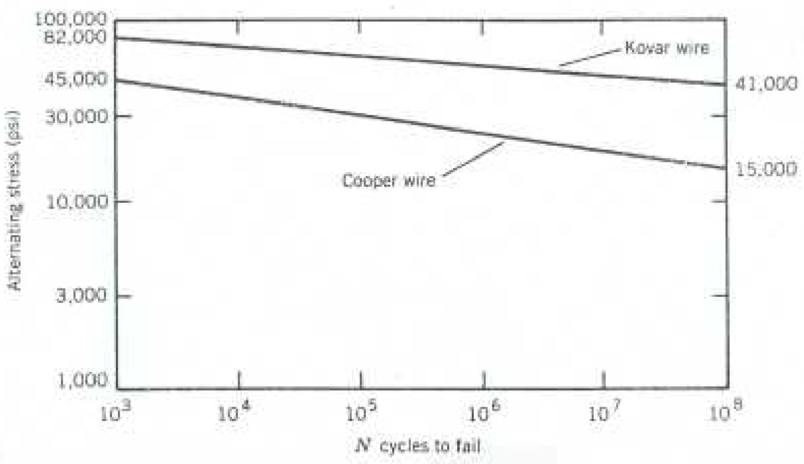

Figure 27.5 Alternating stress fatigue curves for kovar and copper wires with no stress concentrations

$$N = 100 \times 10^6 \text{ cycles for wire to fail}$$

The actual number of thermal cycles (n) expected over the 15 year life can be determined as follows:

$$n = (3 \text{ cycle/day}) (5 \text{ day/wk}) (52 \text{ wk/year}) (15 \text{ year})$$
$$= 11700 \text{ actual thermal cycles expected}$$

Miner's rule can be used to find the fatigue cycle ratio for the lead wire for the thermal cycling condition.

$$R_2 = n / N = 11700 / 100 \times 10^6 = 0.00017 \text{ (wire thermal cycle ration)}$$

This damage accumulation in the lead wires due to thermal cycling is very small compared with the damage obtained from the vibration environment, so it is ignored.

The solder joint shear tear-out stress value can be obtained from Equation 25.9. The solder joint height is based upon the PCB thickness only, assuming there are no solder joint fillets at the top or bottom surfaces of the PCB. The shear tear-out area in the solder joint is based upon the average diameter of the solder joint. This is the average of the 0.018 in wire diameter and a PTH diameter of 0.038 in, resulting in a 0.028 in average diameter.

Given:
M = 0.0117 Ib in (overturning moment)
h = 0.06 in (PCB thickness, ignoring solder fillets)
$A_S = \dfrac{\pi(0.028)^2}{4} = 0.000616 \text{ in}^2$ (solder area)
Substitute into Equation 25.9 for the solder shear tear-out stress level.

$$S_{ST} = \frac{0.0117}{(0.06)(0.000616)} = 316 \frac{\text{Ib}}{\text{in}^2}$$

The approximate number of stress cycles required to produce a failure in the solder joint can be determined from Equations 26.4 and Figure 27.2.

Given:
N_2 = 250 cycles to fail (solder reference point)
S_2 = 2100 Ib/in^2 (solder stress reference point)
S_1 = 316 Ib/in^2 (solder stress)

$$N_1 = 250(2100/316)^{2.5} = 28462 \text{ cycles to fail}$$

Miner's rule can be used to find the fatigue cycle ratio for the solder is:

$$R_3 = n / N = 11700 / 28462 = 0.411 \text{ (solder thermal cycle ratio)}$$

The total damage ratio accumulated during the vibration and thermal cycling is:

$$R = 0.331 + 0.411 = 0.742$$

Although this value is slightly over the maximum acceptable level of 0.7, where public safety is involved the design can be considered safe because the combined damage ratio was very conservative.

Part F: Practical Applications

Indicative Contents

- **Fan-Cooled Enclosure of a PC System**
- **Flow over a Heat Sink**

28. Fan-Cooled Enclosure of a PC System

28.1 Objective

Design of airflow in PC systems is an important problem in electronics packaging. Flow Network Analysis using hand calculations or spreadsheets has been traditionally employed for the prediction of airflow distribution in computer systems. Such analyses are not general in nature and cannot be easily adapted for different types of systems. Ellison [1] has used the network modeling approach for the calculation of air flow in a fan cooled PC system. In the present study, we have repeated this analysis using MacroFlow to illustrate the ease with which the model can be constructed and the speed with which results are obtained. MacroFlow, with its easy-to-use graphical frame work and a generalized network solution methodology, enables use of Flow Network Modeling for expedited airflow design of computer systems.

28.2 Physical System

The physical system of interest is a fan-cooled enclosure containing a Printed Circuit Board (PCB) array and Power Supply. The system configuration represents a computer system package that is typical for personal computers and workstations. A schematic of the configuration is shown below.

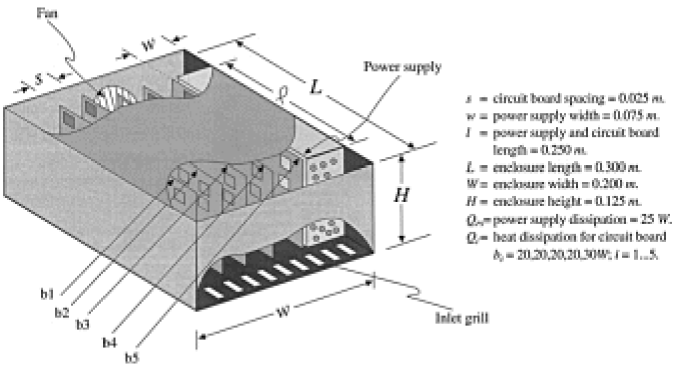

Figure 28.1 Fan-cooled enclosure containing a Printed Circuit Board array and Power Supply

The air flow is driven by an exhaust fan positioned at the back of the computer housing. Air at room temperature is drawn through an inlet screen on the bottom panel of the housing, turns 90 degrees, and spreads over the frontal area of the power supply and the PCB assembly. The PCB assembly contains five boards. In addition, the power supply has a screen at its entry and exit. Air moves over these heat dissipating components and then exits the housing through the exhaust fan.

28.3 Network Representation

The network representation of the flow system is constructed by representing the various paths that the air follows using the component and link library provided in MacroFlow. This representation of the fan-cooled enclosure is shown in Figure 28.2. Important features of the network are described below.

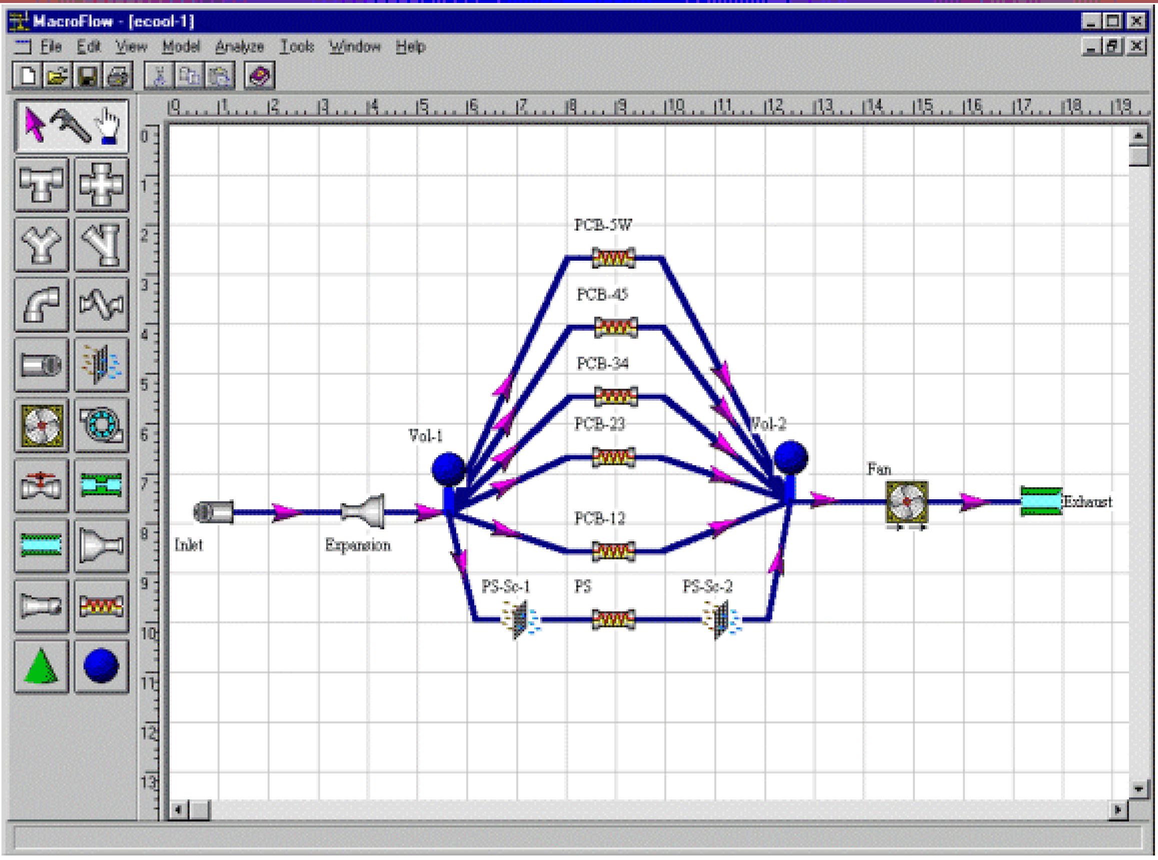

Figure 28.2 Flow network representation of the fan cooled enclosure

- The flow enters the enclosure through a slotted screen. It is represented by the Inlet/Exhaust component within the network.
- After entering the enclosure, the flow turns and faces the frontal area of the PCB array and the power supply. The network model represents the loss in total pressure and the static pressure recovery in this region using the area change component named "Expansion". The corresponding plenum upstream of the PCB and the power supply is represented by "Vol-1".
- The flow then splits into multiple streams corresponding to the passages between the cards of the PCB and the power supply. The five passages in the PCB are represented by the resistances PCB-12, PCB-23, PCB-34, PCB-45, and PCB-5W. (The resistance PCB-34 denotes the flow impedance for the passage formed by the 3rd and the 4th PCB in the array.) The power supply is embedded in a box with screens in the front and the back. These screens are represented by PS-Sc-1 and PS-Sc-2 while the power supply itself is represented by the resistance PS.
- The air streams exiting from the PCB passages and the power supply meet in the plenum named "Vol-2" upstream of the fan Ex-fan.
- The characteristics of the Ex-fan are represented using the piecewise-linear option. The fan provides a maximum head of 0.22 in of water, a maximum flow rate of 34 CFM, and follows a linear fan curve.
- The flow exits the box through the straight Inlet/Exhaust component exit.
- Each of the links connecting successive components serve to direct the flow and do not offer any resistance to flow. Therefore, all the links are zero resistance links.

28.4 Flow Impedance Characteristics

Flow resistance or impedance characteristics of various components need to be specified to complete the network specification. The flow characteristics of the PCB array and the power supply are known from empirical measurements and are expressed in the following form.

$$\Delta P = BQ^2$$

Analysis has been performed for two cases corresponding to even and uneven spacing of the cards in the array. The loss coefficient B for the Power Supply is constant in both cases and is equal to 3.5 x 10^5 Pa/ $(m^3/s)^2$. The loss coefficient for each passage of the PCB array is listed in Table 28.1. As noted above, all links simply direct the flow between components and offer no resistance to flow. The resistance of the screens at the inlet and at the Power Supply (PS-Sc-1, PS-Sc-2) are computed based on the Standard correlations provided in MacroFlow [2, 3,4]. Each of the cards is assumed to dissipate 50W of heat while the power supply dissipates 167 W.

Table 28.1 Flow characteristics of the card array

	Case I		Case II	
Flow Passage	Separation	Resistance Coefficient	Separation	Resistance Coefficient
	cm	$Pa/(m^3/s)^2$	cm	$Pa/(m^3/s)^2$
PCB-12	2.54	1.0e+5	2.54	1.0 x 10^5
PCB-23	2.54	1.0e+5	1.25	4.0 x 10^5
PCB-34	2.54	1.0e+5	1.25	4.0 x 10^5
PCB-45	2.54	1.0e+5	3.75	4.44 x 10^5
PCB-5W	2.54	1.0e+5	3.75	4.44 x 10^5

28.5 Results

The network model predicts the flow distribution and the pressure losses in all parts of the system. Figure 28.3 shows a bar chart for the volumetric flow rate in different parts of the system for Case I (equally spaced PCBs). The flow rate in each passage of the PCB array is identical and much greater than the flow rate through the power supply. This is because the power supply offers a much greater resistance to flow. The pressure losses in various components of the system are shown in Figure28.4. The pressure drop in the inlet grill is a large fraction of the overall pressure drop. The pressure drops across all PCB passages and the power supply is identical since these components are in parallel. The fan creates the head (shown by the negative pressure loss) necessary to create the flow through the enclosure. Figure 28.5 shows the bulk temperatures of the streams exiting the PCB passages and the power supply. The predicted results agree very well with the results of the model presented by Ellison [1].

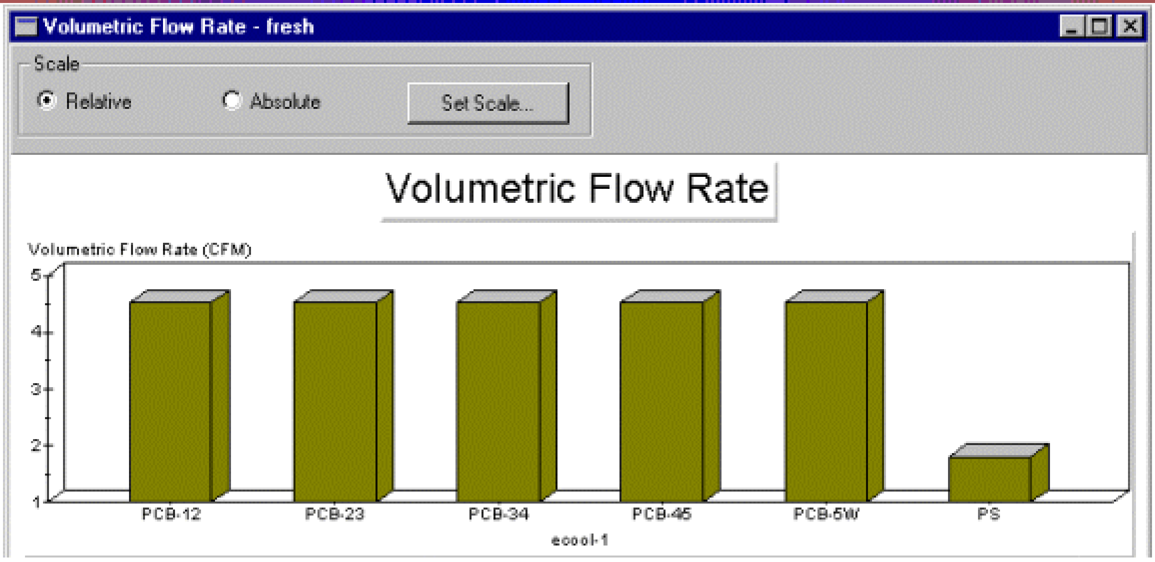

Figure 28.3 Volumetric flow rates for Case I (equally spaced PCB cards)

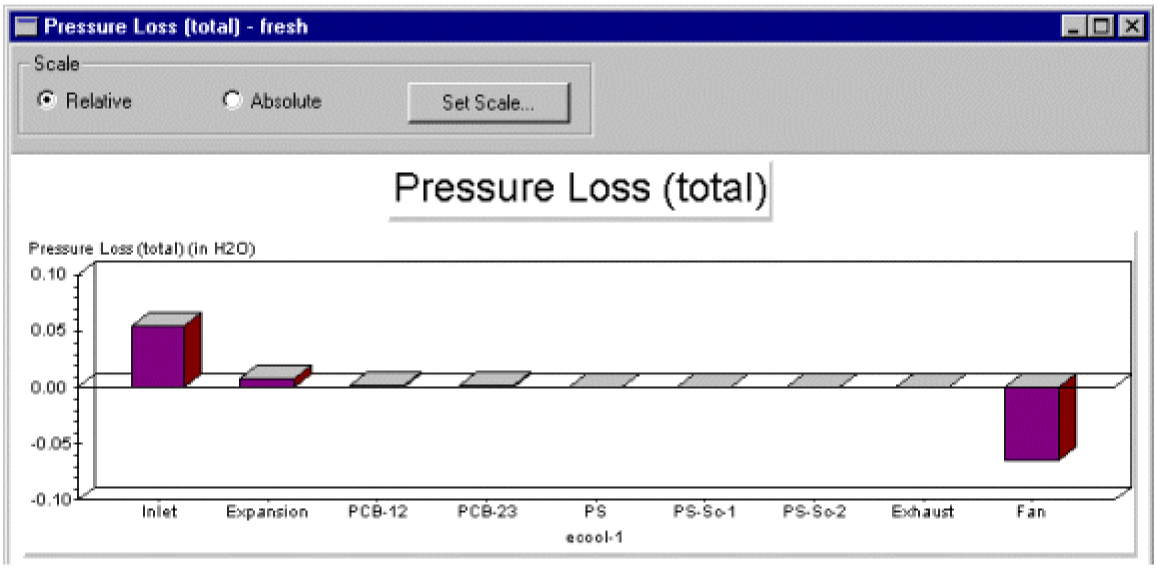

Figure 28.4 Pressure losses for Case I (equally spaced PCB cards)

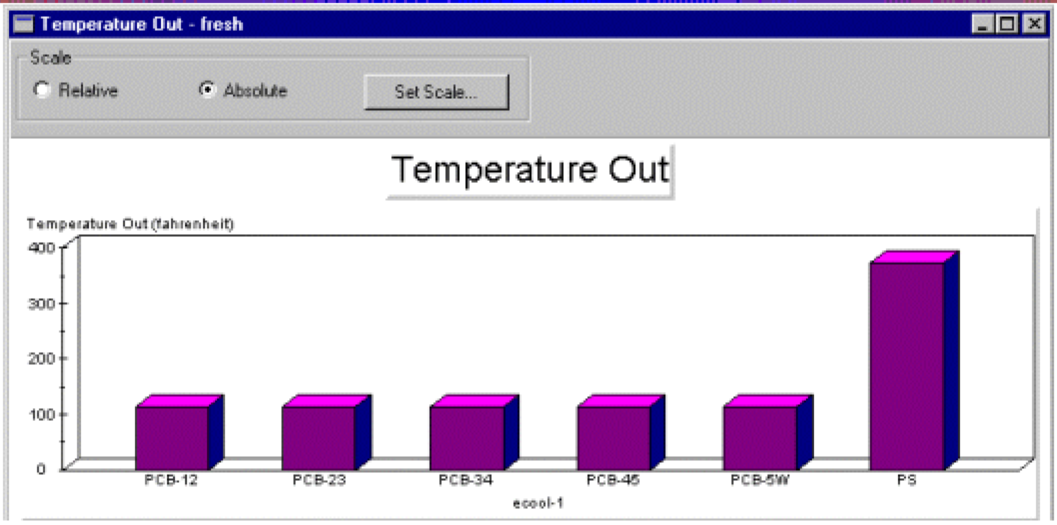

Figure 28.5 Bulk temperatures of the air streams exiting the PCB and the Power Supply for Case I (equally spaced PCB cards)

The volumetric flow rates, pressure losses, and bulk temperatures for Case II are shown in Figures 28.6 and 28.7, and 28.8 respectively. For Case II, an important feature to be observed is that the flow between the PCBs is different due to the unequal separation between them. Since the net system impedance is different than for equally spaced cards, the total induced flow is also different from the configuration with equally spaced cards in Case I. The uneven spacing of the PCBs causes uneven distribution of the bulk temperatures of the air stream exiting the PCB flow passages.

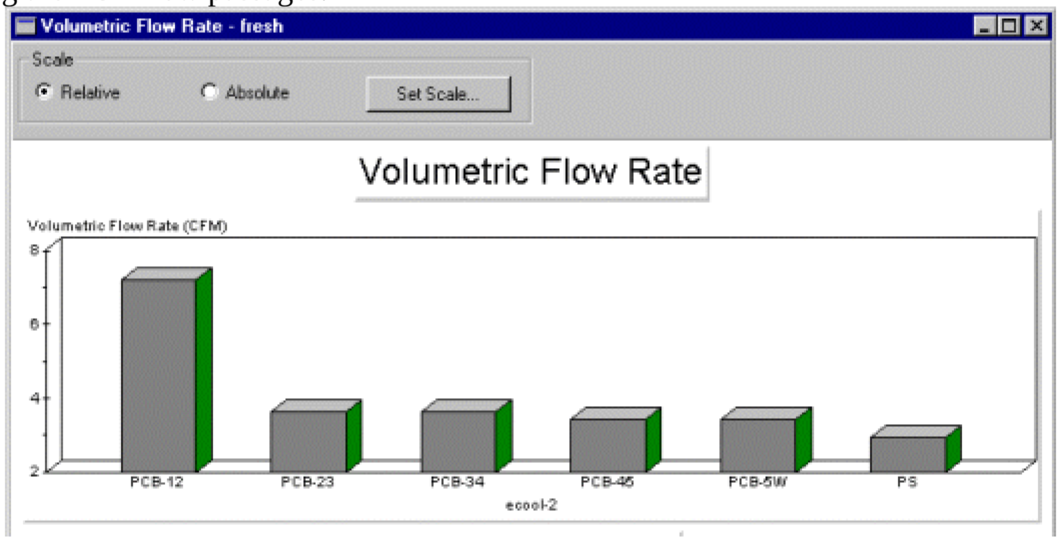

Figure 28.6 Volumetric flow rates for Case II (unequally spaced PCB cards)

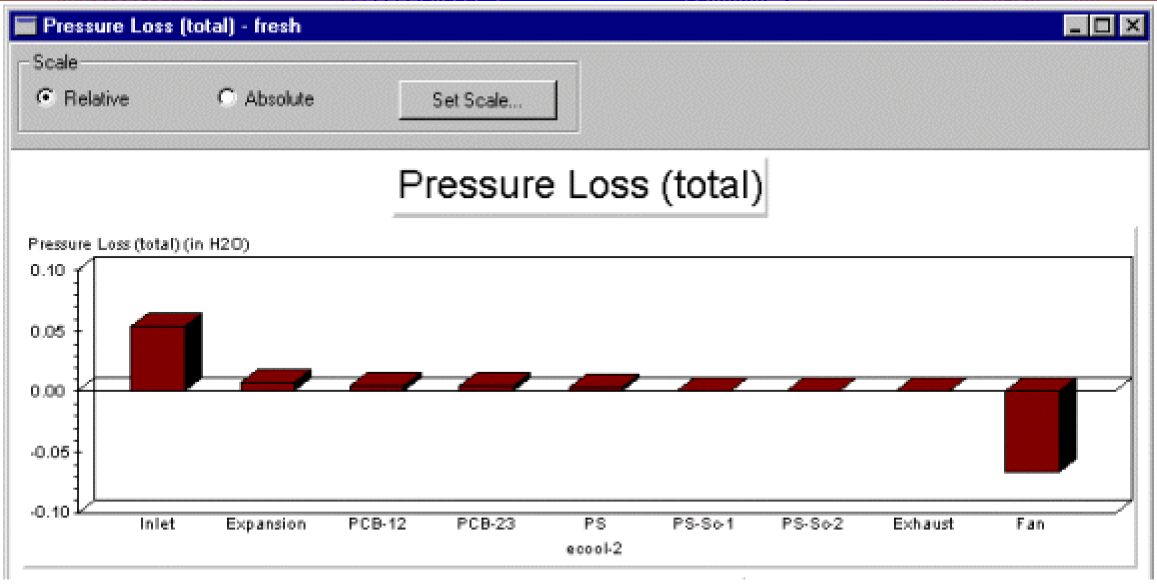

Figure 28.7 Pressure losses for Case II (unequally spaced PCB cards)

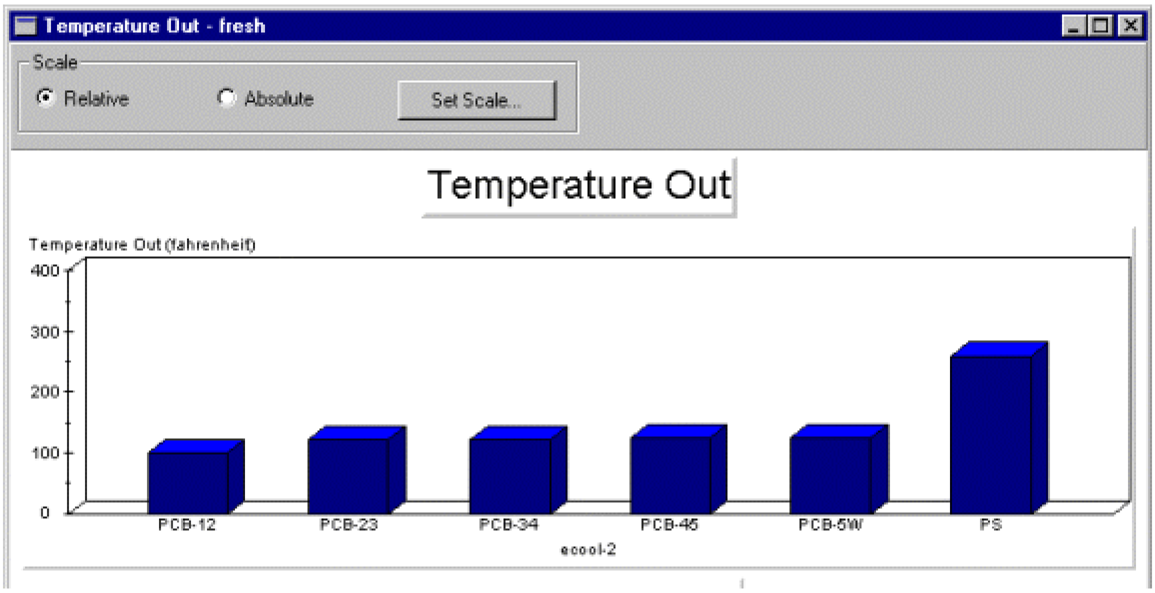

Figure 28.8 Bulk temperatures of the air streams exiting the PCB and the Power Supply for Case II (unequally spaced PCB cards)

28.6 Concluding Remarks

The above example illustrates the simplicity and the speed with which MacroFlow models of practical computer systems can be constructed for accurate predictions of system wide airflow and bulk temperature distributions. MacroFlow-based network modeling enables quick and reliable assessment of the thermal feasibility of competing system layouts and rapid analysis of what-if scenarios. Therefore, use of MacroFlow significantly shortens the overall cycle of designing practical electronic cooling systems and improves the reliability of the system package.

29. Flow over a Heat Sink

29.1 Objective

Heat sinks are mounted in circuit boards to provide additional surface area for heat loss from components that produce a high heat flux. However, heat sinks create additional resistance to flow and the result is that some of the flow bypasses them. This undesirable effect of bypass on the thermal performance of the heat generating component needs to be accurately predicted during the early design stages. Further, the effect of increased flow resistance in PCBs on overall airflow distribution needs to be accurately estimated during the conceptual design stage.

In the present study, MacroFlow is used to construct a model of a test cell used to characterize the performance of heat sinks. It includes a general network model of flow over a heat sink in the presence of bypass as proposed by Butterbaugh and Kang [1]. The predicted flow characteristics of the heat sink are compared with the experimental measurements provided by Biber [2]. The network model is extremely easy to construct, it runs very quickly, and accurately predicts the airflow distribution around the heat sink. The MacroFlow model of the heat sink can be effectively used to determine the benefit of incorporating heat sinks on the component-level thermal performance and also to predict the resulting system-level airflow distribution.

29.2 Physical System

Pressure drop and heat transfer characteristics of heat sinks are determined from wind tunnel testing as shown in Figure 29.1 [3].The heat sink is situated inside a duct (wind tunnel). Screens or perforated plates may cover the inlet and the exit of the duct. The flow within the duct is driven by a fan situated near the inlet and its rate is varied by controlling the opening of the orifice. Further, the duct size can be varied (by moving the walls or using different sized ducts) to study the effect of bypass on the performance of the heat sink. A diffuser is incorporated in the duct to recover the velocity head before the flow exits the system. The cross-sectional view of the duct with the fin sink is shown in Figure 29.2.

The fin sink, manufactured by Wakefield Engineering [2], has the following characteristics.

Table 29.1 Geometry of the fin sink manufactured by Wakefield Engineering

Dimension	Value (in)
Length	2.2
Width	4.6
Fin Height	0.75
Fin Pitch	0.1
Fin Thickness	0.012

Experiments have been carried out at Wakefield Engineering [2] for measuring the pressure drop through the heat sink over a range of air flow rates for the no bypass configuration. In the present study, a MacroFlow model for the wind tunnel test cell has been constructed for the general case of flow over the fin sink with the bypass using the methodology proposed by Butterbaugh and Kang [1]. The results of the model for the no bypass configuration have been compared with experimental measurements.

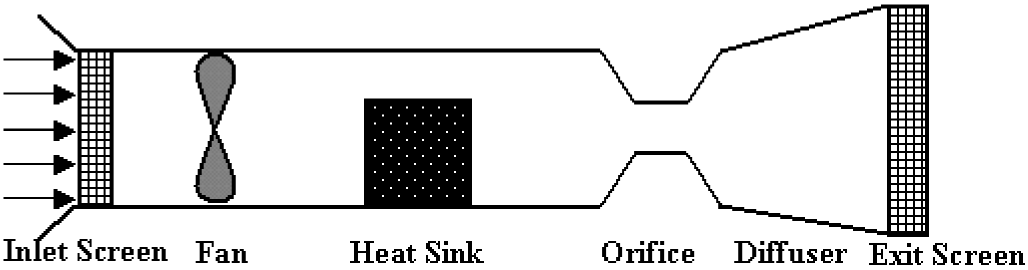

Figure 29.1The wind tunnel test cell for characterizing heat sink performance

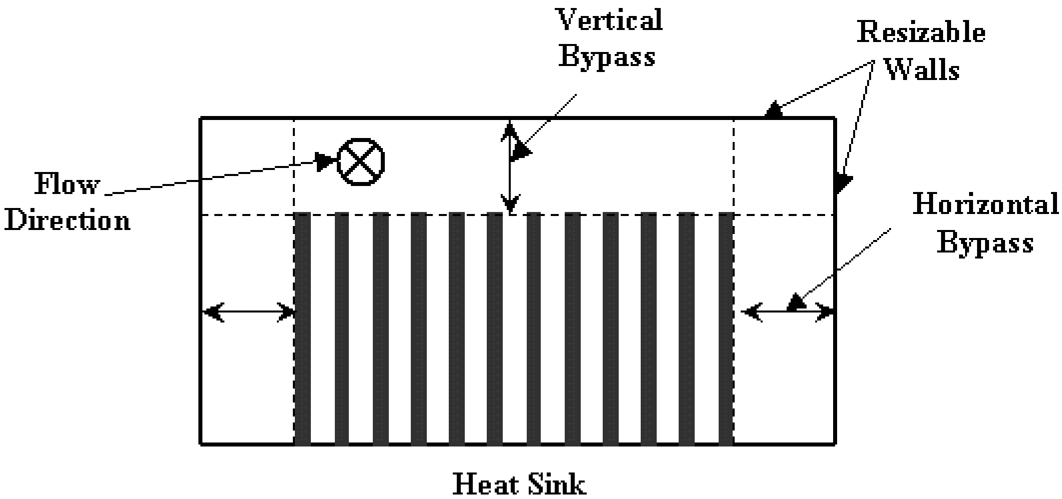

Figure 29.2 Cross-sectional view of the heat sink with bypass

29.3 Network Representation

The network representation of flow passage with the heat sink is shown in Figure 29.3. The important features of the model are as follows:

- The inlet and exit sections of the duct are represented using the Inlet/Exhaust with screen component available in MacroFlow. The screen is characterized by appropriate specification of the fractional open area and the geometry of a representative orifice.
- The fan performance curve is chosen from the library of Rotron fan characteristics provided in MacroFlow.
- The interfin spaces (a total of forty-six) are represented as channels with a rectangular cross-section. Note that as the flow enters each interfin space, it goes through an area contraction. Similarly, the flow goes through an area expansion when it exits an interfin

space. Correspondingly, the flow network contains contraction and expansion components upstream and downstream of each interfin space. A multiplier of forty-six is applied to the assembly of the contraction-interfin channel-expansion passage to signify that there are 46 such channels parallel to each other. The multiplier is a very powerful of MacroFlow that can be used for representing a number of identical flow paths that are in parallel.

- The two horizontal bypasses on the two sides of the sink are represented as passages of the same length as the fin sink, but with appropriate cross-sectional dimensions corresponding to the clearance between the fin wall and the duct wall. A multiplier of two signifies that there are two such bypasses in parallel with each other. A single rectangular channel is specified corresponding to the vertical bypass. The no bypass configuration is simulated by simply specifying the clearance dimension in these passages to be very small.
- The orifice downstream of the sink is a flow control element. The flow through the channel is controlled by the opening of the orifice.
- The portions of the duct before and after the sink are represented as rectangular passages with appropriate dimensions.
- The diffuser enables pressure recovery before the flow leaves the system. The Generic Nodes used in the network represent the junctions where the flow streams meet or from which flow streams divide. Thus, a Generic Node represents junctions in which no losses take place.
- Calculations have been done with ambient air (20 degrees ^{o}C, 1 atm) flowing through the duct.

Analogous to the experimental setup, the operating point of the system is determined by the orifice opening. By running the model for different orifice openings, the variation of the pressure drop in the fin sink with the flow rate is determined for the no bypass situation. Similarly, in presence of the bypass, the flow split as a function of the flow rate can also be determined.

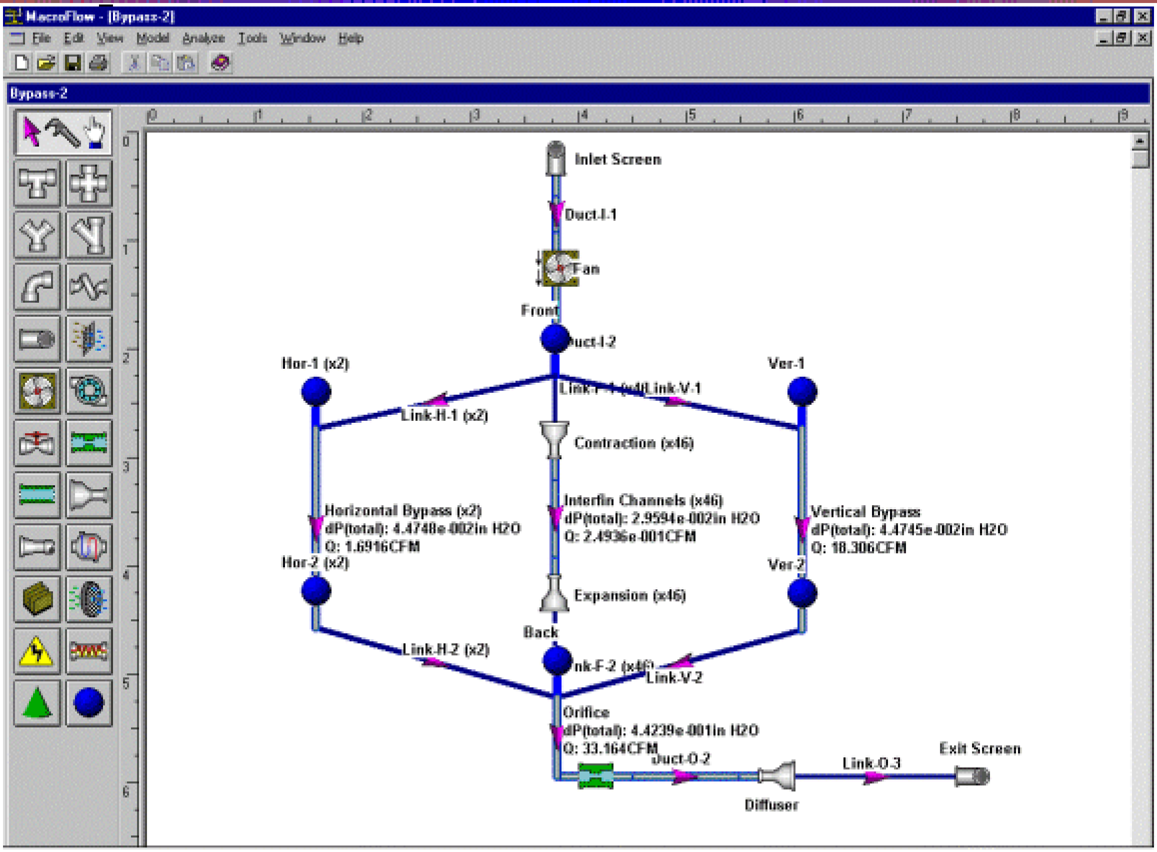

Figure 29.3 MacroFlow representation of the test cell used characterizing the heat sink performance

29.4 Flow Impedance Characteristics

The network representation of the entire test cell has been carried out using the standard components available in MacroFlow components and links. Their flow impedence characteristics are therefore determined internally from the corresponding library of loss coefficients. Note that MacroFlow accurately accounts for losses in laminar and turbulent flows. MacroFlow internally characterizes the flow regime based on the Reynolds number for the flow and chooses the appropriate variation of the pressure losses with the flow rate to determine the flow resistance. For example, since the flow in interfin passages is laminar MacroFlow will use the friction factor for laminar flow in a rectangular channel to characterize the corresponding flow resistance.

29.5 Results

MacroFlow predicts the distribution of the flow through the heat sink and the flow around it in the presence of bypass passages and the pressure drop in all parts of the systems. The predicted pressure drop-flow rate relationship and its comparison with the measurements [2] for the no bypass situation are shown in Figure 29.4. It can be seen that the physically motivated MacroFlow representation of the heat sink as parallel passages in combination with contraction and expansion components accurately predicts the heat sink performance.

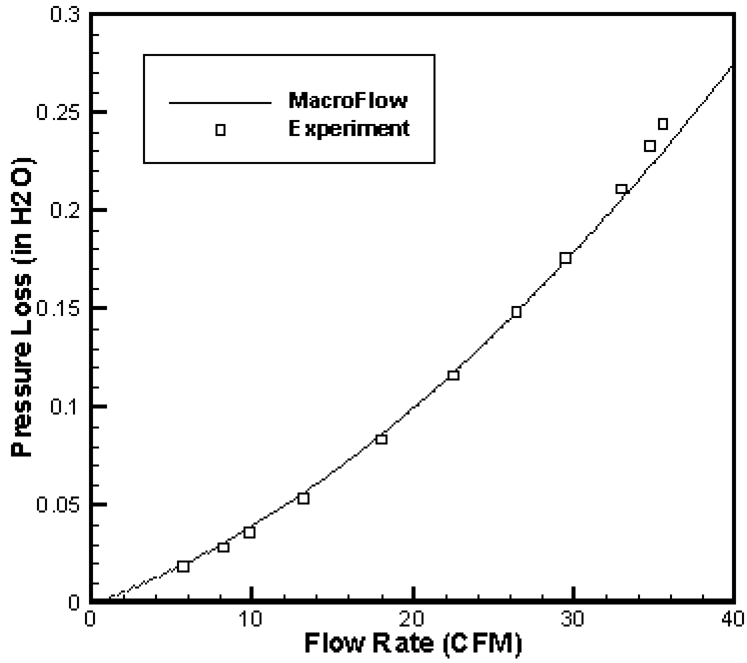

Figure 29.4 Variation of the pressure drop through the fin sink with the flow rate with no bypass

This representation can also be used in presence of bypass to predict the flow split. The bar chart in Figure 29.5 shows the variation of the pressure losses in various parts of the system. Similar plots can be made for any other quantity of interest to examine the flow distribution in the system. Figure 29.6 shows the fraction of the flow going through the heat sink as a function of the total flow rate through the duct for a fixed bypass (0.2 inches on the side and 0.25 inches above the fin tips).

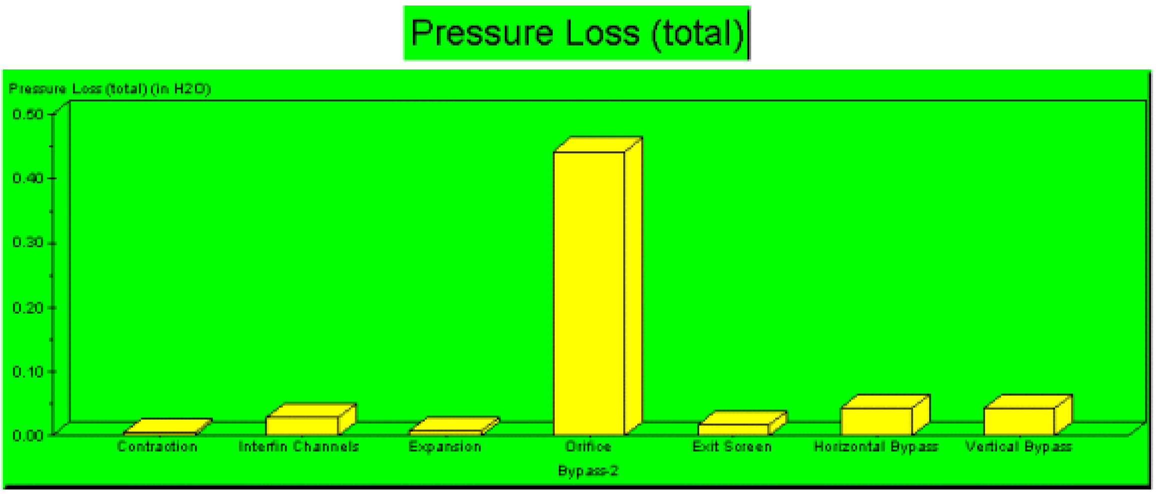

Figure 29.5 Pressure losses through various parts of the flow system with bypass

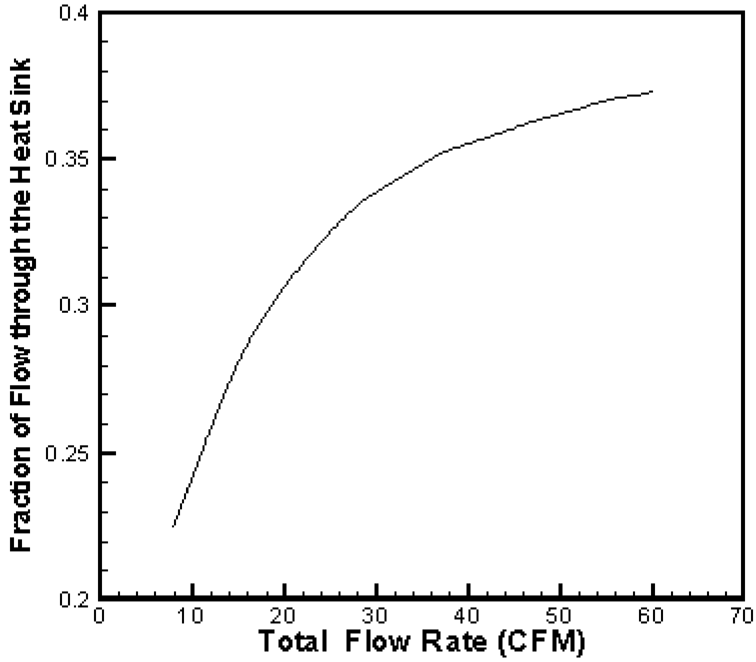

Figure 29.6 Variation of the fraction of the flow passing through the sink as a function of the total flow rate in the passage in presence of a specified bypass

29.6 Conclusions

In the present study, MacroFlow has been used to model a wind tunnel test cell employed for characterizing the performance of heat sinks. The innovative approach in this study is the successful use of a very simple generalized network representation of a heat sink for predicting flow through and around it. The model accurately reproduces the measured pressure drop characteristics of the heat sink under no-bypass conditions. MacroFlow can be used at many levels of the system for quick and accurate prediction of the airflow distribution needed during the Conceptual and Detailed Design stages. First, the heat sink model can be used to evaluate how the placement of a heat sinks affects the flow through the heat sink and hence the thermal performance of heat dissipating components on a particular circuit board. Second, the network model of a passage containing the heat sink can be used to determine the increase in the flow impedence in that passage. Third, these impedence characteristics can be used in the network model of the entire system to determine its airflow performance. The resulting flow distribution can, in turn, be used in the board-level model to determine the thermal performance under actual operating conditions. Finally, MacroFlow can also be used for designing wind tunnel test cells used for determining the flow impedence characteristics of subsysyems such as Power Supplies, Card Arrays, and Disk Units etc. With the user-friendly framework of MacroFlow, the construction of flow networks is extremely easy and accurate results are obtained in a very short time.

Part G-1: Course Specifications

University Cairo University
Faculty of Engineering
Mechanical Power Engineering Department
Course Specifications

Program(s) on which the course is given:	M.Sc. Prerequisites.
Major or minor element of programs:	Heat Transfer and its Applications
Department offering the program:	Mechanical Power Engineering Department
Department offering the course:	Mechanical Power Engineering Department
Academic year /level:	First year in M.Sc. / Level 6

Date of specification approval:

A. Basic Information

Title:	Electronics Cooling
Code:	MPE 635
Credit hours:	2/Term but teaching covers the full year (2 terms)
Lectures:	20
Tutorial:	6
Practicals:	4
Total:	30

B. Professional Information

1. Overall Aims of Course

The course aims to expand the scope of the mechanical engineer to include the importance of effective heat transfer in electronic equipments. This should include the heat transfer processes occurring in electronic equipment, the methods of packaging and cooling and finally the analysis of thermal failure for electronic components.

2. Intended Learning Outcomes of course (ILOs)

a- Knowledge and Understanding:

Heat transfer processes involved in electronics cooling.
Thermal design of electronic packages.

b- Intellectual Skills

Analysis of thermal failure for electronic components and define the solution.

c- Professional and Practical Skills

Assigning the best cooling method for each individual application.
Design of cooling system for any electronic device.
Best packaging approach for any design.

d- General and Transferable skills

Heat transfer basics.

Numerical simulation of heat transfer problems.

3. Contents

Topic	No. of Hours	No. of Lectures	Tutorial /Practical
Part A: Introduction to Electronics Cooling	6	2	1
Part B: Heat Transfer Principals in Electronics Cooling	18	8	1
Part C: Electronics Cooling Methods in Industry	16	7	1
Part D: Packaging of Electronic Equipments	8	2	2
Part E: Analysis of Thermal Failure of Electronic Components	6	1	2
Part F: Practical Applications	4	0	2
Electronics Cooling Survey	2	0	1
Total	**60**	**20**	**10**

4. Teaching and Learning Methods

4.1 Lectures, including slide show and power point presentations

4.2 Case studies ended by discussions

4.3 Tutorial and Practice classes for problems answer.

4.4 Laboratory work and reports

5. Student Assessment Methods

No.	Assessment type	Objective
1	Semester Work	in class performance and attendance
2	Other types of assessment (Reports, Quizzes, ..)	student's performance with time
3	Mid-Term Examination	to assess student's performance and to give him feed back
4	Oral Examination	to assess student's performance and communication skills
5	Practical Examination (case studies, …)	intellectual skills and team performance
6	Final-Term Examination	to assess overall student's performance

Assessment Schedule

Assessment 1:	week (all over the year)
Assessment 2:	week (all over the year)
Assessment 3:	week #15
Assessment 4:	week #20
Assessment 5:	week #25
Assessment 6:	week #30

Weighting of Assessments

Semester Work	10%
Other types of assessment	5%
Mid-Term Examination	10%
Oral Examination	5%
Practical Examination	10%
Final-Term Examination	60%
Total	**100%**

6. List of References

6.1. Course Notes

1- Lecture notes developed by the course coordinator
2- Thermal design of electronic packages, a Graduate Course by Prof. Kamal-Eldin Hassan.

6.2. Essential Books (Text Books)

1. Dave S. Steinberg," Cooling Techniques for Electronic Equipment ", Second Edition, John Wiley & Sons, 1991.
2. Frank P. Incropera, "Introduction to Heat Transfer ", Fourth Edition, John Wiley, 2002.
3. Sung Jin Kim and Sang Woo Lee, "Air cooling Technology for Electronic Equipment", CRC press, London, 1996.
4. Frank P. Incropera, "Liquid Cooling of Electronic Devices by Single-Phase Convection", John Wiley& sons, inc, 1999.

5. Charles A. Harper," Electronic Packaging and Interconnection Hand Book ", Second Edition, McGraw-Hill, 1997.

6.3. Recommended Books

6. Joel L. Sloan, "Design and Packaging of Electronic Equipment", Van Nostrand Reinhold Company, 1985.
7. Belady C., "Standardizing Heat Sink Performance for Forced Convection, Electronics Cooling", Vol. 3, No. 3, September, 1997.
8. Biber C., Wakefield Engineering, Wakefield, Massachusetts, "Characterization of the Performance of Heat Sinks,", Personal Communication, October 1997.
9. Butterbaugh M.A. and Kang S.S., IBM, Rochester, Minnesota, "Effect of Airflow Bypass on the Performance of Heat Sinks in Electronic Cooling," Presented at the ASME Winter Annual Meeting, 1995.

6.4. Periodicals, Web Sites, … etc

http://www.electronics-cooling.com
http://www.me.umn.edu/courses/me5348/index.html
http://www.acktechnology.com/Application%20Notes.htm
http://www.melcor.com/index.html
http://home.socal.rr.com/xsvtoys/articles.htm
http://www.nidec.com/aircooling/fantech.htm
http://www.ferrotec.com/usa/index.html
http://www.desernet.com
http://www.thermalloy.com/catalog/htm/geninfo.htm
http://www.coolingzone.com/Content/SupplierDirectory/index.html
http://www.thermalcooling.com/courses/instrnf.htm
http://www.thermalcomputations.com/#A
http://www.technicalbooks.net/Merchant2/merchant.mv?Screen=PLST&Store_Code=1

7. Facilities Required for Teaching and Learning

Lecture room for 20 students, accommodated with visual aids and data show
Electronic Packaging and Cooling Lab.

Course Coordinator:
Dr. Sayed Kasseb,
Dr. Gamal Al-Hariry

Head of Department:
Prof. Dr. Zeinab Safar

Date: 30/4/2006

Part G-2: Problem Bank

Introduction Problems (Basic Modes of H.T in Electronic Devices)

1. A square silicon chip (k = 150 W/m.K) is of width w = 5 mm on a side and of thickness t = 1 mm. The chip is mounted in a substrate such that its side and back surfaces are insulated, while the front surface is exposed to a coolant. If 4 W are being dissipated in circuits mounted to the back surface of the chip, what is the steady-state temperature difference between back and front surfaces?

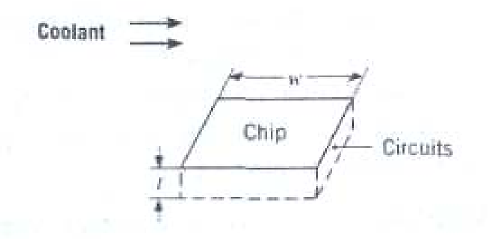

2. A square isothermal chip is of width w = 5 mm on a side and is mounted in a substrate such that its side and back surfaces are well insulated, while the front surface is exposed to the flow of a coolant at T_∞ = 15 °C. From reliability considerations, the chip temperature must not exceed T = 85 °C.

If the coolant is air and the corresponding convection coefficient is h = 200 W/m^2.K. What is the maximum allowable chip power? If the coolant is a dielectric liquid for which h = 3000 W/m^2.K. What is the maximum allowable power?

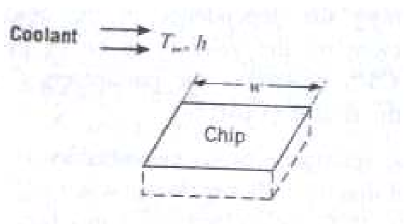

3. The case of a power transistor, which is of length L = 10mm and diameter D = 12 mm, is cooled by an air stream of temperature T_∞ = 25 °C. Under conditions for which the air maintains an average convection coefficient of h = 100 W/m^2.K on the surface of the case, what is the maximum allowable power dissipation if the surface temperature is not to exceed 85 °C?

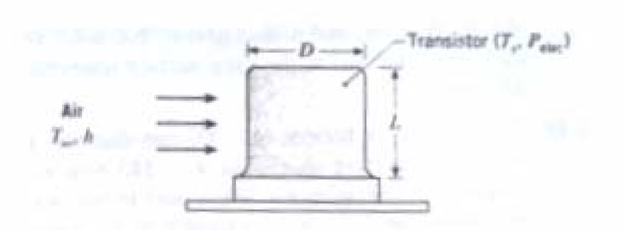

4. The use of impinging air jets is proposed as a means of effectively cooling high-power logic chips in a computer. However, before the technique can be implemented, the convection coefficient associated with jet impingement on a chip surface must be known. Design an experiment that could be used to determine convection coefficients associated with air jet impingement on a chip measuring approximately 10 mm by 10 mm on a side.

5. An instrumentation package has a spherical outer surface of diameter D = 100 mm and emissivity $\varepsilon = 0.25$. The package is placed in a large space simulation chamber whose walls are maintained at 77 K. If operation of the electronic components is restricted to the temperature range $40 \le T \le 85$ °C, what is the range of acceptable power dissipation for the package? Display your results graphically, showing also the effect of variations in the emissivity by considering values of 0.20 and 0.30.

6. Consider the conditions of Problem 2. With heat transfer by convection to air, the maximum allowable chip power is found to be 0.35 W. If consideration is also given to net heat transfer by radiation from the chip surface to large surroundings at 15 °C, what is the percentage increase in the maximum allowable chip power afforded by this consideration?
The chip surface has an emissivity of 0.9.

7. Square chips of width L = 15 mm on a side are mounted to a substrate that is installed in an enclosure whose walls and air are maintained at a temperature of $T_\infty = T_{surr} = 25$ °C. The chips have an emissivity of $\varepsilon = 0.60$ and a maximum allowable temperature of $T_s = 85$ °C.

(a) If heat is rejected from the chips by radiation and natural convection, what is the maximum operating power of each chip? The convection coefficient depends on the chip-to-air temperature difference and may be approximated as $h = C\,(T_s - T_\infty)^{0.25}$, Where $C = 4.2\ W/m^2.K^{5/4}$.
(b) If a fan is used to maintain air flow through the enclosure and heat transfer is by forced convection, with $h = 250\ W/m^2.K$, what is the maximum operating power?

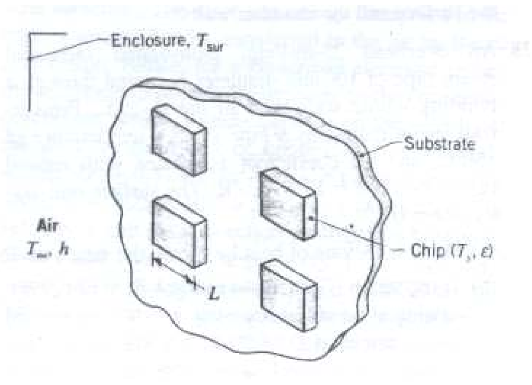

8. A computer consists of an array of five printed circuit boards (PCBs). Each dissipating P_b = 20 W of power. Cooling of the electronic components on a board is provided by the forced flow of air, equally distributed in passages formed by adjoining boards, and the convection coefficient associated with heat transfer from the components to the air is approximately h = 200 $W/m^2.K$. Air enters the computer console at a temperature of $T_i = 20$ °C, and flow is driven by a fan whose power consumption is $P_f = 25$ W.

(a) If the temperature rise of the air flow. (T_o - T_i), is not to exceed 15 °C, what is the minimum allowable volumetric flow rate of the air? The density and specific heat of the air may be approximated as $\rho = 1.161$ kg/m^3 and $C_p = 1007$ J/kg.K, respectively.

(b) The component that is most susceptible to thermal failure dissipates 1 W/cm^2 of surface area. To minimize the potential for thermal failure, where should the component be installed on a PCB? What is its surface temperature at this location?

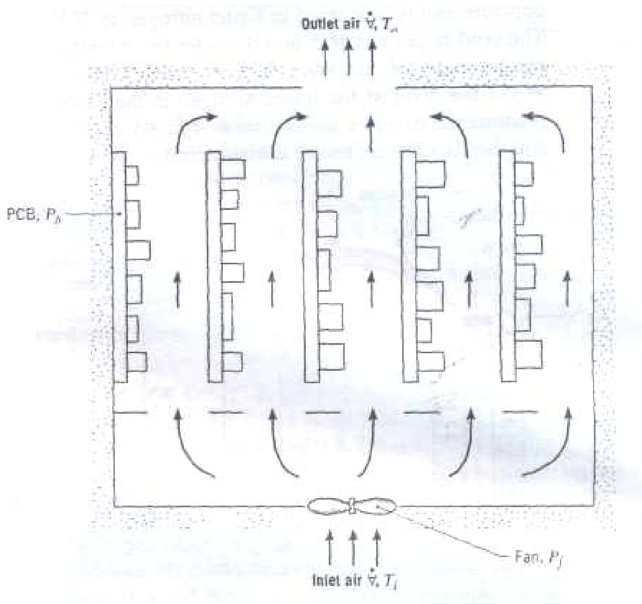

9. Electronic power devices are mounted to a heat sink having an exposed surface area of 0.045 m^2 and an emissivity of 0.80. When the devices dissipate a total power of 20 W and the air and surroundings are at 27 °C, the average sink temperature is 42 ^{o}C. What average temperature will the heat sink reach when the devices dissipate 30 W for the same environmental condition?

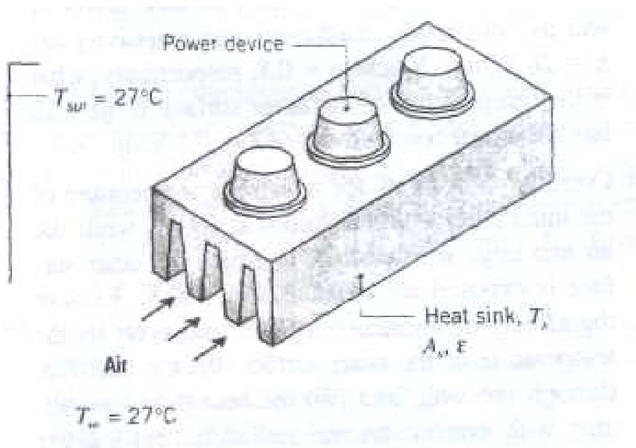

10. Consider a surface-mount type transistor on a circuit board whose temperature is maintained at 35 °C. Air at 20 °C flows over the upper surface of dimensions 4 mm by 8 mm with a convection coefficient of 50 W/m^2.K.Three wire leads, each of cross section 1 mm by 0.25 mm and length 4 mm, conduct heat from the case to the circuit board. The gap between the case and the board is 0.2 mm.

(a) Assuming the case is isothermal and neglecting radiation; estimate the case temperature when 150mW are dissipated by the transistor and (i) stagnant air or (ii) a conductive paste fills the gap. The thermal conductivities of the wire leads, air. And conductive pastes are 25, 0.0263, and 0.12 W/m.K. respectively.

(b) Using the conductive paste to fill the gap, we wish to determine the extent to which increased heat dissipation may be accommodated, subject to the constraint that the case temperature not exceeds 40 °C. Options include increasing the air speed to achieve a larger convection coefficient h and/or changing the lead wire material to one of larger thermal conductivity. Independently considering leads fabricated from materials with thermal conductivities of 200 and 400 W/m.K., compute and plot the maximum allowable heat dissipation for variations in h over the range $50 \leq h \leq 250$ W/m^2.K.

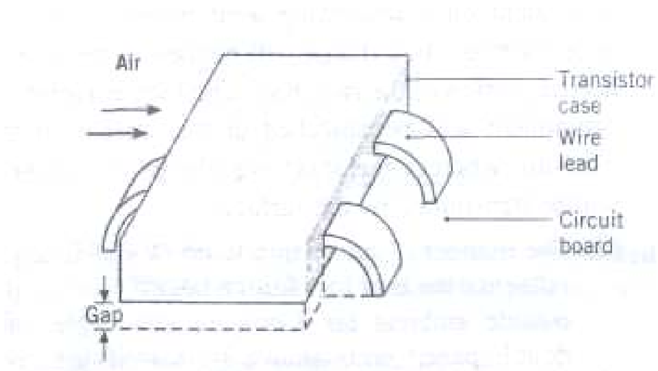

11. A transistor that dissipates10W is mounted on a duralumin heat sink at 50 °C by a duralumin bracket 20 mm wide as shown in the opposite figure. The bracket is attached to the heat sink by a rivet that produces an interface pressure of 12 bar. The surfaces in contact have a roughness of 1.6 μm rms. With convective cooling negligibly small, estimate the surface temperature of the transistor.

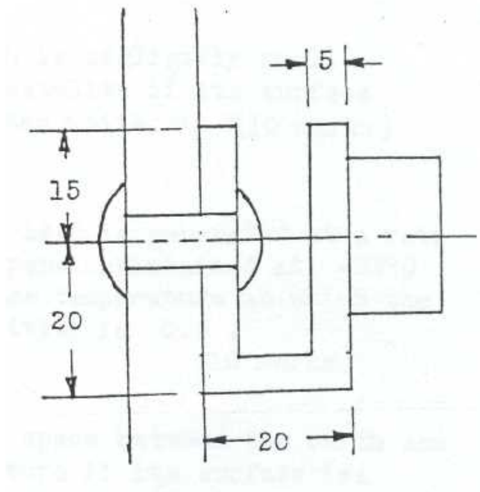

12. A cable 10 mm is to be insulated to maximize its current carrying capacity. For certain reasons, the outside diameter of the insulation should be 30 mm. The heat transfer coefficient for the outer surface is estimated to be 10 W /m^2 .K.

What should be the thermal conductivity of the chosen insulation? By what percentage would the insulation increase the energy carrying capacity of the bare cable?

13. The vertical side of an electronics box is 40 x 30 cm with the 40 cm side vertical. What is the maximum radiation energy that could be dissipated by this side if its temperature is not to exceed 60 °C in an environment of 40 °C, and its emissivity is 0.8?

Conduction H.T and Fins Problems

14. In a manufacturing process, a transparent film is being bonded to a substrate as shown in the sketch. To cure the bond at a temperature T_o, a radiant source is used to provide a heat flux q_o'' (W/m^2), All of which is absorbed at the bonded surface. The back of the substrate is maintained at T_1 while the free surface of the film is exposed to air at T_∞ and a convection heat transfer coefficient h.

(a) Show the thermal circuit representing the steady-state heat transfer situation. Be sure to label all elements, nodes, and heat rates. Leave in symbolic form.

(b) Assume the following conditions: T_∞ = 20 °C, h = 50 $W/m^2.K$ and T_1 = 30 °C. Calculate the heat flux q_o'' that is required to maintain the boded surface at T_o = 60 °C.

(c) Compute and plot the required heat flux as a function of the film thickness for $0 \le L_f \le 1$mm.

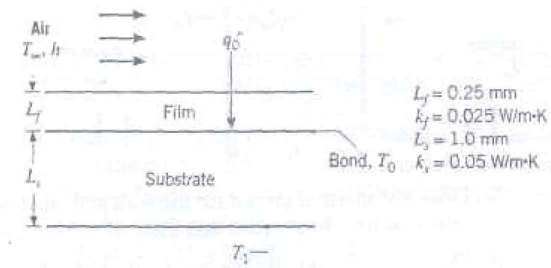

15. A silicon chip is encapsulated such that, under steady-state conditions, all of the power it dissipates is transferred by convection to a fluid stream for which h = 1000 $W/m^2.K$. and T_∞ = 25 °C. The chip is separated from the fluid by a 2-mm-thick aluminum cover plate, and the contact resistance of the chip/aluminum interface is 0.5 x 10^{-4} $m^2.K/W$. If the chip surface area is 100 mm^2 and its maximum allowable temperature is 85 °C, what is the maximum allowable power dissipation in the chip?

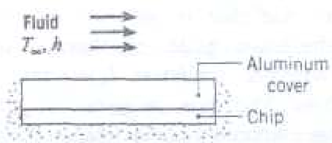

16. Approximately 10^6 discrete electrical components can be placed on a single integrated circuit (chip), with electrical heat dissipation as high as 30,000 W/m^2. The chip, which is very thin, is exposed to a dielectric liquid at its outer surface, with h_o = 1000 W/m^2. K and $T_{\infty,o}$ = 20 °C, and is joined to a circuit board at its inner surface. The thermal contact resistance between the chip and the board is 10^{-4} $m^2.K/W$. and the board thickness and thermal conductivity are L_b = 5 mm and k_b = 1 W/m.K, respectively. The other surface of the board is exposed to ambient air for which h_i = 40 W/m^2.K and $T_{\infty,i}$ = 20 °C.

(a) Sketch the equivalent thermal circuit corresponding to steady-state conditions. In variable form, label appropriate resistances, temperatures, and heat fluxes.
(b) Under steady-state conditions for which the chip heat dissipation is q_c'' = 30,000 W/m^2. What is the chip temperature?
(c) The maximum allowable heat flux $q_{c,m}''$, is determined by the constraint that the chip temperature must not exceed 85 °C. Determine $q_{c,m}''$ for the foregoing conditions. If air is used in lieu of the dielectric liquid, the convection coefficient is reduced by approximately an order of magnitude. What is the value of $q_{c,m}''$ for h_o = 100 W/m^2.K? With air cooling, can significant improvements be realized by using an aluminum oxide circuit board and/or by using a conductive paste at the chip/board interface for which $R_{t,c}''$ = 10^{-5} m^2.K/W.?

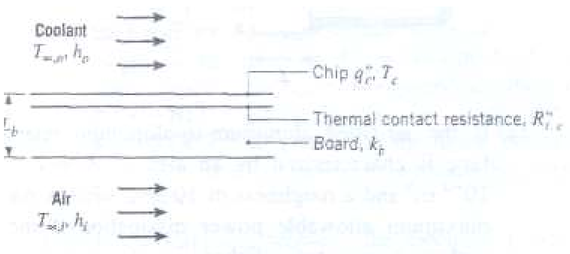

17. Consider a power transistor encapsulated in an aluminum case that is attached at its base to a square aluminum plate of thermal conductivity k = 240 W/m.K., thickness L = 6 mm, and width W = 20 mm. The case is joined to the plate by screws that maintain a contact pressure of 1 bar, and the back surface of the plate transfers heat by natural convection and radiation to ambient air and large surroundings at $T_\infty = T_{sur}$ = 25 °C. The surface has an emissivity of ε = 0.9, and the convection coefficient is h = 4 W/m^2.K. The case is completely enclosed such that heat transfer may be assumed to occur exclusively through the base plate.

(a) If the air-filled aluminum-to-aluminum interface is characterized by an area of A_c = 2 x 10^{-4} m^2 and a roughness of 10 µ.m. what is the maximum allowable power dissipation if the surface temperature of the case, $T_{s,c}$, is not to exceed 85 °C?
(b) The convection coefficient may be increased by subjecting the plate surface to a forced flow of air. Explore the effect of increasing the coefficient over the range 4 ≤ h ≤ 200 W/ m^2.K.

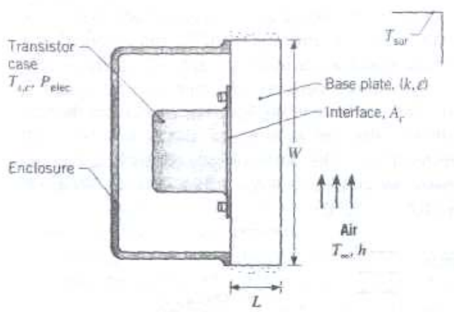

18. A transistor, which may be approximated as a hemispherical heat source of radius $r_o = 0.1$ mm, is embedded in a large silicon substrate (k = 125 W/m.K) and dissipates heat at a rate q. All boundaries of the silicon are maintained at an ambient temperature of $T_\infty = 27°C$, except for a plane surface that is well insulated. Obtain a general expression for the substrate temperature distribution and evaluate the surface temperature of the heat source for q = 4 W.

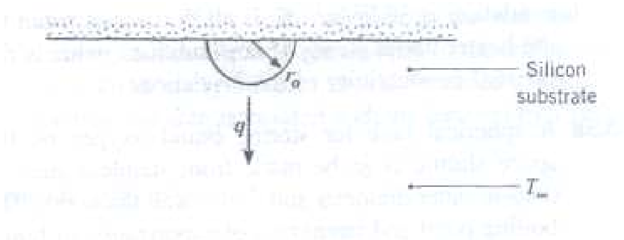

19. A bonding operation utilizes a laser to provide a constant heat flux q_o'', across the top surface of a thin adhesive-backed, plastic film to be affixed to a metal strip as shown in the sketch. The metal strip has a thickness d=1.25 mm and its width is large relative to that of the film. The thermophysical properties of the strip are $\rho = 7850$ kg/m^3, $C_p = 435$ J/kg.K, and k = 60 W/m.K. The thermal resistance of the plastic film of width $w_1 = 40$ mm is negligible. The upper and lower surfaces of the strip (including the plastic film) experience convection with air at 25 ^{o}C and a convection coefficient of 10 W/m^2.K. The strip and film are very long in the direction normal to the page. Assume the edges of the metal strip are at the air temperature (T_∞).

(a) Derive an expression for the temperature distribution in the portion of the steel strip with the plastic film ($-w_1/2 \le x \le +w_1/2$).
(b) If the heat flux provided by the laser is 10,000 W/m^2, determine the temperature of the plastic film at the center (x = 0) and its edges ($x = \pm w_1/2$).
(c) Plot the temperature distribution for the entire strip and point out its special features.

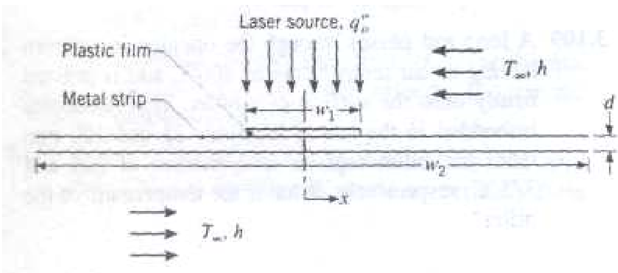

20. A disk-shaped electronic device of thickness L_d, diameter D, and thermal conductivity k_d dissipates electrical power at a steady rate P, along one of its surfaces. The device is bonded to a cooled base at T_o using a thermal pad of thickness L_p and thermal conductivity k_p. A long fin of diameter D and thermal conductivity kf is bonded to the heat-generating surface of the device using an identical thermal pad. The fin is cooled by an air stream, which is at a temperature T_∞ and provides a convection coefficient h.

(a) Construct a thermal circuit of the system.
(b) Derive an expression for the temperature T_d of the heat-generating surface of the device in terms of the circuit thermal resistances, T_o and T_∞. Express the thermal resistances in terms of appropriate parameters.
(c) Calculate T_d for the prescribed conditions.

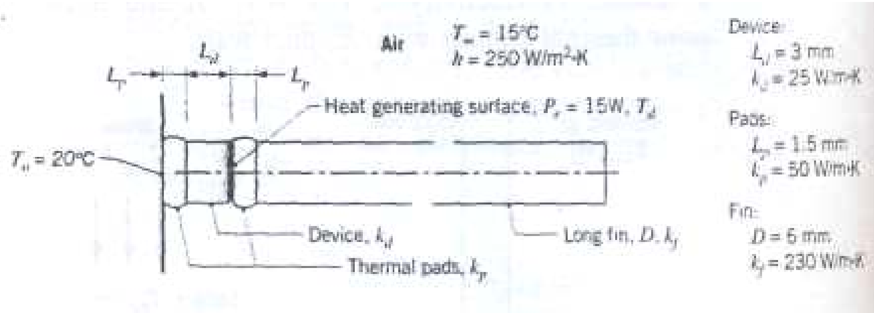

21. An isothermal silicon chip of width W = 20 mm on a side is soldered to an aluminum heat sink (k = 180W/m.K) of equivalent width. The heat sink has a base thickness of L_b =3 mm and an array of rectangular fins, each of length L_f = 15 mm. Air flow at T_∞ = 20°C is maintained through channels formed by the fins and a cover plate, and for a convection coefficient of h = 100 W/m^2.K., a minimum fin spacing of 1.8 mm is dictated by limitations on the flow pressure drop. The solder joint has a thermal resistance of $R''_{t,c}$ = 2 x 10^{-6} m^2.K.

Consider limitations for which the array has N = 11 fins, in which case values of the fin thickness t = 0.182 mm and pitch S = 1.982 mm are obtained from the requirements that W = [(N - 1) S + t] and S - t = 1.8 mm. If the maximum allowable chip temperature is T_c = 85 °C, what is the corresponding value of the chip power q_c? An adiabatic fin tip condition may be assumed, and air flow along the outer surfaces of the heat sink may be assumed to provide a convection coefficient equivalent to that associated with air flow through the channels.

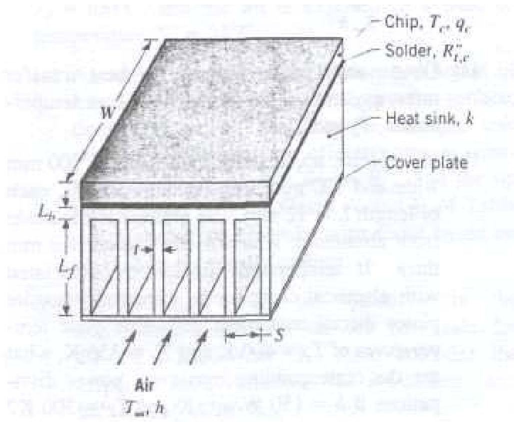

22. A 3 x 3 array of power transistors is attached to an aluminum heat sink (k = 180 W/m.K.) of width W = 150 mm on a side. The thermal contact resistance between each transistor and the heat sink is $R_{t,c}$ = 0.045 K/W. The heat sink has a base thickness of L_b = 6 mm and an array of N_f = 25 rectangular fins, each of thickness t = 3 mm. Cooling is provided by air flow through channels formed by the fins and a cover plate, as well as by air flow along the two sides of the heat sink (the outer surfaces of the outermost fins).

(a) Consider conditions for which the fin length is L_f = 30 mm, the temperature of the air is T_∞ = 27 °C, and the convection coefficient is h = 100 W/m^2.K. If the maximum allowable transistor temperature is T_s = 100 °C, what is the maximum allowable power dissipation, q per transistor? An adiabatic fin tip condition may be assumed.

(b) Explore the effect of variations in the convection coefficient and fin length on the maximum allowable transistor power.

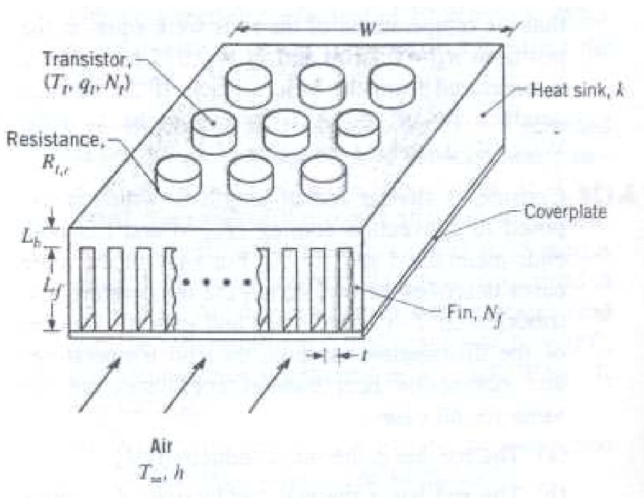

23. As more and more components are placed on a single integrated circuit (chip), the amount of heat that is dissipated continues to increase. However, this increase is limited by the maximum allowable chip operating temperature, which is approximately 75 °C. To maximize heat dissipation, it is proposed that a 4 x 4 array of copper pin fins be metallurgically joined to the outer surface of a square chip that is 12.7 mm on a side.

(a) Sketch the equivalent thermal circuit for the pin-chip-board assembly, assuming one-dimensional, steady-state conditions and negligible contact resistance between the pins and the chip. In variable form, label appropriate resistances, temperatures, and heat rates.
(b) For the conditions prescribed in Problem 16, what is the maximum rate at which heat can be dissipated in the chip when the pins are in place? That is, what is the value of q_c For T_c = 75 °C? The pin diameter and length are D_p= 1.5 mm and L_p = 15 mm.

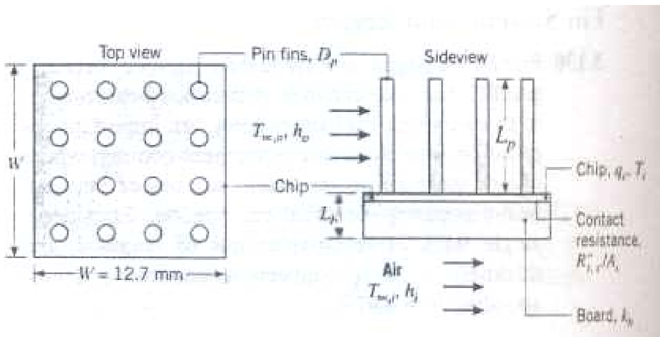

24. As a means of enhancing heat transfer from high-performance logic chips, it is common to attach a heal sink to the chip surface in order to increase the surface area available for convection heat transfer. Because of the ease with which it may be manufactured (by taking orthogonal sawcuts in a block of material), an attractive option is to use a heat sink consisting of an array of square fins of width w on a side. The spacing between adjoining fins would be determined by the width of the sawblade, with the sum of this spacing and the fin width designated as the fin pitch S. The method by which the heat sink is joined to the chip would determine the interfacial contact resistance $R''_{t,c}$.

Consider a chip of width W_c = 16 mm and conditions for which cooling is provided by a dielectric liquid with T_∞ = 25 °C and h = 1500 W/m^2.K. The heat sink is fabricated from copper (k = 400 W/m.K), and its characteristic dimensions are w = 0.25 mm, S = 0.50 mm, L_f = 6 mm, and L_b = 3 mm. The prescribed values of w and S represent minima imposed by manufacturing constraints and the need to maintain adequate flow in the passages between fins.

(a) If a metallurgical joint provides a contact resistance of $R''_{t,c}$ = 5 x 10^{-6} m^2.K/W. and the maximum allowable chip temperature are 85 ^{o}C. What is the maximum allowable chip power dissipation q_c? Assume all of the heat to be transferred through the heat sink.

(b) It may be possible to increase the heat dissipation by increasing w, subject to the constraint that (S - w) ≥ 0.25 mm, and/or increasing L_f (subject to manufacturing constraints that $L_f \le$ 10 mm). Assess the effect of such change.

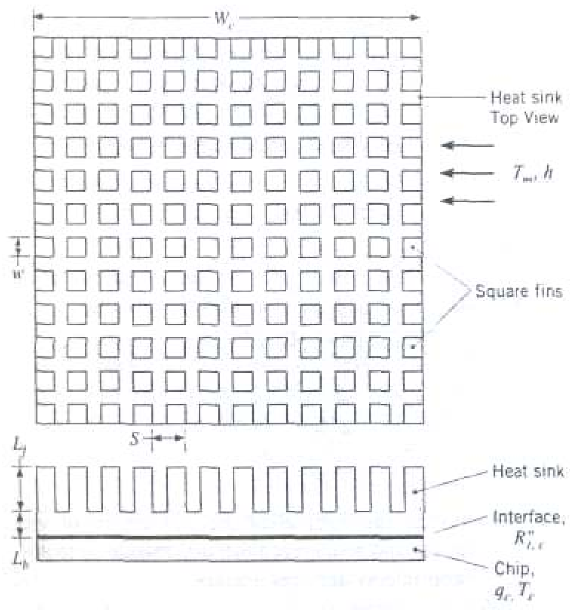

25. Because of the large number of devices in today's PC chips, finned heat sinks are often used to maintain the chip at an acceptable operating temperature. Two fin designs are to be evaluated, both of which have base (unfinned) area dimensions of 53 mm x 57 mm. The fins are of square cross section and fabricated from an extruded aluminum alloy with a thermal conductivity of 175 W/m.K. cooling air may be supplied at 25 °C, and the maximum allowable chip temperature is 75 °C. Other features of the design and operating conditions are tabulated.

Determine which fin arrangement is superior. In your analysis, calculate the heat rate, efficiency, and effectiveness of a single fin, as well as the total heat rate and overall efficiency of the array. Since real estate inside the computer enclosure is important, compare the total heat rate per unit volume for the two designs.

Design	Fin Dimensions: Cross Section $w \times w$ (mm)	Fin Dimensions: Length L (mm)	Number of Fins in Array	Convection Coefficient ($W/m^2 \cdot K$)
A	3×3	30	6×9	125
B	1×1	7	14×17	375

Transient Conduction Problems

26. A duralumin hollow core PCB is 160 x 200 mm with 58 conduits as shown. It has two laminated PCB's of thermal conductivity 0.4 W /m. K and thickness 1 mm each. The electronic components are cemented to the laminated PCB's by an adhesive of thermal conductivity 0.4 W/m. K. and 0.2 mm thick. These components generate heat evenly at a rate of 1.6 KW /m^2 on the two sides. Air at 50 °C and a rate of 25 kg /h is used for cooling.

If the hollow core PCB attains at a uniform temperature of 80 °C, when the electronic components mounted on it are turned off while the cooling air continues to flow, estimate the time necessary for the PCB to reach a temperature of 55 °C. You may consider the laminated PCB's to act as perfect insulators.

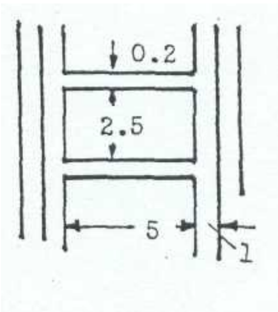

27. A 35 W power transistor is fitted to a duralumin plate 150 x 165 mm and 5 mm thick. The plate is finned on the other side by 15 fins spaced 9 mm apart. The fins are 2 mm thick and protrude 40 mm. In an ambience of 40 °C, how long would it take this transistor, after turning it on, to be within 5 ^{o}C from its final temperature? Neglect effect of radiation.

Free Convection Problems

28. Consider an array of vertical rectangular fins, which is lo be used lo cool an electronic device mounted in quiescent, atmospheric air at T_∞= 27 °C. Each fin has L = 20 mm and H = 150 mm and operates at an approximately uniform temperature of T_s = 77 °C. For the optimum value of fin spacing S and a fin thickness of t = 1.5 mm, estimate the rate of heat transfer from the fins for an array of width W = 355 mm.

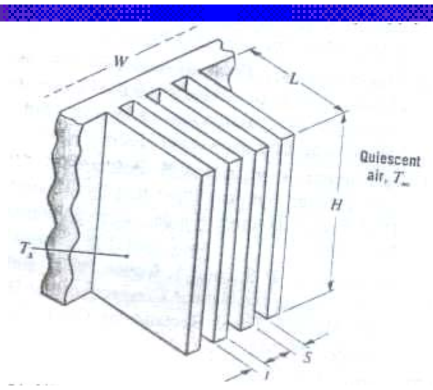

29. The components of a vertical circuit board. 150 mm on a side, dissipate 5 W. The back surface is well insulated and the front surface is exposed to quiescent air at 27 °C. Assuming a uniform surface heat flux, what is the maximum temperature of the board? What is the temperature of the board for an isothermal surface condition?

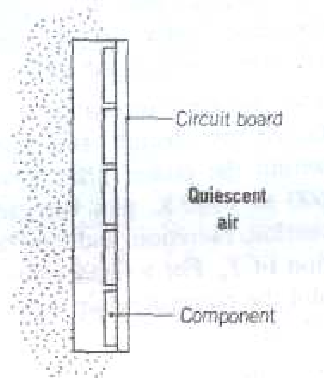

30. Circuit boards are mounted to interior vertical surfaces of a rectangular duct of height H = 400 mm and length L = 800 mm. Although the boards are cooled by forced convection heat transfer to air flowing through the duct, not all of the heat dissipated by the electronic components is transferred to the flow. Some of the heat is instead transferred by conduction to the vertical walls of the duct and then by natural convection and radiation to the ambient (atmospheric) air and surroundings, which are at equivalent temperatures of $T_\infty = T_{sur} = 20$ °C. The walls are metallic and, to a first approximation, may be assumed to be isothermal at a temperature T_s.

(a) Consider conditions for which the electronic components dissipate 200 W and air enters the duct at a flow rate of m = 0.015 kg/s and a temperature of $T_{m,i} = 20$ °C. If the emissivity of the side walls is $\varepsilon_s = 0.15$ and the outlet temperature of the air is $T_{m,o} = 30$ °C, what is the surface temperature T_s?

(b) To reduce the temperature of the electronic components, it is desirable to enhance heat transfer from the side walls. Assuming no change in the air flow conditions, what is the effect on Ts of applying a high emissivity coating ($\varepsilon_s = 0.90$) to the side walls?

(c) If there is a loss of airflow while power continues to be dissipated, what are the resulting values of T_s for $\varepsilon_s = 0.15$ and $\varepsilon_s = 0.90$?

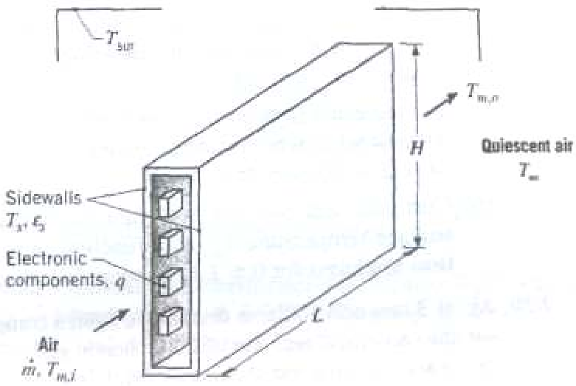

31. A vertical array of circuit boards is immersed in quiescent ambient air at T_∞ = 17 °C. Although the components protrude from their substrates, it is reasonable, as a first approximation, to assume flat plates with uniform surface heat flux q".
Consider boards of length and width L = W = 0.4 m and spacing S = 25 mm. If the maximum allowable board temperature is 77 °C. What is the maximum allowable power dissipation per board?

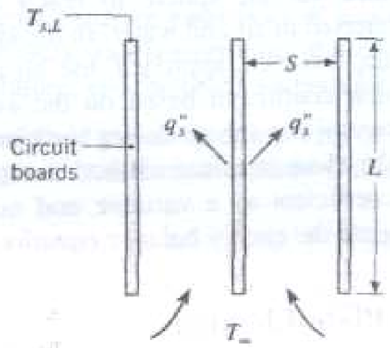

Forced Convection

- **External Flow**

32. A heat sink constructed from 2024 aluminum alloy is used to cool a power diode dissipating 5 W. The internal thermal resistance between the diode junction and the case is 0.8 °C/W, while the thermal contact resistance between the case and the heat sink is 10^{-5} m^2. °C/W. Convection at the fin surface may be approximated as that corresponding to a flat plate in parallel flow.

(a) Assuming that all the diode power is transferred to the ambient air through the rectangular fins; estimate the operating temperature of the diode.

(b) Explore options for reducing the diode temperature, subject to the constraints that the air velocity and fin length may not exceed 25 m/s and 20 mm, respectively, while the fin thickness may not be less than 0.5 mm. All other conditions, including the spacing between fins, remain as prescribed.

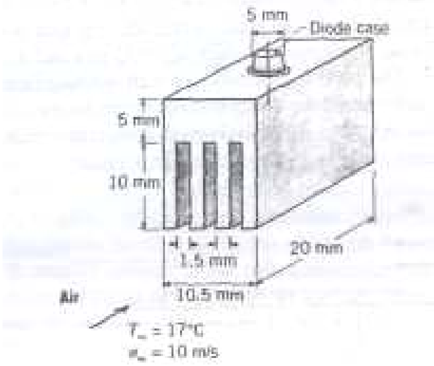

33. An array of electronic chips is mounted within a sealed rectangular enclosure, and cooling is implemented by attaching an aluminum heat sink (k = 180 W/m.K). The base of the heat sink has dimensions of $w_1 = w_2 = 110$ mm, while the 6 fins are of thickness t = 10 mm and pitch S = 20 mm. The fin length is $L_f = 60$ mm, and the base of the heat sink has a thickness of $L_b = 20$mm.

If cooling is implemented by water flow through the heat sink, with $u_\infty = 3$ m/s and $T_\infty = 17$ ^oC, what is the base temperature T_b of the heat sink when power dissipation by the chips is $P_{elec} = 1200$ W? The average convection coefficient for surfaces of the fins and the exposed base may be estimated by assuming parallel flow over a flat plate. Properties of the water may be approximated as k = 0.62 W/m.K, $\nu = 7.73 \times 10^{-7}$ m^2/s, and Pr = 5.2.

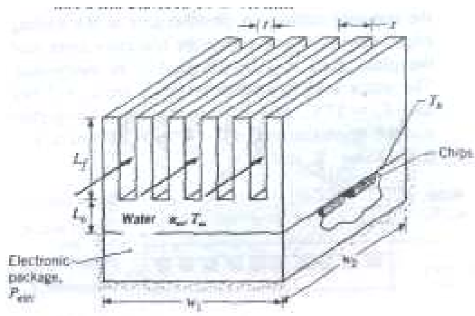

34. An array of heat-dissipating electrical components is mounted on the bottom side of a 1.2 m by 1.2 m horizontal aluminum plate, while the top side is cooled by an air stream for which $u_\infty = 15$ m/s and $T_\infty = 300$ K. The plate is attached to a well-insulated enclosure such that all the dissipated heat must be transferred to the air. Also, the aluminum is sufficiently thick to ensure a nearly uniform plate temperature.

(a) If the temperature of the aluminum is not exceeding 350 K, what is the maximum allowable heat dissipation?

(b) Determine the maximum allowable heal dissipation as a function of air velocity in the range, $5 \leq u_\infty \leq 25$ m/s. With $u_\infty = 25$ m/s, the maximum allowable power may be increased further by using an aluminum plate with longitudinal fins. What is the maximum allowable power if the fin length, thickness, and spacing are 25 mm, 5 mm, and 10 mm, respectively?

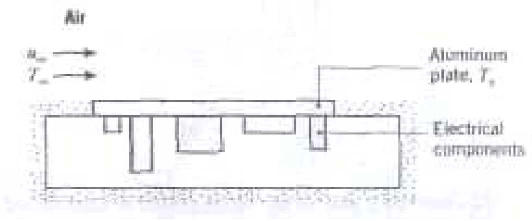

35. One-hundred electrical components, each dissipating 25 W, are attached to one surface of a square (0.2 m x 0.2 m) copper plate, and all the dissipated energy is transferred to water in parallel flow over the opposite surface. A protuberance at the leading edge of the plate acts to trip the boundary layer, and the plate itself may be assumed to be isothermal. The water velocity and temperature are u_∞ = 2 m/s and T_∞ = 17 °C, and its thermophysical properties may be approximated as $\nu = 0.96 \times 10^{-6}$ m/s, k = 0.620 W/m.K, and Pr = 5.2.
(a)What is the temperature of the copper plate?
(b)If each component has a plate contact surface area of 1 cm^2 and the corresponding contact resistance is 2×10^{-4} m^2.K/W, what is the component temperature? Neglect the temperature variation across the thickness of the copper plate.

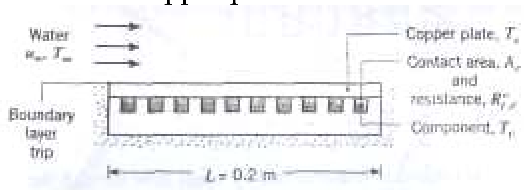

36. Air at 27 °C with a free stream velocity of 10 m/s is used lo cool electronic devices mounted on a printed circuit board. Each device, 4 mm by 4 mm, dissipates 40 mW, which is removed from the top surface. A turbulator is located at the leading edge of the board, causing the boundary layer to be turbulent.

(a) Estimate the surface temperature of the fourth device located 15 mm from the leading edge of the board.
(b) Generate a plot of the surface temperature of the first four devices as a function of the free stream velocity for $5 \le u_\infty \le 15$ m/s.
(c) What is the minimum free stream velocity if the surface temperature of the honest device is not to exceed 80 °C?

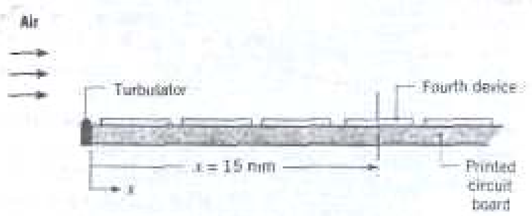

37. Forced air at 25 °C and 10 m/s is used to cool electronic elements mounted on a circuit board. Consider a chip of length 4 mm and width 4 mm located 120 mm from the leading edge. Because the board surface is irregular, the flow is disturbed and the appropriate convection correlation is of the form $Nu_x = Re_x^{0.85} Pr^{0.33}$. Estimate the surface temperature of the chip, T_s, if its heat dissipation rate is 30 mW.

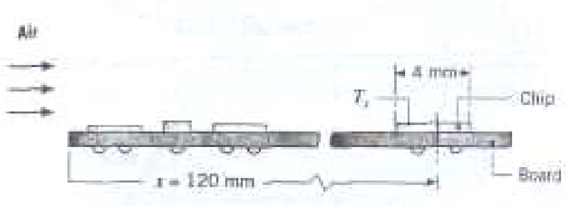

38. To enhance heat transfer from a silicon chip of width W = 4 mm on a side, a copper pin fin is brazed to the surface of the chip. The pin length and diameter are L = 12 mm and D = 2 mm, respectively, and atmospheric air at V = 10 m/s and T_∞ = 300 K is in cross flow over the pin. The surface of the chip, and hence the base of die pin, are maintained at a temperature of T_b = 350 K.

(a) Assuming the chip to have a negligible effect on flow over the pin, what is the average convection coefficient for the surface of the pin?
(b) Neglecting radiation and assuming the convection coefficient at the pin tip to equal that calculated in part (a), determine the pin heat transfer rate.
(c) Neglecting radiation and assuming the convection coefficient at the exposed chip surface to equal that calculated in part (a), determine the total rate of heat transfer from the chip.

39. A silicon chip (k = 150 W/m.K, ρ = 2300 kg/m^3, c_p = 700 J/kg.K), 10 mm on a side and 1 mm thick, is connected to a substrate by solder balls (k = 40 W/m.K, ρ = 10,000 kg/m^3, c_p = 150 J/kg.K) of 1 mm diameter, and during an accelerated thermal stress test, the system is exposed to the flow of a dielectric liquid (k = 0.064 W/m.K, ν= 10^{-6} m^2/s, Pr = 25). As first approximations, treat the top and bottom surfaces of the chip as flat plates in turbulent, parallel flow and assume the substrate and lower chip surfaces to have a negligible effect on flow over the solder balls. Also assume point contact between the chip and the solder, thereby neglecting heat transfer by conduction between the components.

(a) The stress test begins with the components at ambient temperature (T_i = 20 °C) and proceeds with heating by the fluid at T_∞ = 80 °C. If the fluid velocity is V = 0.2 m/s, estimate the ratio of the time constant of the chip to that of a solder ball. Which component responds more rapidly to the heating process?
(b) The thermal stress acting on the solder joint is proportional to the chip-to-solder temperature difference. What is this temperature difference 0.25 s after the start of heating?

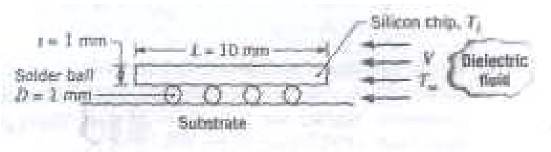

- **<u>Tube Bank</u>**

40. Electrical components mounted to each of two isothermal plates are cooled by passing atmospheric air between the plates, and an in-line array of aluminum pin fins is used to enhance heat transfer to the air. The pins are of diameter D = 2 mm. length L = 100 mm, and thermal conductivity k = 240 W/m.K. The longitudinal and transverse pitches are $S_L = S_T =$ 4 mm. with a square array of 625 pins ($N_T = N_L = 25$) mounted to square plates that are each of width W = 100 mm on a side. Air enters the pin array with a velocity of 10 m/s and a temperature of 300 K.

(a)Evaluating air properties at 300 K, estimate the average convection coefficient for the array of pin fins.

(b)Assuming a uniform convection coefficient overall heat transfer surfaces (plates and pins), use the result of part (a) to determine the air outlet temperature and total heat rate when the plates are maintained at 350 K. Hint: The air outlet temperature is governed by an exponential relation of the form $[(T_s - T_o)/(T_s - T_i)] = \exp[[-(\bar{h}A_t\eta_o)/m^\bullet C_p]$, where $m^\bullet$ = $\rho V L N_T S_T$ is the mass flow rate of air passing through the array, A_t is the total heat transfer surface area (plates and fins), and η_o is the overall surface efficiency defined as $[1-(NA_f / A_t)(1-\eta_f)]$.

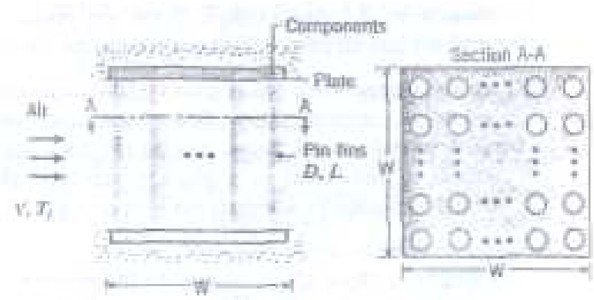

- **<u>Impinging Jet</u>**

41. A circular transistor of 10 mm diameter is cooled by impingement of an air jet exiting a 2-mm diameter round nozzle with a velocity of 20 m/s and a temperature of 15 °C. The jet exit and the exposed surface of the transistor are separated by a distance of 10 mm. If the transistor is well insulated at all but its exposed surface and the surface temperature is not to exceed 85 ^{o}C, what is the transistor's maximum allowable operating power?

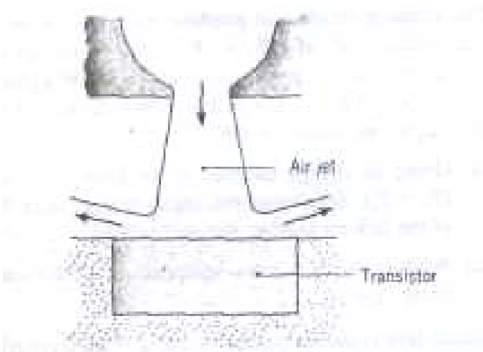

42. You have been asked to determine the feasibility of using an impinging jet in a soldering operation for electronic assemblies. The schematic illustrates the use of a single, round nozzle to direct high velocity, hot air to a location where a surface mount joint is to be formed.

For your study, consider a round nozzle with a diameter of 1 mm located a distance of 2 mm from the region of the surface mount, which has a diameter of 2.5 mm.

(a) For an air jet velocity of 70m/s and a temperature of 400 °C, estimate the average convection coefficient over the area of the surface mount.

(b) For three air jet temperatures of 400, 500, and 600 ^{o}C, calculate and plot the surface temperature as a function of time for $0 \leq t \leq 40$ s. On this plot, identify important temperature limits for the soldering process: the lower limit corresponding to the solder's eutectic temperature, T_{sol} = 183 °C and the upper limit corresponding to the glass transition temperature, T_{gl} = 250 ^{o}C, at which the PCB becomes plastic. Comment on the outcome of your study, the appropriateness of the assumptions, and the feasibility of using the jet for a soldering application.

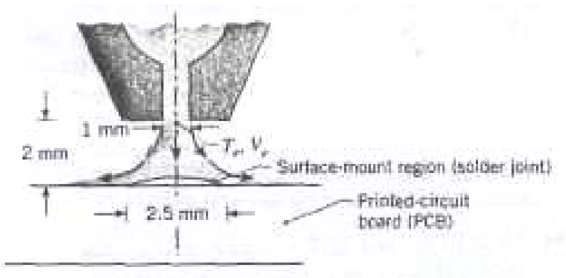

- **Internal Flow**

43. An electrical power transformer of diameter 300 mm and height 500 mm dissipates 1000 W. It is desired to maintain its surface temperature at 47 °C by supplying glycerin at 24 °C through thin-walled tubing of 20 mm diameter welded to the lateral surface of the transformer. All the heat dissipated by the transformer is assumed to be transferred to the glycerin.

(a) Assuming the maximum allowable temperature rise of the coolant to be 6 °C and fully developed flow throughout the tube, determine the required coolant flow rate, the total length of tubing, and the lateral spacing S between turns of the tubing.

(b) For a prescribed tube length of 15 m and a maximum allowable transformer surface temperature of 47 °C, compute and plot the maximum allowable transformer power and the outlet temperature of the glycerin as a function of flow rate for $0.05 \leq \dot{m} \leq 0.25$ kg/s. Account for the fact that the flow is not fully developed.

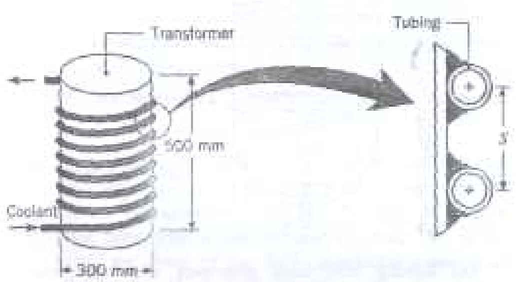

44. A common procedure for cooling a high-performance computer chip involves joining the chip to a heat sink within which circular microchannels are machined. During operation, the chip produces a uniform heal flux q_c'' at its interface with the heat sink, while a liquid coolant (water) is routed through the channels. Consider a square chip and heat sink, each L x L on a side, with microchannels of diameter D and pitch $S = C_1D$, where the constant C_1 is greater than unity.

Water is supplied at an inlet temperature $T_{m,i}$ and a total mass flow rate $m^{\bullet}$ (for the entire heat sink).

(a) Assuming that q_c'' is dispersed in the heat sink such that a uniform heat flux q_c'' is maintained at the surface of each channel; obtain expressions for the longitudinal distributions of the mean fluid, $T_m(x)$, and surface. $T_s(x)$, temperatures in each channel. Assume laminar, fully developed flow throughout each channel, and express your results in terms of $m^{\bullet}$. q_c''. C_1, D, and/or L, as well as appropriate thermophysical properties.

(b) For L = 12 mm, D = 1 mm, $C_1 = 2$, q_c'' = 20 W/cm^2, $m^{\bullet}$ = 0.010 kg/s, and $T_{m,i}$ = 290 K, compute and plot the temperature distributions $T_m(x)$ and T_s (x).

(c) A common objective in designing such heat sinks is to maximize q_c'' while maintaining the heat sink at an acceptable temperature. Subject to prescribed values of L = 12 mm and $T_{m,i}$ = 290 K and the constraint that $T_{s,max} \leq 50°C$, explore the effect on q_c'' of variations in heat sink design and operating conditions.

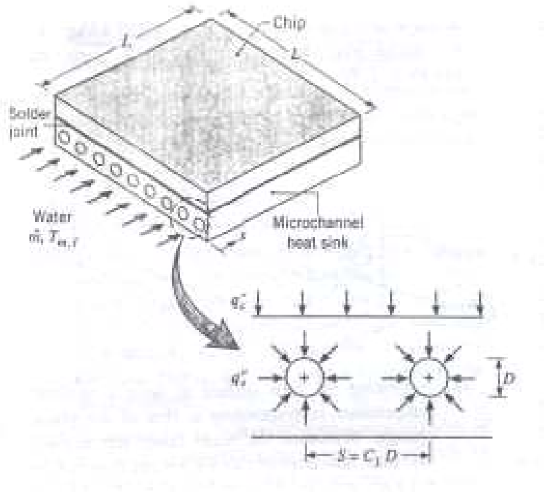

45. One way to cool chips mounted on the circuit boards of a computer is to encapsulate the boards in metal frames that provide efficient pathways for conduction to supporting cold plates. Heat generated by the chips is then dissipated by transfer to water flowing through passages drilled in the plates. Because the plates are made from a metal of large thermal conductivity (typically aluminum or copper), they may be assumed to be at a uniform temperature, $T_{s,cp}$.

(a)Consider circuit boards attached to cold plates of height H = 750 mm and width L = 600 mm, each with N = 10 holes of diameter D = 10mm. If operating conditions maintain plate temperatures of $T_{s,cp}$ = 32 °C with water flow at $\dot{m}_1$= 0.2 kg/s per passage and $T_{m,i}$ = 7 °C, how much heat may be dissipated by the circuit boards?

(b)To enhance cooling, thereby allowing increased power generation without an attendant increase in system temperatures, a hybrid cooling scheme may be used. The scheme involves forced air flow over the encapsulated circuit boards, as well as water flow through the cold plates. Consider conditions for which N_{cb} = 10 circuit boards of width W = 350 mm are attached to cold plates and their average surface temperature is $T_{s,cb}$ = 47 °C when $T_{s,cp}$ = 32°C. If air is in parallel flow over the plates with u_∞ = 10 m/s and T_∞ = 7 °C, how much of the heat generated by the circuit boards is transferred to the air?

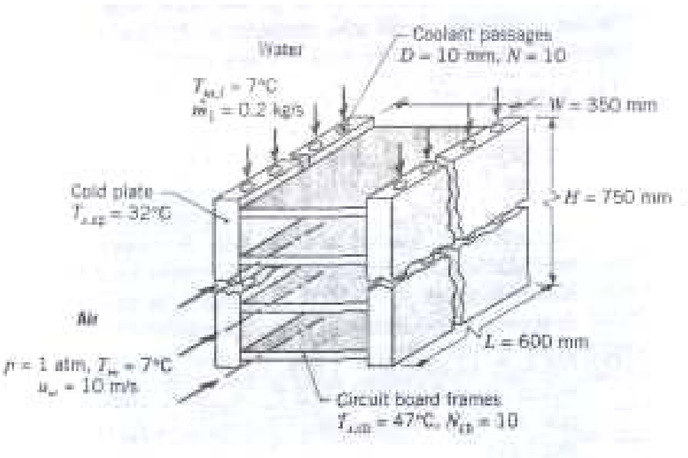

46. Freon is being transported at 0.1 kg/s through a Teflon tube of inside diameter D_i = 25 mm and outside diameter D_o = 28 mm, while atmospheric air at V = 25 m/s and 300 K is in cross flow over the tube. What is the heat transfer per unit length of tube to Freon at 240 K?

47. A novel scheme for dissipating heat from the chips of a multichip array involves machining coolant channels in the ceramic substrate to which the chips are attached. The square chips (L_c = 5 mm) are aligned above each of the channels, with longitudinal and transverse pitches of $S_L = S_T$ = 20 mm. Water flows through the square cross section (W = 5 mm) of each channel with a mean velocity of u_m = 1 m/s, and its properties may be approximated as ρ = 1000 kg/m^3, C_p = 4180 J/kg .K, μ = 855 x 10^{-6} kg/s.m, k = 0.610 W/m.K, and Pr = 5.8. Symmetry in the transverse direction dictates the existence of equivalent conditions for each substrate section of length L_s and width S_T.

(a) Consider a substrate whose length in the flow direction is L_s = 200 mm, thereby providing a total of N_L = 10 chips attached in-line above each flow channel. To a good approximation, all the heat dissipated by the chips above a channel may be assumed to be transferred to the water flowing through the channel. If each chip dissipates 5 W, what is the temperature rise of the water passing through the channel?

(b) The chip-substrate contact resistance is $R''_{t,c}$ = 0.5 x 10^{-4} m^2.K/W, and the three-dimensional conduction resistance for the L_s x S_T substrate section is R_{cond} =

0.120 K/W. If water enters the substrate at 25 °C and is in fully developed flow, estimate the temperature T_c of the chips and the temperature T_s of the substrate channel surface.

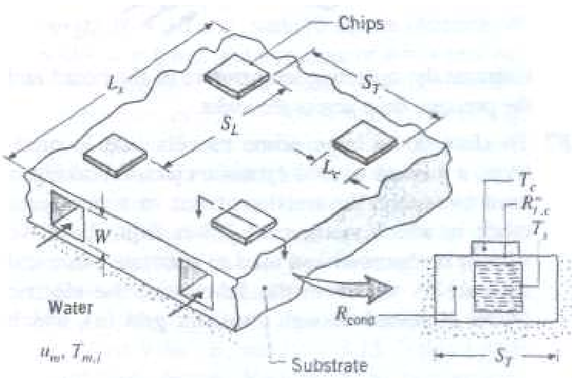

48. To cool electronic components that are mounted to a printed circuit board and hermetically sealed from their surroundings, two boards may be joined to form an intermediate channel through which the coolant is passed. Termed a hollow-core PCB, all of the heat generated by the components may be assumed to be transferred to the coolant. Consider a hollow-core PCB of length L = 300 mm and equivalent width W (normal to the page). Under normal operating conditions, 40 W of power are dissipated on each side of the PCB and a uniform distribution of the attendant heat transfer may be assumed for each of the hollow-core surfaces. If air enters a core of height H = 4 mm at a temperature of $T_{m\ i}$ = 20°C and a flow rate of $m^{\bullet}$ = 0.002 kg/s what is its outlet temperature $T_{m\ o}$? What are the surface temperatures at the inlet and outlet of the core? What are the foregoing temperatures if the flow rate is increased by a factor of five?

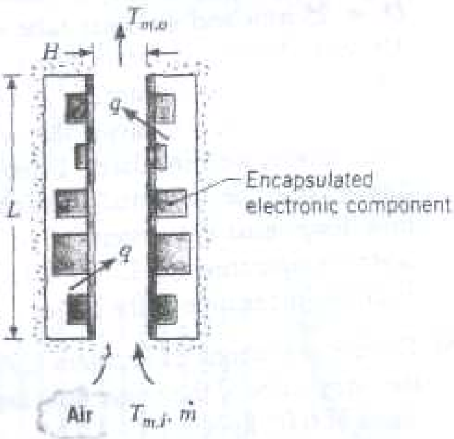

49. A printed circuit board (PCB) is cooled by laminar, fully developed air flow in adjoining, parallel-plate channels of length L and separation distance a. The channels may be assumed to be of infinite extent in the transverse direction, and the upper and lower surfaces are insulated. The temperature T_s, of the PCB board is uniform, and air flow with an inlet temperature of $T_{m,i}$ is driven by a pressure difference, Δp.
Calculate the average heat removal rate per unit area (W/m^2) from the PCB.

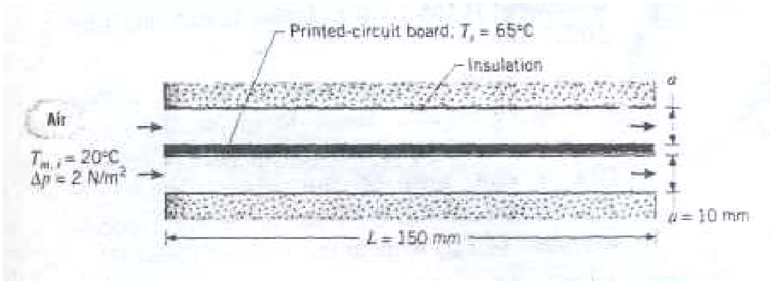

- **<u>Fans Performance</u>**

50. The electronics in a fan cooled box dissipate 450 W. In an environment of 30°C, the cooling air should leave the box at a temperature of no more than 70 °C. Measurements showed that when the air is flowing through the box at a rate of 20 m^3/h, the pressure drop is 40 Pa. *A* fan is available that has the following characteristics

Discharge, m^3/h	0	10	20	30	40	50	60
Pressure drop, Pa	320	225	215	250	200	110	0

Is this fan suitable for the purpose? Under what conditions would it operate?

51. The electronics in a fan cooled box dissipate 600 W in an environment of 30 °C. The cooling air should leave the box at a temperature not exceeding 70 °C. Measurements showed that when the air is flowing through the box at a rate of 30 m^3/h, the pressure drop is 90 Pa. The characteristics of the fan available for the purpose, when operating at 1000 rpm, is given by

$$\Delta p = 320 + 0.7\ V^{\bullet} - 0.1\ V^{\bullet 2}$$

Where $V^{\bullet}$ is the discharge in m^3/h and Δp in Pascal's.
Is this fan suitable for the purpose? If not, suggest a method to make it suitable for the task.

52. The following table gives the performance of a fan that handles air at a speed of 1200 rpm. What would be the performance of this fan when it handles hydrogen at this speed and at a speed of 1800 rpm? (The molecular weight of hydrogen is 2; its apparent value for air is 28.8).

Discharge, m^3/h	0	10	20	30	40	50	60
Pressure drop , Pa	320	225	215	250	200	110	0
Power, W	0.4	1	2	3.5	3.8	2.5	0.4

- **<u>Mixed Convection</u>**

53. A vertical array of circuit boards of 150 mm height is to be air cooled such that the board temperature does not exceed 60 °C when the ambient temperature is 25 °C.
Assuming isothermal surface conditions, determine the allowable electrical power dissipation per board for the cooling arrangements:
(a)Free convection only (no forced airflow).
(b)Airflow with a downward velocity of 0.6 m/s.
(c)Airflow with an upward velocity of 0.3 m/s.
(d)Airflow with a velocity (upward or downward) of 5 m/s.

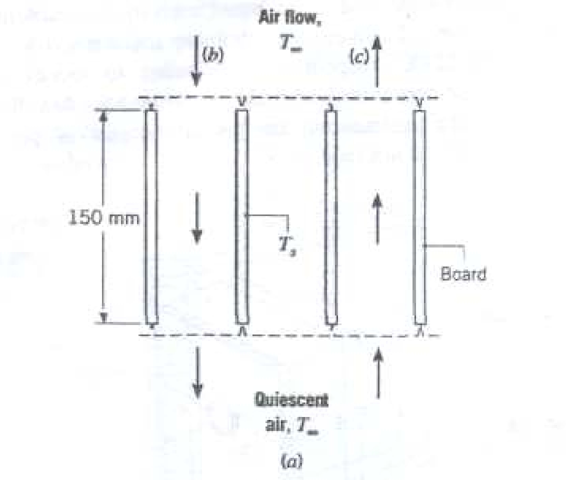

54. Heat-dissipating electrical components are mounted to the inner surface of a long metallic tube. The tube is of 0.10 m diameter and is submerged in a quiescent water bath.

What is the heat dissipation per unit tube length if the tube wall and water temperatures are 350 and 300 K, respectively? What is the heat dissipation per unit length if a forced flow is imposed over the tube, with a cross-flow velocity of 1.0 m/s?

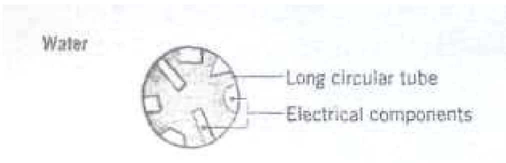

- **Heat Exchangers**

55. In a supercomputer, signal propagation delays are reduced by resorting to high-density circuit arrangements, which are cooled by immersing them in a special dielectric liquid. The fluid is pumped in a closed loop through the computer and an adjoining shell-and-tube heat exchanger having one shell and two tube passes.
During normal operation, heat generated within the computer is transferred to the dielectric fluid passing through the computer at a flow rate of m_f = 4.81 kg/s. In turn, the fluid passes through the tubes of the heat exchanger and the heat is transferred to water passing over the tubes. The dielectric fluid may be assumed to have constant properties of C_p = 1040 J/kg. K, μ = 7.65 x 10^{-4} kg/s. m, k = 0.058 W/m. K, and Pr = 14. During normal operation, chilled water at a flow rate of $\dot{m}_w$ = 2.5 kg/s and an inlet temperature of $T_{w,i}$ = 5 °C passes over the tubes. The water has a specific heat of 4200 J/kg. K and provides an average convection coefficient of 10,000 W/m^2.K over the outer surface of the tubes.

(a) If the heat exchanger consists of 72 thin-walled tubes, each of 10-mm diameter, and fully developed flow is assumed to exist within the tubes, what is the convection coefficient associated with flow through the tubes?
(b) If the dielectric fluid enters the heat exchanger at $T_{f,i}$ = 25 °C and is to leave at $T_{f,o}$ = 15 °C, what is the required tube length per pass?
(c) For the exchanger with the tube length per pass determined in part (b), plot the outlet temperature of the dielectric fluid as a function of its flow rate for $4 \le \dot{m}_w \le 6$ kg/s.

Account for corresponding changes in the overall heat transfer coefficient, but assume all other conditions to remain the same.

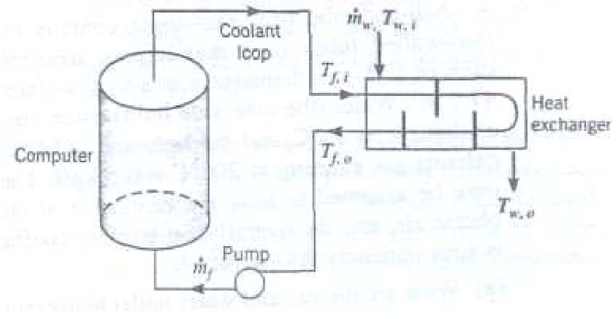

Radiation

- **Radiation Properties Applications**

56. Square plates freshly sprayed with epoxy paint must be cured at 140 °C for an extended period of time. The plates are located in a large enclosure and heated by a bank of infrared lamps. The top surface of each plate has an emissivity of ε = 0.8 and experiences convection with a ventilation air stream that is at T_∞ = 27 °C and provides a convection coefficient of h = 20 W/m^2. K. The irradiation from the enclosure walls is estimated to be G_{wall} = 450 W/m^2, for which the plate absorptivity is α_{wall} = 0.7.

(a) Determine the irradiation that must be provided by the lamps, G_{lamp}. The absorptivity of the plate surface for this irradiation is α_{lamp} = 0.6.

(b) For convection coefficients of h = 15, 20, and 30 W/m^2. K. Plot the lamp irradiation, G_{lamp}, as a function of the plate temperature. Ts, for 100 ≤ Ts ≤ 300 °C.

(c) For convection coefficients in the range from 10 to 30 W/m^2. K and a lamp irradiation of G_{lamp} = 3000 W/m^2. Plot the air stream temperature T_∞ required to maintain the plate at T_s = 140 °C.

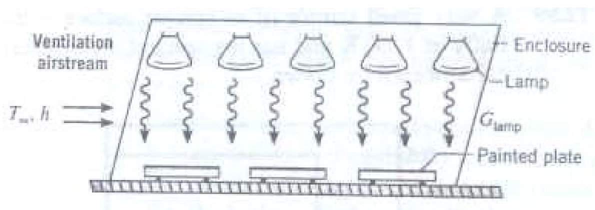

57. An instrumentation transmitter pod is a box containing electronic circuitry and a power supply for sending sensor signals to a base receiver for recording. Such a pod is placed on a conveyor system, which passes through a large vacuum brazing furnace as shown in the sketch. The exposed surfaces of the nod have a special diffuse, opaque coating with spectral emissivity as shown below.

To stabilize the temperature of the pod and prevent overheating of the electronics, the inner surface of the pod is surrounded by a layer of a phase-change material (PCM) having a fusion temperature of 87 °C and a heat of fusion of 25 kJ/kg. The pod has an exposed surface area of 0.040 m^2 and the mass of the PCM is 1.6 kg. Furthermore, it is known that the power dissipated by the electronics is 50 W. Consider the situation when the pod enters the furnace at a uniform temperature of 87 °C and all the PCM are in the solid state. How long will it take before all the PCM changes to the liquid state?

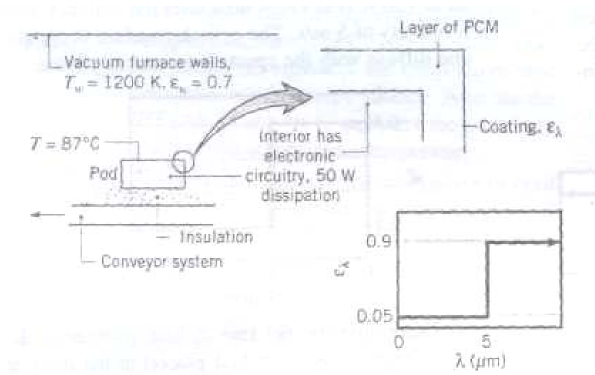

58. Components of an electronic package in an orbiting satellite are mounted in a compartment that is well insulated on all but one of its sides. The uninsulated side consists of an isothermal copper plate whose outer surface is exposed to the vacuum of outer space and whose inner surface is attached to the components. The plate dimensions are 1 m by 1 m on a side.

The exposed surface of the plate, which is opaque and diffuse, has a spectral, hemispherical absorptivity of α_λ = 0.2 for $\lambda \leq 2$ μm and α_λ = 0.8 for $\lambda > 2$ μm. Consider steady-state conditions for which the plate is exposed to a solar flux of q_s'' = 1350 W/m^2, which is incident at an angle of θ = 30° relative to the surface normal. If the plate temperature is T_p = 500 K, how much power is being dissipated by the components?

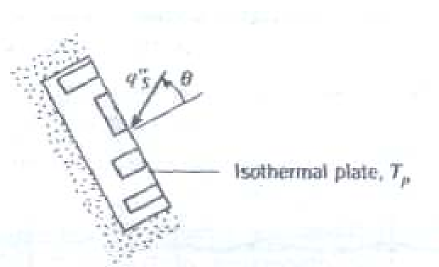

- **<u>Radiation Exchange Between Surfaces</u>**

59. Determine F_{12} and F_{21} for the following configurations using the reciprocity theorem and other basic shape factor relations. Do not use tables or charts.

(a) Long duct

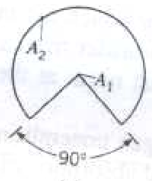

(a)

(b) Small sphere of area A_1 under a concentric hemisphere of area $A_2 = 2A_1$

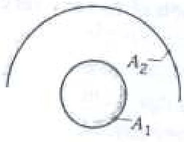

(b)

(c) Long duct. What is F_{22} for this case?

(c)

(d) Long inclined plates (point B is directly above the center of A_1)

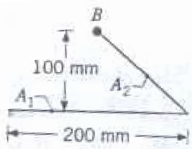

(d)

(e) Sphere lying on infinite plane

(e)

(f) Hemisphere-disk arrangement

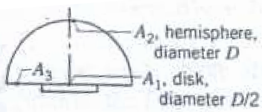

(f)

(g) Long open channel

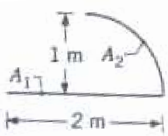

(g)

60. Electrical conductors, in the form of parallel plates of length L = 40 mm, have one edge mounted to a ceramic insulated base and are spaced a distance w = 10 mm apart. The plates are exposed to large isothermal surroundings at T_{sur} = 300 K. The conductor (1) and ceramic (2) surfaces are diffuse and gray with emissivities of $\varepsilon_1 = 0.8$ and $\varepsilon_2 = 0.6$, respectively. For a prescribed operating current in the conductors, their temperature is T_1 = 500 K.

(a) Determine the electrical power dissipated in a conductor plate per unit length $q_1^{'}$ considering only radiation exchange. What is the temperature of the insulated base, T_2?

(b) Determine $q_1^{'}$ and T_2 when the surfaces experience convection with an air stream at 300 K and a convection coefficient of h =25 W/m^2. K

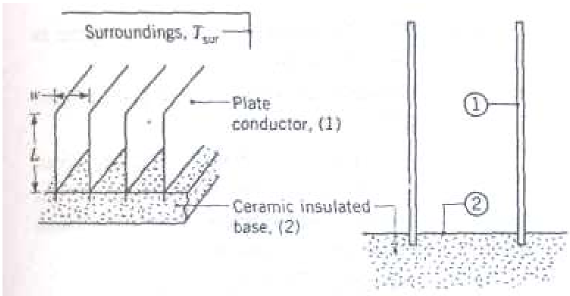

61. A scheme for cooling electronic components involves mounting them to a copper plate that forms one vertical wall of a rectangular cavity containing helium gas at atmospheric pressure.

The cavity width and height are L = 20 mm and H = 160 mm, respectively. The top and bottom surfaces, as well as the back wall of the component compartment, are well insulated. Under steady-state conditions, the copper plate and the adjoining cold plate are maintained at 75 and 15 °C, respectively. The plates each have an emissivity of 0.8.

(a) Determine the rate at which heat is being dissipated by the components per unit distance perpendicular to the cross section (W/m).

(b) Assess the effect of varying the plate spacing L on the heat dissipation rate.

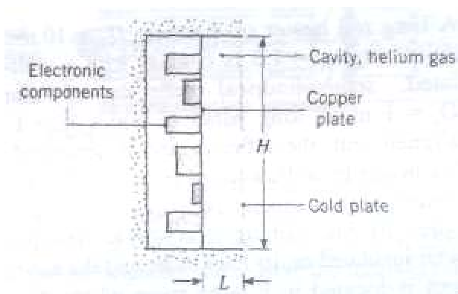

62. In an orbiting space station, an electronic package is housed in a compartment having a surface area, A_S = 1 m^2, which is exposed to space. Under normal operating conditions, the electronics dissipate 1 kW, all of which must be transferred from the exposed surface to space. If the surface emissivity is 1.0 and the surface is not exposed to the sun. What is its steady-state temperature? If the surface is exposed to a solar flux of 750 W/m^2 and its absorptivity to solar radiation is 0.25, what is its steady-state temperature?

63. In the thermal processing of semiconductor materials, annealing is accomplished by heating a silicon wafer according to a temperature-time recipe and then maintaining a fixed elevated temperature for a prescribed period of time. For the process tool arrangement shown as follows, the wafer is in an evacuated chamber whose walls are maintained at 27 °C and within which heating lamps maintain a radiant flux q" at its upper surface. The wafer is 0.78 mm thick, has a thermal conductivity of 30W/m.K. and an emissivity that equals its absorptivity to the radiant flux ($\varepsilon = \alpha = 0.65$). For q"= 3.0 x 10^5 W/m^2, the temperature on its lower surface is measured by a radiation thermometer and found to have a value of $T_{w,l}$ = 997°C. To avoid warping the wafer and inducing slip planes in the crystal structure, the temperature difference across the thickness of the wafer must be less than 2 ^oC. Is this condition being met?

64. A satellite in the form of a cube is in deep space between the earth and the sun. Determine its equilibrium temperature if its surface is: (a) polished aluminum (h) painted grey (c) painted white.

65. In a large electronics panel in outer space, heat is generated at a rate of 300 W/m^2. It is cooled by a parallel panel maintained at -23 °C that has a reflectivity of 0.4.Estimate the temperature at which the electronics panel would operate if its emissivity is 0.8.

66. A polished copper panel is 20 x 30 cm and is used as a heat sink for an electronic package at sea level. The panel is finned to dissipate 25 W when at 70 °C in air at 50 °C. The fins are 1.5 mm thick and 40 mm long. How many fins are required for the purpose? How would you set the panel for best operation?

67. A polished copper panel 30 x 20 cm has 15 fins, 1.5 mm, thick protruding 40 mm along the 20 cm length. Estimate the maximum power that could be dissipated by this panel when its temperature is 70 °C in air at 50 °C.

68. The vertical side of an electronics box is 40 x 30 cm with the 40 cm side vertical. What is the maximum energy that could be dissipated by this side if its temperature is not to exceed 60 °C in an environment of 40 °C, and its emissivity is 0.8?

Boiling and Condensation

69. A silicon chip of thickness L = 2.5 mm and thermal conductivity k_s = 135 W/m. K is cooled by boiling a saturated fluorocarbon liquid (T_{sat} = 57 °C) on its surface. The electronic circuits on the bottom of the chip produce a uniform heat flux of $q_o'' = 5 \times 10^4$ W/m^2, while the sides of the chip are perfectly insulated. Properties of the saturated fluorocarbon are $C_{p,l}$ = 1100 J/kg. K, h_{fg} = 84,400 J/kg, ρ_l = 1619.2 kg/ m^3, ρ_v = 13.4 kg/ m^3, $\sigma = 8.1 \times 10^{-3}$ kg/s^2, $\mu_l = 440 \times 10^{-6}$ kg/m. s, and Pr_l = 9.01. In addition, the nucleate boiling constants are $C_{s,f}$ = 0.005 and n = 1.7.

(a) What is the steady-state temperature T_o at the bottom of the chip? If, during testing of the chip, q_o'' is increased to 90% of the critical heat flux, what is the new steady-state value of T_o?

(b) Compute and plot the chip surface temperatures (top and bottom) as a function of heat flux for $0.20 \leq q_o''/q_{max}'' \leq 0.90$. If the maximum allowable chip temperature is 80 °C, what is the maximum allowable value of q_o''?

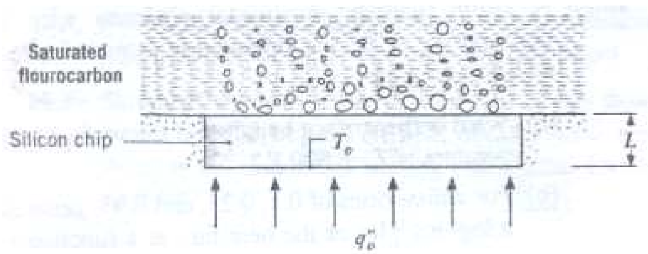

70. A device for performing boiling experiments consists of a copper bar (k = 400 W/m. K), which is exposed to a boiling liquid at one end, encapsulates an electrical heater at the other end, and is well insulated from its surroundings at all but the exposed surface. Thermocouples inserted in the bar are used to measure temperatures at distances of x_1 = 10 mm and x_2 = 25 mm from the surface.

An experiment is performed to determine the boiling characteristics of a special coating applied to the exposed surface. Under steady-state conditions, nucleate boiling is maintained in saturated water at atmospheric pressure and values of T_1 = 133.7 °C and T_2 = 158.6 °C are recorded. If n = 1, what value of the coefficient $C_{s,f}$ is associated with the Rohsenow correlation?

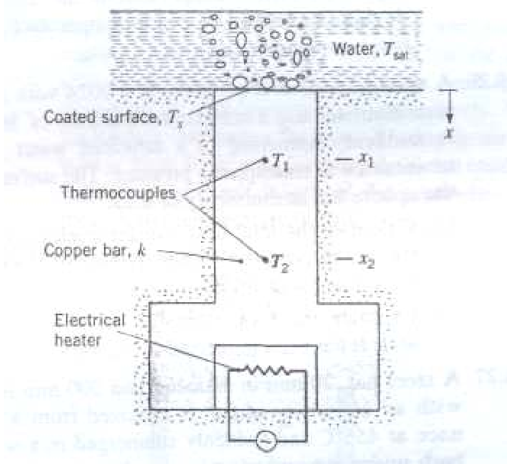

71. A technique for cooling a multichip module involves submerging the module in saturated fluorocarbon liquid. Vapor generated due to boiling at the module surface id condensed on the outer surface of copper tubing suspended in the vapor space above the liquid. the thin-walled tubing is of diameter D = 10 mm and is coiled in a horizontal plane. It is cooled by water that enters at 285 K and leaves at 315 K. All the heat dissipated by the chips within the module is transferred from a 100-mm by 100-mm boiling surface, at which the flux is 10^5 W/m^2, to the fluorocarbon liquid, which is at T_{sat} = 57 °C. Liquid properties are $C_{p,l}$ = 1100 J/kg. K, $h_{fg} = h'_{fg}$ = 84,400 J/kg, ρ_l = 1619.2 kg/m^3, ρ_v = 13.4 kg/m^3, $\sigma = 8.1 \times 10^{-3}$ kg/s^2, $\mu_l = 440 \times 10^{-6}$ kg/m. s, and Pr_l = 9.

(a) For the prescribed heat dissipation, what is the required condensation rate (kg/s) and water flow rate (kg/s)?
(b) Assuming fully developed flow throughout the tube, determine the tube surface temperature at the coil inlet and outlet.
(c) Assuming a uniform tube surface temperature of T_s = 53 °C, determine the required length of the coil.

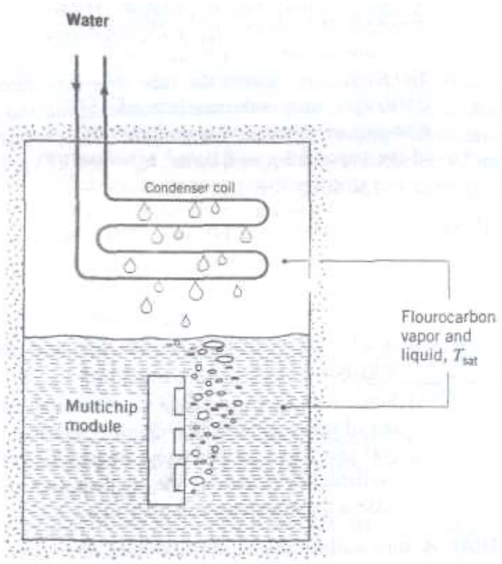

Combined Boiling/Condensation Problems

72. A passive technique for cooling heat-dissipating integrated circuits involves submerging the ICs in a low boiling point dielectric fluid. Vapor generated in cooling the circuits is condensed on vertical plates suspended in the vapor cavity above the liquid. The temperature of the plates is maintained below the saturation temperature, and during steady-state operation a balance is established between the rate of heat transfer to the condenser plates and the rate of heat dissipation by the ICs.

Consider conditions for which the 25-mm^2 surface area of each IC is submerged in a fluorocarbon liquid for which $T_{sat} = 50^oC$, $C_{p,l} = 1005$ J/kg. K, $h_{fg} = 1.05 \times 10^5$ J/kg, $\rho_l = 1700$ kg/m^3, $\sigma = 0.013$ kg/s^2, $\mu_l = 6.80 \times 10^{-4}$ kg/m. s, $k_l = 0.062$ W/m. K and $Pr_l = 11.0$, $C_{s,f} = 0.004$ and $n = 1.7$.

If the integrated circuits are operated at a surface temperature of $T_s = 75\ ^oC$, what is the rate at which heat is dissipated by each circuit? If the condenser plates are of height H = 50 mm and are maintained at a temperature of $T_c = 15$ °C by an internal coolant, and laminar film condensation is assumed, how much condenser surface area must be provided to balance the heat generated by 500 integrated circuits?

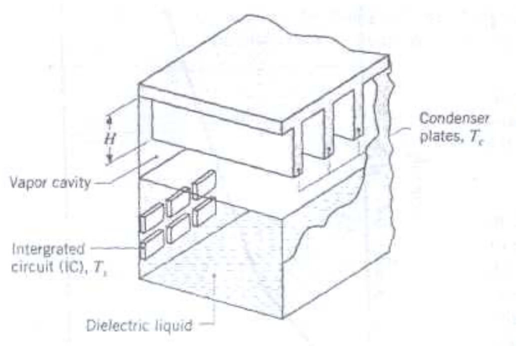

73. A novel scheme for cooling computer chips uses a thermosyphon containing a saturated fluorocarbon. The chip is brazed to the bottom of a cuplike container, within which heat is dissipated by boiling and subsequently transferred to an external coolant (water) via condensation on the inner surface of a thin-walled tube.

The nucleate boiling constants and the properties of the fluorocarbon are provided in Problem 1.0. In addition, $k_l = 0.054$ W/m. K

(a) If the chip operates under steady-state conditions and its surface heat flux is maintained at 90% of the critical heat flux, what is its temperature T? What the total power dissipation if the chip width is $L_c = 20$ mm on a side?

(b) If the tube diameter is D = 30 mm and its surface is maintained at $T_s = 25\ ^oC$ by the water, what tube length L is required to maintain the designated conditions?

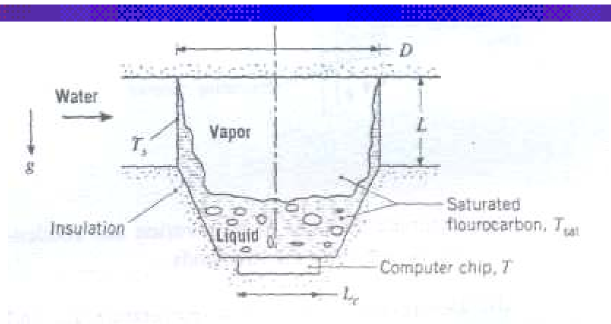

TEC

74. The interface temperature of an electronic assembly dissipating 10 W must be limited to 40 ^oC in a 50 ^oC environment. It is assumed that all of the generated heat will be removed by thermoelectrics and that heat absorbed from the environment is negligible. The interface temperature difference between the assembly and the thermoelectric can be held to 2 ^oC. The temperature difference between the thermoelectric and ambient can be held to 8 ^oC.
The bismuth telluride element used has a length of 0.3 cm and a cross-area of 0.01 cm^2.

Determine the size and performance characteristics of the thermoelectric temperature control device.
Knowing that

- The equivalent material properties of the thermoelectric couples is
  $\rho_e = 0.00267\ \Omega.cm$
  $\alpha_e = 425 \times 10^{-6}$ V/K
  $k_e = 0.00785$ W/cm.K
- Design for maximum refrigeration capacity.

Impinging Jets Problems

75. A circular transistor of 10 mm diameter is cooled by impingement of an air jet exiting a 2- mm diameter round nozzle with a velocity of 20 m/s and a temperature of 15 °C. The jet exit and the exposed surface of the transistor are separated by a distance of 10 mm. If the transistor is well insulated at all but its exposed surface and the surface temperature is not to exceed 85 ^oC, what is the transistor's maximum allowable operating power?

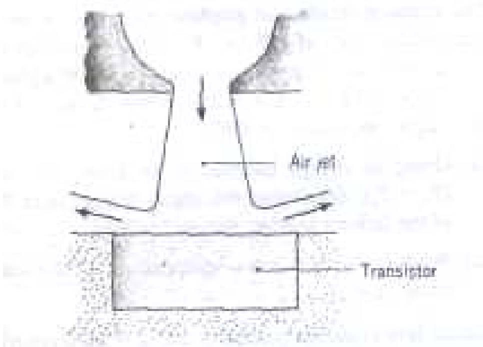

76. You have been asked to determine the feasibility of using an impinging jet in a soldering operation for electronic assemblies. The schematic illustrates the use of a single, round nozzle to direct high velocity, hot air to a location where a surface mount joint is to be

formed.
For your study, consider a round nozzle with a diameter of 1 mm located a distance of 2 mm from the region of the surface mount, which has a diameter of 2.5 mm.

(c) For an air jet velocity of 70m/s and a temperature of 400 °C, estimate the average convection coefficient over the area of the surface mount.
(d) For three air jet temperatures of 400, 500, and 600 ^oC, calculate and plot the surface temperature as a function of time for $0 \le t \le 40$ s. On this plot, identify important temperature limits for the soldering process: the lower limit corresponding to the solder's eutectic temperature, T_{sol} = 183 °C and the upper limit corresponding to the glass transition temperature, T_{gl} = 250 ^oC, at which the PCB becomes plastic. Comment on the outcome of your study, the appropriateness of the assumptions, and the feasibility of using the jet for a soldering application.

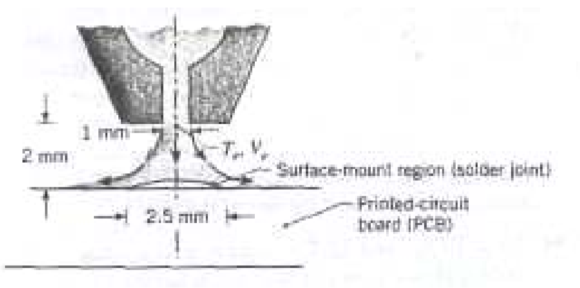

<u>Packaging of Electronic Equipments</u>
<u>Surface Mount Problems</u>
77. An electronic chassis was designed for natural convection cooling, so that a clearance of 0.75 in (1.905 cm) was provided between the PCBs and components. However, a design change required the addition of another PCB, which might reduce the clearance too much unless the new PCB is placed very close to the side wall of the chassis, with a clearance of only 0.20 in (0.51 cm). The PCB measures 6 x 9 in and dissipates 5.5 watts. The electronic chassis must operate at sea level conditions in a maximum ambient temperature of 110 °F (43.3 °C). The maximum allowable component surface temperature is 212 °F (100 °C) with the chassis shown in Figure below. The aluminum chassis has a polished finish that has a low emissivity, so that the heat lost by radiation is small. The PCB construction only allows heat to be removed from the component mounting face. Determine if the design is adequate.

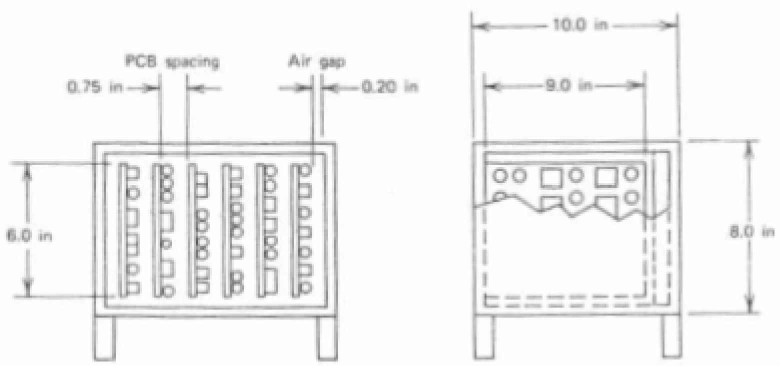

PCB spaced close to an end bulkhead

78. An aluminum (5052) plate is used to support a row of six power resistors. Each resistor dissipates 3 watts, for a total power dissipation of 18 watts. The bulkhead conducts the heat to the opposite wall of the chassis, which is cooled by a multiple fin heat exchanger. The bulkhead has two cutouts for connectors to pass through, as shown in figure below. Determine the temperature rise across the length of the bulkhead.

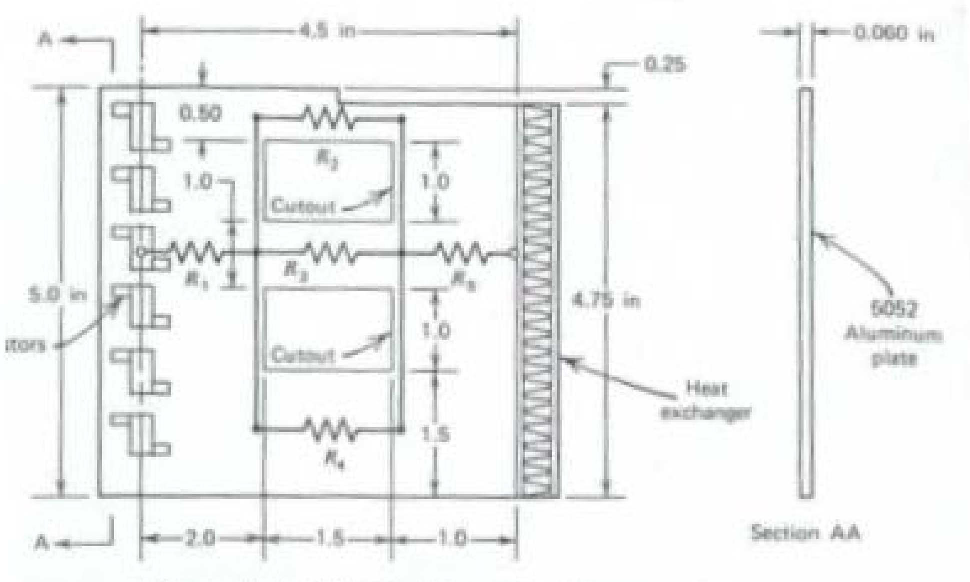

Bulkheads with two cutouts for connectors

79. Several power transistors, which dissipate 7 watts each, are mounted on a power supply circuit board that has a 0.093 in thick 5052 aluminum heat sink plate, as shown in Figure below. Determine how much lower the case temperatures will be when these components are mounted close to the edge of the PCB (new design), instead of the center of the PCB (old design).

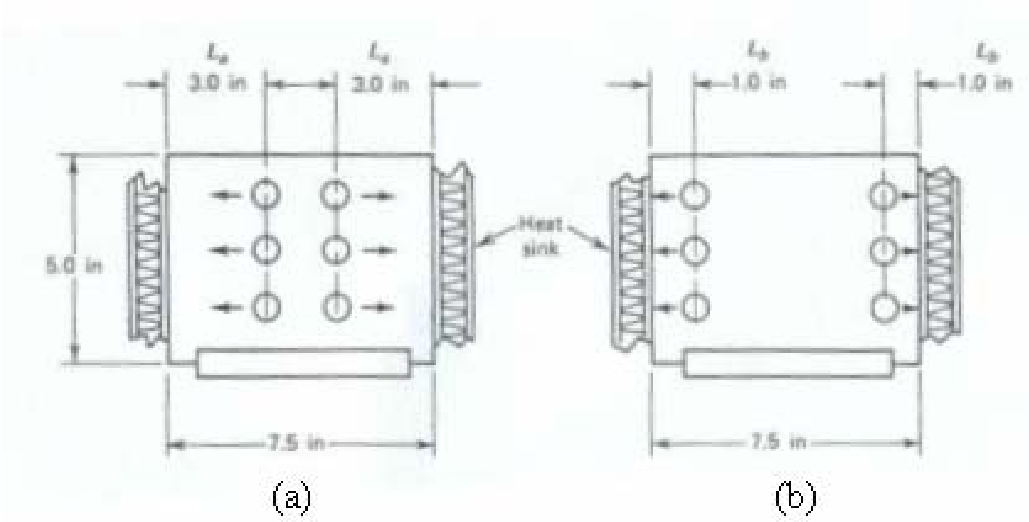

Power transistors mounted on an aluminum heat sink plate. (a) Old design (b) new design

80. Determine the temperature rise across the PCB edge guide (from the edge of the PCB to the chassis wall) for the assembly shown in figure below. The edge guide is 5.0 in long, type d. The total power dissipation of the PCB is 8 watts, uniformly distributed, and the equipment must operate at 100,000 ft.

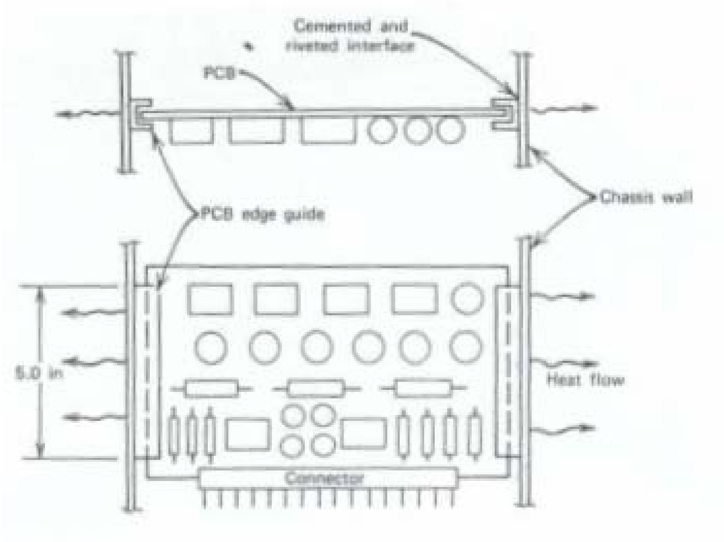

Plug-in PCB assembly with board edge guides

Electronics Cooling Problems

81. Determine the deflections and thermal stresses expected in the lead wires and solder joints of the surface mounted transformer shown in the following figure, when it is mounted on an aluminum composite PCB which experiences in plane (X and Y) thermal expansion during rapid temperature cycling tests over a temperature range from -30 to +80 °C, with no electrical operation. (Note: All dimensions in inches)
Assuming that:
$a_T = 35 \times 10^{-6}$ in/in/°C (average TCE of transformer)
$a_P = 20 \times 10^{-6}$ in/in/°C (average TCE of composite PCB)
$E_W = 16 \times 10^{6}$ psi (modulus of elasticity, copper wire)

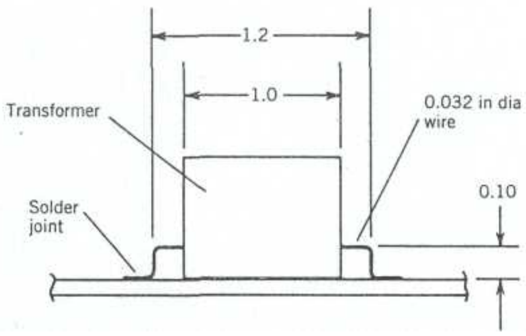

82. Determine the axial force in the lead wire for the resistor shown in figure below, when bending of the PCB is included in the analysis over a temperature cycling range from -50 to +90 °C, which produce total horizontal displacement expected at the top of the wire will be 0.0003 in. (Note: All dimensions in inches)

Assuming that:
$E_W = 16 \times 10^6$ Ib/in^2 (copper wire modulus elasticity)
$E_P = 1.95 \times 10^6$ Ib/in^2 (PCB modulus of elasticity)

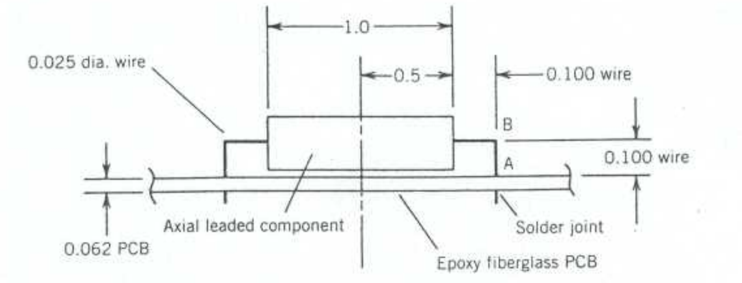

83. Determine the resonant frequency of a rectangular plug-in epoxy fiberglass PCB simply supported (or hinged) on all four sides, 0.080 in thick, with a total weight of 1.0 pounds, as shown in figure. (Note: All dimensions in inches)
Assuming that:
$E = 2 \times 10^6$ Ib/in^2 (PCB modulus of elasticity)
$\mu = 0.12$ (Poisson's ratio, dimensionless)

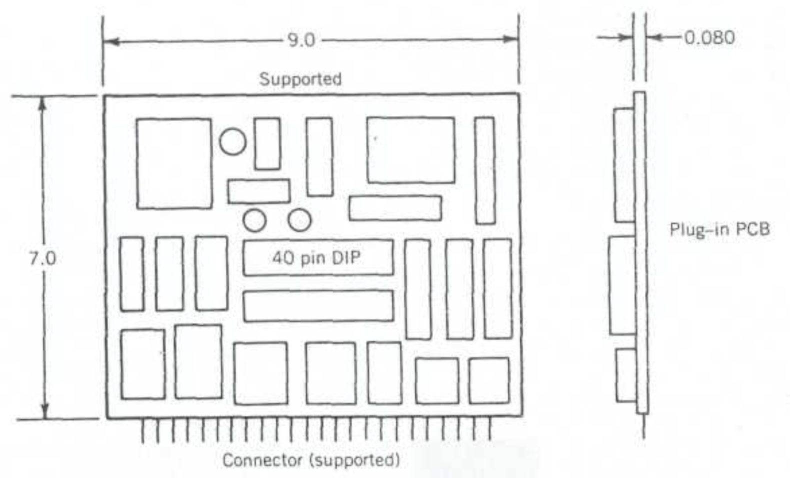

84. A 40 pin DIP (Dual inline package, electronic equipment) with standard lead wires, 2.5 in length will be installed at the center of a 8.0 x 6.0 x 0.080 in plug-in PCB. The DIP will be mounted parallel to the 9 in edge. The assembly must be capable of passing a 4.0G peak sine vibration qualification test with resonant dwell conditions. Determine the minimum desired PCB resonant frequency for a 10 million cycle fatigue life, and the approximate fatigue life.

Part G-3: Solved Problems

1. A square silicon chip (k = 150 W/m. K) is of width w =5 mm on a side and of thickness t = 1 mm. The chip is mounted in a substrate such that its side and back surfaces are insulated, while the front surface is exposed to a coolant. If 4 W are being dissipated in circuits mounted to the back surface of the chip, what is the steady-state temperature difference between back and front surfaces?

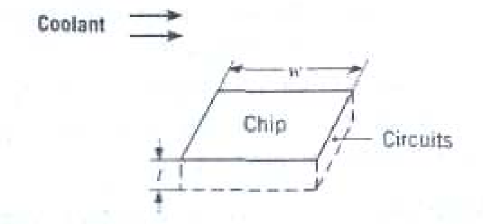

Data given: Chip dimensions, its thermal conductivity, and 4 W input power to the chip from the back surface of the chip.
Require: Temperature difference across the chip.
Assumptions:
(a) Steady-state conductions.
(b) Constant properties.
(c) One-dimensional conduction in the chip.
(d) Neglect heat loss from back and sides.

Solution:
From Fourier's law,

$$q = -kA\frac{dT}{dx}$$

Or,

$$P = q = kA\frac{\Delta T}{t}$$

Then,

$$\Delta T = \frac{tP}{kA} = \frac{0.001 \text{ X } 4}{150 \text{ X } (0.005)^2} = 1.07 \ ^oC$$

2. A square isothermal chip is of width w = 5 mm on a side and is mounted in a substrate such that its side and back surfaces are well insulated, while the front surface is exposed to the flow of a coolant at T_∞ = 15 °C. From reliability considerations, the chip temperature must not exceed T = 85 °C.
If the coolant is air and the corresponding convection coefficient is h = 200 W/m^2 K. What is the maximum allowable chip power? If the coolant is a dielectric liquid for which h = 3000 W/m^2.K. What is the maximum allowable power?

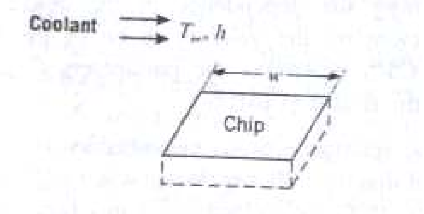

Data given: Chip width, coolant conditions, and maximum allowable chip temperature.
Require: maximum allowable chip power at air and dielectric liquid.
Assumptions:

(a) Steady-state conditions.
(b) Neglect heat loss from back surface and sides.
(c) Neglect the heat transferred by radiation.
(d) Chip is at uniform temperature (isothermal).

Solution:
According to Newton's law,

$$q = hA(T_s - T_\infty) = P$$

For air cooling,

$$P_{\max} = hA(T_{s,\max} - T_\infty) = 200 \text{ X } (0.005)^2 \text{ X } (85-15) = 0.35\,W$$

For dielectric liquid cooling,

$$P_{\max} = hA(T_{s,\max} - T_\infty) = 3000 \text{ X } (0.005)^2 \text{ X } (85-15) = 5.25\,W$$

Comment: at comparison between both air and liquid cooling. It appears the air heat transfer is poorer than the liquid heat transfer but cooling with liquid is higher cost.

3. The case of a power transistor, which is of length L = 10mm and diameter D = 12 mm, is cooled by an air stream of temperature T_∞ = 25 °C. Under conditions for which the air maintains an average convection coefficient of h = 100 W/m^2.K on the surface of the case, what is the maximum allowable power dissipation if the surface temperature is not to exceed 85 °C?

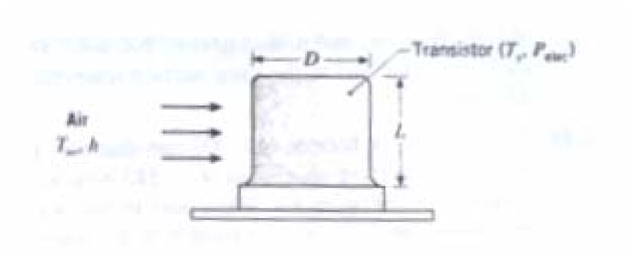

Data given: transistor dimensions, air coolant conditions, and maximum allowable chip temperature.

Require: maximum allowable transistor power.
Assumptions:
(a) Steady-state conditions.
(b) Neglect heat loss from base, and top surfaces.
(c) Neglect the heat transferred by radiation.
(d) Transistor is at uniform temperature (isothermal).

Solution:
According to Newton's law,

$$q = hA(T_s - T_\infty) = P$$

According to the maximum surface transistor temperature, the maximum allowable transistor power is,

$$P_{\max} = hA(T_{s,\max} - T_\infty) = 100 \text{ X } (\pi \text{ X } 0.012 \text{ X} 0.01) \text{ X } (85 - 25) = 2.262\ W$$

4. The use of impinging air jets is proposed as a means of effectively cooling high-power logic chips in a computer. However, before the technique can be implemented, the convection coefficient associated with jet impingement on a chip surface must be known. Design an experiment that could be used to determine convection coefficients associated with air jet impingement on a chip measuring approximately 10 mm by 10 mm on a side.

Given data: chip dimensions.
Required: determine the convection heat transfer coefficients experimentally.
Solution:
We will give the experiment in steps as follow,
1) Construct the system including its components as shown in figure below.
2) Bring voltmeter to measure the electric potential volt.
3) Bring ammeter to measure the electric current.
4) Bring thermometer to measure the surface temperature.
5) Close the electric circuit key.
6) Let constant power supply (IV = const.), plate surface area (A = const.), and free stream air temperature (T_∞ = const.).
7) The heat transfer coefficient depends on Reynolds number, and Prandtl number. Then by changing the jet air velocities according to its flow rates it will gives different heat transfer coefficients, which obtained according to the following relation, by known each measured plate surface temperature T_s (varied with each jet air velocity)..

$$q = IV = hA(T_s - T_\infty)$$

8) Plot the relation between the jet air velocities and heat transfer coefficients.

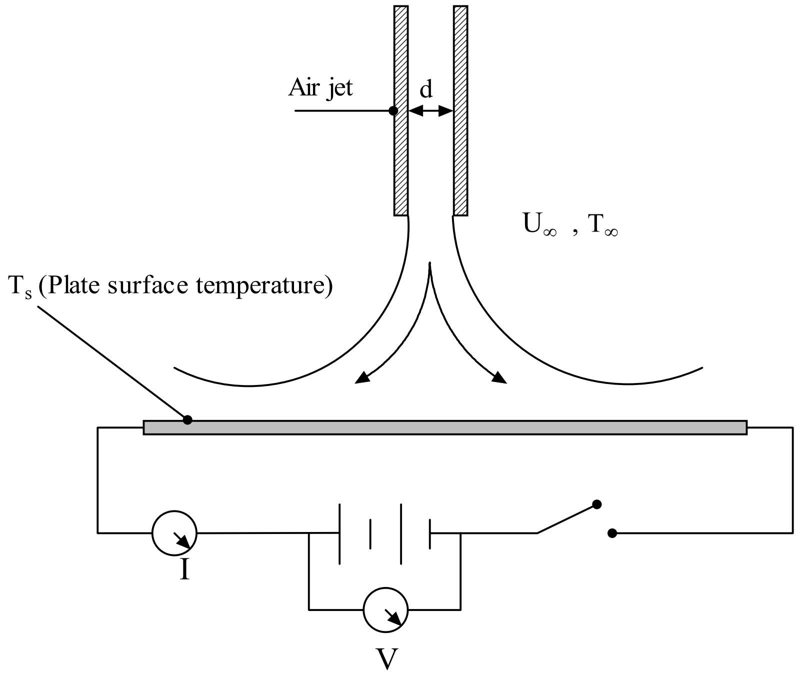

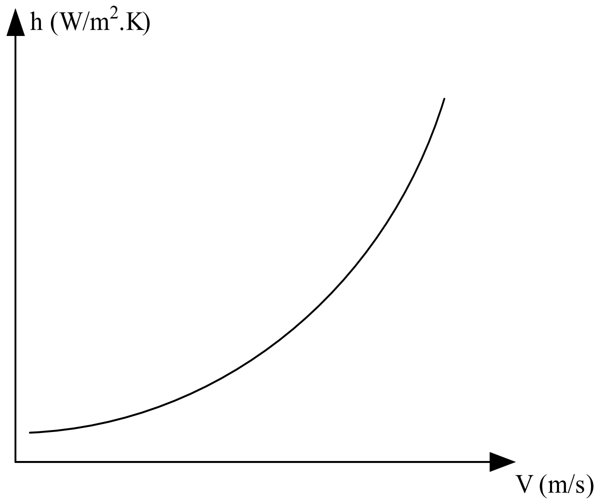

The suggested out put chart: Shows the effect of jet air velocities on heat transfer coefficients.

5. An instrumentation package has a spherical outer surface of diameter D = 100 mm and emissivity ε = 0.25. The package is placed in a large space simulation chamber whose walls are maintained at 77 K. If operation of the electronic components is restricted to the temperature range $40 \leq T \leq 85$ °C, what is the range of acceptable power dissipation for the package? Display your results graphically, showing also the effect of variations in the emissivity by considering values of 0.20 and 0.30.

Given data: Instrumentation emissivities (ε) and its surface temperature range $40 \leq T \leq 85$ °C
Require: The range of acceptable power dissipation for the package
Assumptions:

(a) Steady-state conditions.

(b) The chamber is very large compared to package size.
(c) Constant chamber wall temperature is maintained at 77 K.
(d) The chamber is evacuated.

Solution:

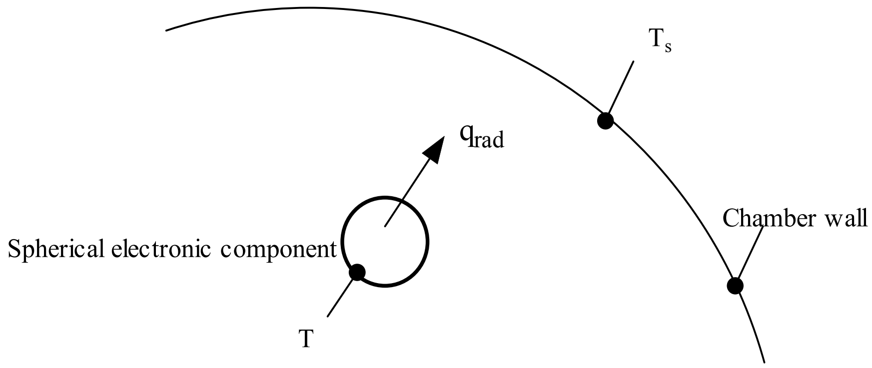

Because the electronic component in a large enclosure then the geometrical factor f = 1. Then the radiation heat transfer from the electronic component to the chamber wall is:

$$q = \sigma\varepsilon fA(T^4 - T_s^4)$$
$$= 5.67 \text{ X } 10^{-8} \text{ X } \varepsilon \text{ X } 1 \text{ X } (\pi \text{ X } 0.1^2)(T^4 - 77^4)$$
$$= 1.7813 \text{ X } 10^{-8} \ \varepsilon\ (T^4 - 77^4)$$

1) The range of acceptable power dissipation for the package at ε = 0.25

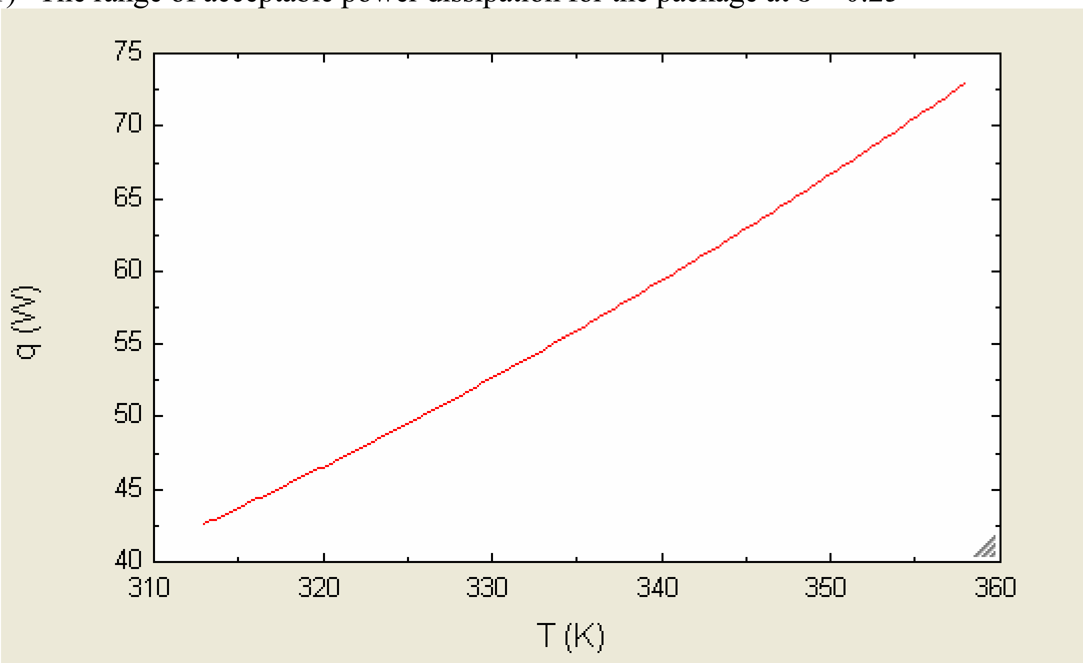

2) The effect of variations in the emissivity

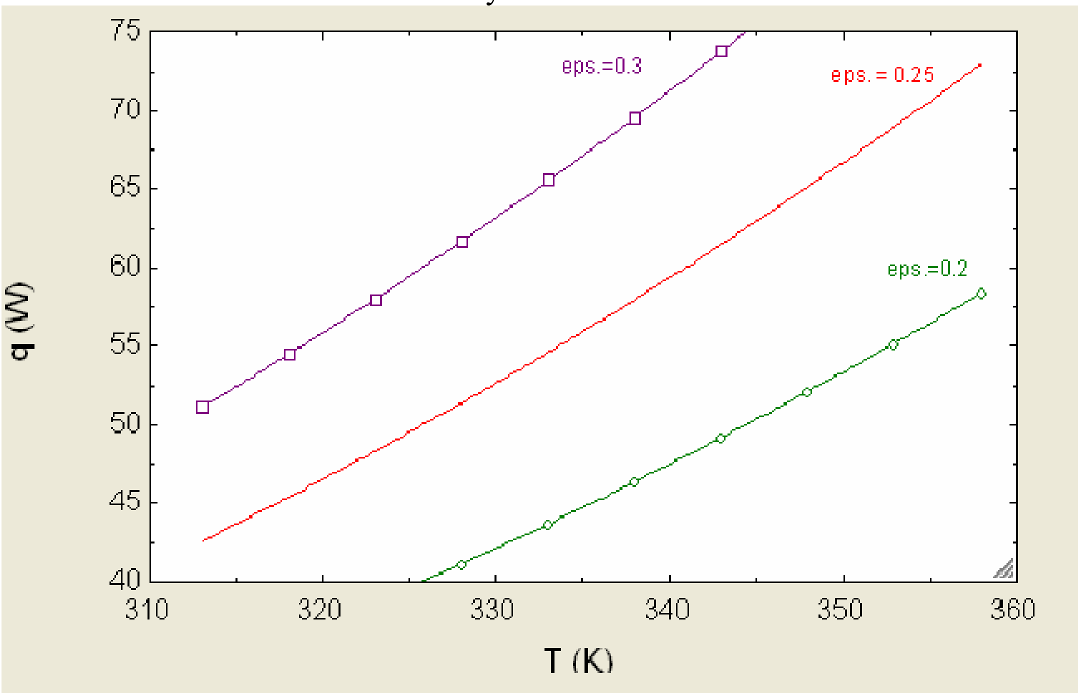

6. Consider the conditions of Problem 2. With heat transfer by convection to air, the maximum allowable chip power is found to be 0.35 W. If consideration is also given to net heat transfer by radiation from the chip surface to large surroundings at 15 °C, what is the percentage increase in the maximum allowable chip power afforded by this consideration?
The chip surface has an emissivity of 0.9.

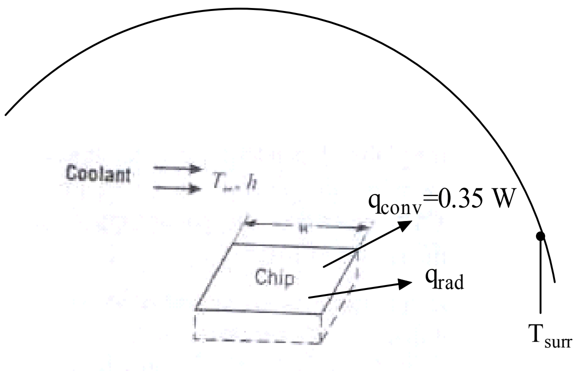

Data given: Chip width, coolant conditions, and maximum allowable chip power due to convective air cooling, maximum allowable chip temperature, and large surroundings temperature.
Require: percentage increase in the maximum allowable chip power due to radiation effect.
Assumptions:
(a) Steady-state conditions.
(b) Radiation exchange between small surface and large enclosure.
(c) Chip is at uniform temperature (isothermal).

Solution:
The radiation heat transfer is

$$\begin{aligned} q &= \sigma\varepsilon f A(T^4 - T_{surr}^4) \\ &= 5.67 \text{ X } 10^{-8} \text{ X } 0.9 \text{ X } 1 \text{ X } (0.005)^2(358^4 - 288^4) \\ &= 0.0122\, W \end{aligned}$$

Percentage increase in chip power due to radiation effect is

$$\%P_{\max} = ((0.35 + 0.0122)/0.35) - 1) * 100 = 3.49\ \%$$

7. A square chips of width L = 15 mm on a side are mounted to a substrate that is installed in an enclosure whose walls and air are maintained at a temperature of $T_\infty = T_{surr} = 25$ °C. The chips have an emissivity of ε = 0.60 and a maximum allowable temperature of $T_s = 85$ °C.

(a) If heat is rejected from the chips by radiation and natural convection, what is the maximum operating power of each chip? The convection coefficient depends on the chip-to-air temperature difference and may be approximated as $h = C\,(T_s - T_\infty)^{0.25}$, Where C = 4.2 W/m^2.K$^{5/4}$.
(b) If a fan is used to maintain air flow through the enclosure and heat transfer is by forced convection, with h = 250 W/m^2.K, what is the maximum operating power?

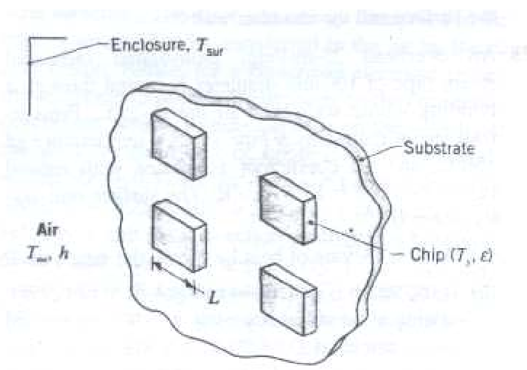

Given data: Chip width, walls and air temperatures, the chip emissivity, and maximum allowable chip temperature.

Require:
- (a) Maximum operating power of each chip.
- (b) Maximum operating power if a fan is used and heat transfer is by forced convection, with h = 250 W/m^2.

Assumptions:
- (a) Steady-state conditions.
- (b) Chip is at uniform temperature (isothermal).

(c) Radiation exchange between small surface and large enclosure.

Solution:

(a) The maximum operating chip power is the summation of heat transfer due to convection and radiation is

$$P_{\max} = q_{tot} = q_{conv} + q_{rad}$$
$$= hA(T_s - T_\infty) + \sigma\varepsilon fA(T_s^4 - T_{surr}^4)$$
$$= 4.2(0.015)^2(85-25)^{1.25} + 5.67 \text{ X } 10^{-8} \text{ X } 0.6 \text{ X } 1 \text{ X}(0.015)^2(358^4 - 298^4)$$
$$= 0.2232\, W$$

(b) Maximum operating power if a fan used is

$$P_{\max} = q_{tot} = q_{conv} + q_{rad}$$
$$= hA(T_s - T_\infty) + \sigma\varepsilon fA(T_s^4 - T_{surr}^4)$$
$$= 250(0.015)^2(85-25) + 5.67 \text{ X } 10^{-8} \text{ X } 0.6 \text{ X } 1 \text{ X}(0.015)^2(358^4 - 298^4)$$
$$= 3.44\, W$$

8. A computer consists of an array of five printed circuit boards (PCBs). Each dissipating P_b = 20 W of power. Cooling of the electronic components on a board is provided by the forced flow of air, equally distributed in passages formed by adjoining boards, and the convection coefficient associated with heat transfer from the components to the air is approximately h = 200 W/m^2.K. Air enters the computer console at a temperature of T_i = 20 °C, and flow is driven by a fan whose power consumption is P_f =25 W.

(a) If the temperature rise of the air flow. (T_o - T_i), is not to exceed 15 °C, what is the minimum allowable volumetric flow rate of the air? The density and specific heat of the air may be approximated as ρ= 1.161kg/m^3 and C_p = 1007J/kg.K, respectively.

(b) The component that is most susceptible to thermal failure dissipates 1 W/cm^2 of surface area. To minimize the potential for thermal failure, where should the component be installed on a PCB? What is its surface temperature at this location?

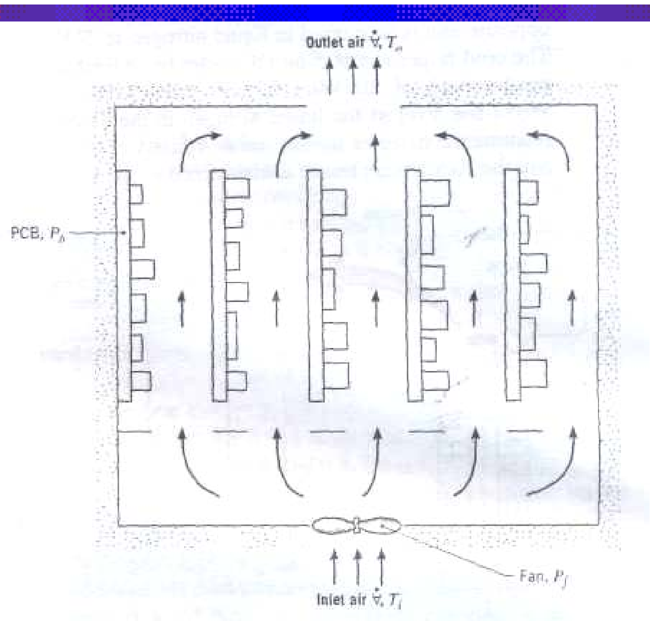

Given data: Five printed circuit boards (PCBs) each dissipating P_b = 20 W of power, convection coefficient associated with heat transfer from the components to the air, Air inlet temperature, and fan power consumption.

Assumptions:

(a) Steady-state conditions.
(b) Neglect the heat transferred by radiation.

Solution:

(a) By overall energy balance on the system including fan power is

$$5P_b + P_f = m_a^{\bullet} C_p (T_o - T_i)$$

$$5 \text{ X } 20 + 25 = 1.161 \text{ X } V_a^{\bullet} \text{ X } 1007(15)$$

The total volumetric flow rate of the air is

$$V_a^{\bullet} = 0.00713 \ m^3 / s$$

(b) To minimize the potential for thermal failure, the component should be installed on a PCB at the coolest air condition which at air entrance.

The board air inlet temperature which equals to temperature leaving the fan is

$$T_{b,i} = (P_f / m_a^{\bullet} C_p) + T_i$$

$$= (25 / 1.161\text{X}0.00713\text{X}1007) + 20 = 23 \ ^oC$$

The heat flux occurs at maximum temperature difference.

$$q'' = h\Delta T_{\max} = h(T_s - T_{b,i})$$
$$10000 = 200(T_s - 23)$$

The surface temperature at this location T_s equals 73 ^{o}C.

9. Electronic power devices are mounted to a heat sink having an exposed surface area of 0.045 m^2 and an emissivity of 0.80. When the devices dissipate a total power of 20 W and the air and surroundings are at 27 °C, the average sink temperature is 42 ^{o}C. What average temperature will the heat sink reach when the devices dissipate 30 W for the same environmental condition?

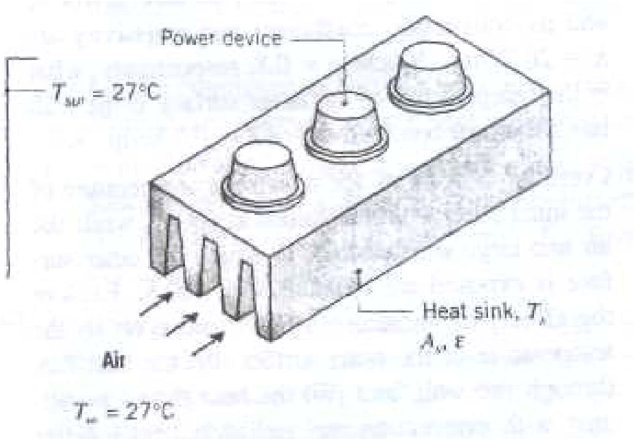

Given data: heat sink surface area, the average sink temperature and its emissivity, total power dissipation, air and surrounding temperatures

Require: Sink temperature when dissipation is 30 W.

Assumptions:

(a) Steady-state conditions.
(b) All dissipated power in devices transferred to the sink.
(c) Sink is at uniform temperature (isothermal).
(d) Radiation exchange between small surface (heat sink) and large enclosure (surrounding) case.
(e) Convective coefficient is the same for both power levels.

Solution:

At a total power device of 20 W.

$$P = q_{tot} = q_{conv} + q_{rad}$$
$$= hA(T_s - T_\infty) + \sigma\varepsilon fA(T_s^4 - T_{surr}^4)$$
$$20 = 0.045h(42 - 27) + 5.67 \text{ X } 10^{-8} \text{ X } 0.8 \text{ X } 1 \text{ X} 0.045(315^4 - 300^4)$$

The convective heat transfer coefficient h is

$$h = 24.35\, W/m^2.K$$

When the devices dissipate 30 W. Using the same value of heat transfer coefficient.

$$30 = 0.045 \text{ X } 24.35(T_s - 300) + 5.67 \text{ X } 10^{-8} \text{ X } 0.8 \text{ X } 1 \text{ X} 0.045(T_s^4 - 300^4)$$

By trial-and-error, the temperature of the heat sink is

$$T_s = 322 \text{ K} = 49\ ^{\circ}\text{C}$$

10. Consider a surface-mount type transistor on a circuit board whose temperature is maintained at 35 °C. Air at 20 °C flows over the upper surface of dimensions 4 mm by 8 mm with a convection coefficient of 50 W/m^2.K.Three wire leads, each of cross section 1 mm by 0.25 mm and length 4 mm, conduct heat from the case to the circuit board. The gap between the case and the board is 0.2 mm.

(a) Assuming the case is isothermal and neglecting radiation; estimate the case temperature when 150 mW are dissipated by the transistor and (i) stagnant air or (ii) a conductive paste fills the gap. The thermal conductivities of the wire leads, air. And conductive pastes are 25, 0.0263, and 0.12 W/m.K. respectively.

(b) Using the conductive paste to fill the gap, we wish to determine the extent to which increased heat dissipation may be accommodated, subject to the constraint that the case temperature not exceeds 40 °C. Options include increasing the air speed to achieve a larger convection coefficient h and/or changing the lead wire material to one of larger thermal conductivity. Independently considering leads fabricated from materials with thermal conductivities of 200 and 400 W/m.K, compute and plot the maximum allowable heat dissipation for variations in h over the range $50 \leq h \leq 250$ W/m^2.K.

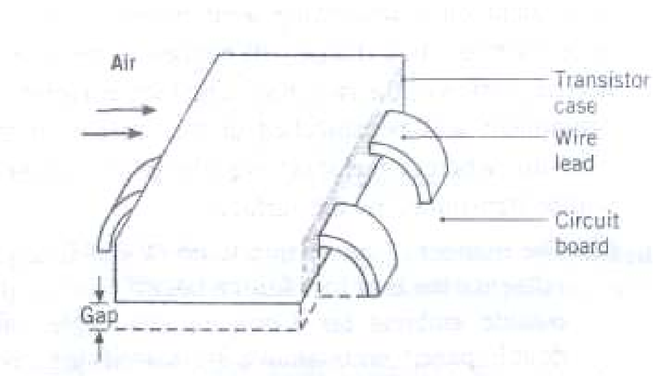

Given data: Surface-mount transistor, power dissipation by conduction and convection

Required:

(a) The case temperature with (i) air-gap and (ii) conductive paste fills the gap.

Assumptions:

(a) Steady-state conductions.
(b) Constant properties.
(c) Transistor case is isothermal.

(d) One-dimensional conduction.
(e) Neglect heat loss from edges.

Solution:
By energy balance across the transistor case

$$P = 3q_{lead} + q_{conv} + q_{cond,gap}$$

$$q_{lead} = k_l A_l (T_c - T_b)/L$$

Where T_c is the case temperature, and T_b is the board temperature

$$q_{conv} = hA_c(T_c - T_\infty)$$

$$q_{cond,gap} = k_g A_g (T_c - T_b)/\delta_{gap}$$

Substitute in the energy equation:

$$P = 3k_l A_l (T_c - T_b)/L + hA_c(T_c - T_\infty) + k_g A_g (T_c - T_b)/\delta_{gap}$$

(i) By substitute in numerical values for air-gap condition

$$0.15 = [3(25)(0.001X0.00025)/0.004 + 0.0263(0.008X0.004)/0.0002](T_c - 35) + 50(0.008X0.004)(T_c - 20)$$

The case temperature with air-gap is

$$T_c = 47\ ^oC$$

(ii) By substitute in numerical values for conductive paste fills the gap condition

$$0.15 = [3(25)(0.001X0.00025)/0.004 + 0.12(0.008X0.004)/0.0002](T_c - 35) + 50(0.008X0.004)(T_c - 20)$$

The case temperature with conductive paste fills the gap is

$$T_c = 40\ ^oC$$

11. A transistor that dissipates10W is mounted on a duralumin heat sink at 50 °C by a duralumin bracket 20 mm wide as shown in the opposite figure. The bracket is attached to the heat sink by a rivet. With convective cooling negligibly small, estimate the surface temperature of the transistor.

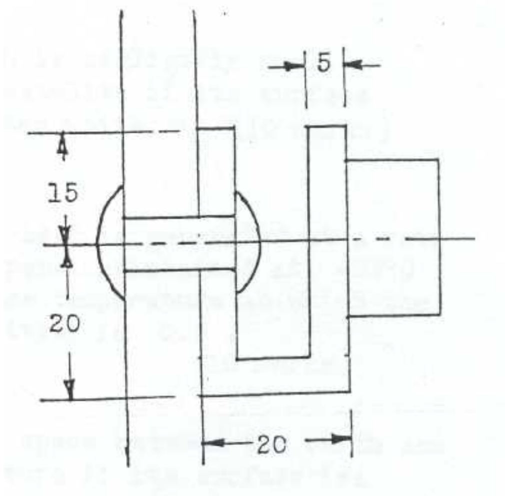

Given data: Transistor power dissipation, and heat sink temperature and bracket dimensions
Require: Surface temperature of the transistor.
Assumptions:

(a) Neglect the convection cooling.
(b) Neglect the contact resistances
(c) One-dimension conduction.
(d) Steady state condition.

Solution:

The heat source is the base of the transistor and the rivets connecting the bracket to the heat sink,
The heat flow path length is

$$L = 20 + 20 + 20 = 60 \text{ mm}$$

The base transistor area equals the heat flow area is

$$A = \text{width x thickness} = 20 \text{ x } 5 = 100 \text{ mm}^2$$

The duralumin thermal conductivity could be obtained from appendix is

$$k = 164 \text{ W/m.K}$$

From Fourier's law,

$$P = q = kA\frac{\Delta T}{L}$$

Then the surface temperature of the transistor is

$$T_s = 50 + (10 \text{ X } 0.06)/(164 \text{ X } 100 \text{ X } 10^{-6}) = 86.58 \ ^oC$$

Comment: Essentially in this case, conduction is not one-dimensional conduction. But the solution based on one-dimensional conduction only for simplicity with loss of accuracy.

12. A cable 10 mm diameter is to be insulated to maximize its current carrying capacity. For certain reasons, the outside diameter of the insulation should be 30 mm. The heat transfer coefficient for the outer surface is estimated to be 10 W /m^2 .K.
What should be the thermal conductivity of the chosen insulation? By what percentage would the insulation increase the energy carrying capacity of the bare cable?

Given data: Cable diameter, insulation diameter and heat transfer coefficient.

Require: thermal conductivity of insulation required to maximize the current carrying capacity, and the percentage increase in the energy carrying capacity due to insulation.

Assumption:

(a) One-dimensional conduction.
(b) Steady-state conditions

Solution:

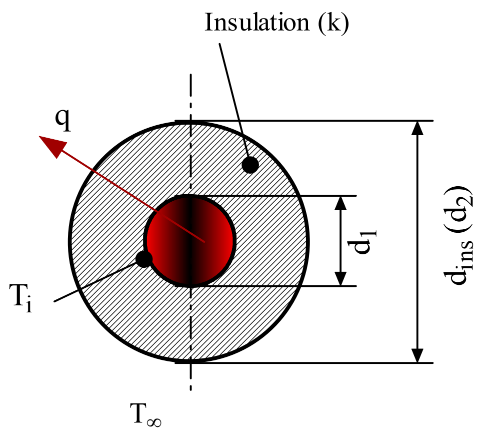

The heat transfer from the cable is

$$q=\frac{\Delta T}{\sum R_{th}}=\frac{T_i-T_\infty}{R_{cond}+R_{conv}}=\frac{T_i-T_\infty}{\ln\left(\frac{r_2}{r_1}\right)/(2\pi kL)+\left(\frac{1}{h(2\pi r_2 L)}\right)}$$

For increasing the radius of insulation the conduction resistance increases, on another hand the convection resistance decreases. So that there's a minimum total thermal resistance causes maximum heat transfer (or current carrying capacity) as shown.

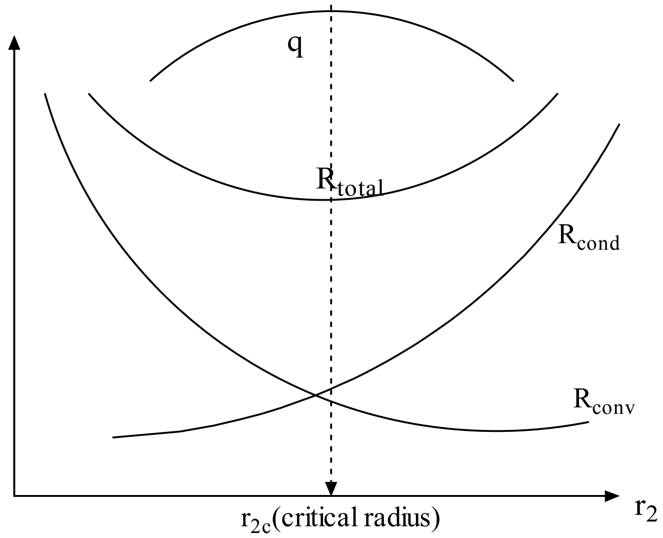

To find the maximum heat transfer: differentiate the heat transfer to the radius of insulation (r_2). Then equal it to zero. It gives

$$r_{2c} = \frac{k}{h}$$

At h = 10 W /m^2 .K. and r_{2c} = 0.015 m

The thermal conductivity of insulation required to maximize the current carrying capacity is

k = 0.015 x 10 = 0.15 W /m .K.

$$q'_{\max} = \frac{\Delta T}{\ln\left(\frac{r_{2c}}{r_1}\right)/(2\pi k)+\left(\frac{1}{h(2\pi r_{2c})}\right)} = \frac{\Delta T}{\ln(15/5)/(2\pi \text{ X } 0.15)+\left(\frac{1}{10(2\pi \text{ X } 0.015)}\right)} = \Delta T/2.2267 \text{ W/m}$$

For bare cable the heat transfer is

$$q'_{bare} = \frac{\Delta T}{\left(\frac{1}{h(2\pi r_1)}\right)} = \frac{\Delta T}{\left(\frac{1}{10(2\pi \text{ X } 0.005)}\right)} = \Delta T/3.183 \text{ W/m}$$

The percentage increase in the energy carrying capacity due to insulation is

$$\%\ q_{increase} = \{(q'_{\max}/q'_{bare})-1\}100 = 43\ \%$$

13. The vertical side of an electronics box is 40 x 30 cm with the 40 cm side vertical. What is the maximum radiation energy that could be dissipated by this side if its temperature is not to exceed 60 °C in an environment of 40 °C, and its emissivity is 0.8?

Given data: electronics box vertical side area, maximum temperature of the electronics box vertical side, its emissivity, and the environment temperature.

Require: maximum radiation energy dissipates from this side of the electronic box

Assumptions:

(a) Steady-state conditions.
(b) Radiation exchange between small surface and large enclosure.
(c) The side is at uniform temperature (isothermal).
(d) The temperature of the enclosure equals the temperature of the environment.

Solution:

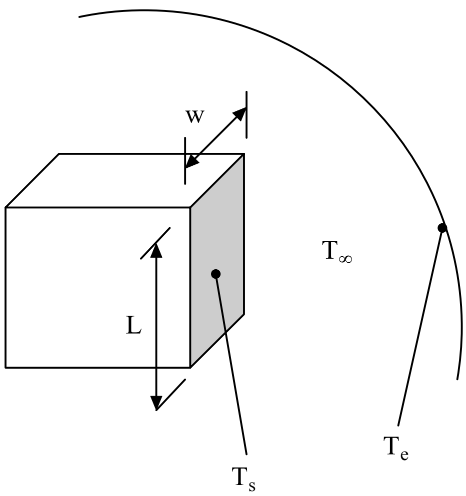

The maximum radiation energy dissipates from this side of the electronic box is

$$\begin{aligned} q_{\max} &= \sigma \varepsilon f A (T_s^4 - T_e^4) \\ &= 5.67 \text{ X } 10^{-8} \text{ X } 0.8 \text{ X } 1 \text{ X} (0.4 \text{ X } 0.3)(333^4 - 313^4) \\ &= 14.7\ W \end{aligned}$$

14. In a manufacturing process, a transparent film is being bonded to a substrate as shown in the sketch. To cure the bond at a temperature T_o, a radiant source is used to provide a heat flux q_o'' (W/m^2), All of which is absorbed at the bonded surface. The back of the substrate is maintained at T_1 while the free surface of the film is exposed to air at T_∞ and a convection heat transfer coefficient h.

(a) Show the thermal circuit representing the steady-state heat transfer situation. Be sure to label all elements, nodes, and heat rates. Leave in symbolic form.

(b) Assume the following conditions: T_∞ = 20 °C, h = 50 W/m^2.K and T_1 = 30 °C. Calculate the heat flux q_o'' that is required to maintain the boded surface at T_o = 60 °C.

(c) Compute and plot the required heat flux as a function of the film thickness for $0 \le L_f \le 1$mm.

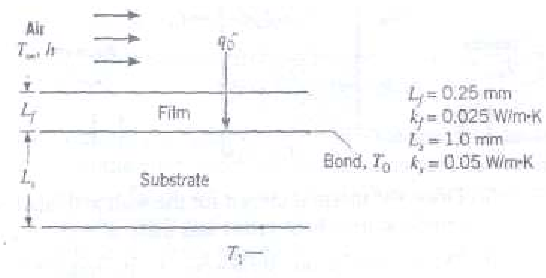

Given data: A radiant source is used to provide a heat flux at the bond to cure the bond at a temperature T_o.

Assumptions:

(a) Steady-state conditions.
(b) Constant properties.
(c) One-dimensional conduction heat transfer.
(d) Neglect the contact resistance.

Solution:

(a) Thermal circuit based on heat flux distribution represented below.

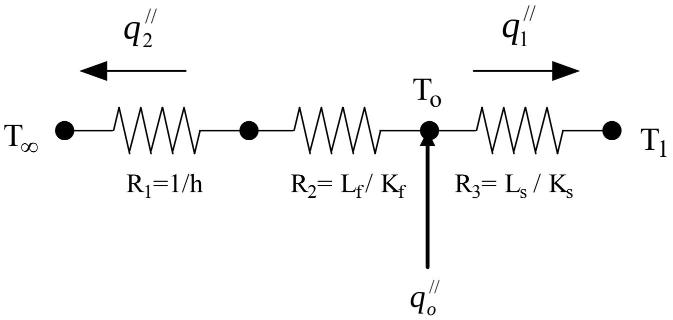

(b) Using this thermal circuit and performing energy balance on film-substrate interface,

$$
\begin{aligned}
q_o'' &= q_1'' + q_2'' \\
&= \frac{(T_o - T_1)}{(L_s / k_s)} + \frac{(T_o - T_\infty)}{(L_f / k_f) + (1/h)} \\
&= \frac{60-30}{(0.001/0.05)} + \frac{60-20}{(0.00025/0.025)+(1/50)} \\
&= 2833 \text{ W/m}^2
\end{aligned}
$$

(c) The heat flux as a function of the film thickness,

$$
\begin{aligned}
q_o^{//} &= q_1^{//} + q_2^{//} \\
&= \frac{(T_o - T_1)}{(L_s / k_s)} + \frac{(T_o - T_\infty)}{(L_f / k_f) + (1/h)} \\
&= 1500 + \frac{40}{40\, L_f + 0.02} \quad \text{W/m}^2
\end{aligned}
$$

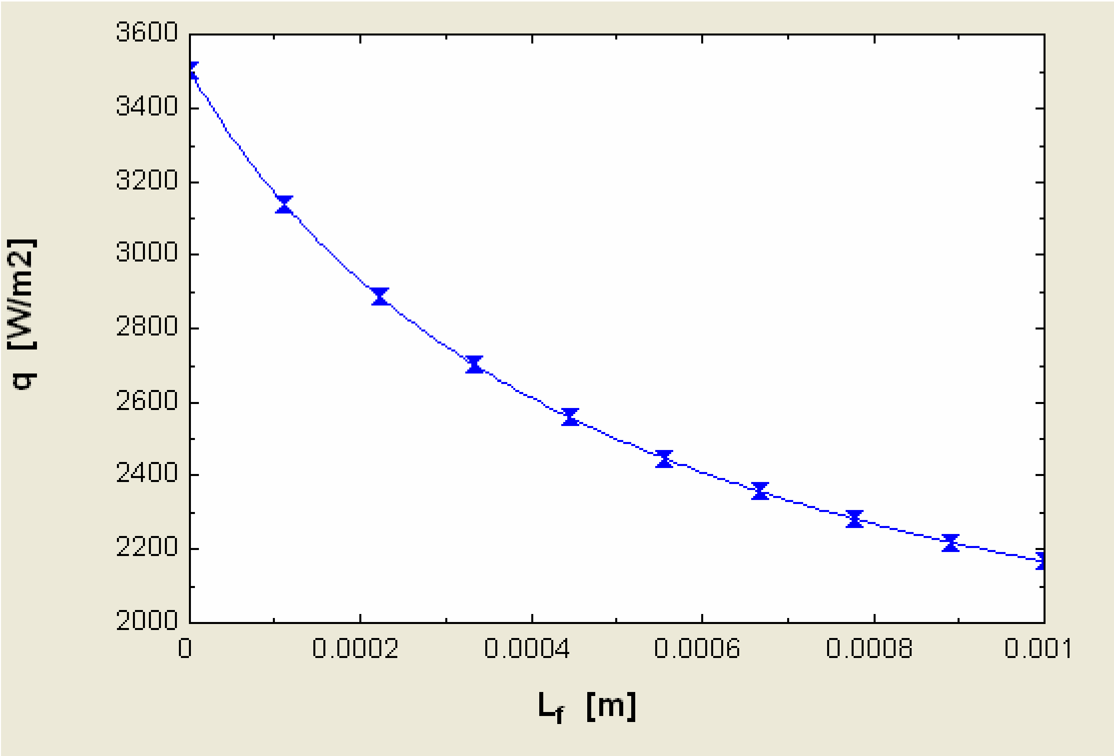

15. A silicon chip is encapsulated such that, under steady-state conditions, all of the power it dissipates is transferred by convection to a fluid stream for which h = 1000 W/m^2.K and T_∞ = 25 °C. The chip is separated from the fluid by a 2-mm-thick aluminum cover plate, and the contact resistance of the chip/aluminum interface is 0.5 x 10^{-4} m^2.K/W. If the chip surface area is 100 mm^2 and its maximum allowable temperature is 85 ^{o}C, what is the maximum allowable power dissipation in the chip?

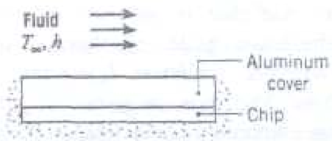

Given data: chip surface area is 100 mm^2 and its maximum allowable temperature, contact resistance of the chip/aluminum interface and fluid stream conditions.

Require: maximum allowable power dissipation in the chip.

Assumption:

(a) Steady-state conditions

(b) Neglect the radiation heat transfer.
(c) One-dimensional conduction.
(d) Neglect the heat loss from the back and side surfaces.
(e) Chip at uniform temperature (isothermal).

Solution:
The thermal circuit of the system represented as shown in the following figure, Conduction heat transfer from the chip equals the convection heat transfer to the fluid stream,

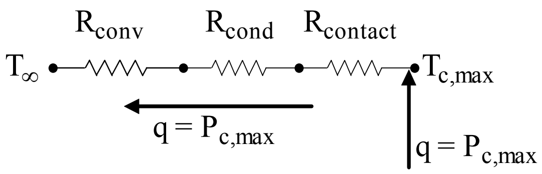

According to the thermal circuit, the maximum allowable power dissipation in the chip is

$$q = P_{c,\max} = \frac{T_{c,\max} - T_\infty}{R_{contact} + R_{cond} + R_{conv}} = \frac{T_{c,\max} - T_\infty}{(1/hA)_{contact} + (L/KA)_{Alu\min um} + (1/hA)_{conv.}}$$

$$= \frac{(85 - 25)\text{ X }10^{-4}}{(0.5\text{ X }10^{-4}) + (0.002/238) + (1/1000)} = 5.667\ W$$

16. Approximately 10^6 discrete electrical components can be placed on a single integrated circuit (chip), with electrical heat dissipation as high as 30,000 W/m^2. The chip, which is very thin, is exposed to a dielectric liquid at its outer surface, with h_o = 1000 W/m^2. K and $T_{\infty,o}$ = 20 °C, and is joined to a circuit board at its inner surface. The thermal contact resistance between the chip and the board is 10^{-4} m^2.K/W. and the board thickness and thermal conductivity are L_b = 5 mm and k_b = 1 W/m.K, respectively. The other surface of the board is exposed to ambient air for which h_i = 40 W/m^2.K and $T_{\infty,i}$ = 20 °C.

(a) Sketch the equivalent thermal circuit corresponding to steady-state conditions. In variable form, label appropriate resistances, temperatures, and heat fluxes.
(b) Under steady-state conditions for which the chip heat dissipation is q_c'' = 30,000 W/m^2. What is the chip temperature?
(c) The maximum allowable heat flux $q_{c,m}''$, is determined by the constraint that the chip temperature must not exceed 85°C. Determine $q_{c,m}''$ for the foregoing conditions. If air is used in lieu of the dielectric liquid, the convection coefficient is reduced by approximately an order of magnitude. What is the value of $q_{c,m}''$ for h_o = 100 W/m^2.K? With air cooling, can significant improvements be realized by using an aluminum oxide circuit board and/or by using a conductive paste at the chip/board interface for which $R_{t,c}''$ = 10^{-5} m^2.K/W?

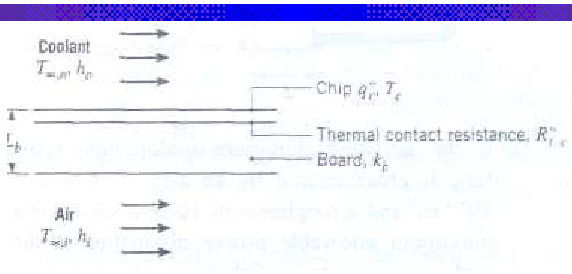

Given data: chip joined to a circuit board and its electrical heat dissipation, board properties, and coolant fluids conditions.

Assumptions:

(a) Steady-state conditions
(b) Neglect the radiation heat transfer.
(c) One-dimensional conduction.
(d) Neglect chip thermal resistance.

Solution:

(a) The equivalent thermal circuit as shown

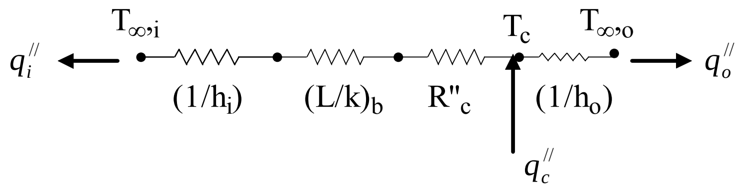

(b) According to the thermal circuit, the chip heat dissipation is

$$q''_c = q''_i + q''_o$$

$$= \frac{T_c - T_{\infty,i}}{R''_c + (L/k)_b + (1/h_i)} + \frac{T_c - T_{\infty,o}}{(1/h_o)}$$

$$30000 = \frac{T_c - 20}{(10^{-4}) + (0.005/1) + (1/40)} + \frac{T_c - 20}{(1/1000)}$$

Then the chip temperature is

$$T_c = 49\ ^{o}\mathrm{C}$$

(c) At chip temperature 85 °C, the maximum allowable heat flux $q''_{c,m}$ is

$$q''_{c,m} = q''_i + q''_o$$

$$= \frac{T_c - T_{\infty,i}}{R''_c + (L/k)_b + (1/h_i)} + \frac{T_c - T_{\infty,o}}{(1/h_o)}$$

$$q''_{c,m} = \frac{85 - 20}{(10^{-4}) + (0.005/1) + (1/40)} + \frac{85 - 20}{(1/1000)} = 67160\ W/m^2$$

The maximum allowable heat flux $q''_{c,m}$ at h_o= 100 W/m^2.k,

$$q''_{c,m} = q''_i + q''_o$$

$$= \frac{T_c - T_{\infty,i}}{R''_c + (L/k)_b + (1/h_i)} + \frac{T_c - T_{\infty,o}}{(1/h_o)}$$

$$q''_{c,m} = \frac{85-20}{(10^{-4}) + (0.005/1) + (1/40)} + \frac{85-20}{(1/100)} = 8660\, W/m^2$$

At an aluminum oxide circuit board (k = 38 W/m.K), the maximum allowable heat flux $q''_{c,m}$ is

$$q''_{c,m} = q''_i + q''_o$$

$$= \frac{T_c - T_{\infty,i}}{R''_c + (L/k)_b + (1/h_i)} + \frac{T_c - T_{\infty,o}}{(1/h_o)}$$

$$q''_{c,m} = \frac{85-20}{(10^{-4}) + (0.005/38) + (1/40)} + \frac{85-20}{(1/100)} = 9076\, W/m^2$$

By using a conductive paste at the chip/board interface for which $R''_{t,c}$ = 10^{-5} m^2.K/W, the maximum allowable heat flux $q''_{c,m}$ is

$$q''_{c,m} = q''_i + q''_o$$

$$= \frac{T_c - T_{\infty,i}}{R''_c + (L/k)_b + (1/h_i)} + \frac{T_c - T_{\infty,o}}{(1/h_o)}$$

$$q''_{c,m} = \frac{85-20}{(10^{-5}) + (0.005/1) + (1/40)} + \frac{85-20}{(1/100)} = 8666\, W/m^2$$

Using an aluminum oxide circuit board gives higher maximum allowable heat flux $q''_{c,m}$ than using conductive paste at the chip/board interface.

17. Consider a power transistor encapsulated in an aluminum case that is attached at its base to a square aluminum plate of thermal conductivity k = 240 W/m.K, thickness L = 6 mm, and width W = 20 mm. The case is joined to the plate by screws that maintain a contact pressure of 1 bar, and the back surface of the plate transfers heat by natural convection and radiation to ambient air and large surroundings at $T_\infty = T_{sur}$ = 25 °C. The surface has an emissivity of ε = 0.9, and the convection coefficient is h = 4 W/m^2.K. The case is completely enclosed such that heat transfer may be assumed to occur exclusively through the base plate.

(a) If the air-filled aluminum-to-aluminum interface is characterized by an area of A_c = 2 x 10^{-4} m^2 and a roughness of 10 µ.m. what is the maximum allowable power dissipation if the surface temperature of the case, $T_{s,c}$, is not to exceed 85 °C?

(b) The convection coefficient may be increased by subjecting the plate surface to a forced flow of air. Explore the effect of increasing the coefficient over the range $4 \le h \le 200$ W/ m^2.K.

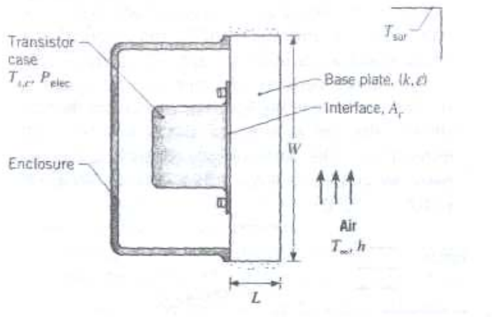

Given data: A power transistor attached at its base to a square aluminum plate with a contact pressure of 1 bar, the plate whose emissivity of ε transfers heat by natural convection and radiation to ambient air and large surroundings.

Assumptions:

(a) Steady-state conditions.
(b) One-dimensional conduction.
(c) Heat transfers occur exclusively through the base plate only.

Solution:

(a) For air interfacial fluid between the aluminum case and the aluminum plate with a roughness 10μ.m, and 1 bar contact pressure. Then the contact resistance $R_c^{//} = 2.75 \text{ x } 10^{-4}$ m^2.K/W.

The thermal circuit represented as shown

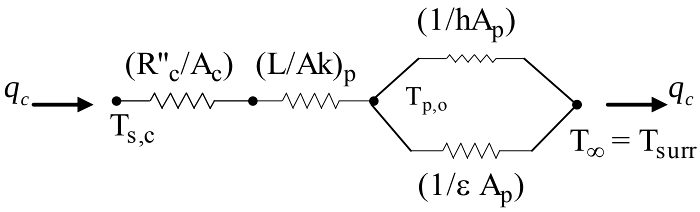

According to the thermal circuit, the maximum allowable power dissipation at $T_{s,c}$ = 85 °C.

$$P_{\max} = q_c = \frac{T_{s,c} - T_{p,o}}{R_c^{//}/A_c + (L/Ak)_p}$$

$$= \frac{T_{p,o} - T_\infty}{(1/hA_p)} + \frac{\sigma(T_{p,o}^4 - T_{surr}^4)}{(1/\varepsilon A_p)}$$

To get the plate out side temperature $T_{p,o}$,

$$\frac{358 - T_{p,o}}{(2.75 \text{ X } 10^{-4})/(2 \text{ X } 10^{-4}) + (0.006/240(0.02)^2)} = \frac{T_{p,o} - 298}{1/4(0.02)^2} + \frac{5.67 \text{ X } 10^{-8}(T_{p,o}^4 - 298^4)}{1/0.9(0.02)^2}$$

By trial and error,

$$T_{p,o} = 357\ ^{o}\mathrm{C}$$

The maximum allowable power dissipation is

$$P_{\max} = q_c = \frac{T_{s,c} - T_{p,o}}{R_c^{//} / A_c + (L / Ak)_p} = \frac{1}{1.4375} = 0.5\ W$$

(b) The effect of increasing the out side convection coefficient

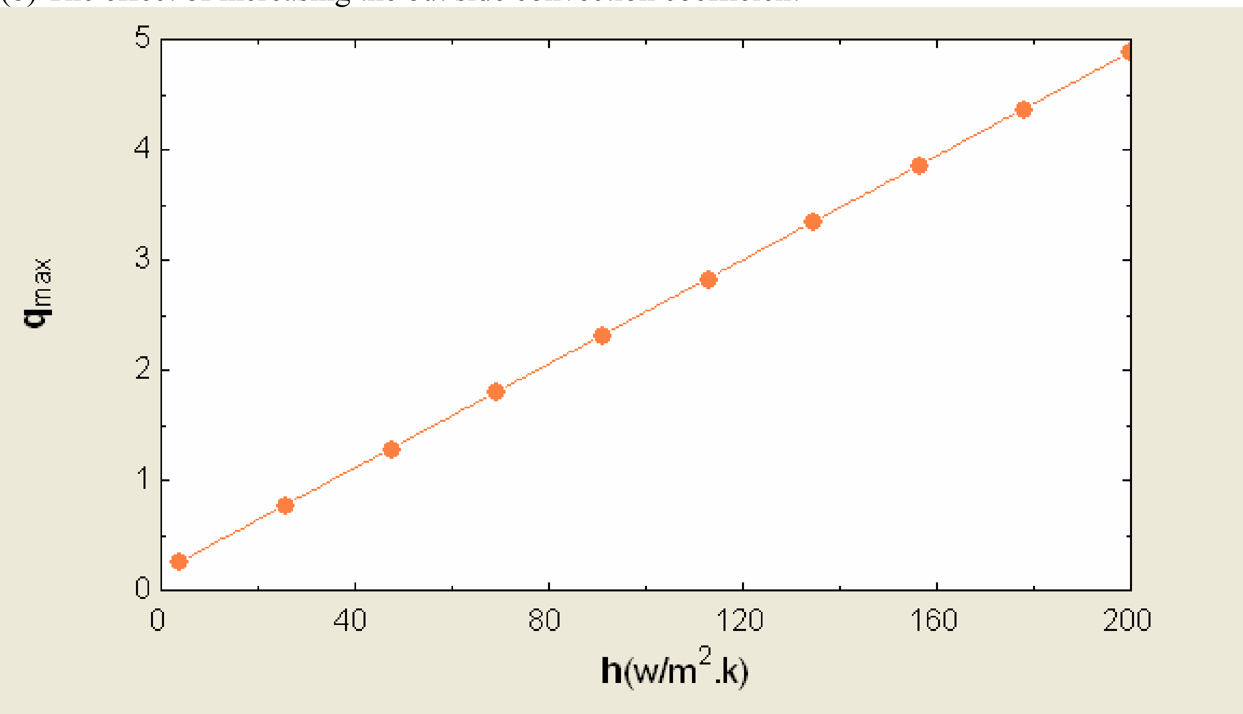

18. A transistor, which may be approximated as a hemispherical heat source of radius $r_o = 0.1$ mm, is embedded in a large silicon substrate (k = 125 W/m.K) and dissipates heat at a rate q. All boundaries of the silicon are maintained at an ambient temperature of $T_\infty = 27$ °C, except for a plane surface that is well insulated. Obtain a general expression for the substrate temperature distribution and evaluate the surface temperature of the heat source for q = 4 W.

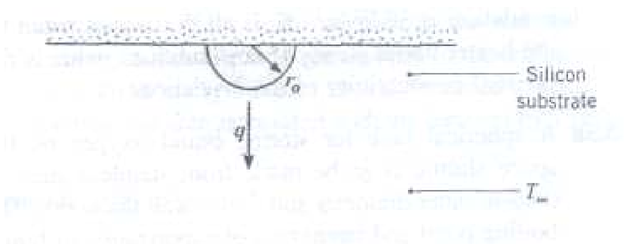

Given data: A heat source embedded in a large silicon substrate, source and substrate boundary conditions.
Require: substrate temperature distribution and surface temperature of heat source for q = 4 W.
Assumption:
(a) Steady-state conditions.
(b) One-dimensional conduction.

Solution:
From energy equation reduced to

$$\frac{1}{r^2}\frac{d}{dr}(kr^2\frac{dT}{dr}) = 0$$

At constant silicon thermal conductivity

$$\frac{d}{dr}(r^2\frac{dT}{dr}) = 0$$

By integration to the substrate radius

$$r^2\frac{dT}{dr} = C_1$$

$$T(r) = -\frac{C_1}{r} + C_2$$

Boundary conditions
$T(\infty) = T_\infty$, and $T(r_o) = T_s$

Then the constants

$C_2 = T_\infty$
$C_1 = r_o(T_\infty - T_s)$

The substrate temperature distribution

$$T(r) = (T_s - T_\infty)r_o / r + T_\infty$$

The heat rate is

$$q = -kA\frac{dT}{dr} = -k(2\pi\, r^2)\left(-(T_s - T_\infty)r_o / r^2\right) = 2\pi\, r_o(T_s - T_\infty)$$

The surface temperature of heat source for q = 4 W is

$$T_s = 4/125(2\pi \text{ X}10^{-4}) + 27 = 78 \ ^oC$$

21. An isothermal silicon chip of width W = 20 mm on a side is soldered to an aluminum heat sink (k = 180W/m.K) of equivalent width. The heat sink has a base thickness of L_b =3 mm and an array of rectangular fins, each of length L_f = 15 mm. Air flow at T_∞ = 20 °C is maintained through channels formed by the fins and a cover plate, and for a convection coefficient of h = 100 W/m^2.K, a minimum fin spacing of 1.8 mm is dictated by limitations on the flow pressure drop. The solder joint has a thermal resistance of $R''_{t,c}$ = 2 x 10^{-6} m^2.K.

Consider limitations for which the array has N = 11 fins, in which case values of the fin thickness t = 0.182 mm and pitch S = 1.982 mm are obtained from the requirements that W= (N - 1) S + t and S - t = 1.8 mm. If the maximum allowable chip temperature is T_c = 85 °C, what is the corresponding value of the chip power q_c? An adiabatic fin tip condition may be assumed, and air flow along the outer surfaces of the heat sink may be assumed to provide a convection coefficient equivalent to that associated with air flow through the channels.

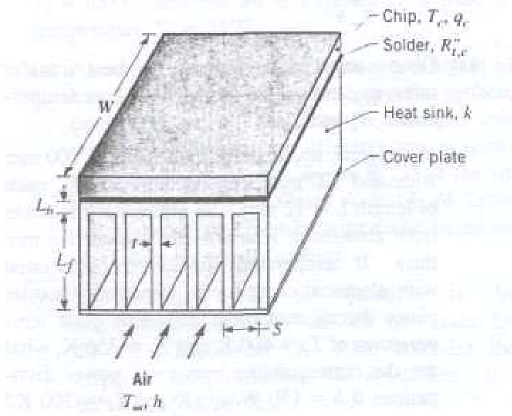

Given data: An isothermal silicon chip produces electric power, and attached to an aluminum heat sink with prescribed dimensions.
Require: (a) The maximum allowable chip power q_c at maximum chip temperature with An adiabatic fin tip condition.
Assumptions:

(a) Steady-state conditions.
(b) One-dimensional conduction.
(c) Heat transfers occur exclusively through the base of the heat sink only.
(d) An adiabatic fin tip condition.

Solution:
The thermal circuit represented as shown

$$q_c \longrightarrow \underset{T_c}{\bullet} \overset{(R''_c/A)}{\text{---}\!\!\wedge\!\!\wedge\!\!\wedge\!\!\text{---}} \underset{T_{b,1}}{\bullet} \overset{(L_b/Ak_b)}{\text{---}\!\!\wedge\!\!\wedge\!\!\wedge\!\!\text{---}} \underset{T_{b,2}}{\bullet} \longrightarrow \quad q_c = N\,q_f + q_{bare}$$

From the thermal circuit, the chip power equals

$$q_c = \frac{\Delta T}{\sum R} = \frac{T_c - T_{b2}}{(R_c^{//}/A) + (L_b/Ak_b)}$$

Also the Chip power equals the summation of the fin array heat transfers and the unfinned (bare) heat transfer area,

$$q_c = N\,q_f + q_{bare} = N\,M\,\tanh mL_f + hA_{bare}(T_{b2} - T_\infty)$$
$$= \frac{T_c - T_{b2}}{(R_c^{//}/A) + (L_b/Ak_b)} = \frac{T_c - T_{b2}}{\Psi}$$

Where:

$$M = (T_{b2} - T_\infty)\sqrt{hPk_f A_c} = (T_{b2} - T_\infty)\sqrt{2h(W+t)k_f Wt}$$

A_c = Fin contact area

$$m = \sqrt{\frac{hP}{k_f A_c}} = \sqrt{\frac{2h(W+t)}{k_f Wt}}$$

$$\Psi = (R_c^{//}/A) + (L_b/Ak_b)$$

A = Cross sectional area of the base flow heat transfer

$$A = [S(N-1)+t]W$$

$$A_{bare} = A - NtW = (s-t)(N-1)W$$

The base-fin temperature T_{b2} equals

$$T_{b2} = T_c - \Psi N\,M\,\tanh mL_f - \Psi hA_{bare}(T_{b2} - T_\infty)$$

For prescribed conditions, the base-fin temperature,

$$T_{b2} = 83.5\ ^oC$$

Then the maximum allowable chip power,

$$q_e = 32\,W$$

22. A 3 x 3 array of power transistors is attached to an aluminum heat sink (k = 180 W/m.K) of width W = 150 mm on a side. The thermal contact resistance between each transistor and the heat sink is $R_{t,c}$ = 0.045 K/W. The heat sink has a base thickness of L_b = 6 mm and an array of N_f = 25 rectangular fins, each of thickness t = 3 mm. Cooling is provided by air flow through channels formed by the fins and a cover plate, as well as by air flow along the two sides of the heat sink (the outer surfaces of the outermost fins).

(a) Consider conditions for which the fin length is L_f = 30 mm, the temperature of the air is T_∞ = 27 °C, and the convection coefficient is h = 100 W/m^2.K. If the maximum allowable transistor temperature is T_s = 100 °C, what is the maximum allowable power dissipation, q per transistor? An adiabatic fin tip condition may be assumed.

(b) Explore the effect of variations in the convection coefficient and fin length on the maximum allowable transistor power.

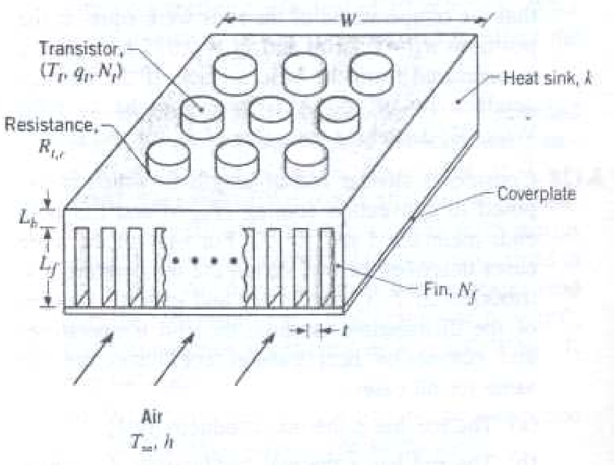

Given data: A 3x3 array of power transistors produces electric power, and attached to an aluminum heat sink with prescribed dimensions.

Require: (a) The maximum allowable power, q_t per transistor at maximum transistor temperature with an adiabatic fin tip condition, (b) effect of variations in the convection coefficient and fin length on the maximum allowable transistor power.

Assumptions:

(a) Steady-state conditions.
(b) One-dimensional conduction.
(c) Heat transfers occur exclusively through the base of the heat sink only.
(d) An adiabatic fin tip condition.
(e) All transistors at same temperatures.

Solution:

(a)The thermal circuit represented as shown

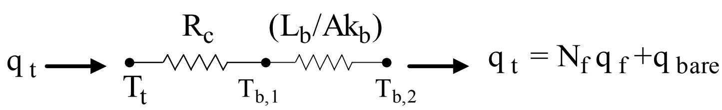

From the thermal circuit, the total transistors power equals

$$q_t = \frac{\Delta T}{\sum R} = \frac{T_t - T_{b2}}{R_c + (L_b / Ak_b)}$$

Also the total transistors power equals the summation of the fins heat transfers and the unfinned (bare) heat transfer area,

$$q_t = N_f\, q_f + q_{bare} = N_f\, M \tanh mL_f + hA_{bare}(T_{b2} - T_\infty)$$
$$= \frac{T_t - T_{b2}}{R_c + (L_b / Ak_b)} = \frac{T_t - T_{b2}}{\Psi}$$

Where:

$$M = (T_{b2} - T_\infty)\sqrt{hPk_f A_c} = (T_{b2} - T_\infty)\sqrt{2h(W+t)k_f Wt}$$

$$A_c = \text{Fin contact area}$$

$$m = \sqrt{\frac{hP}{k_f A_c}} = \sqrt{\frac{2h(W+t)}{k_f Wt}}$$

$$\Psi = R_c + (L_b / Ak_b)$$

$$A = \text{Cross sectional area of the base flow heat transfer}$$

$$A = W^2$$

$$A_{bare} = A - N_f tW$$

The base-fin temperature T_{b2} equals

$$T_{b2} = T_t - \Psi N_f M \tanh mL_f - \Psi h A_{bare}(T_{b2} - T_\infty)$$

For prescribed conditions, the base-fin temperature,

$$T_{b2} = 63.27\ ^oC$$

Then the maximum allowable total transistors power,

$$q_t = 790\ W$$

The maximum allowable transistors power per transistor,

$$q_t = 790/9 = 87.7\ W$$

(b) Effect of variations in the convection coefficient and fin length on the maximum allowable transistor power.

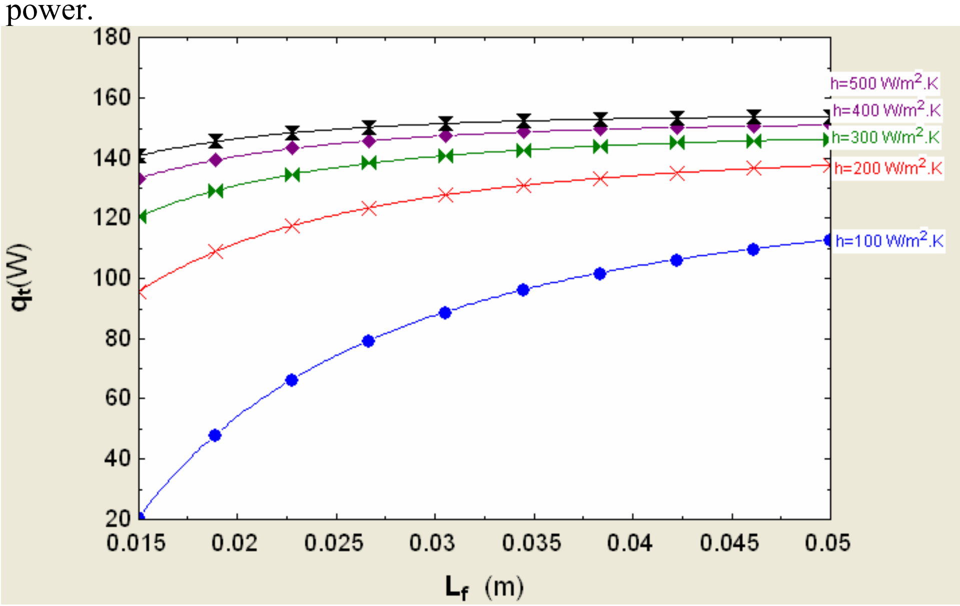

23. The interface temperature of an electronic assembly dissipating 10 W must be limited to 40 ^oC in a 50 ^oC environment. It is assumed that all of the generated heat will be removed by thermoelectrics and that heat absorbed from the environment is negligible. The interface temperature difference between the assembly and the thermoelectric can be held to 2 ^oC. The temperature difference between the thermoelectric and ambient can be held to 8 ^oC.
The bismuth telluride element used has a length of 0.3 cm and a cross-area of 0.01 cm^2.
Determine the size and performance characteristics of the thermoelectric temperature control device.
Knowing that

- The equivalent material properties of the thermoelectric couples is
  $\rho_e = 0.00267$ Ω.cm
  $\alpha_e = 425 \times 10^{-6}$ V/K
  $k_e = 0.00785$ W/cm.K
- Design for maximum refrigeration capacity.

Solution:
$T_h = 58\ ^oC = 331$ K
$T_c = 42\ ^oC = 315$ K
L = 0.3 cm
A = 0.01 cm^2

Overall electric resistance (R) $= (\rho_e)\ (L/A)$
$= 0.00267\ (0.3 / 0.01)$
$= 0.08\ \Omega$
Conduction coefficient (C) $= (k_e)\ (A/L)$
$= (0.00785)\ (0.01 /0.3)$
$= 2.6 \times 10^{-4}$ W/K
Figure of merit (Z) $= \alpha_e^{\ 2}/ RC$
$= (425 \times 10^{-6})^2/ (0.08 \times 2.6 \times 10^{-4})$
$= 8.684 \times 10^{-3}\ K^{-1}$

1- Number of couples required.
$Q_C = Q_C\ (max) = N\ C\ [(Z\ T_c^{\ 2})/2 - (T_h - T_c)]$
$10 = N\ (2.6 \times 10^{-4})\ [0.5\ (8.684 \times 10^{-3} \times (315)^2) - (16)]$
$N \approx 94$ couples

2- Rate of heat rejection to the ambient (Q_h).
$I_{opt.} = (\alpha_e)\ T_c /R$
$= (425 \times 10^{-6}) \times 315/ 0.08$
$= 1.67$ A
Then
$Q_h = N\ [(\alpha_e)\ T_h \times I_{opt} - C\ (T_h - T_c) + I^2_{opt}\ R/2]$
$= 94\ [(425 \times 10^{-6})\ 331 \times 1.67 - 2.6 \times 10^{-4}\ (16) + (1.67)^2\ 0.08 /2]$
$= 32.2$ W

3- The COP.

$COP = Q_C / P_{in}$

P_{in} (Power input by power source to the thermoelectric) = $Q_h - Q_C$

$= 32.2 - 10 = 22.2$ W

$COP = 10 / 22.2$

$= 0.45$

4- The voltage drop across the d.c. power source.

The voltage drop (ΔV) = P_{in} / I

$= 22.2 / 1.67$

$= 13.3$ volt

5- Size of the thermoelectric device.

The module size is approximately three times the element area. Since each couple is composed of two elements, the module area becomes

$A_{module} = 2(0.01)(94) \times 3 = 5.64 \text{ cm}^2$

which can be accommodated in a package measuring 2.38 cm on a side.

24. An electronic chassis was designed for natural convection cooling, so that a clearance of 0.75 in (1.905 cm) was provided between the PCBs and components. However, a design change required the addition of another PCB, which might reduce the clearance too much unless the new PCB is placed very close to the side wall of the chassis, with a clearance of only 0.20 in (0.51 cm). The PCB measures 6 x 9 in and dissipates 5.5 watts. The electronic chassis must operate at sea level conditions in a maximum ambient temperature of 43.3 °C. The maximum allowable component surface temperature is 100 °C with the chassis shown in Figure below. The aluminum chassis has a polished finish that has a low emissivity, so that the heat lost by radiation is small. The PCB construction only allows heat to be removed from the component mounting face. Determine if the design is adequate.

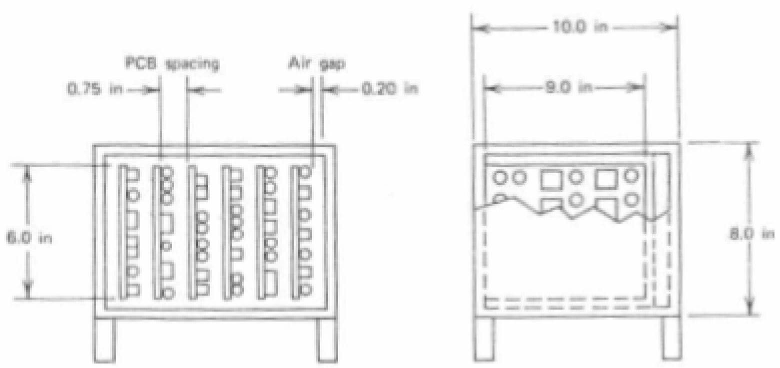

PCB spaced close to an end bulkhead

Solution:
Heat from the components must flow to the outside ambient. This will require the heat to flow across two major resistance areas, the internal air gap of 0.20 in (R_1) and the external convection film (R_2) with neglecting the chassis wall resistance, as shown in the following figure.
The thermal conductivity of the air in the air gap is unknown, so that an average air temperature of 80 °C is assumed and verified later. Determine the resistance with the convection coefficient for the 0.20 in air gap.

$$R_1 = \frac{1}{h_{AG} A}$$

Where:
k = 0.03 W/m.K
L = 0.20 in = 0.005 m

For small space enclosure, the air gap convection coefficient can be obtained as shown

$$h_{AG} = k/L$$
$$= 0.03/0.005 = 6 \text{ W/m}^2\text{.K}$$

A = 6 x 9 = 54 in^2
= 0.035 m^2

Then: $R_1 = \frac{1}{6 \text{ x } 0.035} = 4.762 \ ^o\text{C/W}$

The external convection coefficient must be estimated because the temperature rise from the surface of the chassis to the ambient is unknown.

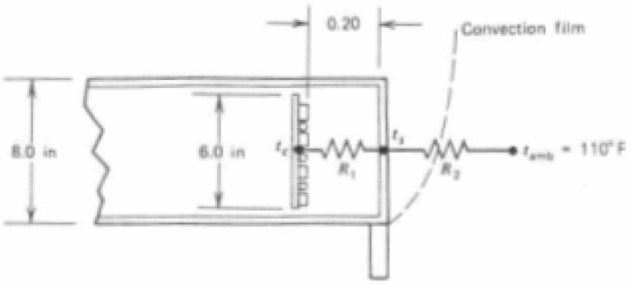

Thermal resistances in the heat flow path from PCB components to the outside ambient

In general, natural convection coefficient for this type of structure will range from about 5 to about 10 W/m^2.K. A value of 7.5 W/m^2.K assumed to start. This can be changed if the analysis shows there is a large error.

$$R_2 = \frac{1}{h_c A}$$

Where:
h_c = 7.5 W/m^2.K
A = 8 x 10 in^2

= 0.052 m^2

Then: $R_2 = \dfrac{1}{7.5\,\text{x}\,0.052} = 2.58 \;\; ^{o}\text{C/W}$

The temperature rise across each thermal resistor is determined as

For resistor R_1: $\Delta t_1 = QR_1 = 5.5\,\text{x}\,4.762 = 26.2 \;\; ^{o}\text{C}$

For resistor R_2: $\Delta t_2 = QR_2 = 5.5\,\text{x}\,2.58 = 14.2 \;\; ^{o}\text{C}$

The natural convection coefficient was assumed to be 7.5 W/m^2.K. The actual value can now be determined from Equation 7.5 using vertical chassis wall height of 8.0 in.

$$\overline{Nu} = \frac{\bar{h}L}{k} = c\left(\text{Gr Pr}\right)^m$$

$$= c(Ra)^m$$

The constants c, m is given in Table 7.1 for the uniform surface temperature case. The fluid properties are evaluated at mean film temperature (T_f) where $T_f = (T_s + T_\infty)/2$.

$$\text{Gr} = \frac{g\beta(T_S - T_\infty)L^3}{v^2}$$

Assume $T_s = T_\infty + \Delta t_2 = 43.3 + 14.2 = 57.5$ ^{o}C

$T_f = 50.4$ ^{o}C = 323.4 K

$\beta = 1/323.4$ K^{-1}

$v = 18.4 \times 10^{-6}$ m^2/s

k = 0.02815 W/m.K

Pr = 0.7035

At $Ra = \dfrac{9.81\,\text{x}\,(1/323.4)\,(14.2)\,(0.203)^3}{(18.4\,\text{x}\,10^{-6})^2}\,\text{x}\,0.7035 = 10.717\,\text{x}\,10^6$

Then: c = 0.59, m= 0.25

The natural convection coefficient is 4.67 W/m^2.K. It nearly far from the assumed value, then by another trial with $h_c = 4.67$ W/m^2.K.

Then: $R_2 = \dfrac{1}{4.67\,\text{x}\,0.052} = 4.12 \;\; ^{o}\text{C/W}$

The temperature rise across each thermal resistor is determined as

For resistor R_1: $\Delta t_1 = QR_1 = 5.5\,\text{x}\,4.762 = 26.2 \;\; ^{o}\text{C}$

For resistor R_2: $\Delta t_2 = QR_2 = 5.5\,\text{x}\,4.12 = 22.66 \;\; ^{o}\text{C}$

Assume $T_s = T_\infty + \Delta t_2 = 43.3 + 22.66 = 65.96$ ^{o}C

$T_f = 54.63$ ^{o}C = 327.63 K

$\beta = 1/327.63$ K^{-1}

$v = 18.67 \times 10^{-6}$ m^2/s

k = 0.02834 W/m.K

Pr = 0.703

At $Ra = \dfrac{9.81\,\text{x}\,(1/327.63)\,(22.66)\,(0.203)^3}{(18.67\,\text{x}\,10^{-6})^2}\,\text{x}\,0.703 = 11.447\,\text{x}\,10^6$

Then: c = 0.59, m= 0.25

Then the natural convection coefficient is 4.8 W/m^2.K.
This compares well with the previous assumed value.
The surface temperature of the component on the end PCB can be determined as follow:

$$t_c = t_\infty + \Delta t_1 + \Delta t_2$$
$$= 43.3 + 26.2 + 22.66 = 92.16\ ^{o}\text{C}$$

The average air temperature in the gap between the wall and the component can now be determined. A temperature of 80 °C is assumed to obtain the air thermal conductivity.
The average air temperature in the gap is obtained as

$$t_{av} = \frac{t_c + t_s}{2} = \frac{92.16 + (43.3 + 22.66)}{2} = 79.06\ °\text{C}$$

This compares well with the assumed value.
Since the component surface temperature is below the maximum value of 100 °C, the design is satisfactory.
If the inside and outside surfaces of the chassis are painted any color except silver, the heat transfer by radiation will be increased and the surface of the PCB will be cooler.

25. Determine the axial force in the lead wire for the resistor shown in figure below, when bending of the PCB is included in the analysis over a temperature cycling range from -50 to +90 °C, which produce total horizontal displacement expected at the top of the wire will be 0.0003 in.
Assuming that:
$E_W = 16 \times 10^6$ Ib/in^2 (copper wire modulus elasticity)
$E_P = 1.95 \times 10^6$ Ib/in^2 (PCB modulus of elasticity)

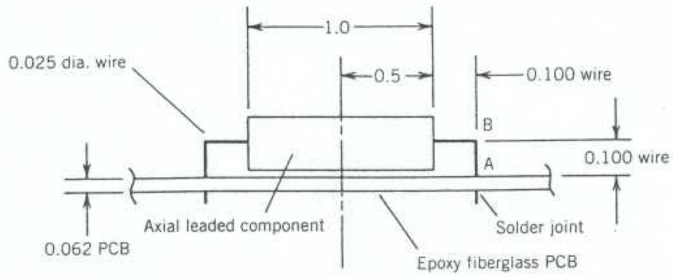

Dimensions of axial leaded resistor throughhole mounted in a PCB (all dimensions in inches)

Solution:
The axial load in the lead wire induced by the different TCE will produce an overturning moment in the PCB and force it to bend. Considering the pivot point to be at the lead wire solder joint, the angular rotation of the lead wire (for small angles) must be the same as the angular rotation of the PCB. The PCB angular rotation will be

$$\theta = \frac{ML_P}{2E_P I_P}$$

Then combined deflection of the bending wire and the rotating PCB is

$$X = \frac{PL_W^3}{7.5E_W I_W} + \frac{RML_P}{2E_P I_P}$$

Reference subscripts W and P are added for the wire and PCB respectively.

Where:
X = 0.0003 in
E_W = 16 x 10^6 Ib/in^2 (copper wire modulus elasticity)
$I_W = \pi\ (d^4)/4 = 1.917\ x10^{-8}\ in^4$
d = 0.025 in
R = height of wire plus one wire diameter into the PCB for wire in bending
= 0.1 + 0.025 = 0.125 in (moment arm length)
L_W = effective wire length = length of wire plus one wire diameter
= 0.1 +0.025 = 0.125 in
E_P = 1.95 x 10^6 Ib/in^2 (PCB modulus of elasticity)
L_P = length of PCB between component lead wires
= 1 + 2(0.1) = 1.2 in (PCB length)
h = 0.062 in (PCB thickness)
b = effective width of PCB for bending = 30 x h = (30) (0.062) = 1.86 in (effective width of PCB assuming no other similar components on PCB)
$I_P = bh^3/12 = (1.86)\ (0.062)^3/12 = 3.694\ x\ 10^{-5}\ in^4$
M = RP = 0.125 P (bending moment on PCB)

Substitute to get the wire load when PCB bends:

$$0.0003 = \frac{P(0.125)^3}{7.5(16x10^6)(1.917x10^{-8})} + \frac{(0.125)(0.125P)(1.2)}{2(1.95x10^6)(3.69x10^{-5})}$$

$$P = 0.3066\ \text{Ib}$$

26. Determine the resonant frequency of a rectangular plug-in epoxy fiberglass PCB simply supported (or hinged) on all four sides, 0.080 in thick, with a total weight of 1.0 pounds, as shown in figure. (Note: All dimensions in inches)
Assuming that:
E = 2 x 10^6 Ib/in^2 (PCB modulus of elasticity)
μ = 0.12 (Poisson's ratio, dimensionless)

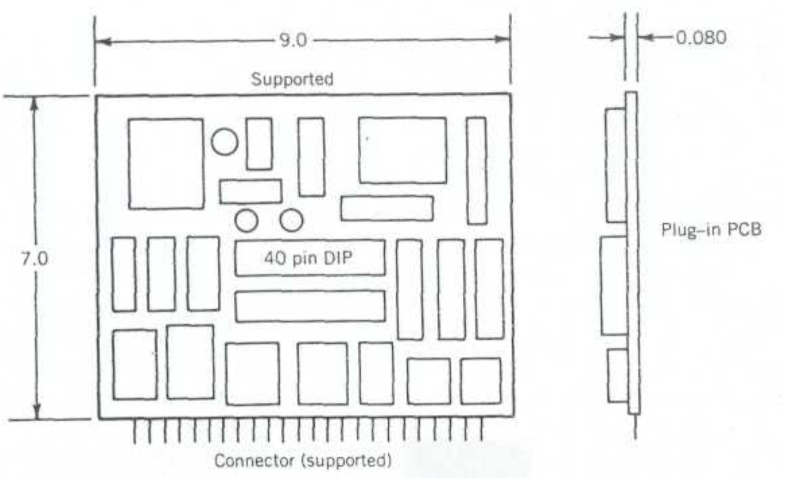

Solution:

The following information is required for a solution:

E = 2 x 10^6 Ib/in^2 (epoxy fiberglass modulus of elasticity)
h = 0.080 in (PCB thickness)
μ = 0.12 (Poisson's ratio, dimensionless)
W = 1.0 Ib (weight)
a = 9.0 in (PCB length)
b = 7.0 in (PCB width)
g = 386 in/sec^2 (acceleration of gravity)

$$D = \frac{(2 \text{ x } 10^6)(0.08)^3 h^3}{12(1-(0.12)^2)} = 86.6 \quad \text{Ib in} \quad \text{(stiffness)}$$

$$\rho = \frac{1.0}{(386)(9)(7)} = 0.431 \text{ x} 10^{-4} \quad \frac{\text{Ibsec}^2}{\text{in}^3}$$

Then the resonant frequency of PCB is

$$f_n = \frac{\pi}{2}\sqrt{\frac{86.6}{0.431 \text{ x } 10^{-4}}}\left(\frac{1}{(9)^2} + \frac{1}{(7)^2}\right)$$
$$= 72.9 \text{ HZ}$$

Part G-4: Sample Exams

Cairo University	M.Sc.: Electronics Cooling
Faculty of Engineering	Final Exam (Sample 1)
Mechanical Power Engineering Dept.	Time allowed 2 Hours

Solve as much as you can.

1. A heat sink constructed from 2024 aluminum alloy is used to cool a power diode dissipating 5 W. The internal thermal resistance between the diode junction and the case is 0.8 °C/W, while the thermal contact resistance between the case and the heat sink is 10^{-5} m^2. °C/W. Convection at the fin surface may be approximated as that corresponding to a flat plate in parallel flow.
a) Assuming that all the diode power is transferred to the ambient air through the rectangular fins; estimate the operating temperature of the diode.
b) Explore options for reducing the diode temperature, subject to the constraints that the air velocity and fin length may not exceed 25 m/s and 20 mm, respectively, while the fin thickness may not be less than 0.5 mm. All other conditions, including the spacing between fins, remain as prescribed.

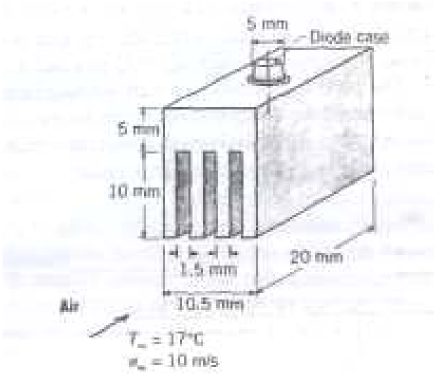

2. Consider an array of vertical rectangular fins, which is lo be used lo cool an electronic device mounted in quiescent, atmospheric air at T_∞= 27 °C. Each fin has L = 20 mm and H = 150 mm and operates at an approximately uniform temperature of T_s = 77 °C. For the optimum value of fin spacing S and a fin thickness of t = 1.5 mm, estimate the rate of heat transfer from the fins for an array of width W = 355 mm.

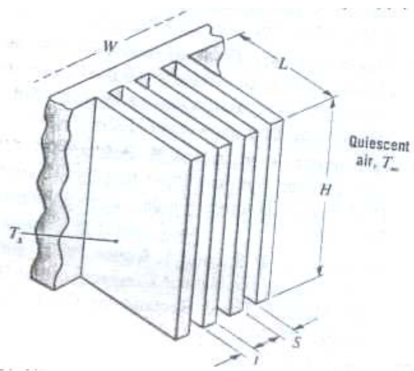

3a. What are the factors affected on filter selection to be mounted on electronic chassis?

3b. What's the difference between active and passive immersion cooling techniques?

4. The interface temperature of an electronic assembly dissipating 10 W must be limited to 40 ^oC in a 50 ^oC environment. It is assumed that all of the generated heat will be removed by thermoelectrics and that heat absorbed from the environment is negligible. The interface temperature difference between the assembly and the thermoelectric can be held to 2 ^oC. The temperature difference between the thermoelectric and ambient can be held to 8 ^oC. The bismuth telluride element used has a length of 0.3 cm and a cross-area of 0.01 cm^2.

Determine the size and performance characteristics of the thermoelectric temperature control device. Knowing that
The equivalent material properties of the thermoelectric couples is

$\rho_e = 0.00267\ \Omega.cm$

$\alpha_e = 425 \times 10^{-6}$ V/K

$k_e = 0.00785$ W/cm.K

NB: Design for maximum refrigeration capacity.

5. Determine the axial force in the lead wire for the resistor shown in figure below, when bending of the PCB is included in the analysis over a temperature cycling range from -50 to +90 °C, which produce total horizontal displacement expected at the top of the wire will be 0.0003 in. (Note: All dimensions in inches)
Assuming that:
$E_W = 16 \times 10^6$ Ib/in^2 (copper wire modulus elasticity)
$E_P = 1.95 \times 10^6$ Ib/in^2 (PCB modulus of elasticity)

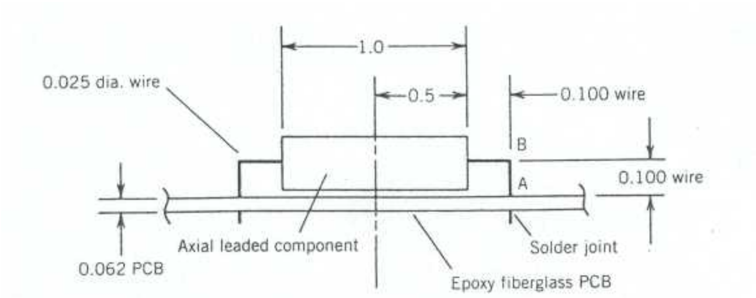

Cairo University	M.Sc.: Electronics Cooling
Faculty of Engineering	Final Exam (Sample 2)
Mechanical Power Engineering Dept.	Time allowed 2 Hours.

Solve as much as you can.

1. Consider a surface-mount type transistor on a circuit board whose temperature is maintained at 35 °C. Air at 20 °C flows over the upper surface of dimensions 4 mm by 8 mm with a convection coefficient of 50 W/m^2.K.Three wire leads, each of cross section 1 mm by 0.25 mm and length 4 mm, conduct heat from the case to the circuit board. The gap between the case and the board is 0.2 mm.

a) Assuming the case is isothermal and neglecting radiation; estimate the case temperature when 150mW are dissipated by the transistor and (i) stagnant air or (ii) a conductive paste fills the gap. The thermal conductivities of the wire leads, air. And conductive pastes are 25, 0.0263, and 0.12 W/m.K. respectively.

b) Using the conductive paste to fill the gap, we wish to determine the extent to which increased heat dissipation may be accommodated, subject to the constraint that the case temperature not exceeds 40 °C. Options include increasing the air speed to achieve a larger convection coefficient h and/or changing the lead wire material to one of larger thermal conductivity. Independently considering leads fabricated from materials with thermal conductivities of 200 and 400 W/m.K., compute and plot the maximum allowable heat dissipation for variations in h over the range $50 \leq h \leq 250$ W/m^2.K.

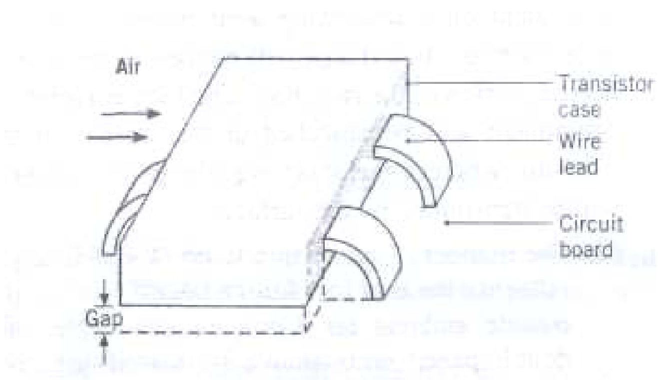

2. A 35 W power transistor is fitted to a duralumin plate 150 x 165 mm and 5 mm thick. The plate is finned on the other side by 15 fins spaced 9 mm apart. The fins are 2 mm thick and protrude 40 mm. In an ambience of 40 °C, how long would it take this transistor, after turning it on, to be within 5 ^{o}C from its final temperature? Neglect effect of radiation.

3a. Describe with neat sketch the components of a heat pipe.

3b. Discuss briefly the types of Printed Wiring Board.

4. A circular transistor of 10 mm diameter is cooled by impingement of an air jet exiting a 2-mm diameter round nozzle with a velocity of 20 m/s and a temperature of 15 °C. The jet exit and the exposed surface of the transistor are separated by a distance of 10 mm. If the transistor is well insulated at all but its exposed surface and the surface temperature is not to exceed 85 °C, what is the transistor's maximum allowable operating power?

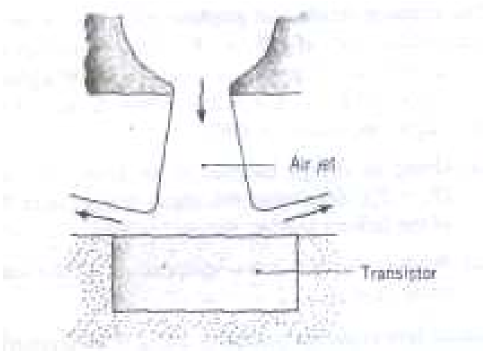

5. Determine the deflections and thermal stresses expected in the lead wires and solder joints of the surface mounted transformer shown in the following figure, when it is mounted on an aluminum composite PCB which experiences in plane (X and Y) thermal expansion during rapid temperature cycling tests over a temperature range from -30 to +80 °C, with no electrical operation. (Note: All dimensions in inches)
Assuming that:
$a_T = 35 \times 10^{-6}$ in/in/°C (average TCE of transformer)
$a_P = 20 \times 10^{-6}$ in/in/°C (average TCE of composite PCB)
$E_W = 16 \times 10^6$ psi (modulus of elasticity, copper wire)

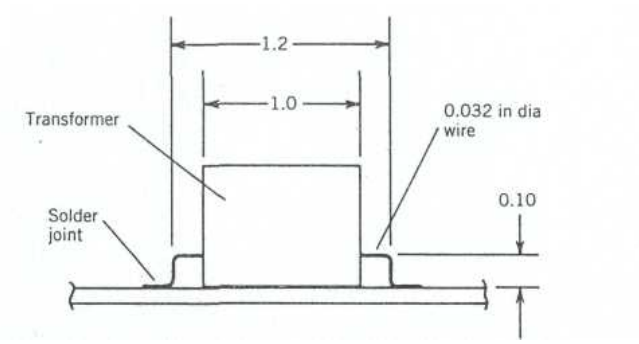

Cairo University Faculty of Engineering Mechanical Power Engineering Dept.	M.Sc.: Electronics Cooling Final Exam (Sample 3) Time allowed 2 Hours.

Solve as much as you can.

1. A square isothermal chip is of width w = 5 mm on a side and is mounted in a substrate such that its side and back surfaces are well insulated, while the front surface is exposed to the flow of a coolant at T_∞ = 15 °C. From reliability considerations, the chip temperature must not exceed T = 85 °C.
If the coolant is air and the corresponding convection coefficient is h = 200 W/m^2.K. What is the maximum allowable chip power? If the coolant is a dielectric liquid for which h = 3000 W/m^2.K. What is the maximum allowable power?

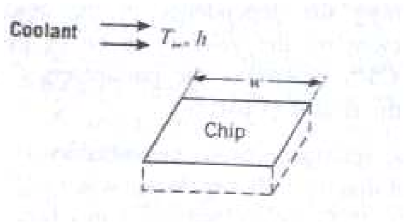

2. A common procedure for cooling a high-performance computer chip involves joining the chip to a heat sink within which circular microchannels are machined. During operation, the chip produces a uniform heal flux q_c'' at its interface with the heat sink, while a liquid coolant (water) is routed through the channels. Consider a square chip and heat sink, each L x L on a side, with microchannels of diameter D and pitch S = C_1D, where the constant C_1 is greater than unity. Water is supplied at an inlet temperature $T_{m,i}$ and a total mass flow rate $m^\bullet$ (for the entire heat sink).

a) Assuming that q_c'' is dispersed in the heat sink such that a uniform heat flux q_c'' is maintained at the surface of each channel; obtain expressions for the longitudinal distributions of the mean fluid, $T_m(x)$, and surface. $T_s(x)$, temperatures in each channel. Assume laminar, fully developed flow throughout each channel, and express your results in terms of $m^\bullet$. q_c''. C_1, D, and/or L, as well as appropriate thermophysical properties.

b) For L = 12 mm, D = 1 mm, C_1 = 2, q_c'' = 20 W/cm^2, $m^\bullet$ = 0.010 kg/s, and $T_{m,i}$ = 290 K, compute and plot the temperature distributions $T_m(x)$ and T_s (x).

c) A common objective in designing such heat sinks is to maximize q_c'' while maintaining the heat sink at an acceptable temperature. Subject to prescribed values of L = 12 mm and $T_{m,i}$ = 290 K and the constraint that $T_{s,max} \leq 50$°C, explore the effect on q_c'' of variations in heat sink design and operating conditions.

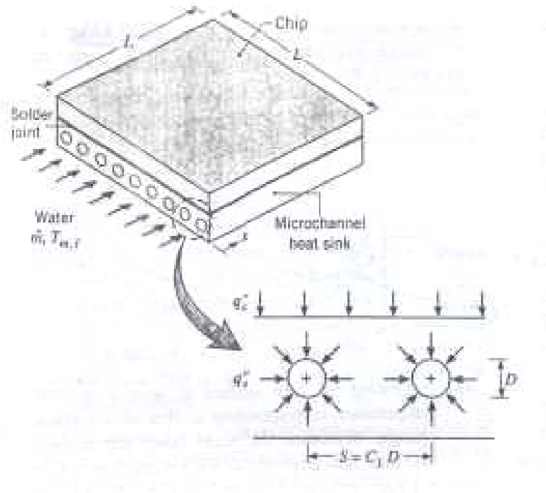

3a. Describe the limitation of operation with heat pipe.

3b. What are the considerations that must be taken in electronics chassis design?

4. A thermoelectric cooling system is to be designed to cool a PCB through cooling a conductive plate mounted on the back surface of the PCB. The thermoelectric cooler is aimed to maintain the external surface of the plate at 40 ^{o}C, when the environment is 48 ^{o}C. Each thermoelectric element will be cylindrical with a length of 0.125 cm and a diameter of 0.1 cm. The thermoelectric properties are:

	p	n
α (V/K)	170×10^{-6}	-190×10^{-6}
ρ (Ω.cm)	0.001	0.0008
k (W/cm K)	0.02	0.02

Assume the cold junction at 38 ^{o}C and the warm junction at 52 ^{o}C, and the electrical resistance of the leads and junctions = 10 % of the element resistance and design for maximum refrigeration capacity. If 10 W are being dissipated through the plate and steady-state conditions then determine:

1- Number of couples required.
2- Rate of heat rejection to the ambient.
3- The COP.
4- The voltage drop across the d.c. power source.

5. Determine the resonant frequency of a rectangular plug-in epoxy fiberglass PCB simply supported (or hinged) on all four sides, 0.080 in thick, with a total weight of 1.0 pounds, as shown in figure. (Note: All dimensions in inches)
Assuming that:
$E = 2 \times 10^6$ Ib/in^2 (PCB modulus of elasticity)
$\mu = 0.12$ (Poisson's ratio, dimensionless)

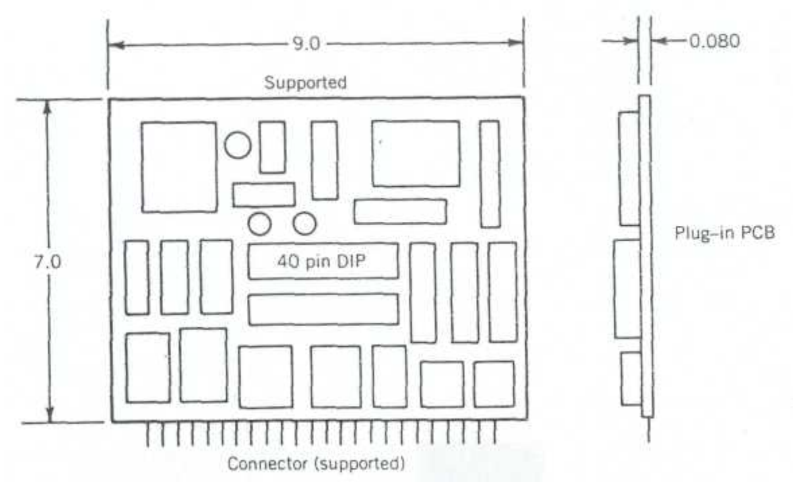

Part G-5: Contents of Courses and Books

Contents of National and International Courses and Books

A. Contents of National and International Courses

University or web site	Course title	Course number	Lecturers	Content
Auburn university	Heat transfer in electronic equipment	ME5348	A.D. Kraus and A. Bar-Cohen	Introduction to Thermal/Fluid Issues in Electronics Manufacturing and Assembly Conduction in Printed Circuit Boards and Chip Packages Natural Convection Cooling of Electronic Systems Forced Convection from Printed Circuit Boards Design & Optimization of Single Fins Heat Sinks Introduction to Boiling and Condensation Passive Immersion Cooling Compact Models of Chip Packages and Heat Sinks Failures and Reliability Strain, Stress, and Fatigue Thermoelectric Cooling Heat Pipes

www.engr.sjsu.edu/ckomives/Courses/Heat%20Transfer%20in%20Electronics/index.htm	Heat transfer in electronics	CHE/ME 109	Dr. Claire F. Komives	Introduction: importance of heat transfer Basic of heat transfer Heat transfer mechanism General 1-D conduction General 3-D conduction Heat generation and variable thermal conductivity & Solution of conduction problems Steady state 1-D conduction Heat transfer from finned surfaces Transient conduction - lumped system analysis 1-D Transient conduction Introduction to forced convection Natural convection over surfaces Natural convection from finned surfaces and PCB's Combined natural and forced convection Thermal radiation
The State University of New Jersey-Science and Engineering Resource Center	Mechanical engineering aspects of electronic cooling	14: 650: 478	Dr. L. S. saxena	Communications/Information industry overview Convergence of telephone, computer, entertainment Communications networks and technologies Traditional telephone, voice & data, LANs, WANs, Internet, IP OSI layers, the physical layer and opto-electronic packaging hierarchy Semiconductors and integrated circuits Integrated circuit packaging Printed circuit boards, backplanes, cabinets, connectors, cables Optical and electronic components Electronic materials Thermal management Thermal design & analysis, free and forced air-cooling etc. Electrical design considerations Parasitics, EMC/EMI etc. Product development and manufacturing Reliability, qualification, environmental stress testing Failure modes, shock & vibration, thermo-mechanical stresses, corrosion etc. Quality standards, ISO 9000 Industrial ecology and design for environment, ISO 14000

University of Oslo	Electronic components, packaging and product	ISBN 82-992193-2-9	Leif Halbo and Per Ohlckers	Introduction to electronic products and electronic packaging Technologies for electronics-overview Materials and basic processes Components for electronic systems Printed wiring board PCB design Production of PCB Hybrid technology and multi ship modules Micro structure technology and micro machined devices
Portland State University	Heat Sinks for Electronic Cooling Applications	ME 449/549	Gerald Recktenwald Associate Professor, Mechanical Engineering Department	What is a Heat Sink? Types of Heat Sinks Simple Model of a Component with a Heat Sink Review of Fin Theory Characterization Experiments: measuring thermal resistance Empirical Data on Heat Sinks

Univ. of Minnesota & Innovative Research, Inc.	System-Level Thermal Design for Electronics Cooling		Dr. Suhas Patankar	Importance of thermal design. Board-level and system-level design. Available software tools for board-level analysis. Computational Fluid Dynamics (CFD). Software tools for CFD. Mass and momentum conservation. Pressure drop and flow resistance. Fan curves. Heat transfer coefficients. Representation of cooling systems as flow networks. Flow resistances for common components.
Cairo University	Thermal Design of Electronic Packaging		Dr. Kamal-Eldien Hassan	Introduction Review of basic principles Packaging of electronic systems Analogy between electric and thermal circuits Thermal networks Thermal contact resistance Heat exchangers Forced air cooling Design for transient conduction

B. Contents International References

Book Title	Authors	Publisher	Contents
Cooling techniques for electronic equipment	Dave S. Steinberg	1991by John Wiley & Sons	• Evaluating the cooling requirements • Designing the electronic chassis • Conduction cooling for chassis and circuit boards • Mounting and cooling techniques for electronic components • Practical guides for natural convection and radiation cooling • Forced air cooling for electronics • Thermal stresses in lead wires, solder joints, and plated through holes • Predicting the fatigue life in thermal cycling and vibration environments • Transient cooling for electronic systems • Effective cooling for large racks and cabinets • Finite element methods for mathematical modeling • Environmental stress screening techniques
Electronic packaging and interconnection hand book	Charles A. Harper	1997 by McGraw-Hill	Materials for electronic packaging Thermal management Connector and interconnection technology Wiring and cabling for electronic packaging Solder technologies for electronic packaging Packaging and interconnection of integrated circuits The hybrid microelectronics technology Rigid and flexible printed wiring boards Surface mount technology Advanced electronic packaging Packaging of high speed and microwave electronic systems Packaging of high voltage systems

Design and packaging of electronic equipment	Joel L. Sloan	1985 by Van Nostrand Reinhold Company	Factors influence equipment design Cooling techniques Mechanics of conduction Mechanics of convection and radiation Thermal elastic effects Force systems in electronic equipment Displacement and stresses in equipment Dynamic characteristics of electronic equipment
Heat transfer	J. P. Holman	1997 by McGraw-Hill	Introduction to heat transfer Steady state conduction-one dimension Steady state conduction-multiple dimension Unsteady state conduction Principles of convection Empirical and practical relation for forced convection heat transfer Natural convection systems Radiation heat transfer Condensation and boiling heat transfer Heat exchangers Mass transfer

Introduction to heat transfer	Frank P. Incropera, and David P. Dewitt	2002 by John Wiley & Sons	Introduction to heat transfer Introduction to conduction One dimensional, steady state conduction Two dimensional, steady state conduction Transient conduction Introduction to convection External flow Internal flow Free convection Boiling and condensation Heat exchangers Radiation
Heat transfer text book	John H. Lienhard IV and John H. Lienhard V	2001 by John H. Lienhard IV and John H. Lienhard V	Introduction to heat transfer Analysis of heat conduction Convective heat transfer Heat exchanger design Thermal radiation heat transfer Mass transfer

Mechanical Engineering Hand book	Ed. Frank Kreith	1999 by Boca Raton	Engineering thermodynamics Fluid mechanics Heat and mass transfer Electrical engineering Electronic packaging
Thermal Management of Microelectronic Equipment	L-T Yeh and R. C. Chu	American Society Of Mechanical engineering 2003	Heat transfer modes thermal interface resistances printed circuit boards air cooling and fans heat exchangers thermoelectric coolers

C. Contents of Books Available in FECU Library

1. Sung Jin Kim and Sang Woo Lee, "Air cooling Technology for Electronic Equipment", CRC press, London, 1996.

Contents:

- Geometric Optimization of Cooling Techniques
- Entrance Design Correlations for Circuit Boards in Forced-Air Cooling
- Forced Air Cooling of Low-Profile Package Arrays
- Conjugate Heat Transfer in Forced Air Cooling of Electronic Components
- Enhancement Air Cooling of Electronic Equipment
- Limits of Air Cooling –A Methodical Approach

2. Jerry E. Sergent Al Krum, "Thermal Management for Electronic Assembues", Mcgraw-Hill London, 1998.

Contents:

- Introduction
- Thermal Effects on Electronic Circuits
- Thermal Properties of Electronic Material
- Heat Generation in Electronic Circuits
- Basic Thermal Analysis
- Computer-Based Thermal Analysis
- Thermal Management
- Electronic Device Cooling

3. Frank P. Incropera, "Liquid Cooling of Electronic Devices by Single-Phase Convection", John Wiley& sons, inc, 1999.

Contents:

- Introduction
- Fundamentals of Heat Transfer and fluid Flow
- Natural Convection
- Channel Flows
- Jet Impingement Cooling
- Heat Transfer Enhancement

4. Roger vizi, "Forced Hot Air Furnaces, Troubleshooting and Repair", mcgraw-Hill, London, 1999.

Contents:

- Introduction
- Listing and Observing
- Components of a Gas Forced Air Heating System
- Electric Circuits
- Operation of a Gas Forced Air Heating System
- Tuning up a Gas Forced Air Heating System
- Troubleshooting a Gas Forced Air Heating System
- Introduction to Humidifiers
- Installation and Maintenance of Humidifiers
- Is an Electronic Air Cleaner Right For You?
- Installation and maintenance of Electronic Air Cleaners
- Introduction to Oil Forced Air Heating Systems
- Electric Circuits for Oil Forced Air Heating Systems
- Protecting Oil Tanks in the Winter
- Operation of an Oil Forced Air Heating Systems
- Tuning Up an Oil Forced Air Heating Systems
- Troubleshooting an Oil Forced Air Heating Systems
- Is Electric Forced Air Heat Right For You?
- Controls for an Electronic Forced Air Heating System
- Circuits for an Electronic Forced Air Heating System
- Operation and Maintenance Electronic Forced Air Heating System
- Troubleshooting Electronic Forced Air Heating System
- Is a Heat Pump Right for You?
- How Does a Heat Pump Work?
- Introduction to Heat Pumps
- Operation and Maintenance of Heat Pumps
- Troubleshooting Heat Pumps

Part G-6: Internet Links

Electronics Cooling Internet Links
(2005-2006)

http://www.electronics-cooling.com/index.html
http://www.wyntec.com.au/coolers.htm
http://www.acktechnology.com/Application%20Notes.htm
http://www.melcor.com/index.html
http://home.socal.rr.com/xsvtoys/articles.htm
http://www.nidec.com/aircooling/fantech.htm
http://www.ferrotec.com/usa/index.html
http://www.desernet.com
http://www.electronics-cooling.com/html/2003_august_a1.html
http://www.me.umn.edu/courses/me5348/manuf00.htm
http://www.msoe.edu/eecs/cese/courses/courses.php?course=MA-231&progcode=IE
http://www.thermalloy.com/catalog/htm/geninfo.htm
http://www.mhhe.com/catalogs/cust_serv/review1.mhtml
http://www.coolingzone.com/Content/SupplierDirectory/index.html
http://www.comsol.com/
http://widget.ecn.purdue.edu/~CTRC/info/wishtv.htm
http://www.amazon.com/exec/obidos/ASIN/0/ref%3Dnosim/bookssites-20/103-9923687-8167014
http://www.globalspec.com/industrial-directory/Evaporative_Cooling_Equipment/#FeaturedProducts
http://www.eriswerks.org/steal.html
http://www.mathcad.com/resources/mathcad_files/
http://www.nmbtc.com/
http://www.rpi.edu/~amitam/Amitay/research.html
www.Knuerr.com
http://www.me.pdx.edu/~gerry/class/ME449/#Description
http://www.thermalcooling.com/courses/instrnf.htm
http://www.cpmt.org/scv/courses/syscooling.html#overview
http://www.ttiedu.com/236cat.html#Outline
http://www.thermalcomputations.com/#A
http://www.me.umn.edu/divisions/tht/tme/pim/
http://www.technicalbooks.net/Merchant2/merchant.mv?Screen=PLST&Store_Code=1
http://www.asme.org/pubs/asmepress
http://www.mhtl.uwaterloo.ca/old/index.html
http://www.electronics-cooling.com/html/2003_august_a1.html

Part G-7: References

References

1. Dave S. Steinberg," Cooling Techniques for Electronic Equipment ", Second Edition, John Wiley & Sons, 1991.
2. Charles A. Harper," Electronic Packaging and Interconnection Hand Book ", Second Edition, McGraw-Hill, 1997.
3. Joel L. Sloan, "Design and Packaging of Electronic Equipment", Van Nostrand Reinhold Company, 1985.
4. J. P. Holman, "Heat Transfer", Eighth Edition, McGraw-Hill, 1997.
5. Frank P. Incropera, "Introduction to Heat Transfer ", Fourth Edition, John Wiley, 2002.
6. Incropera, F. P. and Dewitt, D. P, Fundamentals of Heat and Mass Transfer, John Willey & Sons, New York., 1981.
7. Frank M. White, "Fluid Mechanics", Fourth Edition, McGraw-Hill, 1999.
8. Dave S. Steinberg, "Vibration Analysis for Electronic Equipment", Second Edition, John Wiley & Sons, 1988.
9. Kays, W. M. and London, A.L., "Compact Heat Exchangers", Second Edition, McGraw-Hill, 1964.
10. Gerhart, P. M. and Gross, R. J., "Fundamentals of Fluid Mechanics", Addison-Wesley Publishing Company, Massachusetts, 1985.
11. Chapman, A. J., "Heat Transfer", Macmillan Publishing Company, New York, 1974.
12. Kays, W.M., London, A.L., "Compact Heat Exchangers", Third Edition, Krieger Publishing Company, 1984.
13. Ellison G.N., "Fan Cooled Enclosure Analysis Using a First Order Method, Electronics Cooling", Vol. 1, No. 2, October 1995.
14. Belady C., "Standardizing Heat Sink Performance for Forced Convection, Electronics Cooling", Vol. 3, No. 3, September, 1997.
15. Biber C., Wakefield Engineering, Wakefield, Massachusetts, "Characterization of the Performance of Heat Sinks,", Personal Communication, October 1997.
16. Butterbaugh M.A. and Kang S.S., IBM, Rochester, Minnesota, "Effect of Airflow Bypass on the Performance of Heat Sinks in Electronic Cooling," Presented at the ASME Winter Annual Meeting, 1995.
17. Idelchik, Handbook of Hydraulic Resistance, CRC Press, Florida, 1994.
18. Blevins R.D., Fluid Dynamics Handbook, Krieger Publishing Company, 1984.
19. Miller, D.S., Internal Flow Systems, Gulf Publishing Company, Texas, 1990.
20. Sung Jin Kim and Sang Woo Lee, "Air cooling Technology for Electronic Equipment", CRC press, London, 1996.
21. Jerry E. Sergent Al Krum, "Thermal Management for Electronic Assemblies", Mcgraw-Hill London, 1998.
22. Frank P. Incropera, "Liquid Cooling of Electronic Devices by Single-Phase Convection", John Wiley& sons, inc, 1999.
23. Roger vizi, "Forced Hot Air Furnaces, Troubleshooting and Repair", mcgraw-Hill, London, 1999.